University of South Bohemia

Faculty of Science

Unique and conserved features of the *Trypanosoma brucei* mitochondrion

HABILITATION THESIS

Mgr. Mir Mohamod Hassan Hashimi Ph.D.

2016

Contents

ACKNOWLEDGEMENTS

I thought this was supposed to be the easy part to write. This thesis forced me to take a good look back at my career so far. Wow, what a great ride it's been. Science is a human endeavor, and in its pursuit, I have had the great fortune to come into contact with some excellent, inspiring people on the way. There are simply too many people to thank! Because a habilitation thesis is toward a pedagogical title, I will specifically thank the people directly involved in that process.

But I break that rule now to thank someone, without whom none of this makes any sense: my beautiful (inside and out) and patient wife Baruška, the mother of our wonderful boy Alex. I returned to stay in České Budějovice because of you and I have no regrets. It may not be the best for a scientific career to stay in one place, but it's worth it to spend each wonderful day with you.

I am so fortunate that in Budějovice is University and Biology Center, a wonderful symbiosis that is so important for the region, because the great impact it makes outside of it! I am fortunate that Julius Lukeš contributes to this great environment by establishing and maintaining such a vibrant and interesting laboratory. Thanks Julo for allowing me to partake in this enterprise! It has made me a better person. It wasn't always pleasant, but it was always, always interesting.

But honestly, much of my intellectual development is thanks to great colleagues that sought voyage on the ship captained by Jula. Among those are the students I had the great pleasure of working with over these years. You have been such a motivated (and –ing), interesting and fun bunch! Thanks to (in rough chronological order of when they came into my life): Zdeňka Čičová, Lucie Novotná, Yan-Zi Wen, Lucie Kafková, Sijia Lin, Lukaš Aberhard, Lindsay McDonald, Zhenqiu Huang, Sabine Kaltenbrunner, Sameer Dixit, Adéla Křižová, Josef Kaurov and Hannah Bruce. Thanks to my great colleagues in the lab, many of whose names are not on the publications, but have enriched my scientific thought and life (in no particular order): Eva Horáková, Drahuška Faktorová, Priscila Peña Diaz, Eva Stříbrná, Eva Dobáková, Alex Haindrich, Zdeněk Paris, Zdeněk Verner, Lukáš Trantírek Silva Trantírková, Alena Zíková, Brain Panicucci, Ondra Gahura, Eva Doleželová, Eva Kriegová, Marcela Jungwirthová, Miša Navarová Jirka Černý.

I also learned so much from excellent scientists (and excellent people) I had the real honor to collaborate with. In particular I thank Laurie Read, whose collaboration started from the worst events of my scientific career. The joy from that collaboration outshines that anguish that catalyzed it. Totally worth it! I also thank Juan Alfonso who's sage and benevolent meddling has started the ball rolling on the next phase of my career...I guess it's up to me where that ball lands but it's a tough one to steer. Thanks go to all the people whose names are on the publications of course, especially (and also in no particular order) Sara Zimmer, Michelle Ammerman, Jonathan Fisk, David Staněk, Marina Cristodero, Anton Horváth, Vladislava Benkovičová, Petra Čermáková, De-Hua Lai, Pasha Flegontov and Kenneth Stuart.

I also have been lucky to guarantee an excellent course conceived by Tomaš Doležal (Thanks Tom!) and taught by great lecturers in the past and present: Michal Žurovec, Alena Krejči, Aleš Hampl, Lada Anděra, Roman Sobotka, Pepa Lazar, David Doležel, James Valdes, Ryan Rego, Víta Brya, Masako Asahina and Marek Jindra. I also thank Ondra Prašil for the chance to lecture in his Bioenergetics course and Petr Svoboda for the same in the prestigious Advances in Molecular Biology Course in Prague.

I wanted to keep this to a page. I made the font this obnoxiously low to achieve this goal. I would have to make it infinitely small to thank all those whose lives I've crossed because of science and do them all justice. Science simply rules. Thanks to all of you that I see that.

ABBREVIATIONS

A	Adenosine
A6	ATP synthase subunit 6
aa-tRNA	Aminoacylated trna
Ak	Akinetoplstic
AS	Antipodal site (of kDNA)
BSF (aka BS)	Bloodstream form
C	Cytosine
cI	Respiratory complex I (NADH dehydrogenase)
cII	Respiratory complex II (succinate dehydrogenase)
cIII	Respiratory complex III (ubiquinol:cytochrome *c* oxidoreductase)
cIV	Respiratory complex IV (cytochrome *c*:oxygen oxidoreductase)
Cox	Cytochrome *c* oxidase (subunit #) (cytochrome *c*:oxygen oxidoreductase)
cV	Respiratory complex V (F_0F_1-ATP synthase)
Dk	Dykinetoplstic
dsRNA	Double stranded RNA
EF	Elongation factor
ES	Editing site
ETC	Electron transport chain
Fe-S	Iron-sulfur
FRAP	Fluorescence recovery after photobleaching
G	Guanine
GPI	Glycosylphosphinositol
gRNA	Guide RNA
H^+	Proton
I	Inosine
IM	Mt inner membrane
IMS	Intermembrane space
kDNA	Kinetoplast DNA (kinetoplast)
KFZ	Kinetoflagellar zone
KHE	K^+/H^+ exchange
KREL	Kinetoplastid RNA editing ligase
KREN	Kinetoplastid RNA editing endonuclease
KRET	Kinetoplastid RNA editing terminal U transferase
KREX	Kinetoplastid RNA editing exonuclease
LECA	Last common eukaryotic ancestor
Letm1	Leucine zipper EF hand-containing transmembrane protein 1
LSU	Large (ribosomal) subunit
MCU	Mitochondrial calcium uniporter
MRB1	Mitochondrial RNA binding complex 1
Mt	Mitochondrial
OM	Mt outer membrane
ORF	Open reading frame
OXPHOS	Oxidative phosphorylation
PCF (aka PS)	Procyclic form
PMF	Proton motive force
RECC	RNA editing core complex
RNAi	RNA interference
S	Svedburg

SL	Spliced leader
SSU	Small (ribosomal) subunit
TAC	Tripartite attachment complex
TCA	Tricarboxylic acid
TIM	Translocase of the inner membrane
TLF	Trypanosome lytic factor
TOM	Translocase of the outer membrane
U	Uridine
UTR	Untranslated region
VSG	Variable surface glycoproteins

INTRODUCTION

1. My research so far… an abstract

I am at a crossroads in my research career. For over a decade, my main research focus has been on trypanosome RNA editing. It has been a very valuable academic experience for me, in which I have contributed to the understanding of an interesting, if somewhat esoteric, biological phenomenon. During this time, I have has the great fortune to be exposed to a variety of techniques and methods and have engaged in several stimulating collaborations. In short, due to this experience I have learned a lot.

Because trypanosome RNA editing is a vital maturation step for a majority of mitochondrial (mt) mRNAs, which encode core subunits of the respiratory chain, I became acquainted with the "powerhouse" of eukaryotic cells, the mitochondrion. The biology of this ancient organelle, which qualifies as a eukaryotic hallmark, has been fascinating to me from the beginning. The most intriguing aspect of mitochondria is the different forms the organelle can take in various milieux, from the reduced mitosomes of anaerobic parasites such as *Giardia intestinalis* to the canonical form found in budding yeast and humans. Despite the many differences among these various mitochondria, they all share fundamental properties that are rooted in the endosymbiotic origin of the organelle, as well as its tight integration into the fabric of eukaryotes.

In this introduction to my habilitation thesis, I will discuss the mitochondrion of the parasite *Trypanosoma brucei*, the model on which I have devoted most of my research career. First, I will highlight some of the key differences of the *T. brucei* organelle that illustrate its evolutionary divergence from other mitochondria: kinetoplast (k) DNA, uridine (U)-insertion deletion editing and its fluctuating energy metabolism. These discussions will be brief and to highlight major themes, as this habilitation thesis contains reviews that discuss these topics to more depth. Then I will discuss how this divergence (and its status as a true research model) makes it an excellent system for addressing major questions of mitochondria as a whole, informing its function throughout eukaryotes, including us. This part represents future directions I would like to take to understand this fascinating organelle.

2. A primer to mitochondria and its integration into the fabric of eukaryotes

Mitochondria arose from the acquisition of an α-proteobacterial endosymbiont by the last common eukaryotic ancestor (LECA) (1). A vestige of this event is the double membrane envelope surrounding the organelle, made up of the outer (OM) and inner (IM) membranes (Figure 1). These two lipid-bilayers delineate two internal compartments: the intermembrane space (IMS) between the OM and IM, plus the matrix bound by the latter. The IM is also a rather complicated structure, a substantial portion of which folds into the matrix to form cristae, a mt hallmark that is distributed throughout all major eukaryotic taxa (2).

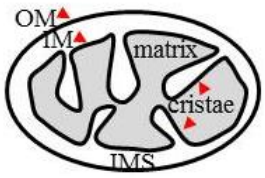

Figure 1. The ultrastructure of mitochondria.
OM, outer membrane; IM, inner membrane;
IMS, intermembrane space

2.1. Mitochondria as the powerhouse of eukaryotes

The textbook function of aerobic mitochondria is to serve as a powerhouse of the eukaryote, generating ATP that eventually powers a number of vital metabolic and physiological processes. The mitochondrial matrix is the seat of the tricarboxylic acid (TCA) cycle, also known as the Krebs or citric acid cycles, which central to the organelle's energy production (3). The catabolic pathways of several carbon sources such as carbohydrates, lipids and amino acids eventually converge into the TCA cycle, ultimately yielding CO_2 and H_2O. While ATP is produced by substrate-level phosphorylation, most of the energy from the breakdown of the chemical bonds occurring in the TCA cycle is harnessed by the reducing equivalents NADH(P) and $FADH_2$, which is generated by constituent dehydrogenase enzymes. NADH(P) and $FADH_2$ in turn shuttles high energy state electrons to the respiratory chain, a series of complexes mostly embedded within the IM, to convert their latent free energy into exploitable chemical energy.

One division of the respiratory chain is the electron transport chain (ETC), made up of four protein complexes, that couples the series of redox reactions that electrons flow to their sink, the reduction of O_2 to H_2O, with the active pumping of protons across the IM to the IMS. This mechanism accumulates the free energy from carbon-source catabolism as a proton (H^+) electrochemical gradient: the potential energy of proton motive force (PMF). The process known as oxidative phosphorylation (OXPHOS) emerges from the coupling of PMF with the production of ATP by F_OF_1-ATP synthase, thus completing the respiratory chain (4).

Both the TCA cycle and respiratory chain are other prominent remnants of the mitochondria's bacterial origin (3). Another vestige is that the organelle maintains its own DNA (5, 6), and therefore also a separate genetic system to express a handful of encoded proteins, which are always represented by subunits of the respiratory chain (1, 3). The often circular topology of mt DNA and also structure of mt ribosomes are thus prokaryotic in character (3, 7, 8).

2.2. Mitochondria as more than a powerhouse

Due to its early origin during eukaryogenesis (9), mitochondria is tightly integrating into the fabric of eukaryotes, doing more than being the renowned powerhouse of the cell. Other functions include the biogenesis of iron-sulfur (Fe-S) clusters, essential cofactors for enzymes playing myriad roles in the cell (10), shaping intracellular Ca^{2+} gradients, a potent secondary messenger in many cell signaling pathways (11) and mediating intrinsic apoptosis in metazoa (12). Fe-S cluster biogenesis appears to be the ultimate essential pathway of mitochondria, since anaerobic organisms such as *G. intestinalis* and the microsporidian *Encephalitozoon cuniculi* keep highly reduced forms called mitosomes for this purpose, despite losing its organellar genome and capacity for OXPHOS (13, 14). The OM represents the interface between mitochondria and the rest of the cell, allowing contact with other organelles like the endoplasmic reticulum to Ca^{2+} microdomains (11, 15) and providing a platform for the Bcl-2 family of pro- and anti-apoptotic proteins to regulate programmed cell death (12).

Both the OM and IM represent diffusion barriers separating mitochondria from the rest of the cell. The bulk of the proteins (~1, 100) required mitochondrial biogenesis are encoded in the nucleus, many of which are products of gene transfer from the endosymbiont to LECA, albeit of a polyphyletic nature (16). A sophisticated system of mt protein import has evolved in eukaryotes (17), populating the mt matrix

and IM via the multiprotein translocases of the OM (TOM) and IM (TIM), mt OM by the sorting and assembly machinery (SAM) plus finally the IMS by members of mitochondria IMS assembly (MIA) pathway (18). Many of the representatives these systems have significantly diverged throughout the evolutionary history of eukaryotes, such as TOM and MIA in *T. brucei* (19-22) or in the case of mitosomes have experienced significant reductive evolution (21-23). Thus, the protein import machineries represent an ancient innovation allowing the perpetuation of mitochondria in eukaryotes.

3. A primer to Trypanosoma brucei

3.1. *Trypanosoma brucei*'s position in the eukaryotic tree of life

T. brucei belongs to the excavate order Kinetoplastida (Figure 2), one of the three clades, along with Dipmlonemida and Euglendida, that comprise the phylum Euglenozoa (24). Several common features support the monophyly of this group of protozoan flagellates, including the addition of small spliced leader (SL) RNA to the 5'-end of all cytoplasmic mRNAs (25) and the presence of the modified base "J" in nuclear DNA (26). In turn, the phylum Euglenozoa is part of the superphylum Discicristata, appropriately named given all its members bear mitochondria with paddle-like, discoidal cristae. This discoidal morphology is different than the tubular or lamellar forms that are found in opisthokonts and plants, demonstrating its large evolutionary distance from these two clades (2). There are two schools of thought as to whether this great divergence is due to Euglenazoa being of an ancient character, in many ways "a living fossil" (20, 27), or just a product of its early divergence and rapid adaptation to extreme ecological niches such as parasitism (28) or oceanic depths (29). Regardless of which opinion prevails, the evolutionarily distance between Euglenozoa such as *T. brucei* and opisthokonts, a taxon containing typical biomedical research models such as the baker's yeast *Saccharomyces cerevisiae*, fruit fly *Drosophila melanogaster* and mouse *Mus musculus*, is vast. Thus, *T. brucei* and its fellow kinetoplastids have independently evolved some interesting characters that distinguish themselves from other eukaryotes. And yet they also share similarities that persist since the endosymbiosis event that gave rise to mitochondria in eukaryotes (1): core pathways that are required for the organelle's biogenesis as well as contributing to fitness of the eukaryotic host (3).

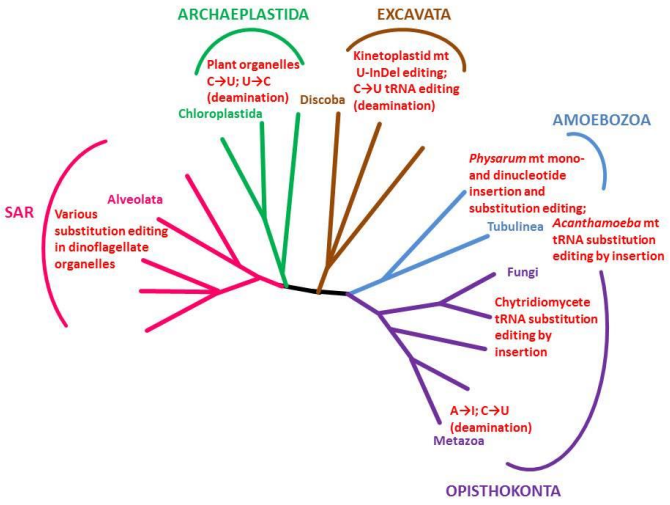

Figure 2. Position of kinetoplastids and distribution of RNA editing in the eukaryotic tree of life. Kinetoplastids are located in the excavate "Discoba" taxon in brown. Note the divergence from opisthokont Fungi and Metazoa taxa in purple. Identified forms of RNA editing are indicated at branches of organisms found. From (46), which in turn was modified from (24).

Like other eukaryotes, members of the order Kinetoplastida have mt DNA, encoding components of the respiratory chain and mt ribosome (30). However, unlike other eukaryotes, the organellar genome is a complex network of thousands of circular DNA that is located at a single location of their sole mitochondrion (31). This structure is called the kinetoplast (kDNA), and because it is an easily observable and unmistakable, it is the defining character of the order.

3.2. The biology *T. brucei*

3.2.1. *T. brucei* the pathogen

T. brucei has been a topic of research since the late 1800's, when Sir David Bruce identified it as the causative agent of nagana, a veterinarian disease of cattle, that is spread by its *Glossina* vector, the tsetse fly (32). The occurrence of tsetse flies in sub-Saharan Africa defines the epidemiological boundaries of the disease. Humans have an innate immunity by to the subspecies *T. brucei brucei* that causes this disease in domesticated ungulates, due to high-density lipoproteins in the serum called trypanosome lytic factors (TLF), a testament to the selection pressure of trypanosomiasis on higher primate evolution (33, 34). However, two subspecies have evolved distinct molecular mechanisms to avoid lysis by TLF: *T. brucei gambiense*, prevalent in western Africa, and *T. brucei rhodesiense*, occurring in the eastern part of the continent (35). These pathogens respectively cause chronic and acute forms of human African trypanosomiasis, commonly referred to as sleeping sickness.

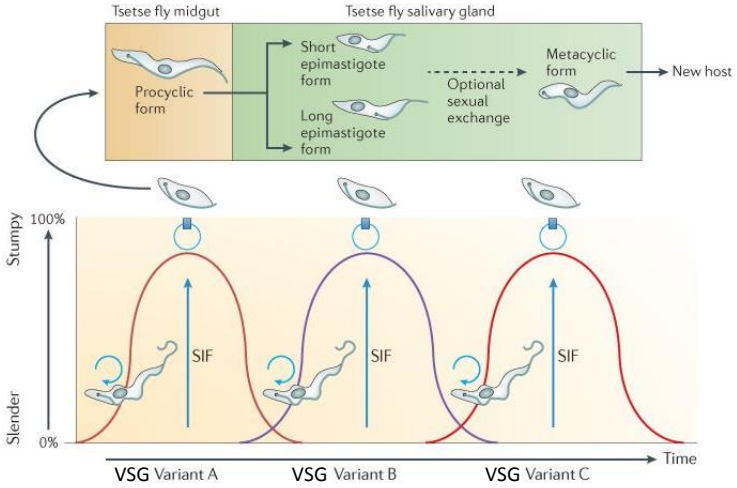

Figure 3. Life cycle of *T.brucei*. The top depicts the various stages of the parasite in the vector, including PCF. The bottom shows the waves of proliferation by the long slender BCF as is switches its VSG coat. Upon a still uncharacterized signal similar to quorum sensing, called the stumpy induction factor (SIF), the parasite switches into the non-proliferative stumpy form that is competent for uptake by the tsetse fly once again. From (36).

The *T. brucei* subspecies complex has a complicated lifecycle involving several stages exquisitely adapted to the different environments of the *Glossina* midgut and salivary glands, where the parasite is taken up from and transmitted to the host, respectively, and the mammalian circulatory system, where the pathogenic bloodstream form (BSF) resides (Figure 3). The long slender BSF represents the proliferative stage of the parasite in the host, which differentiate into non-dividing, stumpy BSF by a quorum-sensing-like mechanism (36). These stumpy forms are competent for uptake into the vector again to complete the lifecycle. The vector serves not only to spread the pathogen, but also the site for sexual

reproduction of the parasite to allowing for emergence of new strains better adapted to current conditions (37).

T. brucei evades the adaptive immunity of the host by a mechanism called antigenic variation (36, 38). Variable surface glycoproteins (VSGs) densely coat the surface of BSF, linked to the plasma membrane by glycosylphosphinositol (GPI) anchors, representing a shield that keeps antibodies from accessing invariant epitopes such as ion channels. VSGs are rapidly turned over, endocytosing antibodies that bind exposed epitopes on the surface protein (39). Antigenic variation occurs when the expression of the current VSG, recognized by the adequately primed immune system to clear the parasite, is switched for another VSG that represents a novel antigen for the host (Figure 3). Since there is estimated to be >1000 VSGs in a given strain of *T. brucei*, the parasite has a vast repertoire for antigenic variation (38). When *T. brucei* differentiates into insect-infective stage, it expresses another GPI-anchored surface protein called procyclin, whose ~10 isoforms facilitate interaction between the flagellate and insect-vector (40). Thus, the midgut-dwelling stage is referred to as the procyclic form (PCF). Other morphological and physiological changes occur in the transition from BSF to PCF (36) , and how these changes impact the *T. brucei* mitochondrion will be discussed in Section 7 of the introduction.

3.2.2. *T. brucei* the research model

The collective efforts to understand *T. brucei* biology have resulted in it becoming a biomedical research model. As with widely used opisthokont models such as *S. cerevisiae* and *D. melanogaster*, *T. brucei* is amenable for genetic manipulations due to its ease of transformation and well developed transgenesis toolkit (41). Among these tools is a tetracycline-controlled system of transgene expression, which is not afflicted by the unintended side-effects of the antibiotic on opisthokont models (7, 8) as well as being the only *in vitro* cultured trypanosomatid with the capacity for RNA interference (RNAi) (42). Furthermore, the simplified cell architecture of *T. brucei* makes it an appealing cell biology model (43). For example, the single Golgi apparatus of the flagellate was exploited as a model for addressing the organelle's duplication (44). Many other discoveries made in *T. brucei* were enlightening for our understanding fundamental eukaryotic processes, such as the biochemistry of GPI anchors (45), the capacity to shape transcriptomes by RNA editing (46) and revealing the evolutionary history of flagella (47) and the nuclear pore (48) and TOM complexes (19). Thus, *T. brucei* is not only a model for understanding Euglenazoa biology, such as unravelling the molecular mechanism of VSG switching (38), but also for eukaryotes as a whole from a highly evolutionarily-diverged perspective.

4. Kinetoplast DNA

As mentioned in section 3.1, the mt genome of *T. brucei* is concentrated in a easily observed spot within its single mitochondrion, in proximity to the basal body from which the flagellum arises (31). In fact, the kDNA is connected to the basal body by cytoskeletal filaments crossing the mt double membrane called the tripartite attachment complex (TAC) (Figure 4). Closer dissection of kDNA reveals that it is a concatenated network of circular DNA, which is made up of two classes based on their size: minicircles

(~1 Kb long in *T. brucei*) and maxicircles (23 Kb) (30, 49). While there are only 30-50 copies of the latter, the former represents the bulk of kDNA, being present in several thousands of copies. The maxicircle is the equivalent of the mt DNA from other eukaryotes as it encodes 2 rRNA and 18 protein-encoding genes. The minicircles are unique to order Kinetoplastida, being a vast, heterogeneous population encoding a majority of the maxicircle-derived mRNAs via RNA editing (Section 5), the minicircles contain essential genetic information that must be faithfully replicated during the cell cycle for mitochondrial biogenesis in progeny cells.

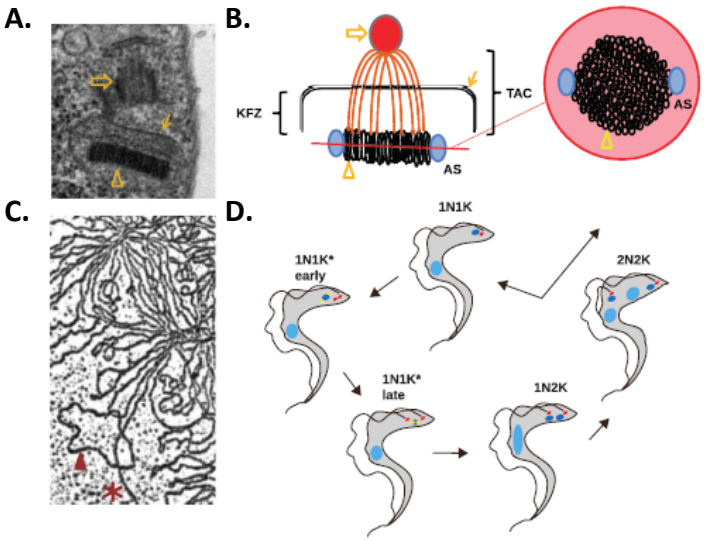

Figure 4. The kinetoplast DNA of *T.brucei* and other trypanosomatids. A. the kDNA disc (hollow arrow head) in proximity to the basal body (hollow arrow) and separated by the mt membrane (arrow). **B.** a schematic depiction of **A** indicated in the same way. Abbreviations as in main text. Concatenated minicircles in black. **C.** Isolated kDNA network from the related *Trypanosoma avium*, showing a minicircle (arrowhead) and maxicircle (*). **D.** kDNA division is synchronized with the cell cycle and S phase. Number of kDNA (K) or nuclei (N) indicated to the top of cell. From (30).

4.1. Kinetoplast DNA replication

The replication of kDNA mini- and maxicircles is a complicated affair compared to other eukaryotes, requiring an estimated 150 proteins, for which only 30 have been characterized (49). Among this machinery are enzymes including ligases, topoisomerases, primases, six helicases and seven polymerases, all acting in concert for proper kDNA replication (Figure 4). Minicircle replication is better understood than maxicircle replication. As a first step, minicircles are freed from the concatenated network by a topoisomerase II into the kinetoflagellar zone (KFZ), which lies between the kDNA and basal body (49). In the KFZ, minicircle replication is initiated by a helicase and primase, followed by elongation of the leading and lagging strands by the same DNA polymerase Pol1B (50). After further processing, the duplicated minicircles are reattached at opposing poles called antipodal sites (ASs), which seeds the daughter kDNA networks. These freshly synthesized minicircles are marked as such by gaps and nicks that are ultimately resealed by another DNA polymerase and ligase when the kDNA is fully replicated. The daughter networks are attached by the nabelschnur, a thread of maxicircles whose decantenation allows the separation of the two kDNAs (51).

kDNA replication is unusual in that occurs once during the cell cycle, preceding nuclear DNA replication during the S phase of mitosis (52) (Figure 4). The prior division and movement of the basal body ultimately safeguards the segregation of daughter kDNA networks via the connecting TAC (51, 53). The

orchestration of the kDNA replication machinery requires the careful regulation of the comprising proteins. Enzymes such as kDNA polymerase ID are dynamically moved to the kDNA at the appropriate time in the cell cycle for their activity (54), while the levels of others is controlled by proteolysis (55). All of these components must be coordinated like clockwork for the fidelity heredity of this fragmented organellar genome.

4.2. Life without kinetoplast DNA

An interesting consequence of faulty kDNA replication is the emergence in the wild of dykinetoplstic (Dk) *T. brucei equiperdum* and akinetoplastic (Ak) *T. brucei evansi*, subspecies that have partially or completely lost their kDNA (56-58). While the morphology of the kDNA of Dk *T. brucei* appears to be normal, the homogenization of minicircle classes lurks under the ultrastructural surface, diminishing their genetic content to a handful of sequences that are not sufficient to decrypt mRNAs needing RNA editing (Section 5). Maxicircles in turn accumulate deletions because of an absence of selection pressure for their maintenance (59), another step on the slippery slope to the Ak state (56).

Due to the loss of most or all of the mt genes required for respiratory chain biogenesis *T. b. evansi* and *T. b. equiperdum* are locked into the long slender BSF stage (56-58), as they cannot transform to PCF, in which survival relies on OXPHOS (the reason is that the PCF has a more active mitochondrion than the BSF, as further discussed in Section 7). These have essentially become the equivalent of petite mutant yeast, in which the mt DNA is aberrant (rho^-) or ablated (rho^0) (60). Just like these petite mutants, Dk and Ak *T. brucei* can only live on fermentable carbon sources, such as the glucose-rich bloodstream.

Because of their monomorphism, *T. b. evansi* and *T. b. equiperdum* have become monoexonous parasites spread mechanically on the mouth parts of biting insects or by coitus in equines, respectively. This discontinuation of the vector-dwelling life cycle stages have allowed these trypanosomatids to escape from the tsetse fly belt throughout the globe (61). However, they also give up the advantages of sex, which may not represent a good long-term life strategy (62).

5. Trypanosome RNA editing and other mitochondrial mRNA maturation steps

5.1. RNA editing

In 1986, Rob Benne and co-workers discovered that 4 Us were post-transcriptionally inserted into specific sites within an mt mRNA encoding cytochrome *c* oxidase (cox) 2, a subunit of respiratory complex IV, to fix a frameshift mutation encoded in the gene's open reading frame (ORF) (63). This discovery stood out since it seemed to contradict the central dogma of molecular biology, strictly dictating that the DNA to RNA flow of information. They dubbed this process RNA editing, which

describes any site-specific change in RNA sequence so that it differs from that of its corresponding gene, excluding RNA splicing and 3´-polyadenylation (64).

In *T. brucei*, transcripts from 12 out of the 18 protein coding genes require RNA editing for the decryption of their ORFs to make a translatable mRNA. These RNAs are edited to different degrees. Three of them, including cox2, are minimally edited, requiring a few U-insertions to fix frameshifts. The rest require pan editing, in which hundreds of Us are inserted into and tens of Us are deleted from the previously guanine-cytosine (GC)-rich transcript to uncover its ORF.

The discovery of RNA editing was important conceptually, because it opened up the possibility of transcriptomes being shaped by such processes. Indeed, other types of RNA editing were discovered (Figure 2), such as adenosine (A) to inosine (I) conversion editing, the most common form found in metazoa (65). While these other forms differ from U-insertion/deletion RNA editing found in kinetoplastids, many mechanistic details are shared among them (46). First is that the central dogma of molecular biology is not betrayed after all: double stranded (ds) RNAs resulting from either hydridization of two trans-acting transcripts or an intramolecular hairpin loop designate the RNA editing site. Second is the interplay between these dsRNA substrates and protein machinery for the catalysis of the given RNA editing event.

5.1.1. Guide RNAs and pan editing

The discovery of small the non-coding gRNAs revealed the genetic component precisely specifying how a subset of trypanosome mt mRNAs are edited to yield a translatable ORF (66). These *trans*-acting molecules hybridize to their cognate mRNAs via their 5’ anchor domains by canonical Watson-Crick and wobble G:U base pairing (67) (Figure 5). At the first base pair mismatch, the gRNA information domain begins, which represents sequence that guides the proper insertion or deletion of U along multiple adjacent editing sites (ESs) in the mRNA until both strands are complementary. The 3’-end of gRNAs are appended post-transcriptionally by a oligo(U) tail (68), which may help to stabilize its duplex with mRNA (69) but not the actual stability of the small transcript affecting their steady state levels (70). The discovery of gRNAs also represents another conceptual breakthrough, being the first case of a small, non-coding and 3’oligo(U) tailed RNA affecting a protein-coding transcriptome, and pre-dating the finding of microRNAs that play a comparable role for nucleus-encoded mRNAs (71).

Strangely, there is no *trans*-acting gRNA for the decoding of *cox2*, the mRNA that sparked the trypanosome RNA editing field (63). The reason for this absence is that the 3’-untranslated region of the transcript contains a sequence that acts like a *cis*-guide RNA by forming an intramolecular loop (72).

Pan-edited mRNAs require dozens of gRNAs for their decryption along their length (73) (Figure 5). The first gRNA:mRNA duplex is formed between the gRNA anchor domain and the small 3’ never-edited sequence present in all pan edited mRNAs. Subsequent gRNAs form anchor duplexes with freshly edited mRNA sequences directed by the previous, 3’-proximal gRNA. Because of this cascade of gRNA binding, pan-editing occurs in a 3’ to 5’ direction along the mRNA (74). This mechanism requires the action of RNA helicases to unwind the utilized gRNA from the mRNA to allow for the binding of the next (75), a process that seemingly leads to degradation of the obsolete gRNA (76-78).

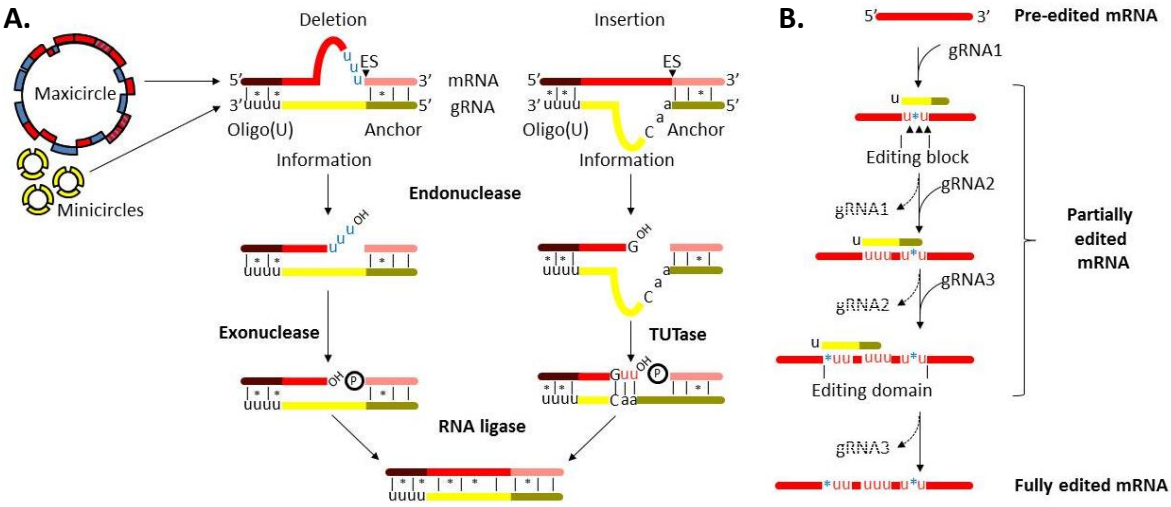

Figure 5. Trypanosome RNA editing. A. The mechanism of a single round of U-deletion (left) or U-insertion (right) RNA editing as mediated by RECC. **B.** 3' to 5' progression of pan editing requires multiple gRNAs. Watson-Crick base pairs, lines; G:U base pairs, dots; OH, 3' hydroxyl group; P, 5' phosphate; inserted Us are in red; Us to be deleted are in blue; position of deleted U, blue *; ESs, black arrow heads; degraded gRNAs are in dashed letters. Please see main text for elaboration of both mechanisms. From (46).

5.1.2. Core catalytic activities of RNA editing

The recapitulation of the U-insertion or U-deletion at a single ES *in vitro* using synthesized dsRNA substrates and mitochondrial lysates supported the hypothesis that trypanosome RNA editing requires a cascade of enzymatic activities (79, 80). These catalytic steps are orchestrated by a fascinating molecular machine called the RNA editing core complex (RECC), also known as the 20 Svedburg (S) editosome or L-complex, the former alias reflecting the sedimentation properties of the enzymatically active complex (46, 81, 82). In *T. brucei*, RECC is made up of about 20 proteins, including two RNA ligases (KREL1 and 2) and U-specific exonucleases (KREX1 and 2), a terminal U transferase (KRET2) and three RNase III endonucleases (KREN1-3). Other subunits serve a structural or RNA binding role.

RECC catalyzes the following steps (Figure 5). First, at the gRNA defined ES, the mRNA is cleaved by one of the KRENs to yield 5' and 3' fragments that are bridged by the bound gRNA. Next, depending on the gRNA information domain sequence, one or more Us are added by KRET2 or removed by KREX2 from the 5'-fragment. Finally, after the ES has been edited to be complementary to the gRNA information domain, the two mRNA fragments are sealed together by KREL1.

The recognition that a given ES requires U-insertion, U-deletion or the editing of *cis*-gRNA-containing *cox2* is mediated by one of the three endonucleases, which specifically cleave only one type of dsRNA substrate (83). Typically, RNase III endonucleases form homodimers to cleave both dsRNA strands (84). Because RNA editing requires only the cleavage of the mRNA strand, each KREN proteins dimerizes with its own unique catalytically inert partner (85). It remains unclear whether these KREN containing RECCs represent different, stable isoforms that specialize in processing a specific ES type, or if they represent

discrete modules that are selectively added onto RECC depending on the bound ES. However, it is clear that editing of several ESs defined by one gRNA and pan editing of mRNAs requiring multiple gRNAs requires a dynamic machinery involving more than RECC.

5.1.3. Multi-core processing: the MRB1 complex

In 2008, a dynamic collection of ~31 proteins were discovered that associate with proteins or activities with established roles in RNA editing, which were called either the mt RNA binding complex 1 (MRB1) (86, 87) or guide RNA binding complex (GRBC) (88). Further work has refined this initial picture to reveal that MRB1 is made up of two subcomplexes with different roles in RNA editing (77, 89) (Figure 6). While there are semantically different opinions as to whether these complexes together with RECC represent the true editosome holoenzyme (90) or that differences in their demonstrated functions and interactions should be considered before such a statement should be made (46, 91), both schools of thought agree that all of these complexes are necessary for the multiple rounds of editing that occur *in vivo*.

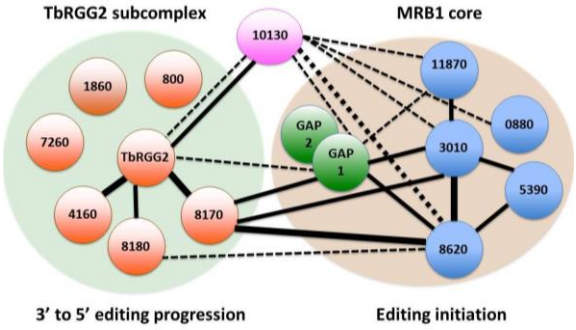

Figure 6. The architecture of the MRB1. MRB1 is made up of two subcomplexes called the MRB1 core, involved in editing initiation and gRNA utilization, and the TbRGG2 subcomplex involved in the 3' to 5' progression of pan editing. The gRNA binding GAP1/2 are depicted in green because they act outside of MRB1 as a separate entity. The two subcomplexes are bridged by a promiscuously interacting MRB1 subunit called 10130. Nomenclature according to the source of this figure (46).

Persistent in all MRB1 purifications are the about ~7 proteins that make up the MRB1 core (46). The paralogous gRNA associated proteins (GAPs) 1 and 2 form a heterotetramer that binds gRNAs, a requisite for their stability, are the only verified RNA binding proteins of the MRB1 core (88, 92). Thus, the editing of *cis*-gRNA-containing *cox2* is not affected by their RNAi-silencing (92). Knockdown of the other core proteins does not destabilize gRNAs, but appears to affect RNA editing initiation when assayed (76, 78, 93, 94). Thus, it has been proposed that the MRB1 core plays a role in editing initiation (46), although a general effect of MRB1 core ablation on gRNA utilization could be masked by an impaired gRNA phenotype. Because the GAP1/2 heterotetramer is present as a separate entity to the MRB1 core, it has been proposed that it may be involved in gRNA delivery to the editing reaction center and pulling GAP1/2 away to allow the gRNA to base pair with its cognate mRNA (46, 78).

The TbRGG2 subcomplex makes up the other major division of MRB1 (46, 91). It contains several RNA binding proteins such as TbRGG2, with motifs often on such proteins such an N-terminal glycine-rich domain containing RG and GWG repeats and C-terminal RNA recognition motif (RRM) (95-97), and the paralogs MRB8170 and MRB4160, which contains novel RNA binding elements as demonstrated by its high isoelectric point (pI) (98). RNAi-silencing of these subunits preferentially leads to a stalling of pan-

editing, which requires a cascade of gRNAs for its 3' to 5' progression (97, 98), suggesting the role of this subcomplex in mediating this process. Consistent with this hypothesis is TbRGG2's RNA annealing and dsRNA melting activities, perhaps facilitated by dynamic intramolecular interactions between its N- and C-terminal domains and the latter's with MRB8170 (95, 96).

5.1.4. Other trypanosome mitochondrial mRNA maturation steps

MRP1 has also been proposed to serve as a bridge between RNA editing and other mt RNA processing machineries (46, 91). The road to mt mRNA maturation from its transcription from kDNA by a single-subunit RNA polymerase, which also transcribes gRNAs (92, 99), is also quite complicated. Maxicircle genes are transcribed polycistronically, with each pre-mRNA being cleaved out for further processing (100). These molecules are first appended with short 3' poly(A) tails before eventually obtaining long 3'poly(A/U) tails (101, 102), features that mark them for subsequent translation (103).

6. Trypanosome mitochondrial translation

6.1. tRNA import

Unlike other mt genomes, the massive kDNA does not encode any tRNA genes, having to import these molecules from the nucleus (104). While kinetoplastids are an extreme case of organisms needing to import all mt tRNAs, even mammalian mitochondria have an innate capacity for this process (105), suggesting the conservation of the required molecules throughout eukaryotes. Surprisingly, even Dk and Ak *T. brucei* import these rendered redundant tRNAs (106, 107). The molecular mechanism(s) behind tRNA import have not been identified yet, although there is evidence for the participation of TIM (108) and the independence of this process on mt membrane potential ($\Delta\Psi p$) (109). Once in the trypanosomatid mitochondrion, one of the tRNAs undergo C to U conversion editing to be compatible with the organelle genetic code (110).

6.2. The mitochondrial ribosome

The structure of the trypanosomatid mt ribosome has is unique among eukaryotes. First, both the large subunit (LSU) and small subunits (SSU) of the ribosome contains the shortest known mt rRNAs (111, 112). To compensate for the loss of sequences are normally important for the ribozyme function and structure of the of the mt ribosomes, kinetoplastids have experienced an expansion in the number of mt ribosomal proteins (113-115). Interestingly, this situation has led to trypanosomatid mitochondrial translation being resistant to tetracycline antibiotics (8), which is a vestige of the prokaryotic origins of bacteria manifested in other eukaryotes (7). A derivative of SSU called SSU* in trypanosomatids represents another kinetoplastid innovation, containing additional proteins and a bilobe structure (115). The precise role of SSU* is still not understood, although there is evidence for its regulation of SSU and LSU association to control the translation of certain transcripts (116).

6.3. Other factors involved translation

As with other translation systems, *T. brucei* requires the participation of elongation factors (EFs) and a release factor for translation termination (117). EF-Tu is a small GTPase that brings and releases aminoacylated (aa)-tRNAs to the ribosome A site by hydrolysis of the nucleoside triphosphate. The *T.*

brucei ortholog of EF-Tu contains a trypanosomatid-specific subdomain, presumably to allow its interaction with the imported, cytoplasmic tRNAs. EF-Ts exchanges EF-Tu bound GDP for GTP for its recycling to participate in another round of aa-tRNA accommodation into the A site. EF-G1 allows the ribosome translocation along the mRNA for incorporation of the next aa-tRNA into the nascent peptide.

7. Regulation of the mitochondrion between the *T. brucei* procyclic and slender bloodstream forms

As *T. brucei* goes through it life cycle from the tsetse fly vector to mammalian host, the cell undergoes many physiological and cytological changes to adapt to these different environments (43). The mitochondrion is significantly remodeled, going from an organelle actively generating ATP via the TCA cycle and OXPHOS in PCF to a significantly reduced one in long slender BSF, in which these processes are shut down and the mitochondrion becomes an ATP consumer to maintain the still essential $\Delta\Psi p$ (57, 118). In the latter stage, energy is derived from abundant glucose in the bloodstream by glycolysis, the enzymes of which are compartmentalized in derived peroxisomes called glycosomes, another kinetoplastid innovation (119).

7.1. The mitochondrion of the procyclic form

The morphology of the PCF mitochondrion resembles that of the fused mitochondrial network observed in healthy mammalian cells (120). It is a reticulated, branching structure that meanders throughout the PCF cytosol. Within, the IM is folded to form discoidal cristae (2, 43), which in yeast are enriched for respiratory chain complexes (121).

The respiratory chain of *T. brucei* contains the whole complement of complexes found in other eukaryotes (30) (Figure 7). The NADH dehydrogenase complex, also known as complex I (cI), appears to have a more limited role in PCF than in mammalian cells as there is a lack of evidence that in contributed to PMF by H^+ pumping to the IMS (122, 123). Succinate dehydrogenase complex II (cII) is also a part of the TCA cycle, directly feeding electrons into ETC without pumping H^+ out of the matrix, which is its typical function in other eukaryotes. H^+ pumping across the IM in PCF is solely achieved by complexes III (cIII) and IV (cIV), whose respective aliases summarize their role in the ETC: ubiquinol:cytochrome *c* oxidoreductase and cytochrome *c*:oxygen oxidoreductase. The downhill flow of H^+ accumulated by PMF generated by ETC is coupled to the uphill synthesis of ATP by F_OF_1-ATP synthase, or complex V (cV), as postulated by chemiosmotic theory (4).

The reducing equivalents needed for generating PMF is produced by the TCA cycle (Figure 7). While all the enzymes typical for this pathway are present in *T. brucei*, they do not act in a cycle as in other eukaryotes (124). Furthermore, while pyruvate from cytosolic glycolysis is typically the metabolic entry point of TCA cycle in eukaryotes, the amino acids proline and glutamine are the major carbon sources for part of the cycle (124, 125). Interestingly, when grown in the presence of ample glucose, PCF prefers its catabolism in the glycosome for energy generation over amino acid utilization (125).

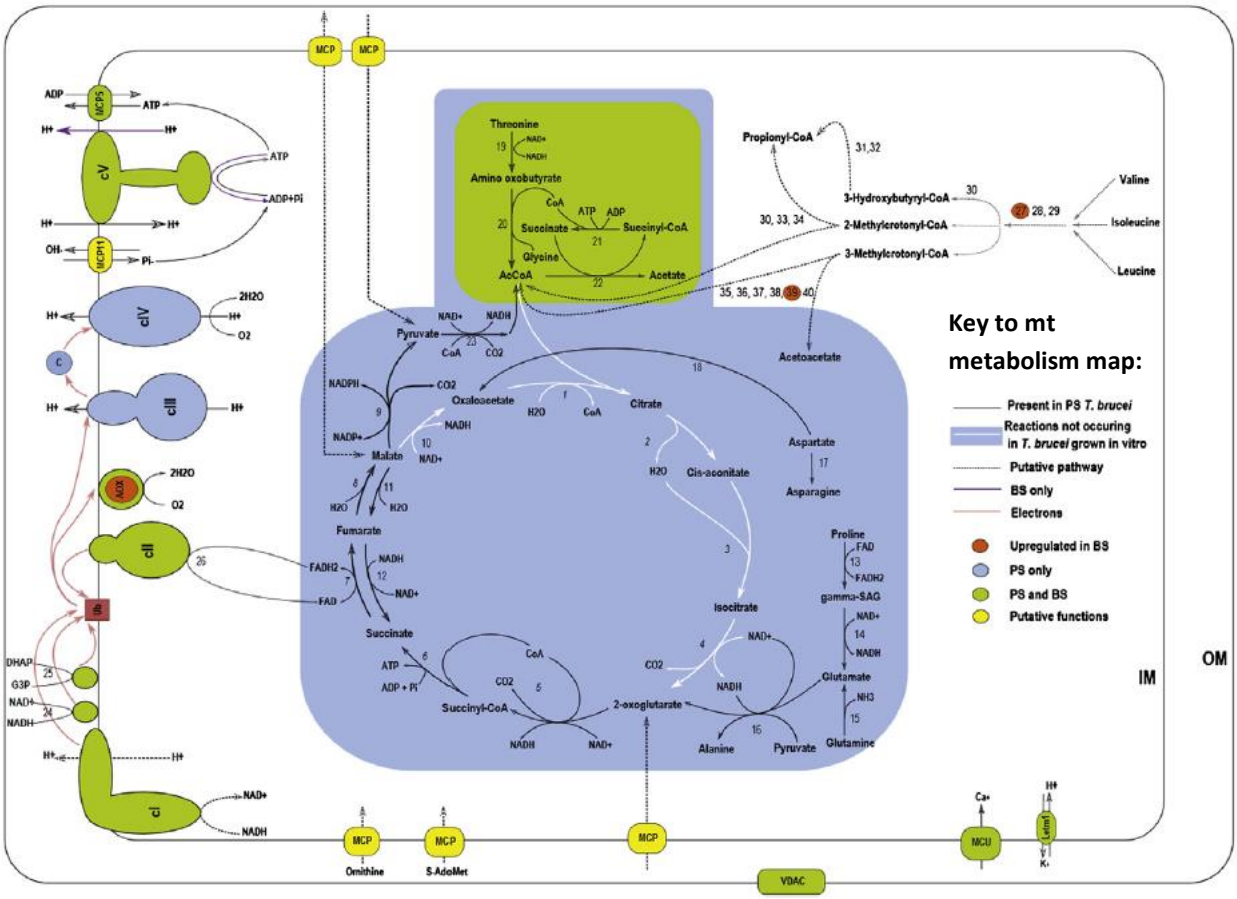

Figure 7. A summary of the procyclic and long slender bloodstream form *T. brucei* mitochondrial metabolism and ion and metabolite import systems. Key to metabolism map indicates at which stage each depicted pathway occurs (BS=BSF; PS=PSF). Enzymes: (1) citrate synthase; (2) and (3) aconitase; (4) isocitrate dehydrogenase; (5) a-ketoglutarate dehydrogenase (2-oxoglutarate); (6) succinyl-CoA synthetase; (7) succinate dehydrogenase/complex II; (8) fumarase; (9) malic enzyme; (10) malate dehydrogenase; (11) fumarase; (12) fumarate reductase; (13) L-proline dehydrogenase; (14) pyrroline-5-carboxylase; (15) L-glutamine deaminase; (16) glutamate dehydrogenase; (17) asparagine synthetase; (18) aspartate aminotransferase; (19) L-threonine dehydrogenase; (20) AcCoA:glycine C-acetyltransferase; (21) succinyl CoA synthetase; (22) acetate:succinate CoA transferase; (23) pyruvate dehydrogenase; (24) alternative NADH:ubiquinone oxidoreductase (rotenone-insensitive); (25) glycerol-3-phosphate dehydrogenase; (26) succinate dehydrogenase; (27) branched-chain aminotransferase; (28) branched-chain keto acid dehydrogenase; (29) and acyl-CoA dehydrogenase; (30) enoyl CoA hydratase; (31) hydroxyisobutyryl CoA hydrolase; (32) 3-hydroxybutyrate dehydrogenase; (33) 3-hydroxyacyl CoA dehydrogenase; (34) acetyl CoA acyltransferase; (35) 2-oxovalerate dehydrogenase; (36) isovaleryl CoA dehydrogenase; (37) methylcrotonyl CoA carboxylase; (38) methylglutaconyl CoA hydratase; (39) hydroxymethyl glutaryl CoA synthase; (40) hydroxymethyl glutaryl CoA lyase. Abbreviations: AcCoA, acetyl Coenzyme A; AOX, alternative oxidase; C, cytochrome C; cI, cII, cIII, cIV, and cV, respiratory chain complexes; DHAP, dihydroxyacetone phosphate; G3P, glycerol 3-phosphate; Letm1, leucine zipper EF-hand-containing transmembrane protein 1; MCP, mitochondrial carrier protein; MCU, mitochondrial calcium uniporter; Pi, inorganic phosphate; OM, mitochondrial outer membrane; S-AdoMet, S-adenosylmethionine; Ub, ubiquinone; VDAC, voltage-dependent anion channel. From (30).

7.2. The mitochondrion of the long slender bloodstream form

The morphology of long slender BSF is quite different to the elaborated organelle found in PCF (43). It is made up of a single tubular structure running from the anterior to posterior ends of the cell. It is also devoid of cristae, which may be due to this stage lacking respiratory complexes cIII and cIV. Since these are the sole H^+ pumping complexes of the *T. brucei* ETC, $\Delta\Psi p$ must be maintained another way for BCF mitochondrial biogenesis. $\Delta\Psi p$ is achieved by the pumping of H^+ out of the mt matrix by cV, which is coupled to ATP hydrolysis, the reverse of its canonical ATP-synthesis function in PCF (57, 118) (Figure 7). Interestingly, both cI and cII remain in BCF for enigmatic reasons, particularly the latter complex that is a part of the TCA cycle, which is absent from this life cycle stage (30, 123). While not involved in energy generation, the BSF nevertheless respiring mitochondrion still is involved in maintaining redox balance in glycosomes (126) and Fe-S biogenesis (127).

Because cIII and cIV are absent in BCF, the RNA editing of some but not all the mt mRNAs are also downregulated by a still unknown mechanism (63, 128). Not surprisingly, the editing of the mRNA that was provisionally assigned to encode ATP synthase subunit 6 (A6), a part of the H^+ pore of the F_O-moiety (129), occurs in both life cycle stages where cV has essential albeit distinct functions (130), making RNA editing an essential process in this lifecycle stage (92, 106, 131). The existence of Dk and Ak *T. brucei*, which still requires cV for its survival (57), ostensibly challenges that kDNA encodes A6. However, empirical evidence supports hypothesis that pan-edited mt mRNA encodes A6 (132, 133). Mutations of a nuclear-encoded cV subunit compensates for the loss of A6 in Dk and Ak *T. brucei* (56, 134), allowing it to contribute to the electrogenic membrane potential ($\Delta\Psi$) in the absence of a H^+ gradient (Δp)(57).

8. *T. brucei* as a model for studying general mitochondrial biology: functional analysis of Letm1

To conclude I would like to discuss how *T. brucei* can serve as model system for studying more conserved mt phenomena, because of features that make it amenable to such type of research. First, it possesses a single mitochondrion, providing a simpler system to study processes whose core mechanisms or regulation may be confounded by the constant fusion and fission of mitochondrial networks in opisthokont models (120). Second, is the evolutionary divergence of *T. brucei* from other eukaryotes can be exploited by integrative studies that bring insight to core mt physiological processes, such as its contribution to the discovery of the mt Ca^{2+} uniporter (MCU) (135). Third is the availability of *in vitro* PCF and BSF cultures to facilitate the study the mitochondrion with and without active OXPHOS, respectively, in one organism. Plus, as in budding yeast, the workhorse of mt research, *T. brucei* has rho^O mutants (134) and the availability of PCF culture growth in fermentable and non-fermentable media (125).

Using these features, we decided to look at the function of a highly conserved IM protein called leucine zipper EF hand-containing transmembrane protein 1 (Letm1) that was serendipitously found in our initial MRB1 purifications (87). Study of this protein in opisthokont models such as *S. cerevisiae*, *D. melanogaster* and *C. elegans* has assigned it with a role in K^+/H^+ exchange (KHE) (136), Ca^{2+}/H^+ antiport

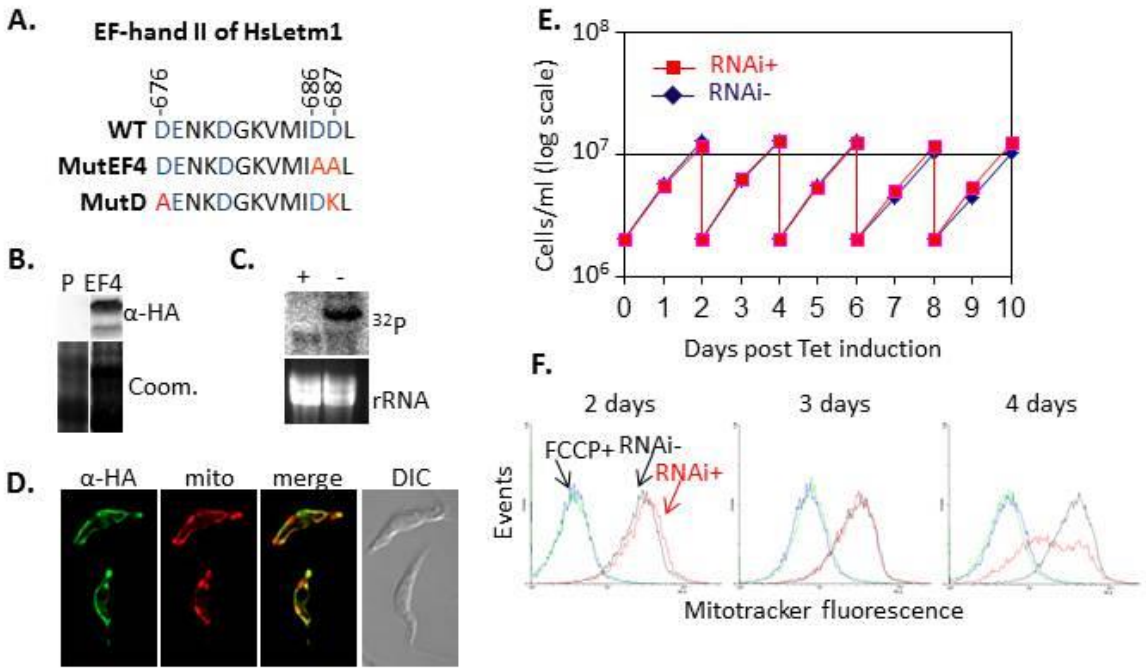

Figure 8. Complementation of RNAi-silenced Letm1 in procyclic *T. brucei* with human Letm1 bearing a EF-hand mutation. The experiment was performed as described in (140) using wild-type (WT) human Letm1 (HsLetm1). **A.** The second and only complete EF-hand of *HsLetm1* (136) in the pABPURO vector was subjected to site directed mutagenesis as depicted to change two adjacent, negatively charged aspartic acid (D) residues to alanine (A) (D686AD687A). This mutation is labelled "MutEF4", was assumed to ablate binding of Ca^{2+}. Another similar mutation employed by another group that had an effect on HsLetm1 function, called "MutD", is shown below (141). The pABPURO-HsLetm1-MutEF4 with a C-terminal HA-tag was electroporated into an existing cell line for regulatable RNAi-silencing of *T. brucei* Letm1 (TbLetm1). **B.** Western blot of total cell lysates immunodecorated with α-HA antibody from the cell line in **A**, confirming that HsLetm1-MutEF4 is expressed. Lysates from the parental cell line (P) was loaded as a control. Coomassie stain of lysates shown below. **C.** Northern blot of total RNA from RNAi-induced (+) and control (-) cell lines hybridized with a ^{32}P 5'-end labelled probe hybridizing *TbLetm1* mRNA confirming its downregulation in the HsLetm1-MutEF4 expressing cell line. Ethidium bromide stained rRNA shown below as a loading control. **D.** Indirect immunofluorescence of *T. brucei* incubated with α-HA antibody to demonstrate targeting of HsLetm1-MutEF4 to the mitochondrion, labelled with MitoTracker Red CMXRos (mito). **E.** Growth of *T. brucei* in which TbLetm1 is downregulated (RNAi+) compared to the non-induced control (RNA-), both of which constitutively express HsLetm1-MutEF4. No effect on growth was detected, in contrast to growth inhibition when TbLetm1 is silenced without any complementation. **F.** Measurement of ΔΨp by flow cytometry of MitoTracker Red CMXRos labelled *T. brucei* from **E.** at 2, 3 and 4 days post-induction. Histograms show no noticeable collapse of ΔΨp (*c.f.* cells treated with the uncoupler FCCP) at time points 2 and 3 days. A reduction in ΔΨp is observed on day 4, albeit to a lesser extent than the FCCP treated cells. Cells and **E** and **F** were grown in ample glucose media.

(137), maintenance of proper mt and cristae morphology (138) and anchoring the mt ribosomes to the IM to facilitate the embedding of highly hydrophobic respiratory chain subunits (139). Taking advantage of its diverged evolutionary position and single mitochondrion, we used *T. brucei* to show its ancestral role is in maintaining mt volume by facilitating KHE, even in the absence of a mt H^+ gradient in Dk *T. b. evansi* (140). RNAi-silencing of Letm1 caused mt swelling that could be mitigated in a dose dependent manner by treatment with the ionophore nigericin, which chemically maintains KHE across the IM. Furthermore, mt translation proceeds normally when Letm1 is depleted but KHE is artificially maintained by nigericin, invalidating it as a player in this process in *T. brucei*, although this observation does not mean it did not acquire this role in yeast (139).

Expression of the human Letm1 ortholog (HsLetm1) complemented the *T. brucei* in which the endogenous protein was depleted, demonstrating its conservation of function over a large evolutionary distance. Complementation was also achieved by expression of HsLetm1 in which Ca^{2+}-binding EF hands were mutated, suggesting these motifs are expendable for its core KHE function in the context of the *T. brucei* mitochondrion (Figure 8A-D). However, assayed $\Delta\Psi p$ shows a decrease at day 4 post-induction, challenging this interpretation (Figure 8F). These motifs appear to be important in for Letm1 function in human HeLa cell cultures (141) (Figure 8A), indicating this motif may serve a unique role in the context of some metazoan mitochondria. However, the absence of the EF-hands in most orthologs throughout eukaryotes, including some metazoa (136), argues against these domains being requisite for its KHE function.

Letm1 came into prominence because its gene locus is often within a hemizygous deletion, occurring to different extents, on the short arm of human chromosome 4, causing Wolf-Hirschhorn syndrome (142). Symptoms of this disease, affecting 1 in 20-50,000 births, are multifarious but often include facial abnormalities, various degrees of mental retardation and seizures (143). The hemizygosity of *Letm1* has been implicated in the development of the final symptom, as patients with deletions that exclude this locus do not exhibit seizures (144, 145). Interestingly, when we knockout one of the *Letm1* alleles in PCF *T. brucei*, we only observe a negative impact on fitness when they are grown in glucose-poor conditions (Figure 9), which requires the active participation of OXPHOS in energy generation (125). This observation suggests that hemizygous deletion of *Letm1* preferentially affects cells with a high bioenergetics flux though the mitochondria across eukaryotic taxa. It is remarkable that this phenotype appear to be so well conserved, affecting a rapidly proliferating protist and the cells of the nervous system.

While having a lot of potential, there are some drawbacks to *T. brucei* as a research model. For example, because of its high motility, the flagellate is difficult to study using many live imaging techniques such as fluorescence recovery after photobleaching experiments (FRAP) to measure the mobility of biomolecules *in vivo* (146). To address this problem, Zheniqu Huang under my supervision has developed a simply implemented, economical immobilization technique that maintains the viability of cells (147) whose motility is essential for its survival (47).

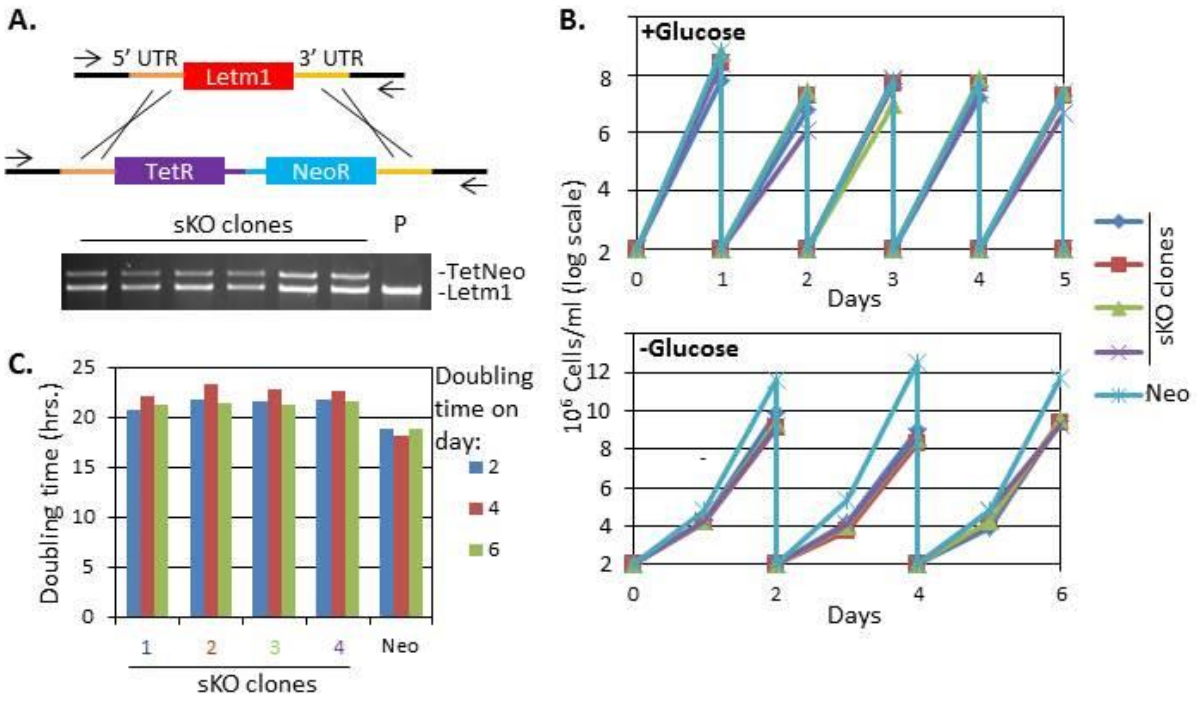

Figure 9. Hemizygous deletion of procyclic *T. brucei* Letm1 results in an inhibition of growth only in glucose-poor media. A. A schema showing integration of the knockout construct replacing the *Letm1* ORF of a single allele is shown on top. The construct undergoes homologous recombination with the *Letm1* 5' and 3' untranslated regions (UTRs). Arrows show the annealing sites of PCR primers to test integration. On the bottom is PCR with these primers on isolated genomic DNA from 6 electroporated clones bearing the single *Letm1* allele knockout (sKO) and the parental cell line (P). The identity of the bands according to size is shown on the right. **B.** Growth of 4 sKO clones in media with ample (+glucose, top) and low (-glucose, bottom) media. Each sKO is color coded. Growth of a cell line bearing a neomycin resistance cassette in an intragenic genome integration site (Neo) was assayed in parallel as a negative a control. **C.** A bar graph showing the doubling times from 0-2 (blue), 2-4 (red) and 4-6 (green) of each cell line from the -glucose growth curve shown in **B**. The number of each clone is color coded as the lines in **B.**

9. References

1. **Andersson SG, Zomorodipour A, Andersson JO, Sicheritz-Ponten T, Alsmark UC, Podowski RM, Naslund AK, Eriksson AS, Winkler HH, Kurland CG.** 1998. The genome sequence of Rickettsia prowazekii and the origin of mitochondria. Nature **396:**133-140.
2. **Munoz-Gomez SA, Slamovits CH, Dacks JB, Baier KA, Spencer KD, Wideman JG.** 2015. Ancient homology of the mitochondrial contact site and cristae organizing system points to an endosymbiotic origin of mitochondrial cristae. Curr Biol **25:**1489-1495.
3. **Vafai SB, Mootha VK.** 2012. Mitochondrial disorders as windows into an ancient organelle. Nature **491:**374-383.
4. **Mitchell P.** 1966. Chemiosmotic coupling in oxidative and photosynthetic phosphorylation. Biol Rev Camb Philos Soc **41:**445-502.
5. **Schatz G, Haslbrunner E, Tuppy H.** 1964. Deoxyribonucleic Acid Associated with Yeast Mitochondria. Biochem Biophys Res Commun **15:**127-132.
6. **Nass MM, Nass S.** 1963. Intramitochondrial Fibers with DNA Characteristics. I. Fixation and Electron Staining Reactions. J Cell Biol **19:**593-611.

7. **Moullan N, Mouchiroud L, Wang X, Ryu D, Williams EG, Mottis A, Jovaisaite V, Frochaux MV, Quiros PM, Deplancke B, Houtkooper RH, Auwerx J.** 2015. Tetracyclines disturb mitochondrial function across eukaryotic models: A call for caution in biomedical research. Cell Rep **10:**1681-1691.
8. **Hashimi H, Kaltenbrunner S, Zíková A, Lukeš J.** 2016. Trypanosome mitochondrial translation and tetracycline: no sweat about Tet. PLoS Pathog **12:**e1005492.
9. **Koonin EV.** 2015. Origin of eukaryotes from within archaea, archaeal eukaryome and bursts of gene gain: eukaryogenesis just made easier? Philos Trans R Soc Lond B Biol Sci **370:**20140333.
10. **Stehling O, Lill R.** 2013. The role of mitochondria in cellular iron-sulfur protein biogenesis: mechanisms, connected processes, and diseases. Cold Spring Harb Perspect Med **3:**1-17.
11. **Rizzuto R, De Stefani D, Raffaello A, Mammucari C.** 2012. Mitochondria as sensors and regulators of calcium signalling. Nat Rev Mol Cell Biol **13:**566-578.
12. **Tait SW, Green DR.** 2010. Mitochondria and cell death: outer membrane permeabilization and beyond. Nat Rev Mol Cell Biol **11:**621-632.
13. **Goldberg AV, Molik S, Tsaousis AD, Neumann K, Kuhnke G, Delbac F, Vivares CP, Hirt RP, Lill R, Embley TM.** 2008. Localization and functionality of microsporidian iron-sulphur cluster assembly proteins. Nature **452:**624-628.
14. **Tovar J, Leon-Avila G, Sanchez LB, Sutak R, Tachezy J, van der Giezen M, Hernandez M, Muller M, Lucocq JM.** 2003. Mitochondrial remnant organelles of Giardia function in iron-sulphur protein maturation. Nature **426:**172-176.
15. **Phillips MJ, Voeltz GK.** 2016. Structure and function of ER membrane contact sites with other organelles. Nat Rev Mol Cell Biol **17:**69-82.
16. **Pagliarini DJ, Calvo SE, Chang B, Sheth SA, Vafai SB, Ong SE, Walford GA, Sugiana C, Boneh A, Chen WK, Hill DE, Vidal M, Evans JG, Thorburn DR, Carr SA, Mootha VK.** 2008. A mitochondrial protein compendium elucidates complex I disease biology. Cell **134:**112-123.
17. **Doležal P, Likic V, Tachezy J, Lithgow T.** 2006. Evolution of the molecular machines for protein import into mitochondria. Science **313:**314-318.
18. **Chacinska A, Koehler CM, Milenkovic D, Lithgow T, Pfanner N.** 2009. Importing mitochondrial proteins: machineries and mechanisms. Cell **138:**628-644.
19. **Mani J, Desy S, Niemann M, Chanfon A, Oeljeklaus S, Pusnik M, Schmidt O, Gerbeth C, Meisinger C, Warscheid B, Schneider A.** 2015. Mitochondrial protein import receptors in Kinetoplastids reveal convergent evolution over large phylogenetic distances. Nat Commun **6:**6646.
20. **Pusnik M, Schmidt O, Perry AJ, Oeljeklaus S, Niemann M, Warscheid B, Lithgow T, Meisinger C, Schneider A.** 2011. Mitochondrial preprotein translocase of trypanosomatids has a bacterial origin. Curr Biol **21:**1738-1743.
21. **Basu S, Leonard JC, Desai N, Mavridou DA, Tang KH, Goddard AD, Ginger ML, Lukeš J, Allen JW.** 2013. Divergence of Erv1-associated mitochondrial import and export pathways in trypanosomes and anaerobic protists. Eukaryot. Cell **12:**343-355.
22. **Eckers E, Petrungaro C, Gross D, Riemer J, Hell K, Deponte M.** 2013. Divergent molecular evolution of the mitochondrial sulfhydryl:cytochrome C oxidoreductase Erv in opisthokonts and parasitic protists. J. Biol. Chem. **288:**2676-2688.
23. **Jedelský PL, Doležal P, Rada P, Pyrih J, Smíd O, Hrdý I, Sedinová M, Marcinciková M, Voleman L, Perry AJ, Beltrán NC, Lithgow T, Tachezy J.** 2011. The minimal proteome in the reduced mitochondrion of the parasitic protist Giardia intestinalis. PLoS One **6:**e17285.
24. **Adl SM, Simpson AG, Lane CE, Lukeš J, Bass D, Bowser SS, Brown MW, Burki F, Dunthorn M, Hampl V, Heiss A, Hoppenrath M, Lara E, Le Gall L, Lynn DH, McManus H, Mitchell EA, Mozley-Stanridge SE, Parfrey LW, Pawlowski J, Rueckert S, Shadwick RS, Schoch CL, Smirnov A, Spiegel FW.** 2012. The revised classification of eukaryotes. J Eukaryot Microbiol **59:**429-493.
25. **Liang XH, Haritan A, Uliel S, Michaeli S.** 2003. trans and cis splicing in trypanosomatids: mechanism, factors, and regulation. Eukaryot. Cell **2:**830-840.
26. **Dooijes D, Chaves I, Kieft R, Dirks-Mulder A, Martin W, Borst P.** 2000. Base J originally found in kinetoplastida is also a minor constituent of nuclear DNA of Euglena gracilis. Nucl. Acids Res. **28:**3017-3021.
27. **Cavalier-Smith T.** 2010. Kingdoms Protozoa and Chromista and the eozoan root of the eukaryotic tree. Biol Lett **6:**342-345.
28. **Mach J, Poliak P, Matušková A, Zarský V, Janata J, Lukes J, Tachezy J.** 2013. An Advanced System of the Mitochondrial Processing Peptidase and Core Protein Family in Trypanosoma brucei and Multiple Origins of the Core I Subunit in Eukaryotes. Genome Biol Evol **5:**860-875.
29. **de Vargas C, Audic S, Henry N, Decelle J, Mahe F, Logares R, Lara E, Berney C, Le Bescot N, Probert I, Carmichael M, Poulain J, Romac S, Colin S, Aury JM, Bittner L, Chaffron S, Dunthorn M, Engelen S, Flegontova O, Guidi L, Horák A, Jaillon O, Lima-Mendez G, Lukeš J, Malviya S, Morard R, Mulot M, Scalco E, Siano R, Vincent F, Zingone A, Dimier C, Picheral M, Searson S, Kandels-Lewis S, Acinas SG, Bork P, Bowler C, Gorsky G, Grimsley N, Hingamp P, Iudicone D, Not F, Ogata H, Pesant S, Raes J, Sieracki ME, Speich S, Stemmann L, Sunagawa S, Weissenbach J, Wincker P, Karsenti E.** 2015. Ocean plankton. Eukaryotic plankton diversity in the sunlit ocean. Science **348:**1261605.
30. **Verner Z, Basu S, Benz C, Dixit S, Dobáková E, Faktorová D, Hashimi H, Horáková E, Huang Z, Paris Z, Pena-Diaz P, Ridlon L, Týč J, Wildridge D, Zíková A, Lukeš J.** 2015. Malleable mitochondrion of *Trypanosoma brucei*. Int Rev Cell Mol Biol **315:**73-151.
31. **Ogbadoyi EO, Robinson DR, Gull K.** 2003. A high-order trans-membrane structural linkage is responsible for mitochondrial genome positioning and segregation by flagellar basal bodies in trypanosomes. Mol Biol Cell **14:**1769-1779.
32. **Joubert JJ, Schutte CH, Irons DJ, Fripp PJ.** 1993. Ubombo and the site of David Bruce's discovery of Trypanosoma brucei. T Roy Soc Trop Med H **87:**494-495.
33. **Pays E, Vanhollebeke B, Uzureau P, Lecordier L, Perez-Morga D.** 2014. The molecular arms race between African trypanosomes and humans. Nat Rev Microbiol **12:**575-584.
34. **Perez-Morga D, Vanhollebeke B, Paturiaux-Hanocq F, Nolan DP, Lins L, Homble F, Vanhamme L, Tebabi P, Pays A, Poelvoorde P, Jacquet A, Brasseur R, Pays E.** 2005. Apolipoprotein L-I promotes trypanosome lysis by forming pores in lysosomal membranes. Science **309:**469-472.

35. **Barrett MP, Burchmore RJ, Stich A, Lazzari JO, Frasch AC, Cazzulo JJ, Krishna S.** 2003. The trypanosomiases. Lancet **362:**1469-1480.
36. **MacGregor P, Szoor B, Savill NJ, Matthews KR.** 2012. Trypanosomal immune evasion, chronicity and transmission: an elegant balancing act. Nat Rev Microbiol **10:**431-438.
37. **Peacock L, Ferris V, Sharma R, Sunter J, Bailey M, Carrington M, Gibson W.** 2011. Identification of the meiotic life cycle stage of Trypanosoma brucei in the tsetse fly. Proc. Natl. Acad. Sci. U.S.A. **108:**3671-3676.
38. **Stockdale C, Swiderski MR, Barry JD, McCulloch R.** 2008. Antigenic variation in Trypanosoma brucei: joining the DOTs. PLoS Biol **6:**e185.
39. **Engstler M, Pfohl T, Herminghaus S, Boshart M, Wiegertjes G, Heddergott N, Overath P.** 2007. Hydrodynamic flow-mediated protein sorting on the cell surface of trypanosomes. Cell **131:**505-515.
40. **Acosta-Serrano A, Vassella E, Liniger M, Kunz Renggli C, Brun R, Roditi I, Englund PT.** 2001. The surface coat of procyclic Trypanosoma brucei: programmed expression and proteolytic cleavage of procyclin in the tsetse fly. Proc. Natl. Acad. Sci. U.S.A. **98:**1513-1518.
41. **Matthews KR.** 2015. 25 years of African trypanosome research: From description to molecular dissection and new drug discovery. Mol. Biochem. Parasitol. **200:**30-40.
42. **Ngo H, Tschudi C, Gull K, Ullu E.** 1998. Double-stranded RNA induces mRNA degradation in Trypanosoma brucei. Proc. Natl. Acad. Sci. U.S.A. **95:**14687-14692.
43. **Matthews KR.** 2005. The developmental cell biology of *Trypanosoma brucei*. J. Cell Sci. **118:**283-290.
44. **He CY, Pypaert M, Warren G.** 2005. Golgi duplication in *Trypanosoma brucei* requires Centrin2. Science **310:**1196-1198.
45. **Ferguson MA.** 1999. The structure, biosynthesis and functions of glycosylphosphatidylinositol anchors, and the contributions of trypanosome research. J. Cell Sci. **112:**2799-2809.
46. **Read LK, Lukeš J, Hashimi H.** 2016. Trypanosome RNA editing: the complexity of getting U in and taking U out. Wiley Interdiscip Rev RNA **7:**33-51.
47. **Broadhead R, Dawe HR, Farr H, Griffiths S, Hart SR, Portman N, Shaw MK, Ginger ML, Gaskell SJ, McKean PG, Gull K.** 2006. Flagellar motility is required for the viability of the bloodstream trypanosome. Nature **440:**224-227.
48. **Obado SO, Brillantes M, Uryu K, Zhang W, Ketaren NE, Chait BT, Field MC, Rout MP.** 2016. Interactome Mapping Reveals the Evolutionary History of the Nuclear Pore Complex. PLoS Biol **14:**e1002365.
49. **Jensen RE, Englund PT.** 2012. Network news: the replication of kinetoplast DNA. Annu Rev Microbiol **66:**473-491.
50. **Bruhn DF, Mozeleski B, Falkin L, Klingbeil MM.** 2010. Mitochondrial DNA polymerase POLIB is essential for minicircle DNA replication in African trypanosomes. Mol Microbiol **75:**1414-1425.
51. **Gluenz E, Povelones ML, Englund PT, Gull K.** 2011. The kinetoplast duplication cycle in Trypanosoma brucei is orchestrated by cytoskeleton-mediated cell morphogenesis. Mol. Cell Biol. **31:**1012-1021.
52. **Woodward R, Gull K.** 1990. Timing of nuclear and kinetoplast DNA replication and early morphological events in the cell cycle of Trypanosoma brucei. J. Cell Sci. **95 (Pt 1):**49-57.
53. **Robinson DR, Gull K.** 1991. Basal body movements as a mechanism for mitochondrial genome segregation in the trypanosome cell cycle. Nature **352:**731-733.
54. **Concepcion-Acevedo J, Luo J, Klingbeil MM.** 2012. Dynamic localization of Trypanosoma brucei mitochondrial DNA polymerase ID. Eukaryot. Cell **11:**844-855.
55. **Li Z, Lindsay ME, Motyka SA, Englund PT, Wang CC.** 2008. Identification of a bacterial-like HslVU protease in the mitochondria of Trypanosoma brucei and its role in mitochondrial DNA replication. PLoS Pathog **4:**e1000048.
56. **Lai DH, Hashimi H, Lun ZR, Ayala FJ, Lukeš J.** 2008. Adaptations of *Trypanosoma brucei* to gradual loss of kinetoplast DNA: *Trypanosoma equiperdum* and *Trypanosoma evansi* are petite mutants of *T. brucei*. Proc. Natl. Acad. Sci. U.S.A. **105:**1999-2004.
57. **Schnaufer A, Clark-Walker GD, Steinberg AG, Stuart K.** 2005. The F1-ATP synthase complex in bloodstream stage trypanosomes has an unusual and essential function. EMBO J. **24:**4029-4040.
58. **Schnaufer A, Domingo GJ, Stuart K.** 2002. Natural and induced dyskinetoplastic trypanosomatids: how to live without mitochondrial DNA. Int. J. Parasitol. **32:**1071-1084.
59. **Speijer D.** 2006. Is kinetoplastid pan-editing the result of an evolutionary balancing act? IUBMB Life **58:**91-96.
60. **Chen XJ, Clark-Walker GD.** 2000. The petite mutation in yeasts: 50 years on. Int Rev Cytol **194:**197-238.
61. **Lun ZR, Desser SS.** 1995. Is the broad range of hosts and geographical distribution of Trypanosoma evansi attributable to the loss of maxicircle kinetoplast DNA? Parasitol Today **11:**131-133.
62. **Weir W, Capewell P, Foth B, Clucas C, Pountain A, Steketee P, Veitch N, Koffi M, De Meeus T, Kabore J, Camara M, Cooper A, Tait A, Jamonneau V, Bucheton B, Berriman M, MacLeod A.** 2016. Population genomics reveals the origin and asexual evolution of human infective trypanosomes. Elife **5**.
63. **Benne R, Van den Burg J, Brakenhoff JP, Sloof P, Van Boom JH, Tromp MC.** 1986. Major transcript of the frameshifted coxII gene from trypanosome mitochondria contains four nucleotides that are not encoded in the DNA. Cell **46:**819-826.
64. **Gott JM, Emeson RB.** 2000. Functions and mechanisms of RNA editing. Annu Rev Genet **34:**499-531.
65. **Bazak L, Haviv A, Barak M, Jacob-Hirsch J, Deng P, Zhang R, Isaacs FJ, Rechavi G, Li JB, Eisenberg E, Levanon EY.** 2014. A-to-I RNA editing occurs at over a hundred million genomic sites, located in a majority of human genes. Genome Res **24:**365-376.
66. **Blum B, Bakalara N, Simpson L.** 1990. A model for RNA editing in kinetoplastid mitochondria: "guide" RNA molecules transcribed from maxicircle DNA provide the edited information. Cell **60:**189-198.
67. **Sturm NR, Simpson L.** 1990. Kinetoplast DNA minicircles encode guide RNAs for editing of cytochrome oxidase subunit III mRNA. Cell **61:**879-884.
68. **Blum B, Simpson L.** 1990. Guide RNAs in kinetoplastid mitochondria have a nonencoded 3' oligo(U) tail involved in recognition of the preedited region. Cell **62:**391-397.
69. **McManus MT, Adler BK, Pollard VW, Hajduk SL.** 2000. *Trypanosoma brucei* guide RNA poly(U) tail formation is stabilized by cognate mRNA. Mol. Cell Biol. **20:**883-891.

70. **Aphasizheva I, Aphasizhev R.** 2010. RET1-catalyzed uridylylation shapes the mitochondrial transcriptome in *Trypanosoma brucei*. Mol. Cell Biol. **30:**1555-1567.
71. **Lee RC, Feinbaum RL, Ambros V.** 1993. The C. elegans heterochronic gene lin-4 encodes small RNAs with antisense complementarity to lin-14. Cell **75:**843-854.
72. **Golden DE, Hajduk SL.** 2005. The 3'-untranslated region of cytochrome oxidase II mRNA functions in RNA editing of African trypanosomes exclusively as a *cis* guide RNA. RNA **11:**29-37.
73. **Koslowsky D, Sun Y, Hindenach J, Theisen T, Lucas J.** 2014. The insect-phase gRNA transcriptome in Trypanosoma brucei. Nucl. Acids Res. **42:**1873-1886.
74. **Maslov DA, Simpson L.** 1992. The polarity of editing within a multiple gRNA-mediated domain is due to formation of anchors for upstream gRNAs by downstream editing. Cell **70:**459-467.
75. **Li F, Herrera J, Zhou S, Maslov DA, Simpson L.** 2011. Trypanosome REH1 is an RNA helicase involved with the 3'-5' polarity of multiple gRNA-guided uridine insertion/deletion RNA editing. Proc. Natl. Acad. Sci. U.S.A. **108:**3542-3547.
76. **Ammerman ML, Tomasello DL, Faktorová D, Kafková L, Hashimi H, Lukeš J, Read LK.** 2013. A core MRB1 complex component is indispensable for RNA editing in insect and human infective stages of *Trypanosoma brucei*. PLoS One **8:**e78015.
77. **Aphasizheva I, Zhang L, Wang X, Kaake RM, Huang L, Monti S, Aphasizhev R.** 2014. RNA binding and core complexes constitute the U-insertion/deletion editosome. Mol. Cell Biol. **34:**4329-4342.
78. **Huang Z, Faktorová D, Křížová A, Kafková L, Read LK, Lukeš J, Hashimi H.** 2015. Integrity of the core mitochondrial RNA-binding complex 1 is vital for trypanosome RNA editing. RNA **21:**2088-2102.
79. **Kable ML, Seiwert SD, Heidmann S, Stuart K.** 1996. RNA editing: a mechanism for gRNA-specified uridylate insertion into precursor mRNA. Science **273:**1189-1195.
80. **Seiwert SD, Heidmann S, Stuart K.** 1996. Direct visualization of uridylate deletion in vitro suggests a mechanism for kinetoplastid RNA editing. Cell **84:**831-841.
81. **Stuart KD, Schnaufer A, Ernst NL, Panigrahi AK.** 2005. Complex management: RNA editing in trypanosomes. Trends. Biochem. Sci. **30:**97-105.
82. **Simpson L, Aphasizhev R, Gao G, Kang X.** 2004. Mitochondrial proteins and complexes in *Leishmania* and *Trypanosoma* involved in U-insertion/deletion RNA editing. RNA **10:**159-170.
83. **Carnes J, Trotter JR, Peltan A, Fleck M, Stuart K.** 2008. RNA editing in *Trypanosoma brucei* requires three different editosomes. Mol. Cell Biol. **28:**122-130.
84. **MacRae IJ, Doudna JA.** 2007. Ribonuclease revisited: structural insights into ribonuclease III family enzymes. Curr Opin Struct Biol **17:**138-145.
85. **Carnes J, Soares CZ, Wickham C, Stuart K.** 2011. Endonuclease associations with three distinct editosomes in *Trypanosoma brucei*. J. Biol. Chem. **286:**19320-19330.
86. **Panigrahi AK, Zíková A, Dalley RA, Acestor N, Ogata Y, Anupama A, Myler PJ, Stuart KD.** 2008. Mitochondrial complexes in *Trypanosoma brucei*: a novel complex and a unique oxidoreductase complex. Mol. Cell Proteomics **7:**534-545.
87. **Hashimi H, Zíková A, Panigrahi AK, Stuart KD, Lukeš J.** 2008. TbRGG1, an essential protein involved in kinetoplastid RNA metabolism that is associated with a novel multiprotein complex. RNA **14:**970-980.
88. **Weng J, Aphasizheva I, Etheridge RD, Huang L, Wang X, Falick AM, Aphasizhev R.** 2008. Guide RNA-binding complex from mitochondria of trypanosomatids. Mol. Cell **32:**198-209.
89. **Ammerman ML, Downey KM, Hashimi H, Fisk JC, Tomasello DL, Faktorová D, Kafková L, King T, Lukeš J, Read LK.** 2012. Architecture of the trypanosome RNA editing accessory complex, MRB1. Nucl. Acids Res. **40:**5637-5650.
90. **Aphasizheva I, Aphasizhev R.** 2016. U-Insertion/Deletion mRNA-Editing Holoenzyme: Definition in Sight. Trends Parasitol. **32:**144-156.
91. **Hashimi H, Zimmer SL, Ammerman ML, Read LK, Lukeš J.** 2013. Dual core processing: MRB1 is an emerging kinetoplast RNA editing complex. Trends Parasitol. **29:**91-99.
92. **Hashimi H, Čičová Z, Novotná L, Wen YZ, Lukeš J.** 2009. Kinetoplastid guide RNA biogenesis is dependent on subunits of the mitochondrial RNA binding complex 1 and mitochondrial RNA polymerase. RNA **15:**588-599.
93. **Ammerman ML, Hashimi H, Novotná L, Čičová Z, McEvoy SM, Lukeš J, Read LK.** 2011. MRB3010 is a core component of the MRB1 complex that facilitates an early step of the kinetoplastid RNA editing process. RNA **17:**865-877.
94. **Acestor N, Panigrahi AK, Carnes J, Zíková A, Stuart KD.** 2009. The MRB1 complex functions in kinetoplastid RNA processing. RNA **15:**277-286.
95. **Ammerman ML, Presnyak V, Fisk JC, Foda BM, Read LK.** 2010. TbRGG2 facilitates kinetoplastid RNA editing initiation and progression past intrinsic pause sites. RNA **16:**2239-2251.
96. **Foda BM, Downey KM, Fisk JC, Read LK.** 2012. Multifunctional G-rich and RRM-containing domains of TbRGG2 perform separate yet essential functions in trypanosome RNA editing. Eukaryot. Cell **11:**1119-1131.
97. **Fisk JC, Ammerman ML, Presnyak V, Read LK.** 2008. TbRGG2, an essential RNA editing accessory factor in two *Trypanosoma brucei* life cycle stages. J. Biol. Chem. **283:**23016-23025.
98. **Kafková L, Ammerman ML, Faktorová D, Fisk JC, Zimmer SL, Sobotka R, Read LK, Lukeš J, Hashimi H.** 2012. Functional characterization of two paralogs that are novel RNA binding proteins influencing mitochondrial transcripts of *Trypanosoma brucei*. RNA **18:**1846-1861.
99. **Grams J, Morris JC, Drew ME, Wang Z, Englund PT, Hajduk SL.** 2002. A trypanosome mitochondrial RNA polymerase is required for transcription and replication. J. Biol. Chem. **277:**16952-16959.
100. **Koslowsky DJ, Yahampath G.** 1997. Mitochondrial mRNA 3' cleavage/polyadenylation and RNA editing in *Trypanosoma brucei* are independent events. Mol. Biochem. Parasitol. **90:**81-94.
101. **Etheridge RD, Aphasizheva I, Gershon PD, Aphasizhev R.** 2008. 3' adenylation determines mRNA abundance and monitors completion of RNA editing in *T. brucei* mitochondria. EMBO J. **27:**1596-1608.

102. **Zimmer SL, McEvoy SM, Menon S, Read LK.** 2012. Additive and transcript-specific effects of KPAP1 and TbRND activities on 3' non-encoded tail characteristics and mRNA stability in *Trypanosoma brucei*. PLoS One **7:**e37639.
103. **Aphasizheva I, Maslov D, Wang X, Huang L, Aphasizhev R.** 2011. Pentatricopeptide repeat proteins stimulate mRNA adenylation/uridylation to activate mitochondrial translation in trypanosomes. Mol. Cell **42:**106-117.
104. **Hancock K, Hajduk SL.** 1990. The mitochondrial tRNAs of Trypanosoma brucei are nuclear encoded. J. Biol. Chem. **265:**19208-19215.
105. **Rubio MA, Rinehart JJ, Krett B, Duvezin-Caubet S, Reichert AS, Soll D, Alfonzo JD.** 2008. Mammalian mitochondria have the innate ability to import tRNAs by a mechanism distinct from protein import. Proc. Natl. Acad. Sci. U.S.A. **105:**9186-9191.
106. **Paris Z, Hashimi H, Lun S, Alfonzo JD, Lukeš J.** 2011. Futile import of tRNAs and proteins into the mitochondrion of *Trypanosoma brucei evansi*. Mol Biochem Parasitol **176:**116-120.
107. **Cristodero M, Seebeck T, Schneider A.** 2010. Mitochondrial translation is essential in bloodstream forms of *Trypanosoma brucei*. Mol Microbiol **78:**757-769.
108. **Tschopp F, Charriere F, Schneider A.** 2011. In vivo study in Trypanosoma brucei links mitochondrial transfer RNA import to mitochondrial protein import. EMBO Rep **12:**825-832.
109. **Paris Z, Rubio MA, Lukeš J, Alfonzo JD.** 2009. Mitochondrial tRNA import in Trypanosoma brucei is independent of thiolation and the Rieske protein. RNA **15:**1398-1406.
110. **Alfonzo JD, Blanc V, Estevez AM, Rubio MA, Simpson L.** 1999. C to U editing of the anticodon of imported mitochondrial tRNA(Trp) allows decoding of the UGA stop codon in Leishmania tarentolae. EMBO J. **18:**7056-7062.
111. **de la Cruz VF, Neckelmann N, Simpson L.** 1984. Sequences of six genes and several open reading frames in the kinetoplast maxicircle DNA of Leishmania tarentolae. J. Biol. Chem. **259:**15136-15147.
112. **de la Cruz VF, Lake JA, Simpson AM, Simpson L.** 1985. A minimal ribosomal RNA: sequence and secondary structure of the 9S kinetoplast ribosomal RNA from Leishmania tarentolae. Proc. Natl. Acad. Sci. U.S.A. **82:**1401-1405.
113. **Zíková A, Panigrahi AK, Dalley RA, Acestor N, Anupama A, Ogata Y, Myler PJ, Stuart K.** 2008. *Trypanosoma brucei* mitochondrial ribosomes: affinity purification and component identification by mass spectrometry. Mol Cell Proteomics **7:**1286-1296.
114. **Sharma MR, Booth TM, Simpson L, Maslov DA, Agrawal RK.** 2009. Structure of a mitochondrial ribosome with minimal RNA. Proc. Natl. Acad. Sci. U.S.A. **106:**9637-9642.
115. **Maslov DA, Sharma MR, Butler E, Falick AM, Gingery M, Agrawal RK, Spremulli LL, Simpson L.** 2006. Isolation and characterization of mitochondrial ribosomes and ribosomal subunits from Leishmania tarentolae. Mol. Biochem. Parasitol. **148:**69-78.
116. **Ridlon L, Škodová I, Pan S, Lukeš J, Maslov DA.** 2013. The importance of the 45 S ribosomal small subunit-related complex for mitochondrial translation in Trypanosoma brucei. J. Biol. Chem. **288:**32963-32978.
117. **Cristodero M, Mani J, Oeljeklaus S, Aeberhard L, Hashimi H, Ramrath DJ, Lukeš J, Warscheid B, Schneider A.** 2013. Mitochondrial translation factors of *Trypanosoma brucei*: elongation factor-Tu has a unique subdomain that is essential for its function. Mol Microbiol **90:**744-755.
118. **Brown SV, Hosking P, Li J, Williams N.** 2006. ATP synthase is responsible for maintaining mitochondrial membrane potential in bloodstream form *Trypanosoma brucei*. Eukaryot. Cell **5:**45-53.
119. **Haanstra JR, Gonzalez-Marcano EB, Gualdron-Lopez M, Michels PA.** 2016. Biogenesis, maintenance and dynamics of glycosomes in trypanosomatid parasites. Biochim Biophys Acta **1863:**1038-1048.
120. **Youle RJ, van der Bliek AM.** 2012. Mitochondrial fission, fusion, and stress. Science **337:**1062-1065.
121. **Vogel F, Bornhovd C, Neupert W, Reichert AS.** 2006. Dynamic subcompartmentalization of the mitochondrial inner membrane. J Cell Biol **175:**237-247.
122. **Verner Z, Čermáková P, Škodová I, Kriegová E, Horváth A, Lukeš J.** 2011. Complex I (NADH:ubiquinone oxidoreductase) is active in but non-essential for procyclic Trypanosoma brucei. Mol. Biochem. Parasitol. **175:**196-200.
123. **Surve S, Heestand M, Panicucci B, Schnaufer A, Parsons M.** 2012. Enigmatic presence of mitochondrial complex I in Trypanosoma brucei bloodstream forms. Eukaryot. Cell **11:**183-193.
124. **van Weelden SW, van Hellemond JJ, Opperdoes FR, Tielens AG.** 2005. New functions for parts of the Krebs cycle in procyclic Trypanosoma brucei, a cycle not operating as a cycle. J. Biol. Chem. **280:**12451-12460.
125. **Coustou V, Biran M, Breton M, Guegan F, Riviere L, Plazolles N, Nolan D, Barrett MP, Franconi JM, Bringaud F.** 2008. Glucose-induced remodeling of intermediary and energy metabolism in procyclic *Trypanosoma brucei*. J. Biol. Chem. **283:**16342-16354.
126. **Clarkson AB, Jr., Bienen EJ, Pollakis G, Grady RW.** 1989. Respiration of bloodstream forms of the parasite Trypanosoma brucei brucei is dependent on a plant-like alternative oxidase. J. Biol. Chem. **264:**17770-17776.
127. **Changmai P, Horáková E, Long S, Cernotíková-Stříbrná E, McDonald LM, Bontempi EJ, Lukeš J.** 2013. Both human ferredoxins equally efficiently rescue ferredoxin deficiency in Trypanosoma brucei. Mol Microbiol **89:**135-151.
128. **Feagin JE, Jasmer DP, Stuart K.** 1987. Developmentally regulated addition of nucleotides within apocytochrome b transcripts in *Trypanosoma brucei*. Cell **49:**337-345.
129. **Velours J, Arselin G.** 2000. The Saccharomyces cerevisiae ATP synthase. J Bioenerg Biomembr **32:**383-390.
130. **Bhat GJ, Koslowsky DJ, Feagin JE, Smiley BL, Stuart K.** 1990. An extensively edited mitochondrial transcript in kinetoplastids encodes a protein homologous to ATPase subunit 6. Cell **61:**885-894.
131. **Schnaufer A, Panigrahi AK, Panicucci B, Igo RP, Jr., Wirtz E, Salavati R, Stuart K.** 2001. An RNA ligase essential for RNA editing and survival of the bloodstream form of *Trypanosoma brucei*. Science **291:**2159-2162.
132. **Hashimi H, Benkovičová V, Čermáková P, Lai DH, Horváth A, Lukeš J.** 2010. The assembly of F(1)F(O)-ATP synthase is disrupted upon interference of RNA editing in *Trypanosoma brucei*. Int J Parasitol **40:**45-54.
133. **Škodová-Sveráková I, Horváth A, Maslov DA.** 2015. Identification of the mitochondrially encoded subunit 6 of F1FO ATPase in Trypanosoma brucei. Mol. Biochem. Parasitol. **201:**135-138.
134. **Dean S, Gould MK, Dewar CE, Schnaufer AC.** 2013. Single point mutations in ATP synthase compensate for mitochondrial genome loss in trypanosomes. Proc. Natl. Acad. Sci. U.S.A. **110:**14741-14746.
135. **Docampo R, Lukeš J.** 2012. Trypanosomes and the solution to a 50-year mitochondrial calcium mystery. Trends Parasitol **28:**31-37.

136. **Nowikovsky K, Froschauer EM, Zsurka G, Samaj J, Reipert S, Kolisek M, Wiesenberger G, Schweyen RJ.** 2004. The LETM1/YOL027 gene family encodes a factor of the mitochondrial K+ homeostasis with a potential role in the Wolf-Hirschhorn syndrome. J. Biol. Chem. **279:**30307-30315.
137. **Jiang D, Zhao L, Clapham DE.** 2009. Genome-wide RNAi screen identifies Letm1 as a mitochondrial Ca2+/H+ antiporter. Science **326:**144-147.
138. **Hasegawa A, van der Bliek AM.** 2007. Inverse correlation between expression of the Wolfs Hirschhorn candidate gene Letm1 and mitochondrial volume in C. elegans and in mammalian cells. Hum Mol Genet **16:**2061-2071.
139. **Frazier AE, Taylor RD, Mick DU, Warscheid B, Stoepel N, Meyer HE, Ryan MT, Guiard B, Rehling P.** 2006. Mdm38 interacts with ribosomes and is a component of the mitochondrial protein export machinery. J Cell Biol **172:**553-564.
140. **Hashimi H, McDonald L, Stříbrná E, Lukeš J.** 2013. Trypanosome Letm1 protein is essential for mitochondrial potassium homeostasis. J. Biol. Chem. **288:**26914-26925.
141. **Doonan PJ, Chandramoorthy HC, Hoffman NE, Zhang X, Cardenas C, Shanmughapriya S, Rajan S, Vallem S, Chen X, Foskett JK, Cheung JY, Houser SR, Madesh M.** 2014. LETM1-dependent mitochondrial Ca2+ flux modulates cellular bioenergetics and proliferation. Faseb J **28:**4936-4949.
142. **Endele S, Fuhry M, Pak SJ, Zabel BU, Winterpacht A.** 1999. LETM1, a novel gene encoding a putative EF-hand Ca(2+)-binding protein, flanks the Wolf-Hirschhorn syndrome (WHS) critical region and is deleted in most WHS patients. Genomics **60:**218-225.
143. **Battaglia A, Filippi T, Carey JC.** 2008. Update on the clinical features and natural history of Wolf-Hirschhorn (4p-) syndrome: experience with 87 patients and recommendations for routine health supervision. Am J Med Genet C Semin Med Genet **148C:**246-251.
144. **South ST, Bleyl SB, Carey JC.** 2007. Two unique patients with novel microdeletions in 4p16.3 that exclude the WHS critical regions: implications for critical region designation. Am J Med Genet A **143A:**2137-2142.
145. **Zollino M, Lecce R, Fischetto R, Murdolo M, Faravelli F, Selicorni A, Butte C, Memo L, Capovilla G, Neri G.** 2003. Mapping the Wolf-Hirschhorn syndrome phenotype outside the currently accepted WHS critical region and defining a new critical region, WHSCR-2. Am J Hum Genet **72:**590-597.
146. **Gordon GW, Berry G, Liang XH, Levine B, Herman B.** 1998. Quantitative fluorescence resonance energy transfer measurements using fluorescence microscopy. Biophys. J. **74:**2702-2713.
147. **Huang Z, Kaltenbrunner S, Šimková E, Staněk D, Lukeš J, Hashimi H.** 2014. Dynamics of mitochondrial RNA-binding protein complex in *Trypanosoma brucei* and its petite mutant under optimized immobilization conditions. Eukaryot. Cell **13:**1232-1240.

SUMMARY OF ARTICLES IN THE THESIS

This habilitation thesis covers my career in studying mitochondrial RNA editing in *Trypanosoma brucei* as well as other aspects of mitochondrial biogenesis that affects the biology of this parasite as a whole. This encompasses 14 primary research articles, 5 reviews, 1 book chapter and 1 popular article. The papers are grouped into categories: Trypanosome RNA Editing, Dyskinetoplastic *Trypansoma brucei*, Trypanosome Mitochondrial Translation and Trypanosome Mitochondrial Physiology. All of these are attached to the thesis, although one review is abbreviated to sections I (co-)wrote directly due to its length.

*Mentioned here but not included in the thesis due to length and/or limited current relevance

**Only a relevant portion of the review is included in thesis due to length.

I. TRYPANOSOME RNA EDITING

Primary research articles:

1. **Hassan Hashimi, Alena Zíková, Aswini K. Panigrahi, Kenneth D. Stuart and Julius Lukeš (2008). TbRGG1, a component of a novel multi-protein complex involved in kinetoplastid RNA editing. *RNA* 14: 970-980.** This paper is among the first to describe the discovery of the mitochondrial RNA binding complex 1 (MRB1), the investigation of which is the major topic of this section of the thesis.

2. **Hassan Hashimi, Zdeňka Čičová, Lucie Novotná, Yan-Zi Wen and Julius Lukeš (2009). Kinetoplastid guide RNA biogenesis is dependent on subunits of the mitochondrial RNA binding complex 1 and mitochondrial RNA polymerase. *RNA* 15: 588-599.** This paper describes the functional analysis of 4 MRB1 subunits. Two of which are called gRNA associated proteins (GAPs) 1 and 2 because they are essential for the stability of these small non-coding transcripts that are essential for RNA editing. It also demonstrates the mt RNA polymerase transcribes minicircle gRNA genes as well as maxicircle transcripts.

3. **Michelle L. Ammerman, Hassan Hashimi, Lucie Novotná, Zdeňka Čičová, Sarah M. McEvoy, Julius Lukeš, and Laurie K. Read (2011). MRB3010 is a core component of the MRB1 complex that facilitates an early step of the kinetoplastid RNA editing process. *RNA* 17: 865-877.** This paper helps to further define the architecture of MRB1 and shows that what will eventually be demonstrated to be a core MRB1 subunit is involved early steps of RNA editing. I am co-first author of this publication.

4. **Michelle L. Ammerman, Kurtis M. Downy, Hassan Hashimi, John C. Fisk, Danielle L. Tomasello, Drahomíra Faktorová, Lucie Kafková, Tony King, Julius Lukeš and Laurie K. Read (2012). Architecture of the trypanosome RNA editing complex, MRB1. *Nucleic Acids Res.* 40: 5637-5650.** This paper maps the interactions among the MRB1 subunits *in vitro* by a yeast 2-hybrid screen and *in vivo* by a series of pull-downs of selected MRB1 proteins. MRB1 is established to be made up of two

subcomplexes involved in either RNA editing initiation (MRB1 core) or pan-editing progression (TbRGG2 subcomplex).

5. **Lucie Kafková, Michelle L. Ammerman, Drahomíra Faktorová, John C. Fisk, Sara L. Zimmer, Roman Sobotka, Laurie K. Read, Julius Lukeš and Hassan Hashimi (2012). Functional characterization of two paralogs that are novel RNA binding proteins influencing mitochondrial transcripts of *Trypanosoma brucei*. *RNA* 18: 1846-1861. [Erratum: 18:2345-2345].** This paper describes two paralogs called MRB8170 and MRB4160 that are subunits of the TbRGG2 subcomplex of MRB1. They represent almost novel RNA binding proteins that influence pan-edited RNAs to differing degrees. They are the product of a chromosome duplication event happening in *T. brucei*, thus sharing sequence identity on the DNA level throughout most of the genes. Functional analysis of each individual protein was a challenge that was overcome by targeting small, unique regions of the encoding mRNAs by RNAi.

6. **Michelle L. Ammerman, Danielle L.Tomasello, Drahomíra Faktorová, Lucie Kafková, Hassan Hashimi, Julius Lukeš, and Laurie K. Read (2013). A core MRB1 complex component is indispensable for RNA editing in insect and human infective stages of *Trypanosoma brucei*. *PLoS One* 8: e78015.** This paper describes the functional analysis of another core MRB1 subunit. It is also the first paper to observe the accumulation of gRNAs upon the interference of RNA editing, suggesting that these small transcripts are consumed during the process.

7. **Zhenqiu Huang, Drahomíra Faktorová, Adéla Křížová, Lucie Kafková, Laurie K. Read, Julius Lukeš, Hassan Hashimi (2015). Integrity of the core mitochondrial RNA-binding complex 1 is vital for trypanosome RNA editing. *RNA* 21:2088-2102.** This paper describes the functional analysis of the last core MRB1 subunit to be examined by RNAi called MRB8620. The protein was not amenable to RNAi under standard culturing conditions, but its subtle effect on RNA editing was observed to affect cells when grown in media without glucose. Furthermore, the *MRB8620* gene was deleted in induced Dk *T. brucei* since it could not be done in cells in which kDNA expression was essential, confirming its necessary role in RNA editing. A new model mechanistic model of MRB1 is presented.

8. ***Vojtěch David, Pavel Flegontov, Evgeny Gerasimov, Goro Tanifugi, Hassan Hashimi, Maria D. Logacheva, Michael W. Gray, John M. Archibald, Julius Lukeš (2015). Gene loss and error-prone RNA editing in the mitochondrion of Perkinsela, an endosymbiotic kinetoplastid. *mBio* 6: e01498-15.** This paper describes RNA editing of *Perkinsella*, an early-branching kinetoplastid that is an endosymbiont of marine amoeba genera *Paramoeba* and *Janickina*. It provides tools for analysis of next generation sequences of mitochondrial transcriptomes shaped by U-insertion/deletion RNA editing. Some but not all RECC and MRB1 subunits were identified by hidden Markov models.

Reviews:

9. ***Julius Lukeš, Hassan Hashimi and Alena Zíková (2005). Unexplained complexity of the mitochondrial genome and transcriptome in kinetoplastid flagellates. *Curr. Genet.* 48:277-299.** This well cited review summarizes what had been known about the genetic system of kinetoplastids and *T. brucei*. This review predates the discovery of MRB1.

10. **Hassan Hashimi, Sara L. Zimmer, Michelle L. Ammerman, Laurie K. Read and Julius Lukeš (2013). Dual core processing: MRB1 is an emerging kinetoplast RNA editing complex. *Trends in Parasitol.* 29: 91-99.** This review summarizes the current state of knowledge of MRB1 in light of the newly elucidated architecture of the complex in paper 4. It puts forth working hypotheses of how MRB1 may also help integrate RNA editing to other processing events in the mitochondrion of kinetoplastids.

11. ***Zdeněk Verner, Somsuvro Basu, Corinna Benz, Sameer Dixit, Eva Dobáková, Drahomíra Faktorová, Hassan Hashimi, Eva Horáková, Zhenqiu Huang, Zdeněk Paris, Priscila Peña-Diaz, Lucie Ridlon, Jiří Týč, David Wildridge, Alena Zíková, Julius Lukeš (2015). Malleable mitochondrion of Trypanosoma brucei. *Int. Rev. Cell Mol. Biol.* 315:73-151.** A review about trypanosome mitochondrial biology, which includes a succinct summary of the current state of knowledge about RNA editing.

12. **Laurie K. Read, Julius Lukeš, Hassan Hashimi (2016). Trypanosome RNA editing: the complexity of getting U in and taking U out. *Wiley Interdiscip. Rev. RNA* 7: 33-51.** A review that brings together the latest data from our laboratories and others studying the complexes involved in RNA editing, RECC and MRB1.

Book chapter:

13. ***Julius Lukeš, Hassan Hashimi, Zdeněk Verner and Zdeňka Čičová (2010). The remarkable mitochondrion of trypanosomes and related flagellates. In: Structures and organelles in pathogenic protists (ed. Wanderley De Souza) Springer-Verlag, Berlin: pp. 228-252.** A book chapter that summarizes the genetic system and energy metabolism of the trypanosome mitochondrion.

Popular article:

14. ***Hassan Hashimi and Julius Lukeš (2010). Editování RNA: od obskUrnosti k všUdzpřítomnosti. *Živa* 6: 249-253.** A popular article written in Czech about trypanosome RNA editing. The title translated into English is “RNA editing: from obscUrity to Ubiquity”

II. DYSKINETOPLASTIC TRYPANOSOMA BRUCEI

Primary research articles:

15. **De-Hua Lai, Hassan Hashimi, Zhao-Rong Lun, Francisco J. Ayala and Julius Lukeš (2008). Adaptations of Trypanosoma brucei to gradual loss of kinetoplast DNA: Trypanosoma equiperdum and Trypanosoma evansi are petite mutants of T. brucei. *Proc. Natl. Acad. Sci. U.S.A.* 105:1999-2004.** This paper examines several strains of *T. brucei evansi* and *T. brucei equiperdum* to demonstrate the many stages that these subspecies undergo to get from the Dk state, in which kDNA minicircles are homogenized and maxicircles accumulate deletions, to the Ak state when all kDNA is gone. The paper identifies several compensatory mutations to the γ subunit of F_OF_1-ATP synthase that were later verified to allow these trypanosomes to achieve the Dk and Ak condition.

16. **Hassan Hashimi, Vladislava Benkovičová, Petra Čermáková, De-Hua Lai, Anton Horváth and Julius Lukeš (2010). The assembly of F_OF_1-ATP synthase is disrupted upon interference of RNA editing in Trypanosoma brucei. *Int. J. Parasitol.* 40: 45-54.** This paper experimentally proves, albeit indirectly, that kDNA maxicircles indeed encode the A6 subunit, which is important to establish in light of the existence of Dk and Ak *T. brucei*. The study gets around the problem of net being able to directly manipulate the trypanosome mt genome by taking advantage of the differential phenotypes of RNAi-silencing of proteins involved in RNA editing and stability.

17. **Zdeněk Paris, Hassan Hashimi, Sijia Lun, Juan D. Alfonzo and Julius Lukeš (2011). Futile import of tRNAs and proteins into the mitochondrion of *Trypanosoma brucei evansi*. *Mol. Biochem. Parasitol.* 176: 116-120.** This paper shows that mtRNA polymerase, GAPs 1 and 2 plus even tRNAs are imported into the mitochondrion of *Trypanosoma brucei evansi* even though the substrates for their function, mRNA, gRNA and fully assembled ribosomes (due to a lack of rRNA) are not present. I am co-first author on this publication.

18. **Zhenqiu Huang, Sabine Kaltenbrunner, Eva Šimková, David Staněk, Julius Lukeš, Hassan Hashimi (2014). The Dynamics of Mitochondrial RNA-binding Protein Complex in *Trypanosoma brucei* and its Petite Mutant Under Optimized Immobilization Conditions. *Euk. Cell* 13: 1232-40.** This paper describes how RNA can affect the *in vivo* dynamics of mt RNA binding proteins in *T. brucei* and Ak *T. brucei evansi*. In order to perform this study, a method to immobilize these highly motile cells without compromising their viability was established.

III. TRYPANOSOME MITOCHONDRIAL TRANSLATION

Primary research article:

19. **Marina Cristodero, Jan Mani, Silke Oeljeklaus, Lukas Aeberhard, Hassan Hashimi, David J. F. Ramrath, Julius Lukeš, Bettina Warscheid and André Schneider (2013). Mitochondrial translation factors of *Trypanosoma brucei*: Elongation factor-Tu has a unique subdomain that is essential for its function. *Mol. Microbiol.* 90: 744-755.** This paper describes the functional analysis of elongation factors EF-Tu, EF-Ts and EF-G1 plus the release factor RF1 in trypanosome mitochondrial translation.

All of these proteins are essential for the process, and surprisingly, EF-Tu has a unique subdomain that may allow this protein to interact with tRNAs that must be imported from the cytosol. Furthermore, interference of mitochondrial translation leads to a downregulation of nucleus-encoded subunits of the respiratory chain and upregulation of cytosolic ribosome proteins.

Review/Opinion:

20. **Hassan Hashimi, Sabine Kaltenbrunner, Alena Zíková, Julius Lukeš (2016). Trypanosome mitochondrial translation and tetracycline: No sweat about Tet. *PLoS Pathog.* 12: e1005492.** In this PLoS Pearl article, we discuss the recent finding the tetracycline affects mitochondrial translation in opisthokonts and plants, causing the "mitonuclear" imbalance that has both positive and negative consequences for these organisms. This side-effect however complicates the interpretation of data using Tet-On/Off systems of gene control in biomedical research. We show experimentally and with cited literature that *T. brucei* mitochondrial translation is not sensitive to the antibiotic. We hypothesize that this insensitivity is due to the lack of mitochondrial rRNA elements, present in opisthokonts and plants, which are the binding sites of tetracycline.

IV. TRYPANOSOME MITOCHONDRIAL PHYSIOLOGY

Primary research article:

21. **Hassan Hashimi, Lindsay McDonald, Eva Střibrná and Julius Lukeš (2013). Trypanosome Letm1 Protein Is Essential for Mitochondrial Potassium Homeostasis. *J. Biol Chem.* 288: 26914-25.** In this paper, we demonstrate that the ancestral role of the highly conserved Letm1 is K^+/H^+ antiport to prevent the sequestering of the abundant monovalent cation in the negatively charged mitochondrial matrix, which would lead to osmotic swelling of the organelle. Moreover, the RNAi-silencing of *T. brucei* Letm1 is complemented by the human ortholog. This paper may help to clear up the controversy surrounding the function of this protein, which has been implicated in seizure symptoms of the human congenital disease Wolf-Hirschhorn syndrome.

Review:

22. ****Zdeněk Verner, Somsuvro Basu, Corinna Benz, Sameer Dixit, Eva Dobáková, Drahomíra Faktorová, Hassan Hashimi, Eva Horáková, Zhenqiu Huang, Zdeněk Paris, Priscila Peña-Diaz, Lucie Ridlon, Jiří Týč, David Wildridge, Alena Zíková, Julius Lukeš (2015). Malleable mitochondrion of *Trypanosoma brucei*. *Int. Rev. Cell Mol. Biol.* 315:73-151.** An excerpt from a review about trypanosome mitochondrial biology summarizing the current state of knowledge of mitochondrial Ca^{2+} and K^+ uptake and homeostasis.

Attached Publications

Part I.

Trypanosome RNA editing

Attached Publications

Part I. Trypanosome RNA editing

Hassan Hashimi, Alena Zíková, Aswini K. Panigrahi, Kenneth D. Stuart and Julius Lukeš (2008). TbRGG1, a component of a novel multi-protein complex involved in kinetoplastid RNA editing. *RNA* 14: 970-980.

This paper is among the first to describe the discovery of the mitochondrial RNA binding complex 1 (MRB1), the investigation of which is the major topic of this section of the thesis.

TbRGG1, an essential protein involved in kinetoplastid RNA metabolism that is associated with a novel multiprotein complex

HASSAN HASHIMI,[1] ALENA ZÍKOVÁ,[2] ASWINI K. PANIGRAHI,[2] KENNETH D. STUART,[2] and JULIUS LUKEŠ[1]

[1]Biology Centre, Institute of Parasitology, Czech Academy of Sciences, and Faculty of Sciences, University of South Bohemia, České Budějovice (Budweis), Czech Republic
[2]Seattle Biomedical Research Institute, Seattle, Washington 98109, USA

ABSTRACT

The uridine insertion/deletion RNA editing of kinetoplastid mitochondrial transcripts is performed by complex machinery involving a number of proteins and multiple protein complexes. Here we describe the effect of silencing of *TbRGG1* gene by RNA interference on RNA editing in procyclic stage of *Trypanosoma brucei*. TbRGG1 is an essential protein for cell growth, the absence of which results in an overall decline of edited mRNAs, while the levels of never-edited RNAs remain unaltered. Repression of TbRGG1 expression has no effect on the 20S editosome and MRP1/2 complex. TAP-tag purification of TbRGG1 coisolated a novel multiprotein complex, and its association was further verified by TAP-tag analyses of two other components of the complex. TbRGG1 interaction with this complex appears to be mediated by RNA. Our results suggest that the TbRGG1 protein functions in stabilizing edited RNAs or editing efficiency and that the associated novel complex may have a role in mitochondrial RNA metabolism. We provisionally name it putative mitochondrial RNA-binding complex 1 (put-MRB complex 1).

Keywords: RNA editing; mitochondrion; trypanosome; RNA binding

INTRODUCTION

Trypanosoma brucei is a flagellate protist of the order Kinetoplastida responsible for African sleeping sickness in humans and nagana in livestock. As one of the early diverged eukaryotes, it contains an array of remarkable biological properties that are not present in other eukaryotic cells. A prominent example is post-transcriptional uridine (U) insertion/deletion RNA editing of the mitochondrial (mt) transcripts. Only after being edited, the mRNAs become translatable, mainly encoding subunits of the respiratory complexes. The numerous insertions and deletions of Us are performed by the 20S editosome (also known as L-complex). The extensively characterized editosomes (for recent reviews, see Simpson et al. 2004; Lukeš et al. 2005; Stuart et al. 2005; Aphasizhev 2007) contain at least 20 proteins, and there are three types of 20S editosomes present in the organelle, each unique to one type of endonucleases (Panigrahi et al. 2006).

During editing, the sequence information is provided by small RNA molecules termed guide (g) RNAs. The role of mt RNA-binding proteins in this processing event is an anticipated feature that entails RNA/RNA hybridization. In addition to component proteins, proteins that are not stably associated with the editosome may be involved in the process and those proteins have been labeled as accessory factors (Stuart and Panigrahi 2002). There is a growing family of such proteins with multiple functions in mt RNA metabolism. The mt RNA-binding proteins (MRPs) are present in the MRP1/2 heterotetrameric complex that serves in the initial stage of RNA editing as a matchmaker by facilitating the hybridization of gRNA with its cognate pre-edited mRNA (Aphasizhev et al. 2003a; Schumacher et al. 2006). Moreover, a pleimorphic phenotype caused by the down-regulation of MRP1 and/or MRP2 indicated that apart from a role in editing, both proteins may also function in other aspects of RNA metabolism (Vondrušková et al. 2005). RBP16 is an RNA-binding protein that plays a role in RNA editing in vivo (Pelletier and Read 2003) and is able to stimulate insertion editing in vitro (Miller et al.

Reprint requests to: Julius Lukeš, Biology Centre, Institute of Parasitology, Branišovská 31, 37005 České Budějovice, Czech Republic; e-mail: jula@paru.cas.cz; fax: 00420-38-5310388.

Article published online ahead of print. Article and publication date are at http://www.rnajournal.org/cgi/doi/10.1261/rna.888808.

2006). Furthermore, it also influences the stability of never-edited RNAs as well as some of their edited counterparts (Pelletier and Read 2003) and is subject to arginine methylation that regulates its functions (Goulah et al. 2006). Another member of this rather heterogeneous family is REAP-1, a protein initially found to specifically bind to pre-edited mRNAs, thus being proposed to recruit pre-mRNAs to the editing complex (Madison-Antenucci et al. 1998). However, a recent study of REAP-1 knock-out cells implies a role in RNA stability rather than editing (Hans et al. 2007). Although RBP38 was first identified as a protein that binds gRNA–mRNA duplexes (Sbicego et al. 2003), its function seems to be in the initiation of kinetoplast DNA replication (Liu et al. 2006).

TbRGG1 is another protein ranked in the category of associated factors in RNA editing (Vanhamme et al. 1998). It contains the arginine-glycine-glycine (RGG) tripeptide, which is repeated within close proximity of each other and interspersed with aromatic residues, comprising a motif that is present in a number of RNA-binding proteins (Burd and Dreyfuss 1994). The positively charged arginines are thought to electrostatically interact with the negatively charged amino acids, thus facilitating RNA binding. TbRGG1 in *T. brucei* is an 85-kDa protein that is equally present in the procyclic and bloodstream stages. In glycerol gradients, TbRGG1 sedimented in 35–40 S fractions that also exhibited in vitro deletion activity, implying both association with a macromolecular complex and RNA editing (Vanhamme et al. 1998). The recombinant protein bound poly(U) with high affinity, a capacity suggestive of gRNA binding, since these molecules have 3′ oligo(U) tails (Blum and Simpson 1992). Interestingly, UV cross-linking of radiolabeled gRNAs to mitochondrial lysates yielded this protein (Leegwater et al. 1995). However, the evidence for function of TbRGG1 in RNA editing is ultimately circumstantial. Another mitochondrial RGG protein was initially identified by mass spectrometric analysis of the monoclonal antibody affinity purified editosome and the protein was called TbRGGm because of its homology with a *Trypanosoma cruzi* protein dubbed TcRGGm (Panigrahi et al. 2003a). Here, we present the resulting effect of the repression of TbRGG1 by RNA interference (RNAi) in *T. brucei*. Moreover, we report its RNase-sensitive association with a novel complex and identification of the components by mass spectrometry.

RESULTS

Silencing of TbRGG1 inhibits cell growth

An inhibition of growth is apparent 5 d after the induction of RNAi silencing of TbRGG1 (Fig. 1A). Thereafter, the induced cells grew approximately two times slower than the culture in which tetracycline induction was absent, and virtually stopped growing by day 12. The RNAi knock-

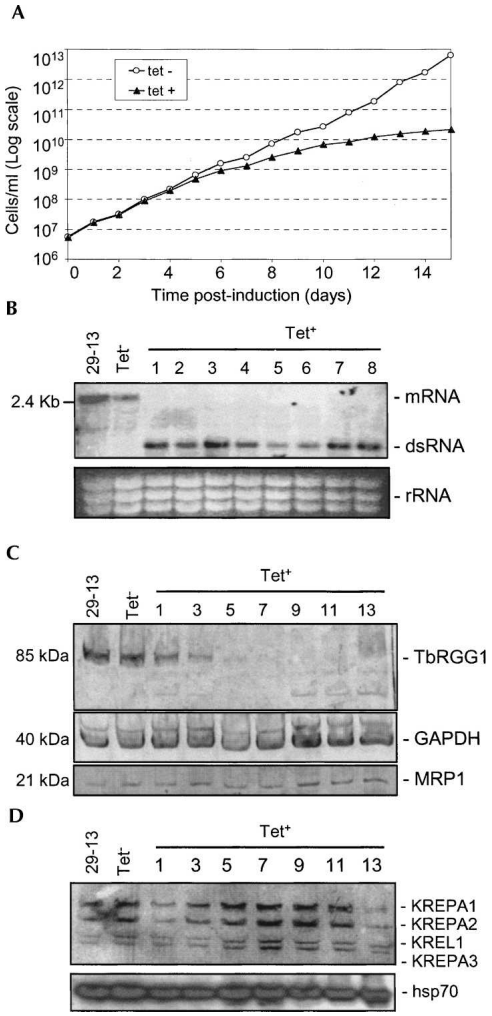

FIGURE 1. RNAi of TbRGG1 inhibits cell growth, and decreases protein and mRNA levels. (*A*) Growth effect. The numbers of noninduced cells (○) and those after induction by the addition of 1 μg/mL tetracycline (▲) were plotted logarithmically as the product of cell density and total dilution. Growth curves are one representative set from three independent experiments. (*B*) Effect on the TbRGG1 mRNA. Its levels were analyzed by blotting 10 μg of total RNA extracted from 29-13, noninduced (Tet−) and induced (Tet+) cells (days 1–8 post-induction of RNAi). The position of the targeted mRNA and the dsRNA synthesized following induction are indicated. As a loading control, the gel was stained with ethidium bromide to visualize rRNA bands. (*C*) Effect on the TbRGG1 protein. Its levels were analyzed by Western blot in extracts from 29-13, noninduced (Tet−) and induced (Tet+) cells lysed from day 1–13 every 48 h. Each lane was loaded with protein from ~5 × 10^6 cells and blots were immunodecorated using polyclonal antibody against TbRGG1, cytosolic glyceraldehyde-3-phosphate dehydrogenase (GAPDH), and mitochondrial RNA-binding protein 1 (MRP1). (*D*) 20 S editosome is unchanged. The editosome protein levels were analyzed by Western blots in mitochondrial extracts from 29-13 noninduced and induced cells lysed from day 1–13 every 48 h. Western blots were simultaneously probed with α-KREPA1, KREPA2, KREL1, and KREPA3 monoclonal antibodies (*top*), and polyclonal antibodies against the mitochondrial heat shock protein 70 (hsp-70) (*bottom*).

down cells showed no recovery even 2 wk after RNAi induction. The extent of TbRGG1 mRNA silencing, as well as the tightness of its inducible down-regulation, was determined by Northern analysis on RNA collected from parental 29-13, noninduced and 1–8 d post-induction cells (Fig. 1B). The target message was undetectable by 24 h after induction with tetracycline and remained so for at least 8 d. In addition, no leaky transcription from the p2T7-177 vector was evident, because dsRNA appeared only after RNAi induction (Fig. 1B). This observation is consistent with Western analysis, showing that the level of TbRGG1 protein significantly drops around day 5 postinduction (Fig. 1C), which corresponds nicely with the appearance of growth inhibition (Fig. 1A), and that its down-regulation persists over the 2 wk time course. In contrast, the signal from the GAPDH antibody, which was used as a loading control (Fig. 1C), persisted throughout the time course. Western analysis using monoclonal antibodies against the core editosome proteins KREPA1, KREPA2, KREL1, and KREPA3 (Fig. 1D) and the accessory complex protein MRP1 (Fig. 1C) showed no effect on abundance of these proteins consequent to TbRGG1 silencing.

It was originally reported that the ORF of TbRGG1 is present in steady-state levels on a dicistronic transcript, which contains another upstream ORF, as well as the expected processed monocistronic RNA (Vanhamme et al. 1998). Northern analysis was performed to confirm that the fully processed mRNA of the upstream ORF was not affected by the dsRNA targeting TbRGG1, and thus, that the observed growth inhibition was due only to TbRGG1 down-regulation (data not shown).

Reduction of edited RNAs upon TbRGG1 down-regulation

To determine whether TbRGG1 has a role in RNA editing, levels of several mt RNA species were compared between cultures growing for 4 d in the presence and absence of the RNAi induction agent tetracycline. This time point was chosen since it is just before observable growth inhibition (Fig. 1A), with the TbRGG1 protein being virtually eliminated (Fig. 1C). Quantitative real-time (q) PCR on cDNA from these cultures was performed with primers against several pre-edited, edited, and never-edited RNAs, as previously described (Carnes et al. 2005). Moreover, newly designed primers amplifying mt 9S and 12S rRNAs, as well as TbRGG1, were used. All qPCR reactions were performed in triplicate, including those for determination of the expression of β-tubulin and 18S rRNA, with an average and median standard deviation of the measured cycle threshold (C_t) values of 0.1 and 0.07, respectively (data not shown). The transcription levels of these housekeeping genes were unaltered by TbRGG1-interference, and thus served as references for calculation of the relative abundances of the other examined transcripts. The qPCR allowed quantification of the elimination of the TbRGG1 mRNA, which is reduced to about 20% of its normal level (Fig. 2).

The analysis of mt mRNAs revealed an overall decline of the levels of edited transcripts (Fig. 2). The edited cytochrome oxidase subunit 3 (co3) and NADH dehydrogenase subunit 7 (ND7) mRNAs decreased by about 50%, while the decline was less pronounced for ATPase subunit 6 (A6), maxicircle unknown reading frame 2 (MURF2), ribosomal protein S12 (RPS12), and co2 mRNAs (about 30%–40%), and only a subtle decrease was noted for edited cytochrome reductase subunit B (cyB). The decrease of edited molecules correlated with an increase of respective pre-edited mRNAs, especially for co3. There was virtually no change in the levels of never-edited ND4 and co1 mRNAs. The abundant mt 9S rRNA remained unaffected, while a slight decrease was apparent in 12S rRNA.

To investigate whether repression of TbRGG1 leads to any changes of the gRNA population, the same RNA used for qPCR assays was labeled with guanylyltransferase, an enzyme that specifically labels gRNAs, which can be subsequently visualized on a denaturing acrylamide gel (Fig. 3). A top band corresponding to a cytosolic RNA also labeled in this reaction (Aphasizhev et al. 2003b) was used as a

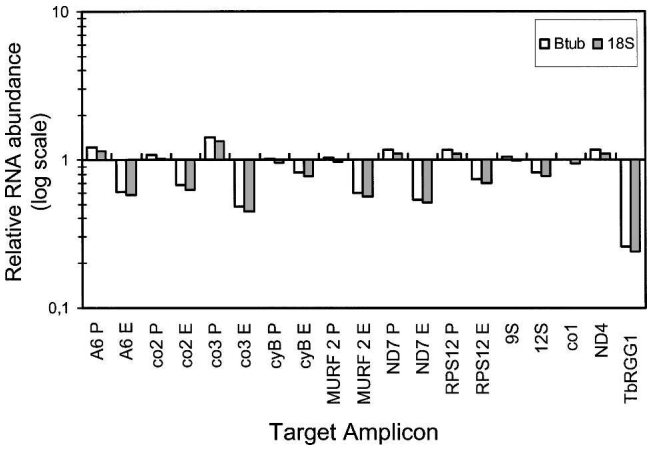

FIGURE 2. RNAi of TbRGG1 affects RNA editing. Real-time PCR analysis of pre-edited, edited, and never-edited mRNAs and ribosomal RNAs encoded in the mt genome. Analysis was performed in triplicate on cDNAs generated from cells grown for 4 d in the presence or absence of tetracycline. For each target amplicon, the relative change in RNA abundance due to induction of RNAi silencing of TbRGG1 was determined by using cytosolic transcripts of β-tubulin (white bar) and 18S rRNA (gray bar) as internal references, since their transcription was not affected. The relative abundance of each examined transcript upon synthesis of the TbRGG1 dsRNA was plotted on a logarithmic scale: 1.0 represents the wild-type level; levels above and below 1.0 mean an increase or decrease of a given RNA, respectively. The following pre-edited (P) and edited (E) mRNAs were assayed: ATPase subunit 6 (A6), cytochrome oxidase subunits 2 (co2), and 3 (co3), cytochrome reductase subunit b (cyB), maxicircle unknown reading frame 2 (MURF2), NADH dehydrogenase subunit 7 (ND7), and ribosomal protein S12 (RPS12). The following never-edited RNAs were assayed: 9S RNA, 12S RNA, co1, and ND4. The levels of the nuclear-encoded TbRGG1 mRNA were also tested (TbRGG1).

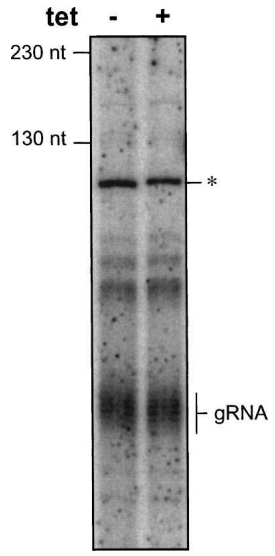

FIGURE 3. RNAi of TbRGG1 does not affect gRNAs. The total population of minicircle-encoded gRNAs was visualized in a high-resolution acrylamide-urea gel by labeling 2.5 μg of total RNA with guanylyltransferase and [γ-^{32}P]GTP. The *left* and *right* lane contains RNA from noninduced (Tet−) and induced (Tet+) TbRGG1 RNAi cells (4 d of induction), respectively. The gRNAs, which range in size mainly due to the variable lengths of their 3′-oligo(U) tails, are indicated on the *right*. The *top* band marked by the "*" is a cytosolic RNA that is concurrently labeled by the enzyme and is used as a loading control. The sizes of two in vitro-transcribed RNAs, which were end-labeled in separate reactions, are indicated on the *left*.

loading control between the samples from induced and noninduced cells. As judged by this assay, TbRGG1 repression does not significantly affect steady-state levels of gRNAs.

TbRGG1 is associated with a multiprotein complex

The sedimentation profile of TbRGG1 on a glycerol gradient as determined by Western analysis indicated that it is part of a large protein complex (Vanhamme et al. 1998). To explore this possibility, the TAP-tagged TbRGG1 protein was expressed in procyclic *T. brucei* cells under the control of a tetracycline-inducible promoter. Expression of the tagged protein was monitored on glycerol gradients using the PAP reagent, which specifically recognizes the Protein A domain of the tag. A strong band of 105 kDa showed the distribution of protein in fractions 3–13, with the bulk being present in fractions 5–9 (Fig. 4). Two additional bands are apparent below the major uppermost band, which may correspond to modification of TbRGG1 by proteolysis or other means, as observed and postulated in the original report (Vanhamme et al. 1998). The same gradient probed with anti-KREPA3 antibody showed the peak 20 S editosome signal in fraction 11 (Fig. 4). The sedimentation properties of the tagged TbRGG1 protein suggest its incorporation into a complex that overlaps with the 20 S editosome, although it sedimented at a somewhat lower "S" value than originally reported (Vanhamme et al. 1998), but consistently with earlier observation from our laboratory (Vondrušková et al. 2005).

The clarified lysate with the expressed TAP-tagged TbRGG1 was subjected to the tandem-affinity purification protocol. Western analysis of aliquots from the final four TAP eluates showed the presence of the tagged protein (Fig. 5A), and SYPRO Ruby staining of SDS-PAGE separated sample showed at least nine visible protein bands in the tagged TbRGG1 complex (Fig. 5B). The same fraction was also probed with a mix of monoclonal antibodies against the four core editosome proteins (KREPA1, KREPA2, KREL1, and KREPA3), and none of these reacted with the protein complex containing TbRGG1 (Fig. 5C). Thus, the tagged TbRGG1 complex does not associate with the editosomes.

Mass spectrometry analysis of the tagged TbRGG1 complex identified several proteins (Table 1; Supplemental Tables 1 and 2), including two proteins, Tb927.2.3800 and Tb927.7.2570, that have no known motifs but have 31% sequence identity and 48% similarity over 432 amino acids between them. These two proteins were identified in the sample with high peptide coverage (data not shown), thus, were selected for reciprocal TAP-tag analyses. Calmodulin elution fractions of Tb927.2.3800 and Tb927.7.2570 TAP-tag purifications were stained by SyproRuby (Fig. 6) and analyzed by LC-MS/MS, in which the TbRGG1 protein was also detected.

To assign the protein to this complex, the data from all three TAP-tag cell lines were compiled. Fourteen proteins that were identified with probability of ≥0.9 in all three TAP-tags, and at least by two unique peptide matches in one of them, were assigned as the component of the complex (Table 1). Seven other proteins that were identified using the above-mentioned conditions, but are known subunits of different mt complexes and/or are abundant mitochondrial and nonmitochondrial proteins, were operationally

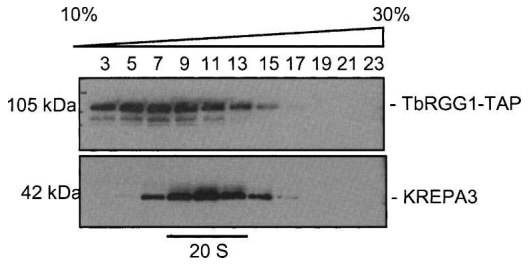

FIGURE 4. Sedimentation profile of the protein complex containing TbRGG1. The cleared lysate of hypotonically isolated mitochondria from cells containing the TAP-tagged TbRGG1 grown for 2 d in the presence of 500 ng/mL tetracycline were loaded onto glycerol gradients and fractionated as described in Materials and Methods. Fractions were immunodecorated with the PAP reagent, which binds the protein A domain of the TAP-tag (*top*), and the anti-KREPA3 (*bottom*) antibody as a marker of the 20 S fractions. The lower two bands visualized by the PAP reagent may correspond to modification of the TAP-tagged TbRGG1 protein by proteolysis or other means.

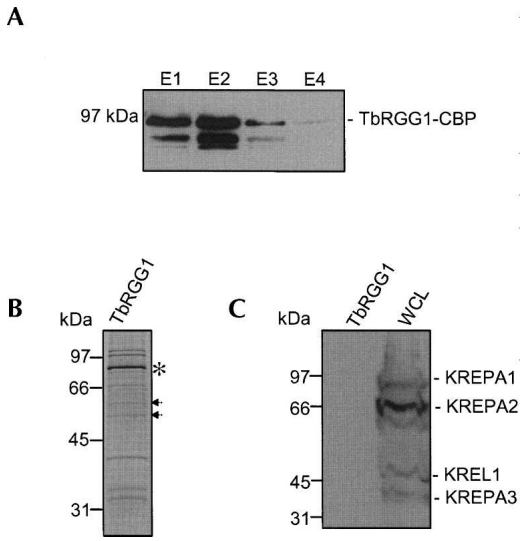

FIGURE 5. Identification of proteins associated with the TAP-tagged TbRGG1 protein. (*A*) Eluates E1–E4 from the TAP-tag purification using the TbRGG1 protein as bait were visualized by Western analysis using the anti-his antibody, recognizing the his-epitope present on the remaining part of the TAP-tag along with the calmodulin binding peptide (TbRGG1-CBP). The eluate most enriched for the TAP-tagged protein (E2) was subjected to LC-MS/MS. As in the glycerol gradient, two lower bands are apparent in the eluates enriched for the tagged protein, possibly products of the modification of the TbRGG1 portion of the fusion. (*B*) Eluate E2 was stained with Sypro Ruby. The predicted position of TbRGG1-CBP and the copurified proteins Tb927.2.3800 and Tb927.7.2570 are indicated on the *right* by the "*" and by the arrows, respectively. (*C*) The purified proteins from the E2 fraction were subjected to simultaneous immunoanalysis using the anti-KREPA1, KREPA2, KREL1, and KREPA3 monoclonal antibodies, using whole-cell lysates (WCL) from *T. brucei* as a positive control.

regarded as contaminants (Supplemental Table 1). We also list numerous proteins that were identified in one or two of the tagged complexes or identified only with one peptide match and were not considered as part of the complex (Supplemental Table 2).

Results from detailed sequence analysis of the component proteins with public databases are presented in Table 1. Some of the proteins in the complex have a high degree of conservation to other eukaryotic RNA helicases and RNA-binding proteins. Moreover, motifs involved in RNA–protein and protein–protein interactions, such as RRM, GRP, and ankyrin repeat were found within some of the polypeptide sequences. Interestingly, TbRGGm (Tb10.406.0050), a protein previously identified to be associated with an affinity purified editosome (Panigrahi et al. 2003a), was also among the RNA-binding motif containing proteins present in the complex. It is noteworthy that two pairs of closely related proteins were identified in the complex (Table 1).

Association of TbRGG1 with the multiprotein complex is RNA mediated

To test whether association of the TbRGG1 is mediated via RNA interactions, hypotonically isolated mitochondria from the 29-13 cell line were lysed in the presence or absence of RNase A, and the lysates were fractionated by sedimentation in glycerol gradients (Fig. 7A). As evident from Western analysis using the anti-TbRGG1 antibody, there is a pronounced shift in the localization of the TbRGG1 protein to the lighter fractions of the gradient upon RNase treatment, peaking in fractions 5 through 7 and absent after fraction 9. TbRGG1 in untreated samples peaks in fractions 7 through 11, and is detected throughout the gradient. The peak of fractionation of two subunits of the 20 S editosome, KREPA1 and KREPA2, was unaffected by RNase treatment (Fig. 7A).

In light of this result, the initial IgG affinity selection step was repeated for the TAP-tagged TbRGG1 in the presence and absence of RNase A. The eluates resulting from TEV cleavage, which releases protein(s) bound to the IgG matrix by the TAP-tag, were resolved by glycerol gradient centrifugation. A shift in the sedimentation of TAP-tagged TbRGG1 to the lighter fractions is apparent when the ribonuclease is present during the first purification step (Fig. 7B). SyproRuby staining of the calmodulin eluates directly separated on SDS-PAGE gel reveals that the abundant bands corresponding in size to the Tb927.2.3800 and Tb927.7.2570 proteins disappear in the presence of RNase A (Fig. 7C). Furthermore, only TbRGG1 peptides were detected in these eluates by mass spectroscopy analysis. Reciprocally, TbRGG1 was not detected by this method in Tb927.2.3800 TAP eluates purified in the presence of RNase A, while other component proteins of the complex were present, as compared with parallel untreated purifications (data not shown). We propose that this novel multiprotein complex is involved in mt RNA metabolism based on the observations that TbRGG1, a protein with such a role, interacts with it in an RNA-mediated manner, and that it contains several proteins with RNA-binding and processing motifs.

DISCUSSION

Since its serendipitous discovery almost 10 yr ago (Vanhamme et al. 1998), TbRGG1 has remained among the least-characterized proteins putatively associated with RNA editing, while the functions of other RNA editing accessory factors have been elucidated, at least to some extent. It was proposed that TbRGG1 may have a role in RNA editing and that it is part of a macromolecular complex based on its reported biochemical properties (Vanhamme et al. 1998; Simpson et al. 2004; Lukeš et al. 2005; Stuart et al. 2005). Here, we test both of these hypotheses in vivo using reverse genetics and TAP-purification approaches that have been established in *T. brucei* subsequent to the discovery of this protein.

Using an RNAi-based approach, we have generated cells deficient for TbRGG1 and showed that editing of all analyzed mRNAs is down-regulated, though to varying degrees, whereas the assayed never-edited mRNAs remain at their wild-type levels. A similar phenotype has been

TABLE 1. Mitochondrial proteins associated with the TAP-tagged TbRGG1 protein, Tb927.2.3800, and Tb927.7.2570 protein in procyclic *T. brucei*

Protein name	GeneDB	TbRGG1	Tb927.2.3800	Tb927.2.2570	Homology (*E*-value)	Motif/domain (*E*-value)
Tb927.6.2230^{tag}	TbRGG1	√	√	√	*Caenorhabditis* hypothetical protein (4e-13)	—
Tb927.7.2570^{tag}	HP*	√	√	√	Tb927.2.3800[1]	—
Tb927.2.3800^{tag}	HP*	√	√	√	Tb927.7.2570[1]	—
Tb927.5.3010	HP	√	√	√	*Babesia* hypothetical protein (9e-09); bacterial putative RNA-binding protein (6e-06)	Ribosomal S2 protein signature
Tb927.4.1500	HP	√	√	√	*Oryza* ATP-dependent RNA helicase (1e-121)	dsrm (9e-07); Helicase C (2e-13)
Tb11.02.5390	HP	√	√	√	—	Ankyrin repeat (0.83)
Tb11.01.8620	HP	√	√	1	—	—
Tb10.406.0050	RBP$^{\#}$	√	√	√	*Caenorhabditis* RNA helicase (1e-09)	RRM (6.3e-11)
Tb927.8.8170	HP	√	√	1	Tb927.4.4160[2]	—
Tb927.4.4160	HP	√	1	√	Tb927.8.8170[2]	—
Tb927.3.1820	HP	√	√	√	—	GRP (0.028)
Tb11.01.7290	Nudix hydr*	√	√	1	—	NUDIX (4e-05)
Tb927.3.4920	HP	1	√	√	*Arabidopsis* calcium binding mt protein (9e-06)	LETM1 (4e-08)
Tb927.6.2140	HP	1	√	1	Bacterial hydratase (6e-05)	2-keto-4 pentenoate hydratase (5e-07)

(√) Protein was identified with more than two unique tryptic peptides; (1) protein was identified with 1 unique tryptic peptide; (*) proteins also known as LtAP1-3 identified in *L. tarentolae* MRP1/2 complex (3); (superscript "tag") tagged proteins in this study; (superscript "#") protein also known as TbRGGm (20); (superscript "1") proteins have 31% sequence identity and 48% similarity over 432 amino acids between them; and (superscript "2") proteins have 77% sequence identity and 85% similarity over 904 amino acids between them.

observed when subunits of the 20 S editosome are silenced, which have a direct role in RNA editing (Carnes et al. 2005; Trotter et al. 2005; Salavati et al. 2006). This result is noteworthy when compared with studies in which the expression of other RNA editing accessory factors is disrupted. In the procyclic stages, RNAi knock-down of either of the two subunits of the MRP1/2 complex decreased the levels of a subset of edited and never-edited mRNAs (Vondrušková et al. 2005). Gene knock-out of *MRP1* in the bloodstages had a comparable effect (Lambert et al. 1999), while silencing of RBP16 caused a reduction of edited cyB and never-edited RNAs (Pelletier and Read 2003). Such a pleimorphic effect on mt transcripts is not observed when TbRGG1 is silenced.

Because of its in vitro poly(U)–RNA binding activity, the TbRGG1 protein was suggested to have an alternate role in the synthesis and/or processing of those mt RNAs (Leegwater et al. 1995; Vanhamme et al. 1998) that contain the post-transcriptionally added 3′-oligo(U) extension (Aphasizhev 2007). This possibility was also tested by assaying the levels of the mitoribosomal RNAs in parallel with the other mRNAs by qPCR. In the induced cells, the levels of the 9S and 12S rRNAs remain unchanged and slightly reduced, respectively, implying that TbRGG1 does not have the proposed role in mt rRNA synthesis.

Another prominent class of mt RNAs with added 3′-oligo(U) tails are the gRNAs, which supply the essential information for proper U-insertion/deletion into the cognate mRNA (Blum and Simpson 1992). Because of its aforementioned affinity for poly(U), it was suggested that TbRGG1 interacts directly with gRNAs, perhaps functioning in their stabilization or maturation. As judged by the

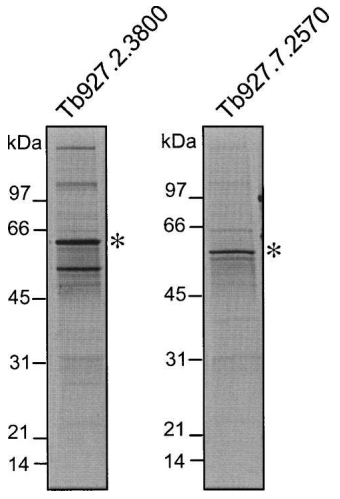

FIGURE 6. Sypro Ruby staining of purified Tb927.2.3800 (*left*) and Tb927.7.2570 (*right*) complexes. The predicted position of the tagged proteins (Tb927.2.3800-CBP or Tb927.7.2570-CBP) are indicated on the *right*.

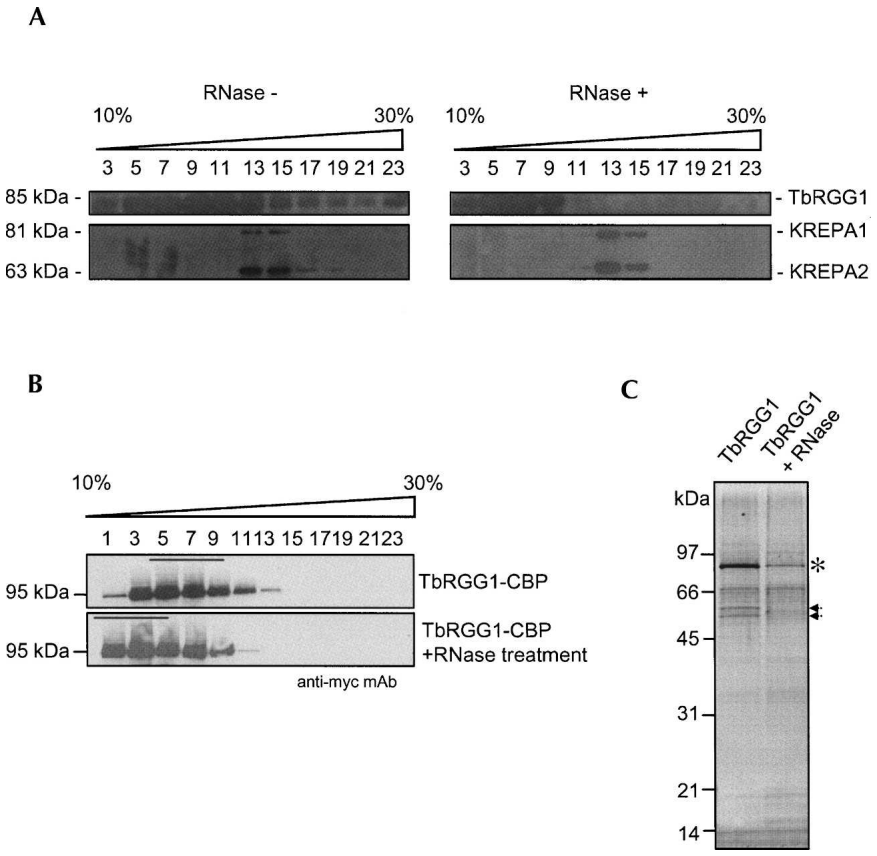

FIGURE 7. TbRGG1 association with the MRB complex 1 appears to be RNase sensitive. (*A*) Hypotonically isolated mitochondria from the 29-13 cell line were lysed in the absence (*left*, RNase-) or presence (*right*, RNase+) of 0.1 mg/mL RNase A. The latter lysates were loaded onto glycerol gradients containing the same concentration of the enzyme. Western analysis was done on resulting fractions with the anti-TbRGG1 antibodies, as well as the anti-KREPA1 and anti-KREPA2 antibodies as markers of the 20 S fractions. (*B*) IgG purification of the TAP-tagged TbRGG1 in the presence and absence of RNase A. The eluates resulting from TEV cleavage, which releases protein(s) bound to the IgG matrix by the TAP-tag, were resolved by glycerol gradient centrifugation. A shift in the sedimentation of TAP-tagged TbRGG1 to the lighter fractions is apparent when the ribonuclease is present during the first purification step. The peak fraction designated by a black line was pooled and further subjected to the second affinity purification step. (*C*) SyproRuby staining of the calmodulin eluates purified from pooled glycerol gradient fractions separated on 10.5%–14% SDS-PAGE gel shows that the abundant bands corresponding in size to the Tb927.2.3800 and Tb927.7.2570 proteins disappear in the presence of RNase A, which are indicated by arrows. TbRGG1-CBP is designated with "*."

guanylyltransferase labeling assay, no significant changes are observed to the steady-state levels of gRNAs or their processing upon TbRGG1 silencing.

One plausible interpretation of these results is that TbRGG1 has a role in RNA editing, since the effect of its silencing is limited to a decrease in edited mRNAs as compared with the other assayed transcripts. However, it most likely does not have a direct role in the process, since the observed down-regulation occurs without a corresponding accumulation of pre-edited RNAs, as observed when multiround editing is disrupted by silencing of the components of the 20 S editosome (Carnes et al. 2005; Trotter et al. 2005; Salavati et al. 2006). An indirect role of TbRGG1 in this process may be via interaction with the gRNAs requisite for decrypting the appropriate mRNAs. Although the guanylyltransferase labeling of these molecules has shown that their stability and processing remain intact upon repression of TbRGG1, the possibility that the protein binds the gRNAs in order to facilitate their utilization, a role proposed for RBP16 (Pelletier and Read 2003), remains open. However, the reduction of edited co2 mRNA in the TbRGG1 knockdowns is quite telling, since its gRNA is located within its 3′-UTR, thus not requiring the independent *trans*-acting gRNA molecules (Kim et al. 1994). TbRGG1 binding to gRNAs, which are heterogeneous in sequence, would most likely involve conserved features such as the 3′ oligo(U) tail, which are absent in the co2 *cis*-gRNA, as implied by its incapacity to act in *trans* (Golden and Hajduk 2005). Thus, based on the observation that co2-edited RNAs are affected by TbRGG1 depletion, while gRNA levels are not, we conclude that the protein does not act through these small RNAs. An explanation that is consistent with the in vivo data is that TbRGG1 may be involved in the stabilization of edited RNAs. Alternately, it may have a role in editing efficiency, since depletion of a protein with such a function would also result in a decrease of edited RNAs.

It was postulated that TbRGG1 is associated with a protein complex performing key editing activities, which is now the well-known 20 S editosome or L-complex. Yet, detailed analyses of the composition of the editosome(s) in *T. brucei* failed to identify TbRGG1 in them (Aphasizhev et al. 2003b; Panigrahi et al. 2003a,b, 2006). Indeed, RNAi silencing of TbRGG1 did affect neither the editosome nor the MRP1/2 complex, since subunits incorporated into either of these complexes remained at wild-type levels, an indication of their integrity (Wang et al. 2003; Vondrušková et al. 2005). To characterize the composition of the complex predicted to interact with TbRGG1, overexpression of the TAP-tagged protein was performed with the intention of identifying any copurified subunits by mass spectrometry. The sedimentation properties in glycerol gradients of tagged TbRGG1 suggest incorporation into a complex, although in lower density fractions than initially reported (Vanhamme et al. 1998). The discrepancy in the described sedimentation

properties of TbRGG1 may be due to technical differences in gradient preparation in the two studies, as the localization of in vitro editing activity, found in the same fractions as TbRGG1 originally (Vanhamme et al. 1998), was at a higher density than is typically observed (Stuart et al. 2005).

The association of TbRGG1 with proteins that may represent a separate complex was demonstrated by the coisolation of a novel set of proteins with TAP-purified TbRGG1, as detected by mass spectrometry. The association was further validated by tagging two other component proteins of the complex. Based on the TAP-tag analyses, we assigned 14 proteins to this novel putative complex, which include a Nudix hydrolase, RNA helicase, TbRGGm, and hypothetical proteins with and without identifiable motifs. A probable TbRGG1 interaction with this complex via RNA was also revealed. This association is likely to be biologically relevant, as it is reproducibly detected in TbRGG1, Tb927.2.3800, and Tb927.7.2570 TAP purifications, without consistently revealing other RNA-binding proteins such as the MRPs, RBP16, REAP1, subunits of the 20 S editosome or ribosomal proteins that may potentially associate with the TAP-tagged proteins nonspecifically due to their affinity for nucleic acids. However, because the complex interacts in an RNase-sensitive manner with TbRGG1 and contains multiple proteins with RNA-binding domains suggestive of roles in RNA processing, we provisionally name it the putative mitochondrial RNA-binding complex 1 (put-MRB complex 1).

Interestingly, three of the proteins identified to be components of the MRB complex 1 were previously encountered in substoichiometric amounts in TAP-purifications of the MRP1/2 complex from *Leishmania tarentolae*: Tb927.2.3800 (LtAP-1), Tb927.7.2570 (LtAP-2), and Nudix hydrolase (LtAP-3) (Aphasizhev et al. 2003a). In contrast, TAP or monoclonal antibody affinity purification of the MRP1/2 complex in *T. brucei* did not copurify these proteins (Panigrahi et al. 2008; Zíková et al. 2008), and we have not identified the MRP1 or MRP2 proteins as part of put-MRP complex 1. Another purification of the putative complex, using a slightly different approach and yielding an overlapping subunit composition also did not contain any MRP peptides (Panigrahi et al. 2008). This discrepancy may be due to RNA-based interactions between these proteins; technical differences in the manner the purifications were performed, such as the amount of cells used, or it simply reflects the different types of associations that take place in the two species.

In conclusion, the 14 proteins identified using tagged TbRGG1, Tb927.2.3800, and Tb927.7.2570 seem to be genuine components of a novel ribonucleoprotein complex or a collection of complexes and/or monomers that associate via RNA linkers. We have termed it here the put-MRB complex 1, since it has features that suggest a function in RNA processing activities in *T. brucei* procyclics, and perhaps an indirect role in RNA editing. This working hypothesis is supported by the effect of RNAi silencing of TbRGG1 on edited RNAs as well as by its association with proteins containing motifs that mediate RNA metabolism and/or protein–protein interactions. In addition, we provide evidence that the association of TbRGG1 with this complex may be mediated through RNA. We are in the process of extensive characterization of the function and composition of this enigmatic protein complex.

MATERIALS AND METHODS

Plasmid construction, cell culture, transfection, RNAi induction, and growth curves

A 543-nt long N-terminal region of the TbRGG1 gene overlapping the RGG motif was PCR amplified using primers RG-F (5′-GGATCCACTACCGAGATCAGCGCAAC) and RG-R (5′-AAGCTTGCATCCATTCTGTAGCCTG) (added BamHI and HindIII restriction sites underlined) from genomic DNA of the *T. brucei* strain 29-13. The amplified fragment was cloned into the p2T7-177 vector, which was electroporated into procyclic *T. brucei* strain 29-13 and selected following a protocol described elsewhere (Vondrušková et al. 2005). The synthesis of dsRNA was induced by the addition of 1 μg/mL tetracycline and the cell density was measured every 24 h. Cell growth rate was determined using the Beckman Z2 Coulter counter over a period of 15 d after the induction of RNAi.

To create a construct for the inducible expression of C-terminally TAP-tagged proteins, the full-length TbRGG1 gene was amplified with primers RG-TAP-Fw (5′-GGGCACAAGCTTATGGTGTGTAGC) and RG-TAP-Rv (5′-GGCGGAGGATCCGCTGTCTTCCAGCC) (added HindIII and BamHI restriction sites underlined) and inserted into the pLew79-MHTAP plasmid (Panigrahi et al. 2003b; Jensen et al. 2006). Similarly, Tb927.2.3800 and Tb927.7.2570 genes were PCR amplified and cloned into pLew79-MHTAP plasmid. The Tb927.2.3800 ORF was PCR amplified from genomic DNA of the 29-13 strain using primers Zah1-TAP-Fw2 (5′-ATTTCATGCTGCGCGCGCGCCTG) and Zah1-TAP-Rv (5′-AAAGGATCCGTATGCCGAAACGGCAGTC). This PCR product was used as a template for PCR with primers Zah1-TAP-Fw (5′-CTGTACTATATTGAAGCTTATGCTGCG) and the aforementioned Zah1-TAP-Rv containing the appropriate HindIII and BamHI restriction sites for cloning, as indicated with underlines. The Tb927.7.2570 ORF was PCR amplified from genomic DNA with primers Zah2-TAP-Fw (5′-TTGACCTCGAGATGCTTCGC) and Zah2-TAP-Rv (5′-GAGATCCAGATCTCAACTTCGC) (XhoI and BglII sites are underlined). The NotI-linearized constructs were introduced into the 29-13 cells and phleomycin-resistant clones were selected.

Northern blot analyses

Total RNA was isolated using Trizol (Sigma) from cells collected at regular intervals and 10 μg were loaded on a 1% formaldehyde agarose gel, blotted, and cross-linked following standard protocols. After prehybridization in Church–Gilbert solution for 1 h at 65°C, hybridization with a radiolabeled probe was performed overnight in the same solution and at the same temperature. Membranes were washed with 2x SSC + 0.1% SDS for 15 min at room temperature, followed by two washes with 0.2x SSC + 0.1%

SDS for 20 min each at 55°C. The radioactive signals were visualized using the PhosphorImager Storm 860.

Western blot analyses

Lysates in SDS-PAGE loading buffer from an equivalent of 5 × 10^6 cells/lane were separated either on 10% or 4%–15% SDS-PAGE gradient gels. Proteins were transferred onto nitrocellulose membrane by electroblotting, blocked overnight with 5% (w/v) nonfat milk in the same solution, and probed with either the anti-TbRGG1 antiserum (provided by L. Vanhamme) or the polyclonal rabbit antisera against *T. brucei* MRP1 (Vondrušková et al. 2005), GAPDH (provided by P.A.M. Michels) and hsp70, all at dilution 1:5000. Monoclonal antibodies against KREPA1 (TbMP81), KREPA2 (TbMP63), KREL1, and KREPA3 (TbMP42) were used as described elsewhere (Panigrahi et al. 2001b) on lysates from hypotonically isolated mitochondria.

Small-scale isolation of mitochondria

A pellet of 10^8 cells was resuspended in 1.5 mL of cold hypertonic NET buffer (100 mM NaCl, 100 mM EDTA at pH 8.0, 10 mM Tris-HCl at pH 7.9), incubated on ice for 10 min, then spun down, and the supernatant was discarded. The pellet was resuspended in cold hypotonic DTE buffer (1 mM Tris-HCl at pH 7.9, 1 mM EDTA at pH 8.0), which disrupts the plasma membrane, and the suspension was passed through a 25-gauge needle into 170 μL of 60% sucrose. The mitochondrial vesicles were spun down and the cytosolic content in the supernatant was discarded. The pelleted mitochondria were resuspended in 500 μL of STM buffer (250 mM sucrose, 20 mM Tris-HCl at pH 7.9, 2 mM $MgCl_2$) supplemented with 3 mM $MgCl_2$ and 5 U DNase I and left on ice for 1 h. Half a mL of STE was added to stop the reaction and the mitochondria were pelleted and washed two more times in 500 μL of STE (250 mM sucrose, 20 mM Tris-HCl at pH 7.9, 2 mM EDTA at pH 8.0) in the same manner. The mitochondrial pellets were stored at −80°C until use.

Quantitative real-time PCR

Ten micrograms of total RNA isolated from noninduced TbRGG1 RNAi cells and cells following 4 d of RNAi induction were treated with the Turbo DNA free kit (Ambion) following the manufacturer's protocol. After the DNase step, 1 μg of RNA was run on a formaldehyde gel to check the integrity of the treated RNA. To prepare templates for quantitative real time (q) PCR, cDNA was synthesized from 4.5 μg of RNA with the SuperScript III reverse transcriptase (Invitrogen) using random hexamers in a volume of 20 μL. A parallel reverse transcription reaction was also performed with the same amount of RNA and omitting the reverse transcriptase as a control for genomic DNA contamination. Both cDNA reactions were diluted 1:10 in H_2O prior to qPCR.

The qPCR reactions were performed using the Rotor-Gene 3000 Real-Time DNA Detection System thermocycler, and data, including PCR efficiencies, were acquired using the Rotor-Gene v6.1 software (Corbett Life Science). The primer pairs used to detect mt transcripts were described previously (Carnes et al. 2005), as are those amplifying 18S rRNA and β-tubulin cDNAs, which were used as reference genes. Primer pairs to detect the 9S and 12S mitochondrial rRNAs and TbRGG1 transcripts were designed for this study and are as follows:

9S Forward (5′-AATGCTATTAGATGGGTGTGGAA-3′);
9S Reverse (5′-GCTGGCATCCATTTCTGACT-3′);
12S Forward (5′-GGGCAAGTCCTACTCTCCTTT-3′);
12S Reverse (5′-TGCCCCAATCAAACATACAA-3′);
TbRGG1 Forward (5′-TTTGACGACCCAAGCACTATGTT-3′); and
TbRGG1 Reverse (5′-GCCTCCCAGCGGTCCTAT-3′).

The TbRGG1 primer pair is not complementary to the dsRNA region targeting the transcript. For each primer, 4 μL of a 1.5 μM stock was added to a 20-μL reaction, in addition to 10 μL of the Power SYBR Green PCR Master Mix (Applied Biosystems) and 2 μL of the cDNA. In the case of reference gene qPCR reactions, the cDNA was additionally diluted 1:50. The qPCR program is as follows: 2 min at 50°C, 10 min at 95°C, and 40 cycles of 15 sec at 95°C and 60 sec at 60°C, in which fluorescence were detected at the end of the latter step. The correctness of the amplicon was verified both by a final dissociation step and electrophoresis of the qPCR product on a 2% agarose gel. The relative abundance of RNAs between the two samples was determined by the Pfaffl method (Pfaffl 2001).

Guanylyltransferase labeling

To visualize gRNAs, 2.5 μg of total RNA from the noninduced and induced (4 d) cells was DNase treated as described above and labeled using guanylyltransferase. A 15-μL reaction contained 1.5 μL of the 10x Capping Reaction Buffer (500 mM Tris at pH 8.0, 60 mM KCl, 12.5 mM DTT, 12.5 $MgCl_2$, 0.5 mg/mL BSA, 45 μCi of [α-^{32}P]GTP, 40 U RNaseOUT Ribonuclease Inhibitor (Invitrogen), and 5 U of guanylyltransferase (Ambion). The reaction was incubated for 1 h at 37°C and stopped by the addition of 0.1% SDS and 10 mM EDTA. The reaction products were phenolchloroform extracted, ethanol precipitated, and dissolved in 8 μL of 60% formamide. They were incubated at 80°C for 2 min, and 4 μL were loaded on a high-resolution denaturing 12% acrylamide-8 M urea gel.

Glycerol gradient sedimentation

For hypotonic purification of the mitochondria, the pellet from 10^{10} cells was washed in 35 mL of the SBG buffer (100 mM NaCl; 20 mM glucose; 20 mM $NaHPO_4$ at pH 7.9) and then dounce homogenized in 35 mL of the DTE solution. Next, 5.85 mL of 60% sucrose was added and the hypotonically isolated mt vesicles were pelleted and resuspended in 6.8 mL of the STM buffer, which was supplemented with 21 μL each of 1 M $MgCl_2$ and 0.1 M $CaCl_2$, and 61.2 μg of DNase. The DNase treatment was stopped with equal volume of the STE buffer. The enriched mitochondria were then lysed in 1 mL of the lysis buffer (10 mM Tris at pH 7.2, 10 mM $MgCl_2$, 100 mM KCl, 1 mM DTT, 1 μg/mL pepstatin, 2 μg/mL leupeptin, 1 mM pefabloc) containing 1% Triton X-100, for 15 min at 4°C. The lysate was cleared by centrifugation and loaded onto a 10%–30% glycerol gradient containing the same concentration of DTT and protease inhibitors as the lysis buffer. The gradient was spun at 38,000 rpm in a SW 40 Ti rotor (Beckman) for 5 h at 4°C, and 500-μL fractions were subsequently collected from the top. In experiments testing RNase sensitivity of TbRGG1 interaction with macromolecular complexes, 0.1 mg/mL of RNase A was introduced into the lysis buffer and glycerol gradient, which was spun using the previously mentioned rotor at

38,000 rpm for 12 h at 4°C or 0.1 mg/mL of RNase A was added during IgG affinity step, and TEV eluates were loaded on glycerol gradients and spun at 38,000 rpm for 5 h at 4°C.

TAP-purification of TbRGG1

Either the whole cell pellet or hypotonically isolated mitochondria (scaled up from the protocol described above) from 4×10^{10} cells containing the TbRGG1 gene with a tandem affinity purification (TAP) tag, whose expression was induced by 500 ng/mL tetracycline, were lysed on ice for 20 min in 20 mL of the IPP150 buffer (10 mM Tris-HCl at pH 8.0, 150 mM NaCl, 0.1% NP40) containing 1% Triton X-100 and two tablets of Complete EDTA-free protease inhibitors (Roche). After centrifugation at 9000*g* for 30 min, the cleared supernatant was incubated with 200 μL of the IgG Sepharose Fast Flow beads (Pharmacia) for 2 h at 4°C. After draining the supernatant and wash in IPP150, beads were incubated with 100 U of TEV protease (Invitrogen) in 1 mL of the TEVCB buffer (10 mM Tris-HCl at pH 8.0, 150 mM NaCl, 0.1% NP40, 0.5 mM EDTA, 1 mM DTT) for 2 h at 16°C. The TEV eluate was combined with three times the volume of calmodulin resin (Stratagene) in the CBB buffer (10 mM Tris-Hcl at pH 8.0, 150 mM NaCl, 0.1% NP40, 10 mM β-mercaptoethanol [ME], 1 mM Mg acetate, 1 mM imidazole, 2 mM $CaCl_2$), which was incubated for 1 h at 4°C. The tagged complexes were eluted with $4 \times$ 250 μL of the CEB buffer (10 mM Tris-Hcl at pH 8.0, 150 mM NaCl, 0.1% NP40, 10 mM ME, 1 mM Mg acetate, 1 mM imidazole, 2 mM EGTA). The same protocol was used to purify proteins associated with TAP-tagged Tb927.2.3800 and Tb927.7.2570 proteins in corresponding cell lines induced with tetracycline. TAP purification Tb927.2.3800 was performed in parallel in the presence and absence of 0.1 mg/mL RNase A during the initial incubation of the cleared lysate with the IgG Sepharose beads. The proteins from isolated complexes were separated in 10.5%–14% SDS-PAGE gel and visualized by SYPRO Ruby (Invitrogen) staining.

Mass spectrometry analysis

Proteins were analyzed by mass spectrometry as described (Panigrahi et al. 2001a). Briefly, proteins in 100 μL of the TAP eluate were precipitated with 600 μL of acetone, resuspended in 8 M urea/1 mM DTT, and denatured at 50°C for 1 h The sample was diluted 1:7 with 50 mM NH_4-HCO_3 and treated with 100 ng of mass spectrometry grade trypsin (Promega) at 37°C overnight. The mixture was dried in a speedvac and dissolved in 5% acetonitrile/0.4% acetic acid. The resulting peptides were purified using a C18 ZipTip (Millipore) following the manufacturer's protocol. The peptides were analyzed using a LTQ Linear Ion Trap Mass Spectrometer. The CID spectra were compared with the *T. brucei* protein database downloaded from GeneDB using TurboSequest software, and protein matches were determined using PeptideProphet and ProteinProphet programs (Keller et al. 2002; Nesvizhskii et al. 2003).

Sequence analysis

The protein sequences were compared with the NCBI nr database using PSI-BLAST and motif, and domain searches were carried out by CDD, PFAM, and Prosite searches.

SUPPLEMENTAL DATA

Supplemental material can be found at http://www.rnajournal.org.

ACKNOWLEDGMENTS

We thank Zdeňka Číčová (Biology Centre) for help with some experiments and Yuko Ogata (Seattle Biomedical Research Institute) for help with mass spectrometry analysis. Paul A.M. Michels (De Duve Institute of Cellular Pathology, Brussels) and Luc Vanhamme (Free University of Brussels, Gosselies) kindly provided antibodies. This work was supported by the Grant Agency of the Czech Republic 204/06/1558, Grant Agency of the Czech Academy of Sciences A500960705, and the Ministry of Education of the Czech Republic (LC07032, 2B06129, and 6007665801) to J.L., the Ph.D. student grant 524/03/H133 to H.H., and National Institutes of Health Grants 5R03TW6445 (to K.D.S. and J.L.) and AI14102 (to K.S.).

Received October 23, 2007; accepted February 15, 2008.

REFERENCES

Aphasizhev, R. 2007. RNA editing. *Mol. Biol.* **41:** 227–239.

Aphasizhev, R., Aphasizheva, I., Nelson, R.E., and Simpson, L. 2003a. A 100-kDa complex of two RNA-binding proteins from mitochondria of *Leishmania tarentolae* catalyzes RNA annealing and interacts with several RNA editing components. *RNA* **9:** 62–76.

Aphasizhev, R., Aphasizheva, I., Nelson, R.E., Gao, G., Simpson, A.M., Kang, X., Falick, A.M., Sbicego, S., and Simpson, L. 2003b. Isolation of a U-insertion/deletion editing complex from *Leishmania tarentolae* mitochondria. *EMBO J.* **22:** 913–924.

Blum, B. and Simpson, L. 1992. Formation of guide RNA messenger-RNA chimeric molecules in vitro, the initial step of RNA editing, is dependent on an anchor sequence. *Proc. Natl. Acad. Sci.* **89:** 11944–11948.

Burd, C.G. and Dreyfuss, G. 1994. Conserved structures and diversity of functions of RNA-binding proteins. *Science* **265:** 615–621.

Carnes, J., Trotter, J.R., Ernst, N.L., Steinberg, A.G., and Stuart, K. 2005. An essential RNase III insertion editing endonuclease in *Trypanosoma brucei*. *Proc. Natl. Acad. Sci.* **102:** 16614–16619.

Golden, D.E. and Hajduk, S.L. 2005. The 3′-untranslated region of cytochrome oxidase II mRNA functions in RNA editing of African trypanosomes exclusively as a *cis* guide RNA. *RNA* **11:** 29–37.

Goulah, C.C., Pelletier, M., and Read, L.K. 2006. Arginine methylation regulates mitochondrial gene expression in *Trypanosoma brucei* through multiple effector proteins. *RNA* **12:** 1545–1555.

Hans, J., Hajduk, S.L., and Madison-Antenucci, S. 2007. RNA-editing-associated protein 1 null mutant reveals link to mitochondrial RNA stability. *RNA* **13:** 881–889.

Jensen, B.C., Kifer, C.T., Brekken, D.L., Randall, A.C., Wang, Q., Drees, B.L., and Parsons, M. 2006. Characterization of protein kinase CK2 from *Trypanosoma brucei*. *Mol. Biochem. Parasitol.* **151:** 28–40.

Keller, A., Nesvizhskii, A.I., Kolker, E., and Aebersold, R. 2002. Empirical statistical model to estimate the accuracy of peptide identifications made by MS/MS and database search. *Anal. Chem.* **74:** 5383–5392.

Kim, K.S., Teixeira, S.M., Kirchhoff, L.W., and Donelson, J.E. 1994. Transcription and editing of cytochrome oxidase II RNAs in *Trypanosoma cruzi*. *J. Biol. Chem.* **269:** 1206–1211.

Lambert, L., Muller, U.F., Souza, A.E., and Göringer, H.U. 1999. The involvement of gRNA-binding protein gBP21 in RNA editing-an

in vitro and in vivo analysis. *Nucleic Acids Res.* **27:** 1429–1436.

Leegwater, P., Speijer, D., and Benne, R. 1995. Identification by UV cross-linking of oligo(U)-binding proteins in mitochondria of the insect trypanosomatid *Crithidia fasciculata*. *Eur. J. Biochem.* **227:** 780–786.

Liu, B., Molina, H., Kalume, D., Pandey, A., Griffith, J.D., and Englund, P.T. 2006. Role of p38 in replication of *Trypanosoma brucei* kinetoplast DNA. *Mol. Cell. Biol.* **26:** 5382–5393.

Lukeš, J., Hashimi, H., and Zíková, A. 2005. Unexplained complexity of the mitochondrial genome and transcriptome in kinetoplastid flagellates. *Curr. Genet.* **48:** 277–299.

Madison-Antenucci, S., Sabatini, R.S., Pollard, V.W., and Hajduk, S.L. 1998. Kinetoplastid RNA-editing-associated protein 1 (REAP-1): A novel editing complex protein with repetitive domains. *EMBO J.* **17:** 6368–6376.

Miller, M.M., Halbig, K., Cruz-Reyes, J., and Read, L.K. 2006. RBP16 stimulates trypanosome RNA editing in vitro at an early step in the editing reaction. *RNA* **12:** 1292–1303.

Nesvizhskii, A.I., Keller, A., Kolker, E., and Aebersold, A. 2003. A statistical model for identifying proteins by tandem mass spectrometry. *Anal. Chem.* **75:** 4646–4658.

Panigrahi, A.K., Gygi, S., Ernst, N.L., Igo Jr., R.P., Palazzo, S.S., Schnaufer, A., Weston, D., Carmean, N., Salavati, R., Aebersold, R., et al. 2001a. Association of two novel proteins, *Tb*MP52 and *Tb*MP48, with the *Trypanosoma brucei* RNA editing complex. *Mol. Cell. Biol.* **21:** 380–389.

Panigrahi, A.K., Schnaufer, A., Carmean, N., Igo Jr., R.P., Gygi, S.P., Ernst, N.L., Palazzo, S.S., Weston, D.S., Aebersold, R., Salavati, R., et al. 2001b. Four related proteins of the *Trypanosoma brucei* RNA editing complex. *Mol. Cell. Biol.* **21:** 6833–6840.

Panigrahi, A.K., Allen, T.E., Haynes, P.A., Gygi, S.P., and Stuart, K. 2003a. Mass spectrometric analysis of the editosome and other multiprotein complexes in *Trypanosoma brucei*. *J. Am. Soc. Mass Spectrom.* **14:** 728–735.

Panigrahi, A.K., Schnaufer, A., Ernst, N.L., Wang, B., Carmean, N., Salavati, R., and Stuart, K. 2003b. Identification of novel components of *Trypanosoma brucei* editosomes. *RNA* **9:** 484–492.

Panigrahi, A.K., Ernst, N.L., Domingo, G.J., Fleck, M., Salavati, R., and Stuart, K.D. 2006. Compositionally and functionally distinct editosomes in *Trypanosoma brucei*. *RNA* **12:** 1038–1049.

Panigrahi, A.K., Zíková, A., Dalley, R.A., Acestor, N., Ogata, Y., Anupama, A., Myler, P.J., and Stuart, K.D. 2008. Mitochondrial complexes in *Trypanosoma brucei:* A novel complex and a unique oxidoreductase complex. *Mol. Cell. Proteom* **7:** 534–545. doi: 10.1074/mcp.M700430-MCP200.

Pelletier, M. and Read, L.K. 2003. RBP16 is a multifunctional gene regulatory protein involved in editing and stabilization of specific mitochondrial mRNAs in *Trypanosoma brucei*. *RNA* **9:** 457–468.

Pfaffl, M.W. 2001. A new mathematical model for relative quantification in real-time RT-PCR. *Nucleic Acids Res.* **29:** e45. doi: 10.1093/nar/29.9.e45.

Sbicego, S., Alfonzo, J.D., Estevez, A.M., Rubio, M.A., Kang, X., Turck, C.W., Peris, M., and Simpson, L. 2003. RBP38, a novel RNA-binding protein from trypanosomatid mitochondria, modulates RNA stability. *Eukaryot. Cell* **2:** 560–568.

Schumacher, M.A., Karamooz, E., Zíková, A., Trantírek, L., and Lukeš, J. 2006. Crystal structures of *Trypanosoma brucei* MRP1/MRP2 guide-RNA-binding complex reveals RNA matchmaking mechanism. *Cell* **126:** 701–711.

Simpson, L., Aphasizhev, R., Gao, G., and Kang, X. 2004. Mitochondrial proteins and complexes in *Leishmania* and *Trypanosoma* involved in U-insertion/deletion RNA editing. *RNA* **10:** 159–170.

Stuart, K. and Panigrahi, A.K. 2002. RNA editing: Complexity and complications. *Mol. Microbiol.* **45:** 591–596.

Stuart, K.D., Schnaufer, A., Ernst, N.L., and Panigrahi, A.K. 2005. Complex management: RNA editing in trypanosomes. *Trends Biochem. Sci.* **30:** 97–105.

Trotter, J.R., Ernst, N.L., Carnes, J., Panicucci, B., and Stuart, K. 2005. A deletion site editing endonuclease in *Trypanosoma brucei*. *Mol. Cell* **20:** 403–412.

Vanhamme, L., Perez-Morga, D., Marchal, C., Speijer, D., Lambert, L., Geuskens, M., Alexandre, S., Ismaïli, N., Göringer, U.H., Benne, R., et al. 1998. *Trypanosoma brucei* TBRGG1, a mitochondrial oligo(U)-binding protein that co-localizes with an in vitro RNA editing activity. *J. Biol. Chem.* **273:** 21825–21833.

Vondrušková, E., van den Burg, J., Zíková, A., Ernst, N.L., Stuart, K., Benne, R., and Lukeš, J. 2005. RNA interference analyses suggest a transcript-specific regulatory role for mitochondrial RNA-binding proteins MRP1 and MRP2 in RNA editing and other RNA processing in *Trypanosoma brucei*. *J. Biol. Chem.* **280:** 2429–2438.

Wang, B.B., Ernst, N.L., Palazzo, S.S., Panigrahi, A.K., Salavati, R., and Stuart, K. 2003. TbMP44 is essential for RNA editing and structural integrity of the editosome in *Trypanosoma brucei*. *Eukaryot. Cell* **2:** 578–587.

Zíková, A., Kopečná, J., Schumacher, M.A., Stuart, K., Trantírek, L., and Lukeš, J. 2008. Structure and function of the native and recombinant mitochondrial MRP1/MRP2 complex from *Trypanosoma brucei*. *Int. J. Parasitol.* doi: 10.1016/j.ijpara.2007.12.009.

Attached Publications

Part I. Trypanosome RNA editing

Hassan Hashimi, Zdeňka Čičová, Lucie Novotná, Yan-Zi Wen and Julius Lukeš (2009). Kinetoplastid guide RNA biogenesis is dependent on subunits of the mitochondrial RNA binding complex 1 and mitochondrial RNA polymerase. *RNA* 15: 588-599.

This paper describes the functional analysis of 4 MRB1 subunits. Two of which are called gRNA associated proteins (GAPs) 1 and 2 because they are essential for the stability of these small non-coding transcripts that are essential for RNA editing. It also demonstrates the mt RNA polymerase transcribes minicircle gRNA genes as well as maxicircle transcripts.

Kinetoplastid guide RNA biogenesis is dependent on subunits of the mitochondrial RNA binding complex 1 and mitochondrial RNA polymerase

HASSAN HASHIMI, ZDEŇKA ČIČOVÁ, LUCIE NOVOTNÁ, YAN-ZI WEN,[1] and JULIUS LUKEŠ

Biology Centre, Institute of Parasitology, Czech Academy of Sciences and Faculty of Natural Sciences, University of South Bohemia, České Budějovice (Budweis), Czech Republic

ABSTRACT

The mitochondrial RNA binding complex 1 (MRB1) is a recently discovered complex of proteins associated with the TbRGG1 and TbRGG2 proteins in *Trypanosoma brucei*. Based on the phenotype caused by down-regulation of these two proteins, it was proposed to play an unspecified role in RNA editing. RNAi silencing of three newly characterized protein subunits, guide RNA associated proteins (GAPs) 1 and 2 as well as a predicted DExD/H-box RNA helicase, show they are essential for cell growth in the procyclic stage. Furthermore, their down-regulation leads to inhibition of editing in only those mRNAs for which minicircle-encoded guide (g) RNAs are required. However, editing remains unaffected when the maxicircle-encoded *cis*-acting gRNA is employed. Interestingly, all three proteins are necessary for the expression of the minicircle-encoded gRNAs. Moreover, down-regulation of a fourth assayed putative MRB1 subunit, Nudix hydrolase, does not appear to destabilize gRNAs, and down-regulation of this protein has a general impact on the stability of maxicircle-encoded RNAs. GAP1 and 2 are also essential for the survival of the bloodstream stage, in which the gRNAs become eliminated upon depletion of either protein. Immunolocalization revealed that GAP1 and 2 are concentrated into discrete spots along the mitochondrion, usually localized in the proximity of the kinetoplast. Finally, we demonstrate that the same mtRNA polymerase known to transcribe the maxicircle mRNAs may also have a role in expression of the minicircle-encoded gRNAs.

Keywords: RNA editing; guide RNA; mitochondrion; trypanosome

INTRODUCTION

Kinetoplastid flagellates, the most studied of which are causative agents of African sleeping sickness, Chagas disease, and leishmaniases in humans, have a strikingly complex mitochondrial (mt) DNA, also termed kinetoplast (k) DNA. It is composed of two types of molecules—maxicircles and minicircles. In the single mitochondrion, maxicircles are present in about a dozen copies and represent the equivalents of classical mtDNA, bearing genes for subunits of respiratory complexes, mitoribosomal RNAs, and one mitoribosomal subunit (for a recent review, see Simpson et al. 2004; Lukeš et al. 2005; Stuart et al. 2005). A unique feature of these flagellates is that the transcripts of some of the maxicircle-encoded genes are post-transcriptionally altered by additions and/or deletions of uridylate (U) residues by a process termed RNA editing (Benne et al. 1986).

The function of kDNA minicircles had remained mysterious for decades. These molecules are concatenated in a network, number in the thousands, and their heterogeneous sequence make up the bulk of the mt genome (Liu et al. 2005). The seminal discovery that they encode genes for small RNA molecules called guide (g) RNAs revealed their biological role as a genetic reservoir complementing the maxicircles (Sturm and Simpson 1990). It is these gRNAs that provide information for multiple and specific insertions and deletions of uridines into pre-edited maxicircle mRNAs. Each gRNA is composed of three regions, differing in their function and content. The 5′ anchor region hybridizes to a complementary sequence of the pre-edited mRNA, while the downstream information region of the RNA molecule provides the template for U insertions/deletions in the

[1]**Present address:** Center for Parasitic Organisms, School of Life Sciences, Sun Yat-Sen (Zhongshan) University, Guangzhou 510275, Peoples Republic of China.

Reprint requests to: Julius Lukeš, Biology Centre, Institute of Parasitology, Czech Academy of Sciences and Faculty of Natural Sciences, Branišovská 31, 37005 České Budějovice, Czech Republic; e-mail: jula@paru.cas.cz; fax: 0042-38-5310388.

Article published online ahead of print. Article and publication date are at http://www.rnajournal.org/cgi/doi/10.1261/rna.1411809.

cognate mRNA via both Watson-Crick and noncanonical G:U base-pairing. The 3′ end of the gRNA is comprised of the post-transcriptionally added oligo(U) tail (Blum and Simpson 1990). While the identity of the RNA components of editing was established almost 20 years ago, the identification of the myriad of proteins involved in mtRNA metabolism remains an ongoing endeavor.

The core RNA editing process has been ascribed to the 20S editosome, a multiprotein complex composed of 20 proteins (Simpson et al. 2004; Lukeš et al. 2005; Stuart et al. 2005). It has been firmly established by in vitro and in vivo experiments that editing is carried out by this complex, which contains all catalytic activities necessary for the cleavage of the pre-mRNA, addition or deletion of the U(s), and ligation of the processed RNA molecules. The 20S editosome appears to be represented by a population of at least three dynamic protein complexes slightly differing in their composition and specific role in this process (Panigrahi et al. 2006; Carnes et al. 2008).

Mitochondrial RNA binding proteins have been a focus of intense research. The MRP1/2 complex is a heterotetrameric structure composed of the MRP1 and MRP2 proteins, with positively charged residues concentrated at one face, to which the gRNAs anneal (Schumacher et al. 2006). Data obtained with the in vivo purified as well as in vitro reconstituted MRP1/2 complexes are consistent with a role in matchmaking the gRNAs with cognate pre-edited mRNAs (Müller et al. 2001; Zíková et al. 2008). RBP16 is another RNA binding protein that appears to have an in vivo role in editing (Pelletier and Read 2003), perhaps via its demonstrated ability to stimulate insertion editing in vitro (Miller et al. 2006).

The initial characterization of TbRGG1, so-called because it possesses the RGG RNA binding motif, suggested the existence of another protein complex with a role in RNA editing (Vanhamme et al. 1998). The down-regulation of TbRGG1 in the procyclic (insect) stage of *Trypanosoma brucei* caused an overall decline of edited mRNAs, but the never-edited transcripts were unaffected (Hashimi et al. 2008). This protein is stably associated with a putative protein complex composed of about 14 different subunits (Hashimi et al. 2008; Panigrahi et al. 2008), provisionally named the mitochondrial RNA binding complex 1 (MRB1 complex). Several of its components have features that point to RNA processing activities associated in an RNA-mediated manner (Hashimi et al. 2008; Panigrahi et al. 2008). Another component of this complex, TbRGG2 (also known as TbRGGm), has affinity for poly(U), and its depletion leads to a dramatic decrease in edited mRNAs (Fisk et al. 2008). Interestingly, a recent report on the newly discovered KPAP1 protein, poly(A) polymerase that polyadenylates maxicircle transcripts, shows that it is associated with a complex of proteins of overlapping composition with the MRB1 complex (Etheridge et al. 2008; Weng et al. 2008).

From these data, the role of the MRB1 complex is not obvious. However, its importance is underscored by the fact that orthologs of its subunits are found in all trypanosomatid genomes sequenced thus far. Here, we attempt to ascertain the function of the MRB1 complex by analysis of four subunits of this complex by RNAi silencing in the procyclic stage. The examined subunits are summarized in Table 1, including a nomenclature introduced in a similar study performed by Weng et al. (2008). Two of these subunits, Tb927.2.3800 and Tb927.7.2570, are paralogs that have no known protein motifs or domains (Hashimi et al. 2008). They will be referred to herein as guide RNA associated proteins (GAP) 1 and 2, respectively, since we provide evidence for their participation in the biogenesis of these molecules. The third subunit, Tb927.4.1500, is predicted to be an ~240-kDa protein with DExD/H-box RNA helicase domains (Hashimi et al. 2008), and is referred to as such in this paper. The last studied subunit, Tb927.11.7290, is annotated as a Nudix hydrolase due to its conservation to other such proteins. Moreover, we show that mtRNA polymerase (mtRNAP), known to transcribe the maxicircle-encoded protein-coding genes (Grams et al. 2002), appears to have a similar role for minicircle-encoded gRNAs.

RESULTS

Subunits of the MRB1 complex are essential for the procyclic stage

Comparison of the growth of noninduced and RNAi-induced GAP1, GAP2, RNA helicase, and Nudix hydrolase cell lines revealed that these proteins are essential for the growth of *T. brucei* procyclics. In these cell lines, growth inhibition is apparent 3 to 4 d after addition of the RNAi-induction agent tetracycline (Fig. 1). In the case of the GAP knockdowns, the cells became increasingly resistant to the dsRNA and recovered around day 12 (Fig. 1A,B), as previously reported in the *T. brucei* system (Pelletier and Read 2003). However, the RNA helicase and Nudix hydrolase knockdowns did not recover their wild-type growth over the 14-d time course. Based on these data, the time points after 3 to 4 d of RNAi induction were

TABLE 1. Nomenclature of examined MRB1 complex proteins

Nomenclature introduced in this study	Nomenclature introduced by Weng et al. (2008)	GeneDB accession number
GAP1	GRBC1	Tb927.2.3800
GAP2	GRBC2	Tb927.7.2570
Nudix hydrolase	MERS1	Tb927.11.7290
RNA helicase	—	Tb927.4.1500

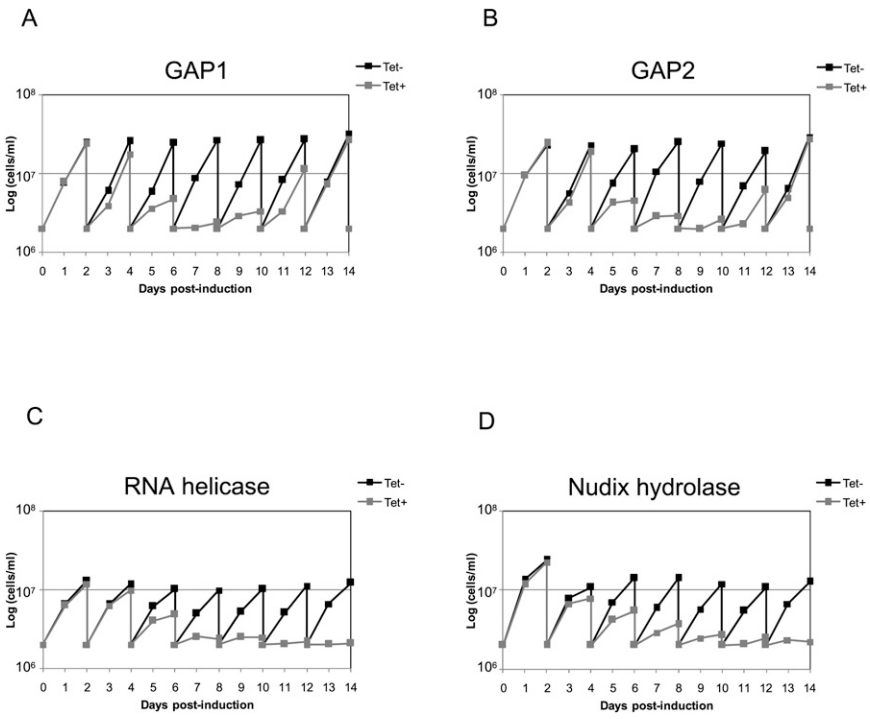

FIGURE 1. Subunits of the MRB1 complex are essential for growth of procyclic stage trypanosomes. Cell densities (cells/mL) that were measured every 24 h are plotted on a logarithmic scale on the *y*-axis over 14 d. Cells were diluted to 2×10^6 cells/mL every 2 d. Cells grown in the presence or absence of the RNAi-induction agent 1 μg/mL tetracycline are indicated by gray (tet+) or black (tet−) lines, respectively. Growth curves of knockdowns of (*A*) GAP1, (*B*) GAP2, (*C*) RNA helicase, and (*D*) Nudix hydrolase are shown.

selected for all subsequent experiments with the knockdowns.

Stability of GAP1 and 2 is mutually dependent

To confirm the mutual association of the GAP proteins as predicted by the mass spectrometry analysis (Hashimi et al. 2008), the mt lysates of cells with a single down-regulated GAP were probed with polyclonal antibodies against both proteins. The specificity of each α-GAP antibody for the appropriate target protein was verified by probing recombinant GAPs overexpressed in *Escherichia coli* (data not shown). Indeed, elimination of the target protein by RNAi was followed by the disappearance of the other GAP protein (Fig. 2A), testifying to their mutual dependence. Furthermore, we checked whether the GAPs are also destabilized upon silencing of either the RNA helicase or Nudix hydrolase. In either of these backgrounds, both proteins persisted (Fig. 2B).

RNAi silencing of MRB1 complex subunits affects maxicircle transcripts

Since TbRGG1 and TbRGG2 from the MRB1 complex were shown to be essential for RNA editing (Fisk et al. 2008; Hashimi et al. 2008), we decided to investigate in detail the effect of down-regulation of the studied subunits in procyclic cells on the stability and editing of mt-encoded mRNAs. The levels of several pre-edited, edited, and never-edited RNAs were measured by a quantitative real-time (q) PCR-based assay, using cDNA from RNAi-induced and noninduced cells. Primers amplifying the pre-edited and edited mt mRNAs of ATPase subunit 6 (A6), cytochrome oxidase subunits 2 and 3 (cox2 and cox3), cytochrome reductase subunit B (cyB), maxicircle unknown reading frame 2 (MURF2), NADH dehydrogenase subunit 7 (ND7), and mitoribosomal protein S12 (RPS12) were used. The levels of two never-edited mRNAs (ND4 and cox1) and, in some cases, the 9S and 12S mitoribosomal RNAs were also measured, as were the mRNAs targeted by RNAi. The obtained values were normalized to the measured levels of the cytoplasmic β-tubulin and 18S rRNA transcripts, since they are unaffected by RNAi. All qPCR reactions with a given primer pair were done in triplicate, and the average and median standard deviations of the measured cycle threshold values are given in Figure 3.

The qPCR assay revealed a virtually identical phenotype for both GAP1 and 2 knockdowns (Fig. 3A,B). With a single but important exception (see below), all examined pre-edited mRNAs (A6, cox3, cyB, MURF2, ND7, and RPS12) were up-regulated between 1.5-fold and up to 20-fold, as compared to RNA from the noninduced cells. Importantly, this up-regulation was correlated to the decrease of the respective edited transcripts. No effect was observed on the never-edited mRNAs (cox1 and ND4) and rRNAs (9S and 12S) (Fig. 3A,B). Significantly, pre-edited and edited cox2 mRNAs were also not affected by RNAi-mediated elimination of either GAP. This transcript is unique in that its single gRNA is contained in its 3′-untranslated region, acting as a guide for insertion editing in *cis* (Golden and Hajduk 2005). The assay also shows that dsRNAs specifically target only the intended GAP RNA (Fig. 3A,B).

This assay revealed a similar effect on maxicircle transcripts in cells with silenced RNA helicase: the combined increase and decrease of pre-edited and edited transcripts, respectively, with the exception of cox2 transcripts (Fig. 3C). However, it should be noted that while never-edited transcripts were unaffected, so were the levels of pre-edited and edited ND7. In contrast, silencing of Nudix hydrolase

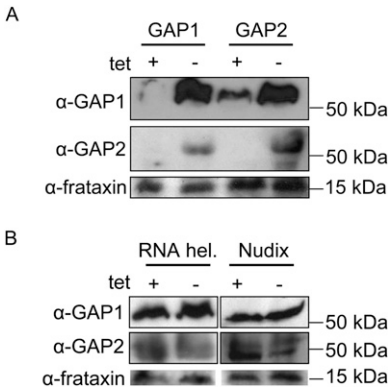

FIGURE 2. The stability of the GAP proteins is dependent on their mutual association. (*A*) Crude mt lysates from 10^8 cells were loaded per lane on a SDS-PAGE gel and transferred onto a PVDF membrane for immunodecoration with either α-GAP1 or α-GAP2 polyclonal antibody, as indicated on the *left*. Antibody against the mitochondrial protein frataxin was used as a loading control. Lysates from cells grown for 3 d in the presence or absence of 1 μg/mL tetracycline are indicated at the *top* ("+" or "−") for either the GAP1 or GAP2 RNAi knockdown. Fifty-kDa and 15-kDa protein markers are indicated on the *right*. (*B*) Samples from the RNA helicase and Nudix hydrolase RNAi knockdown cells grown for 4 d in the presence and absence of 1 μg/mL tetracycline were prepared and labeled as described above.

showed a general effect on almost all maxicircle-encoded transcripts (Fig. 3D). Most never-edited, pre-edited, and edited mRNAs and rRNAs are down-regulated upon depletion of this protein. This phenotype represents a highly significant departure from the otherwise relatively uniform phenotype of the other examined knockdowns.

The MRB1 complex has a role in gRNA expression

The disruption of RNA editing, observed in cells in which either GAP1, GAP2, or RNA helicase is down-regulated, appears to be independent of the core editing activities of the 20S editosome since cox2 mRNA editing proceeds normally. Another component of this process is the small 30–60-nt gRNAs. To see whether these primary transcripts are affected, they were capped with guanylyltransferase and [α-^{32}P]GTP and visualized on a high-resolution denaturing acrylamide gel. An upper band corresponding to a cytoplasmic RNA is used as a loading control. Indeed, repression of GAP1 and 2 as well as RNA helicase in the procyclic cells leads to a decrease of the steady-state level of gRNAs (Fig. 4A–C). In contrast, neither the abundance nor the 3′-oligo(U) tail of gRNAs is affected upon depletion of Nudix hydrolase (Fig. 4D).

GAP1 assembly into macromolecular complexes is affected in the knockdowns for subunits of the MRB1 complex

To further study the sedimentation properties of GAP1 in cells with down-regulated MRB1 subunits, lysates from hypotonically isolated mitochondria from noninduced and RNAi-induced cultures were loaded onto 10% to 30% glycerol gradients. Gradient fractions were first probed with monoclonal antibodies against three of the core editosome proteins, KREPA2, REL1, and KREPA3 (Panigrahi et al. 2001), used as markers for 20S. As an additional control, the fractions were immunodecorated with an antibody binding Tbmp45, a protein previously labeled REAP1, as a marker for 40S sedimentation (Madison-Antenucci et al. 1998; Fisk et al. 2008). A representative immunoblot performed on GAP1-induced and noninduced samples is in agreement with previous studies, as all proteins recognized by these antibodies localized to fractions 13 thru 17, the peak of 20S editosome sedimentation (Fig. 5A, top panel). Furthermore, it has been demonstrated that this complex is not disrupted when substrate RNAs are absent since it is held together by protein–protein interactions (Domingo et al. 2003; Fisk et al. 2008; Hashimi et al. 2008). The Tbmp45 protein was found to be localized in the lowest fractions, as expected (Fig. 5A, bottom panel). The other gradients depicted in Figure 5B were also validated in this fashion (data not shown).

In the separated mt lysates from the noninduced cell lines, GAP1 is distributed throughout the gradient, although with some variation in the pattern as revealed by Western analysis (Figs. 5B; see, also, Fig. 7B, below). A broad distribution of GAP2 has been previously reported (Panigrahi et al. 2008). As expected, GAP1 is reduced upon interference of expression of either GAP subunit (Fig. 5B). A dramatic shift of the *S*-value of GAP1 is observed in the RNA helicase-silenced cells, in which it is concentrated in the lighter fractions (Fig. 5B). Such a striking difference in GAP1 sedimentation is not observed in the induced and noninduced Nudix hydrolase knockdowns (Fig. 5B). In the hydrolase-silenced sample, a reduction of GAP1 immunopositive signal in the dense fractions is apparent (Fig. 5B).

mtRNA polymerase appears to transcribe minicircles

The participation of a multiprotein complex in the transcription of minicircle gRNA genes, independent of mtRNAP, has been hypothesized (Grams et al. 2002). In the inducible mtRNAP knockdowns (kindly provided by P.T. Englund, Johns Hopkins University), we have first verified the RNAi effect by Northern analysis, as antibodies against the *T. brucei* mtRNAP are not available. As shown in Figure 6A, the mtRNAP mRNA is undetectable 3 d after tetracycline induction, the time point at which growth inhibition is first observed (Grams et al. 2002). Next, we have hybridized blots containing mtRNA with a probe against *cox1* mRNA. In agreement with the previous study (Grams et al. 2002), this never-edited transcript is undetectable 3 d after RNAi is triggered (Fig. 6B). To test whether this polymerase is responsible for the transcription of minicircles, the initial step in expression of gRNA

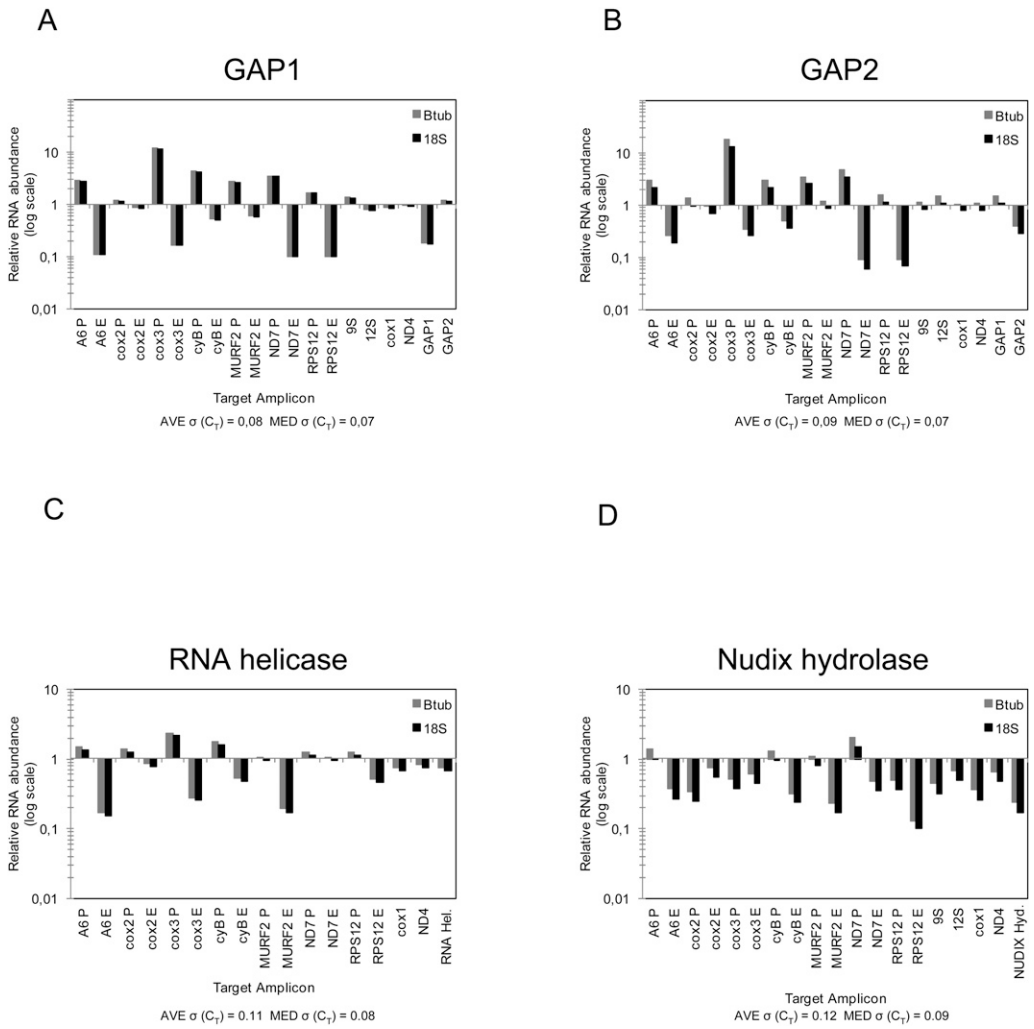

FIGURE 3. Effects of RNAi silencing of the MRB1 complex subunits on maxicircle transcripts. Quantitative real-time PCR analysis of pre-edited, edited, and never-edited mRNAs and rRNAs was performed on knockdowns of (*A*) GAP1, (*B*) GAP2, (*C*) RNA helicase, and (*D*) Nudix hydrolase. The reaction for each amplicon was done in triplicate on cDNA generated from cells grown in the presence or absence of the RNAi-inducer tetracycline. The relative abundance of each of the examined RNAs upon the synthesis of interfering dsRNA was plotted on a logarithmic scale: 1 represents the wild-type levels, while a value above or below this number signifies an increase or decrease of a given RNA, respectively. These values were normalized to the cytosolic transcripts β-tubulin or 18S rRNA, whose levels are not affected by RNAi. The average [AVE $\sigma(C_T)$] and median standard deviations [MED $\sigma(C_T)$] of the measured cycle threshold (C_T) values for all the reactions performed for each knockdown are indicated under each bar graph. The following pre-edited (P) and edited (E) RNAs were assayed: ATPase subunit 6 (A6), cytochrome oxidase subunits 2 (cox2) and 3 (cox3), cytochrome reductase subunit b (cyB), maxicircle unknown reading frame 2 (MURF2), NADH dehydrogenase subunit 7 (ND7), and ribosomal protein S12 (RPS12). The following never-edited RNAs were assayed: 9S RNA, 12S RNA, cox1, and ND4. The appropriate cytoplasmic mRNA targeted by RNAi were assayed for each knockdown and are indicated on the *right*.

molecules, we have performed the guanylyltransferase labeling assay on total RNA isolated from noninduced and induced knockdowns for mtRNAP. Clearly, the gRNA population is decreased in cells lacking the enzyme (Fig. 6C).

MRB1 complex is disrupted upon down-regulation of mtRNA polymerase

The similarity in the effect on gRNA expression of the knockdowns for mtRNAP and MRB1 subunits GAP1, GAP2, and RNA helicase inspired us to investigate the integrity of this complex in the absence of the polymerase. For this purpose, total lysates prepared from noninduced cells as well as from cells in which mtRNAP was targeted by RNAi for 3 d were loaded on glycerol gradients, and the obtained fractions were screened with the α-GAP1 antibody. The quality of the gradient was tested by Western blot analysis, using antibodies against the editosome KREL1 and Tbmp45 (Fig. 7A). GAP1 is broadly distributed in the noninduced cells in fractions 7–17 (Fig. 7B). Indeed, an apparent shift toward the lighter density fractions (with a marked peak in fractions 7 and 9) of the gradient in the

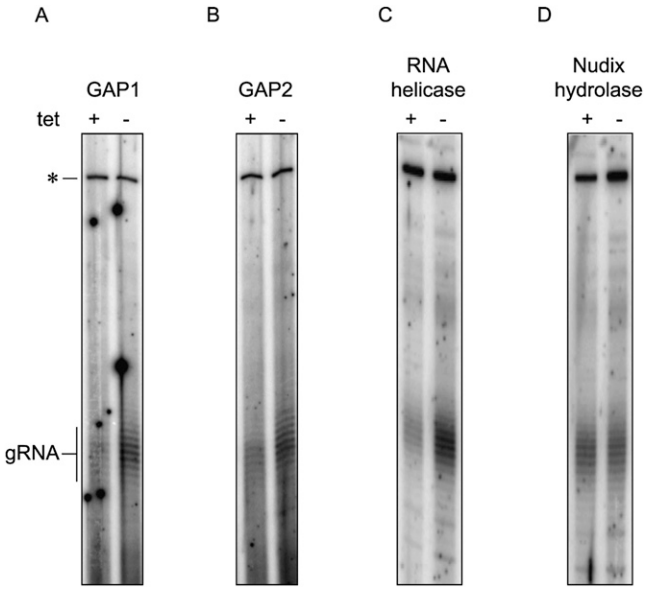

FIGURE 4. Effects of RNAi silencing of the MRB1 complex subunits on minicircle transcripts. The total population of minicircle-encoded gRNAs were labeled in knockdowns of (*A*) GAP1, (*B*) GAP2, (*C*) RNA helicase, and (*D*) Nudix hydrolase. Labeling reactions were performed with guanylyltransferase, [α-^{32}P]GTP and either (*A*,*B*) 2.5 μg or (*C*,*D*) 5 μg of RNA. The gRNAs, appearing as a ladder mainly because of their heterogeneous 3′-oligo(U) tails, are indicated on the *left*. The *top* band marked with the "*" is a cytosolic RNA that is also labeled in this reaction and is used as a loading control.

GAP1 distribution occurs when mtRNAP is down-regulated. This result indicates that in the absence of mtRNAP, the MRB1 complex is disrupted in the same manner as in the absence of RNA helicase (Fig. 5B).

GAP1 and 2 and gRNAs are essential for the bloodstream stage

Since RNA editing is essential also in the bloodstream stage (Schnaufer et al. 2001), we decided to test whether the absence of GAP1 and 2, and consequently gRNA expression, are also lethal in this stage. The constructs containing the same GAP1 or 2 gene fragments as those used for RNAi in the procyclics were transfected into the bloodstream stage. Western blot analysis revealed that in the GAP1 and 2 knockdowns, the targeted protein was undetectable after 2 d of induction (Fig. 8A). Moreover, as in the procyclic stage, the ablation of GAP1 leads to the reduction of GAP2, and vice versa, testifying to their mutual dependence.

Down-regulation of either GAP1 or 2 results in growth inhibition, indicating that these proteins are also essential in this life cycle stage. When compared with the noninduced cells, the growth of the induced clones decreases at day 3 and stops at day 4 (Fig. 8B). Both induced cell lines recovered from the effect of RNAi at day 7 post-induction. Labeling of total RNA collected at days 2 and 3 post-induction with guanylyltransferase revealed that steady-state levels of gRNAs are decreased when either GAP1 or 2 is silenced in the bloodstream stage (Fig. 8C). This result indicates that the function of these proteins is conserved between the two major life stages of *T. brucei,* and that gRNAs are also required for survival of the infective blood forms.

GAP1 and GAP2 have a novel localization within the mitochondrion

Previous data provided evidence for localization of the MRB1 complex in the mitochondrion (Hashimi et al. 2008; Panigrahi et al. 2008). We therefore have resorted to indirect immunofluorescence experiments to determine

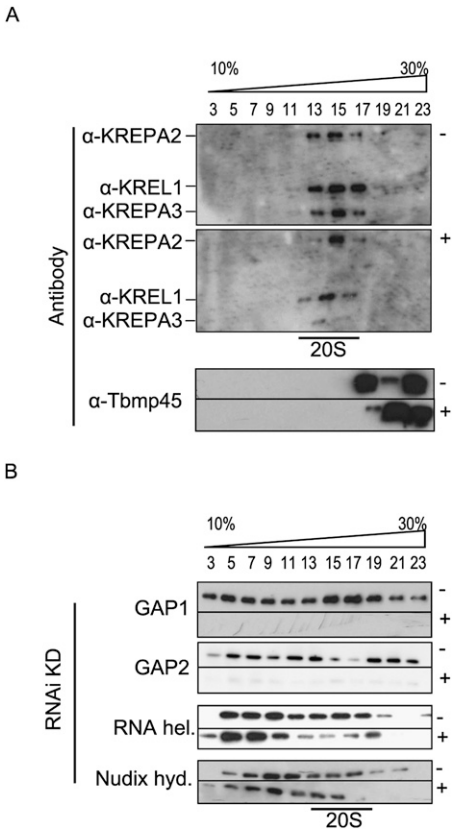

FIGURE 5. GAP1 assembly into macromolecular complexes is affected in the knockdowns for subunits of the MRB1 complex. Cleared lysates from hypotonically isolated mitochondria are separated by sedimentation in glycerol gradients. Odd fractions from the gradients were run on SDS-PAGE gels and transferred onto PVDF membranes. (*A*) All gradients were verified by immunodecoration with monoclonal antibodies against editosome subunits (*top* panel) KREPA2, KREL1, and KREPA3, as well as (*bottom* panel) Tbmp45. A representative blot for GAP1 samples is shown here in which the appropriate antibody signals are indicated on the *left*. The presence (+) or absence (−) of tetracycline is specified on the *right*. (*B*) α-GAP1 antibody was used to probe the glycerol gradient fractions from knockdown cell lines grown in the absence (−) or presence (+) of tetracycline as indicated on the *right*. The GAP1, GAP2, RNA helicase, and Nudix hydrolase cell lines are indicated on the *left*.

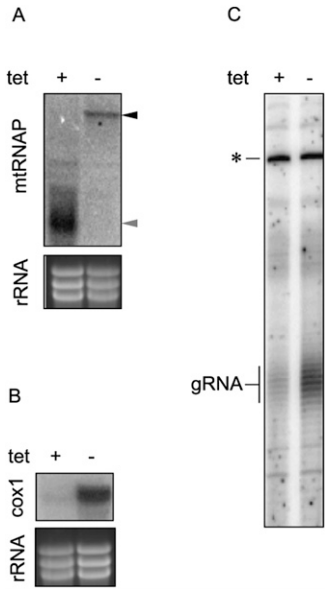

FIGURE 6. Evidence that mtRNAP transcribes kDNA minicircles. (*A*) Effect of RNAi induction on the mtRNAP mRNA was followed by Northern blot analysis. Its levels were analyzed by blotting 10 μg of total RNA extracted from noninduced cells (−) and cells 3 d after RNAi induction (+) with a probe hybridizing to the gene fragment used for generation of dsRNA. The position of (black arrowhead) the targeted mRNA and (gray arrowhead) the inducibly synthesized dsRNA are indicated. To visualize characteristic rRNA bands, used here as a loading control, the gel was stained with ethidium bromide. (*B*) The same RNA was hybridized with a labeled probe for never-edited mRNA encoding cytochrome oxidase subunit 1 (cox1). (*C*) Guanylyltransferase labeling of gRNAs using same RNA samples as used in *A* and *B* are performed and marked as in Figure 4. Five micrograms of total RNA was used per lane.

where these proteins are located in the organelle. Using the α-GAP1 antibody, we show that in the procyclic cells, the protein is confined to several discrete foci, distributed throughout the reticulated mitochondrion (Fig. 9A, top row), often in the proximity of the kDNA disk. Specificity of the used antibody was confirmed by its failure to detect target protein in RNAi-silenced GAP1 cells (Fig. 9A, bottom row). The polyclonal α-GAP2 antibodies proved to be less useful in the immunolocalization studies.

To corroborate this unexpected observation, cells were transfected with a construct for tetracycline-inducible expression of either GAP1 or 2 proteins bearing an HA_3-epitope tag. Immunocytochemistry and DAPI staining performed on cells grown in the presence of the antibiotic for 2 d confirmed that both epitope-tagged proteins are confined to multiple discrete punctuate loci unevenly distributed throughout the organelle (Fig. 9B). As observed with the α-GAP1 antibody, an immunopositive signal is also often observed near the kinetoplast.

Although attachment of the HA_3 tag to the C terminus of the protein should not interfere with the mt import signal located at the N terminus, possible extra-mitochondrial localization had to be ruled out. Therefore, the 29-13 procyclics containing the HA_3-tagged GAP1 or 2 were fractionated by extraction with increasing concentrations of digitonin. Indeed, probing the obtained cytosolic and mt fractions, as well as the total cell lysate, with antibodies against the HA_3 tag showed that both tagged GAP proteins are properly imported into the organelle (Fig. 9C).

DISCUSSION

Since the discovery of RNA editing in 1986 (Benne et al. 1986), considerable efforts have been directed at understanding the molecular mechanisms underlying what was initially an enigmatic biological process. A major breakthrough was the discovery of gRNAs, which revealed that the information for U insertion/deletion events resides in these molecules, and a function of the thousands of minicircles is to encode them (Blum and Simpson 1990). The establishment of an in vitro editing assay led to the validation that proteins provided the enzymatic machinery for RNA editing (Seiwert et al. 1996). The isolation and characterization of the 20S editosome have dissected how a multi-protein complex can orchestrate the catalytic steps required for the maturation of most mtRNAs in trypanosomes (Simpson et al. 2004; Lukeš et al. 2005; Stuart et al. 2005).

Studies focusing on identifying proteins involved in other aspects of mtRNA metabolism have uncovered the MRB1 complex in three different instances (Etheridge et al. 2008; Hashimi et al. 2008; Panigrahi et al. 2008). Although the subunit composition in these studies is not identical, the degree of overlap is quite significant. The MRB1 complex contains up to 14 proteins, some of which possess known motifs and domains involved in RNA processing or protein interactions (Hashimi et al. 2008; Panigrahi et al. 2008). Two

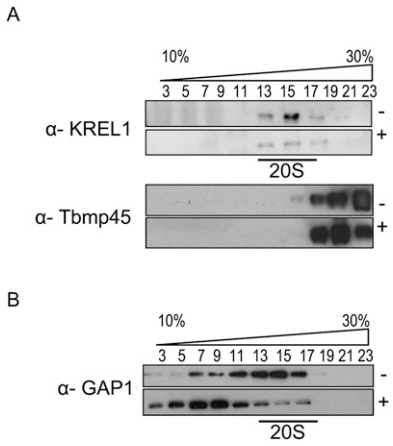

FIGURE 7. GAP1 assembly into large macromolecular complexes is reduced in cells with RNAi-silenced mtRNAP. Western blot analysis of glycerol gradients was performed and labeled as described in Figure 5. (*A*) Western blots of fractions were verified using the (*top* panel) α-KREL1 or (*bottom* panel) α-Tbmp45 monoclonal antibodies or (*B*) probed using the α-GAP1 polyclonal antibody.

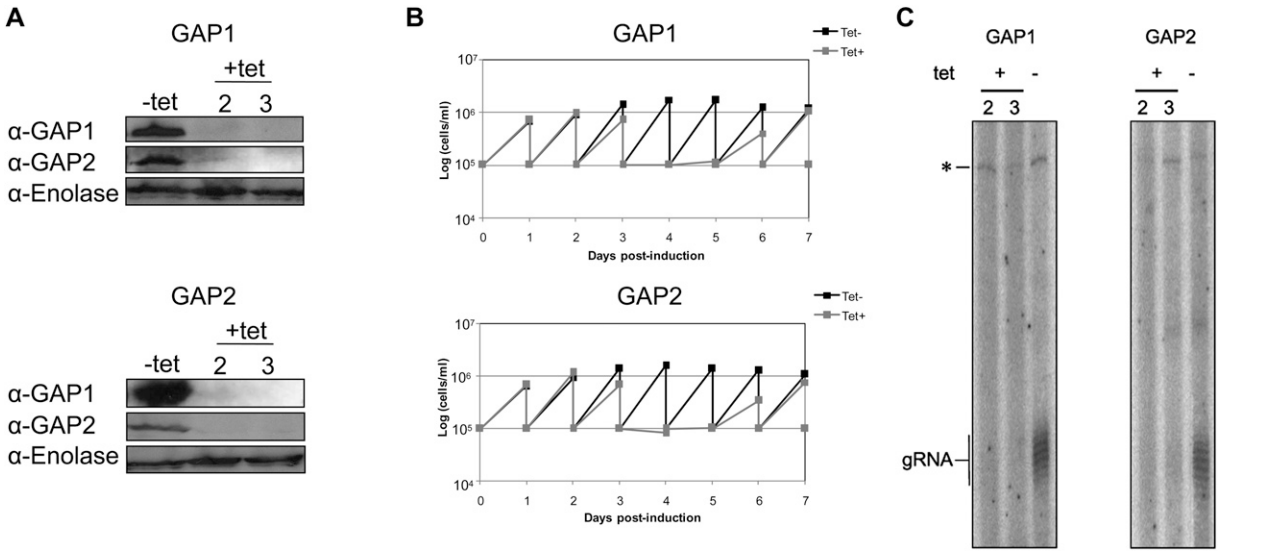

FIGURE 8. GAP1 and GAP2 are essential for gRNA biogenesis in the bloodstream stage. (*A*) Whole cell lysates from 1.5×10^7 cells were immunoblotted with either the α-GAP1 or α-GAP2 antibody for each of the (*top*) GAP1 and (*middle*) GAP2 cell lines. Cells grown in the absence (−) or presence (+) of 1 μg/mL tetracycline are indicated, as well as the days post-induction in the latter samples. (*Bottom*) An antibody decorating the cytosolic enolase was used as a loading control. All antibodies are indicated on the *left*. (*B*) RNAi silencing of the GAP proteins in the bloodstream stage results in growth inhibition. Growth curves over 7 d are shown for the (*top*) GAP1 and (*bottom*) GAP2 knockdown cell lines and are labeled as in Figure 1. Cells were diluted every 24 h to a density of 10^5 cells/mL. (*C*) Guide RNA levels are diminished in the GAP-silenced bloodstream stage. The guanylyltransferase assay was performed on 5 μg of total RNA as described in Figure 4. The gels shown for (*left*) GAP1 and (*right*) GAP2 are also labeled as in Figure 4, with the days post-induction by tetracycline indicated below the "+."

components of the MRB1 complex have been already characterized to some extent, namely, TbRGG1 and TbRGG2, the latter of which was suggested to be a transiently associated editing factor required for the processivity of RNA editing (Fisk et al. 2008). RNAi silencing of both proteins leads to a down-regulation of edited transcripts, suggesting some kind of a role in RNA editing (Fisk et al. 2008; Hashimi et al. 2008). However, these data do not adequately address a possible role of the MRB1 complex.

Here we addressed the question of function by examining the phenotype resulting from RNAi silencing of four subunits of this complex: GAP1, GAP2, RNA helicase, and Nudix hydrolase. We have shown that a subset of the MRB1 complex, GAP1, GAP2 and RNA helicase, is involved in gRNA biogenesis. This notion is supported by the absence of gRNAs when any of these proteins is depleted as a consequence of RNAi. Furthermore, editing of the maxicircle-encoded RNAs is subsequently reduced, with the notable exception of cox2. This transcript contains its own *cis*-gRNA in the 3′-untranslated region, thus circumventing the requirement for minicircle-encoded gRNAs acting *in trans* (Golden and Hajduk 2005). The independence of *cox2* mRNA editing, in the *trans*-acting gRNA-deficient background, on these MRB1 proteins clearly indicates that they are not involved in core RNA editing activities.

The question is specifically what role do these proteins play in the expression of gRNAs? It was hypothesized that a multiprotein complex may be involved in the transcription of minicircle-encoded genes, independent of the canonical mtRNAP involved in maxicircle transcription (Grams et al. 2002). Here we provide evidence that mtRNAP is the most likely candidate for the transcription of gRNA genes as well as maxicircle genes. This observation indicates that the MRB1 complex may have a distinct role in gRNA synthesis, since mtRNAP was not demonstrated to be associated with this complex in any of the published reports (Etheridge et al. 2008; Hashimi et al. 2008; Panigrahi et al. 2008). Furthermore, the possibility that the mtRNAP transcribes both minicircle-encoded gRNAs and maxicircle-encoded mRNAs is surprising given the requirement of the multiple DNA ligases and DNA polymerases for kDNA maintenance and replication (Klingbeil et al. 2002; Sinha et al. 2004; Liu et al. 2005).

The GAPs and RNA helicase do appear to be involved in some aspect of gRNA processing and/or stability. The most established processing event in the biogenesis of a gRNA is its post-transcriptional addition of the 3′-oligo(U) tail (Blum and Simpson 1990) by the KRET1 enzyme (Aphasizhev et al. 2003). It was also proposed that functional gRNAs are spliced from the 5′ ends of polycistronic minicircle transcripts (Grams et al. 2000). However, a corresponding accumulation of these large precursor RNAs was not detected in the GAP knockdowns (data not shown), suggesting that if this processing step does exist, it is not mediated by these proteins.

Another proposed feature of gRNA is the presence of two intramolecular hairpin structures with single-stranded ends

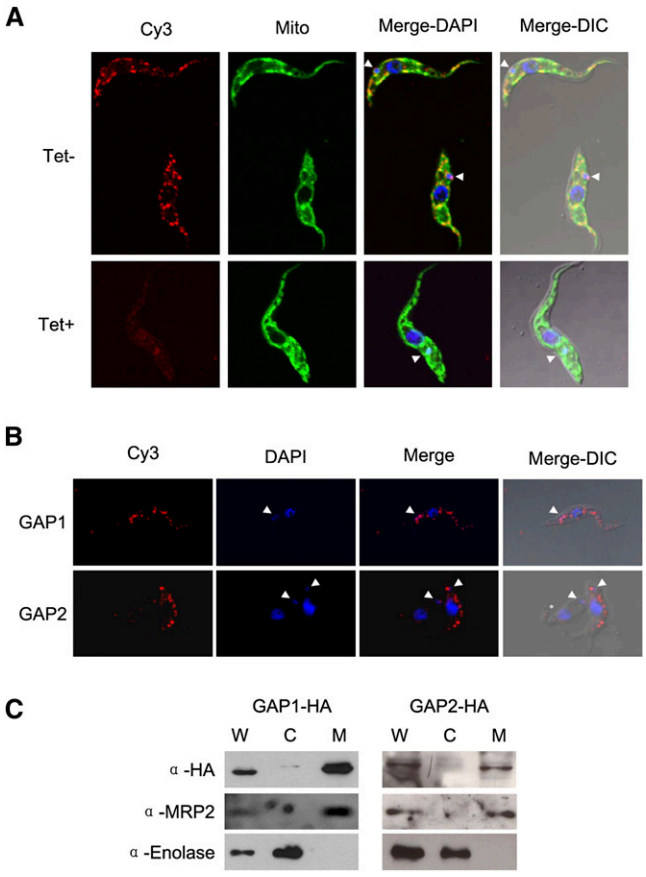

FIGURE 9. The GAP proteins are localized in punctuate loci along the reticulated mitochondrion of procyclic *T. brucei*. (*A*) Immunolocalization using rabbit α-GAP1 antibody in the (*top* row, labeled Tet−) GAP1 noninduced and (*bottom* row, Tet+) RNAi-induced cells. Signal from cy3-conjugated α-rabbit antibody (Cy3), MitoTracker Green FM (Mito), the two images merged with DAPI staining of nucleus, and kDNA (Merge-DAPI) and a composite image with a differential interference contrast image (Merge-DIC) are indicated along the *top*. (White arrowheads) Position of kDNA. (*B*) Immunolocalization of the HA_3-tagged versions (*top* row) GAP1 and (*bottom* row) GAP2, which is immunodecorated with rabbit polyclonal antibody against the epitope. Signal from cy3-conjugated α-rabbit antibody (Cy3), DAPI staining of nucleus and kDNA (DAPI), a merged image of the two (Merge), and a composite image with a differential interference contrast image (Merge-DIC) are indicated along the *top*. (White arrowheads) Position of kDNA. (*C*) Immunoblot analysis of the localization of overexpressed HA_3-tagged (*left*) GAP1 and (*right*) GAP2 proteins. (W) Whole cell lysates and digitonin extracted (C) cytosolic and (M) mitochondrial fractions of these cell lines grown for 2 d in the presence of 1 μg/mL tetracycline. Antibody against the HA_3-tag was used as well as those against the MRP2 and enolase proteins, serving as mitochondrial and cytosolic markers, respectively. Ten micrograms of protein of each digitonin fraction was loaded per lane.

(Schmid et al. 1995; Hermann et al. 1997). The presence of a predicted DExD/H-box RNA helicase in the gRNA-expression component of the MRB1 complex raises the possibility that these proteins may play a role in facilitating the formation of this secondary structure in these small transcripts. Perhaps these thermodynamically unfavorable loops (Schmid et al. 1995) are not formed in the absence of the GAPs or RNA helicase, leading to the apparent destabilization of the gRNAs. However, this speculative model is tempered by the involvement of the DExD/H box RNA helicases in diverse roles in RNA metabolism not restricted just to processing, such as transcription regulation and RNA turnover (for review, see Fuller-Pace 2006).

We show that the GAP proteins are essential for the bloodstream stage, where they appear to have the same role in gRNA processing/stability as they do in the procyclic stage. Although an active RNA metabolism has been established as a requirement for survival of this infective stage (Schnaufer et al. 2001; Fisk et al. 2008), to our knowledge, this result is the first to indicate that the gRNA biogenesis is required in this part of the life cycle as well. This result is significant in light of the existence of naturally occurring dyskinetoplastic and akinetoplastic trypanosomes (Lai et al. 2008), which must circumvent the lack of the requisite repertoire of gRNAs for the expression of normally essential mt-encoded genes, such as the ATPase subunit 6 (Schnaufer et al. 2005). Apparently, in both stages, all kDNA is transcribed, and any regulation occurs at the post-transcriptional level, a situation strikingly similar to what is known for the expression of nuclear genes in trypanosomes and other kinetoplastid flagellates (Haile and Papadopoulou 2007).

We also establish here that the group of proteins that we designate to the MRB1 complex do not share an overall function. While GAP1, GAP2, and RNA helicase are involved in gRNA expression, TbRGG1 and 2 clearly are not (Fisk et al. 2008; Hashimi et al. 2008). Furthermore, we show here that the Nudix hydrolase is also not involved in gRNA expression, since these molecules persist in a background deficient of this protein. The family of Nudix hydrolases has a diverse array of functions in the cell, such as decapping mRNAs (Cohen et al. 2005) and clearance of oxidized nucleosides (for review, see McClennan 2006). Designation of a specific role of this hydrolase is still not feasible based on the observed destabilization of most of the maxicircle transcripts upon its depletion. However, these results counter those of Weng et al. (2008) indicating a specific decrease in edited RNAs.

The array of phenotypes affecting different aspects of mtRNA metabolism upon down-regulation of various putative subunits of the MRB1 complex, along with the assortment of associating proteins, is quite striking (Etheridge et al. 2008; Fisk et al. 2008; Hashimi et al. 2008; Panigrahi et al. 2008; Weng et al. 2008). These observations raise the question whether it represents a single bona fide complex, held together by protein–protein interactions, or a collection of monomers and/or smaller complexes connected by substrate RNAs. Indeed, the latter situation has been proposed (Weng et al. 2008), and incorporation of both TbRGG proteins into large complex(es) appears to be RNase sensitive, while the 20S editosome complex remains intact (Fisk et al. 2008; Hashimi et al. 2008). Interestingly, RNAi silencing

of either RNA helicase or mtRNAP clearly disrupts the GAP1 assembly into macromolecular complexes. This result may reflect a genuine interaction of these proteins with GAP1 or be a result of the consequent decrease of RNA molecules via which these proteins seem to associate.

We conclude by discussing the unique localization of the GAP proteins to discrete points along the reticulated mitochondrion, often proximal to the kDNA network. To our knowledge, such a pattern has not been reported for other proteins involved in mt nucleic acid metabolism (Vanhamme et al. 1998; Klingbeil et al. 2002; Liu et al. 2005; Etheridge et al. 2008). Panigrahi et al. (2008) have previously reported a more uniform distribution of different subunits of the MRB1 complex throughout the mitochondrion. However, given the aforementioned diversity of RNAi-silencing phenotypes for the MRB1 complex proteins, it is possible that they may also exhibit diverse yet overlapping sites in the organelle as well. Nevertheless, as the GAP proteins have a demonstrated role in gRNA biogenesis, we imagine these loci may represent centers where gRNAs are processed and distributed for their participation in RNA editing as catalyzed by the 20S editosome.

MATERIALS AND METHODS

Generation of RNAi-knockdown and transgenic cell lines

Primers for generation of 400–600-base pair (bp) gene fragments for cloning into the p2T7-177 vector were designed using the RNAit online tool available on the TrypanoFAN website (http://trypanofan.path.cam.ac.uk/software/RNAit.html). The following primer pairs (with restriction site underlined and indicated in parentheses) were used: GAP1 gene, GAP1-F (5′-CTCCTCGAGCCTTTCAGC-3′) (XhoI) and GAP1-R (5′-GGCAAGCTTCTGCGAATGTAG-3′) (HindIII), amplified a 533-bp-long fragment; GAP2 gene, GAP2-F (5′-CGAGGATCCACAACGGCATT-3′) (BamHI) and GAP2-R (5′-CATCATCAGCAAGCTTTATGATG-3′) (HindIII), amplified a 580-bp-long fragment; Hel1-F (5′-GGATCCGTAGGAACTGGCAGAGACGC-3′) (BamHI) and He1-R (5′-CTCGAGGCTACTGATTGCACGCAAAA-3′) (XhoI), amplified a 453-bp-long fragment; and Hyd1-F (5′-GGATCCCGTAAGGTGTCAGGACCGAT-3′) (BamHI) and Hyd1-R (5′-CTCGAGTCTACGGTAATGCCCGTTTC-3′) (XhoI) amplified a 467-bp-long fragment. All amplified fragments were cloned into the p2T7-177 vector creating constructs, which were upon linearization electroporated into the procyclic *T. brucei* strain 29-13, and the clones were obtained by limiting dilution at 27°C as described elsewhere (Vondrušková et al. 2005). Synthesis of dsRNA was induced by the addition of 1 μg/mL tetracycline to six clonal cell lines for each knockdown. For further experiments, clones were selected based on the tightness of tetracycline expression of dsRNA and the robust elimination of target mRNA, as determined by Northern blot analysis using the appropriate gene fragment as a probe. The procyclic knockdown generated by cloning a fragment of the mtRNAP gene in the pZJM vector (Grams et al. 2002) was kindly provided by P.T. Englund (Johns Hopkins University, Baltimore).

Linearized p2T7-177 vectors containing the GAP1 and 2 gene fragments were electroporated using the Amaxa Nucleofector II electroporator into the 427 bloodstream *T. brucei* strain. About 3×10^7 cells of exponentially growing culture were used for transfection, following the protocol of Vassella et al. (2001) with minor modifications. Transfectants were selected with 1.25 μg/mL phleomycin and cloned by limiting dilution. RNAi was triggered and assessed in six clonal cell lines by the addition of 1 μg/mL tetracycline using the same strategy as that described for the procyclics.

The full-length open reading frames of the GAP1 and 2 genes were cloned into the pJH54 plasmid containing the C-terminal HA_3-tag (a gift from Christine Clayton, University of Heidelberg). The PCR-amplified insert was digested with either HindIII and XbaI (GAP1) or just XbaI (GAP2). The orientation of the latter insert was verified by diagnostic restriction digests and sequencing. The utilized PCR primers were (with restriction site underlined): GAP1-HA-F (5′-AAGCTTATGCTGCGCGCGCGCCTG-3′) and GAP1-HA-R (5′-TCTAGAGTATGCCGAAACGGCAGT-3′); GAP2-HA-F (5′-TCTAGAATGCTTCGCTTATTGCGG-3′) and GAP2-HA-R (5′-TCTAGACAACTTCGCCTCACAGCC-3′).

Generation of antibodies

Affinity-purified polyclonal rabbit antibodies against GAPs 1 and 2 were raised against synthetic oligopetides by GenScript. The GAP1 synthetic oligopeptide (EYGDWGAEPGFEDRC) corresponds to the 137–150-amino-acid region of the *T. brucei* protein, while the GAP2 oligopeptide (TIKRSKDQLHVDLDC) is derived from the 297–310 amino acid region.

Western and Northern blot analyses

For Western blot analysis, cell lysates corresponding to 5×10^6 procyclics/lane or 1×10^7 bloodstreams/lane were separated on a 12% SDS-PAGE gel. The polyclonal rabbit antibodies against the MRP2 protein (Vondrušková et al. 2005), enolase (provided by P.A.M. Michels), and frataxin (Long et al. 2008) were used at 1:2000, 1:150,000, and 1:1000 dilutions, respectively. The antibodies against GAP1 and GAP2 were used at the respective dilutions 1:2000 and 1:500. Monoclonal antibodies against KREPA2, KREL1, KREPA3, and Tbmp45 were used as described elsewhere (Madison-Antenucci et al. 1998; Panigrahi et al. 2001). Commercial antibodies against the HA_3 tag were used according to the manufacturer's protocol (Sigma).

For Northern blot analysis, ~10 μg per lane of total RNA from procyclic or bloodstream cells was loaded on a 1% formaldehyde agarose gel, blotted, and cross-linked as published elsewhere (Vondrušková et al. 2005). After pre-hybridization in NaPi solution (0.25 M Na_2HPO_4 and 0.25 M NaH_2PO_4 at pH 7.2, 1 mM EDTA, 7% SDS) for 2 h at 55°C, hybridization was performed overnight in the same solution at 55°C. A wash in 2× SSC + 0.1% SDS for 20 min at room temperature was followed by two washes in 0.2× SSC + 0.1% SDS for 20 min each at 55°C.

Growth curves

Following Northern blot analysis of several clones for each knockdown, one clone was selected for further experiments. Growth curves were obtained over a period of 14 d in the presence or absence of the RNAi-induction agent tetracycline for transfected

procyclics or 8 d for transfected bloodstreams. Cell density was measured every 24 h using the Beckman Z2 Cell Counter.

Cell fractionation, glycerol gradients, digitonin fractionation

For separation on glycerol gradients, mitochondria from 10^9 procyclic cells were purified following the protocol detailed in Hashimi et al. (2008). Digitonin fractionation and glycerol gradient sedimentation were performed as described elsewhere (Smíd et al. 2006).

Quantitative real-time PCR and guanylyltransferase labeling

RNA for quantitative real-time (q) PCR and guanylyltransferase labeling were collected and DNased as described in Hashimi et al. (2008). After checking the integrity by running an aliquot on a formaldehyde gel, 4.5 μg of RNA was used as a template for cDNA synthesis for subsequent qPCR analysis (for details, see Hashimi et al. 2008). A parallel cDNA synthesis reaction was set up with the same amount of RNA but without the reverse transcriptase to serve as a control for effective DNase treatment. Primers for maxicircle mRNAs, as well as the housekeeping β-tubulin and 18S rRNA transcripts serving as reference genes, are listed in Carnes et al. (2005) and Hashimi et al. (2008). New primer pairs amplifying cDNAs corresponding to transcripts of the subunits of the MRB1 complex are GAP1-qPCR-Fw (5′-AACGTATTGCG GATGCTTAC-3′) and Rv (5′-GAACCACACGCTCACAACAG-3′); GAP2-qPCR-Fw (5′-CGGCTCATATTCCTGCCAATG-3′) and Rv (5′-CGAAGTCCTCAGCAACCAACC-3′); Hel-qPCR-Fw (5′-ATC GCGTTAGGTGAAGCAGT-3′) and Rv (5′-AAATGGGGATCCCT AAGGTG-3′); and Hyd-qPCR-Fw (5′-ATTTTTCACCCTTGCACGT C-3′) and Rv (5′-TCGATGGATTTGTTGTCACC-3′). Relative abundances of maxicircle transcripts were calculated using the Pfaffl method (Pfaffl 2001).

Guanylyltransferase reactions were performed on 2.5–5 μg of total RNA to cap gRNAs with [α-^{32}P]GTP as previously described (Hashimi et al. 2008). The recombinant enzyme was either purchased from Ambion or provided by Ruslan Aphasizhev (University of California, Irvine). The reactions were separated on a denaturing 12% acrylamide–8 M urea gel.

Immunolocalization

In order to visualize mitochondria, 5×10^6 to 1×10^7 cells were incubated in SDM-79 media supplemented with 1 mM of MitoTracker Green FM (Molecular Probes) for 20 min at 27°C. Cells were subsequently washed 3× in phosphate-buffered saline (PBS) and then spread on slides, fixed, and permeabilized as described in Klingbeil et al. (2002). All subsequent steps were carried out in a humid chamber. The slides were first blocked for 1 h at room temperature with 10% goat serum diluted in PBS. Afterward, the primary rabbit antibody was applied to the slides at the appropriate dilution in 10% goat serum + PBS for 90 min. After washing 3× for 10 min each in PBS, the slides were incubated with secondary goat α-rabbit antibody conjugated to the cy3 fluorophore (Jackson Immunoresearch) at a 1:800 dilution for 1 h. The slides were then washed 3× for 10 min each in PBS and mounted in Vectashield containing DAPI. The α-GAP1 antibody was used at a dilution of 1:100, and the α-HA_3 antibody was used according to the manufacturer's protocol (Sigma). Samples probed with the latter antibody were not pre-treated with MitoTracker. Cells were examined on the Olympus Fluoview FV1000 confocal microscope using the accompanying Fluoview v1.7 software. A composite of the Z-stack of the fluorescent images was rendered using the ImageJ software and processed using Adobe Photoshop v6.0.

ACKNOWLEDGMENTS

We thank Lucie Hanzálková and Julius Lukeš IV for help with some experiments, and Paul T. Englund (Johns Hopkins University), Paul A.M. Michels (Université catholique de Louvain), Ken Stuart (Seattle Biomedical Research Institute), Stephen Hajduk (University of Georgia), Christine Clayton (Heidelberg University), and Ruslan Aphasizhev (University of California at Irvine) for sharing the mtRNA polymerase knockdowns, the α-enolase antibody, antibodies against 20S editosome subunits, α-Tbmp45 antibody, pJH54 plasmid, and recombinant guanylyltransferase, respectively. We also thank Aswini Panigrahi and Alena Zíková (Seattle Biomedical Research Institute) for critical reading of the manuscript. This work was supported by the Grant Agency of the Czech Republic 204/09/1667, Grant Agency of the Czech Academy of Sciences A500960705, and the Ministry of Education of the Czech Republic (LC07032 and 2B06129) to J.L. and the Ph.D. student grant 524/03/H133 to H.H.

Received October 8, 2008; accepted January 9, 2009.

REFERENCES

Aphasizhev, R., Aphasizheva, I., and Simpson, L. 2003. A tale of two TUTases. *Proc. Natl. Acad. Sci.* **100:** 10617–10622.

Benne, R., van den Burg, J., Brakenhoff, J.P., Sloof, P., Van Boom, J.H., and Tromp, M.C. 1986. Major transcript of the frameshifted coxII gene from trypanosome mitochondria contains four nucleotides that are not encoded in the DNA. *Cell* **46:** 819–826.

Blum, B. and Simpson, L. 1990. Guide RNAs in kinetoplastid mitochondria have a nonencoded 3′ oligo(U) tail involved in recognition of the preedited region. *Cell* **62:** 391–397.

Blum, B., Bakalara, N., and Simpson, L. 1990. A model for RNA editing in kinetoplastid mitochondria: "Guide" RNA molecules transcribed from maxicircle DNA provide the edited information. *Cell* **60:** 189–198.

Carnes, J., Trotter, J.R., Ernst, N.L., Steinberg, A.G., and Stuart, K. 2005. An essential RNase III insertion editing endonuclease in *Trypanosoma brucei*. *Proc. Natl. Acad. Sci.* **102:** 16614–16619.

Carnes, J., Trotter, J.R., Peltan, A., Fleck, M., and Stuart, K. 2008. RNA editing in *Trypanosoma brucei* requires three different editosomes. *Mol. Cell. Biol.* **28:** 122–130.

Cohen, L.S., Mikhli, C., Jiao, X., Kiledjian, M., Kunkel, G., and Davis, R.E. 2005. Dcp2 decaps $m^{2,2,7}$ GpppN-capped RNAs, and its activity is sequence and context dependent. *Mol. Cell. Biol.* **25:** 8779–8791.

Domingo, G.J., Palazzo, S.S., Wang, B., Panicucci, B., Salavati, R., and Stuart, K.D. 2003. Dyskinetoplastic *Trypanosoma brucei* contains functional editing complexes. *Eukaryot. Cell* **2:** 569–577.

Etheridge, R.D., Aphasizheva, I., Gershon, P.D., and Aphasizhev, R. 2008. 3′ adenylation determines mRNA abundance and monitors completion of RNA editing in *T. brucei* mitochondria. *EMBO J.* **27:** 1596–1608.

Fisk, J.C., Ammerman, M.L., Presnyak, V., and Read, L.K. 2008. TbRGG2, an essential RNA editing accessory factor in two

Trypanosoma brucei life cycle stages. *J. Biol. Chem.* **283:** 23016–23025.

Fuller-Pace, F.V. 2006. DExD/H box RNA helicases: Multifunctional proteins with important roles in transcriptional regulation. *Nucleic Acids Res.* **34:** 4206–4215.

Golden, D.E. and Hajduk, S.L. 2005. The 3′-untranslated region of cytochrome oxidase II mRNA functions in RNA editing of African trypanosomes exclusively as a *cis* guide RNA. *RNA* **11:** 29–37.

Grams, J., McManus, M.T., and Hajduk, S.L. 2000. Processing of polycistronic guide RNAs is associated with RNA editing complexes in *Trypanosoma brucei*. *EMBO J.* **19:** 5525–5532.

Grams, J., Morris, J.C., Drew, M.E., Wang, Z.F., Englund, P.T., and Hajduk, S.L. 2002. A trypanosome mitochondrial RNA polymerase is required for transcription and replication. *J. Biol. Chem.* **277:** 16952–16959.

Haile, S. and Papadopoulou, B. 2007. Developmental regulation of gene expression in trypanosomatid parasitic protozoa. *Curr. Opin. Microbiol.* **10:** 569–577.

Hashimi, H., Zíková, A., Panigrahi, A.K., Stuart, K.D., and Lukeš, J. 2008. TbRGG1, a component of a novel multi-protein complex involved in kinetoplastid RNA editing. *RNA* **14:** 970–980.

Hermann, T., Schmid, B., Heumann, H., and Göringer, H.U. 1997. A three-dimensional working model for a guide RNA from *Trypanosoma brucei*. *Nucleic Acids Res.* **25:** 2311–2318.

Klingbeil, M.M., Motyka, S.A., and Englund, P.T. 2002. Multiple mitochondrial DNA polymerases in *Trypanosoma brucei*. *Mol. Cell* **10:** 175–186.

Lai, D.-H., Hashimi, H., Lun, Z.-R., Ayala, F.J., and Lukeš, J. 2008. Adaptations of *Trypanosoma brucei* to gradual loss of kinetoplast DNA: *Trypanosoma equiperdum* and *Trypanosoma evansi* are petite mutants of *T. brucei*. *Proc. Natl. Acad. Sci.* **105:** 1999–2004.

Liu, B.Y., Liu, Y.N., Motyka, S.A., Agbo, E.E.C., and Englund, P.T. 2005. Fellowship of the rings: The replication of kinetoplast DNA. *Trends Parasitol.* **21:** 363–369.

Long, S., Jirků, M., Mach, J., Ginger, M.L., Sutak, R., Richardson, D., Tachezy, J., and Lukeš, J. 2008. Ancestral roles of eukaryotic frataxin: mitochondrial frataxin function and heterologous expression of hydrogenosomal *Trichomonas* homologues in trypanosomes. *Mol. Microbiol.* **69:** 94–109.

Lukeš, J., Hashimi, H., and Zíková, A. 2005. Unexplained complexity of the mitochondrial genome and transcriptome in kinetoplastid flagellates. *Curr. Genet.* **48:** 277–299.

Madison-Antenucci, S., Sabatini, R.S., Pollard, V.W., and Hajduk, S.L. 1998. Kinetoplastid RNA-editing-associated protein 1 (REAP-1): A novel editing complex protein with repetitive domains. *EMBO J.* **21:** 6368–6376.

McClennan, A.G. 2006. The Nudix hydrolase superfamily. *Cell. Mol. Life Sci.* **63:** 123–143.

Miller, M.M., Halbig, K., Cruz-Reyes, J., and Read, L.K. 2006. RBP16 stimulates trypanosome RNA editing in vitro at an early step in the editing reaction. *RNA* **12:** 1292–1303.

Müller, U.F., Lambert, L., and Göringer, H.U. 2001. Annealing of RNA editing substrates facilitated by guide RNA-binding protein gBP21. *EMBO J.* **20:** 1394–1404.

Panigrahi, A.K., Schnaufer, A., Carmean, N., Igo Jr., R.P., Gygi, S.P., Ernst, N.L., Palazzo, S.S., Weston, D.S., Aebersold, R., Salavati, R., et al. 2001. Four related proteins of the *Trypanosoma brucei* RNA editing complex. *Mol. Cell. Biol.* **21:** 6833–6840.

Panigrahi, A.K., Ernst, N.L., Domingo, G.J., Fleck, M., Salavati, R., and Start, K.D. 2006. Compositionally and functionally distinct editosomes in *Trypanosoma brucei*. *RNA* **12:** 1038–1049.

Panigrahi, A.K., Zíková, A., Halley, R.A., Acestor, N., Ogata, Y., Myler, P.J., and Stuart, K. 2008. Mitochondrial complexes in *Trypanosoma brucei*: A novel complex and a unique oxidoreductase complex. *Mol. Cell. Proteomics* **7:** 534–545.

Pelletier, M. and Read, L.K. 2003. RBP16 is a multifunctional gene regulatory protein involved in editing and stabilization of specific mitochondrial mRNAs in *Trypanosoma brucei*. *RNA* **9:** 457–468.

Pfaffl, M.W. 2001. A new mathematical model for relative quantification in real-time RT-PCR. *Nucleic Acids Res.* **29:** e45. doi: 10.1093/nar/29.9.e45.

Schmid, B., Riley, G.R., Stuart, K., and Göringer, H.U. 1995. The secondary structure of guide RNA molecules from *Trypanosoma brucei*. *Nucleic Acids Res.* **23:** 3093–3102.

Schnaufer, A., Panigrahi, A.K., Panicucci, B., Igo Jr., R.P., Wirtz, E., Salavati, R., and Stuart, K. 2001. An RNA ligase essential for RNA editing and survival of the bloodstream form of *Trypanosoma brucei*. *Science* **291:** 2159–2162.

Schnaufer, A., Clark-Walker, G.D., Steinberg, A.G., and Stuart, K. 2005. The F_1-ATP synthase complex in bloodstream stage trypanosomes has an unusual and essential function. *EMBO J.* **24:** 4029–4040.

Schumacher, M.A., Karamooz, E., Zíková, A., Trantírek, L., and Lukeš, J. 2006. Crystal structures of *T. brucei* MRP1/MRP2 guide-RNA-binding complex reveals RNA matchmaking mechanism. *Cell* **126:** 701–711.

Seiwert, S.D., Heidmann, S., and Stuart, K. 1996. Direct visualization of uridylate deletion in vitro suggests a mechanism for kinetoplastid RNA editing. *Cell* **84:** 831–841.

Simpson, L., Aphasizhev, R., Gao, G., and Kang, X. 2004. Mitochondrial proteins and complexes in *Leishmania* and *Trypanosoma* involved in U insertion/deletion RNA editing. *RNA* **10:** 159–170.

Sinha, K.M., Hines, J.C., Downey, N., and Ray, D.S. 2004. Mitochondrial DNA ligase in *Crithidia fasciculata*. *Proc. Natl. Acad. Sci.* **101:** 4361–4366.

Smíd, O., Horáková, E., Vilímová, V., Hrdý, I., Cammack, R., Horváth, A., Lukeš, J., and Tachezy, J. 2006. Knockdowns of mitochondrial iron-sulfur cluster assembly proteins IscS and IscU down-regulate the active mitochondrion of procyclic *Trypanosoma brucei*. *J. Biol. Chem.* **281:** 28679–28686.

Stuart, K.D., Schnaufer, A., Ernst, N.L., and Panigrahi, A.K. 2005. Complex management: RNA editing in trypanosomes. *Trends Biochem. Sci.* **30:** 97–105.

Sturm, N. and Simpson, L. 1990. Kinetoplast DNA minicircles encode guide RNAs for editing of cytochrome oxidase subunit III mRNA. *Cell* **61:** 879–884.

Vanhamme, L., Peréz-Morga, D., Marechal, C., Speijer, D., Lambert, L., Geuskens, M., Alexandre, S., Ismaili, N., Göringer, U., Benne, R., et al. 1998. *Trypanosoma brucei* TBRGG1, a mitochondrial oligo(U)-binding protein that co-localizes with an in vitro RNA editing activity. *J. Biol. Chem.* **273:** 21825–21833.

Vassella, E., Kramer, R., Turner, C.M.R., Wankell, M., Modes, C., Van den Bogaard, M., and Boshart, M. 2001. Deletion of a novel protein kinase with PX and FYVE-related domains increases the rate of differentiation of *Trypanosoma brucei*. *Mol. Microbiol.* **41:** 33–46.

Vondrušková, E., van den Burg, J., Zíková, A., Ernst, N.L., Stuart, K., Benne, R., and Lukeš, J. 2005. RNA interference analyses suggest a transcript-specific regulatory role for MRP1 and MRP2 in RNA editing and other RNA processing in *Trypanosoma brucei*. *J. Biol. Chem.* **280:** 2429–2438.

Weng, J., Aphasizheva, I., Etheridge, R.D., Huang, L., Wang, X., Falick, A.M., and Aphasizhev, R. 2008. Guide RNA-binding complex from mitochondria of trypanosomatids. *Mol. Cell* **32:** 1–12.

Zíková, A., Kopečná, J., Schumacher, M.A., Stuart, K.D., Trantírek, L., and Lukeš, J. 2008. Structure and function of the native and recombinant mitochondrial MRP1/MRP2 complex from *Trypanosoma brucei*. *Int. J. Parasitol.* **38:** 901–912.

Attached Publications

Part I. Trypanosome RNA editing

Michelle L. Ammerman[†], Hassan Hashimi[†], Lucie Novotná, Zdeňka Čičová, Sarah M. McEvoy, Julius Lukeš, and Laurie K. Read (2011). MRB3010 is a core component of the MRB1 complex that facilitates an early step of the kinetoplastid RNA editing process. *RNA* 17: 865-877.

This paper helps to further define the architecture of MRB1 and shows that what will eventually be demonstrated to be a core MRB1 subunit is involved early steps of RNA editing. I am co-first author of this publication.

[†]Co-first author

MRB3010 is a core component of the MRB1 complex that facilitates an early step of the kinetoplastid RNA editing process

MICHELLE L. AMMERMAN,[1,3] HASSAN HASHIMI,[2,3] LUCIE NOVOTNÁ,[2] ZDEŇKA ČIČOVÁ,[2,4] SARAH M. MCEVOY,[1] JULIUS LUKEŠ,[2] and LAURIE K. READ[1]

[1]Department of Microbiology and Immunology, School of Medicine, State University of New York at Buffalo, Buffalo, New York 14214, USA
[2]Biology Centre, Institute of Parasitology, Czech Academy of Sciences and Faculty of Sciences, University of South Bohemia, České Budějovice (Budweis), Czech Republic

ABSTRACT

Gene expression in the mitochondria of the kinetoplastid parasite *Trypanosoma brucei* is regulated primarily post-transcriptionally at the stages of RNA processing, editing, and turnover. The mitochondrial RNA-binding complex 1 (MRB1) is a recently identified multiprotein complex containing components with distinct functions during different aspects of RNA metabolism, such as guide RNA (gRNA) and mRNA turnover, precursor transcript processing, and RNA editing. In this study we examined the function of the MRB1 protein, Tb927.5.3010, which we term MRB3010. We show that MRB3010 is essential for growth of both procyclic form and bloodstream form life-cycle stages of *T. brucei*. Down-regulation of MRB3010 by RNAi leads to a dramatic inhibition of RNA editing, yet its depletion does not impact total gRNA levels. Rather, it appears to affect the editing process at an early stage, as indicated by the accumulation of pre-edited and small partially edited RNAs. MRB3010 is present in large (>20S) complexes and exhibits both RNA-dependent and RNA-independent interactions with other MRB1 complex proteins. Comparison of proteins isolated with MRB3010 tagged at its endogenous locus to those reported from other MRB1 complex purifications strongly suggests the presence of an MRB1 "core" complex containing five to six proteins, including MRB3010. Together, these data further our understanding of the function and composition of the imprecisely defined MRB1 complex.

Keywords: RNA editing; trypanosome; MRB1 complex; mitochondria; kinetoplast

INTRODUCTION

Trypanosoma brucei, the causative agent of African sleeping sickness in humans and nagana in animals, is a member of the clade Kinetoplastida within the phylum Euglenozoa. Members of this order are so named for their kinetoplast (k) DNA, the mitochondrial genome that is a dense catenated network of several dozen DNA maxicircles and thousands of minicircles. The maxicircles encode the traditional mitochondrial genes including ribosomal RNAs and proteins that are components of the respiratory complexes. Twelve of the 18 protein-coding genes present in the kDNA of *T. brucei* require post-transcriptional editing by uridine insertion and deletion to generate translatable mRNAs. Editing is directed by small (~60 nt) *trans*-acting guide RNAs (gRNAs) that are encoded primarily on the minicircles (Blum and Simpson 1990; Sturm and Simpson 1990). The editing reaction is catalyzed by related 20S editosomes or RECCs (RNA editing core complexes), which include the required endonucleolytic, exonucleolytic, nucleoside transferase, and ligase activities (Rusché et al. 1997; Simpson et al. 2004; Lukeš et al. 2005; Stuart et al. 2005; Carnes et al. 2008).

Additional proteins that are not stably associated with the 20S editosomes act as direct or indirect editing accessory factors by affecting the editing process itself, substrate production, and RNA turnover. For example, the heterotetrameric MRP complex (MRP1/2) exhibits RNA annealing activity and is thought to affect editing by facilitating hybridization of some gRNAs to their cognate pre-mRNAs (Aphasizhev et al. 2003; Schumacher et al. 2006). RBP16, another RNA editing accessory factor, has

[3]These authors contributed equally to this work.
[4]**Present address:** University of Munich (LMU), Institute of Genetics, Martinsried, Germany.

Reprint requests to: Laurie K. Read, Department of Microbiology and Immunology, School of Medicine, State University of New York at Buffalo, Buffalo, NY 14214, USA; e-mail: lread@buffalo.edu; fax: (716) 829-2158.

Article published online ahead of print. Article and publication date are at http://www.rnajournal.org/cgi/doi/10.1261/rna.2446311.

also been shown to facilitate gRNA/pre-mRNA annealing in vitro (Ammerman et al. 2008). Individual knockdown of MRP1/2 and RBP16 demonstrates a role for these proteins in the editing of cytochrome b (CYb) and the stability of certain never-edited transcripts (Pelletier and Read 2003; Vondrušková et al. 2005). Recently, knockdown of MRP1/2 and RBP16 concurrently showed that they contained distinct and overlapping roles in editing and stability that are transcript and life-cycle stage dependent (Fisk et al. 2009a). Another protein, REAP-1, was believed to recruit pre-edited RNAs to the editosome (Madison-Antenucci and Hajduk 2001), but a more recent study of REAP-1 knockout cells suggests a role in RNA stability instead of editing (Hans et al. 2007).

Studies originally performed by Panigrahi et al. (2008) using monoclonal antibodies against mitochondrial proteins, and later confirmed by tandem affinity purification chromatography and mass spectrometry, identified a complex containing numerous proteins with RNA-binding and macromolecular interaction motifs. The complex was named the mitochondrial RNA-binding complex 1 (MRB1). Other groups have also identified this complex (a.k.a. guide RNA-binding complex [GRBC]) (Weng et al. 2008); however, both common and distinct components were reported in the MRB1 complex preparations from different laboratories (Hashimi et al. 2008; Panigrahi et al. 2008; Weng et al. 2008; Hernandez et al. 2010). Additionally, some of the MRB1 complex components are also associated with the mitochondrial polyadenylation (kPAP1) complex (Weng et al. 2008). Several proteins associated with MRB1 have been characterized by RNAi-mediated knockdowns and found to impact diverse aspects of mitochondrial RNA metabolism. GAP1 and GAP2 (a.k.a. GRBC2 and GRBC1, or Tb927.2.3800 and Tb927.7.2570, respectively) as well as the REH2 RNP complex (Tb927.4.1500) bind gRNAs and are necessary for the expression and/or stability of the minicircle-encoded gRNAs (Weng et al. 2008; Hashimi et al. 2009; Hernandez et al. 2010). TbRGG2 (a.k.a. TbRGGm and Tb927.10.10830) is a protein with two RNA-binding domains (RRM and RGG), which is required for editing of extensively (pan) edited transcripts (Fisk et al. 2008; Acestor et al. 2009). Moreover, recent evidence suggests that TbRGG2 facilitates editing initiation and 3′–5′ progression of editing by affecting gRNA utilization (Ammerman et al. 2010). The RNA-binding protein, TbRGG1, functions in stabilizing edited RNAs and/or editing efficiency, and has an RNA-dependent interaction with the MRB1 complex (Vanhamme et al. 1998; Hashimi et al. 2008). NUDIX hydrolase (a.k.a. MERS1 or Tb11.01.7290) is required for the stability of edited and potentially pre-edited mRNAs (Weng et al. 2008; Hashimi et al. 2009). Two other MRB1 complex proteins, a C2H2 Zn finger motif containing protein Tb927.6.1680 and Tb11.02.5390 also affect edited mRNA levels (Acestor et al. 2009), but the roles of these proteins and many other MRB1 complex components have yet to be elucidated. Although all of these MRB1 proteins are essential for growth in the insect midgut stage of the parasite (procyclic form; PF) (Fisk et al. 2008; Hashimi et al. 2008, 2009; Weng et al. 2008; Acestor et al. 2009), they appear to have varied affects on mitochondrial RNA metabolism, and may not all be genuine components of all MRB1 complexes. Here, the term MRB1 complex is loosely defined by copurification, and we note that the roles of RNA-dependent interactions, subcomplex associations, and life-cycle stage-dependent interactions in defining this complex have to be addressed.

In all reported MRB1 complex purifications, five proteins are consistently present: GAP1, GAP2, Tb11.02.5390, Tb11.01.8620, and Tb927.5.3010 (Hashimi et al. 2008; Panigrahi et al. 2008; Weng et al. 2008; Hernandez et al. 2010). In this study, we utilize RNAi and in vivo tagging and coimmunoprecipitation to examine the function of one of these common MRB1 proteins, Tb927.5.3010, which we term MRB3010. We show here that MRB3010 is essential for growth of both PF and pathogenic bloodstream form (BF) life-cycle stages of *T. brucei*. Downregulation of MRB3010 leads to a dramatic inhibition of RNA editing with minimally edited RNAs being somewhat less affected than pan-edited RNAs. MRB3010 depletion does not impact total gRNA levels, but appears to affect editing at early stages of the process. Finally, we identify both RNA-dependent and RNA-independent interactions between MRB3010 and other MRB1 complex proteins. These studies increase our understanding of the function and composition of the imprecisely defined MRB1 complex.

RESULTS

MRB3010 is essential for growth of PF and BF life-cycle stage *T. brucei*

MRB3010 is a common component of all reported MRB1 complex purifications (Hashimi et al. 2008; Panigrahi et al. 2008; Weng et al. 2008; Hernandez et al. 2010). The protein is highly conserved in trypanosomatids with homologs in *Trypanosoma cruzi* (Tc00.1047053510173.40), *Trypanosoma vivax* (TvY486_0502380), *Trypanosoma congolense* (TcIL3000.5.3280), *Leishmania braziliensis* (LbrM08_V2.0940), *Leishmania infantum* (LinJ08_V3.1080), and *Leishmania major* (LmjF08.1170) (Weng et al. 2008). The 57.7-kDa predicted MRB3010 protein exhibits at least 85% amino acid identity to these orthologs over the majority of its primary structure; however, the *Trypanosoma* proteins are distinguished by a 7-kDa extension at their N-termini, which is absent in *Leishmania* spp. (Supplemental Fig. 1). MRB3010 contains a ribosomal S2 signature domain, although the significance of this motif is unclear as the protein was not identified in purified mitochondrial ribosomes (Maslov et al. 2006; Zíková et al. 2008).

Several components of the MRB1 complex are required for optimal growth of PF (Fisk et al. 2008; Hashimi et al. 2008, 2009; Weng et al. 2008; Acestor et al. 2009) and BF *T. brucei* (Fisk et al. 2008; Hashimi et al. 2009). To determine whether MRB3010 is similarly important for growth of either life-cycle stage, we generated PF and BF cell lines expressing tetracycline (tet) regulatable RNAi against MRB3010. The online tool, RNAit, was used to determine an MRB3010 gene fragment that is suitable for RNAi and prevents off-target effects (Redmond et al. 2003). MRB3010 RNA levels in PF were reduced to ~25% of wild-type levels upon tet induction, whereas levels in BF were reduced to ~70% of those in uninduced cells as measured by qRT–PCR (Fig. 1). Because no antibodies are available for detection of MRB3010, we were unable to directly monitor changes in protein levels. Nevertheless, a dramatic growth defect was observed in both life-cycle stages upon MRB3010 depletion. In both PF and BF, cell growth began to slow between days 3 and 4 post-induction and ceased by days 8 and 5 in PF and BF, respectively. Thus, MRB3010 is essential for growth of both PF and BF *T. brucei*.

MRB3010 depletion impacts RNA editing

We next asked whether MRB3010 depletion affects the abundance of edited mRNAs, and if so, whether specific classes are altered. RNA from PF and BF cells was isolated after 4 d of tet-induction for use in quantitative PCR. In PF, we measured the levels of three pan-edited and three minimally edited mRNAs (Fig. 2A). Edited versions of pan-edited A6, RPS12, and COIII mRNAs were significantly decreased to levels 15%–35% of those of uninduced cells. The corresponding pre-edited versions were all increased in induced cells. Editing of minimally edited CYb, MURF2, and COII mRNAs was also affected, albeit more modestly, with edited RNA levels in induced cells between 50% and 70% of those in uninduced cells, and the corresponding pre-edited RNAs increased. We also analyzed the abundance of 9S and 12S mitochondrial rRNAs, which do not undergo editing, as well as four never-edited mRNAs. All never-edited RNAs were unchanged upon MRB3010 depletion, with the exception of a small decrease in COI RNA. To ask whether MRB3010 plays a role in precursor RNA processing we measured the levels of three precursors. Levels of 9S/ND8 and A6/CYb precursors were unchanged, while the RPS12/ND5 precursor was increased slightly. qRT–PCR analysis of a smaller panel of RNAs in BF MRB3010 RNAi cells revealed a similar pattern, with all three pan-edited RNAs examined exhibiting a dramatic decrease upon MRB3010 depletion. The edited versions of the minimally edited transcripts COII and MURF2 were also decreased, although to a lesser extent than were the pan-edited RNAs. Never-edited transcripts ND4 and COI were essentially unaffected. To determine whether the inhibition of editing observed upon MRB3010 depletion is a result of destabilization of the total gRNA population, as in knockdowns of the GAP1/2 and REH2 proteins (Weng et al. 2008; Hashimi et al. 2009), we assessed the levels of total gRNAs in PF MRB3010-depleted cells by guanylyltransferase labeling (Fig. 2C). We observed no change in the levels of gRNAs between uninduced and induced cells, demonstrating that MRB3010 has a function distinct from that of GAP1/2 or REH2. Together, these results indicate that MRB3010 plays a role in the RNA editing process. The accumulation of pre-edited mRNAs suggests that this role manifests, at least in part, at the initial stages of the process.

Having shown that MRB3010 depletion affects RNA editing, we wanted to further explore which steps in this process are compromised. To this end, we performed gene-specific RT–PCRs using primers to the constant 5′ and 3′ never-edited regions of pan-edited RNAs, which flank the large edited regions. This approach allows us to visualize the overall 3′–5′ progression of editing within the population of a given mRNA, because increased size of the PCR products correlates with increased U insertion (Schnaufer et al. 2001; Ammerman et al. 2010). We compared the defect in RNA editing in MRB3010-depleted cells with that in cells with ablated TbRGG2, in which both initiation and 3′–5′ progression of editing are compromised (Ammerman et al. 2010). When we analyzed the pan-edited COIII

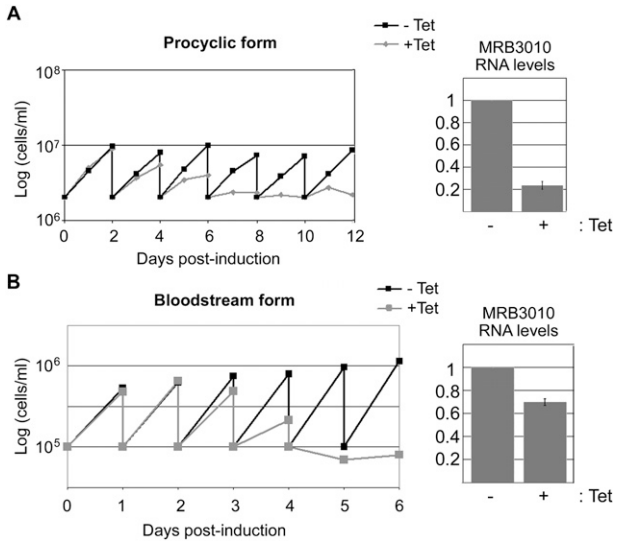

FIGURE 1. MRB3010 is essential for growth in both PF and BF life-cycle stages. (*A*) Growth was measured in PF MRB3010 RNAi cells that were uninduced (black) or induced with 1 μg/mL tet (gray). Cell growth, plotted here on a logarithmic scale, was measured every 24 h. Cells were diluted every 2 d to a starting concentration of 2×10^6 cells/mL. The bar graph on the *right* indicates the relative MRB3010 RNA levels in the tet-induced vs. uninduced cells as determined by quantitative RT–PCR. (*B*) Growth was measured in BF MRB3010 RNAi cells that were uninduced (black) or induced with 1 μg/mL tet (gray). Cell growth was measured every 24 h, followed by dilution of cells to a starting concentration of 1×10^5 cells/mL. The bar graph on the *right* indicates the relative MRB3010 RNA levels in the tet-induced vs. uninduced cells as determined by quantitative RT–PCR.

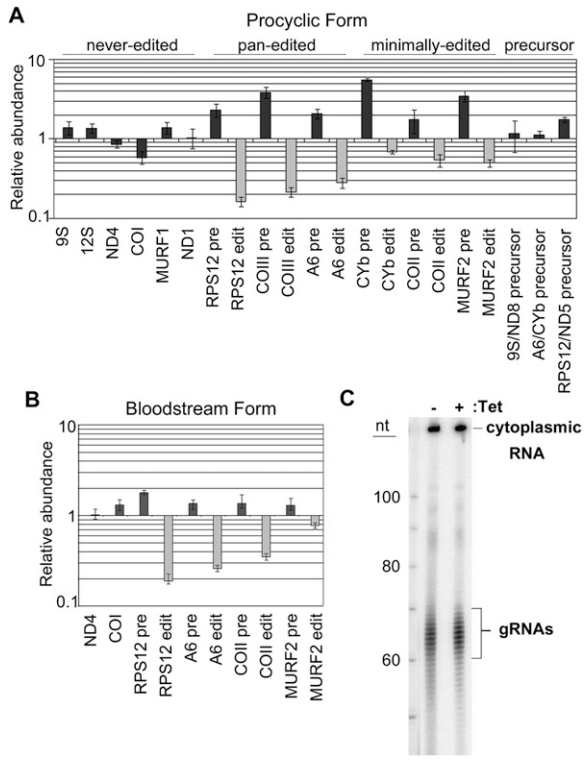

FIGURE 2. Effect of MRB3010 depletion on the abundance of mitochondrial RNAs. (*A*) Quantitative RT–PCR analysis of mitochondrial maxicircle transcripts from PF MRB3010 RNAi cells 4 d post-induction. Abundance of a given RNA in induced cells relative to that in the uninduced cells is plotted on a log scale. RNA levels were standardized against 18S rRNA, and the numbers represent the mean and standard deviation of at least six determinations. (*B*) Quantitative RT–PCR analysis of mitochondrial maxicircle transcripts from BF MRB3010 RNAi cells 4 d post-induction. RNA levels were standardized against 18S rRNA and numbers represent the mean and standard deviation of at least three determinations. (*C*) Guanylyl transferase labeling of the total gRNA population from the PF MRB3010 RNAi cells 4 d post-induction. Fifteen micrograms of total RNA were labeled with [α-^{32}P]GTP using guanylyl transferase and resolved on a denaturing gel. RNA input was standardized against the quantity of a labeled cytoplasmic RNA (indicated).

mRNA population by gene-specific RT–PCR, we found that depletion of MRB3010 results in accumulation of both pre-edited and small partially edited RNAs (Fig. 3A). It was striking that many of the partially edited mRNAs accumulating upon MRB3010 depletion cells are smaller than those in TbRGG2-depleted cells. We next analyzed the pan-edited A6 transcript. To confirm that the observed differential effect on editing between the MRB3010 and TbRGG2 RNAi cells is not the result of analysis of RNAs from different post-induction time points, we isolated RNA from MRB3010 and TbRGG2 cells on days 2, 4, and 6 post-induction. Similar to the results we obtained with COIII RNA, we observed accumulation of partially edited A6 mRNAs in MRB3010 depleted cells that are smaller than those seen upon the ablation of TbRGG2, in addition to products of the same size in both cell lines (Fig. 3B). The observation that the editing effect in MRB3010 knockdown cells manifests later than that in TbRGG2 knockdown cells may reflect distinct protein functions or simply different levels of target protein reduction. Together, these data indicate that MRB3010 affects both initiation and progression of RNA editing and that MRB3010 and TbRGG2 impact somewhat different aspects of the editing process.

Association of MRB3010 with MRB1 complex components

To directly examine the interaction of MRB3010 with MRB1 complex components, we generated a PF cell line expressing C-terminally PTP-tagged MRB3010 from the endogenous locus. The PF PTP-MRB3010 cells exhibited similar growth rates to the parental cells. The PTP tag allows the protein to be detected by anti-Protein C antibody (Fig. 4A) and to be subjected to tandem affinity purification (TAP) via sequential Protein A and Protein C chromatography (Schimanski et al. 2005). All previous MRB1 complex purifications have entailed overexpressed proteins (Hashimi et al. 2008; Panigrahi et al. 2008; Weng et al. 2008; Hernandez et al. 2010). Here, expression of tagged MRB3010 from an endogenous locus alleviates any concerns regarding either spurious associations with abundant proteins or lack of association with true partners that are unavailable due to interaction with endogenous protein. We performed two PTP-MRB3010 tandem affinity purifications and examined aliquots of the purified proteins by SDS-PAGE (Fig. 4B) and LC-MS/MS (Table 1). In addition to MRB3010, LC-MS/MS identified a total of 11 previously described MRB1 components. Of these 11 proteins, five were found in both experiments. In two cases (Tb927.4.4160/Tb927.8.8170 and Tb927.4.4150/Tb927.8.8180) we were unable to distinguish the origin of a given peptide that could have arisen from either two of two highly homologous proteins. The 11 proteins we identified as copurifying with PTP-MRB3010 have been previously reported in one or more TAP purifications of exogenously expressed MRB1 components, including GAPs, REH2, TbRGG1, MRB10130 (Tb927.10.10130), or MRB3010, and our set of proteins included all seven of the proteins previously purified with MRB3010-TAP (Hashimi et al. 2008; Panigrahi et al. 2008; Weng et al. 2008; Hernandez et al. 2010) (Table 2). It was surprising that we failed to identify REH2 in PTP-MRB3010 purifications, because MRB3010 was purified with TAP-tagged REH2 (Hernandez et al. 2010) and REH2 was present in all GAP1/2 purifications (Table 1). However, REH2 was also absent from the MRB3010-TAP purification, which could be the result of the C-terminal tag of PTP-MRB3010 blocking this association, the MRB3010–REH2 interaction being transient, or the interaction being RNA dependent. The remaining proteins identified in tandem affinity purified MRB3010 eluates were presumed contaminants that are

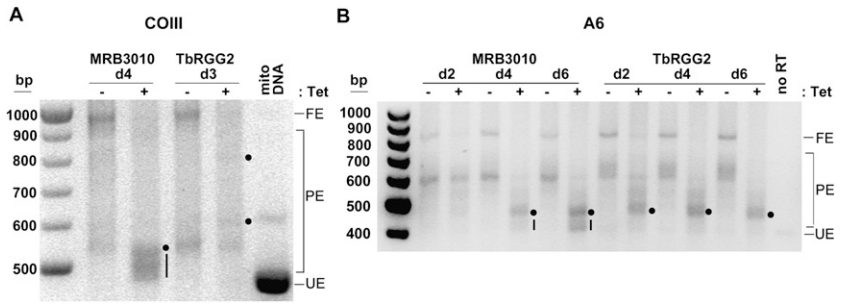

FIGURE 3. MRB3010 impacts an early step of the editing process. (*A*) Gel analysis of COIII RT–PCR reactions using RNAs from MRB3010 and TbRGG2 RNAi cells that were grown in the absence (−) or presence (+) of tet for 4 (MRB3010) or 3 (TbRGG2) d. Primers specific to the 5′ and 3′ ends of the COIII gene amplify the entire population of the mRNAs including pre-edited (or unedited) (UE), partially edited (PE), and fully edited (FE) transcripts. Mitochondrial (Mito) DNA was used as a template control for sizing the pre-edited COIII transcript. Dots and dashes represent major editing pause sites in cells depleted for MRB3010 or TbRGG2. (*B*) Gel analysis of A6 RT–PCR reactions that were performed essentially as described in *A*, except that primers were specific to the 3′ and 5′ ends of the A6 gene and RNA was collected from MRB3010 and TbRGG2 RNAi cells that were grown in the absence (−) or presence (+) of tet for 2, 4, and 6 d.

commonly observed in TAP purifications and/or have a nonmitochondrial localization (Supplemental Fig. 2). Notably, comparison of the cohorts of proteins identified by different groups with different tagged MRB1 complex components reveals five proteins present in all nine purifications: MRB3010, GAP1, GAP2, Tb11.02.5390, and Tb11.01.8260. These data suggest that the latter five proteins, potentially together with REH2, represent a core MRB1 subcomplex (see Fig. 7, below).

To confirm the LC-MS/MS findings and to determine whether some MRB3010 interactions depend on an RNA bridge, we performed coimmunoprecipitation experiments. To avoid spurious RNase activity that may occur during tandem affinity purification (M Ammerman, unpubl.), we isolated PTP-MRB3010 solely through Protein A Sepharose chromatography, and released bound proteins by TEV protease cleavage. To assess the impact of RNA bridges, we compared samples that were untreated with those that were incubated with an RNase cocktail prior to purification. We then utilized available antibodies to detect proteins associated with MRB3010. Anti-Protein C was used to visualize CBP-MRB3010 and confirm equal recovery and loading. Two bands of CBP-MRB3010 of 55 kDa and 50 kDa were detected (Fig. 4C); the 50-kDa band is likely a breakdown product as it was not present in all preparations and its abundance increased with increasing manipulations of a sample. Immunoblot analysis with antibodies against selected MRB1 components shows that MRB3010 interacts with GAP1, GAP2, and TbRGG2 (Fig. 4C). The interactions with GAP1 and GAP2 appear to involve direct protein–protein contacts, as they are largely refractory to RNase treatment. In contrast, the interaction between MRB3010 and TbRGG2 is primarily RNA mediated and may have been disrupted during the tandem affinity purification used for the LC-MS/MS study. We also confirmed the LC-MS/MS results suggesting that PTP-MRB3010 does not stably interact with REH2 or Tb927.3.1590 (here called MRB1590).

Because MRB3010 is required for efficient RNA editing (Figs. 2, 3), we next asked whether the integrity or activity of the RECC is affected by MRB3010 depletion. Mitochondria isolated from tetracycline-induced and uninduced PF MRB3010 RNAi cells were fractionated on 10%–30% glycerol gradients. The sedimentation pattern of the core RECC component KREPA6 was largely unchanged upon depletion of MRB3010 (Fig. 5A), demonstrating that RECC integrity is unaffected by MRB3010 depletion. To determine whether MRB3010 knockdown affects the activity of the RECC complex, editing assays were carried out on a precleaved deletion substrate using mitochondrial protein extract prepared from uninduced or induced PF MRB3010 RNAi cells. Extracts were analyzed on Coomassie-stained denaturing protein gels to confirm an equal recovery and overall protein profile (Fig. 5B). Precleaved editing assays were performed with the mRNA fragments U5-5″CL and U5-3″CL and gRNA gA6[14]PC-del (Igo et al. 2002). The 5′ and 3′ mRNA fragments are based on the A6 mRNA sequence immediately upstream of and downstream from the first editing site (ES1). The gA6[14]PC-del gRNA is complementary to the U5-5″CL and U5-3″CL fragments and specifies the deletion of four U's. Addition of mitochondrial extract to the RNA substrates resulted in the removal of four U's from the radiolabeled 5′ mRNA fragment 3′end (shift of the input 5′ mRNA down to −4 in Fig. 5C) and ligation of the 3′ mRNA fragment with the processed 5′ mRNA fragment from which four U's had been removed (shift of the 5′ mRNA up to ligated –4 in Fig. 5C). The assays shown in Figure 5C demonstrate that equal amounts of mitochondrial extracts from MRB3010 RNAi-uninduced or induced cells have equivalent amounts of precleaved editing activity (Fig. 5C). The resistance of RECC activity and integrity to MRB3010 depletion mirrors that seen upon knockdown of GAP1, GAP2, and MERS1 (Weng et al. 2008), and support the idea that the MRB1 complex is physically separate from the RECC, yet has a functional role in editing.

We next investigated the integrity of MRB1 complex(es) upon MRB3010 depletion. Mitochondrial lysates from uninduced and induced MRB3010 RNAi cells were fractionated on 10%–30% glycerol gradients, and the resulting fractions were analyzed by immunoblot for alterations in the sedimentation profiles of MRB1 components (Fig. 6A).

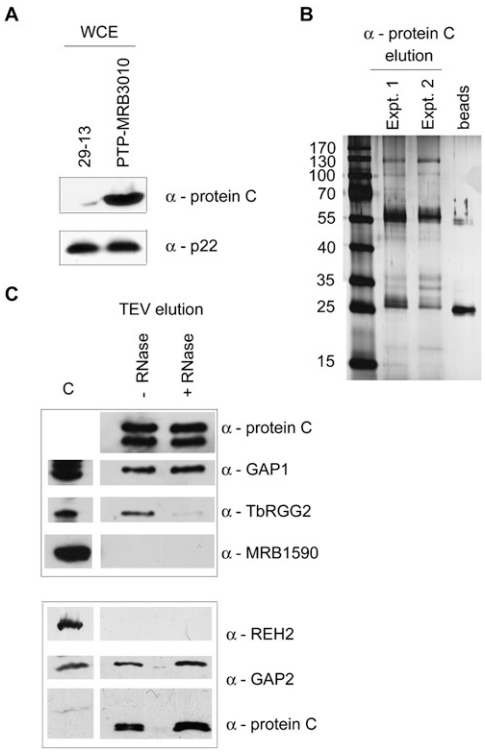

FIGURE 4. MRB3010 undergoes RNA-dependent and RNA-independent interactions with MRB1 complex components. (*A*) Western blot analysis of 29-13 or PTP-MRB3010 PF cells with anti-Protein C antibody confirms expression of the tandem affinity tagged MRB3010 protein (*top*). The p22 protein was used as a loading control (*bottom*). (*B*) Ten percent of two PTP-purified MRB3010 samples were separated on a 10% SDS–polyacrylamide gel and visualized by silver staining. Anti-Protein C beads were run as a control for unintended antibody elution. (*C*) IgG affinity purification of PTP-MRB3010 from cell extracts that were either RNase treated (+ RNase) or left untreated (− RNase). Proteins were eluted from IgG Sepharose 6 Fast Flow columns by TEV protease cleavage and electrophoresed on 10% (*top*) or 6% (*bottom*) SDS–polyacrylamide gels, followed by Western blotting with antibodies specific to Protein C (to detect MRB3010-ProtC) and various MRB complex components. (C) Control whole-cell extract, which is from either 29-13 PF cells (*top*) or PTP-MRB3010 cells (*bottom*).

TbRGG2 sedimented almost entirely in fractions 15–23, corresponding to particles of >20S, and its sedimentation was unaffected by MRB3010 levels. We note that the sedimentation of TbRGG2 is slightly different from what was previously published (Fisk et al. 2008); this may be the result of different sedimentation conditions or differential disruption of RNA-mediated interactions. In contrast, GAP1 and GAP2 sedimented broadly in fractions 7–17 (~11S to >20S) of the gradient in uninduced cells, and upon depletion of MRB3010 their sedimentation shifted to fractions 5–13. MRB1590 exhibited a broad distribution (fractions 7–19) whose peak broadened from fractions 11–13 to fractions 7–13 (11S–20S) upon MRB3010 knockdown. Overall, the discernible change in sedimentation of GAP1 and GAP 2-containing complexes upon depletion of MRB3010 demonstrates a requirement for MRB3010 for the integrity of large complexes containing GAP1 and GAP2 proteins. The extension of the sedimentation of MRB1590 to lower fractions upon MRB3010 knockdown may suggest that MRB3010 and MRB1590 are in a common complex, or perhaps knockdown of MRB3010 made available additional proteins or complexes that can interact with MRB1590. Overall, the broad distributions of the different MRB1 complex component proteins on the gradients indicate heterogeneity in MRB1 complexes. MRB3010 appears to be required for stability of some, but not all of the complexes that contain MRB components.

With the obvious heterogeneity of MRB1 complexes demonstrated in Figure 6A, it became important to analyze the sedimentation profile of PTP-MRB3010 to determine the size(s) of the complex(es) with which it associates. To this end, mitochondria from PTP-MRB3010 cells were fractionated on 10%–30% glycerol gradients and analyzed by immunoblot, with KREPA6 marking the 20S region of the gradient (Fig. 6B). An anti-Protein C antibody detected the same two bands observed in PTP-MRB3010 pull downs (Fig. 4). The full-length PTP-MRB3010 protein is detected in fractions 14–24, where complexes of 20S or larger sediment. To determine whether MRB3010 association with some or all of these macromolecular complexes is RNA mediated, mitochondrial extracts were treated with a combination of RNases prior to glycerol gradient sedimentation. In Figure 6B, we show that upon RNase treatment, sedimentation of PTP-MRB3010 protein shifts to regions of 20S and lower, consistent with a disruption of PTP-MRB3010-containing complexes via removal of RNA-mediated interactions. This redistribution of MRB3010 demonstrates that the protein exists in complex(es) with RNA-dependent interactions. However, upon RNase treatment we did not observe any PTP-MRB3010 protein shifting to the very top of the gradient, indicating that in addition to engaging in RNA-dependent interactions, MRB3010 also makes RNA-independent contacts with a subset of proteins. Interestingly, comparison of the sedimentation profiles of MRB3010, MRB1590, TbRGG2, GAP1, and GAP2, particularly in uninduced samples (Fig. 6A), reveals substantially different patterns for the five proteins. Collectively, these data are consistent with an MRB1 complex comprising multiple subcomplexes connected by a network of protein–protein and protein–RNA interactions.

DISCUSSION

MRB3010 is a protein common to all MRB1 complex purifications. In this work, we demonstrate that this core MRB1 component is essential for growth and RNA editing in both PF and BF life-cycle stages of *T. brucei*. Depletion of MRB3010 resulted in a large reduction in the levels of pan-edited mRNAs and a smaller reduction in minimally edited mRNA levels. Total gRNA abundance is unaltered

TABLE 1. PTP-MRB3010-associated proteins identified by mass spectrometry

		Expt 1		Expt 2	
Locus tag	Name	Unique peptides	Coverage	Unique peptides	Coverage
Tb927.5.3010	MRB3010	8	15.7%	13	22.9%
Tb11.02.5390		12	14.1%	24	20.6%
Tb927.2.3800	GAP1/GRBC2	7	15.4%	8	16.5%
Tb927.7.2570	GAP2/GRBC1	5	11.8%	9	21.8%
Tb11.01.8620		5	8.3%	9	16.0%
Tb927.10.11870		3	13.5%	4	17.7%
Tb11.01.0880		3	19.0%		
Tb927.4.4160/ Tb927.8.8170[a]		1	1.5%		
Tb10.6k15.0150				4	9.3%
Tb927.7.800				3	7.2%
Tb927.2.1860				2	3.1%
Tb927.4.4150/ Tb927.8.8180[a]				1	0.9%

[a]Peptides that could have arisen from either of the two highly homologous proteins.

in MRB3010 knockdown cells. Further, MRB3010 depletion similarly affects the editing of COII and MURF2 minimally edited mRNAs, which utilize *cis* and *trans* acting gRNAs, respectively. Data indicate that MRB3010 exerts its effect on the editing process indirectly as the integrity and activity of the RECC appear unaltered upon MRB3010 depletion. Nevertheless, MRB3010 functions early in the editing process, as evidenced by the dramatic accumulation of pre-edited and small partially edited mRNAs in MRB3010 knockdown cells. Indeed, this phenotype is reminiscent of that observed upon depletion of several editosome components (Carnes et al. 2005; Salavati et al. 2006; Babbarwal et al. 2007; Tarun et al. 2008; Guo et al. 2010). We also showed that MRB3010 is required for the integrity of some complex(es) that contain MRB1 component proteins, and that it engages in both RNA-independent and RNA-dependent interactions with other MRB1 complex components.

The effect of MRB3010 on RNA editing is distinct from that of other MRB1 components

It is striking that the effects of MRB3010 on RNA editing differ from those of other characterized MRB1 complex components. Even though GAP1 and GAP2 are also common to all MRB1 complex purifications, their apparent function in gRNA stabilization is distinct from the function of MRB3010, which does not impact gRNA stability. The function of MRB3010 also differs from that of TbRGG2, another MRB1 component studied by one of our laboratories (Fisk et al. 2008; Acestor et al. 2009; Ammerman et al. 2010). While depletion of either MRB3010 or TbRGG2 results in a dramatic decrease in the abundance of pan-edited mRNAs, TbRGG2 knockdown does not affect the abundance of minimally edited transcripts whose levels are reduced upon MRB3010 knockdown. Additionally, down-regulation of MRB3010 generally results in greater accumulation of pre-edited mRNAs than does TbRGG2 knockdown as evidenced by qRT–PCR. Gene-specific RT–PCR assays designed to assess the degree of 3′–5′ editing progression also revealed that editing is inhibited at earlier stages in the process in MRB3010-depleted cells than in TbRGG2-depleted cells. Comparisons of the relative levels of various mitochondrial RNAs between MRB3010 RNAi cells and those depleted for other MRB1 complex components, such as TbRGG1, MERS1, Tb927.6.1680, and Tb11.02.5390, also suggest a distinct effect of MRB3010 on mitochondrial RNA metabolism (Hashimi et al. 2008, 2009; Weng et al. 2008; Acestor et al. 2009). How these physically associated proteins impact editing at different stages, and how their effects are coordinated, will be a fascinating subject for future study.

The requirement for MRB3010 in maintaining the stability of complexes containing MRB1 components suggests a structural role for the protein, but we cannot rule out additional functions for MRB3010. An effect on early stages of editing suggests MRB3010 may impact gRNA and/or mRNA utilization, although recombinant MRB3010 does not appear to directly bind gRNAs or mRNAs in vitro using filter-binding assays (M. Ammerman, unpubl.). Moreover, because editing of COII mRNA is affected by MRB3010 knockdown, its effect cannot be restricted to *trans*-acting gRNAs. One likely possibility is that MRB3010, in the context of a subcomplex containing GAP1/2 proteins that bind gRNAs, is required for proper association of gRNA and/or mRNA with the editosome. In addition, we cannot rule out that the cumulative impact of MRB3010 knockdown on editing may reflect a combination of proteins and processes that have been affected, perhaps resulting from a role for MRB3010 in maintaining the stability of multiple MRB1 subcomplexes.

Macromolecular interactions within the MRB1 complex

Glycerol gradient sedimentation demonstrates that MRB3010 is associated with a large complex, greater than 20S, and that this complex has both RNA-dependent and RNA-independent interactions. Our coimmunoprecipitation experiments demonstrated that GAP1 and GAP2 are associated with PTP-MRB3010 following RNase treatment, while the interaction between MRB3010 and TbRGG2 is apparently

TABLE 2. Proteins purified by different laboratories using various tagged MRB1 complex components or anti-MRB1 complex antibodies

Protein ID	Other ID	Name/Motif	PTP-3010[a]	TAP-3010[b]	TAP-GAP1[c]	TAP-GAP1[e]	TAP-GAP2[b]	GAP2 mIP43[b]	TAP-GAP2[c]	TAP-GAP2[e]	TAP-10130[b]	TAP-REH2[d]	TAP-RGG1[c]
Tb927.5.3010		MRB3010/ Ribosomal S2	+	+	+	+	+	+	+	+	+	+	+
Tb11.02.5390			+	+	+	+	+	+	+	+	+	+	+
Tb927.2.3800		GRBC2/GAP1	+	+	+	+	+	+	+	+	+	+	+
Tb927.7.2570		GRBC1/GAP2	+	+	+	+	+	+	+	+	+	RD	+
Tb11.01.8620			+	+	+	+	+	+	+	+	+	+	+
Tb927.10.10130	Tb10.6k15.0150		+	+		RD	+	+		RD	+	RD	
Tb927.4.4160			*		+	RD		+	+	+		+	+
Tb927.8.8170			*		+	NC	+	+	+	NC		+	+
Tb927.2.1860			+					+			+	+	
Tb927.7.800			+	+				+			+	+	
Tb927.8.8180	Tb927.4.4150		+		+	+	+	+		+	+		+
Tb927.10.11870	Tb10.389.1910		+		+	+			+	+		+	
Tb11.01.0880			+									+	
Tb927.4.1500		REH2/Helicase			+	+	+	+	+	+		+	+
Tb927.2.6070		RBZ zinc finger						+				RD	
Tb927.3.1590		ATPase					+	+				RD	+
Tb927.10.10830	Tb10.406.0050	TbRGG2/RRM			+	+	+	+	+	+	+	+	+
Tb927.6.1680		C2H2 Znf			+	+		+		+		+	+
Tb927.6.2230		TbRGG1/RGG			+	RD			+	RD		RD	+
Tb927.6.2140		Hydratase			+				+			+	+
Tb927.3.4920		LETM1			+				+				+
Tb927.3.1820					+				+			RD	+
Tb11.01.7290		MERS1/ Nudix hydrolase			+	RD			+	RD		RD	+
Tb11.55.0009		MRP1				RD				RD		+	
Tb11.01.4860		MRP2				+				RD		RD	
Tb927.2.3180		PPR1				+				+		RD	
Tb927.10.380	Tb10.70.7960	PPR5				+				+			
Tb11.02.3180		PPR repeats				+				+			
Tb11.02.5120		PPR repeats				+				RD			
Tb927.10.6850	Tb10.67.3900	TbMRPS18				+				+		RD	
Tb11.02.0130						+				+			

(RD) RNA-dependent interaction, where there is a complete loss of peptides present in mass spectrometry results after RNase treatment of samples. (NC) No comparison, purifications (Weng et al. 2008) were done in *Leishmania* spp. where there is no homolog to Tb927.8.8170. The asterisk (*) denotes that the single peptide obtained by mass spectrometry is present in both Tb927.4.4160 and Tb927.8.8170, as these proteins exhibit 77% amino acid identity. The proteins targeted for purification in each immunoprecipitation are indicated by gray boxes.

[a]This study.
[b]Panigrahi et al. (2008).
[c]Hashimi et al. (2008).
[d]Hernandez et al. (2010).
[e]Weng et al. (2008).

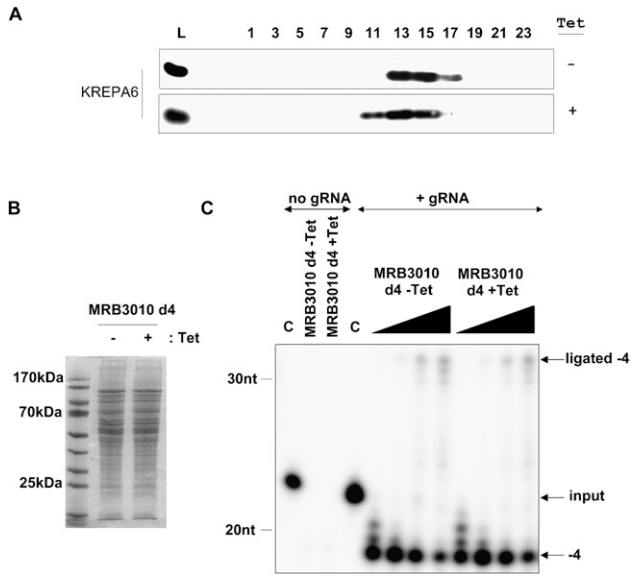

FIGURE 5. MRB3010 knockdown does not affect RNA editing core complexes. (*A*) The effect of MRB3010 depletion on the sedimentation of the RNA editing core complex (RECC). Mitochondrial extracts from uninduced (− tet) or tet-induced (+ tet) PF MRB3010 RNAi cells 4 d post-induction were fractionated on 10%–30% glycerol gradients. Alternate gradient fractions were electrophoresed on SDS–polyacrylamide gels and immunoblotted with anti-KREPA6 antibody. The mitochondrial extracts loaded on the gradient are shown on the *left* (abbreviated as L). (*B*) Equivalent amounts of mitochondrial extract purified from PF MRB3010 cells uninduced (−) or tet induced (+) for 4 d were separated on a 10% SDS-PAGE, followed by Coomassie staining. (*C*) Precleaved deletion editing assays were performed with [γ-^{32}P]ATP-radiolabeled 5′ mRNA fragment and 3′ mRNA fragment, but no gRNA (no gRNA); or radiolabeled 5′ mRNA fragment, 3′ mRNA fragment, and gRNA (+ gRNA). In the no gRNA experiments either a control with no protein (C) or 2.5 μL of the indicated extract was added. Nonspecific ribonucleases in the extracts degraded the radiolabeled 5′ mRNA fragment when gRNA was not present. In the experiments where gRNA was added either no protein (C) or 1, 2.5, 5, and 7.5 μL of the indicated extracts were added. The migration position of the input radiolabeled 5′ mRNA fragment is indicated. The −4 nonligated deletion product is labeled −4 and the ligated deletion product is labeled ligated −4.

RNA mediated. LC-MS/MS analysis of proteins purified by tandem affinity purification of endogenously tagged MRB3010 identified all of the proteins found when MRB3010 was overexpressed and purified in addition to six other MRB1 components, one of which was only previously reported to be associated with REH2 (Panigrahi et al. 2008; Hernandez et al. 2010).

Numerous groups have characterized the MRB1 complex with the different purifications containing overlapping and distinct components (Table 2), making the exact composition of the MRB1 complex unclear. Figure 7 summarizes the proteins found in the various MRB1 purifications. Most purifications were done in the absence of RNase treatment; however, in the purifications where −/+ RNase treatment were compared we noted RNA-dependent (RD) protein associations in the cases where there was a complete loss of peptides in LC-MS/MS in RNase-treated samples (Table 2). The results from this study, in combination with those of previous groups, suggest that there is a set of proteins that form a core subcomplex of the MRB1 complex. This core includes GAP1, GAP2, Tb11.02.5390, Tb11.01.8620, Tb927.5.3010, and REH2 (Fig. 7, blue oval). While REH2 was not identified in pulldowns with either endogenously or exogenously tagged MRB3010, purifications of TAP-REH2 did contain MRB3010 (Hernandez et al. 2010). Whether the large C-terminal tag on MRB3010 prevents its normal association with REH2, or whether MRB3010 exists predominantly in a complex without REH2, has to be more closely examined. The consistent copurification of these six proteins suggests that they form a stable particle.

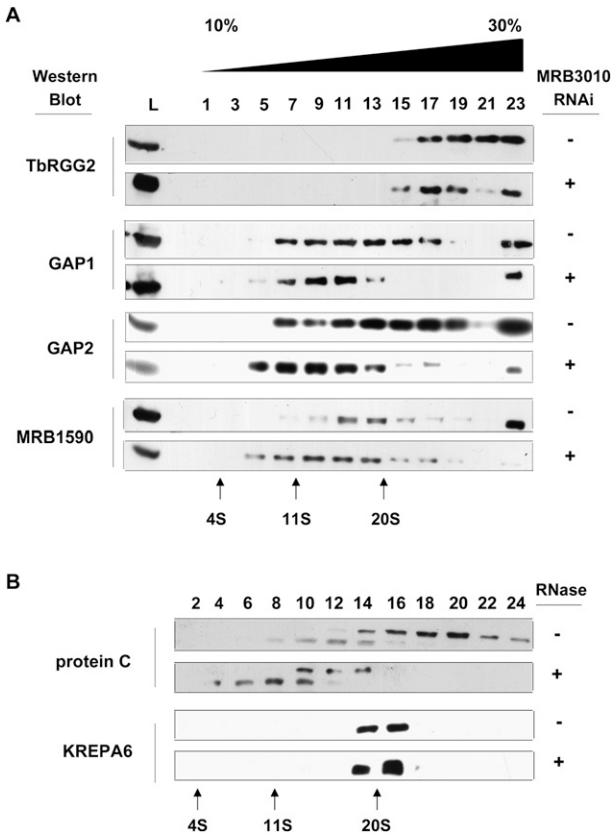

FIGURE 6. Glycerol gradient sedimentation of MRB complex components. (*A*) The effect of MRB3010 depletion on the sedimentation of TbRGG2, GAP1, GAP2, and MRB1590-containing complexes. Mitochondrial extracts from uninduced (− tet) or tet-induced (+ tet) PF MRB3010 RNAi cells 4 d post-induction were fractionated on 10%–30% glycerol gradients. Alternate gradient fractions were electrophoresed on SDS–polyacrylamide gels and immunoblotted with the indicated antibodies. The mitochondrial extracts loaded on the gradient are shown on the *left* (abbreviated as L). (*B*) MRB3010 is part of a macromolecular complex that sediments at >20S and has RNA-dependent interactions. Mitochondrial extracts from PF PTP-MRB3010 cells that were either treated with an RNase cocktail (+) or left untreated (–) were fractionated and analyzed as described in *A*. The position of KREPA6-containing complexes is shown here as a 20S size standard.

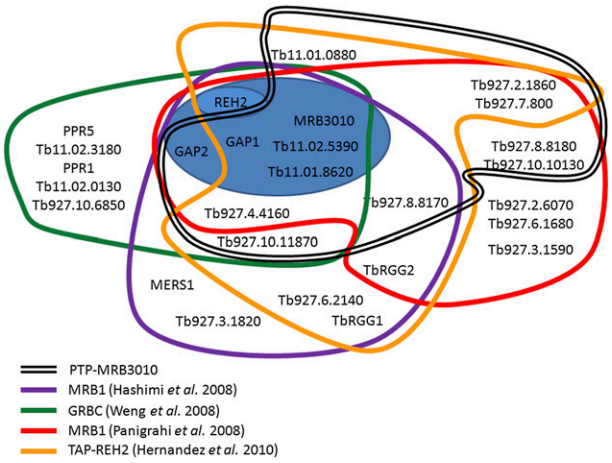

FIGURE 7. Overlapping and distinct components of MRB1 complexes isolated by different methods. Gene DB numbers or common names of proteins identified by affinity purification and mass spectrometry from this study and previous studies are outlined in different colors. The blue oval indicates proteins that were identified in the majority of TAP purifications performed with tagged MRB1 components, which may constitute a core subcomplex. GAP2 was identified, but shown to be RNA dependent in the REH2-based purification (Hernandez et al. 2010). REH2 is highlighted because it was not detected with either MRB3010-based purification (Panigrahi et al. 2008; this study); however, the latter may be due to the C-terminal tag, since MRB3010 was detected in the reciprocal REH2-based purification (Hernandez et al. 2010). MRB1 complexes purified by Weng et al. (2008), Hernandez et al. (2010), and in this study were RNase treated, while MRB1 complexes purified by Panigrahi et al. (2008) and Hashimi et al. (2009) were not.

However, it is also clear that these proteins do not function exclusively in this context. Copurification of the core subcomplex suggests that the proteins have a common activity when together, but this does not exclude the possibility that these proteins have other activities when they are outside the core subcomplex.

Another set of proteins, including Tb927.4.4160, Tb927.8.8170, and Tb927.10.11870, are present in most, but not all of the MRB1 purifications (Hashimi et al. 2008; Panigrahi et al. 2008; Weng et al. 2008; Hernandez et al. 2010). These proteins may associate with the MRB1 core subcomplex individually and/or as components of another subcomplex(es). The observed variation in the composition of the MRB1 complex in preparations purified by tagging of different components likely reflects participation of these proteins in different subcomplexes that can affect more than one step of RNA editing and/or RNA metabolism. In addition, temporal association and disassociation of proteins and subcomplexes is also likely to contribute to the observed heterogeneity in MRB1. Moreover, some of the proteins may not be part of a complex, but may have dynamic and transient interactions with subunits of the complex or RNA. Additional data obtained in this study allow us to refine previous models of the MRB1 complex (Weng et al. 2008; Hernandez et al. 2010). Further analysis is necessary to define the direct protein–protein interactions and subcomplex compositions and to understand the role of the component proteins in this fascinating complex.

MATERIALS AND METHODS

Cell culture, RNA interference, and growth curves

The RNAi vector was prepared by amplifying a 506-bp fragment from nucleotides 832 to 1337 of the MRB3010 open reading frame with forward (GGATCCCTAAGCAAGAGGTTCGCCAC) and reverse (CTCGAGGTCTCCCCTGCATCCAGTAA) primers (BamHI and XhoI restriction sites are underlined) and introduced into the BamHI–XhoI restriction sites of p2T7-177. This DNA was transfected into procyclic form (PF) 29-13 and bloodstream form (BF) 427 cells, and transformants were selected with phleomycin. Clonal cell lines were selected by limiting dilution.

For integration of the tandem affinity purification PTP tag into the endogenous MRB3010 locus, primers ApaI 5′ RibS2 (PTP) (5′-CACGGGCCCATGCAAGCACAGAAAGCCG-3′) and NotI 3′ RibS2 (5′-CACGCGGCCGCGCTTGCGGTGTAGACCCACG-3′), encompassing nucleotides 502–1547 of the MRB3010 open reading frame, were used to amplify the 3′-end of MRB3010 and introduce it into the ApaI–NotI restriction sites of pC-PTP PURO (Fisk et al. 2009b). pC-PTP-MRB3010 was then restricted at the unique BpiI site within MRB3010 and transfected into 29-13 PF *T. brucei* cells. Cells harboring the insert were selected with puromycin and cloned by limiting dilution.

Quantitative real-time PCR

RNA from uninduced and tet-induced PF and BF MRB3010 RNAi cells was collected at day 4 following induction. Ten micrograms of RNA were treated with a DNA-free DNase kit (Ambion) to remove any residual DNA and reverse transcribed using random hexamer primers and the Taq-Man reverse transcription kit (Applied Biosciences). Twenty-five microliters of real time RT–PCR reactions were then performed with primers specific to pre-edited, edited, and never-edited mitochondrial transcripts as previously described (Carnes et al. 2005; Carnes and Stuart 2007) using a MyiQ real time PCR detection system (Bio-Rad). Primers that flank the junctions of *9S/ND8*, *A6/CYb*, and *RPS12/ND5* adjacent genes were previously described (Acestor et al. 2009). Primers RibS2 qPCR Fwd (5′-CCGCTTTTCCTACTGTTGTG-3′) and RibS2 qPCR Rev (5′-ATATTGCGAGCAGAGAGGTG-3′), which amplify nucleotides 68–197 of the MRB3010 open reading frame, were designed to analyze MRB3010 mRNA levels. Results from PF cells were analyzed using iQ5 software (Bio-Rad). Data presented here are normalized using 18S rRNA, although many of the mRNA levels were also confirmed using a β-tubulin standard and found to be comparable to those standardized against 18S rRNA. The level of each RNA is represented as the mean and standard deviation of at least six determinations. Quantitative RT–PCR reactions using BF MRB3010 RNAi cells were performed essentially as described for the PF cells, except reactions were performed using a Rotorgene RG-3000 real time PCR detection system (Corbett Research) with at least three determinations, and data were quantified by the Pfaffl method (Carnes and Stuart 2007).

Guanylyltransferase labeling

Total RNA from the PF MRB3010 RNAi cells uninduced or induced for 4 d with 1μg/mL of tet was purified using Trizol (Invitrogen) as per the manufacturer's instructions. Contaminating DNA was removed from the RNA samples using the DNA-free kit (Ambion) following the accompanying protocol. Fifteen micrograms of RNA was labeled with 5 μCi [α-^{32}P]GTP (800 Ci/mmol) in the presence of 1.5 pmol of guanylyltransferase DIR$^{1-545}$ 50 mM Tris-HCl (pH 8.0), 1.5 mM $MgCl_2$, 6 mM KCl, 2.5mM DTT, and 20 U of SUPERase-In (Ambion) for 30 min at room temperature (Hayman and Read 1999). Reactions were phenol:chloroform extracted twice, chloroform extracted once, and precipitated in the presence of 2 M ammonium acetate, 20 μg of glycogen, and ethanol. Samples were resuspended in 90% formamide loading buffer and resolved on an 8% acrylamide/7 M urea gel in 1X TBE.

RT–PCR analysis of mitochondrial mRNAs

A total of 30 mL of mid-log trypanosome culture were harvested and resuspended in 1 mL of Trizol (Invitrogen). Total RNA was isolated as per the manufacturer instructions. Contaminating DNA was removed from the RNA using the DNA-free kit (Ambion) and subsequent phenol:chloroform extraction. The following primers that anneal to the never-edited 5′ and 3′ regions of the genes were used for RT–PCR analysis (restriction site underlined):

A6 5′ full NE (5′-AAAAATAAGTATTTTGATATTATTAAAGT AAA-3′),
A6 3′ (5′-ATTAACTTATTTGATCTTATTCTATAACTCC-3′),
COIII 3′ long (5′-AACTTCCTACAAACTACCAATAC-3′) (this primer includes the first two editing sites),
COIII 5′NE (5′-GCGAATTCATTGAGGATTGTTTAAAATTGA-3′).

A total of 50 μL of reverse transcription reactions were performed with 150 pmoles of oligo(dT) primer for COIII and 60 pmoles of A6 3′ primer for A6, and 1 μg of DNase-treated RNA in a 10-μL reaction by incubation at 70°C for 5 min, and slow cooling (30 min) to 20°C. The annealed primer was extended with Superscript III Reverse Transcriptase (Invitrogen) for 1 h at 42°C. PCR reactions were carried out with 3.5 μL of the RT reaction and 20 pmol of gene-specific upstream and downstream primers. PCR was performed using an annealing temperature of 45°C, and products were analyzed on 2.5% agarose gels. Mitochondrial DNA was used as a template control for sizing the pre-edited COIII transcript.

Editing assays

Mitochondrial extracts were prepared by a rapid extract protocol from day 4-uninduced and tet-induced PF MRB3010 RNAi cells as described previously (Rusché et al. 2001; Law et al. 2005). Precleaved deletion assays were performed with the U5-5″CL 5′ mRNA fragment, the U5-3″CLpp 3′ mRNA fragment, and gA6[14]PC-del gRNA (Igo et al. 2002). The U5-5″CL RNA (5″-GGAAAGGGAAAGUUGUGAUUUU-3″) and the U5-3″CLpp RNA (5″-pGCGAGUUAUAGAAUAp-3″) were synthesized by Integrated DNA Technologies. The gRNA gA6[14]PC-del was prepared by annealing the A6comp1 antisense oligo (GGAAAGGGAAAGTTG TGAGCGAGTTATAGAACCTATAGAACCTATAGTGAGTCGTAT TAC) to the T7 oligo (GTAATACGACTCACTATA) to act as a template for T7 transcription. The U5-5″CL RNA was labeled with [γ-^{32}P]ATP using T4 polynucleotide kinase (Fermentas). RNAs were purified on 12% polyacrylamide/7 M urea gels. Precleaved editing reactions were carried out as previously described (Igo et al. 2002).

Glycerol gradients

Hypotonic purifications of mitochondria from 7.5×10^9-uninduced and tet-induced PF MRB3010 RNAi cells and 5×10^9 PTP-MRB3010 cells were carried out as described previously (Hashimi et al. 2008). The enriched mitochondria were lysed in 1 mL of the lysis buffer (10 mM Tris at pH 7.2, 10 mM $MgCl_2$, 100 mM KCl, 1 mM DTT, 1 μg/mL pepstatin, 2 μg/mL leupeptin, 1 mM pefabloc) with 1% Triton X-100, for 15 min at 4°C. Lysates were cleared and loaded on 11-mL 10%–30% glycerol gradients and centrifuged at 38,000 rpm in a Beckman SW41 rotor for 12 h at 4°C. Individual 0.5-mL fractions were then collected from the top.

PTP purification and protein analysis

Then, 1.5×10^{10} PTP-MRB3010 PF cells were collected and PTP-MRB3010 was purified by tandem affinity chromatography as described previously (Schimanski et al. 2005; Günzl and Schimanski 2009), except for one minor modification. Prior to binding the IgG Sepharose 6 Fast Flow column, the supernatant was either treated with 40 U of RNaseOUT or with a RNase cocktail containing RNase A (0.1 U/μL), T1 (0.125 U/μL), V1 (0.001/μL), and micrococcal nuclease (0.03 U/μL) for 60 min in ice. TEV elutions from the IgG Sepharose 6 Fast Flow column were analyzed by Western blot. Elutions from the Protein C affinity column were subjected to tandem mass spectrometry (LC-MS/MS; Seattle BioMed). LC-MS/MS was performed using LTQ linear ion trap mass spectrometer (Thermo Fisher Scientific). The LC system consisted of a fused-silica nanospray needle packed in-house with C18 reverse-phase material. The peptide samples were loaded onto the reversed phase column using a two-mobile-phase solvent system consisting of 0.4% acetic acid in water (A) and 0.4% acetic acid in acetonitrile (B). The mass spectrometer operated in a data-dependent MS/MS mode over the *m/z* range of from 400 to 2000. For each cycle, the five most abundant ions from each MS scan were selected for MS/MS analysis using 45% normalized collision energy. Dynamic exclusion was used to exclude ions that had been detected twice in a 30-sec window for 3 min. Data analysis involved submitting raw MS/MS data to Bioworks 3.3 (ThermoElectron) and searched using the Sequest algorithm against *T. brucei* protein database v. 4.0 (ftp://ftp.sanger.ac.uk/pub/databases/T.brucei_sequences/T.brucei_genome_v4/), which included additional common contaminants such as human keratin. The Sequest output files were analyzed and validated by PeptideProphet (Keller et al. 2002). Proteins and peptides with a probability score of ≥0.9 were accepted.

Antibodies and Western blots

Fractions from glycerol gradients were electrophoresed on 10% or 12% SDS–polyacrylamide gels. Proteins were transferred onto nitrocellulose membrane and probed with polyclonal antibodies against GAP1, which was produced against recombinant GAP1

protein (Bethyl Laboratories), GAP2 (Hashimi et al. 2009), TbRGG2 (Fisk et al. 2008), KREPA6 (Tarun et al. 2008) (a generous gift from Ken Stuart, Seattle Biomedical Research Institute), and MRB1590 (antibodies were produced against the peptide [CILPRDAGNSDKPLRD] of Tb927.3.1590 [Bethyl Laboratories]).

Whole-cell lysates from the 29-13 and PTP-MRB3010 cells (equivalent of 1×10^7 cells) were electrophoresed on 12% SDS–polyacrylamide gels, transferred to nitrocellulose membrane, and probed with monoclonal anti-Protein C antibody (Sigma P7058) and polyclonal anti-p22 (Hayman et al. 2001). TEV elutions from tandem affinity purifications of PTP-MRB3010 were run on 6% and 10% SDS–polyacrylamide gels, transferred to nitrocellulose membranes, and probed with anti-MRB1590 (described above), anti-Protein C, anti-GAP1, and anti-GAP2 (Hashimi et al. 2009), anti-TbRGG2 (Fisk et al. 2008), and anti-REH2 antibodies (Hernandez et al. 2010) (a generous gift from Jorge Cruz-Reyes, Texas A&M University).

SUPPLEMENTAL MATERIAL

Supplemental material is available for this article.

ACKNOWLEDGMENTS

We thank Yuko Ogata for performing the mass spectrometric analysis. We thank Jorge Cruz-Reyes and Ken Stuart for providing antibodies and Sara Zimmer for critical reading of this manuscript. This work was supported by NIH grant number RO1 AI061580 to L.K.R. and by the Grant Agency of the Czech Republic 204/09/1667, the Ministry of Education of the Czech Republic (2B06129, LC07032, and 6007665801), and the Praemium Academiae award to J.L.

Received August 31, 2010; accepted February 17, 2011.

REFERENCES

Acestor N, Panigrahi AK, Carnes J, Zíková A, Stuart KD. 2009. The MRB1 complex functions in kinetoplastid RNA processing. *RNA* **15:** 277–286.

Ammerman ML, Fisk JC, Read LK. 2008. gRNA/pre-mRNA annealing and RNA chaperone activities of RBP16. *RNA* **14:** 1069–1080.

Ammerman MA, Presnyak V, Fisk JC, Foda BM, Read LK. 2010. TbRGG2 facilitates kinetoplastid RNA editing initiation and progression past intrinsic pause sites. *RNA* **16:** 2239–2251.

Aphasizhev R, Aphasizheva I, Nelson RE, Simpson L. 2003. A 100-kD complex of two RNA-binding proteins from mitochondria of *Leishmania tarentolae* catalyzes RNA annealing and interacts with several RNA editing components. *RNA* **9:** 62–76.

Babbarwal VK, Fleck M, Ernst NL, Schnaufer A, Stuart K. 2007. An essential role of KREPB4 in RNA editing and structural integrity of the editosome in *Trypanosoma brucei*. *RNA* **13:** 737–744.

Blum B, Simpson L. 1990. Guide RNAs in kinetoplastid mitochondria have a nonencoded 3′ oligo(U) tail involved in recognition of the preedited region. *Cell* **62:** 391–397.

Carnes J, Stuart KD. 2007. Uridine insertion/deletion editing activities. *Methods Enzymol* **424:** 25–54.

Carnes J, Trotter JR, Ernst NL, Steinberg A, Stuart K. 2005. An essential RNase III insertion editing endonuclease in *Trypanosoma brucei*. *Proc Natl Acad Sci* **102:** 16614–16619.

Carnes J, Trotter JR, Peltan A, Fleck M, Stuart K. 2008. RNA editing in *Trypanosoma brucei* requires three different editosomes. *Mol Cell Biol* **28:** 122–130.

Fisk JC, Ammerman ML, Presnyak V, Read LK. 2008. TbRGG2, an essential RNA editing accessory factor in two *Trypanosoma brucei* life cycle stages. *J Biol Chem* **283:** 23016–23025.

Fisk JC, Presnyak V, Ammerman ML, Read LK. 2009a. Distinct and overlapping functions of MRP1/2 and RBP16 in mitochondrial RNA metabolism. *Mol Cell Biol* **29:** 5214–5225.

Fisk JC, Sayegh J, Zurita-Lopez C, Menon S, Presnyak V, Clarke SG, Read LK. 2009b. A type III protein arginine methyltransferase from the protozoan parasite *Trypanosoma brucei*. *J Biol Chem* **284:** 11590–11600.

Günzl A, Schimanski B. 2009. Tandem affinity purification of proteins. *Curr Protoc Protein Sci* **55:** 19.19.1–19.19.16.

Guo X, Ernst NL, Carnes J, Stuart KD. 2010. The zinc-fingers of KREPA3 are essential for the complete editing of mitochondrial mRNAs in *Trypanosoma brucei*. *PLoS ONE* **5:** e8913. doi: 10.1371/journal.pone.0008913.

Hans J, Hajduk SL, Madison-Antenucci S. 2007. RNA-editing-associated protein 1 null mutant reveals link to mitochondrial RNA stability. *RNA* **13:** 881–889.

Hashimi H, Zíková A, Panigrahi AK, Stuart KD, Lukeš J. 2008. TbRGG1, an essential protein involved in kinetoplastid RNA metabolism that is associated with a novel multiprotein complex. *RNA* **14:** 970–980.

Hashimi H, Čičová Z, Novotná L, Wen YZ, Lukeš J. 2009. Kinetoplastid guide RNA biogenesis is dependent on subunits of the mitochondrial RNA binding complex 1 and mitochondrial RNA polymerase. *RNA* **15:** 588–599.

Hayman ML, Read LK. 1999. *Trypanosoma brucei* RBP16 is a mitochondrial Y-box family protein with guide RNA binding activity. *J Biol Chem* **274:** 12067–12074.

Hayman ML, Miller MM, Chandler DM, Goulah CC, Read LK. 2001. The trypanosome homolog of human p32 interacts with RBP16 and stimulates its gRNA binding activity. *Nucleic Acids Res* **29:** 5216–5225.

Hernandez A, Madina BR, Ro K, Wohlschlegel JA, Willard B, Kinter MT, Cruz-Reyes J. 2010. REH2 RNA helicase in kinetoplastid mitochondria: ribonucleoprotein complexes and essential motifs for unwinding and guide RNA (gRNA) binding. *J Biol Chem* **285:** 1220–1228.

Igo RP Jr, Weston DS, Ernst NL, Panigrahi AK, Salavati R, Stuart K. 2002. Role of uridylate-specific exoribonuclease activity in *Trypanosoma brucei* RNA editing. *Eukaryot Cell* **1:** 112–118.

Keller A, Nesvizhskii AI, Kolker E, Aebersold R. 2002. Empirical statistical model to estimate the accuracy of peptide identifications made by MS/MS and database search. *Anal Chem* **74:** 5383–5392.

Law JA, Huang CE, O'Hearn SF, Sollner-Webb B. 2005. In *Trypanosoma brucei* RNA editing, band II enables recognition specifically at each step of the U insertion cycle. *Mol Cell Biol* **25:** 2785–2794.

Lukeš J, Hashimi H, Zíková A. 2005. Unexplained complexity of the mitochondrial genome and transcriptome in kinetoplastid flagellates. *Curr Genet* **48:** 277–299.

Madison-Antenucci S, Hajduk SL. 2001. RNA editing-associated protein 1 is an RNA binding protein with specificity for preedited mRNA. *Mol Cell* **7:** 879–886.

Maslov DA, Sharma MR, Butler E, Falick AM, Gingery M, Agrawal RK, Spremulli LL, Simpson L. 2006. Isolation and characterization of mitochondrial ribosomes and ribosomal subunits from *Leishmania tarentolae*. *Mol Biochem Parasitol* **148:** 69–78.

Panigrahi AK, Zíková A, Dalley RA, Acestor N, Ogata Y, Anupama A, Myler PJ, Stuart KD. 2008. Mitochondrial complexes in *Trypanosoma brucei*: a novel complex and a unique oxidoreductase complex. *Mol Cell Proteomics* **7:** 534–545.

Pelletier M, Read LK. 2003. RBP16 is a multifunctional gene regulatory protein involved in editing and stabilization of specific mitochondrial mRNAs in *Trypanosoma brucei*. *RNA* **9:** 457–468.

Redmond S, Vadivelu J, Field MC. 2003. RNAit: an automated web-based tool for the selection of RNAi targets in *Trypanosoma brucei*. *Mol Biochem Parasitol* **128:** 115–118.

Rusché LN, Cruz-Reyes J, Piller KJ, Sollner-Webb B. 1997. Purification of a functional enzymatic editing complex from *Trypanosoma brucei* mitochondria. *EMBO J* **16:** 4069–4081.

Rusché LN, Huang CE, Piller KJ, Hemann M, Wirtz E, Sollner-Webb B. 2001. The two RNA ligases of the *Trypanosoma brucei* RNA editing complex: cloning the essential band IV gene and identifying the band V gene. *Mol Cell Biol* **21:** 979–989.

Salavati R, Ernst NL, O'Rear J, Gilliam T, Tarun S Jr, Stuart K. 2006. KREPA4, an RNA binding protein essential for editosome integrity and survival of *Trypanosoma brucei*. *RNA* **12:** 819–831.

Schimanski B, Nguyen TN, Günzl A. 2005. Highly efficient tandem affinity purification of trypanosome protein complexes based on a novel epitope combination. *Eukaryot Cell* **4:** 1942–1950.

Schnaufer A, Panigrahi AK, Panicucci B, Igo RP Jr, Wirtz E, Salavati R, Stuart K. 2001. An RNA ligase essential for RNA editing and survival of the bloodstream form of *Trypanosoma brucei*. *Science* **291:** 2159–2162.

Schumacher MA, Karamooz E, Zíková A, Trantírek L, Lukeš J. 2006. Crystal structures of *T. brucei* MRP1/MRP2 guide-RNA binding complex reveal RNA matchmaking mechanism. *Cell* **126:** 701–711.

Simpson L, Aphasizhev R, Gao G, Kang X. 2004. Mitochondrial proteins and complexes in *Leishmania* and *Trypanosoma* involved in U-insertion/deletion RNA editing. *RNA* **10:** 159–170.

Stuart KD, Schnaufer A, Ernst NL, Panigrahi AK. 2005. Complex management: RNA editing in trypanosomes. *Trends Biochem Sci* **30:** 97–105.

Sturm NR, Simpson L. 1990. Kinetoplast DNA minicircles encode guide RNAs for editing of cytochrome oxidase subunit III mRNA. *Cell* **61:** 879–884.

Tarun SZ Jr, Schnaufer A, Ernst NL, Proff R, Deng J, Hol W, Stuart K. 2008. KREPA6 is an RNA-binding protein essential for editosome integrity and survival of *Trypanosoma brucei*. *RNA* **14:** 347–358.

Vanhamme L, Perez-Morga D, Marechal C, Speijer D, Lambert L, Geuskens M, Alexandre S, Ismaili N, Göringer U, Benne R, et al. 1998. *Trypanosoma brucei* TbRGG1, a mitochondrial oligo(U)-binding protein that co-localizes with an in vitro RNA editing activity. *J Biol Chem* **273:** 21825–21833.

Vondrušková E, van den Burg J, Zíková A, Ernst NL, Stuart K, Benne R, Lukeš J. 2005. RNA interference analyses suggest a transcript-specific regulatory role for mitochondrial RNA-binding proteins MRP1 and MRP2 in RNA editing and other RNA processing in *Trypanosoma brucei*. *J Biol Chem* **280:** 2429–2438.

Weng J, Aphasizheva I, Etheridge RD, Huang L, Wang X, Falick AM, Aphasizhev R. 2008. Guide RNA-binding complex from mitochondria of trypanosomatids. *Mol Cell* **32:** 198–209.

Zíková A, Panigrahi AK, Dalley RA, Acestor N, Anupama A, Ogata Y, Myler PJ, Stuart K. 2008. *Trypanosoma brucei* mitochondrial ribosomes: affinity purification and component identification by mass spectrometry. *Mol Cell Proteomics* **7:** 1286–1296.

Attached Publications

Part I. Trypanosome RNA editing

Michelle L. Ammerman, Kurtis M. Downy, Hassan Hashimi, John C. Fisk, Danielle L. Tomasello, Drahomíra Faktorová, Lucie Kafková, Tony King, Julius Lukeš and Laurie K. Read (2012). Architecture of the trypanosome RNA editing complex, MRB1. *Nucleic Acids Res.* 40: 5637-5650.

This paper maps the interactions among the MRB1 subunits in vitro by a yeast 2-hybrid screen and in vivo by a series of pull-downs of selected MRB1 proteins. MRB1 is established to be made up of two subcomplexes involved in either RNA editing initiation (MRB1 core) or pan-editing progression (TbRGG2 subcomplex).

Nucleic Acids Research Advance Access published March 6, 2012

Nucleic Acids Research, 2012, 1–14
doi:10.1093/nar/gks211

Architecture of the trypanosome RNA editing accessory complex, MRB1

Michelle L. Ammerman[1], Kurtis M. Downey[1], Hassan Hashimi[2,3], John C. Fisk[1], Danielle L. Tomasello[1], Drahomíra Faktorová[2], Lucie Kafková[3], Tony King[1], Julius Lukeš[2,3] and Laurie K. Read[1,*]

[1]Department of Microbiology and Immunology, School of Medicine, State University of New York at Buffalo, Buffalo, NY 14214, USA, [2]Biology Centre, Institute of Parasitology and [3]Faculty of Science, University of South Bohemia, 37005 České Budějovice (Budweis), Czech Republic

Received November 21, 2011; Revised February 1, 2012; Accepted February 16, 2012

ABSTRACT

***Trypanosoma brucei* undergoes an essential process of mitochondrial uridine insertion and deletion RNA editing catalyzed by a 20S editosome. The multiprotein mitochondrial RNA-binding complex 1 (MRB1) is emerging as an equally essential component of the trypanosome RNA editing machinery, with additional functions in gRNA and mRNA stabilization. The distinct and overlapping protein compositions of reported MRB1 complexes and diverse MRB1 functions suggest that the complex is composed of subcomplexes with RNA-dependent and independent interactions. To determine the architecture of the MRB1 complex, we performed a comprehensive yeast two-hybrid analysis of 31 reported MRB1 proteins. We also used *in vivo* analyses of tagged MRB1 components to confirm direct and RNA-mediated interactions. Here, we show that MRB1 contains a core complex comprised of six proteins and maintained by numerous direct interactions. The MRB1 core associates with multiple subcomplexes and proteins through RNA-enhanced or RNA-dependent interactions. These findings provide a framework for interpretation of previous functional studies and suggest that MRB1 is a dynamic complex that coordinates various aspects of mitochondrial gene regulation.**

INTRODUCTION

The Order Kinetoplastida includes numerous human and animal pathogens such as *Trypanosoma brucei, T. cruzi* and *Leishmania* spp., which are the causative agents of African sleeping sickness and nagana, Chagas' disease and several forms of leishmaniasis, respectively. The kinetoplastids are named for their unique mitochondrial DNA, called the kinetoplast, which is comprised of a catenated network of approximately 50 maxicircles and thousands of minicircles (1). Maxicircles encode two mitochondrial rRNAs and 18 proteins, the majority of which are components of the respiratory complexes. Of 18 mitochondrial mRNAs, 12 undergo post-transcriptional modification through an exceptional process of RNA editing entailing specific uridine (U) insertion and deletion that can double the size of the primary transcript. U insertion/deletion editing is essential for creation of translatable open reading frames in kinetoplastid mitochondria (2,3). Sequence information governing the sites and numbers of uridines to be inserted and deleted is provided by the mostly (with two exceptions) minicircle-encoded guide RNAs (gRNAs). RNA editing is catalyzed by the multiprotein RNA editing core complex (RECC), also known as the editosome. Pre-mRNA and cognate gRNA form an anchor duplex, with the sites to be edited located upstream of the anchor duplex. The central region of the gRNA then acts as the template to direct the editing by the RECC, in a series of reactions including endonucleolytic cleavage of the mRNA, U insertion or deletion, and RNA ligation. Some mRNAs are minimally edited, while a number of mRNAs are extensively edited (pan-edited) and require dozens of gRNAs to act sequentially in the 3′- to 5′-direction along the mRNA to produce the fully edited translatable mRNAs (2,3). In addition to the RECC, a number of editing accessory factors are required for efficient editing. These accessory proteins can modulate editing through substrate production, substrate delivery, and editing processivity, as well as associated gene regulatory processes including RNA turnover. For example, MRP1/2 and RBP16 are essential for editing of a subset of mRNAs, a function that may involve their RNA–RNA annealing properties (4–7).

*To whom correspondence should be addressed. Tel: +1 716 829 3307; Fax: +1 716 829 2158; Email: lread@buffalo.edu

The helicase REH1 facilitates RNA editing progression when multiple gRNAs are involved (8). Another protein, p22, transiently interacts with the editosome and is specifically required for editing of cytochromes oxidase subunit II (9).

A number of other accessory proteins have been characterized, and these were either subsequently or simultaneously identified as components of an ill-defined RNA editing accessory complex. Three groups independently identified this multiprotein accessory complex by immunopurification and mass spectrometry of tagged gRNA-associated proteins, GAP1 and GAP2. This complex was named the mitochondrial RNA-binding complex 1 (MRB1) in *T. brucei* and gRNA-binding complex (GRBC) in *Leishmania major* (10–12). This MRB1/GRBC complex, hereafter called MRB1, has an imprecisely defined composition because the initial and subsequent MRB1 purifications identified both common and distinct components (10–14). MRB1 complex proteins characterized to date are essential for growth and affect RNA editing directly or indirectly at multiple steps including initiation (MRB3010, TbRGG2), 3′- to 5′-editing progression (TbRGG2), gRNA stabilization (GAP1/2 and REH2), as well as undefined steps of RNA editing (Tb11.02.5390 and Tb927.6.1680) (12,14–17). Additionally, some MRB1 pulldowns contain components of the MERS1 (mitochondrial edited mRNA stability) and kPAP1 (mRNA polyadenylation) complexes (12,17). The kPAP1 complex protein PPR1, also known as KPAF1, stimulates kPAP1 and RET1 post-editing 3′ A/U long tail addition, which marks the transcripts for translation (18). Thus, the MRB1 complex may play a central role in coordinating RNA editing, stability, polyadenylation and translation.

MRB1 pulldowns consistently identify a common set of proteins; however, copurification of other proteins varies depending on the component of MRB1 that is tagged and the laboratory (10–14). This variability suggests that the MRB1 complex is composed of subcomplexes that have different temporal and physical associations. Characterization of the MRB1 complex is further complicated by the RNA-dependent associations that are likely taking place. To understand the functional roles of this complex, we must first determine the physical associations that make up the MRB1 complex and its component subcomplexes and proteins. To this end, we undertook a large scale yeast two-hybrid analysis to characterize direct protein–protein interactions in the MRB1 complex. Additional affinity purifications of MRB1 components in the presence and absence of nuclease treatment, followed by immunoblots and mass spectrometric analysis, were used to confirm associations *in vivo,* and determine their RNA dependence. We identify a core MRB1 complex containing six proteins, GAP1, GAP2, MRB3010, MRB5390 (Tb11.02.5390), MRB8620 (Tb11.01.8620) and MRB11870 (Tb927.10.11870). The MRB1 core complex interacts with additional subcomplexes and proteins directly or in a manner enhanced by the presence of RNA. Yet other proteins associate with the MRB1 complex in a completely RNA-dependent manner. This work reveals the basic structural architecture of the MRB1 complex, which is essential in understanding its functions and their spatial and temporal organization. Overall, our results suggest a model in which the MRB1 core complex participates in multifaceted dynamic and RNA-dependent associations that coordinate the numerous roles of the MRB1 complex in mitochondrial RNA biogenesis and editing.

MATERIALS AND METHODS

Yeast two-hybrid screen

The complete open reading frames of 31 putative MRB1 genes were PCR amplified from either *T. brucei* procyclic form (PF) strains 29–13 genomic DNA or cDNA using Pfx (Invitrogen) or Phusion (Finnzymes) polymerase with the primers listed in the Supplementary Materials and Methods. PCR products were cloned into the yeast two-hybrid Gal4 activation domain (AD) vector pGADT7 and into the Gal4-binding domain (BD) vectors pAS2-1 or pGBKT7 (Clontech). Binary combinations of the plasmids (1 μg each) were cotransformed into the *Saccharomyces cerevisiae* strain PJ69-4 A using the lithium acetate method. Cotransformed yeast was plated to synthetically defined (SD) media lacking leucine (–leu) and tryptophan (–trp), and incubated for 3 days at 30°C. Next, 5–10 colonies of cotransformed yeast were inoculated onto SD (−leu/−trp) media, to select for the two cotransformed plasmids, and onto SD (−leu/−trp) also lacking histidine (−his), to select for protein–protein interaction. SD (−leu/−trp/−his) plates were supplemented with 1, 2, 3.5 and 5 mM 3-amino-1,2,4-triazole (3-AT), which inhibits PJ69-4 A yeast growth due to leaky expression of the HIS gene. The inoculated plates were incubated 3 days at 30°C. The entire procedure was repeated for each binary combination yielding growth.

Tagged cell line construction (plasmid construction, cell culture, transfection)

For PTP tagging, The C-terminal 400 bp of MRB6070 were cloned into the ApaI and NotI sites of pC-PTP (19) that was previously modified to contain the puromycin resistance gene (pC-PTP-PURO) (20), and the resulting pC-PTP-PURO-MRB6070 was digested at the unique MRB6070 cut site BoxI. The C-terminal 569 bp of MRB5390 were cloned into pC-PTP-PURO ApaI and NotI sites, and the resulting pC-PTP-PURO-MRB5390 was linearized at the unique BsgI site. The C-terminal 583 bp of MRB10130 were cloned into pC-PTP-PURO HindIII and NotI sites and the resulting pC-PTP-PURO-MRB10130 was linearized at the unique NcoI site. The C-terminal 518 bp of MRB11870 were cloned into pC-PTP-PURO using the ApaI and NotI sites, and the resulting pC-PTP-PURO-MRB11870 was linearized at the unique MfeI site. All plasmids were subsequently transfected into procyclic form *T. brucei* strain 29–13. To construct an RNAi vector for TbRGG2, a 350-nt DNA fragment corresponding to the TbRGG2 3′-UTR was cloned into the BamHI and HindIII sites of p2T7-177 vector. An amount of 50 μg of NotI linearized p2T7-177-TbRGG2 3′-UTR was transfected by

electroporation into 29–13 cells, and transformants were selected with phleomycin (2.5 μg/ml). Growth effects of TbRGG2-3′-UTR RNAi were monitored for at least 10 days in the absence or presence of 2.5 μg/ml tetracycline and protein downregulation was verified by immunoblotting. To construct the addback vector for myc-TbRGG2, the entire ORF of TbRGG2 was amplified and cloned into Zero blunt-end vector (Invitrogen). This TbRGG2 fragment was excised and cloned into HindIII and XbaI sites of p2Myc-100 vector (21). An amount of 50 μg of NotI linearized p2Myc-TbRGG2 was transfected into TbRGG2-3′-UTR RNAi cells. Transformants were selected with blasticidin (20 μg/ml) and downregulation of the endogenous TbRGG2 as well as expression of the exogenous myc-TbRGG2 was confirmed by immunoblotting. All primers used in this study are listed in Supplementary Table S1.

PTP purification and immunoprecipitation

Tandem affinity purification was carried out using 5×10^{10} procyclic cells containing the PTP-tagged proteins as described previously (19,22) except for minor modifications. Prior to binding the IgG Sepharose 6 Fast Flow column the supernatant was split in half. One-half was incubated with 50 U of the RNase inhibitor SuperaseIn (Ambion). The other half was treated with a nuclease cocktail containing RNase A (0.1 U/μl), RNase T1 (0.1 U/μl), RNase H (0.01 U/μl), RNase 1 (0.1 U/μl), RNase V1 (0.002 U/μl), DNase 1 (0.002 U/μl) and micrococcal nuclease (0.25 U/μl) (Fermentas) for 60 min on ice. The TEV eluates from the first step of the tandem affinity purification were analyzed by western blot. The tandem affinity purified eluates from the anti-protein C columns were analyzed by mass spectrometry. Myc affinity purification of TbRGG2 was carried out under similar conditions to the published PTP and TAP purification schemes. Mitochondrial extract from Day 4 TbRGG2-2myc overexpression PF cells was incubated with anti-myc polyclonal antibody (ICL laboratories) cross-linked to protein A sepharose beads (GE Healthcare) for 2 h at 4° in the presence of the SuperaseIn inhibitor and Complete Protease inhibitor (Roche). The flow through was collected and the column washed extensively with PBST (phosphate buffered saline with 0.1% NP-40). The antibody-antigen complex was disrupted using elutions of 100 mM glycine (pH 2.5). The eluted complexes were neutralized using 1 M Tris buffer (pH 8.7) and analyzed using western blotting.

Glycerol gradient

Mitochondria were enriched from 1×10^{10} PTP-MRB3010 RNAi procyclic cells as described previously (11). The enriched mitochondria were lysed in 1 ml of the lysis buffer (10 mM Tris at pH 7.2, 10 mM $MgCl_2$, 100 mM KCl, 1 mM DTT, 1 mg/ml pepstatin, 2 mg/ml leupeptin) with 1% Triton X-100 and treated with the nuclease cocktail described above for 60 min at 4°C. The lysate was cleared and loaded on a 11-ml 10–30% glycerol gradient and the gradient centrifuged at 32 000 rpm in a Beckman SW41 rotor for 16 h at 4°C. Twelve 0.5-ml fractions were then collected from the top and sedimentation of MRB proteins was analyzed by western blot.

Western blots

Proteins were transferred onto nitrocellulose membrane and probed with polyclonal antibodies against GAP1 (14), GAP2 (17), TbRGG2 (23) and KREPA6 (24) (a kind gift from Ken Stuart, Seattle BioMed) described previously. Polyclonal antibodies were produced against recombinant MRB11870 and the oligopeptides CNLSNETTSDLKGKENSEESQ (MRB6070) and CGNGPKDGTTIHSGPGGREK (MRB8170) (Bethyl Laboratories). Anti-MRB11870 antibodies were further affinity purified against recombinant MRB11870.

Mass spectrometry

LC–MS/MS analysis was performed by Dr Yuko Ogata at the Fred Hutchinson Cancer Research Center using LTQ mass spectrometer (Thermo Fisher Scientific). The LC system configured in a vented format (25) consisted of a fused-silica nanospray needle packed in-house with Magic C18 AQ 100 A reverse-phase media (Michrom Bioresources Inc.) and a trap containing Magic C18 AQ 200 A reverse-phase media. The peptide samples were loaded onto the column and chromatographic separation was performed using a two-mobile-phase solvent system consisting of 0.1% formic acid in water (A) and 0.1% acetic acid in acetonitrile (B). The mass spectrometer operated in a data-dependent MS/MS mode over the m/z range of 400–1800. For each cycle, the five most abundant ions from each MS scan were selected for MS/MS analysis using 35% normalized collision energy. Selected ions were dynamically excluded for 45 s. For data analysis, raw MS/MS data were submitted to the Computational Proteomics Analysis System (CPAS), a web-based system built on the LabKey Server (26) and searched using the X! Tandem search engine (27) against *T. brucei* protein database v. 4.0 (ftp://ftp.sanger.ac.uk/pub/databases/T.brucei_sequences/T.brucei_genome_v4/), which included additional common contaminants such as human keratin. The search output files were analyzed and validated by ProteinProphet (28). Proteins and peptides with a probability scores of ≥0.9 were accepted.

RESULTS

Identifying direct protein–protein interactions in the MRB1 complex by yeast two-hybrid analysis

The MRB1 complex has been ascribed multiple functions and overlapping protein compositions (10–14,16,17). However, these functional analyses of individual MRB1 complex components are difficult to interpret without an understanding of the RNA-dependent and RNA-independent protein–protein interactions and subcomplexes that comprise the large MRB1 complex. To gain an understanding of the architecture of this complex, or possibly a consortium of subcomplexes, we began by performing a comprehensive yeast two-hybrid

Table 1. *Trypanosoma brucei* mitochondrial MRB1 and MRB1-associated proteins analyzed in the comprehensive yeast two-hybrid screen

Tb Name	GeneDB #	Other Name or #	Complex(es)	Predicted Size (kDa)	LmjF homolog
MRB3010	Tb927.5.3010		MRB1 (10–14)[a,b,c,d,e]	57	LmjF08.1170
MRB5390	Tb11.02.5390		MRB1 (10–14)[a,b,c,d,e]	120	LmjF28.0340
MRB4160[f]	Tb927.4.4160		MRB1 (10–14)[a,b,c,d,e]	100[g]	LmjF31.0640
MRB8620	Tb11.01.8620		MRB1 (10–14)[a,b,c,d,e]	53[g]	LmjF32.3180
MRB8170[f]	Tb927.8.8170		MRB1 (10–14)[a,b,c,d,e]	100	LmjF31.0640
TbRGG2	Tb927.10.10830	Tb10.406.0050, RGGm	MRB1 (10,11,13)[a,b,d]	32	LmjF33.0260
GAP1	Tb927.2.3800	GRBC2	MRB1 (10–14)[a,b,c,d,e]	55	LmjF33.2730
GAP2	Tb927.7.2570	GRBC1	MRB1 (10–12,14)[a,b,c,e]	52	LmjF22.0650
Helicase	Tb927.4.1500	Hel1500, REH2	MRB1 (10–13)[a,b,d,e]	241	LmjF34.3230
MRB11870	Tb927.10.11870	Tb10.389.1910	MRB1 (11–14)[b,c,d,e]	34	LmjF33.1250
MERS1	Tb11.01.7290	NUDIX Hydrolase	MERS1 (12)[e] MRB1 (11)[b]	44	LmjF32.2440
MRB1820	Tb927.3.1820		MRB1 (11)[b]	25[g]	LmjF25.1740
MRB1860	Tb927.2.1860		MRB1 (10,13,14)[a,c,d]	96	LmjF33.1730
MRB6070	Tb927.2.6070		MRB1 (10)[a]	31[g]	
MRB800	Tb927.7.800		MRB1 (10,13,14)[a,c,d]	60	LmjF26.1140
MRB10130	Tb927.10.10130	Tb10.6k15.0150	MRB1 (10,14)[a,c]	61	LmjF36.4770
MRB8180[h]	Tb927.8.8180	Tb927.4.4150[h]	MRB1 (10,12,14)[a,c,e]	103	LmjF31.0630
MRB1680	Tb927.6.1680		MRB1 (10)[a]	58[g]	LmjF30.0260
MRB1590	Tb927.3.1590		MRB1 (10,11)[a,b]	72	LmjF25.1540
MRB0880	Tb11.01.0880		MRB1 (10,13,14)[a,c,d]	18	LmjF28.1810
kPAP1	Tb11.02.5820		kPAP (12)[e]	58	LmjF28.0780
7510	Tb11.01.7510		kPAP (12)[e]	86	LmjF32.2670
0024	Tb11.47.0024		kPAP (12)[e] MERS1 (12)[e]	98	LmjF27.0630
PPR5	Tb927.10.380	Tb10.70.7960	MRB1 (12)[e]	39	LmjF21.1620
3180	Tb11.02.3180		MRB1 (12)[e] kPAP (12)[e] MERS1 (12)[e]	94	LmjF24.0830
PPR1	Tb927.2.3180	kPAF1	MRB1 (12)[e] kPAP (12)[e]	114	LmjF18.0010
0130	Tb11.02.0130		MRB1 (12)[e] kPAP (12)[e] MERS1 (12)[e]	84	LmjF33.2510
3900	Tb927.10.6850	Tb10.6k15.3900	MRB1 (12)[e] kPAP (12)[e] MERS1 (12)[e]	36	LmjF36.2310
5120	Tb11.02.5120		MERS1 (12)[e]	104	LmjF28.0040
MRB2140	Tb927.6.2140	Hydratase	MRB1 (11,13)[b,d]	28	LmjF30.0705
TbRGG1	Tb927.6.2230	RGG1	MRB1 (11)[b]	88[g]	LmjF30.0780

MRB1 and MRB1-associated proteins identified by multiple groups in five manuscripts:
[a,b,c,d]Proteins are identified as components of indicated complex if present after RNase treatment.
[e]Proteins are identified as components of indicated complex if at least three peptides were identified and greater than half remained after RNase treatment.
[f]Both MRB8180/MRB4150 and MRB8170/MRB4160 are the result of a chromosomal duplication in *T. brucei* (but not *L. major*), and therefore these two proteins have the same single *L. major* homolog.
[g]Some of the predicted sizes for the *T. brucei* proteins are different from those listed on TriTrypDB because of alternative initiation site utilization.
[h]MRB8180/MRB4150 are 99% identical and thus are considered identical for the purpose of this study.
Tb, *T. brucei*; LmjF, *L. major*.

screen to identify direct protein–protein interactions. Here, we included 26 components reported in the three original MRB1 (also known as GRBC) purifications (10–12) and Tb11.01.0880, which was subsequently isolated with the REH2 helicase (13) and MRB3010 (14). In addition, some components of the kPAP1 polyadenylation and MERS1 RNA stability complexes were also associated with the MRB1 complex (12), prompting us to include four additional proteins reported to be components of the kPAP1 and/or MERS1 (but not MRB1) complexes. A complete list of the 31 proteins tested by yeast two-hybrid analysis is shown in Table 1. Throughout the manuscript, we refer to MRB1 components with the last four or five digits of their TriTrypDB designation, preceded by MRB, or by previously reported descriptive names. Unnamed proteins that are kPAP1 or MERS1 components are only listed by the last four digits of their TriTrypDB accession number.

For yeast two-hybrid analysis, genes encoding each of the 31 proteins were cloned into bait and prey vectors, and the resulting plasmids were cotransformed into yeast to screen for all 961 possible binary combinations. Selection was carried out on SD (−leu/−trp/−his) plates containing 1, 2, 3.5 or 5 mM 3-AT to eliminate background growth and establish increasingly stringent growth conditions. We categorized each interaction as strong or weak based on reproducible growth patterns as follows. Strong interactions were defined as those for which cotransformants grew robustly on plates containing 3.5 mM 3-AT, and weak interactions were defined as those for which cotransformants grew on plates containing 2 mM 3-AT, but not at higher 3-AT concentrations. An example of the selection and scoring scheme is shown in Figure 1A, where plasmid cotransformation was confirmed by growth on SD (−leu/−trp) and protein–protein interaction was screened on SD (−leu/−trp/−his) supplemented with 3-AT inhibitor. Interactions between TbRGG2-activation domain (AD) and MRB8180-BD, MRB8620-BD and TbRGG2-BD were scored as strong [shown as (+) in Figure 1] based on their robust growth at 3.5 mM 3-AT. Interactions

A

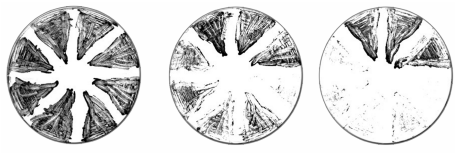

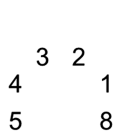

	Activation Domain	Binding Domain	Growth
1	RGG2	RGG2	+
2	RGG2	8180	+
3	RGG2	8620	+
4	RGG2	7510	wk
5	RGG2	0024	wk
6	RGG2	PPR5	wk
7	RGG2	GAP1	wk
8	RGG2	PPR1	--

B

	MRB3010	GAP1	Tb927.4.4160	Tb927.8.8170	Tb11.01.8620	TbRGG2	Tb11.02.5390	Tb927.10.11870	Tb927.3.1820	Tb927.3.1590	Tb927.10.10130	Tb927.8.8180	Tb11.01.0880	Tb11.01.7510	Tb11.47.0024	PPR5	Tb11.02.3180	PPR1	Tb11.02.0130
MRB3010	+	--	--	--	+	+	--	--	wk	--	--	--	--	--	--	--	--	--	--
GAP1	+	--	--	+	+	wk	--	wk	+	--	wk	--	--	--	--	--	--	--	--
Tb927.4.4160	--	--	--	--	wk	+	--	--	--	--	--	--	--	--	--	--	--	--	--
Tb927.8.8170	+	--	+	+	+	+	--	--	wk	--	--	--	--	--	--	wk	--	--	--
Tb11.01.8620	+	--	+	+	+	+	--	--	+	--	wk	--	--	--	--	--	--	--	--
TbRGG2	wk	--	+	+	--	+	--	--	--	--	wk	--	--	--	--	--	--	--	--
Tb11.02.5390	+	--	--	--	+	--	--	--	--	--	--	--	--	--	--	--	--	--	--
Tb927.10.11870	+	--	--	--	--	--	--	--	--	--	wk	--	--	--	--	--	--	--	--
Tb927.3.1820	--	+	--	--	--	wk	--	--	+	--	--	--	--	--	--	--	--	--	--
Tb927.3.1590	--	--	--	--	--	--	--	--	--	wk	--	--	--	--	--	--	--	--	--
Tb927.10.10130	wk	--	--	--	wk	+	--	--	--	--	--	--	--	--	--	--	--	--	--
Tb927.8.8180	--	--	--	--	wk	+	--	--	--	--	--	--	--	--	--	--	--	--	--
Tb11.01.0880	--	--	--	--	--	--	--	--	--	--	wk	--	--	--	--	--	--	--	--
Tb11.01.7510	wk	--	--	--	wk	wk	--	--	--	--	wk	--	--	--	--	--	--	--	--
Tb11.47.0024	wk	--	--	--	wk	wk	--	--	--	--	wk	--	--	--	--	--	--	--	--
PPR5	--	--	--	--	--	wk	--	--	--	--	wk	--	--	--	--	--	--	--	--
Tb11.02.3180	--	--	--	--	wk	--	--	--	--	--	--	--	--	--	--	--	--	--	--
PPR1	+	--	--	+	wk	--	--	--	--	--	--	--	--	--	--	--	--	--	--
Tb11.02.0130	wk	--	--	--	+	--	--	--	--	--	wk	--	--	--	--	--	--	--	--

Figure 1. Yeast two-hybrid analysis of direct interactions in the MRB1 complex. (**A**) Representative plates showing yeast cotransformed with bait (BD) and prey (activation domain). Yeast cells were grown on synthetically defined (SD) media (−leu/−trp) plates to select for cotransformants and subsequently grown on SD (−leu/−trp/−his) plates with 2 or 3.5 mM 3-AT to select for bait-prey interaction. Growth on 2 mM 3-AT but not 3.5 mM 3-AT was scored as a weak (wk) interaction, and growth on both 2 and 3.5 mM 3-AT was scored as a strong (+) interaction. (**B**) Summary of yeast two-hybrid results for all proteins showing at least one interaction (19 out of 31). The prey proteins are on the *x*-axis and the bait proteins are on the *y*-axis.

between TbRGG2-AD and GAP1-BD, 7510-BD and PPR5-BD (latter two are members of the kPAP1 complex proteins), and 0024-BD (member of the kPAP1 and MERS1 complexes) were scored as weak [shown as (wk) in Figure 1], based on growth at 2 mM, but not 3.5 mM 3-AT. The TbRGG2-AD/PPR1-BD interaction was scored as negative due to the absence of growth on 2 mM 3-AT. Using this scoring system, we designated each of the 961 binary interactions as strong, weak, or negative. In Figure 1B, we show a summary of the interactions only for those proteins that exhibited at least one interaction. Of the 31 proteins tested, 19 displayed interactions in at least one direction. The 12 proteins that showed no interactions are GAP2 (Tb927.7.2570), REH2 (Tb927.4.1500), MERS1 (Tb11.01.7290), Tb927.2.1860, Tb927.2.6070, Tb927.7.800, Tb927.6.1680, kPAP1 (Tb11.02.5820), Tb927.10.6850, Tb11.02.5120, Tb927.6.2140 and TbRGG1 (Tb927.6.2230). The absence of interactions in the yeast two-hybrid screen may reflect an RNA-dependent association between a given protein and the MRB1 complex. However, we cannot rule out that poor protein expression or the presence of the AD or BD tag precluded interactions in this assay.

In total, we observed 62 protein–protein interactions, 31 strong and 31 weak. Strikingly, a small number of proteins are responsible for the majority of interactions. The proteins MRB3010, GAP1, TbRGG2, MRB8620, MRB8170 and MRB4160 are involved in 30 of 31 strong interactions and 24 of 31 weak interactions. Notably, the protein MRB10130 is involved in many of the weak interactions (Figures 1B and 3). These results suggest these proteins are important binding partners in the MRB1 complex.

MRB1 contains a core subcomplex

We next set out to confirm a subset of the strong protein–protein interactions identified by the yeast two-hybrid screen using *in vivo* pull downs, followed by western blot, glycerol gradient, and mass spectrometry analysis. We generated PF *T. brucei* cell lines in which MRB5390 and MRB11870 were tagged at one endogenous locus with a C-terminal PTP (Protein A-TEV cleavage-Protein C) tag (19). We also utilized PTP-MRB3010 cell lines, which were previously described (14). Initially, we employed all available antibodies to detect proteins that copurify with the PTP-tagged proteins by western blot. Extracts were either incubated with RNase inhibitor (− RNases) or were pretreated with a cocktail containing RNases A, T1, V1, H and 1, DNase 1, and micrococcal nuclease (+ RNases). Untreated and nuclease treated extracts were subjected to IgG Sepharose chromatography and TEV protease cleavage, a protocol that avoids RNases that often contaminate proteins subjected to a second affinity chromatography step (29). Comparison of copurifying proteins from both RNase inhibited and nuclease treated extracts allows us to distinguish RNA-dependent, RNA-enhanced and RNA-independent interactions. Western blot analysis of proteins associated with PTP-MRB3010, MRB5390 and MRB11870 revealed numerous RNA-independent protein–protein

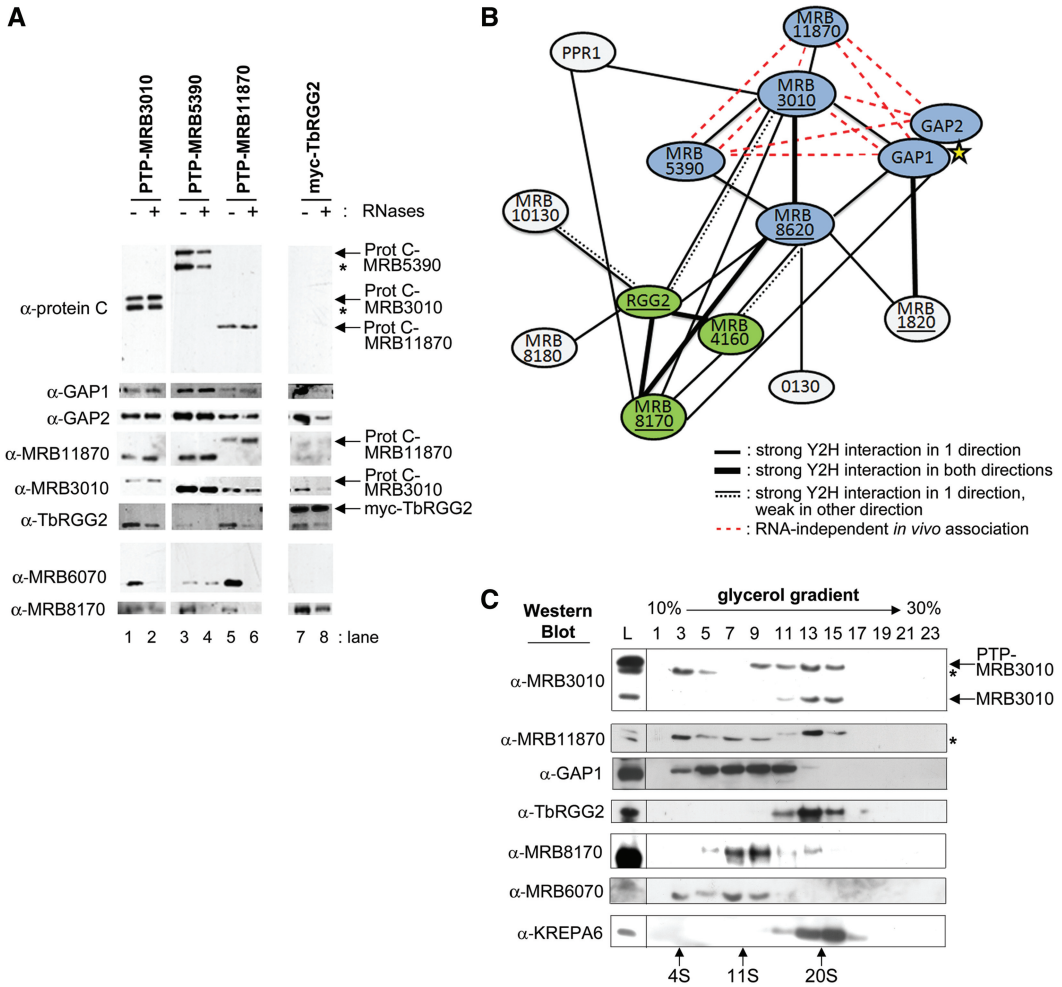

Figure 2. The MRB1 core complex and TbRGG2 subcomplex have RNA-independent and RNA-enhanced interactions. **(A)** Purification of MRB1 complexes from extracts of cells expressing PTP- or myc-tagged MRB1 components that were either nuclease treated (+ RNases) or left untreated (− RNases). Proteins were eluted from IgG Sepharose 6 Fast Flow columns by TEV protease cleavage or immunoprecipitated with anti-myc antibody and electrophoresed on SDS–PAGE gels, followed by immunoblot analysis using an antibody specific to protein C (to detect the PTP-tagged proteins) or antibodies specific to MRB1 complex proteins. Asterisks indicate breakdown products. **(B)** Schematic representation of all yeast two-hybrid (Y2H) strong interactions. Thin black lines represent a strong interaction in one direction, thick black lines represent strong interactions in both directions, a thin black line with a dashed line represents a strong interaction in one direction and a weak interaction in the other direction, and an underline represents self-interaction. The yellow star is used to indicate that the GAP1 and GAP2 interaction is based on previous work (12,17), not yeast two-hybrid results. The MRB1 core complex is shown in blue and the TbRGG2 subcomplex is shown in green. Red dashed lines represent RNA-independent interactions between core proteins identified in *in vivo* purifications in (A). **(C)** Glycerol gradient sedimentation of MRB components after RNase treatment. Mitochondrial extract from PF PTPMRB3010 cells was treated with RNases and fractionated on a 10–30% glycerol gradient. Alternate gradient fractions were electrophoresed on SDS–PAGE and immunoblotted with the indicated antibodies. The mitochondrial extract loaded on the gradient is shown on the left (abbreviated as L). Asterisks indicate breakdown products or a nonspecific band.

interactions, several of which confirmed direct interactions detected by yeast two-hybrid screen. Affinity purified PTP-MRB3010 associated *in vivo* with GAP1 and MRB11870 in an RNA-independent manner (Figure 2A, lanes 1 and 2), consistent with the direct MRB3010-GAP1 and MRB3010-MRB11870 interactions identified by yeast two-hybrid assay (Figures 1B and 2B). The latter interaction was corroborated by the reciprocal RNA-independent copurification of MRB3010 with PTP-MRB11870 (Figure 2A, lanes 5 and 6). Western blot analysis of affinity purified PTP-MRB5390 demonstrated an RNA-independent association between this protein and MRB3010 (Figure 2A, lanes 3 and 4), again supporting the direct interaction identified by yeast two-hybrid assay.

Unexpectedly, western blot analysis of nuclease treated extracts also revealed numerous RNA-independent interactions between GAP1, GAP2, MRB3010, MRB5390 and MRB11870 that were not detected by the yeast two-hybrid assay. For example, we observed RNA-independent associations between GAP2 and PTP-MRB3010, PTP-MRB5390 and PTP-MRB11870, although GAP2 showed no two-hybrid interactions (Figure 2A, lanes 1–6). Likewise, PTP-MRB5390 and PTP-MRB11870 associated with GAP1 in an RNA-independent manner even though these proteins lacked direct interactions by

yeast two-hybrid analysis (Figure 2A, lanes 3–6). These results suggest that the *in vivo* interactions between MRB5390, MRB11870 and GAP2 are indirect and mediated by other proteins such as MRB3010. The diagram in Figure 2B summarizes all strong yeast two-hybrid interactions, which are shown with solid black lines, and incorporates RNA-independent associations identified by *in vivo* tagged protein pulldowns as shown by dashed red lines. Collectively, the yeast two-hybrid screening and *in vivo* pulldown analyses support the presence of an RNA-independent subcomplex containing at least MRB5390, MRB3010, MRB11870, GAP1 and GAP2, which entails numerous direct and indirect interactions between these proteins (Figure 2B, shown in blue). The existence of such a subcomplex is consistent with all previous MRB1 complex pulldowns, the majority of which contained these five proteins [summarized in (14)]. We were not able to obtain an antibody against MRB8620 to test its copurification with the subcomplex proteins by western blot. However, yeast two-hybrid results demonstrating direct interactions between MRB8620 and MRB5390, MRB3010 and GAP1 (Figures 1B and 2B) in combination with mass spectrometric analyses of MRB1 complex components performed by our laboratories and others are consistent with MRB8620 constituting a sixth member of the subcomplex (Table 2) (10–14).

To further confirm the core complex composition and identify additional RNA-independent interactions within the MRB1 complex, we performed mass spectrometric analysis of proteins that associate with PTP-tagged MRB5390 and MRB11870 in an RNA-independent manner. PTP-MRB5390 and PTP-MRB11870 were isolated from nuclease treated extracts by tandem affinity purification via sequential IgG Sepharose chromatography, TEV cleavage and mAb anti-Protein C chromatography. PTP pulldowns contained likely contaminants including characterized nuclear and cytoplasmic proteins, and these additional proteins are listed in Supplementary Table S2. Of the 14 unlikely contaminant proteins identified in PTP-MRB5390 purifications, the six proteins with the highest amino acid sequence coverage were PTP-MRB5390 itself along with GAP1, GAP2, MRB3010, MRB8620 and MRB11870 (Table 2). Thus, the proposed core subcomplex components make up the six proteins with the highest coverage. These results are consistent with previous mass spectrometry results for PTP-MRB3010, in which these six proteins were also isolated with the highest amino acid coverage (14). In MRB11870 purifications, the six core subcomplex components were present, comprising 6 of the 10 proteins with the highest amino acid coverage (Table 2), again supporting RNA-independent interactions between these proteins. Mass spectrometry also revealed nuclease-resistant interactions between both PTP-MRB5390 and PTP-MRB11870 and reported MRB1 components TbRGG2, MRB8170/4160, MRB8180, MRB10130 and MRB800. In addition, PTP-MRB5390 copurified with MRB0880, while PTP-MRB11870 copurified with MRB1860, possibly reflecting specific or higher affinity interactions. Taken together, our yeast two-hybrid and *in vivo* copurification results indicate that a particle comprising MRB5390, MRB3010, MRB11870, MRB8620, GAP1 and GAP2 constitutes an RNA-independent core subcomplex of the larger MRB1 complex.

Next we wanted to determine if the core proteins function only within the core subcomplex, or if they have additional functions outside of the core. We fractionated mitochondrial lysates from nuclease treated PTP-MRB3010 cells on 10–30% glycerol gradients, and analyzed MRB component sedimentation by immunoblot. PTP-MRB3010 sediments in fractions 9–15 and endogenous MRB3010 appears in fractions 11–15, which corresponds to a size of $\leq$20 S as compared to the 20 S editosome marker, KREPA6 (Figure 2C, bottom) (14). A breakdown product of PTP-MRB3010 is also evident in fractions 3–5 (Figure 2C, top, asterisk) (14). MRB11870 cosediments with both endogenous and PTP-tagged MRB3010 primarily in fractions 11–15 (Figure 2C). Together with the pull down results in Figure 2B, this suggests that MRB3010 and MRB11870 exist primarily, if not exclusively, in the MRB1 core subcomplex. In contrast, GAP1 (and therefore its heterotetramer partner GAP2) sediments broadly in fractions 3–13 after nuclease treatment (Figure 2C). The small degree of cosedimentation of the GAP proteins with other core complex components suggests GAP1 and GAP2 have additional functions outside of the core subcomplex.

TbRGG2 exhibits RNA-enhanced interactions with core subcomplex and other proteins

TbRGG2 is an RNA-binding protein that impacts both initiation and 3′- to 5′-progression of RNA editing (15,23). In the yeast two-hybrid screen, TbRGG2 displayed numerous strong interactions with both the core subcomplex, as well as with MRB8170, MRB4160, MRB8180 and MRB10130 (Figures 1B and 2B). Regarding interactions with the core, in the yeast two-hybrid screen TbRGG2 bound strongly both MRB3010 and MRB8620 (Figure 1B). In the glycerol gradient fractionation of nuclease treated mitochondrial lysates TbRGG2 cosedimented in fractions 13–17 with the core proteins MRB3010 and MRB11870 (Figure 2C). To further examine interactions between TbRGG2 and the above-described MRB1 core *in vivo*, we performed anti-TbRGG2 western blots of affinity purified MRB3010, MRB5390 and MRB11870. PTP-MRB3010 pulled down TbRGG2 in both untreated and nuclease treated extracts, although the signal in nuclease treated extracts was markedly diminished (Figure 2A, lanes 1 and 2). Thus, we define the MRB3010–TbRGG2 interaction as RNA-enhanced. Notably, PTP-MRB11870 also pulled down TbRGG2 in an RNA-enhanced manner (Figure 2A, lanes 5 and 6), although these proteins did not interact in the yeast two-hybrid screen. This presumably reflects an indirect MRB11870–TbRGG2 interaction mediated through MRB3010. The core protein PTP-MRB5390 also pulled down TbRGG2 (Figure 2A, lanes 3 and 4), although the interaction appears to be weaker than that observed between TbRGG2 and other core components. In addition, the MRB5390-TbRGG2

Table 2. Proteins associated with RNase-treated MRB1 components were identified by LC–MS/MS

Locus tag	Name/motif	Unique peptides	Amino acid coverage (%)
PTP-MRB5390			
Tb927.7.2570	GAP2	18	50.30
Tb927.5.3010	MRB3010	19	47.10
Tb11.02.5390	MRB5390	47	46.20
Tb927.10.11870	MRB11870	11	43.90
Tb11.01.8620	MRB8620	17	30.40
Tb927.2.3800	GAP1	15	30.30
Tb927.10.10130	MRB10130	8	18.90
Tb11.01.0880	MRB0880	2	13.20
Tb09.160.5320	PhyH	2	11.70
Tb927.7.800	MRB800	4	11.20
Tb927.8.8180	MRB8180	7	8.50
Tb10.406.0050	TbRGG2	1	4.10
Tb927.8.8170	MRB8170/MRB4160	1	2.40
Tb927.4.4160			
Tb927.1.1730		1	2.30
PTP-MRB11870			
Tb11.02.5390	MRB5390	32	33.10
Tb927.5.3010	MRB3010	15	32.60
Tb11.01.0880	MRB0880	3	32.20
Tb927.10.11870	MRB11870	10	31.90
Tb927.10.10130	MRB10130	11	26.40
Tb09.160.5320	PhyH	4	25.70
Tb11.01.8620	MRB8620	12	24.70
Tb927.7.800	MRB800	9	21.90
Tb927.2.3800	GAP1	10	19.70
Tb927.7.2570	GAP2	8	18.80
Tb927.8.8180, Tb927.4.4150	MRB8180/MRB4150	10	13.10
Tb10.406.0050	TbRGG2	3	12.80
Tb927.2.1860	MRB1860	5	10.00
Tb927.7.5120	rRNA methylase	1	3.30
Tb927.8.8170, Tb927.4.4160	MRB8170/MRB4160	1	2.40
PTP-MRB10130			
Tb927.10.11870	MRB11870	11	48.40
Tb927.5.3010	MRB3010	21	46.50
Tb927.10.10130	MRB10130	19	45.90
Tb927.2.1860	MRB1860	22	34.20
Tb927.8.8180/ Tb927.4.4150	MRB8180/ MRB4150	26	32.30
Tb11.01.0880	MRB0880	4	32.20
Tb10.406.0050	TbRGG2	5	24.10
Tb927.7.800	MRB800	11	23.60
Tb927.2.3800	GAP1	8	22.80
Tb09.160.5320	PhyH	5	22.10
Tb11.02.5390	MRB5390	15	16.30
Tb927.7.2570	GAP2	6	15.60
Tb11.01.8620	MRB8620	6	13.70
Tb11.01.7290	MERS1	4	12.20
Tb927.3.1590	MRB1590	3	5.10
PTP-MRB6070			
Tb927.2.6070	MRB6070	12	*36.50*
Tb10.70.0820	UMSBP, ZnF	2	30.50
Tb10.406.0050	TbRGG2	6	28.10
Tb927.10.7910		3	20.60
Tb927.7.2570	GAP2	5	19.00
Tb10.389.1410	ZnF	3	18.30
Tb11.01.7290	Nudix	4	15.70
Tb927.2.3800	GAP1	4	15.00
Tb927.4.4160	MRB4160	11	12.10
Tb927.8.8180, Tb927.4.4150	MRB8180/MRB4150	8	11.30
Tb927.8.8170	MRB8170	8	9.60
Tb927.3.1590	MRB1590	3	8.50
Tb11.01.0880	MRB0880	1	8.00
Tb927.10.11870	MRB11870	2	5.50
Tb10.61.1690	ZnF	1	4.60
Tb927.3.2300	ZnF	1	4.50
Tb927.5.3010	MRB3010	1	2.90
Tb927.7.800	MRB800	1	1.80
Tb11.02.5390	MRB5390	1	1.50

Mass spectrometric analysis of proteins identified in tandem affinity purifications of nuclease treated extracts from PF cells containing endogenously PTP-tagged MRB1 complex components; MRB5390, MRB11870, MRB10130 and MRB6070. The numbers of unique peptides and amino acid coverage for each protein are shown. Proteins highlighted in gray are components of the MRB1 core complex.

interaction may be RNA-dependent, although the apparent absence of signal in the nuclease treated sample may reflect the overall weak signal. It is possible that different core components interact with TbRGG2 somewhat differently, or the PTP tag on MRB5390 may perturb its interaction with TbRGG2. Nevertheless, this interaction is likely indirect as MRB5390 and TbRGG2 did not interact in the yeast two-hybrid screen. The RNA-enhanced nature of the *in vivo* interactions between TbRGG2 and core components is in striking contrast to the RNA-independent interactions observed between the core components themselves, and further supports the composition of the core. Together, these results suggest that TbRGG2 interacts with the core subcomplex (through MRB3010 and perhaps MRB8620, as suggested by yeast two-hybrid results), but it is not part of the core.

To confirm the numerous TbRGG2 interactions detected in the yeast two-hybrid screen, we generated a PF *T. brucei* line overexpressing exogenous myc-tagged TbRGG2 in a 3′-UTR-based knockdown background, such that the tagged protein constitutes a large percentage of mitochondrial TbRGG2. Initially, we generated a PTP-tagged TbRGG2 cell line, but the cells had severely altered growth rates, likely a result of improper function of TbRGG2 with the larger tag. Immunopurification of myc-TbRGG2 was carried out using untreated or nuclease treated cell extracts, as previously described for the PTP-tagged proteins. Interestingly, myc-TbRGG2 coprecipitated endogenous TbRGG2 in an RNA-enhanced manner (Figure 2A, lanes 7 and 8). This result suggests that multiple TbRGG2 proteins, or TbRGG2-containing complexes, can bind the same RNA or associated RNAs. The core subcomplex proteins GAP1, GAP2 and MRB3010 also demonstrate RNA-enhanced associations with myc-TbRGG2 (Figure 2A, lanes 7 and 8), consistent with the reciprocal PTP-MRB3010 pulldown described above. The signal for MRB11870 in myc-TbRGG2 immunoprecipitates is low, and it is difficult to discriminate between an RNA-enhanced or RNA-dependent association. These data further support an RNA-enhanced interaction between TbRGG2 and the core subcomplex.

In addition to its interactions with the core subcomplex, TbRGG2 also exhibited strong yeast two-hybrid interactions with MRB8180, MRB10130, MRB4160 and MRB8170, with the latter two displaying strong interactions in both directions. The result of gene duplication unique to *T. brucei*, MRB4160 and MRB8170 display >80% homology and show a number of the same interactions in yeast two-hybrid screens, including the core protein MRB8620, TbRGG2 and MRB8170 itself (Figure 1B). In addition, MRB8170 interacts with PPR1 and the core proteins MRB3010 and GAP1 (Figures 1B and 2B). Interestingly, the existence of a subcomplex comprising TbRGG2, MRB8170 and MRB4160 (green in Figure 2B) was suggested by Madina *et al.* (29) based on the isolation of these three proteins with the endonuclease mRNP1, a non-MRB1 complex protein. The TbRGG2-MRB8170 interaction is supported by western blot analysis of myc-TbRGG2 pulldown, which shows an RNA-enhanced TbRGG2-MRB8170 interaction, with a large amount remaining after nuclease treatment (Figure 2A, lanes 7 and 8). Indeed, the diminished signal upon nuclease treatment may reflect in part RNA-dependent interactions between myc-TbRGG2 and TbRGG2–MRB8170–MRB4160 complexes formed with the endogenous TbRGG2 (Figure 2A, compare α-TbRGG2 and α-8170 in myc-TbRGG2 pull down lane).

Interactions between MRB8170 and the MRB1 core subcomplex were probed by anti-MRB8170 western blot analysis of PTP-MRB3010, PTP-MRB5390 and PTP-MRB11870 purifications. The latter two proteins exhibit an RNA-dependent association with MRB8170, while PTP-MRB3010 demonstrated an RNA-enhanced interaction with MRB8170 (Figure 2A, lanes 1–4). These results are consistent with MRB8170 (and perhaps MRB4160 and TbRGG2 in a subcomplex with it) associating with the core, but not comprising part of the core complex. Similar to TbRGG2, yeast two-hybrid results indicate that the interaction of MRB8170 with the core may be mediated by MRB3010 and MRB8620 (Figures 1B and 2B). Collectively, the yeast two-hybrid screen and *in vivo* pulldown results suggest a model in which TbRGG2, MRB8170, MRB4160 comprise a subcomplex with primarily RNA-enhanced interactions with the core subcomplex. In glycerol gradients, MRB8170 partially cosedimented with the core proteins MRB3010 and MRB11870 and TbRGG2 in fractions 11 and 13; however, MRB8170 peaked in fractions 7 and 9 (Figure 2C). These results suggest that MRB8170 engages in dynamic interactions with the core and TbRGG2.

ARM/HEAT repeat protein MRB10130 mediates multiple protein–protein interactions

In addition to the 31 strong interactions, yeast two-hybrid analysis identified 31 weak interactions amongst the MRB1 complex proteins (Figure 1B, diagrammed in Figure 3A). MRB10130 is involved in 11 of these interactions, demonstrating weak association with nine other proteins, including numerous core components (GAP1, MRB3010, MRB11870, MRB8620), TbRGG2, MRB0880 [identified through its interactions with the

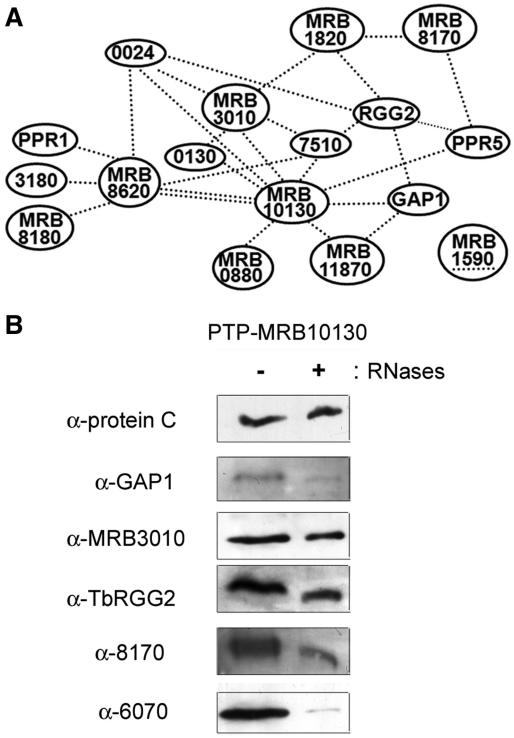

Figure 3. MRB10130 mediates multiple protein–protein interactions in the MRB1 complex. (**A**) Schematic representation of all protein–protein pairs exhibiting only weak interactions in the yeast two-hybrid screen. Each black dashed line represents a weak interaction in one direction and an underline represents self-interaction. (**B**) Purification of PTP-tagged MRB10130 from cell extracts that were either nuclease treated (+ RNases) or left untreated (− RNases). TEV protease eluates of IgG Sepharose 6 Fast Flow columns were analyzed by immunoblot as described in Figure 2.

REH2 RNA helicase (13) and MRB3010 (14)], PPR5 [a component of both MRB1 and kPAP1 complexes (12)], MRB0130 [also a MERS1 complex component (12)] and 0024 [a component of both kPAP1 and MERS1 complexes (12)]. The observation that MRB10130 mediates numerous, diverse interactions is particularly striking because analysis using the $(PS)^2$-v2 protein structure prediction server predicts that MRB10130 is almost entirely composed of ARM/HEAT repeat units, which often act as a protein–protein interaction platforms (30,31). To determine if these weak interactions involving MRB10130 are relevant *in vivo*, we generated PF *T. brucei* cells expressing PTP-tagged MRB10130 and performed pulldowns as described above. Mass spectrometric analysis of PTP-MRB10130 that had been tandem affinity purified from nuclease treated cell extracts identified a number of proteins that associated with MRB10130 in the yeast two-hybrid analysis (Table 2). This included TbRGG2, the only protein with which MRB10130 showed strong interaction, as well as 5 of the 9 proteins with which this protein exhibited weak two-hybrid interactions (MRB11870, MRB3010, GAP1, MRB8620 and MRB0880). PPR5, MRB0130, 7510 and 0024 were not identified in the pulldowns by mass spectrometry, yet they interacted with MRB10130 in

two-hybrid assays. Whether these four proteins have transient *in vivo* interactions with MRB10130 that are lost in the two-step purification, or are simply false positives, has yet to be determined. However, it is notable that we did identify MERS1 by mass spectrometry of MRB10130 purifications, which could reflect an interaction mediated by MRB0130 and/or 0024. Western blot analysis of TEV eluates from PTP-MRB10130 purifications reveals RNA-enhanced interactions between this protein and MRB3010, GAP1, MRB8170 and TbRGG2 (Figure 3B). These pulldowns thus support the *in vivo* relevance of the weak yeast two-hybrid interactions with both the MRB1 core and the TbRGG2 subcomplex. Collectively, the yeast two-hybrid and *in vivo* pulldown results suggest a role for MRB10130 in mediating numerous protein–protein interactions in the MRB1 complex, and possibly between MRB1 and other RNA-modifying complexes.

RNA-dependent associations in the MRB1 complex

As stated above, 12 of the 31 proteins tested by yeast two-hybrid analysis exhibited no interactions in this assay, although most have been identified in more than one MRB1 complex pulldown. This suggests that interaction of at least some of these proteins with the MRB1 core is entirely RNA-mediated. To test the RNA-dependent associations of a protein lacking direct interactions by yeast two-hybrid screen, we generated antibodies against MRB6070 (10,13), and analyzed its presence in untreated and nuclease treated MRB1 component pulldowns. MRB6070 was present in pulldowns of core components PTP-MRB3010 and PTP-MRB11870, as well as PTP-MRB10130 pulldowns, when extracts were untreated. However, MRB6070 was essentially absent if the same pulldowns were performed after nuclease treatment (Figure 2A, lanes 1 and 2, 5 and 6; Figure 3B). Western blots of TEV elutions from PTP-MRB5390 pulldowns showed a very weak association with MRB6070 in the presence or absence of RNase treatment; however, no MRB6070 peptides were identified in the mass spectrometric results (Figure 2A, lanes 3 and 4). This is similar to the relatively weak interaction between MRB5390 and TbRGG2, again suggesting that the tag on MRB5390 may affect some of its *in vivo* interactions. These results show that core proteins, MRB3010 and MRB11870, as well as MRB10130 associate with MRB6070 in a strictly RNA-dependent manner. Consistent with these results, MRB6070 fractionated on glycerol gradients in complexes of ≤11 S, smaller than the core proteins MRB3010 and MRB11870 (Figure 2C).

To further examine the interactions involving MRB6070 in the MRB1 complex, we generated a PF cell line expressing PTP-tagged MRB6070 and examined eluates of tandem affinity purification by western blot and mass spectrometry. Western blots of TEV elutions reveal RNA-dependent interactions with core subcomplex GAP1 and GAP2, RNA-enhanced interactions with TbRGG2, MRB8170 and endogenous MRB6070, but no interactions with the core subcomplex proteins MRB3010 and MRB11870 (Figure 4). Consistent with these results, mass spectrometry of the anti-protein C elution from

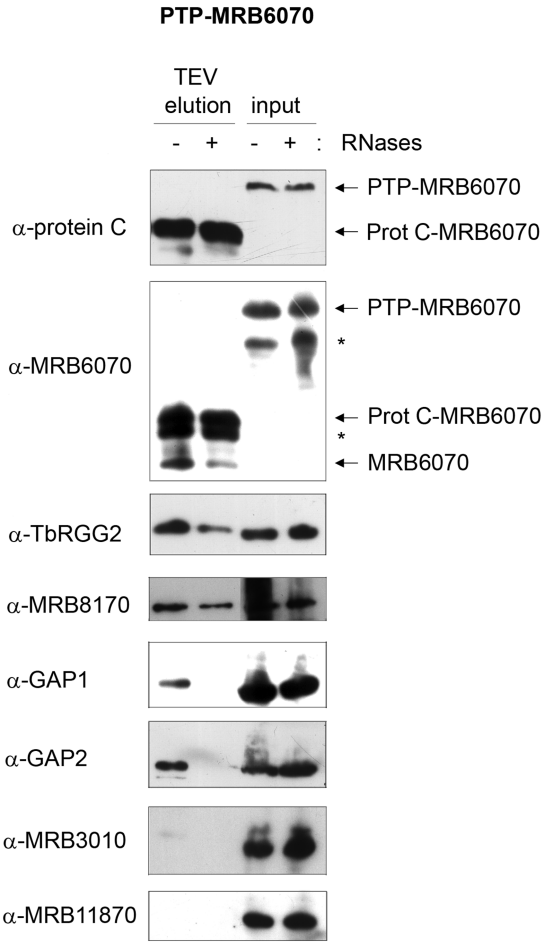

Figure 4. MRB6070 exhibits RNA-dependent interactions with MRB1 complex proteins. Purification of PTP-tagged MRB6070 from cell extracts that were either nuclease treated (+ RNases) or left untreated (− RNases). Both the cell extracts (input) and the eluates from TEV protease cleavage off IgG Sepharose columns (TEV elution) were analyzed by immunoblot as described in Figure 2. Asterisks indicate breakdown products.

RNase-treated PTP-MRB6070 extracts shows higher coverage for GAP1, GAP2, TbRGG2 and MRB8170, while MRB3010 and MRB11870 were identified by only 1 and 2 unique peptides, respectively (Table 2). The apparent preferential association of GAP1 and GAP2 with PTP-MRB6070 as compared to other core components supports our conclusion that the GAP1/2 heterotetramer can engage in interactions apart from the core subcomplex. MRB6070 also pulled down MRB8180 and MRB4150, which may be a TbRGG2-interacting protein (as suggested by yeast two-hybrid screen), and MRB4160 which is believed to be in a subcomplex with MRB8170 and TbRGG2 [Figure 1 and (29)]. Additional MRB1 components MRB1590 and MERS1, which only rarely copurify with the MRB1 complex are here pulled down with MRB6070 (Table 2). Mass spectrometry also identified a number of additional proteins that are not members of the MRB1 complex copurifying with PTP-MRB6070; most of these proteins contain zinc finger (ZnF) motifs, including the universal

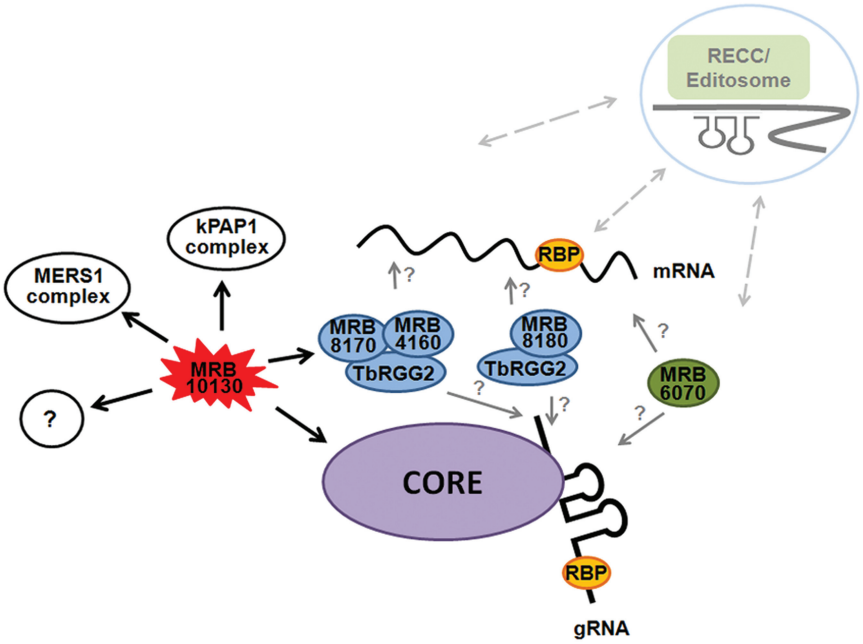

Figure 5. Model for MRB1 complex interactions. The core complex binds gRNA through GAP1/2. The TbRGG2 subcomplexes interact with the core and RNA. MRB6070 associates with the MRB1 complex in an RNA-dependent manner. The gray arrows and question marks indicate remaining questions regarding whether TbRGG2 subcomplexes and MRB6070 bind gRNA, mRNA, or both. MRB10130 binds the core, TbRGG2 subcomplex, MERS1 complex and kPAP1 complex and may coordinate association of these proteins. Because repression of numerous MRB1 components affects RNA editing, the MRB1 complex presumably interacts transiently with the RECC, as suggested by several studies.

minicircle-sequence binding protein (UMSBP). These results are consistent with a model in which MRB6070 interacts with the MRB1 complex through association with a common RNA. It is likely that a number of the other proteins that only purify with a subset of the MRB1 pulldowns also have RNA-dependent associations with the MRB1 complex.

DISCUSSION

MRB1 is a multifunctional complex with reported roles in numerous aspects of mitochondrial gene expression, including RNA editing and differing reported protein compositions (10–17). In this study, we address the architecture of the MRB1 complex by identifying the direct and indirect (protein- and RNA-mediated) interactions between its component proteins to provide a roadmap for understanding the function of the MRB1 complex and constituent subcomplexes and proteins. We identified a six-protein core subcomplex, containing GAP1, GAP2, MRB3010, MRB5390, MRB8620 and MRB11870 that interacts with other subcomplexes and proteins through RNA-enhanced and RNA-dependent interactions. Yeast two-hybrid and immunoblot analyses of affinity purified MRB1 complex proteins confirmed numerous direct and indirect interactions between the core complex proteins, which are independent of RNA. These results validate the consistent copurification of these six proteins in MRB1 pulldowns from various groups (10–14). The core complex also has numerous and likely dynamic interactions with other subcomplexes and proteins involved in various processes including RNA processing, polyadenylation, stabilization and editing (Figure 5). What is unclear at this point is whether the core is a structural coordinator for all of the functions associated with the MRB1 complex, whether it has a distinct function of its own, or if the core is responsible for both of these activities.

Although the function of the core complex as a whole is not known, some of its component proteins have been characterized. Knockdown experiments show that both MRB5390 and MRB3010 affect RNA editing of most transcripts, with MRB3010 having a role at an early step in the editing process (14,16). Knockdowns of GAP1 and GAP2 primarily cause destabilization of gRNAs, which was not seen with the MRB3010 knockdowns (12,14,17). Thus, while these proteins are all components of the core MRB1 complex, they appear to affect different steps of the editing process. This may in part be a result of using knockdowns to analyze protein function. With this method, not only do we observe the *in vivo* effect of the direct loss of the protein's activity, but if the protein has binding partners we may also see the effect of the loss of these interactions. Therefore, knocking down the protein results in phenotypes summarizing compromised function of some or all of the proteins it touches, highlighting the critical nature of the structural analysis undertaken in this study.

GAP1 and GAP2 form an α2/β2 heterotetramer that binds gRNAs *in vitro* and *in vivo* (12,32), and is likely responsible for mediating the interaction of the core complex with gRNAs. The inhibition of editing at an early stage by MRB3010 knockdowns suggests that one function of the core may be to recruit GAP1/2-bound

gRNA to the editing complex. However, it appears that GAP1/2 can also exist as a subcomplex apart from the core as evidenced by their enriched purification in the MRB6070 pulldown separate from the rest of the core (Table 2) as well as sedimentation separate from other core complex components (Figure 2C). Perhaps GAP1/2 exists as a heterotetramer when it initially binds the gRNA and then brings it to the core complex, although additional core proteins could facilitate GAP1/2-gRNA interaction. Interestingly, although GAP1 and GAP2 have 31% sequence identity and 48% sequence similarity, only GAP1 displayed interactions in the yeast two-hybrid screen. Although false negative results occur in yeast two-hybrid screens, our results may indicate that GAP1 is responsible for all protein interactions of the heterotetramer.

A number of other proteins demonstrated interaction with the core complex in our study, including TbRGG2. Indeed, apart from the core complex proteins, TbRGG2 and its interacting proteins are responsible for most of the remaining strong interactions by yeast two-hybrid screen. TbRGG2 and the paralogs MRB8170 and MRB4160 exhibited multiple interactions with each other and, thus, may exist as a subcomplex, although we cannot distinguish between multiple binary complexes or a single subcomplex containing these proteins from our results. Support for a TbRGG2 subcomplex, or subcomplexes, comes from the recent report that only TbRGG2, MRB8170 and MRB4160 copurified with the endoribonuclease mRNP1, which is involved in gRNA processing (29). Together, these data suggest these three proteins exist together apart from the rest of the MRB1 complex. Interestingly, the TbRGG2 subcomplex(es) containing MRB8170 and MRB4160 may not be the only subcomplex carrying TbRGG2. Mass spectrometry results from tandem affinity purifications of MRB10130 (a protein that has a strong interaction with TbRGG2 by yeast two-hybrid) revealed high amino acid coverage for TbRGG2; however, MRB8170 and MRB4160 were not present (Table 2). Rather, in these MRB10130 pulldowns, another protein that had a strong interaction with TbRGG2 in the yeast two-hybrid screen, MRB8180, exhibited high amino acid coverage comparable to that of TbRGG2 (Table 2). Additionally, TbRGG2 and MRB8170 had overlapping but distinct sedimentation patterns (Figure 2C). Thus, TbRGG2 may have multiple subcomplex associations within the MRB1 complex. The complexity of the TbRGG2 interactions in the MRB1 complex adds to the difficulty in determining the role of TbRGG2 in RNA editing. It is known that TbRGG2 is a multifunctional protein that affects gRNA utilization and editing processivity (15). However, the specific functions of the TbRGG2 subcomplex(es) or its binding partners including MRB8170, MRB4160, MRB8180 and MRB10130 are unknown. Although the TbRGG2 subcomplex(es) containing MRB8170 and MRB4160 was found associated with mRPN1, an endonuclease involved in gRNA processing, RNAi results for TbRGG2 suggest that gRNA processing is not one of its primary functions (15). TbRGG2 has two putative RNA-BDs, and *in vitro* binds RNA (23), so we postulate that TbRGG2 is one of the proteins responsible for MRB1 complex binding to RNA, possibly facilitating gRNA or mRNA association and utilization during editing. Where and when the different TbRGG2-binding partners play a role has yet to be determined, and we speculate that there may be temporal differences in these TbRGG2 associations.

The results discussed thus far suggest the occurrence of dynamic associations within the MRB1 complex, particularly with the core. Likely there are proteins whose purpose is to coordinate these interactions and processes, and an attractive candidate for this role is MRB10130. This protein is predicted on TriTrypDB to consist mostly of an ARM repeat Superfamily SSF48371 domain, and modeling analysis reveals that the majority of the protein forms HEAT repeats. ARM Superfamily proteins (which includes HEAT motif-containing proteins), often act as organizers of protein complexes because the superhelix of α-helices and hydrophobic core formed by tandem ARM repeat units creates a versatile platform for interactions with numerous partners (33–37). In fact, MRB10130 has numerous yeast two-hybrid interacting partners, all of which display weak interactions except for TbRGG2. Immunopurification experiments demonstrate clear association of MRB10130 with the core complex, TbRGG2 subcomplex(es), other MRB proteins and the MERS1 Nudix hydrolase. Could MRB10130 be facilitating binding of specific proteins with the core or the TbRGG2 subcomplex (Figure 5)? Could MRB10130 be coordinating association of the core and TbRGG2 subcomplex with each other? Does MRB10130 play a role in coordinating association of the kPAP1 and MERS1 complexes with the core? Further analysis is necessary to determine if MRB10130 is acting as an MRB1 complex organizer and how cooperative and/or competitive protein binding to MRB10130 plays a role.

Finally, a number of proteins previously identified in MRB1 pulldowns were included in our yeast two-hybrid screen, but exhibited no direct interactions in this assay. In some cases, this may be the result of false negatives; however, we anticipate that a number of these proteins have only RNA-dependent or transient interactions with the MRB1 complex. Likely, numerous RNA-binding proteins interact with gRNAs and mRNAs and through this associate with the MRB1 complex. Whether these proteins are essential for some of the functions carried out by the MRB1 complex has not been addressed. In this study, we identified an RNA-dependent component of the MRB1 complex, termed MRB6070. MRB6070 is predicted to contain 5–6 repeats of a Ran-binding protein 2 type ZnF domain which can act as either a protein recognition motif or a single-stranded RNA-binding motif (38). The fact that the yeast two-hybrid screen revealed no direct protein interactions with MRB6070, yet in pulldown experiments this protein consistently displayed RNA-dependent and RNA-enhanced interactions with other MRB1 proteins, suggests the ZnF motifs in MRB6070 function in RNA binding. Western blot analysis provided additional evidence for RNA-dependent association of MRB6070 with the MRB1 complex (Figures 2A and 3B), yet it remains

unknown if MRB6070 is interacting through mRNA, gRNA, or both (Figure 5). When MRB6070 was tandem affinity purified, mass spectrometry of associated proteins revealed primarily the RNA-binding proteins of the MRB1 complex (GAP1, GAP2, TbRGG2). The copurification of TbRGG2 and MRB8170 with PTP-MRB6070 after RNase treatment suggests these proteins are in close proximity on the same RNA, and thus the interactions are partially resistant to RNAse treatment (Figure 4), although we cannot exclude a direct interaction undetected by yeast two-hybrid analysis. The tandem affinity purification of PTP-MRB6070 also identified a number of other likely nucleic acid-binding proteins that were not previously identified as part of the MRB1 complex, including the UMSBP. The association of MRB6070 with UMSBP may be a result of either MRB6070 binding to nascent minicircle-encoded RNA, DNA-binding activity of MRB6070 and resultant interaction with UMSBP on the minicircle, or a role for UMSBP outside of DNA replication in which it interacts with MRB6070.

In conclusion, the present study provides significant insight into the direct and indirect interactions within the MRB1 complex. Our results suggest a dynamic complex comprised of subcomplexes and RNA-binding proteins that are likely subject to temporal and spatial regulation as they carry out numerous functions in mitochondrial gene regulation. The interaction studies described here illuminate potential functions of the MRB1 complex components, such as a direct role for the core in gRNA recruitment during RNA editing and a role for MRB10130 in MRB1 complex organization. They further provide a framework for the future interpretation of functional studies of proteins that comprise this enigmatic complex.

SUPPLEMENTARY DATA

Supplementary Data are available at NAR Online: Supplementary Tables S1 and S2.

ACKNOWLEDGEMENTS

The authors thank Drs Achim Schnaufer and Fred Ponticelli for advice on yeast two-hybrid screens and Dr Ken Stuart for the gift of anti-KREPA6 antibodies.

FUNDING

National Institutes of Health grants (RO1 AI061580 and RO1 AI077520 to LKR, F32 AI07718501 to J.C.F.); the Grant Agency of the Czech Republic (204/09/1667 to J.L.); the Praemium Academiae award to J.L.; and RNPnet FP7 program (289007 to J.L.). Funding for open access charge: NIH (grant NIAID AI077520).

Conflict of interest statement. None declared.

REFERENCES

1. Liu,T. and Bundschuh,R. (2005) Model for codon position bias in RNA editing. *Phys. Rev. Lett.*, **95**, 088101.
2. Lukeš,J., Hashimi,H. and Zíková,A. (2005) Unexplained complexity of the mitochondrial genome and transcriptome in kinetoplastid flagellates. *Curr. Genet.*, **48**, 277–299.
3. Stuart,K.D., Schnaufer,A., Ernst,N.L. and Panigrahi,A.K. (2005) Complex management: RNA editing in trypanosomes. *Trends Biochem Sci*, **30**, 97–105.
4. Fisk,J.C., Presnyak,V., Ammerman,M.L. and Read,L.K. (2009) Distinct and overlapping functions of MRP1/2 and RBP16 in mitochondrial RNA metabolism. *Mol. Cell Biol.*, **29**, 5214–5225.
5. Schumacher,M.A., Karamooz,E., Zíková,A., Trantírek,L. and Lukeš,J. (2006) Crystal structures of T. brucei MRP1/MRP2 guide-RNA binding complex reveal RNA matchmaking mechanism. *Cell*, **126**, 701–711.
6. Aphasizhev,R., Aphasizheva,I., Nelson,R.E. and Simpson,L. (2003) A 100-kD complex of two RNA-binding proteins from mitochondria of Leishmania tarentolae catalyzes RNA annealing and interacts with several RNA editing components. *RNA*, **9**, 62–76.
7. Ammerman,M.L., Fisk,J.C. and Read,L.K. (2008) gRNA/pre-mRNA annealing and RNA chaperone activities of RBP16. *RNA*, **14**, 1069–1080.
8. Li,F., Herrera,J., Zhou,S., Maslov,D.A. and Simpson,L. (2011) Trypanosome REH1 is an RNA helicase involved with the 3'-5' polarity of multiple gRNA-guided uridine insertion/deletion RNA editing. *Proc. Natl Acad. Sci. USA*, **108**, 3542–3547.
9. Sprehe,M., Fisk,J.C., McEvoy,S.M., Read,L.K. and Schumacher,M.A. (2010) Structure of the Trypanosoma brucei p22 protein, a cytochrome oxidase subunit II-specific RNA-editing accessory factor. *J. Biol. Chem.*, **285**, 18899–18908.
10. Panigrahi,A.K., Zíková,A., Dalley,R.A., Acestor,N., Ogata,Y., Anupama,A., Myler,P.J. and Stuart,K.D. (2008) Mitochondrial complexes in Trypanosoma brucei: a novel complex and a unique oxidoreductase complex. *Mol. Cell. Proteomics*, **7**, 534–545.
11. Hashimi,H., Zíková,A., Panigrahi,A.K., Stuart,K.D. and Lukeš,J. (2008) TbRGG1, an essential protein involved in kinetoplastid RNA metabolism that is associated with a novel multiprotein complex. *RNA*, **14**, 970–980.
12. Weng,J., Aphasizheva,I., Etheridge,R.D., Huang,L., Wang,X., Falick,A.M. and Aphasizhev,R. (2008) Guide RNA-binding complex from mitochondria of trypanosomatids. *Mol. Cell*, **32**, 198–209.
13. Hernandez,A., Madina,B.R., Ro,K., Wohlschlegel,J.A., Willard,B., Kinter,M.T. and Cruz-Reyes,J. (2010) REH2 RNA helicase in kinetoplastid mitochondria: ribonucleoprotein complexes and essential motifs for unwinding and guide RNA (gRNA) binding. *J. Biol. Chem.*, **285**, 1220–1228.
14. Ammerman,M.L., Hashimi,H., Novotná,L., Čičová,Z., McEvoy,S.M., Lukeš,J. and Read,L.K. (2011) MRB3010 is a core component of the MRB1 complex that facilitates an early step of the kinetoplastid RNA editing process. *RNA*, **17**, 865–877.
15. Ammerman,M.L., Presnyak,V., Fisk,J.C., Foda,B.M. and Read,L.K. (2010) TbRGG2 facilitates kinetoplastid RNA editing initiation and progression past intrinsic pause sites. *RNA*, **16**, 2239–2251.
16. Acestor,N., Panigrahi,A.K., Carnes,J., Zíková,A. and Stuart,K.D. (2009) The MRB1 complex functions in kinetoplastid RNA processing. *RNA*, **15**, 277–286.
17. Hashimi,H., Čičová,Z., Novotná,L., Wen,Y.Z. and Lukeš,J. (2009) Kinetoplastid guide RNA biogenesis is dependent on subunits of the mitochondrial RNA binding complex 1 and mitochondrial RNA polymerase. *RNA*, **15**, 588–599.
18. Aphasizheva,I., Maslov,D., Wang,X., Huang,L. and Aphasizhev,R. (2011) Pentatricopeptide repeat proteins stimulate mRNA adenylation/uridylation to activate mitochondrial translation in trypanosomes. *Mol. Cell*, **42**, 106–117.
19. Schimanski,B., Nguyen,T.N. and Gunzl,A. (2005) Highly efficient tandem affinity purification of trypanosome protein complexes based on a novel epitope combination. *Eukaryot. Cell*, **4**, 1942–1950.

20. Fisk,J.C., Sayegh,J., Zurita-Lopez,C., Menon,S., Presnyak,V., Clarke,S.G. and Read,L.K. (2009) A type III protein arginine methyltransferase from the protozoan parasite Trypanosoma brucei. *J. Biol. Chem.*, **284**, 11590–11600.
21. Goulah,C.C., Pelletier,M. and Read,L.K. (2006) Arginine methylation regulates mitochondrial gene expression in Trypanosoma brucei through multiple effector proteins. *RNA*, **12**, 1545–1555.
22. Gunzl,A. and Schimanski,B. (2009) Tandem affinity purification of proteins. *Curr. Protoc. Protein Sci.*, Chapter 19, Unit 19 19.
23. Fisk,J.C., Ammerman,M.L., Presnyak,V. and Read,L.K. (2008) TbRGG2, an essential RNA editing accessory factor in two Trypanosoma brucei life cycle stages. *J. Biol. Chem.*, **283**, 23016–23025.
24. Tarun,S.Z. Jr, Schnaufer,A., Ernst,N.L., Proff,R., Deng,J., Hol,W. and Stuart,K. (2008) KREPA6 is an RNA-binding protein essential for editosome integrity and survival of Trypanosoma brucei. *RNA*, **14**, 347–358.
25. Licklider,L.J., Thoreen,C.C., Peng,J. and Gygi,S.P. (2002) Automation of nanoscale microcapillary liquid chromatography-tandem mass spectrometry with a vented column. *Anal. Chem.*, **74**, 3076–3083.
26. Rauch,A., Bellew,M., Eng,J., Fitzgibbon,M., Holzman,T., Hussey,P., Igra,M., Maclean,B., Lin,C.W., Detter,A. *et al.* (2006) Computational Proteomics Analysis System (CPAS): an extensible, open-source analytic system for evaluating and publishing proteomic data and high throughput biological experiments. *J. Proteome Res.*, **5**, 112–121.
27. Craig,R. and Beavis,R.C. (2004) TANDEM: matching proteins with tandem mass spectra. *Bioinformatics*, **20**, 1466–1467.
28. Nesvizhskii,A.I., Keller,A., Kolker,E. and Aebersold,R. (2003) A statistical model for identifying proteins by tandem mass spectrometry. *Anal. Chem.*, **75**, 4646–4658.
29. Madina,B.R., Kuppan,G., Vashisht,A.A., Liang,Y.H., Downey,K.M., Wohlschlegel,J.A., Ji,X., Sze,S.H., Sacchettini,J.C., Read,L.K. *et al.* (2011) Guide RNA biogenesis involves a novel RNase III family endoribonuclease in Trypanosoma brucei. *RNA*, **17**, 1821–1830.
30. Tewari,R., Bailes,E., Bunting,K.A. and Coates,J.C. (2010) Armadillo-repeat protein functions: questions for little creatures. *Trends Cell Biol.*, **20**, 470–481.
31. Andrade,M.A., Petosa,C., O'Donoghue,S.I., Muller,C.W. and Bork,P. (2001) Comparison of ARM and HEAT protein repeats. *J. Mol. Biol.*, **309**, 1–18.
32. Aphasizheva,I. and Aphasizhev,R. (2010) RET1-catalyzed uridylylation shapes the mitochondrial transcriptome in Trypanosoma brucei. *Mol. Cell Biol.*, **30**, 1555–1567.
33. Giesecke,A. and Stewart,M. (2010) Novel binding of the mitotic regulator TPX2 (target protein for Xenopus kinesin-like protein 2) to importin-alpha. *J. Biol. Chem.*, **285**, 17628–17635.
34. Xu,W. and Kimelman,D. (2007) Mechanistic insights from structural studies of beta-catenin and its binding partners. *J. Cell Sci.*, **120**, 3337–3344.
35. Zhao,G., Li,G., Schindelin,H. and Lennarz,W.J. (2009) An Armadillo motif in Ufd3 interacts with Cdc48 and is involved in ubiquitin homeostasis and protein degradation. *Proc. Natl Acad. Sci. USA*, **106**, 16197–16202.
36. Sampietro,J., Dahlberg,C.L., Cho,U.S., Hinds,T.R., Kimelman,D. and Xu,W. (2006) Crystal structure of a beta-catenin/BCL9/Tcf4 complex. *Mol. Cell*, **24**, 293–300.
37. Nardozzi,J., Wenta,N., Yasuhara,N., Vinkemeier,U. and Cingolani,G. (2010) Molecular basis for the recognition of phosphorylated STAT1 by importin alpha5. *J. Mol. Biol.*, **402**, 83–100.
38. Nguyen,C.D., Mansfield,R.E., Leung,W., Vaz,P.M., Loughlin,F.E., Grant,R.P. and Mackay,J.P. (2011) Characterization of a family of RanBP2-type zinc fingers that can recognize single-stranded RNA. *J. Mol. Biol.*, **407**, 273–283.

Attached Publications

Part I. Trypanosome RNA editing

Lucie Kafková, Michelle L. Ammerman, Drahomíra Faktorová, John C. Fisk, Sara L. Zimmer, Roman Sobotka, Laurie K. Read, Julius Lukeš and Hassan Hashimi[†] (2012). Functional characterization of two paralogs that are novel RNA binding proteins influencing mitochondrial transcripts of Trypanosoma brucei. *RNA* 18: 1846-1861. [Erratum: 18:2345-2345].

This paper describes two paralogs called MRB8170 and MRB4160 that are subunits of the TbRGG2 subcomplex of MRB1. They represent almost novel RNA binding proteins that influence pan-edited RNAs to differing degrees. They are the product of a chromosome duplication event happening in *T. brucei*, thus sharing sequence identity on the DNA level throughout most of the genes. Functional analysis of each individual protein was a challenge that was overcome by targeting small, unique regions of the encoding mRNAs by RNAi.

[†]Corresponding author

Functional characterization of two paralogs that are novel RNA binding proteins influencing mitochondrial transcripts of *Trypanosoma brucei*

LUCIE KAFKOVÁ,[1,2,5] MICHELLE L. AMMERMAN,[3,5] DRAHOMÍRA FAKTOROVÁ,[2] JOHN C. FISK,[3] SARA L. ZIMMER,[3] ROMAN SOBOTKA,[2,4] LAURIE K. READ,[3] JULIUS LUKEŠ,[1,2] and HASSAN HASHIMI[1,2,6]

[1]Biology Center, Institute of Parasitology, Czech Academy of Sciences, University of South Bohemia, 370 05 České Budějovice (Budweis), Czech Republic
[2]Faculty of Sciences, University of South Bohemia, 370 05 České Budějovice (Budweis), Czech Republic
[3]Department of Microbiology and Immunology, School of Medicine, State University of New York at Buffalo, Buffalo, New York 14214, USA
[4]Institute of Microbiology, Czech Academy of Sciences, 379 81 Třeboň, Czech Republic

ABSTRACT

A majority of *Trypanosoma brucei* proteins have unknown functions, a consequence of its independent evolutionary history within the order Kinetoplastida that allowed for the emergence of several unique biological properties. Among these is RNA editing, needed for expression of mitochondrial-encoded genes. The recently discovered mitochondrial RNA binding complex 1 (MRB1) is composed of proteins with several functions in processing organellar RNA. We characterize two MRB1 subunits, referred to herein as MRB8170 and MRB4160, which are paralogs arisen from a large chromosome duplication occurring only in *T. brucei*. As with many other MRB1 proteins, both have no recognizable domains, motifs, or orthologs outside the order. We show that they are both novel RNA binding proteins, possibly representing a new class of these proteins. They associate with a similar subset of MRB1 subunits but not directly with each other. We generated cell lines that either individually or simultaneously target the mRNAs encoding both proteins using RNAi. Their dual silencing results in a differential effect on moderately and pan-edited RNAs, suggesting a possible functional separation of the two proteins. Cell growth persists upon RNAi silencing of each protein individually in contrast to the dual knockdown. Yet, their apparent redundancy in terms of cell viability is at odds with the finding that only one of these knockdowns results in the general degradation of pan-edited RNAs. While MRB8170 and MRB4160 share a considerable degree of conservation, our results suggest that their recent sequence divergence has led to them influencing mitochondrial mRNAs to differing degrees.

Keywords: RNA editing; RNA binding protein; ribonuclear protein (RNP); mitochondria; trypanosome

INTRODUCTION

Trypanosoma brucei subspecies are the etiological agents of several neglected human and veterinary diseases that mainly impact sub-Saharan Africa, as epitomized by sleeping sickness and nagana. Our understanding of the underlying biology of this flagellate has certainly been advanced by the release of its genome, along with those of its parasitic cohorts *Trypanosoma cruzi* and *Leishmania major*. However, there is much fertile ground for future research because more than half of the predicted *T. brucei* proteins are of unknown function (El-Sayed et al. 2005).

The unfamiliar nature of the *T. brucei* proteome is not surprising given that it belongs to the order Kinetoplastida, a clade that has several unusual biological features due to its long and independent evolutionary history (Philippe et al. 2000). Most notable of these is the kinetoplast (k) DNA that ultimately lends its name to the whole order (Shlomai 2004; Lukeš et al. 2005). This DNA, usually arranged in the form of a network, represents the mitochondrial (mt) genome, which is made up of two types of circular molecules. In *T. brucei*, thousands of ~1 kb-long minicircles, heterogeneous in sequence, constitute the bulk of kDNA, while the dozens of ~23 kb-long maxicircles resemble the mt genomes of other aerobic eukaryotes because they contain rRNA and protein-coding genes, which predominantly encode subunits of the respiratory complexes (Shlomai 2004; Lukeš et al. 2005).

The complicated affair that is maxicircle gene expression is also a distinguishing feature of kinetoplastid flagellates.

[5]These authors contributed equally to this work.
[6]**Corresponding author**
E-mail hassan@paru.cas.cz

Article published online ahead of print. Article and publication date are at http://www.rnajournal.org/cgi/doi/10.1261/rna.033852.112.

Twelve out of the 18 protein-coding mt genes in *T. brucei* are encrypted, and their mRNAs require for their maturation a post-transcriptional process called kinetoplastid (k) RNA editing (Simpson et al. 2004; Lukeš et al. 2005; Stuart et al. 2005). Uridine (U) residues are inserted into or deleted from preordained sites of the edited mRNA to render a meaningful open reading frame (ORF). The extent of this process varies from the so-called pan-edited mRNAs that require the insertions of hundreds and deletions of dozens of U's throughout the molecule to minimally edited mRNAs that bear short regions where U insertions occur. Numerous 50- to 70-bp-long noncoding guide (g) RNAs encoded predominantly in the minicircles act true to their name by directing the kRNA editing machinery to the appropriate sites of U-insertion/deletion on the mRNA. For pan-edited mRNAs, a series of gRNA:mRNA annealing events decodes the ORFs from a 3′-to-5′ direction (Maslov and Simpson 1992).

Many proteins, usually as subunits of macromolecular complexes, make up the kRNA editing machinery. Among the best characterized of these components is the RNA editing core complex (RECC), also known as the 20S editosome (Simpson et al. 2010). This complex encompasses the cascade of enzymatic activities for U-insertion/deletion events: An endonuclease cleaves the mRNA at the editing site dictated by the gRNA, which also provides information to RECC for how many U's are inserted or deleted here by a terminal uridylyltransferase (TUTase) or exonuclease, respectively; in the last step, the processed site is sealed within the mRNA by an RNA ligase. These activities are being explored as potential drug targets for treating these pathogens in their mammalian hosts (Durrant et al. 2010; Moshiri et al. 2011).

RECC actually occurs in three forms that, while containing overlapping subunits, are distinguished by others that confer specificity to a particular type of editing event (Panigrahi et al. 2006; Carnes et al. 2008, 2011). Notably, each RECC bears one of three types of endonucleases that are able to exclusively cleave U-insertion or U-deletion editing sites, plus one that is created by a unique *cis*-acting gRNA element within the 3′-UTR of an edited mRNA (Golden and Hajduk 2005). As implied by the name RECC, other proteins play a role in kRNA editing as well as other aspects of kinetoplastid mtRNA metabolism. The heterotetrameric complex that is formed by the two mtRNA binding proteins MRP1/2 is believed to facilitate gRNA:mRNA duplex formation (Schumacher et al. 2006; Zíková et al. 2008), as is the RBP16 protein (Ammerman et al. 2008). RNAi-mediated depletion of either of these entities affects only a subset of edited mRNAs (Pelletier and Read 2003; Vondrušková et al. 2005), while their simultaneous down-regulation leads to a more pronounced reduction of the overall panel of these transcripts (Fisk et al. 2009). RNA editing helicase (REH) 1 comes into play after editing of a given site is completed by unwinding the utilized gRNA from its cognate mRNA, a particularly important task in maturation of pan-edited mRNAs that require many of these small molecules (Li et al. 2011). TbRGG1 is a poly(U) binding protein that appears to have a role in the stability of mRNAs that have completed editing (Vanhamme et al. 1998; Hashimi et al. 2008). An enzyme called RNA editing TUTase 1 (RET1) is responsible for the post-transcriptional addition of a short 3′-poly(U) tail onto the *trans*-acting gRNAs, an essential feature of these molecules (Aphasizhev et al. 2003).

The gRNAs are not the only species in the mt transcriptome that is modulated by RET1, because polyuridylylation is a widespread processing event in the organelle (Ryan and Read 2005; Aphasizheva and Aphasizhev 2010). The mRNAs occur in two populations distinguished by 3′-extensions that are composed of short poly(A) (~20 nt) or long A/U tails (~200 nt) (Bhat et al. 1992; Militello and Read 1999; Etheridge et al. 2008). A mt poly(A) polymerase (KPAP1) is responsible for the former structure while KPAP1 and RET1 act in concert with two pentatricopeptide repeat (PPR) proteins to produce the latter, a feature that marks mature mRNAs for translation (Ryan and Read 2005; Etheridge et al. 2008; Aphasizheva et al. 2011). In contrast to such a plethora of polyuridylylation events, a novel RNase D exoribonuclease targets the gRNA poly(U) tail, perhaps serving to fine-tune this heterogeneous population of molecules (Zimmer et al. 2011). A close homolog of the RECC endonucleases has been recently shown to process polycistronic minicircle transcripts to yield functional gRNAs of the appropriate size and has thus been dubbed mtRNA precursor-processing endonuclease 1 (mRPN1) (Madina et al. 2011).

Contributing to kRNA metabolism is the recently discovered mtRNA binding complex 1 (MRB1), whose subunits appear to have diverse functions (Hashimi et al. 2008; Panigrahi et al. 2008; Weng et al. 2008). MRB1 was so named because among its constituent proteins are those having motifs that clearly indicate a role in mtRNA metabolism. However, most MRB1 subunits lack these features or orthologs outside of the kinetoplastid flagellates, obscuring their specific roles in kRNA processing/maintenance. A further impediment to understanding MRB1 is that reported isolations from different groups contain both overlapping as well as differing proteins (summarized in Ammerman et al. 2011). However, recent work based on a pairwise yeast two-hybrid screen of 31 putative MRB1 subunits has defined the architecture of MRB1 (Ammerman et al. 2012). It is composed of a core, which persisted in all reported isolations, of the following proteins: the two gRNA-associated proteins GAP1 and 2 (also known as GRBC), MRB3010, MRB5390, MRB8620, and MRB11870 (Ammerman et al. 2012). Furthermore, there are peripheral subcomplexes that interact with this core in an RNA-enhanced or -dependent manner, possibly reflecting a dynamic assembly onto kRNAs undergoing processing.

Adding to the difficulty in pinpointing the role of MRB1 is the variety of apparent functions of its studied subunits. The two paralogous GAPs partner with each other in a way reminiscent of the aforementioned MRP1/2 complex and

promote the stability of these short RNAs (Weng et al. 2008; Hashimi et al. 2009). The REH2 RNA helicase, which has been identified in some MRB1 isolates, also appears to have a still-undefined role during the lifetime of the gRNAs that also affects their stability (Hashimi et al. 2009; Hernandez et al. 2010). Ablation of the core MRB3010 by RNAi indicates that it facilitates an early step in RNA editing while not directly affecting gRNAs (Ammerman et al. 2011). TbRGG2, a peripheral MRB1 protein outside of the core, participates in the progression of multi-round editing required by pan-edited transcripts in an evocative fashion of the previously mentioned REH1 (Fisk et al. 2008; Acestor et al. 2009; Ammerman et al. 2010). A Nudix hydrolase (also called MERS1) has a role in the stability of potentially all mRNAs (Weng et al. 2008; Hashimi et al. 2009).

In this study, we investigate the functions of two MRB proteins called MRB8170 and MRB4160 that are paralogs sharing striking sequence similarity on the DNA level, a result of a duplication event that occurred during or after the speciation of *T. brucei* (Jackson 2007). MRB8170 and MRB4160 have no known motifs or orthologs outside the sequenced kinetoplastid flagellates. They have been shown to interact with the pre-gRNA processing endonuclease mRPN1 in an RNA-independent manner, although their direct contact with this enzyme was not verified by yeast two-hybrid analysis (Madina et al. 2011). However, it is known that their association with the MRB1 core is mediated by their interaction with TbRGG2 (Ammerman et al. 2012). We found that each protein associates with a highly similar subset of core and peripheral MRB1 subunits, while showing no direct interaction with each other, thus clarifying their status within the MRB1 complex. Very significantly, MRB8170 and MRB4160 bind RNA and thus represent a novel, kinetoplastid-restricted class of nucleic acid binding proteins. Finally, to elucidate their function within MRB1, we used RNAi-silencing techniques. Single knockdown of MRB8170 or MRB4160 did not affect procyclic cell growth, although mild effects on abundance of some edited and pre-edited transcripts were observed with MRB8170 depletion only. In contrast, tandem MRB8170/4160 RNAi silencing inhibits cell growth, coinciding with a substantial depletion of pan-edited RNAs and a significant, although qualitatively and quantitatively different effect on moderately edited transcripts. Thus, we conclude that while these proteins do have a fair degree of functional redundancy in their critical role in the MRB1 complex, although some suggestions of functional divergence are evident.

RESULTS

The two paralogous *MRB8170* and *MRB4160* genes share a highly conserved sequence

The *MRB8170 and MRB4160* genes are located within regions of chromosomes 8 and 4, respectively, that are products of a large 0.5-Mb duplication event that occurred solely in the *T. brucei* lineage (Jackson 2007) and is absent from the other Trypanosomatids such as *Leishmania* species and *T. cruzi*. These genes are among the 47% of such duplicated coding sequences (CDS) retained in both locations. In the immediate genomic neighborhood of the *MRB8170/MRB4160* genes, they can be thought of as being the first in an array of five genes that are found on both chromosomes (Fig. 1A). Using chromosome 4 as a reference, this array is bounded downstream from *MRB4160* by *Tb927.4.4170*, encoding a putative rRNA methyltransferase that has been lost in chromosome 8. This pair of genes is present in a syntenic block on chromosome 8 of *Trypanosoma congolense*, a species closely related to *T. brucei* that is the major causative agent of nagana, and thus can be considered the ancestral state of this locus. Interestingly, it is the *MRB8170* CDS that shares slightly higher sequence identity to the *T. congolense* ortholog than *MRB4160* (Fig. 1A).

The translated *MRB8170 and MRB4160* genes have a predicted molecular weight of 100 kDa and share 77.3% amino acid sequence identity, taking into account that the ORF of the latter gene actually starts at the first ATG internal to the annotated start codon (Supplemental Fig. 1; Nilsson et al. 2010; Siegel et al. 2010). However, most of the sequence divergence is restricted to a 5′ region comprising 15% of the ORFs (Fig. 1B). The remaining 85% of the two CDSs exhibit high conservation with 90.2% sequence DNA identity, which is similar to the 90.1% identity between the two predicted 3′-untranslated regions (UTRs) (Jackson 2007). The similarity of the two 3′-UTRs implies that MRB8170 and MRB4160 mRNAs have comparable degrees of post-transcriptional regulation (Jackson 2007).

It should be noted that MRB8170 and MRB4160 are not the only two MRB1 proteins whose genes are located in these paralogous loci (Fig. 1A). A subunit designated MRB8180 (Tb927.8.8180) is encoded in the 3′-CDS adjacent to MRB8170, while MRB4150 (Tb927.4.4150) is located directly downstream from MRB4160. Interestingly, *MRB4150* and *MRB8170* are virtually indistinguishable from each other as they share 99.1% sequence identity, in contrast to the divergence between *MRB8170* and *MRB4160* (Fig. 1B).

Both MRB8170 and MRB4160 have in vitro RNA binding activity

The amino acid compositions of MRB8170 and MRB4160 confer basic theoretical isoelectric points (pI) 9.48 and 9.64, respectively. This property is suggestive of RNA binding ability, since it signifies a net positive charge of the polypeptide at physiological pH, which would promote interaction with negatively charged nucleic acids. To test whether MRB8170 and MRB4160 are indeed RNA binding proteins, recombinant MRB8170 and MRB4160 were isolated from *E. coli* via an incorporated GST tag. Surprisingly,

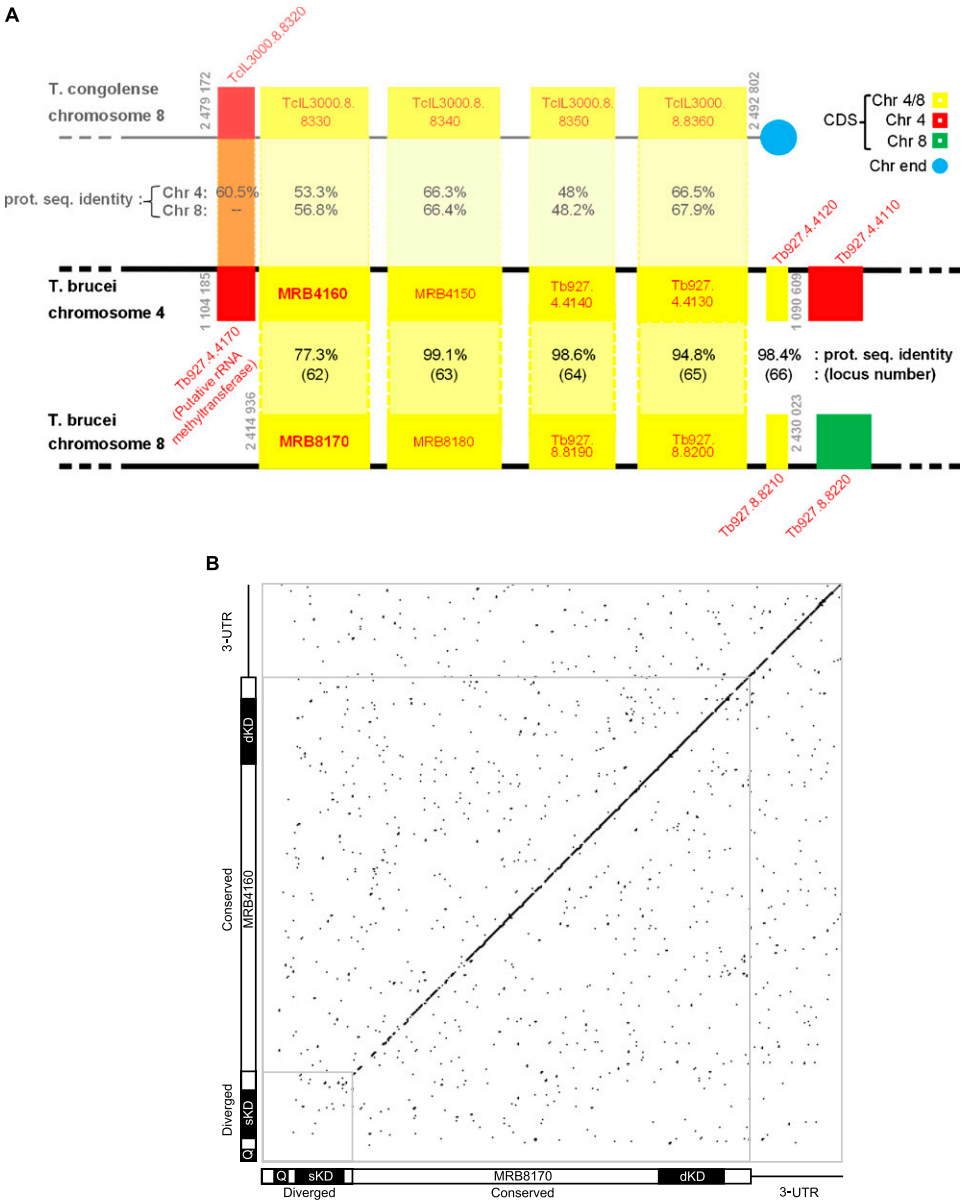

FIGURE 1. The paralogous *MRB8170* and *MRB4160* genes. (*A*) Scheme showing that the *kMAP* genes are part of an array of five paralogs retained on both chromosomes 4 and 8 arising from a duplication event (*bottom* two black lines). In addition, a syntenic region of *T. congolense* chromosome 8 (*top* gray line) is aligned to the gene array present on *T. brucei* chromosome 4. CDSs are depicted as boxes with either its name or locus tag given inside or adjacently just above or below the box in red letters. *MRB8170* and *MRB4160* loci are in bold. Paralogs retained on both *T. brucei* chromosome 4 and 8 are yellow, only on the former in red and the latter in green. The *top* number in the shaded region between the duplicated CDSs is the percentage protein sequence identity between them according to a ClustalW alignment performed in the BioEdit program. The *bottom* number in parentheses is the locus number as given by Jackson (2007), from which this figure is adapted. The numbers in the shaded region between *T. congolense* chromosome 8 and *T. brucei* chromosome 4 represent the protein sequence identity of the CDSs from the former with *T. brucei* chromosomes 8 (*top*) and 4 (*bottom*) as calculated previously. The chromosome location at the beginning and end of the array of genes in question is given in gray adjacent to the relevant bounding CDS. (*B*) Dot-plot comparing the CDSs plus 3′-UTRs of *MRB8170* (*x*-axis) and *MRB4160* (*y*-axis) to reveal regions of nucleotide sequence identity. Nucleotide matches are represented as a black dot. The diagonal represents the identical regions of the two sequences. The small gray square in the lower *left-hand* corner encloses the diverged region of two sequences. Schemes depicting the relevant regions of *MRB8170 and MRB4160* are provided along the axes. The diverged and conserved regions are indicated, while the 3′-UTR is shown as a black line. The regions targeted for the single (sKD) and double (dKD) knockdowns and regions amplified by quantitative real-time PCR primers (Q) are shown.

MRB4160 exhibited a considerably lower level of overexpression compared with MRB8170 under the same conditions despite sharing 77.3% amino acid identity. These proteins were subsequently incubated with radiolabeled RNA corresponding to 102 nt of the 5′ end of the preedited cyB mRNA followed by UV cross-linking to capture

any direct interactions. After these reactions were treated with RNase to degrade the unbound polyribonucleotide, they were resolved on a SDS-polyacrylamide gel and assayed for overlapping radioactive RNA and protein signals.

Figure 2A (lane 1) shows that the radiolabeled RNA does not bind bovine serum albumin (BSA), visualized by the Coomassie stain as an ~67-kDa band (Fig. 2B), which is a constituent of the RNA binding buffer. The motilities of the recombinant MRB8170, p22, and TbRGG2 proteins in the absence of bound RNA are shown in Figure 2B (lanes 2–5). The MRB8170 protein with the 30-kDa GST tag has a predicted molecular weight of ~125 kDa. The p22 protein with the ~64-kDa MBP-tag migrates as a band just below the BSA band, which served as a negative control because it does not bind RNA (Fig. 2, lanes 4,6; Sprehe et al. 2010). TbRGG2-GST acted as a positive control for RNA binding (Fisk et al. 2008). This recombinant protein exhibited the same mobility as BSA, which is apparent from the increased intensity of the 75-kDa band (Fig. 2, lanes 4,7). Both MRB8170 and MRB4160 bind RNA, because they meet the criteria of yielding strong radioactive signals (Fig. 2A, lanes 5,8) that correspond with the recombinant proteins in Figure 2B. While we attempted to use an equal amount of recombinant protein in all the reactions, it is clear from the ~130-kDa band intensity that less of the poorly expressing recombinant MRB4160 was present. The copious amount of the free GST-tag in this isolation compared with the others (Fig. 2B, lane 8) indicates that this contaminant represented a significant portion of the utilized protein.

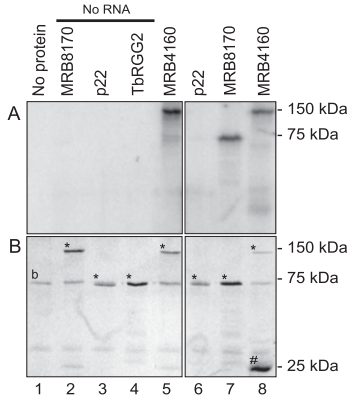

FIGURE 2. The MRB8170 and MRB4160 proteins bind RNA. Proteins incubated with the first 102 nt of pre-edited cyB sequence body-labeled with [α-^{32}P]UTP were UV-cross-linked, treated with RNase A, and separated on a 10% SDS-acrylamide gel. (*A*) Autoradiograph of recombinant proteins binding radiolabeled single-stranded RNA. (*B*) Coomassie-stained 10% SDS-acrylamide gel. The band indicated as "b" in lane *1* is BSA, a component of the binding buffer. (*) Bands corresponding to recombinant proteins indicated at the *top* of the lanes. (#) The 25-kDa band in lane *8* that stains the free GST-tag. Protein ladder sizes are indicated on the *right* of both panels.

MRB8170 has an apparent higher affinity for mRNAs than guide RNAs

Since both MRB8170 and MRB4160 exhibit in vitro RNA binding activities, we decided to address whether there is a preferential binding to mRNA or gRNA. To this end, we used the double filter binding assay (Wong and Lohman 1993; Hall and Kranz 1999) to quantify recombinant MRB8170 binding to radiolabeled pre-edited and edited RPS12 mRNAs (Kao and Read 2005) as well as a oligo(U) tail containing gRNA (gA6[14]) (Koslowsky et al. 1992). A constant concentration of one of these substrate RNAs was incubated with a range of concentrations of MRB8170 and at least a 2000-fold molar excess of torula yeast RNA. The RNA:protein complex was filtered via a nitrocellulose membrane from the unbound RNA, which was subsequently captured by a nylon membrane. The apparent dissociation constant (K_d) of MRB8170 RNA binding was determined by measuring the percent RNA bound for each protein concentration. The aforementioned poor expression of MRB4160 precluded its use in this assay.

As shown in Figure 3, A and B, the apparent $K_d \pm$ SE of MRB8170 binding for pre-edited and edited RPS12 mRNA is 15 ± 1 nM and 21 ± 2 nM, respectively. These values are about five times more than the K_d of MRB8170 association with the U-tail bearing gRNA, which is 117 ± 22 nM (Fig. 3C). These results suggest that MRB8170 has an higher affinity for mRNAs than gRNAs.

MRB8170 is incorporated into a macromolecular complex in RNA-dependent manner

Several MRB1 subunits have been shown to be incorporated into macromolecular complexes (Panigrahi et al. 2008; Acestor et al. 2009; Hashimi et al. 2009; Hernandez et al. 2010; Ammerman et al. 2011). Because MRB8170 and MRB4160 have been found in several MRB1 isolations (Ammerman et al. 2011), we decided to test whether MRB8170, the only paralog against which specific antibodies are available, also associates with a macromolecular complex(es). To this end, mt proteins were separated on a 10%–30% glycerol gradient in the presence or absence of an RNase cocktail. The odd fractions from the gradient were loaded onto a SDS-PAGE gel, and the resolved proteins were detected by immunodecoration with α-MRB8170 polyclonal and α-KREPA1 and α-KREL1 monoclonal antibodies. The latter two antigens served as markers for the sedimentation of the RECC (Fig. 4). A strong α-MRB8170 signal sediments in the denser fractions (15–23), with a peak around 20S, while a weaker signal appears in fractions 7–13 (Fig. 4). This pattern indicates that MRB8170 is primarily incorporated into a large complex(es). This association is abolished upon RNase treatment, as sedimentation shifts to the lighter fractions, with a somewhat equal distribution of signal in fractions 1–15 and a weaker band trailing from here to the bottom of

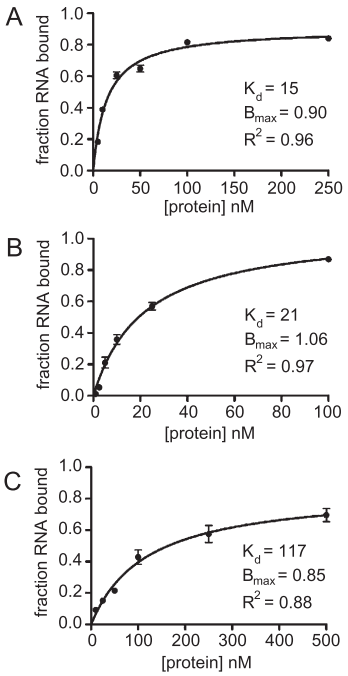

FIGURE 3. MRB8170 appears to preferentially bind mRNA in vitro. Binding curves of MRB8170 binding to (*A*) pre-edited RPS12 mRNA, (*B*) edited RPS12 mRNA, and (*C*) gA6[14] gRNA, which possesses a U_{17} 3′-oligomer tail. The range of protein concentrations used is given on the *x*-axis in nanomolars and the fraction of bound RNA on the *y*-axis. The apparent K_d determined from the fitted curves is given along with the B_{max} of MRB8170 RNA binding and coefficient of determination (R^2) of each curve. Whiskers at each data point represent standard deviation over two separate experiments done in triplicate.

the gradient. Thus, this association of MRB8170 appears to have an RNA component, which is consistent with both its RNA binding activity and the RNase sensitivity of the incorporation of other subunits into MRB1.

MRB8170 and MRB4160 interact with a highly similar subset of MRB1 subunits

Next, we set about determining whether the MRB8170-containing complex(es) contains the characteristic MRB1 subunits described from pull-down isolations in other studies (Hashimi et al. 2008; Panigrahi et al. 2008; Weng et al. 2008; Hernandez et al. 2010; Ammerman et al. 2011), as well as ascertaining whether the composition of the likely MRB4160 RNP(s) is equivalent to that of its paralog. *T. brucei* cell lines inducibly overexpressing either the MRB8170 or MRB4160 ORF bearing a C-terminal TAP tag were generated. This method allowed the affinity purification of MRB8170 or MRB4160 and identification of copurified proteins in the TAP eluates by mass spectroscopy or Western blot analysis with specific antibodies immunodecorating MRB1 subunits.

As depicted in Table 1 and Figure 5A, both proteins pulled down a highly similar subset of MRB1 subunits in the absence of any nuclease treatment. The core proteins comprising MRB11870, MRB3010, MRB5390, GAP1, and 2 (Ammerman et al. 2012) were present in both isolations, while MRB8620 was identified only in the MRB4160 isolation. When the number of unique peptides and their coverage of the identified interacting partners are taken into account for both MRB8170 and MRB4160 TAP experiments, the similarity between the two RNPs is even more striking. The MRB4150/8180 protein is highly represented in both isolations using this criteria, as well as MERS1, which has a role in mRNA stability and has been proposed to be in a discrete complex apart from MRB1 (Table 1; Weng et al. 2008). TbRGG2, the MRB1 protein involved in the 3′-to-5′ progression of pan-edited RNAs, was also observed in both purifications to the same extent as was Tb927.10.11870. Overall, more proteins were distinguished in the MRB4160 TAP isolation as compared with MRB8170, including the RNA binding MRP2 protein (Fig. 5A; Table 1). However, it should be noted that neither the polycistronic gRNA endonuclease mRPN1, which was demonstrated to associate with either MRB8170 or MRB4160 (Madina et al. 2011), nor the REH2 RNA helicase was observed in any of the TAP experiments.

Since many of these interactions could be mediated by RNA linkers, we decided to compare the presence of some MRB1 subunits against which we have antibody, namely, GAP1, MRB3010, and TbRGG2, in both MRB8170 and MRB4160 TAP isolations performed with or without RNases (Fig. 5B) as previously described (Ammerman et al. 2012). The efficiency of RNase degradation was confirmed by running on an ethidium-bromide-stained gel RNA extracted from an equal volume sample of treated and untreated lysates before application onto the first affinity column (data not shown). While GAP1 interaction with MRB8170 or MRB4160 was abolished due to RNase treatment, interaction with MRB3010 and TbRGG2 was significantly reduced, but not eliminated, in both cases. These results suggest that while MRB8170 and MRB4160 contact MRB3010 and TbRGG2 directly, this interaction is enhanced by the presence of RNA. Furthermore, this

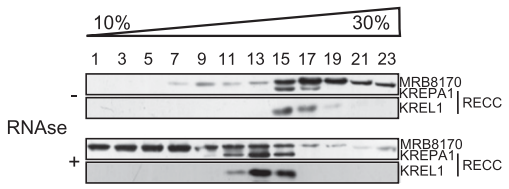

FIGURE 4. MRB8170 is incorporated into a macromolecular complex(es) in an RNase-sensitive manner. Mitochondria isolated from 10^{10} cells of the *T. brucei* 29-13 strain were lysed and separated on a 10%–30% glycerol gradient by ultracentrifugation. The gradient was divided into 24 fractions, out of which all odd ones were run on a 10% SDS-acrylamide gel and transferred onto a PVDF membrane that was immunoprobed with the α-MRB8170 antibody. The lysate used in the *top* panels was treated with RNase inhibitor (RNase-), while that used in the *bottom* panel was treated with an RNase cocktail that disrupted interactions mediated by both single- and double-stranded RNAs (RNase+).

TABLE 1. TAP-MRB8170- and TAP-MRB4160-associated proteins identified by mass spectrometry ordered according to the number of unique peptides from MRB4160 TAP tag elutions

		MRB8170 TAP tag		MRB4160 TAP tag	
Locus tag	Name	Unique peptides	Coverage	Unique peptides	Coverage
Tb927.8.8170[a]	MRB8170	28	32.7%	7	11.5%
Tb927.4.4160	MRB4160	12	16.5%	26	32.7%
Tb927.8.8170/ Tb927.4.4160[b]	MRB8170/ MRB4160	18	19.7%	13	13.5%
Tb927.4.4150/ Tb927.8.8180[c]	MRB4150/ MRB8180	22	33.0%	29	40.7%
Tb927.2.1860		9	13.8%	20	29.8%
Tb927.5.3010	MRB3010	10	25.2%	17	41.5%
Tb11.02.5390		10	10.8%	17	20.3%
Tb11.01.7290	MERS1/Nudix hydrolase	14	50.9%	14	50.9%
Tb927.7.2570	GRBC1/GAP2	10	30.4%	14	37.6%
Tb927.10.10130	Tb10.6k15.0150	5	13.2%	13	30.8%
Tb927.10.11870	Tb10.389.1910	12	50.0%	12	46.5%
Tb927.3.1590		7	11.7%	10	18.0%
Tb927.10.10830	TbRGG2	8	26.6%	9	28.1%
Tb927.7.800		—	—	9	20.8%
Tb927.2.3800	GRBC2/GAP1	5	13.6%	8	26.6%
Tb11.01.8620		—	—	7	15.5%
Tb927.2.6070		—	—	3	8.8%
Tb11.01.0880		—	—	2	27.0%
Tb11.01.4860	MRP2	—	—	2	10.7%

[a]Peptides that distinguish between MRB8170 or MRB4160.
[b]Peptides that could have arisen from both MRB8170 and MRB4160.
[c]Peptides that could have arisen from either of the two highly conserved proteins.

observation is consistent with reciprocal experiments that show that MRB8170 is less abundant in MRB3010 or TbRGG2 pull-downs in the presence of ribonucleases (Ammerman et al. 2012).

Finally, we provide here some evidence that while MRB8170 and MRB4160 may interact with a matching subset of MRB1 proteins in a nearly identical manner, each protein may represent a distinct complex(es). Upon mass spectroscopy of either TAP isolation, there is an under-representation of unique peptides attributable to its paralog (Table 1, top two rows); this analysis excludes peptides that can arise from both MRB8170 and MRB4160 (Table 1, third row). Furthermore, interaction of the tagged MRB8170 with its endogenous counterpart persists despite RNase treatment, indicating self-binding, while the interaction of endogenous MRB8170 with tagged MRB4160 is abolished under such conditions (Fig. 5B), indicating that their association is RNA-mediated only and not due to any protein–protein contact.

The RNAi silencing of either MRB8170 or MRB4160 is compensated by the presence of the other to maintain cell growth

To facilitate functional analysis of the MRB8170 and MRB4160, procyclic *T. brucei* cell lines were generated with the capacity for tetracycline-inducible RNAi silencing of the expression of either protein individually as single knock-downs (sKDs) or both simultaneously as a double knock-down (dKD). We targeted a portion of the diverged 5′ regions of the two ORFs for the sKDs and sequence from the conserved 3′ part for the dKD (Fig. 1B; Supplemental Table 1). To assay the specificity and robustness of RNAi silencing of either MRB8170 or MRB4160 transcripts in these cell lines, qPCR was used using primers annealing to their distinct regions (Fig. 1B; Supplemental Table 1). The dKD equally down-regulated both mRNAs to roughly 57%–66% as compared with their wild-type abundance. In the sKDs, MRB8170 or MRB4160 was reduced to ∼28%–38% of their ordinary levels in their respective KDs, while the other untargeted paralog was not significantly affected (Fig. 6A). This result was confirmed by Western blot analysis with the α-MRB8170 antibody, showing that the protein was undetectable in both the MRB8170 sKD and dKD, while it remained unaffected in the RNAi-induced MRB4160 sKDs (Fig. 6B). The persistence of MRB8170 when MRB4160 is depleted is in contrast to the situation when one of the GAPs or MRPs is silenced, which leads to the reciprocal instability of the other partner protein (Vondrušková et al. 2005; Hashimi et al. 2009).

To ascertain whether the MRB8170 and MRB4160 is essential for the viability of procyclic *T. brucei*, the growth

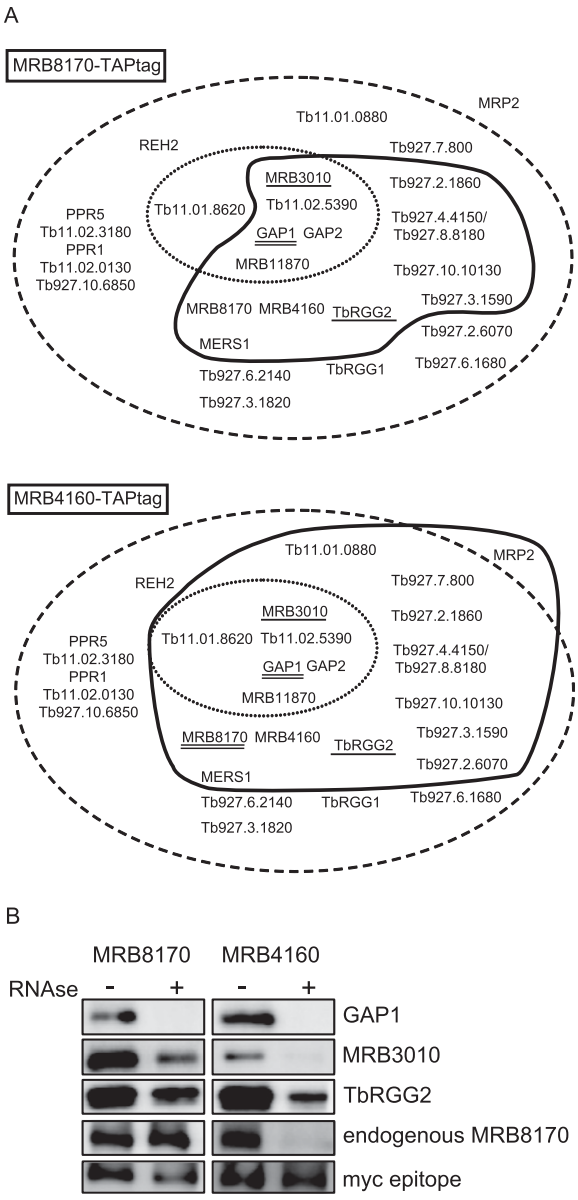

FIGURE 5. MRB1 proteins interacting with MRB8170 and MRB4160. (*A*) The proteins identified by mass spectroscopy of the TAP purification of MRB8170 and MRB4160 described in Table 1 are depicted in the scheme introduced by Ammerman and colleagues (Ammerman et al. 2011). The names or gene tags of all proteins described from various MRB1 purifications (Ammerman et al. 2011) are enclosed in the large dashed oval, while the core MRB1 proteins are depicted in the small dotted oval. The proteins associated with either of the TAP-tagged MRB8170 and MRB4160 in the absence of RNase is enclosed by a thick dark line. Proteins that were demonstrated to have RNA-dependent or -enhanced interactions are with double and single underlines, respectively. (*B*) Immunoblot of TEV eluates from the first column of the TAP purification of MRB8170 and MRB4160, performed in the absence (−) and presence (+) of an RNase cocktail degrading both single- and double-stranded RNAs, The membrane was probed with antibodies recognizing MRB1 proteins GAP1, MRB3010, TbRGG2, and MRB8170. The band recognizing the endogenous and not the larger TAP-tagged MRB8170 protein is shown for this purification. An antibody recognizing the myc-epitope present in the TAP-tag was used as a loading control between the RNase-untreated and -treated purifications.

of the sKD and dKD cell lines in the presence and absence of tetracycline was monitored over the course of 2 wk. Simultaneous ablation of MRB8170 and MRB4160 resulted in slower growth, which was apparent 5 d after RNAi induction and persisted until the end of the time course (Fig. 6C). This retardation of growth was also observed when both MRB8170 and MRB4160 were ablated in the bloodstream stage of the parasite (data not shown). However, no effect on cell growth was observed when only one of these proteins was silenced in the procyclics (Fig. 6C). Thus, while both MRB8170 and MRB4160 together are essential for maintaining normal cell growth, the absence of one of them is compensated by the presence of the other. Based on these data, we decided to perform subsequent experiments on the dKD and sKDs 4 and 5 d after RNAi induction, respectively.

The influence of MRB8170 and MRB4160 ablation on the integrity of MRB1 subunit-containing complexes

Next, we wanted to determine whether the functional redundancy apparent in the sKDs in terms of growth also influences the integrity of MRB1 subunits-containing complexes. The mt proteins from the tetracycline-treated and -untreated dKD and sKD cells were resolved by ultracentrifugation in a 10%–30% glycerol gradient, and the resulting fractions were analyzed as described previously (Fig. 4), using antibodies against the MRB1 subunits GAP1, MRB3010, and TbRGG2. The α-MRB8170 antibody was also used in the analysis of the MRB4160 sKD. In the dKD, a clear shift to lighter fractions was observed in the sedimentation of the core MRB1 subunits GAP1 and MRB3010, indicating that the integrity of macromolecular complexes encompassing these two proteins was compromised. The sedimentation of TbRGG2 was much less affected (Fig. 7A), because only the protein in the two densest fractions was shifted upon simultaneous RNAi silencing.

In both of the sKDs, the integrity of the TbRGG2 complex remained unaltered (Fig. 7B,C). The sedimentation of the MRB3010 subunit in the denser fractions was also retained when only one of the MRB8170 and MRB4160 proteins was depleted, although there was a slight shift to lighter fractions in the peak of the antibody signal in the MRB8170 sKD (Fig. 7B). An effect on GAP1 sedimentation to less dense fractions was slightly more apparent in the case of the MRB8170 silencing (Fig. 7B) as compared to that in the MRB4160 sKD (Fig. 7C). Interestingly, the sedimentation of MRB8170 is unchanged when MRB4160 is depleted, consistent with the notion that they are in a distinct complex(es) (Fig. 7C). Thus, it appears that the assembly of MRB1-containing complexes is most affected in the dKD. The integrity of RECC, as represented by the α-KREPA6 antibody signal, is unaffected in all of the KDs.

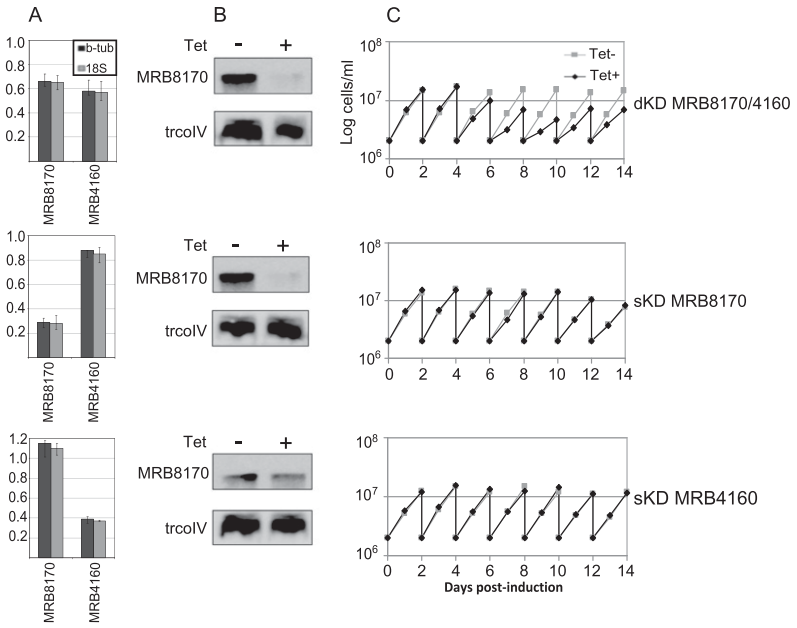

FIGURE 6. Growth is inhibited upon simultaneous down-regulation of MRB8170 and MRB4160 but persists when each is individually RNAi-silenced. (*A*) A bar graph on a linear scale showing the mean relative transcript abundance as determined by qRT-PCR in MRB8170/4160 double- and single-knockdown cell lines treated with the RNAi-induction agent tetracycline in comparison to those grown in the absence of the antibiotic. Data were normalized to cytosolic β-tubulin (black) and 18S rRNA (gray) levels. A value of 1 indicates no change, while a value <1 signifies depletion of the assayed transcript. The range of obtained relative abundances is signified by whiskers around the *top* of the bars. (*B*) Western analysis of resolved mitochondrial proteins from the studied cell lines was performed to assay the depletion of MRB8170 in kMAP double and single knockdowns. The mitochondrial protein trCoIV was used as a loading control. (*C*) The growth rate of cells grown in the presence (black diamond and line) or absence (gray square and line) of tetracycline for the MRB8170/4160 double and single knockdowns over a 14-d course. Cell density (cells/mL) was measured every 24 h, and the cells were diluted to the starting density of 2×10^6 cells/mL every second day.

MRB8170/4160 RNAi silencing does not appreciably alter minicircle-encoded guide RNAs

Because some MRB1 proteins have been demonstrated to affect gRNA stability (Weng et al. 2008; Hashimi et al. 2009; Hernandez et al. 2010) and MRB8170 and MRB4160 were shown to associate with the pre-gRNA processing endonuclease mRPN1 (Madina et al. 2011), we decided to inspect whether MRB8170/4160 RNAi silencing affects the levels of these small transcripts. Guanylyltransferase labeling of gRNAs revealed no changes in the steady-state level or size distribution of these molecules when both proteins were simultaneously down-regulated (Fig. 8A). Further investigation of a panel of four individual gRNAs by Northern analysis in the dKD, using a probe against a cytoplasmic tRNA as a loading control, shows that none are completely degraded, although there appears to be a small but discernible decrease in the molecules directing co3 and ATP synthase subunit 6 (A6) mRNA editing (Fig. 8B). However, the levels of these gRNAs were not greatly affected in either sKD (Fig. 8B). We conclude from these results that MRB8170 and MRB4160 do not play a major role in gRNA biogenesis.

Depletion of MRB8170/4160 differentially influences maxicircle-encoded mRNAs

We then turned our attention to whether levels of maxicircle-encoded never-edited and edited mRNAs were impacted in the MRB8170/4160 dKD and sKDs by an established qPCR-based assay (Carnes et al. 2005). The levels of never-edited transcripts were not dramatically affected in any of the RNAi knockdowns (Fig. 9, NE). In fact, the depletion of MRB4160 does not significantly affect any maxicircle transcripts examined (Fig. 9C). In contrast, ablation of MRB8170 exerts a mild effect on many pan-edited and two moderately edited mRNAs. Most of these are depleted in abundance (edited MURF2, A6, and ND7, and both pre-edited and edited co3), while pre-edited cyB is actually more abundant (Fig. 9B; Supplemental Fig. 2). However, the most striking changes in maxicircle edited RNA abundances were obtained upon the dual silencing of MRB8170 and MRB4160 (Fig. 9A). In this case, both pre-edited and edited species of most pan-edited RNAs were clearly less abundant, and to a greater extent than observed in the MRB8170 sKD. Changes in abundance of almost all examined moderately edited RNAs were also observed. Thus it seems that MRB8170 and MRB4160 exhibit a synergistic effect on the stability of pan-edited RNAs, since the dKD affects these molecules more than the sKDs. This synergy in their influence is strikingly demonstrated when nascently edited A6 and RPS12 molecules are assayed by poisoned primer extension (Ammerman et al. 2010). The severity of the down-regulation of edited A6 and RPS12 RNAs decreases steadily from the dKD to the MRB8170 sKD, with the mildest effect in the MRB4160 sKD (Supplemental Fig. 2). Together, these results suggest an apparent functional divergence between the two paralogs since MRB8170 appears to influence mtmRNAs to a higher degree than MRB4160.

Interestingly, we noted in the dKD a qualitative difference between pan-edited and moderately edited transcripts. In moderately edited transcripts, the manifested effect was reminiscent of the consequences of the disruption of core RNA editing activities: an accumulation of pre-edited mRNAs and a decrease of fully edited molecules

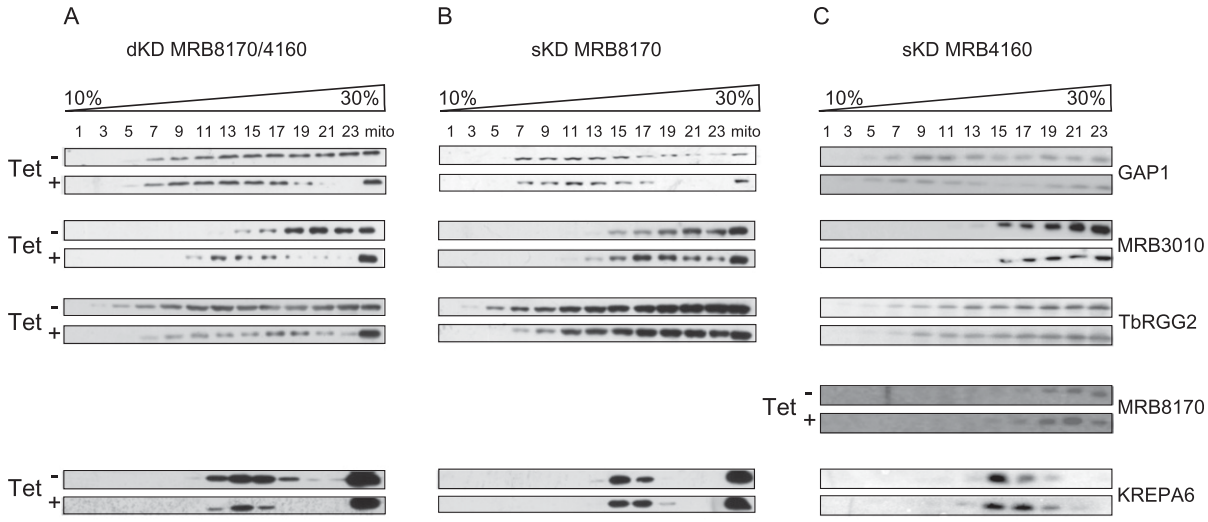

FIGURE 7. Simultaneous down-regulation of MRB8170 and MRB4160 leads to disruption of macromolecular complexes containing some MRB1 subunits. Mitochondrial vesicles from the double and single MRB8170/4160 knockdown cell lines were isolated following RNAi induction by tetracycline (Tet+). Parallel samples grown for this time in the absence of the antibiotic were also analyzed (Tet−). The mitochondrial proteins from MRB8160/MRB4160 dKD (*A*), MRB8170 sKD (*B*), and MRB4160 sKD (*C*) were resolved by glycerol gradient sedimentation and analyzed by Western blot as described in Figure 4. The column marked as "mito" contains total mitochondrial lysate. The identity of the antibody used is indicated at the *right*.

(Carnes et al. 2005; Tarun et al. 2008; Weng et al. 2008; Hashimi et al. 2009; Ammerman et al. 2011). The cytochrome oxidase subunit (co) 2 and cyB transcripts exhibited such a phenotype, while the pre-edited MURF2 mRNA exhibited an increase without the concurrent decrease of the respective edited transcripts (Fig. 9A, moderately edited).

In contrast, pan-edited transcript abundances in the dKD were affected in a fashion that is reminiscent of an effect on RNA stability, namely, that both pre-edited and edited forms of various transcripts are often less abundant (Fig. 9A, pan-edited; Hashimi et al. 2008, 2009). The effects observed here ranged from a similar degree of down-regulation of edited and pre-edited co3, to the marginally affected or unaltered pre-edited NADH dehydrogenase subunit (ND) 7 and RPS12 mRNAs, respectively (Fig. 9A) with coincident depletion of both edited forms. The fully edited ribosomal protein S12 (RPS12) mRNA was further analyzed to determine whether the long A/U appended population, which stabilizes and marks these transcripts for translation (Ryan and Read 2005; Etheridge et al. 2008; Aphasizheva et al. 2011), was preferentially degraded over the short poly(A) forms; both types were equally down-regulated in the dKDs (Supplemental Fig. 3). Thus, it is some feature other than the long A/U tail that results in the differential effect on abundance of fully edited and pre-edited RPS12 resulting from MRB8170 and MRB4160 codepletion. Finally, we note that the steady-state levels of fully processed pan-edited molecules were more reduced (25%–45% relative abundance, average 35%) as compared with those from the moderately edited population (60%–94% relative abundance, average 75%) (Fig. 9A, pan-edited). This phenotype, in addition to all of the other mRNA phenotypes described above, hints at a role of MRB8170 and MRB4160 in mRNA stability and/or processing.

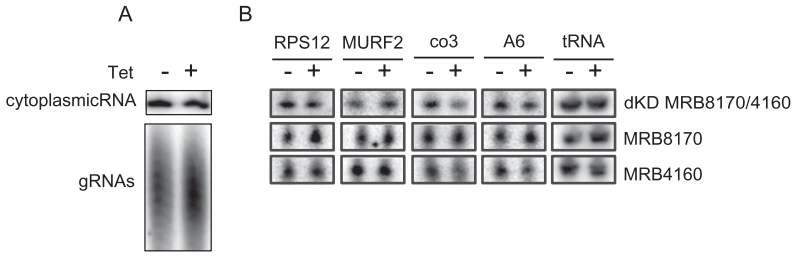

FIGURE 8. The effect of simultaneous and individual MRB8170/4160 RNAi silencing on minicircle-encoded gRNAs. (*A*) RNA from the double MRB8170/4160 knockdown grown in the presence (+) and absence (−) of the RNAi-induction agent tetracycline was capped with [α-^{32}P]GTP by the recombinant guanylyltransferase enzyme. The homogeneous population of small gRNA molecules in the samples was resolved as a ladder of bands on a denaturing 7 M urea/8%-acrylamide gel (*bottom* panel). A cytosolic RNA that is simultaneously labeled by this reaction is shown (*top* panel) as a loading control. (*B*) Individual gRNAs directing editing of RPS12, MURF2, co3, and A6 mRNAs (using the abbreviations as defined in Fig. 9) were detected by Northern blot. A probe against a cytoplasmic tRNA^{Cys} (GCA) was used as a loading control. The "+" and "−" above the lanes indicate the state of tetracycline induction.

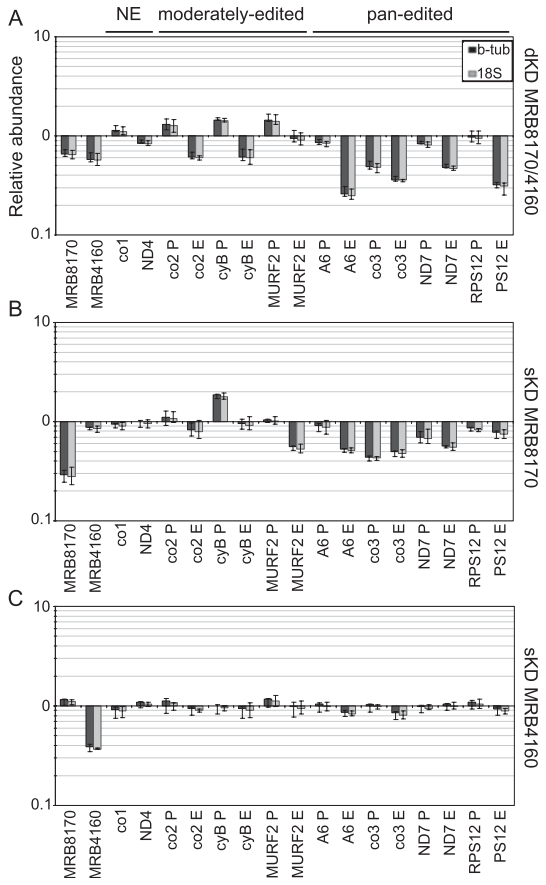

FIGURE 9. The influence of simultaneous and individual MRB8170/4160 depletion on the steady-state levels of maxicircle-encoded mRNAs. qRT-PCR analysis of pre-edited (P), edited (E), and never-edited (NE) mRNAs encoded on maxicircle DNA. Analysis was performed in the presence or absence of the RNAi-induction agent tetracycline for the double (*A*) and single knockdowns of MRB8170 (*B*) and MRB4160 1 (*C*). For each target amplicon, the relative change in RNA abundance due to the depletion of both or one of the MRB8170/4160 proteins as compared with the untreated controls, which were processed in parallel, was determined by using the cytosolic transcripts β-tubulin and 18S rRNA as internal references. The mean relative abundance of each amplicon is plotted as a bar graph on a logarithmic scale on the *y*-axis, in which levels above and below the middle axis signify an up- or down-regulation, respectively, while no bar indicates that there was no change in steady-state levels of the transcript upon RNAi silencing; whiskers denote the range of obtained relative abundances within the triplicates. The following pre-edited and edited mRNAs were assayed: ATPase subunit 6 (A6), cytochrome oxidase subunits 2 (co2) and 3 (co3), cytochrome reductase subunit b (cyB), maxicircle unknown reading frame 2 (MURF2), NADH dehydrogenase subunit 7 (ND7), and ribosomal protein S12 (RPS12). The following never-edited RNAs were assayed: cytochrome oxidase subunit (co1) and NADH dehydrogenase subunit 4 (ND4).

DISCUSSION

The MRB1 complex proteins are among the bewildering number of proteins that play a role in the unique process of U-insertion/deletion RNA editing. As such, not only are many MRB1 subunits exclusive to the order Kinetoplastida, but they also exhibit a variety of RNAi phenotypes, complicating the determination of their roles in mediating this massive processing event and integrating it into the RNA metabolism required for mt gene expression. Here, we expand our knowledge about MRB1 by functional characterization of its subunits MRB8170 and MRB4160. They are paralogs in *T. brucei* while occurring only as a single locus in other sequenced trypanosomatid lineages. The proteins share a large conserved C terminus while having divergent sequence in a relatively smaller N-terminal region. In this work, we show that although these proteins share many biological properties due to their significant conservation, they also differ in a key aspect.

Both MRB8170 and MRB4160 proteins have basic pIs, a biophysical feature that facilitates their ability to bind RNA in vitro. Because neither of them has any identifiable domains or orthologs outside of kinetoplastids, they represent novel RNA binding proteins that will be an interesting topic of future study. As a start toward this endeavor, we investigated whether MRB8170 has higher affinity in vitro for RNA species that are well represented in the mt transcriptome: gRNAs, pre-edited or edited mRNAs. The results from the filter binding assay used suggest that MRB8170 exhibits ∼5× higher affinity for mRNAs than gRNAs. To ensure that any observed differences in binding are not caused by varying numbers of nucleotides in assayed binding substrates, a molar excess of torula yeast RNA was included during the incubation of the tested substrate RNAs. Not much is known about the structure of mt mRNAs, in contrast to studies demonstrating three-helical structures in mRNA:gRNA duplexes (Reifur and Koslowsky 2008) and the presence of two hairpin loops in gRNAs, including gA6[14] (Schmid et al. 1995). While our data do not indicate which structural features of the mRNAs are exploited by the 100-kDa MRB8170 for binding, one possible structural determinant of the apparent preference for mRNAs is that they may have significant stretches that are single-stranded compared with gRNA. Nevertheless, these data are consistent with the RNAi silencing of MRB8170 influencing pan-edited mRNAs but not gRNAs.

A common feature of MRB8170 and MRB4160 is that they interact with a highly overlapping subset of the MRB1 subunits, as evidenced by the very similar peptide composition profiles of proteins pulled down with either TAP-MRB8170 or TAP-MRB4160. In both cases, interaction with GAP1 is mediated completely by RNA linkers, while that with MRB3010 and TbRGG2 is RNA-enhanced, consistent with a direct contact. This finding agrees with other studies reporting the existence of a complex containing TbRGG2 and either MRB8170 or MRB4160 (Madina et al. 2011; Ammerman et al. 2012), interacting with the core MRB1 proteins via MRB3010 and MRB8620 (Ammerman et al. 2012). Furthermore, when both MRB8170 and MRB4160 are down-regulated simultaneously, the assembly of the three MRB1 subunits GAP1, MRB3010,

and TbRGG2 into macromolecular complexes appears to be hindered, albeit to different degrees, further supporting the notion that they interact with each other via RNAs slated for editing, which are also reduced in this background, and/or protein–protein binding.

We also show that MRB8170 and MRB4160 do not interact directly with each other, as evidenced by RNase-treated TAP-MRB4160 failing to pull down MRB8170. Furthermore, the stability of MRB8170 is not dependent on the presence of MRB4160, as observed for the GAP paralogs (Hashimi et al. 2009) and the MRP1/2 proteins (Zíková et al. 2008), and even the integrity of the MRB8170-containing complex(es) is not affected in the MRB4160 sKD. Thus it appears that the MRB8170 and MRB4160 proteins function independently.

Current evidence suggests that proteins within the MRB1 complex undergo numerous transient and dynamic interactions (Hashimi et al. 2008; Panigrahi et al. 2008; Weng et al. 2008; Ammerman et al. 2012). Interestingly, MRB8170 and MRB4160 along with TbRGG2 were recently shown to associate with the gRNA endonuclease mRPN1 (Madina et al. 2011). We did not detect mRPN1 in mass spectrometry of the MRB8170 or MRB4160 TAP purifications described here. Since neither we, nor other laboratories, have detected this endonuclease by mass spectrometry analyses of purified MRB1 subunits, we speculate that mRNP1 is not amenable to such a technique, either due to its intrinsic properties or an association with these MRB1 subunits in substoichiometric amounts. Our data also indicate that the primary role of MRB8170 and MRB4160 is not the processing of gRNAs, because the dKD does not significantly affect the steady-state levels or sizes of these molecules. Rather, our data are more consistent with a role for TbRGG2/MRB8170/4160 in a hand-over mechanism between the biogenesis of gRNAs and their utilization in the RNA editing process as proposed by Madina et al. (2011).

MRB8170 and MRB4160 are among 74 paralogs that have arisen due to a massive duplication of a 0.5-Mb-long region between chromosomes 4 and 8 that occurred after the *T. brucei* clade branched off from the other trypanosomes. As described by Jackson (2007), the affected loci were either lost from one of the chromosomes only or retained on both, the latter event resulting in paralogs that either remained conserved or diverged in sequence. The CDSs of *MRB8180* and *MRB4150*, which are immediately downstream from the topics of this work, *MRB8170* and *MRB4160*, respectively, are loci that fit into the category of conserved paralogs, sharing 99.1% translated sequence identity. On the other hand, *MRB8170* and *MRB4160* are considered to be divergent, because their amino acid sequence identity is 77.3%. The question is whether this divergence in sequence has resulted in two functionally divergent proteins. The similarities between MRB8170 and MRB4160 discussed so far seem to argue against this. Their functional redundancy is also implied by our finding that cell growth persists upon RNAi silencing of either MRB8170 or MRB4160 alone, at least under the culture condition used, while their simultaneous down-regulation leads to substantial growth inhibition.

However, MRB8170 and MRB4160 do differ in one key aspect: They influence pan-edited RNAs to differing degrees. When MRB8170 is ablated, pan-edited RNAs appear to be destabilized because their levels are decreased. This is in contrast to the MRB4160 sKD in which neither pan-edited RNAs nor any other classes of maxicircle transcripts are affected, despite equally efficient RNAi. When both proteins are silenced in the dKD, the pan-edited RNAs exhibit a more severe decrease than that observed in the MRB8170 sKD. Together, these results suggest that after their divergence, MRB8170 retained more influence on the stability of pan-edited transcripts than MRB4160, but that both proteins may act synergistically on these transcripts.

The picture is somewhat different with regard to moderately edited RNAs. Here, MRB8170 and MRB4160 display a clearly redundant function. Neither of the sKDs exhibited alterations in the abundances of moderately edited transcripts, while these RNAs were affected in the dKD. Moreover, this redundant MRB8170/4160 function appears to be at the level of RNA editing, since in the dKD moderately edited RNAs were affected in a manner reminiscent of that observed when core editing processes are interfered with: an accumulation of pre-edited mRNAs and a depletion of edited mRNAs. This phenotype may reflect a redundant structural role of MRB8170/4160 in the assembly of partner MRB1 subunits that impact RNA editing, resulting in a downstream effect on moderately edited RNAs. The profound disassembly of the MRB complex in the dKD, in contrast to either sKD, agrees with this scenario.

Although the pan-editing phenomenon has been reported in several kinetoplastids, it seems most prevalent in the *Trypanosoma* clade, as exemplified by the nine maxicircle genes that require extensive editing in *T. brucei* as compared with only six such transcripts in *Leishmania tarentolae* (Arts and Benne 1996; Alfonzo et al. 1997; Speijer 2006). Thus, we propose that this milieu could be conducive to retain both *MRB8170* and *MRB4160* in the duplicon and perhaps the subsequent divergence of the two paralogs. Since both MRB8170 and MRB4160 function independently of each other, one of them can be modified in the background of the other maintained paralog, as long as any potential innovations fit within the context of the other MRB1 subunits. Indeed, there is evidence for some of the codons being positively selected between the two loci (Jackson 2007). Such a situation could then give rise to a functionally distinct MRB8170 that plays a bigger role in the stability of pan-edited RNAs than its paralog.

MATERIALS AND METHODS

Dot-plot analysis of MRB8170 and MRB4160 ORFs and 3′-UTRs

The MRB8170 and MRB4160 ORFs plus predicted 3′-UTR DNA sequences (Jackson 2007) from the 927 *T. brucei* strain (available at TriTrypDB: http://tritrypdb.org/tritrypdb/) were entered into the CLC Main Workbench 6.1.1 program (CLC Bio). The included dot-plot function was used to create the similarity matrix using the default window size setting of 9. The output was further adjusted manually in the program to reduce the background noise, which did not affect the signal on the diagonal of the plot. The corrected MRB4160 ORF from recent spliced leader trapping studies (Nilsson et al. 2010; Siegel et al. 2010), which was confirmed by spliced leader-mediated PCR (Supplemental Fig. 1), was used in this analysis, as was the annotated MRB8170 ORF that was also confirmed with this method (data not shown).

Expression and purification of recombinant MRB8170 and MRB4160

The MRB8170 and MRB4160 ORFs were PCR-amplified using Pfx polymerase (Invitrogen) from genomic DNA extracted from procyclic form (PF) *T. brucei* (strain 29-13) using primers incorporating the restriction sites described in Supplemental Table 1. The resultant PCR products were cloned into the pGBD-C2 vector using the In-Fusion cloning kit (Clontech). The inserts were then shuttled into the expression vector pGEX4T-1 (Novagen) and transformed into the Rosetta strain of *Escherichia coli* (Novagen). Cells were grown to an OD_{600} of ~0.4 at 37°C and induced with 0.1 mM IPTG, while the temperature was reduced to 17°C overnight. GST-tagged MRB8170 and MRB4160 were purified using glutathione-agarose (Invitrogen) and a standard single-step GST purification protocol.

RNA cross-linking assay

To generate substrate RNA, a previously described BamHI-linearized construct containing the 5′ 102 nt of pre-edited cytochrome B (cyB) sequence (Koslowsky et al. 1996) was in vitro transcribed with a MAXIscript kit (Ambion) using unlabeled and [α-^{32}P]-labeled UTP (800 Ci/mmol) at a 1:1 molar ratio in a 20-μL volume. DNase-treated RNA was resuspended in an equal volume of 90% formamide and run on a 8%-acrylamide/7 M urea gel, after which the band of appropriate size was excised. RNA was eluted from the cut gel by constant rotation overnight in elution buffer (10 mM Tris-HCl at pH 8.0, 1 mM EDTA at pH 8, 0.75 M NH_4oAc, 0.1% SDS) and subsequently precipitated with isopropanol. Five femtomoles of RNA and 7.5 pmol of protein were incubated in cross-linking buffer (4.5 mM HEPES, 1.6 mM $MgCl_2$, 0.38 mM DTT, 1.13 mM ATP, 3.75 mM creatine phosphate, 0.075 mM EDTA, 7.5 μg /mL torula yeast RNA type VI [Sigma-Aldrich], 4.5% glycerol, 15 μg/mL BSA, 6 U RNaseOUT [Invitrogen]) for 20 min at room temperature, UV cross-linked for 10 min on ice, and treated with 30 μg of RNase A for 15 min at 37°C. These reactions were run on a 10% SDS-acrylamide gel, stained with Coomassie dye, and dried. The radioactive signal on the gel was detected using the Storm PhosphorImager (Molecular Dynamics).

RNA double filter binding assay

The untailed, full-length pre-edited and edited RPS12 mRNAs used in this assay were 221 and 325 nt in length (Kao and Read 2005). The 79-nt gA6[14] substrate gRNA consisted of a previously reported sequence (Koslowsky et al. 1992) with a 17-nt 3′ U tail and 10 nt of 5′ vector-derived sequence. These RNAs were body-labeled as described above and subsequently gel-purified. RNAs were then renatured by incubation for 3 min at 70°C, slow cooling at a rate of 2°C per min to 27°C, at which they remained for 30 min, followed by quenching on ice to allow them to most closely achieve their native secondary state. RNA with an invariant concentration of 30 pM was incubated with different concentrations of protein for 30 min at room temperature in two separate experiments each performed in triplicate. Buffer conditions during binding were 0.2× PBS, 2 mM $MgCl_2$, 0.5 mM DTT, 0.1 mM EDTA, 10 μg/mL torula yeast RNA (type VI [Sigma-Aldrich]), 50 μg/mL BSA, and 6% glycerol. Filter binding was performed as previously described (Wong and Lohman 1993; Hall and Kranz 1999) to determine the percent of RNA bound at each concentration, and results were combined and plotted using GraphPad Prism 5 software. Apparent K_d and B_{max} were calculated by nonlinear regression assuming single-site specific binding and using the equation $Y = B_{max} \times X/(K_d + X)$, fitting by the method of least squares.

Generation of cell lines and growth curves

Gene fragments cloned into the p2T7-177 RNAi vector (Wickstead et al. 2002) for generating single and double MRB8170 and MRB4160 knockdown cell lines were PCR-amplified from the *T. brucei* genomic DNA using the primers given in Supplemental Table 1, which also indicates the restriction sites used for ligation into the construct as well as the corresponding region of the fragment in ORF (Fig. 2). This table also lists the primers used to amplify the whole ORFs of MRB8170 and MRB4160 1 and 2 that were cloned into the pLew79-MHTAP vector (Jensen et al. 2007). Both types of constructs were linearized with the NotI restriction enzyme and electroporated as previously described (Hashimi et al. 2008) into the parental procyclic strain 29-13, and clones obtained by limiting dilution were selected for phleomycin (2.5 μg/mL) resistance. The 29-13-derived cell lines were grown in SDM-79 medium supplemented with hygromycin (50 μg/mL) and G418 (15 μg/mL). RNAi was induced by the addition of 1 μg/mL tetracycline. The growth dynamics of the tetracycline-induced cells compared with their noninduced counterparts was performed as described elsewhere (Hashimi et al. 2009).

Western blot analysis and antibodies

Proteins were separated on 10% or 12% SDS-polyacrylamide gels and transferred onto PVDF membranes. Forty micrograms of proteins from hypotonically isolated mt vesicles were loaded on gels for assessing of single and double knockdowns with the affinity-purified MRB8170 (Tb927.8.8170) antibody by Western analysis, which is described by Ammerman and coworkers (2012). The other polyclonal antibodies used is this study were generated against MRB3010, in particular, its oligopeptide CEALQMKKLHQERGGNPM (Bethyl Laboratories), GAP1 (Hashimi et al. 2009; Ammerman et al. 2011), TbRGG2 (Fisk et al. 2008), KREPA6 (Tarun et al. 2008),

trCoIV (Maslov et al. 2002), and the Myc protein (Sigma-Aldrich). In addition, monoclonal antibodies immunodecorating KREPA1 and KREL1 (Panigrahi et al. 2001) were also used. All antibodies against RECC proteins (KREPA1 and 6; KREL1) were kindly provided by Ken Stuart (Seattle Biomed).

Glycerol gradient fractionation of mitochondrial lysates

The resolution of MRB1 and RECC macromolecular particles by ultracentrifugation on 10%–30% glycerol gradients was performed as described previously (Ammerman et al. 2011). Hypotonically isolated mt vesicles (Hashimi et al. 2008) from 10^{10} cells were lysed in a lysis buffer (1% Triton-X, 10 mM Tris at pH 7.2, 10 mM $MgCl_2$, 100 mM KCl, 1 mM DTT, 1 μg/mL pepstatin, 2 μg/mL leupeptin, 1 mM pefabloc) supplemented with either 40 units of RNaseOUT or an RNase cocktail (0.1 unit/μL RNase A, 0.125 unit/μL T1, 0.001 unit/μL V1, 0.03 unit/μL micrococcal nuclease) to eliminate both single-stranded (ss) and double-stranded (ds) RNAs.

Tandem affinity purification and protein analysis

Tandem affinity purification (TAP) of MRB8170 and MRB4160 was performed on $\sim 5 \times 10^9$ tetracycline-induced cells using the protocol described in Hashimi et al. (2008). In the case of RNase treatment during the TAP purification, cleared lysates were split equally in IPP150 buffer (10 mM Tris at pH 8.0, 150 mM NaCl, 0.1% Igepal) that was supplemented either with 40 units of RNaseOUT (Invitrogen) or an RNase cocktail (0.1 unit/μL RNase A, 0.1 unit/μL RNase I, 0.001 unit/μL RNase V1), before loading onto the initial IgG-Sepharose columns. TEV eluates were collected for Western blot analyses, while they were completely processed via a second calmodulin-Sepharose column for submission to mass spectroscopy (LC-MS/MS).

The eluates were scored for the presence of the TAP-tagged MRB8170/4160 protein by Western blot probed with an α-Myc antibody. The positive samples were pooled, acetone-precipitated, and resuspended in an appropriate digestion overnight at 37°C with 20 μg/mL proteomic grade trypsin (Sigma-Aldrich), and the digested peptides were purified using a C18 ZipTip (Millipore) according to the manufacturer's protocol. Subsequent LC-MS/MS was performed on a NanoAcuity ultra performance liquid chromatography device coupled on-line to an electrospray ionization (ESI) Q-Tof Premier mass spectrometer (Waters). One microliter of sample was diluted in 3% acetonitrile/0.1% formic acid (v/v) and subjected to reverse-phase HPLC with a flow rate of 0.4 μL/min through a BEH300 C18 analytical column (Waters). A linear solvent gradient was applied—initially 3% (v/v) solvent B (0.1% (v/v) formic acid in acetonitrile diluted with solvent A (0.1% [v/v] formic acid in water) was gradually increased to 40% solvent B over 30 min. The peptides were then eluted by increasing the concentration of solvent B to 85% over a 2-min period, where it was maintained for another 5 min and then lowered to 3% for the next run. All eluted peptides were applied directly into the ESI source. Raw data were acquired in data-independent MS^e Identity mode. Precursor ion spectra were acquired with a 5 V collision energy and fragment ion spectra with a 20–35 V collision energy ramp in alternating 1-sec scans. The data-dependent analysis mode was subsequently used for secondary analysis. Peptide spectra were acquired with a 5 V collision energy, and peptides with charge states of +2–4 were selected for MS/MS analysis. Fragment spectra were collected with a 20–40 V collision energy ramp. In both modes, peptide and fragment spectra were acquires with a 2- and 5-ppm tolerance, respectively. Raw data were then used to interrogate the *T. brucei* Uniprot and NCBI protein databases, as well as the one described in Panigrahi et al. (2008), using the PLGS v2.3 program (Waters). Acetyl N-terminal deamidation of N and Q, carbamidomethyl C, and M oxidation were set as variable modifications. Identification of three consecutive y- or b-ions was set as a prerequisite for a positive peptide match.

Quantitative real-time PCR

RNA was isolated and processed for subsequent reverse transcription into cDNA as described previously by Hashimi et al. (2008, 2009) from single and double MRB8170 and MRB4160 knockdown cell lines for 5 and 4 d, respectively, in the presence or absence of tetracycline. The resulting random hexamer-primed cDNA was used as a template for quantitative real-time (q) PCR as described in the aforementioned references using previously designed primers that anneal to the maxicircle mRNA sequences (Carnes et al. 2005). Primers that amplify MRB8170 or MRB4160 encoding cDNAs were designed specifically for this study and are given in Supplemental Table 1. All qPCRs were performed in triplicate and also with a negative control template from a mock reverse transcription reaction to ensure that genomic DNA was adequately degraded before cDNA production. The raw qPCR was used in Pfaffl analysis (Pfaffl 2001) to obtain the relative abundance of the examined transcripts in the RNAi cell lines as compared with those in the untreated controls grown and processed in parallel.

Guanylyltransferase and gRNA Northern analyses

RNA for these assays were isolated and treated as for the above-described qPCR procedure. For the guanylyltransferase-mediated 5′-capping of the gRNAs, 15 μg of total RNA was incubated with the enzyme and 5 μCi of [α-^{32}P]GTP (800 Ci/mmol) and then extracted as described elsewhere (Ammerman et al. 2011). The radiolabeled products of both of these assays were separated on a denaturing 8% acrylamide/7 M urea gel in 1× TBE. For gRNA Northerns, 10 μg of total RNA was run on the aforementioned gel and transferred onto a Zeta-probe membrane (Bio-Rad), which was probed with specific 5′-^{32}P-labeled oligonucleotides hybridizing specific gRNAs as previously performed (Madina et al. 2011).

SUPPLEMENTAL MATERIAL

Supplemental material is available for this article.

ACKNOWLEDGMENTS

Much gratitude is given to Andrew Jackson (Sanger Institute) for enlightening discussions about the nature of the MRB8170/4160 paralogs in the context of the chromosome 4 and 8 duplication event that he described in *T. brucei*. The efforts of Yan-Zi Wen, Lucie Novotná, and Zdeňka Čičová (Institute of Parasitology) at early stages of this project are appreciated. We thank Ken Stuart

(Seattle Biomed) for his kind gift of antibodies and Peter Koník (University of South Bohemia) for help with mass spectrometry. This work was supported by the Grant Agency of the Czech Republic 204/09/1667, the RNPnet FP7 program (289007), and the Praemium Academiae award to J.L.; NIH grants RO1 AI061580 and RO1 AI077520 to L.K.R.; the NIH Postdoctoral Fellowship F32 AI07718501 to J.C.F.; and the Institutional Research Concept AV0Z50200510 to R.S. J.L. is a Fellow of the Canadian Institute for Advanced Research.

Received April 13, 2012; accepted July 11, 2012.

REFERENCES

Acestor N, Panigrahi AK, Carnes J, Zíková A, Stuart KD. 2009. The MRB1 complex functions in kinetoplastid RNA processing. *RNA* **15:** 277–286.

Alfonzo JD, Thiemann O, Simpson L. 1997. The mechanism of U insertion/deletion RNA editing in kinetoplastid mitochondria. *Nucleic Acids Res* **25:** 3751–3759.

Ammerman ML, Fisk JC, Read LK. 2008. gRNA/pre-mRNA annealing and RNA chaperone activities of RBP16. *RNA* **14:** 1069–1080.

Ammerman ML, Presnyak V, Fisk JC, Foda BM, Read LK. 2010. TbRGG2 facilitates kinetoplastid RNA editing initiation and progression past intrinsic pause sites. *RNA* **16:** 2239–2251.

Ammerman ML, Hashimi H, Novotná L, Čičová Z, McEvoy SM, Lukeš J, Read LK. 2011. MRB3010 is a core component of the MRB1 complex that facilitates an early step of the kinetoplastid RNA editing process. *RNA* **17:** 865–877.

Ammerman ML, Downey KM, Hashimi H, Fisk JC, Tomasello DL, Faktorová D, Kafková L, King T, Lukeš J, Read LK. 2012. Architecture of the trypanosome RNA editing accessory complex, MRB1. *Nucleic Acids Res* **40:** 5637–5650.

Aphasizheva I, Aphasizhev R. 2010. RET1-catalyzed uridylylation shapes the mitochondrial transcriptome in *Trypanosoma brucei*. *Mol Cell Biol* **30:** 1555–1567.

Aphasizhev R, Aphasizheva I, Simpson L. 2003. A tale of two TUTases. *Proc Natl Acad Sci* **100:** 10617–10622.

Aphasizheva I, Maslov D, Wang X, Huang L, Aphasizhev R. 2011. Pentatricopeptide repeat proteins stimulate mRNA adenylation/uridylation to activate mitochondrial translation in trypanosomes. *Mol Cell* **42:** 106–117.

Arts GJ, Benne R. 1996. Mechanism and evolution of RNA editing in kinetoplastida. *Biochim Biophys Acta* **1307:** 39–54.

Bhat GJ, Souza AE, Feagin JE, Stuart K. 1992. Transcript-specific developmental regulation of polyadenylation in *Trypanosoma brucei* mitochondria. *Mol Biochem Parasitol* **52:** 231–240.

Carnes J, Trotter JR, Ernst NL, Steinberg A, Stuart K. 2005. An essential RNase III insertion editing endonuclease in *Trypanosoma brucei*. *Proc Natl Acad Sci* **102:** 16614–16619.

Carnes J, Trotter JR, Peltan A, Fleck M, Stuart K. 2008. RNA editing in *Trypanosoma brucei* requires three different editosomes. *Mol Cell Biol* **28:** 122–130.

Carnes J, Soares CZ, Wickham C, Stuart K. 2011. Endonuclease associations with three distinct editosomes in *Trypanosoma brucei*. *J Biol Chem* **286:** 19320–19330.

Durrant JD, Hall L, Swift RV, Landon M, Schnaufer A, Amaro RE. 2010. Novel naphthalene-based inhibitors of *Trypanosoma brucei* RNA editing ligase 1. *PLoS Negl Trop Dis* **4:** e803. doi: 10.1371/journal.pntd.0000803.

El-Sayed NM, Myler PJ, Blandin G, Berriman M, Crabtree J, Aggarwal G, Caler E, Renauld H, Worthey EA, Hertz-Fowler C, et al. 2005. Comparative genomics of trypanosomatid parasitic protozoa. *Science* **309:** 404–409.

Etheridge RD, Aphasizheva I, Gershon PD, Aphasizhev R. 2008. 3′ adenylation determines mRNA abundance and monitors completion of RNA editing in *T. brucei* mitochondria. *EMBO J* **27:** 1596–1608.

Fisk JC, Ammerman ML, Presnyak V, Read LK. 2008. TbRGG2, an essential RNA editing accessory factor in two *Trypanosoma brucei* life cycle stages. *J Biol Chem* **283:** 23016–23025.

Fisk JC, Presnyak V, Ammerman ML, Read LK. 2009. Distinct and overlapping functions of MRP1/2 and RBP16 in mitochondrial RNA metabolism. *Mol Cell Biol* **29:** 5214–5225.

Golden DE, Hajduk SL. 2005. The 3′-untranslated region of cytochrome oxidase II mRNA functions in RNA editing of African trypanosomes exclusively as a *cis* guide RNA. *RNA* **11:** 29–37.

Hall KB, Kranz JK. 1999. Nitrocellulose filter binding for determination of dissociation constants. *Methods Mol Biol* **118:** 105–114.

Hashimi H, Zíková A, Panigrahi AK, Stuart KD, Lukeš J. 2008. TbRGG1, an essential protein involved in kinetoplastid RNA metabolism that is associated with a novel multiprotein complex. *RNA* **14:** 970–980.

Hashimi H, Čičová Z, Novotná L, Wen YZ, Lukeš J. 2009. Kinetoplastid guide RNA biogenesis is dependent on subunits of the mitochondrial RNA binding complex 1 and mitochondrial RNA polymerase. *RNA* **15:** 588–599.

Hernandez A, Madina BR, Ro K, Wohlschlegel JA, Willard B, Kinter MT, Cruz-Reyes J. 2010. REH2 RNA helicase in kinetoplastid mitochondria: Ribonucleoprotein complexes and essential motifs for unwinding and guide RNA (gRNA) binding. *J Biol Chem* **285:** 1220–1228.

Jackson AP. 2007. Tandem gene arrays in *Trypanosoma brucei*: Comparative phylogenomic analysis of duplicate sequence variation. *BMC Evol Biol* **7:** 54. doi: 10.1186/1471-2148-7-54.

Jensen BC, Kifer CT, Brekken DL, Randall AC, Wang Q, Drees BL, Parsons M. 2007. Characterization of protein kinase CK2 from *Trypanosoma brucei*. *Mol Biochem Parasitol* **151:** 28–40.

Kao CY, Read LK. 2005. Opposing effects of polyadenylation on the stability of edited and unedited mitochondrial RNAs in *Trypanosoma brucei*. *Mol Cell Biol* **25:** 1634–1644.

Koslowsky DJ, Riley GR, Feagin JE, Stuart K. 1992. Guide RNAs for transcripts with developmentally regulated RNA editing are present in both life cycle stages of *Trypanosoma brucei*. *Mol Cell Biol* **12:** 2043–2049.

Koslowsky DJ, Kutas SM, Stuart K. 1996. Distinct differences in the requirements for ribonucleoprotein complex formation on differentially regulated pre-edited mRNAs in *Trypanosoma brucei*. *Mol Biochem Parasitol* **80:** 1–14.

Li F, Herrera J, Zhou S, Maslov DA, Simpson L. 2011. Trypanosome REH1 is an RNA helicase involved with the 3′–5′ polarity of multiple gRNA-guided uridine insertion/deletion RNA editing. *Proc Natl Acad Sci* **108:** 3542–3547.

Lukeš J, Hashimi H, Zíková A. 2005. Unexplained complexity of the mitochondrial genome and transcriptome in kinetoplastid flagellates. *Curr Genet* **48:** 277–299.

Madina BR, Kuppan G, Vashisht AA, Liang YH, Downey KM, Wohlschlegel JA, Ji X, Sze SH, Sacchettini JC, Read LK, et al. 2011. Guide RNA biogenesis involves a novel RNase III family endoribonuclease in *Trypanosoma brucei*. *RNA* **17:** 1821–1830.

Maslov DA, Simpson L. 1992. The polarity of editing within a multiple gRNA-mediated domain is due to formation of anchors for upstream gRNAs by downstream editing. *Cell* **70:** 459–467.

Maslov DA, Zíková A, Kyselová I, Lukeš J. 2002. A putative novel nuclear-encoded subunit of the cytochrome *c* oxidase complex in trypanosomatids. *Mol Biochem Parasitol* **125:** 113–125.

Militello KT, Read LK. 1999. Coordination of kRNA editing and polyadenylation in *Trypanosoma brucei* mitochondria: Complete editing is not required for long poly(A) tract addition. *Nucleic Acids Res* **27:** 1377–1385.

Moshiri H, Acoca S, Kala S, Najafabadi HS, Hogues H, Purisima E, Salavati R. 2011. Naphthalene-based RNA editing inhibitor blocks RNA editing activities and editosome assembly in *Trypanosoma brucei*. *J Biol Chem* **286:** 14178–14189.

Nilsson D, Gunasekera K, Mani J, Osteras M, Farinelli L, Baerlocher L, Roditi I, Ochsenreiter T. 2010. Spliced leader trapping reveals

widespread alternative splicing patterns in the highly dynamic transcriptome of *Trypanosoma brucei*. *PLoS Pathog* **6:** e1001037. doi: 10.1371/journal.ppat.1001037.

Panigrahi AK, Schnaufer A, Carmean N, Igo RP Jr, Gygi SP, Ernst NL, Palazzo SS, Weston DS, Aebersold R, Salavati R, et al. 2001. Four related proteins of the *Trypanosoma brucei* RNA editing complex. *Mol Cell Biol* **21:** 6833–6840.

Panigrahi AK, Ernst NL, Domingo GJ, Fleck M, Salavati R, Stuart KD. 2006. Compositionally and functionally distinct editosomes in *Trypanosoma brucei*. *RNA* **12:** 1038–1049.

Panigrahi AK, Zíková A, Dalley RA, Acestor N, Ogata Y, Anupama A, Myler PJ, Stuart KD. 2008. Mitochondrial complexes in *Trypanosoma brucei*: A novel complex and a unique oxidoreductase complex. *Mol Cell Proteomics* **7:** 534–545.

Pelletier M, Read LK. 2003. RBP16 is a multifunctional gene regulatory protein involved in editing and stabilization of specific mitochondrial mRNAs in *Trypanosoma brucei*. *RNA* **9:** 457–468.

Pfaffl MW. 2001. A new mathematical model for relative quantification in real-time RT-PCR. *Nucleic Acids Res* **29:** e45. doi: 10.1093/nar/29.9.e45.

Philippe H, Lopez P, Brinkmann H, Budin K, Germot A, Laurent J, Moreira D, Muller M, Le Guyader H. 2000. Early-branching or fast-evolving eukaryotes? An answer based on slowly evolving positions. *Proc Biol Sci* **267:** 1213–1221.

Reifur L, Koslowsky DJ. 2008. *Trypanosoma brucei* ATPase subunit 6 mRNA bound to gA6-14 forms a conserved three-helical structure. *RNA* **14:** 2195–2211.

Ryan CM, Read LK. 2005. UTP-dependent turnover of *Trypanosoma brucei* mitochondrial mRNA requires UTP polymerization and involves the RET1 TUTase. *RNA* **11:** 763–773.

Schmid B, Riley GR, Stuart K, Goringer HU. 1995. The secondary structure of guide RNA molecules from *Trypanosoma brucei*. *Nucleic Acids Res* **23:** 3093–3102.

Schumacher MA, Karamooz E, Zíková A, Trantírek L, Lukeš J. 2006. Crystal structures of *T. brucei* MRP1/MRP2 guide-RNA binding complex reveal RNA matchmaking mechanism. *Cell* **126:** 701–711.

Shlomai J. 2004. The structure and replication of kinetoplast DNA. *Curr Mol Med* **4:** 623–647.

Siegel TN, Hekstra DR, Wang X, Dewell S, Cross GA. 2010. Genome-wide analysis of mRNA abundance in two life-cycle stages of *Trypanosoma brucei* and identification of splicing and polyadenylation sites. *Nucleic Acids Res* **38:** 4946–4957.

Simpson L, Aphasizhev R, Gao G, Kang X. 2004. Mitochondrial proteins and complexes in *Leishmania* and *Trypanosoma* involved in U-insertion/deletion RNA editing. *RNA* **10:** 159–170.

Simpson L, Aphasizhev R, Lukeš J, Cruz-Reyes J. 2010. Guide to the nomenclature of kinetoplastid RNA editing: A proposal. *Protist* **161:** 2–6.

Speijer D. 2006. Is kinetoplastid pan-editing the result of an evolutionary balancing act? *IUBMB Life* **58:** 91–96.

Sprehe M, Fisk JC, McEvoy SM, Read LK, Schumacher MA. 2010. Structure of the *Trypanosoma brucei* p22 protein, a cytochrome oxidase subunit II-specific RNA-editing accessory factor. *J Biol Chem* **285:** 18899–18908.

Stuart KD, Schnaufer A, Ernst NL, Panigrahi AK. 2005. Complex management: RNA editing in trypanosomes. *Trends Biochem Sci* **30:** 97–105.

Tarun SZ Jr, Schnaufer A, Ernst NL, Proff R, Deng J, Hol W, Stuart K. 2008. KREPA6 is an RNA-binding protein essential for editosome integrity and survival of *Trypanosoma brucei*. *RNA* **14:** 347–358.

Vanhamme L, Perez-Morga D, Marchal C, Speijer D, Lambert L, Geuskens M, Alexandre S, Ismaili N, Goringer U, Benne R, et al. 1998. *Trypanosoma brucei* TBRGG1, a mitochondrial oligo(U)-binding protein that co-localizes with an in vitro RNA editing activity. *J Biol Chem* **273:** 21825–21833.

Vondrušková E, van den Burg J, Zíková A, Ernst NL, Stuart K, Benne R, Lukeš J. 2005. RNA interference analyses suggest a transcript-specific regulatory role for mitochondrial RNA-binding proteins MRP1 and MRP2 in RNA editing and other RNA processing in *Trypanosoma brucei*. *J Biol Chem* **280:** 2429–2438.

Weng J, Aphasizheva I, Etheridge RD, Huang L, Wang X, Falick AM, Aphasizhev R. 2008. Guide RNA-binding complex from mitochondria of trypanosomatids. *Mol Cell* **32:** 198–209.

Wickstead B, Ersfeld K, Gull K. 2002. Targeting of a tetracycline-inducible expression system to the transcriptionally silent minichromosomes of *Trypanosoma brucei*. *Mol Biochem Parasitol* **125:** 211–216.

Wong I, Lohman TM. 1993. A double-filter method for nitrocellulose-filter binding: application to protein–nucleic acid interactions. *Proc Natl Acad Sci* **90:** 5428–5432.

Zíková A, Kopečná J, Schumacher MA, Stuart K, Trantírek L, Lukeš J. 2008. Structure and function of the native and recombinant mitochondrial MRP1/MRP2 complex from *Trypanosoma brucei*. *Int J Parasitol* **38:** 901–912.

Zimmer SL, McEvoy SM, Li J, Qu J, Read LK. 2011. A novel member of the RNase D exoribonuclease family functions in mitochondrial guide RNA metabolism in *Trypanosoma brucei*. *J Biol Chem* **286:** 10329–10340.

ERRATUM

RNA 18: 1846–1861

Functional characterization of two paralogs that are novel RNA binding proteins influencing mitochondrial transcripts of *Trypanosoma brucei*

LUCIE KAFKOVÁ, MICHELLE L. AMMERMAN, DRAHOMÍRA FAKTOROVÁ, JOHN C. FISK, SARA L. ZIMMER, ROMAN SOBOTKA, LAURIE K. READ, JULIUS LUKEŠ, AND HASSAN HASHIMI

The labels *above* the lanes in Figure 2A (page 1850) were mislabeled and should instead read as follows:

Lane 1: no RNA, no protein
Lane 2: no RNA, MRB8170
Lane 3: no RNA, p22
Lane 4: no RNA, TbRGG2
Lane 5: plus RNA, MRB8170
Lane 6: plus RNA, p22
Lane 7: plus RNA, TbRGG2
Lane 8: plus RNA, MRB4160

The authors apologize for any confusion this mislabeling may have caused, though they note that these errors do not affect the results of the figure or any conclusions of the manuscript.

Attached Publications

Part I. Trypanosome RNA editing

Michelle L. Ammerman, Danielle L.Tomasello, Drahomíra Faktorová, Lucie Kafková, Hassan Hashimi, Julius Lukeš, and Laurie K. Read (2013). A core MRB1 complex component is indispensable for RNA editing in insect and human infective stages of *Trypanosoma brucei*. *PLoS One* 8: e78015.

This paper describes the functional analysis of another core MRB1 subunit. It is also the first paper to observe the accumulation of gRNAs upon the interference of RNA editing, suggesting that these small transcripts are consumed during the process.

A Core MRB1 Complex Component Is Indispensable for RNA Editing in Insect and Human Infective Stages of *Trypanosoma brucei*

Michelle L. Ammerman[1¤], Danielle L. Tomasello[1], Drahomíra Faktorová[2], Lucie Kafková[1], Hassan Hashimi[2], Julius Lukeš[2], Laurie K. Read[1*]

1 Department of Microbiology and Immunology, University at Buffalo School of Medicine, Buffalo, New York, United States of America, **2** Institute of Parasitology, Biology Center, Czech Academy of Sciences and Faculty of Science, University of South Bohemia, České Budějovice (Budweis), Czech Republic

Abstract

Uridine insertion/deletion RNA editing is a unique and vital process in kinetoplastids, required for creation of translatable open reading frames in most mitochondrially-encoded RNAs. Emerging as a key player in this process is the mitochondrial RNA binding 1 (MRB1) complex. MRB1 comprises an RNA-independent core complex of at least six proteins, including the GAP1/2 guide RNA (gRNA) binding proteins. The core interacts in an RNA-enhanced or -dependent manner with imprecisely defined TbRGG2 subcomplexes, Armadillo protein MRB10130, and additional factors that comprise the dynamic MRB1 complex. Towards understanding MRB1 complex function in RNA editing, we present here functional characterization of the pentein domain-containing MRB1 core protein, MRB11870. Inducible RNAi studies demonstrate that MRB11870 is essential for proliferation of both insect vector and human infective stage *T. brucei*. MRB11870 ablation causes a massive defect in RNA editing, affecting both pan-edited and minimally edited mRNAs, but does not substantially affect mitochondrial RNA stability or processing of precursor transcripts. The editing defect in MRB1-depleted cells occurs at the initiation stage of editing, as pre-edited mRNAs accumulate. However, the gRNAs that direct editing remain abundant in the knockdown cells. To examine the contribution of MRB11870 to MRB1 macromolecular interactions, we tagged core complexes and analyzed their composition and associated proteins in the presence and absence of MRB11870. These studies demonstrated that MRB11870 is essential for association of GAP1/2 with the core, as well as for interaction of the core with other proteins and subcomplexes. Together, these data support a model in which the MRB1 core mediates functional interaction of gRNAs with the editing machinery, having GAP1/2 as its gRNA binding constituents. MRB11870 is a critical component of the core, essential for its structure and function.

Citation: Ammerman ML, Tomasello DL, Faktorová D, Kafková L, Hashimi H, et al. (2013) A Core MRB1 Complex Component Is Indispensable for RNA Editing in Insect and Human Infective Stages of *Trypanosoma brucei*. PLoS ONE 8(10): e78015. doi:10.1371/journal.pone.0078015

Editor: Ziyin Li, University of Texas Medical School at Houston, United States of America

Received August 1, 2013; **Accepted** September 11, 2013; **Published** October 18, 2013

Funding: This work was supported by NIH grant RO1 AI061580 to LKR, and by the Grant Agency of the Czech Republic (P305/11/2179 and P305/12/2261), the RNPnet FP7 program (289007), and a Praemium Academiae award to J.L., who is a Fellow of the Canadian Institute for Advanced Research. The funders had no role in study design, data collection and analysis, decision to publish, or preparation of the manuscript.

Competing interests: The authors have declared that no competing interests exist.

* E-mail: lread@buffalo.edu

¤ Current address: Department of Chemistry and Biochemistry, Kettering University, Flint, Michigan, United States of America

Introduction

The mitochondrial genome of the kinetoplastid flagellate *Trypanosoma brucei* is comprised of dozens of maxicircles and thousands of minicircles that are concatenated into a dense network [1]. Maxicircles contain 18 protein-encoding genes, the majority of which represent subunits of the respiratory chain, as well as two rRNAs. Two-thirds of maxicircle-encoded mRNAs require dramatic remodeling by specific uridine (U) insertion/deletion RNA editing for the creation of translatable open reading frames. This process is essential for both insect procyclic form (PF) and mammalian bloodstream form (BF) *T. brucei* [2,3]. A few mRNAs are edited only within discrete regions, and are referred to as minimally-edited. However, in the majority of mRNAs, termed pan-edited, the degree of U insertion is so extreme that it doubles the size of the primary transcript. *Trans*-acting guide RNAs (gRNAs), primarily encoded within the minicircle components of the mitochondrial DNA network, specify the precise insertion and deletion of Us into mRNAs through gRNA/mRNA base-pairing interactions. The enzymatic reactions of the RNA editing process (endonuclease, terminal uridylyl transferase, U-specific 3' exoribonuclease and RNA ligase activities) are catalyzed by

multiprotein complexes termed editosomes or RNA editing core complexes (RECCs) [3,4].

In addition to the editosome, several non-editosome proteins facilitate the editing of one or more mRNAs *in vivo* [5-11]. Most importantly, a large, dynamic macromolecular complex termed the MRB1 (mitochondrial RNA binding 1) complex, otherwise known as GRBC (gRNA binding complex), has recently emerged as essential for mitochondrial RNA editing [10]. Three groups originally isolated MRB1 through immunoaffinity purification of the GAP1 or GAP2 proteins (for gRNA associated proteins; a.k.a. GRBC1 and 2) [9,12,13]. Purifications of GAP1/2 associated proteins performed in different laboratories resulted in overlapping, but substantially different, sets of proteins. We recently elucidated the architecture of the MRB1 complex and defined its component subcomplexes through a combination of directed yeast two-hybrid screen and *in vivo* pulldowns with numerous endogenously tagged proteins [14]. We found that MRB1 contains a core associating in an RNA-independent manner, composed of GAP1/2 and the MRB11870, MRB3010, MRB5390 and MRB8620 proteins (nomenclature based on TriTrypDB numbers; http://tritrypdb.org/tritrypdb/). GAP1/2, which function as a heterotetramer that binds and stabilizes gRNA [15], may interact with the rest of the core in a dynamic fashion and thereby serve to deliver gRNA to the core. These two proteins are essential for RNA editing, presumably due to their gRNA stabilizing function [13,16]. Repression of the core protein MRB3010 also causes a broad disruption of RNA editing; however, this takes place in the face of normal gRNA levels [17]. Moreover, in the MRB3010 knockdown cells, RNA editing is impaired at an early step in the process, as shown by the accumulation of pre-edited mRNAs, but not partially edited mRNAs. Repression of core protein MRB5390 also disrupts editing, although to a lesser extent as compared to the MRB3010 knockdown [18]. Collectively, the current data are consistent with a model in which the MRB1 core is critical for the functional association of gRNA with the editosome, and GAP1/2 are the gRNA-binding components of the core.

A second important component of the MRB1 complex is TbRGG2, an RNA binding protein that forms mutually exclusive subcomplexes with two paralogous proteins MRB8170 and MRB4160, and also interacts with other proteins including MRB8180 [19-22]. Repression of TbRGG2 dramatically affects editing of pan-edited mRNAs, but does not affect minimally-edited mRNAs [18,19]. TbRGG2 silencing modestly impacts editing initiation, but has a more significant effect on the 3' to 5' progression of editing along pan-edited mRNAs, resulting in the accumulation of partially edited RNAs [23]. Recombinant TbRGG2 preferentially binds pre-edited mRNAs compared to edited mRNAs or gRNAs and catalyzes gRNA/mRNA annealing [20]. *In vivo* complementation studies implicate the RNA annealing activity of the protein as being essential for RNA editing [20]. The TbRGG2-associated proteins, MRB8170 and MRB4160, are paralogues with redundant functions in editing that also impact pan-edited mRNAs to a greater degree than minimally edited mRNAs [21]. These proteins both bind RNA, and like TbRGG2, display a marked preference for mRNA over gRNA [20,21]. TbRGG2/MRB8170/MRB4160 subcomplexes may be multifunctional, as they have also been reported in association with the gRNA processing endonuclease, mRPN1 [22]. Together, results to date implicate the TbRGG2 subcomplex(es) in productive gRNA/mRNA interaction, especially during editing progression.

An additional protein that is present in the majority of MRB1 purifications is MRB10130, a protein almost entirely composed of Armadillo repeats. In yeast two-hybrid screens, MRB10130 exhibits weak interactions with a large number of MRB1 components and a strong direct interaction with TbRGG2 [14]. As Armadillo proteins often act as organizers of multiprotein complexes, our data suggest that MRB10130 may play a similar role, organizing interactions between the MRB1 core, TbRGG2 subcomplexes, and additional subcomplexes and proteins that comprise the dynamic MRB1 complex. All components of the MRB1 complex that have been tested thus far are essential for growth of PF *T. brucei* (the paralogous MRB8170/4160 are redundant such that only the double knockdown impairs growth) [10,13,16-19,21]. Those that have been examined in BF are essential for growth in this life cycle stage as well [16,17,19].

In addition to the essential functions of the MRB1 complex in RNA editing, numerous lines of evidence link MRB1 to other aspects of mitochondrial gene regulation such as RNA maturation, stability and translation [10]. For example, *in vivo* pulldown experiments demonstrate an interaction between enzymes involved in mRNA 3' tail addition and the MRB1 complex, namely KPAP1, a mitochondrial poly(A) polymerase, and KPAF1, a PPR-motif bearing RNA-binding protein [13,24,25]. Accordingly, yeast two-hybrid studies identified direct interactions between KPAF1 and both the MRB1 core and TbRGG2 subcomplex(es) [14]. The MRB1 complex also occasionally co-purifies with MERS1, a NUDIX hydrolase domain-containing protein thought to be involved in stabilizing edited mRNAs [9,13]. Finally, substoichiometric levels of several ribosomal proteins are often identified in association with MRB1, and a more detailed study demonstrated the association of the GAP1/2 proteins with the large ribosomal subunit [26]. Thus, the MRB1 complex connects RNA editing to other aspects of mitochondrial gene expression in a manner whose temporal and spatial details are yet to be uncovered.

In this study, we present a functional characterization of an MRB1 complex protein, MRB11870. Previous *in vivo* pulldown experiments clearly demonstrated that MRB11870 is a component of the MRB1 complex core as it engages in RNA-independent interactions with numerous core components [14]. Yeast two-hybrid studies identified a strong direct interaction of this protein only with MRB3010, suggesting some of these interactions are likely indirect. MRB11870 also engages in weak two-hybrid interactions with the core protein GAP1 and the Armadillo repeat protein MRB10130 [14]. Importantly, the function of MRB11870 cannot be implied simply from its residence in the MRB1 core, as RNAi studies mentioned above reveal different phenotypes upon knockdown of different core components. Repression of GAP1/2 leads to destabilization of the entire gRNA population and a resultant halt in editing [13,16]. In contrast, knockdown of MRB3010 does not affect gRNA levels, but severely impacts editing of the majority of

mRNAs [17], while MRB5390 repression has a more modest effect on RNA editing [18]. Here, we show that MRB11870 is essential for growth of both PF and BF *T. brucei*. Quantitative (q) RT-PCR analyses demonstrate that MRB11870 repression leads to a very strong editing defect that impacts both pan-edited and minimally-edited mRNAs. Editing in MRB11870-ablated cells appears to be halted at an early step in the process, although gRNAs remain abundant, similar to the phenotype observed upon repression of the core protein, MRB3010. Analysis of protein-protein interactions in MRB11870-depleted cells demonstrates that this protein is critical for association of GAP1/2, MRB10130, and TbRGG2 subcomplexes with the core. Thus, MRB11870 is a key protein involved in numerous structural interactions of the core as well as in initial stages of editing in both human and insect stage *T. brucei*.

Results

MRB11870 is a pentein protein highly conserved among Kinetoplastida

MRB11870 is a kinetoplastid-specific protein of 310 amino acids with a predicted molecular mass of 34.7 kDa and pI of 6.7. It is highly conserved across the kinetoplastid flagellates, exhibiting 92% identity/95% similarity to its *Trypanosoma cruzi* homologue and 64% identity/78% similarity to its homologue in *Leishmania major*. Divergence between the *T. brucei* and *L. major* proteins stems in large part from an 18 amino acid-long insertion in the latter. The bulk of the protein, with the exception of the N terminal 12 and C terminal 27 residues, comprises a pentein domain (Superfamily SSF55909, E value $5.1x10^{-15}$). Pentein superfamily proteins are defined by their similar beta/alpha propeller structural folds [27]. The family contains both catalytic proteins, including many proteins that modify guanidines, as well as non-catalytic proteins such as eukaryotic initiation factor 6 (eIF6), which plays key roles in both 60S ribosomal subunit assembly and preventing premature association of 60S and 40S subunits during translation [27,28]. Since the pentein fold arises from disparate primary protein sequences, and this domain plays several catalytic and structural roles in the cell, it is difficult to assign a function to MRB11870 based on this information alone [27]. Furthermore, BLAST searches performed with MRB11870 do not identify any convincing homologues outside the Kinetoplastida.

MRB11870 is essential for growth in PF and BF trypanosomes

MRB11870 is a component of the MRB1 complex core, and other members of this complex are indispensible for growth and RNA editing in PF and BF *T. brucei* [10,13,16-19,21,24]. To determine whether MRB11870 is likewise essential for PF and/or BF proliferation, we silenced MRB11870 expression by conditional tetracycline-regulated RNAi in both life cycle stages and monitored cell growth for 14 days. Two clonal PF lines were isolated, and these behaved similarly. A representative growth curve is shown in Figure 1A. On day 4 following tetracycline addition to the medium, MRB11870 transcript levels were reduced to approximately 25% of wild type levels (Figure 1A, right). Uninduced and RNAi-induced cells grew similarly through day 6, at which time the MRB11870-repressed cells ceased growth. Starting on day 10 post-induction the MRB11870-repressed cells rapidly died. This is one of the most severe growth phenotypes reported for a protein involved in RNA editing to date. In the BF clone, MRB11870 mRNA was reduced to about 50% of wild type levels by day 4 upon RNAi-induction (Figure 1B, right). Proliferation slowed dramatically between days 4 and 8 post-induction, after which the cells appeared to escape the RNAi (Figure 1B, left), which is a typical phenomenon in this life stage [16,19]. Thus, MRB11870 is essential for proliferation of two *T. brucei* life cycle stages.

MRB11870 is required for RNA editing

We next asked whether the essential phenotype of MRB11870 reflects a function for this protein in RNA editing. To examine the effect of MRB11870 repression on RNA editing, we isolated RNA from PF and BF trypanosomes in which the protein was either normally expressed or repressed via RNAi. We then measured the levels of numerous mitochondrial RNAs by quantitative (q) RT-PCR. We used a panel of primer sets that distinguish edited from pre-edited versions of a given mRNA [29]. We also measured RNAs that do not undergo editing, the so-called never-edited RNAs, and dicistronic pre-processed RNAs, to ask whether MRB11870 effects were specific to editing or extended to other aspects of RNA processing or stability [18]. Because editing of some RNAs is developmentally regulated, we examined a slightly different panel of RNAs in the two life cycle stages. Figure 2A shows the results from PF cells. This analysis demonstrated that the levels of never-edited 9S and 12S rRNAs, as well as never-edited ND4 and COI mRNAs, were unaffected by MRB11870 repression. Likewise, the levels of three dicistronic precursor transcripts spanning the 9S/ND8, A6/CYb and RPS12/ND5 genes remained unaltered. In contrast, all six edited mRNAs tested were dramatically impacted by repression of the MRB11870 protein. Edited versions of the pan-edited RPS12, COIII, and A6 mRNAs were decreased to between 10-20% of wild type levels. At the same time, the pre-edited versions of these same mRNAs were increased 2.2 to 4.5-fold. We also analyzed three mRNAs that are edited only within a small region, termed minimally-edited. This is of interest because some MRB1 complex proteins, such as TbRGG2, impact only pan-edited mRNAs, while core components reportedly affect the majority of edited mRNAs [13,16-19]. MRB11870 repression leads to a decrease in the levels of edited CYb, COII, and MURF2 mRNAs and a corresponding increase in pre-edited CYb mRNA. Thus, MRB11870 is required for editing of both pan-edited and minimally-edited mRNAs in PF trypanosomes, and appears to have little if any impact on RNA stability or processing.

In BF trypanosomes, MRB11870 repression had a similar impact on RNA editing as that observed in PF. Editing of pan-edited A6, RPS12, and ND8 mRNAs and minimally-edited MURF2 mRNA was essentially abolished upon MRB11870 depletion. The corresponding pre-edited mRNAs accumulated to 5 to 6-fold their normal levels in the cases of A6 and RPS12

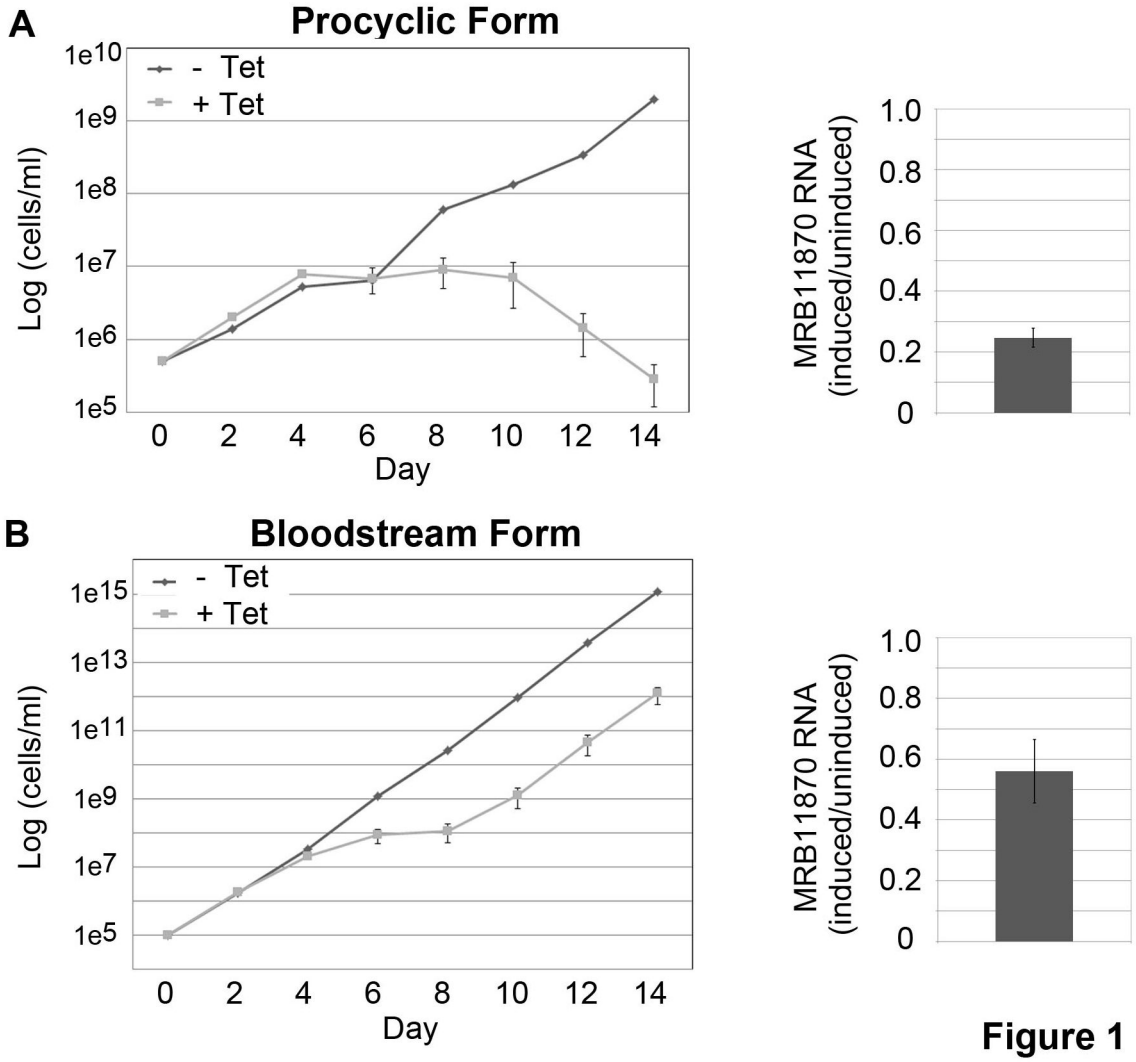

Figure 1. MRB11870 is essential for proliferation of both procyclic and bloodstream form *T. brucei*. MRB11870 was repressed by tetracycline-regulated RNAi in procyclic (A) and bloodstream (B) form *T. brucei*, and cell growth was monitored in triplicate cultures of uninduced and induced cells for 14 days. MRB11870 knockdown on day 4 post-induction was verified by qRT-PCR (n = 6) normalized to tubulin RNA.

doi: 10.1371/journal.pone.0078015.g001

mRNAs, while ND8 and MURF2 pre-edited mRNAs exhibited minimal increases. We also observed that the abundance of three dicistronic precursors spanning the 9S/ND8, A6/CYb and RPS12/ND5 genes and the never-edited COI and ND4 mRNAs were largely unaffected by MRB11870 repression, again indicating the MRB11870 does not play any role in the processing or stabilization of these RNAs in this life cycle stage. However, we did observe an approximately 75% decrease in the levels of both 9S and 12S rRNAs upon MRB11870 repression in BF, although it is unclear whether this is a primary effect of MRB11870 as the same phenomenon was not observed in PF. Collectively, these data indicate that MRB11870 plays a broad and essential role in RNA editing in two stages of the *T. brucei* life cycle.

MRB11870 impacts editing initiation, but does not dramatically affect gRNA levels

Having shown that MRB11870 is essential for editing of both minimally-edited and pan-edited mRNAs, we next addressed which point of the process is affected when this protein is repressed. The qRT-PCR analysis of edited mRNAs described above monitors editing in regions near the 5' ends of these RNAs [23,29]. Because editing takes place in a 3' to 5' direction, this analysis does not distinguish between impacts of protein repression at the initiation vs. progression stages of editing. Our observation that pre-edited mRNAs increase concomitantly for most transcripts (Figure 2) suggests some effect at the initiation of editing [17]. To further assess the effect of MRB11870 down-regulation at both the initiation and

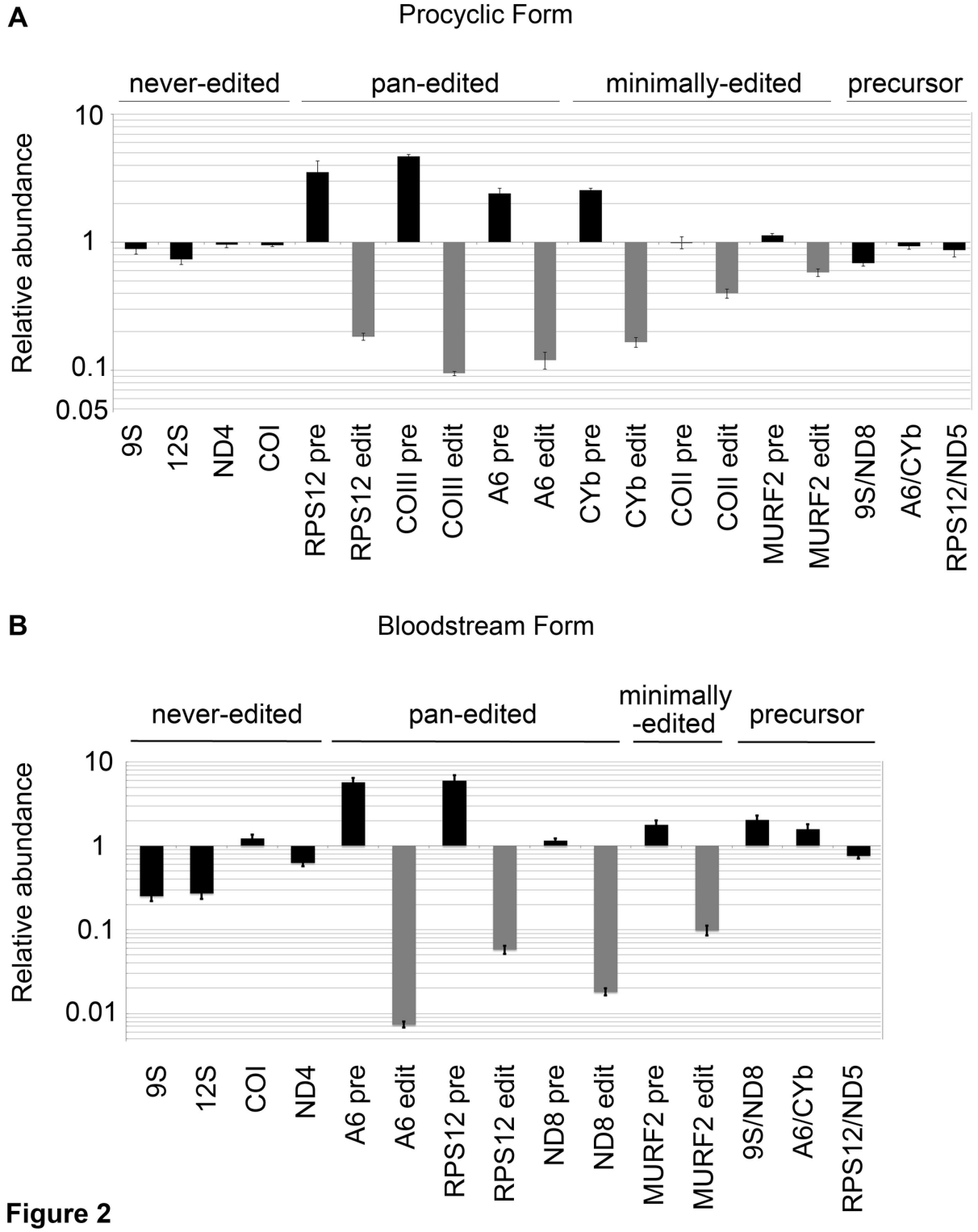

Figure 2

Figure 2. MRB11870 is required for editing of both pan-edited and minimally-edited mRNAs. RNA was isolated from procyclic (A) and bloodstream (B) form *T. brucei* on day 4 post-induction. RNAs were quantified by qRT-PCR using primer sets specific for selected never-edited, pan-edited, minimally-edited and dicistronic precursor RNAs. Relative RNA abundance indicates RNA levels in tetracycline-induced cells compared to those in uninduced cells. RNA levels were standardized to tubulin RNA and numbers represent the mean and standard error of 6-15 determinations.

doi: 10.1371/journal.pone.0078015.g002

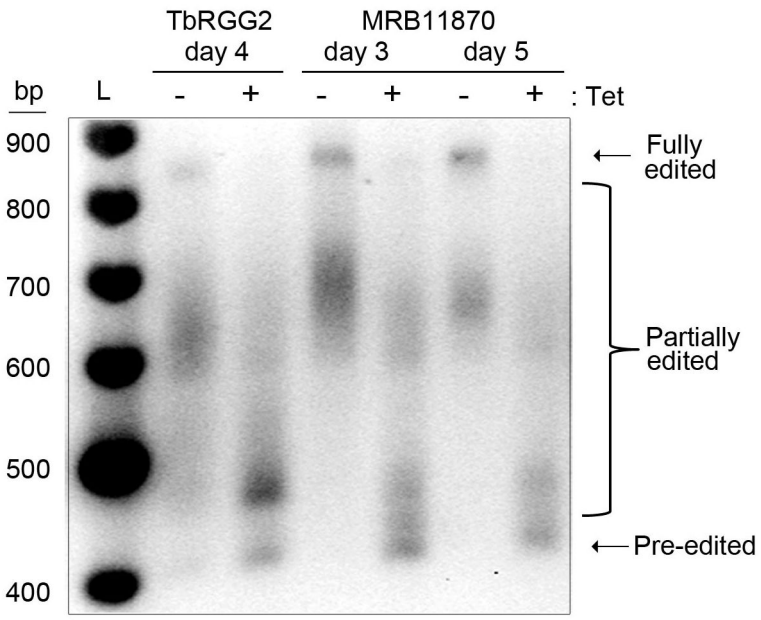

Figure 3

Figure 3. MRB11870 impacts an early step of the editing process. Agarose gel analysis of RT-PCR reactions using RNAs isolated from TbRGG2 and MRB11870 RNAi cells that were grown in the absence or presence of tetracycline (Tet) for the indicated number of days. Primers specific to the never-edited 5' and 3' ends of A6 mRNA, which flank the edited region, amplify the entire population of transcripts, including pre-edited, partially edited, and fully edited. L, size ladder.

doi: 10.1371/journal.pone.0078015.g003

progression phases of the editing process, we analyzed the complete population of A6 mRNA from PF MRB11870 RNAi cells by RT-PCR using primers specific to the small 5' and 3' never-edited regions of the RNA, which flank the pan-edited region. This assay permits us to compare the relative amounts of pre-edited, partially edited, and fully edited mRNAs in uninduced and induced MRB11870 RNAi cells on the same gel [23,30]. We used this assay to compare the effect of MRB11870 repression to that of TbRGG2, which leads to a small decrease in editing initiation and a dramatic effect on the 3' to 5' progression of editing that manifests as accumulation of specific partially edited mRNAs even 6 days following induction of RNAi [17,23] (Figure 3). Compared to TbRGG2-repressed cells, flagellates ablated for MRB11870 exhibit a greater increase in pre-edited mRNA and lower accumulation of partially edited mRNA. This effect was evident by day 3 post-induction, and by day 5 pre-edited mRNA was the dominant species. Thus, because intermediate products do not build up, our results suggest that MRB11870 repression affects RNA editing initiation, perhaps due to an impact on utilization of the first gRNA. This phenotype is reminiscent of that observed upon MRB3010 depletion [17].

Another MRB1 core component, the GAP1/2 heterotetramer, also affects RNA editing at the initiation stage, but this is a secondary effect of global gRNA destabilization upon GAP1/2 repression [13,16]. In contrast, repression of the MRB3010 core protein blocks editing initiation although gRNA levels remain normal [17]. To address whether the effect of MRB11870 on editing initiation reflects a decrease in gRNA abundance, we examined the levels of both the global gRNA population and specific gRNAs in the respective RNAi cells. In the experiment shown in Figure 4A, we isolated RNA from uninduced cells and cells that had been tetracycline-induced for 4 days. The total gRNA population was labeled by incubation of the RNA with alpha-[^{32}P]-GTP and guanylyltransferase; a labeled cytoplasmic RNA serves as a loading control. These data clearly show that total gRNA levels are not decreased upon MRB11870 repression, and in fact gRNA abundance may be slightly increased. To further examine the impact of MRB11870 knockdown on gRNAs, we analyzed three specific gRNAs by Northern blot on days 3 and 4 after induction of RNAi, and normalized RNA abundance determined by densitometry to that of 5.8S rRNA (Figure 4B). Following quantification and normalization of specific gRNA levels, it was clear that gA6[14], gCYb[558], and gMURF2[II] levels were essentially unchanged on day 3 post-induction. The levels of these gRNAs increased on day 4 post-induction, with levels compared to uninduced cells ranging from 1.3 to 2.2-fold depending on the gRNA. From these data, we conclude that MRB11870 facilitates an early step in the editing process in a manner that is independent of gRNA stabilization.

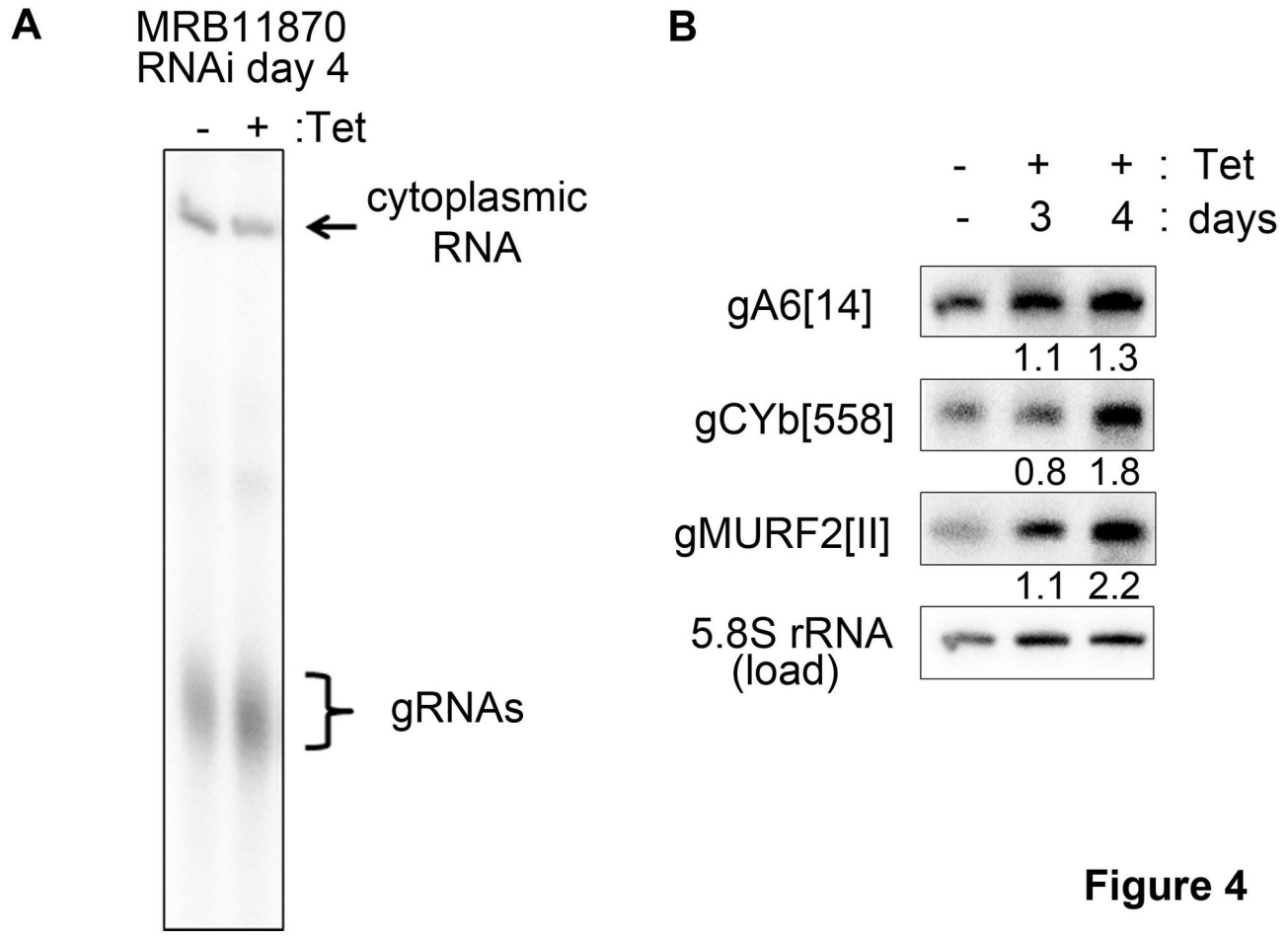

Figure 4. MRB11870 repression does not lead to a decrease in gRNA levels. (A) RNA was isolated from MRB11870 RNAi cells either uninduced (-) or induced with tetracycline (+) for 4 days, and labeled with alpha-[32P]-GTP and guanylyltransferase. The labeled gRNA population is indicated, as is a labeled cytoplasmic RNA used for normalization. (B) Six µg of RNA isolated from MRB11870 RNAi cells either uninduced (-) or induced with tetracycline (+) for 3 or 4 days was electrophoresed on 10% acrylamide/8 M urea gels and transferred to a nylon membrane. Membranes were probed with 5'-end labeled oligonucleotides complementary to gA6[14], CYb[558] or gMURF2[II] gRNAs plus 5.8S rRNA as a loading control. Signals were quantified by phosphorimaging and gRNA levels were normalized to the levels of 5.8S RNA from the same sample. The change in normalized gRNA levels at days 3 and 4 after RNAi induction are indicated below the blots.

doi: 10.1371/journal.pone.0078015.g004

MRB11870 is essential for MRB1 complex protein-protein interactions

We previously defined the architecture of the MRB1 complex, which includes a core complex of at least 6 proteins, including GAP1/2; the latter may also exist as a separate heterotetramer and recruit gRNAs to the core [14] (Figure 5A). Yeast two-hybrid data indicate that MRB11870 interacts within the core primarily through a strong direct interaction with MRB3010, with a possible contribution from a weak direct interaction with GAP1. Additional components of the MRB1 complex include the TbRGG2 subcomplex(es), which contain the eponymous protein and a still imprecisely characterized combination of the MRB8170, MRB4160 and/or MRB8180 proteins [14,21]. MRB10130 is an Armadillo repeat protein that interacts with a large number of MRB1 proteins, including components of both the core and the TbRGG2 subcomplex(es), and may serve as an MRB1 organizer. Towards understanding the function of MRB11870 in RNA editing, we next wanted to address its macromolecular interactions within the MRB1 complex. To this end, we generated PF cells harboring both an endogenously PTP-tagged allele of the MRB3010 core component and the MRB11870 RNAi construct (Figure 5B). This set up allowed us to perform pulldowns of the MRB1 core in the presence and absence of MRB11870 and determine whether the depletion of the latter protein dramatically impacts the composition of the core and/or its interactions with other MRB1 subcomplexes and proteins.

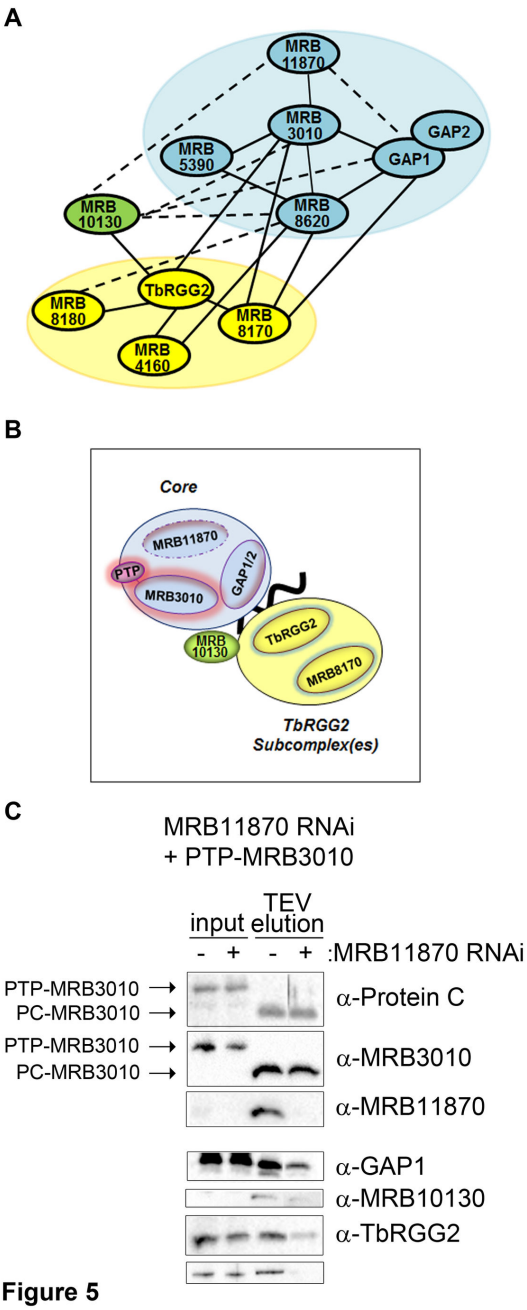

Figure 5

Figure 5. MRB11870 is required for numerous MRB1 complex macromolecular interactions. (A) Schematic showing the known strong (solid line) and weak (dotted line) yeast two-hybrid interactions between MRB1 components examined here (14). MRB1 core is indicated by the blue oval and TbRGG2 subcomplexes by the yellow oval. We omitted the strong two-hybrid interaction between MRB4160 and MRB8170 as these two proteins were later shown to engage in mutually exclusive interactions with TbRGG2 (21). (B) Cartoon of selected MRB1 complex components in cells harboring both MRB11870 RNAi (dotted line) and MRB3010 PTP-tagged at an endogenous allele (pink highlight). Shown in the figure is the MRB1 core (blue), from which GAP1/2 may transiently dissociate. Blank oval indicates additional core proteins including MRB5390 and MRB8620. Also depicted are the TbRGG2 subcomplex(es) (yellow), a subset of which contain MRB8170 as depicted. The MRB10130 protein, which may act as an MRB1 complex organizer is shown in green. Black line indicates RNA, which may include gRNA, mRNA or both. (C) PTP-MRB3010 and associated proteins were isolated by IgG Sepharose chromatography and TEV protease cleavage from RNase-treated extracts of cells either uninduced (-) or tetracycline-induced (+) for MRB11870 RNAi. PTP-MRB3010 and PC-MRB3010 indicate the tagged protein before and after TEV cleavage, respectively. Both input and TEV elutions were analyzed by western blot for MRB1 complex components using the antibodies indicated on the right.

doi: 10.1371/journal.pone.0078015.g005

PTP-MRB3010 and associated proteins were isolated from RNase-treated MRB11870-expressing or repressed cell extracts by affinity chromatography on IgG Sepharose, which binds the Protein A moiety of the PTP tag, followed by a subsequent TEV protease cleavage (Figure 5C). The resulting Protein C (PC)-tagged MRB3010 was detected in the eluates by both anti-Protein C and anti-MRB3010 antibodies, and MRB11870 knockdown was verified using anti-MRB11870 antibodies. Eluates from uninduced and MRB11870-ablated cells were normalized to PC-MRB3010 levels, and the abundance of selected MRB1 complex components was analyzed by western blot. Since GAP1/2 is a critical, gRNA binding component of the core that weakly interacts with MRB11870, we first asked whether association with the MRB1 core of GAP1, serving as a proxy for both GAP proteins, was affected by MRB11870 repression. Figure 5C shows that the amount of GAP1 associated with the MRB1 core was significantly decreased when MRB11870 was repressed, although the steady state level of the protein remains unaffected (input). MRB11870 may be directly involved in the association of GAP1/2 with the core, as suggested by the yeast two-hybrid data showing a weak direct MRB11870-GAP1 interaction [14]. Additionally, the absence of MRB11870 may cause a general destabilization of the MRB1 core, or it may perturb the structures of MRB3010 and/or MRB8620, core proteins that display strong direct interactions with GAP1. We next asked whether association of the MRB1 core with MRB10130, the putative organizer protein, is impacted by MRB11870 repression. As shown in Figure 5C, core-associated levels of MRB10130 are also substantially decreased upon MRB11870 repression, possibly reflecting the direct interaction between these two proteins and/or global disruption of core structure.

Finally, we asked whether association of TbRGG2 subcomplexes with the core was impacted by MRB11870 repression. Western blot analysis of TbRGG2 and its binding partner MRB8170 revealed a strong disruption of the core-TbRGG2 subcomplex association in the absence of MRB11870. Interestingly, MRB11870 does not appear to engage in direct interactions with either TbRGG2 or MRB8170 [14]. Thus, the dramatic decrease in the association of these proteins with the core may be a secondary consequence of MRB10130 reduction, since this putative organizer directly contacts both the core and TbRGG2 (Figure 5A) [14]. Additionally, loss of GAP1/2 and its associated gRNAs may lead to decreased interaction with TbRGG2-bound mRNA that promotes the association of core and TbRGG2 subcomplexes [20]. Together, the protein-protein interaction studies reveal a pivotal role for MRB11870 in the MRB1 complex structure and highlight the intricate nature of the macromolecular interactions that comprise the MRB1 complex.

Discussion

MRB1 is a dynamic multiprotein complex in trypanosome mitochondria, numerous components of which are critical for the vital and unique RNA editing process [10]. Our previous studies, employing yeast two-hybrid and *in vivo* pulldown analyses, defined an MRB1 complex core of at least six proteins that interact in an RNA independent manner [14]. In this manuscript, we characterize MRB11870, a protein component of the MRB1 core, and demonstrate that it is essential for growth and RNA editing in two *T. brucei* life cycle stages. MRB11870 affects the initiation of the editing process, despite the presence of abundant gRNAs. Comparative *in vivo* pulldown studies in cells with normal or repressed MRB11870 levels also reveal a key structural role for MRB11870 within the MRB1 complex.

Proteins comprising the MRB1 complex core that have been characterized to date have two distinct phenotypes. The GAP1/2 heterotetramer binds and stabilizes gRNAs [13,15,16]. Repression of either GAP1 or GAP2 destabilizes both proteins, leading to a dramatic decrease in gRNA levels and a consequent halt in RNA editing [13,16]. On the other hand, repression of MRB3010 does not affect gRNA levels, but nevertheless leads to a significant inhibition of RNA editing of both pan- and minimally-edited mRNAs [17]. The phenotype of cells repressed for MRB11870 reported here is similar to that of MRB3010 knockdowns, with a broad and significant effect on editing initiation but no decrease in gRNA levels. This observation is consistent with our reported protein-protein interaction studies, in which the only MRB1 component exhibiting a strong, direct interaction with MRB11870 was MRB3010 [14]. Thus, the functional analysis of MRB11870 reported here validates aspects of our previously published model of MRB1 architecture derived from comprehensive yeast two-hybrid and *in vivo* pulldown studies. Together, the current data support a model in which GAP1/2 are the gRNA binding component of the core, while additional core components, including MRB11870 and MRB3010, are required for the functional association of gRNA with the editing machinery. Interestingly, gRNA levels are modestly increased by day 4 following MRB11870 RNAi induction, representing a hitherto unseen phenotype. This increase in gRNAs may be a consequence of their decreased utilization in the editing process when MRB11870 is repressed, suggesting that gRNAs are consumed during editing and accumulate if editing is abrogated. The mechanisms governing the fate of gRNAs used in editing are not understood. The gRNA cycle and the precise roles of MRB1 complex components in gRNA utilization, and possibly destruction, will be important avenues for future research.

Downregulation of MRB11870 dramatically affected macromolecular interactions within the MRB1 complex. Western blot analysis of GAP1 revealed that, while its total levels in the organelle are unaffected by MRB11870 repression, the fraction of GAP1 associated with the MRB3010 core protein is significantly diminished when MRB11870 is repressed. MRB11870 may be directly involved in maintaining GAP1/2 association with the core, through a weak direct interaction between the GAP1 and MRB11870 [14]. Alternatively or in addition, the inability of GAP1 to properly associate with the core in the absence of MRB11870 may be indicative of an overall disturbance of the core structure. These data also demonstrate that the ability of GAP1/2 to stabilize the total gRNA population is not dependent on the proteins'

interaction with the rest of the MRB1 core, since gRNAs remain abundant when the GAP1/2 association with MRB3010 is impaired in MRB11870-repressed cells. The decreased interaction of Armadillo repeat protein MRB10130 with the core upon MRB11870 ablation may also reflect the reported weak direct interaction between these two proteins and/or altered core structure. While neither TbRGG2 nor MRB8170 interact directly with MRB11870, both make direct contact with other core proteins, and so their decreased interaction with the core could result from global core disruption [14]. Moreover, MRB10130 directly interacts with both TbRGG2 and numerous core components and may serve as a bridge or promote their interaction (Figures 5A and B) [14]. Finally, decreased association of TbRGG2/MRB8170 with the core could result, at least in part, from disruption of gRNA/mRNA interactions responsible for the RNA-enhanced association of core with TbRGG2 subcomplexes [14]. Although the pulldown experiments reported here were performed in RNase-treated extracts, RNA may still facilitate interaction between the MRB1 core and TbRGG2 subcomplex *in vivo*, but be dispensable once this interaction is established. Both TbRGG2 and MRB8170 exhibit RNA binding activity *in vitro*, with significantly stronger affinities for mRNA than for gRNA, suggesting that TbRGG2/MRB8170 containing subcomplexes may play a role in mRNA utilization during editing, including a role in gRNA/mRNA annealing [20,21]. Thus, loss of GAP1-bound gRNA from the core upon MRB11870 repression could impact association of mRNAs bound to TbRGG2 and/or MRB8170. Regardless of the precise mechanisms, the dramatic disruption of macromolecular associations within the MRB1 complex when MRB11870 is repressed highlights the many coordinated interactions comprising this dynamic complex.

The biochemical function of MRB11870 is not known, but its characterization as a member of the pentein superfamily may yield some clues in this regard. The non-catalytic eIF6, which functions in both ribosome assembly and translation [28,31], represents the simplest form of a pentein domain-containing protein. In the nucleus, eIF6 associates with pre-60S ribosomal subunits and is necessary for biogenesis of mature 60S subunits, including the proper processing of pre-rRNA precursors [32]. An analogous role for MRB11870 in MRB1 core assembly would be consistent with the broken MRB3010-GAP1 interaction that we demonstrate in MRB11870 repressed cells. The second function of eIF6 is to act as a ribosome anti-association factor, sterically blocking the interaction between 60S and 40S ribosomal subunits at critical points in the ribosome cycle. During protein synthesis, GTP hydrolysis catalyzed by 60S-bound ELF1 causes a conformational change in the 60S subunit, promoting eIF6 release and subunit joining [33]. One could envision a similar role for MRB11870 in regulating interactions between MRB1 subcomplexes. Catalytic pentein proteins are larger than non-catalytic members of the family due to the appendage of numerous loops and extensions, and they range from approximately 400-660 amino acids [27]. Interestingly, MRB11870 is significantly larger (310 amino acids) than the minimal pentein protein eIF6 (108 amino acids), suggesting it might have a catalytic function. Catalytic pentein proteins include diverse guanidine-modifying enzymes, such as hydrolases, amidinotransferases, and dihydrolases. Peptidylarginine demininases (PADs) are one member of this family. PADs convert arginine and monomethylarginine (MMA) residues in proteins to citrullines, with a subsequent dramatic effect on protein function [34]. We have identified methylarginine on several MRB1 complex proteins, including TbRGG2, MRB10130, and MRB4160 [35]. While the functions of these modifications are currently unknown, both citrullination of the arginine residues, which would preclude their methylation, as well as citrullination of MMA would likely modulate macromolecular interactions. Investigating the potential enzymatic activities of MRB11870 and determining its precise role in modulating the dynamic interactions that comprise the MRB1 complex will be exciting topics for future research.

Materials and Methods

Generation of cell lines and growth curves

To generate MRB11870 RNAi cells, the entire open reading frame of MRB11870 was amplified with forward primer CAGGATCCATGCTGCGCCACACATCACG and reverse primer CAAAGCTTTTTCTGCAGTTGATGCGTCTGC and cloned into the BamHI and HindIII restriction sites (underlined) of the p2T7-177 plasmid [36] between opposing tetracycline-regulated T7 RNA polymerase promoters. The resulting construct was linearized with NotI and transfected into parental procyclic strain 29-13 and bloodstream form single marker strain *T. brucei* [37]. Transformants were selected with 2.5 μg/ml phleomycin and clones were obtained by limiting dilution. To generate the cell line harboring constructs for both MRB11870 RNAi and PTP-tagged MRB3010, a previously described PTP-MRB3010 plasmid [17] was linearized with BpiI and electroporated into the clonal MRB11870 RNAi line. Cells were selected with 2.5 μg/ml phleomycin and 1 μg/ml puromycin and cloned by limiting dilution. Repression of MRB11870 was induced in all cell lines by adding 2.5 μg/ml tetracycline to cell cultures. TbRGG2 RNAi cells were previously described [19].

Quantitative real time PCR

RNA was isolated from uninduced and tetracycline-induced PF and BF MRB11870 RNAi cells on day 4 post-induction using Trizol, and qRT–PCR reactions were performed with primers specific to mitochondrial transcripts as previously described [19,29]. The level of MRB11870 mRNA depletion was analyzed by qRT-PCR (n = 6) with primers MRB11870 qRT-UTR Rev 5' CGATCTGATACGTTCGTGGTTTGC 3' and MRB11870 qRT-UTR Fwd 5' GTGTGCTCATGGTTGTGGTTAG 3'. These primers target the nts 42-135 following the stop codon within the reported 3' UTR [38,39]. Reactions were normalized to the level of tubulin cDNA.

RT-PCR analysis of A6 transcripts

RNA was isolated from uninduced and tetracycline-induced PF TbRGG2 RNAi cells and MRB11870 RNAi cells and

DNase-treated as described previously [23]. Oligo-dT primed cDNA was prepared by reverse transcription with Superscript III (Invitrogen) by the manufacturer's instructions. A6-specific primers A6 5' NE (5' GCGAATTCAAATAAGTATTTTGATATTATTAAAG 3') and A6 3' (5' ATTAACTTATTTGATCTTATTCTATAACTCC 3') that anneal to the never edited 5' and 3' regions that flank the edited part of the A6 mRNA were used for RT-PCR analysis (restriction site underlined).

Guanyltransferase labeling and northern blot analyses of RNA

Quantification of the total gRNA population by guanylyltransferase labeling was performed as previously described [17]. For northern blot analysis, total RNA (6 µg) was dissolved in loading dye (90% formamide, 10 mM EDTA, 0.05%xylene cyanol, 0.05% bromophenol blue), heated for 5 min to 65°C and resolved by 8 M urea/10% PAGE. RNA was transferred to positively charged nylon membrane (Boehringer Mannheim) by electrotransfer in 0.5X TBE and UV crosslinked using a Stratalinkner (Stratagene). DNA oligonucleotide probes (10 pmol) were labeled with ϒ-[^{32}P] ATP (6000 Ci/mmol) using T4 kinase. Membranes were prehybridized in ULTRAhyb-oligo solution (Ambion) for 30 minutes and then hybridized with the probe overnight at 42°C. The membrane was washed 3 times for 30 minutes each with 20 mL of 4xSSPE, 0.5%SDS at 42°C and was exposed to a phosphor screen overnight. The screen was scanned with the Bio-Rad Personal Imager FX and the quantitation of the density of bands in northern blots was performed with the Quantity One software (Bio-Rad). The following 5'- ^{32}P-labeled oligonucleotides were used:

gA6[14]:
ATAATTATCATATCACTGTCAAAATCTGATTCGTTATCGGAGTTATAGTATAT

gMURF2[II] gRNA (maxicircle encoded):
CATTCAATTACTCTAATTTAATTTTATTTTTGTGC

gCYb[558]: GCGGATCCTTATTCCCTTTATCACC

Pre-5.8S rRNA: CCATCGCGACACGTTGTGGGAGCCG

Immunoprecipitation and western blot analysis

PF cells expressing both the endogenous PTP-MRB3010 and the tetracycline-inducible MRB11870 RNAi constructs were either grown in the presence or absence of the tetracycline for 4 days. Expression of PTP-MRB3010 was verified by western blot using affinity purified rabbit anti-protein C (ICL). MRB11870 knockdown was verified by qRT-PCR at the RNA level as described above and by western blot with anti-MRB11870 antibodies (which are effective only in partially purified samples but not in whole cell extracts). Whole cell extracts were nuclease treated and MRB3010 and its associated proteins were affinity purified by IgG Sepharose 6 Fast Flow chromatography and TEV protease cleavage as described previously [14]. Input and TEV cleavage samples were subsequently analyzed by western blot. Whole cell extracts and TEV elutions were electrophoresed on 10% SDS-polyacrylamide gels and proteins were transferred onto nitrocellulose membrane. Membranes were probed with previously described polyclonal antibodies against MRB3010 [14], MRB11870 [14], MRB8170 [14], GAP1 [17] and TbRGG2 [19]. Polyclonal antibodies against MRB10130 were produced by Bethyl laboratories against the oligopeptide CDLQVLLQRGAVEPGAAPGVM. Western blots were analyzed by chemiluminescence using a Chemidoc MP System (Bio-Rad). Normalization of PC-MRB3010 protein amounts using anti-Protein C antibody was performed with Image lab Software. This experiment was performed twice, using biological replicates, with similar results.

Acknowledgements

We thank Dr. Natalie Merlino for critical reading of the manuscript.

Author Contributions

Conceived and designed the experiments: MLA HH JL LKR. Performed the experiments: MLA DLT DF LK. Analyzed the data: MLA HH JL LKR. Wrote the manuscript: MLA LKR.

References

1. Jensen RE, Englund PT (2012) Network news: the replication of kinetoplast DNA. Annu Rev Microbiol 66: 473-491. doi:10.1146/annurev-micro-092611-150057. PubMed: 22994497.
2. Aphasizhev R, Aphasizheva I (2011) Uridine insertion/deletion editing in trypanosomes: a playground for RNA-guided information transfer. Wiley Interdiscip Rev RNA 2: 669-685. doi:10.1002/wrna.82. PubMed: 21823228.
3. Stuart KD, Schnaufer A, Ernst NL, Panigrahi AK (2005) Complex management: RNA editing in trypanosomes. Trends Biochem Sci 30: 97-105. doi:10.1016/j.tibs.2004.12.006. PubMed: 15691655.
4. Simpson L, Aphasizhev R, Lukes J, Cruz-Reyes J (2010) Guide to the nomenclature of kinetoplastid RNA editing: a proposal. Protist 161: 2-6. doi:10.1016/j.protis.2009.10.001. PubMed: 19945343.
5. Pelletier M, Read LK (2003) RBP16 is a multifunctional gene regulatory protein involved in editing and stabilization of specific mitochondrial mRNAs in *Trypanosoma brucei*. RNA 9: 457-468. doi:10.1261/rna.2160803. PubMed: 12649497.
6. Fisk JC, Presnyak V, Ammerman ML, Read LK (2009) Distinct and overlapping functions of MRP1/2 and RBP16 in mitochondrial RNA metabolism. Mol Cell Biol 29: 5214-5225. doi:10.1128/MCB.00520-09. PubMed: 19620277.
7. Vondrušková E, van den Burg J, Zíková A, Ernst NL, Stuart K et al. (2005) RNA interference analyses suggest a transcript-specific regulatory role for mitochondrial RNA-binding proteins MRP1 and MRP2 in RNA editing and other RNA processing in *Trypanosoma brucei*. J Biol Chem 280: 2429-2438. PubMed: 15504736.
8. Sprehe M, Fisk JC, McEvoy SM, Read LK, Schumacher MA (2010) Structure of the *Trypanosoma brucei* p22 protein, a cytochrome oxidase subunit II-specific RNA-editing accessory factor. J Biol Chem 285: 18899-18908. doi:10.1074/jbc.M109.066597. PubMed: 20392699.
9. Hashimi H, Zíková A, Panigrahi AK, Stuart KD, Lukes J (2008) TbRGG1, an essential protein involved in kinetoplastid RNA metabolism that is associated with a novel multiprotein complex. RNA 14: 970-980. doi:10.1261/rna.888808. PubMed: 18369185.
10. Hashimi H, Zimmer SL, Ammerman ML, Read LK, Lukeš J (2013) Dual core processing: MRB1 is an emerging kinetoplast RNA editing complex. Trends Parasitol 29: 91-99. doi:10.1016/j.pt.2012.11.005. PubMed: 23305619.
11. Li F, Herrera J, Zhou S, Maslov DA, Simpson L (2011) Trypanosome REH1 is an RNA helicase involved with the 3'-5' polarity of multiple gRNA-guided uridine insertion/deletion RNA editing. Proc Natl Acad Sci U S A 108: 3542-3547. doi:10.1073/pnas.1014152108. PubMed: 21321231.

12. Panigrahi AK, Zíková A, Dalley RA, Acestor N, Ogata Y et al. (2008) Mitochondrial complexes in *Trypanosoma brucei*: a novel complex and a unique oxidoreductase complex. Mol Cell Proteomics 7: 534-545. PubMed: 18073385.
13. Weng J, Aphasizheva I, Etheridge RD, Huang L, Wang X et al. (2008) Guide RNA-binding complex from mitochondria of trypanosomatids. Mol Cell 32: 198-209. doi:10.1016/j.molcel.2008.08.023. PubMed: 18951088.
14. Ammerman ML, Downey KM, Hashimi H, Fisk JC, Tomasello DL et al. (2012) Architecture of the trypanosome RNA editing accessory complex, MRB1. Nucleic Acids Res 40: 5637-5650. doi:10.1093/nar/gks211. PubMed: 22396527.
15. Aphasizheva I, Aphasizhev R (2010) RET1-catalyzed uridylylation shapes the mitochondrial transcriptome in Trypanosoma brucei. Mol Cell Biol 30: 1555-1567. doi:10.1128/MCB.01281-09. PubMed: 20086102.
16. Hashimi H, Čičová Z, Novotná L, Wen YZ, Lukes J (2009) Kinetoplastid guide RNA biogenesis is dependent on subunits of the mitochondrial RNA binding complex 1 and mitochondrial RNA polymerase. RNA 15: 588-599. doi:10.1261/rna.1411809. PubMed: 19228586.
17. Ammerman ML, Hashimi H, Novotná L, Čičová Z, McEvoy SM et al. (2011) MRB3010 is a core component of the MRB1 complex that facilitates an early step of the kinetoplastid RNA editing process. RNA 17: 865-877. doi:10.1261/rna.2446311. PubMed: 21451155.
18. Acestor N, Panigrahi AK, Carnes J, Zíková A, Stuart KD (2009) The MRB1 complex functions in kinetoplastid RNA processing. RNA 15: 277-286. doi:10.1261/rna.1353209. PubMed: 19096045.
19. Fisk JC, Ammerman ML, Presnyak V, Read LK (2008) TbRGG2, an essential RNA editing accessory factor in two *Trypanosoma brucei* life cycle stages. J Biol Chem 283: 23016-23025. doi:10.1074/jbc.M801021200. PubMed: 18583347.
20. Foda BM, Downey KM, Fisk JC, Read LK (2012) Multifunctional G-rich and RRM-containing domains of TbRGG2 perform separate yet essential functions in trypanosome RNA editing. Eukaryot Cell 11: 1119-1131. doi:10.1128/EC.00175-12. PubMed: 22798390.
21. Kafková L, Ammerman ML, Faktorová D, Fisk JC, Zimmer SL et al. (2012) Functional characterization of two paralogs that are novel RNA binding proteins influencing mitochondrial transcripts of *Trypanosoma brucei*. RNA 18: 1846-1861. doi:10.1261/rna.033852.112. PubMed: 22898985.
22. Madina BR, Kuppan G, Vashisht AA, Liang YH, Downey KM et al. (2011) Guide RNA biogenesis involves a novel RNase III family endoribonuclease in *Trypanosoma brucei*. RNA 17: 1821-1830. doi:10.1261/rna.2815911. PubMed: 21810935.
23. Ammerman ML, Presnyak V, Fisk JC, Foda BM, Read LK (2010) TbRGG2 facilitates kinetoplastid RNA editing initiation and progression through intrinsic pause sites. RNA 16: 2239-2251. doi:10.1261/rna.2285510. PubMed: 20855539.
24. Hernandez A, Madina BR, Ro K, Wohlschlegel JA, Willard B et al. (2010) REH2 RNA helicase in kinetoplastid mitochondria: ribonucleoprotein complexes and essential motifs for unwinding and guide RNA (gRNA) binding. J Biol Chem 285: 1220-1228. doi:10.1074/jbc.M109.051862. PubMed: 19850921.
25. Etheridge RD, Aphasizheva I, Gershon PD, Aphasizhev R (2008) 3' adenylation determines mRNA abundance and monitors completion of RNA editing in *T. brucei* mitochondria. EMBO J 27: 1596-1608. doi:10.1038/emboj.2008.87. PubMed: 18464794.
26. Aphasizheva I, Maslov D, Wang X, Huang L, Aphasizhev R (2011) Pentatricopeptide repeat proteins stimulate mRNA adenylation/uridylation to activate mitochondrial translation in trypanosomes. Mol Cell 42: 106-117. doi:10.1016/j.molcel.2011.02.021. PubMed: 21474072.
27. Linsky T, Fast W (2010) Mechanistic similarity and diversity among the guanidine-modifying members of the pentein superfamily. Biochim Biophys Acta 1804: 1943-1953. doi:10.1016/j.bbapap.2010.07.016. PubMed: 20654741.
28. Miluzio A, Beugnet A, Volta V, Biffo S (2009) Eukaryotic initiation factor 6 mediates a continuum between 60S ribosome biogenesis and translation. EMBO Rep 10: 459-465. doi:10.1038/embor.2009.70. PubMed: 19373251.
29. Carnes J, Trotter JR, Ernst NL, Steinberg A, Stuart K (2005) An essential RNase III insertion editing endonuclease in *Trypanosoma brucei*. Proc Natl Acad Sci U_S_A 102: 16614-16619. doi:10.1073/pnas.0506133102. PubMed: 16269544.
30. Schnaufer A, Panigrahi AK, Panicucci B, Igo RP Jr., Wirtz E et al. (2001) An RNA ligase essential for RNA editing and survival of the bloodstream form of *Trypanosoma brucei*. Science 291: 2159-2162. doi:10.1126/science.1058655. PubMed: 11251122.
31. Brina D, Grosso S, Miluzio A, Biffo S (2011) Translational control by 80S formation and 60S availability: the central role of eIF6, a rate limiting factor in cell cycle progression and tumorigenesis. Cell Cycle 10: 3441-3446. doi:10.4161/cc.10.20.17796. PubMed: 22031223.
32. Basu U, Si K, Warner JR, Maitra U (2001) The *Saccharomyces cerevisiae* TIF6 gene encoding translation initiation factor 6 is required for 60S ribosomal subunit biogenesis. Mol Cell Biol 21: 1453-1462. doi:10.1128/MCB.21.5.1453-1462.2001. PubMed: 11238882.
33. Finch AJ, Hilcenko C, Basse N, Drynan LF, Goyenechea B et al. (2011) Uncoupling of GTP hydrolysis from eIF6 release on the ribosome causes Shwachman-Diamond syndrome. Genes Dev 25: 917-929. doi:10.1101/gad.623011. PubMed: 21536732.
34. Bicker KL, Thompson PR (2013) The protein arginine deiminases: Structure, function, inhibition, and disease. Biopolymers 99: 155-163. doi:10.1002/bip.22127. PubMed: 23175390.
35. Fisk JC, Li J, Wang H, Aletta JM, Qu J et al. (2013) Proteomic analysis reveals diverse classes of arginine methylproteins in mitochondria of trypanosomes. Mol Cell Proteomics 12: 302-311. doi:10.1074/mcp.M112.022533. PubMed: 23152538.
36. Wickstead B, Ersfeld K, Gull K (2002) Targeting of a tetracycline-inducible expression system to the transcriptionally silent minichromosomes of *Trypanosoma brucei*. Mol Biochem Parasitol 125: 211-216. doi:10.1016/S0166-6851(02)00238-4. PubMed: 12467990.
37. Wirtz E, Leal S, Ochatt C, Cross GA (1999) A tightly regulated inducible expression system for conditional gene knock-outs and dominant-negative genetics in *Trypanosoma brucei*. Mol Biochem Parasitol 99: 89-101. doi:10.1016/S0166-6851(99)00002-X. PubMed: 10215027.
38. Kolev NG, Franklin JB, Carmi S, Shi H, Michaeli S et al. (2010) The transcriptome of the human pathogen *Trypanosoma brucei* at single-nucleotide resolution. PLOS Pathog 6: e1001090. PubMed: 20838601.
39. Siegel TN, Hekstra DR, Wang X, Dewell S, Cross GA (2010) Genome-wide analysis of mRNA abundance in two life-cycle stages of *Trypanosoma brucei* and identification of splicing and polyadenylation sites. Nucleic Acids Res 38: 4946-4957. doi:10.1093/nar/gkq237. PubMed: 20385579.

Attached Publications

Part I. Trypanosome RNA editing

Zhenqiu Huang, Drahomíra Faktorová, Adéla Křížová, Lucie Kafková, Laurie K. Read, Julius Lukeš, Hassan Hashimi† (2015). Integrity of the core mitochondrial RNA-binding complex 1 is vital for trypanosome RNA editing. *RNA* 21:2088-2102.

This paper describes the functional analysis of the last core MRB1 subunit to be examined by RNAi called MRB8620. The protein was not amenable to RNAi under standard culturing conditions, but its subtle effect on RNA editing was observed to affect cells when grown in media without glucose. Furthermore, the MRB8620 gene was deleted in induced Dk *T. brucei* since it could not be done in cells in which kDNA expression was essential, confirming its necessary role in RNA editing. A new model mechanistic model of MRB1 is presented.

Integrity of the core mitochondrial RNA-binding complex 1 is vital for trypanosome RNA editing

ZHENQIU HUANG,[1,2] DRAHOMÍRA FAKTOROVÁ,[1,2] ADÉLA KŘÍŽOVÁ,[2] LUCIE KAFKOVÁ,[3] LAURIE K. READ,[3] JULIUS LUKEŠ,[1,2,4] and HASSAN HASHIMI[1,2]

[1]Biology Center, Institute of Parasitology, Czech Academy of Sciences, České Budějovice (Budweis), 370 05, Czech Republic
[2]Faculty of Sciences, University of South Bohemia, České Budějovice (Budweis), 370 05, Czech Republic
[3]Department of Microbiology and Immunology, School of Medicine, State University of New York at Buffalo, Buffalo, New York 14214, USA
[4]Canadian Institute for Advanced Research, Toronto, Ontario M5G 1Z8, Canada

ABSTRACT

***Trypanosoma brucei* is the causative agent of the human and veterinarian diseases African sleeping sickness and nagana. A majority of its mitochondrial-encoded transcripts undergo RNA editing, an essential process of post-transcriptional uridine insertion and deletion to produce translatable mRNA. Besides the well-characterized RNA editing core complex, the mitochondrial RNA-binding 1 (MRB1) complex is one of the key players. It comprises a core complex of about six proteins, guide RNA-associated proteins (GAPs) 1/2, which form a heterotetramer that binds and stabilizes gRNAs, plus MRB5390, MRB3010, and MRB11870, which play roles in initial stages of RNA editing, presumably guided by the first gRNA:mRNA duplex in the case of the latter two proteins. To better understand all functions of the MRB1 complex, we performed a functional analysis of the MRB8620 core subunit, the only one not characterized so far. Here we show that MRB8620 plays a role in RNA editing in both procyclic and bloodstream stages of *T. brucei*, which reside in the tsetse fly vector and mammalian circulatory system, respectively. While RNAi silencing of MRB8620 does not affect procyclic *T. brucei* fitness when grown in glucose-containing media, it is somewhat compromised in cells grown in the absence of this carbon source. MRB8620 is crucial for integrity of the MRB1 core, such as its association with GAP1/2, which presumably acts to deliver gRNAs to this complex. In contrast, GAP1/2 is not required for the fabrication of the MRB1 core. Disruption of the MRB1 core assembly is followed by the accumulation of mRNAs associated with GAP1/2.**

Keywords: RNA editing; mitochondrion; trypanosome

INTRODUCTION

In the kinetoplastid *Trypanosoma brucei*, 12 of 18 mitochondrial-encoded mRNAs undergo RNA editing for their maturation. In this process, uridines (U) are inserted into, or less frequently deleted from, specific positions in the transcript to decrypt open reading frames (ORFs), which subsequently serve as templates for the mitochondrial (mt) translation machinery. Because most of resulting proteins are subunits of the mt respiratory chain, RNA editing is essential for the survival of *T. brucei* throughout its life cycle, in which it circulates between the insect vector and mammalian host (Schnaufer et al. 2001).

Small noncoding transcripts called guide (g) RNAs, ranging from 50 to 70 nucleotides (nts) in size, represent the informational component of RNA editing (Blum et al. 1990). A 5′-proximal region on the gRNA called the anchor domain hybridizes to a cognate mRNA to be edited. The downstream information domain defines several editing sites (ESs) on the mRNA that undergo either a U-insertion or U-deletion event. When all the ESs have been edited, the information domain and mRNA are complementary via Watson-Crick and noncanonical U:G base-pairing. A post-transcriptionally added 3′-oligo(U) tail on the gRNA likely stabilizes its interaction with mRNA during duplex formation (McManus et al. 2000).

Moreover, several protein complexes also play various essential roles in editing. The RNA editing core complex (RECC), also referred to as the 20S editosome, provides the requisite catalytic activities needed for U-insertion/deletion at a given ES. One of three RECC endonucleases cuts the mRNA strand of the duplex at a base pair mismatch to yield

Corresponding author: hassan@paru.cas.cz
Article published online ahead of print. Article and publication date are at http://www.rnajournal.org/cgi/doi/10.1261/rna.052340.115.

5′ and 3′ fragments bridged by a gRNA (Carnes et al. 2008). An ES cut by the deletion site-specific endonuclease is processed by a 3′ to 5′ exonuclease, whose activity is restricted to the extra U's from the 5′ fragment (Ernst et al. 2009). If the ES is an insertion site, the RECC terminal U transferase (KRET2) appends the 5′ fragment with the titular nucleotide (Ernst et al. 2003). The mRNA encoding cytochrome *c* oxidase (cox) 2 is cut by the third RECC endonuclease that recognizes this unique substrate, which contains a gRNA-like element in its 3′ UTR that guides the addition of 4 U's within the ORF by KRET2 (Golden and Hajduk 2005). After the appropriate editing event is finished at the ES, an RNA ligase reseals the two mRNA fragments (Schnaufer et al. 2001; Verner et al. 2015).

The cascade of core enzymatic steps encapsulated by RECC can be recapitulated in vitro for the editing of a single ES. However, the lack of RECC processivity in vitro suggests that essential components for editing progression are lacking. This aspect of RNA editing is especially important for pan-editing, the decryption of an ORF throughout a transcript with a 3′ to 5′ polarity as facilitated by multiple gRNAs (Maslov and Simpson 1992). We have proposed that these and other facets of in vivo RNA editing may be facilitated by another protein complex discovered after RECC that has been named the mitochondrial RNA-binding complex 1 (MRB1) (Hashimi et al. 2013). Its elucidated architecture shows that it is composed of a core complex and the TbRGG2 subcomplex (Ammerman et al. 2012). The MRB1 core is made up of six proteins with a still undefined stoichiometry. The gRNA-associated proteins (GAPs) 1 and 2 (also known as GRBC2 and 1, respectively) form a heterotetramer that binds and stabilizes these small transcripts (Weng et al. 2008; Hashimi et al. 2009). The GAP1/2 proteins also represent the only bona fide RNA-binding components of the complex identified to date. RNAi silencing of three other subunits called MRB5390, MRB3010, and MRB11870 (nomenclature by Ammerman et al. 2012) also impacts editing without destabilizing gRNAs, with editing stalling at initial stages of pan-editing, presumably guided by the first gRNA:mRNA duplex, in the case of the latter two proteins (Acestor et al. 2009; Ammerman et al. 2011, 2013).

Although there are complex protein–protein interactions between the TbRGG2 subcomplex and the MRB1 core, this association is greatly enhanced by the presence of RNA (Ammerman et al. 2012; Aphasizheva et al. 2014). This phenomenon may in part be due to the subcomplex containing TbRGG2 and one of the two highly similar paralogs MRB8170 and MRB4160, all of which bind RNA (Fisk et al. 2008; Kafková et al. 2012). The TbRGG2 subcomplex also contains a protein called MRB8180 (Ammerman et al. 2012), whose RNA-binding properties and functional analysis have still not been addressed. RNAi silencing of the subcomplex primarily impacts pan-edited mRNAs (Fisk et al. 2008; Ammerman et al. 2010; Kafková et al. 2012), leading to the view that they are specific for transcripts requiring multiple gRNAs for their processing (Hashimi et al. 2013). The finding that TbRGG2 has RNA annealing and unwinding activities is consistent with this notion. Indeed, they could facilitate the formation of gRNA:mRNA duplexes, as well as melting them after the editing of all ESs encoded by given gRNA to allow the annealing of the next upstream gRNA on the cognate mRNA and/or facilitate the utilization of a single gRNA as editing proceeds through one gRNA-directed block (Ammerman et al. 2010; Foda et al. 2012).

In a highly concerted fashion, the MRB1 core, the TbRGG2 subcomplex, and RECC maturate mRNAs for their eventual translation into subunits of the mt respiratory chain. In the *T. brucei* procyclic stage (PS), living within the *Glossina* fly midgut, the cytochrome *c*-containing electron transport chain complexes III and IV pump protons out of the mt matrix to create electrochemical gradient across the inner membrane, which is used by the F_OF_1-ATP synthase complex to generate ATP (Schnaufer et al. 2005). The reducing equivalents for this process are primarily supplied by the catabolism of proline in the mt matrix, although PS cells grown in glucose-containing SDM79 medium (Brun and Schönenberger 1979) circumvent this pathway, as they preferentially generate ATP via glycolysis (Coustou et al. 2008). This situation is reminiscent of the energy metabolism of the pathogenic slender *T. brucei* bloodstream stage (BS), which generates ATP exclusively by glycolysis.

Although BS *T. brucei* does not utilize the mt respiratory chain for energy generation and the cytochrome *c*-containing complexes III and IV are absent, the electrochemical gradient across the inner membrane is still required for cell viability. To achieve this condition, the ATP synthase consumes ATP to pump protons out of the mt matrix (Schnaufer et al. 2005; Brown et al. 2006). As such, pan-editing of the mRNA encoding ATP synthase subunit 6 (A6) is required for the complete assembly of this complex in BS (Hashimi et al. 2010). Interestingly, dyskinetoplastic (DK) strains of *T. brucei* that have lost the capacity for RNA editing exist in nature (Schnaufer et al. 2005; Lai et al. 2008). The DK strains emerged independently several times (Carnes et al. 2005). To compensate for the loss of A6, these DK trypanosomes have acquired mutations in the ATP synthase F_1-moiety γ-subunit, allowing their survival in the bloodstream of vertebrate hosts (Dean et al. 2013).

In this report, we describe the functional analysis of MRB8620 (TriTrypDB accession number: Tb927.11.16860; formerly "Tb11.01.8620"), the last remaining MRB1 core subunit as defined by Ammerman et al. (2012), by virtue of its consistent presence in various MRB1 core isolations, to be studied this way. This study was performed in the various physiological states of *T. brucei* in vitro cultures: PS grown in the presence and paucity of glucose and BS that has been rendered kDNA-independent due to bearing a γ-subunit site mutation that allows this condition.

RESULTS

MRB8620 interacts with other MRB1 subunits

MRB8620 has been shown to interact with the MRB1 core complex and the TbRGG2 subcomplex by yeast two-hybrid analysis and various tandem affinity purification (TAPs) of tagged MRB1 subunits (Hashimi et al. 2008; Weng et al. 2008; Hernandez et al. 2010; Ammerman et al. 2011, 2012; Kafková et al. 2012). To confirm that MRB8620 is an integral component of the MRB1 complex, we analyzed proteins co-purifying with the C-terminally PTP-tagged MRB8620 without nuclease treatment by LC-MS/MS mass spectroscopy. As shown in Table 1, MRB8620 interacts with all the other MRB1 core proteins (GAP 1/2, MRB5390, MRB3010, and MRB11870) plus subunits of the TbRGG2 subcomplex, and thus comprises an integral part of MRB1. Some common contaminants were also detected in the PTP eluates and are listed in Supplemental Table 1.

MRB8620 associates with the inner mitochondrial membrane

Using an updated gene model based on spliced leader trapping studies (Nilsson et al. 2010; Siegel et al. 2010), in silico-translated *MRB8620* contains a predicted hydrophobic stretch of amino acids toward the N-terminus that may serve as a transmembrane domain (Fig. 1A), as determined using the TMHMM 2.0 program (Möller et al. 2001). To test whether MRB8620 is indeed a membrane-associated protein, digitonin fractionated mitochondria isolated from the MRB8620-PTP-tag cell line were further processed into soluble and insoluble fractions by 0.1% Triton X-100. The resulting fractions were probed with antibodies against PTP-tag constituent protein A, HSP70 as an mt matrix marker, and respiratory complex IV subunit (trCOIV) as an inner membrane marker. As expected, HSP70 and trCOIV localized to the soluble matrix and insoluble membrane fractions, respectively (Fig. 1B). The protein A signal from the C-terminally tagged MRB8620, expressed from its endogenous locus by RNA polymerase II, is in the membrane fraction. Thus, MRB8620 is associated with the mt membrane.

RNAi silencing of MRB8620 inhibits growth in glucose-poor media

To facilitate the functional analysis of MRB8620 by reverse genetics, a PS cell line was generated that allows for the tetracycline-inducible expression of double-stranded (ds) RNA, which subsequently directs the RNAi machinery to degrade MRB8620 mRNA. To follow depletion of the protein, this cell line bears the MRB8620-PTP-tagged allele, which is also targeted by the dsRNA complementary to sequence within ORF. Upon depletion of MRB8620, no growth retardation was observed in the glucose-containing SDM-79 medium (Fig. 2A). The efficiency of RNAi was verified by Western blot analysis detecting the PTP-tagged protein via the α-protein A antibody (Fig. 2B). Indeed, MRB8620-PTP is considerably down-regulated 2 and 4 d after RNAi induction, although there is a slight recovery of its steady-state levels 6 d after tetracycline addition to the medium. Down-regulation at the RNA level was also confirmed on Day 4 post-induction by qRT-PCR (Fig. 2C).

RNA editing is required for the maturation of mRNAs encoding several subunits of respiratory chain complexes, and the ablation of proteins involved in this process therefore negatively impacts oxidative phosphorylation in PS (Neboháčová et al. 2004; Zíková et al. 2006; Hashimi et al. 2010). Yet, oxidative phosphorylation does not contribute to energy metabolism when the *T. brucei* resides in SDM79,

TABLE 1. MRB8620-PTP associated proteins identified by mass spectrometry and ordered according to the number of unique peptides from PTP-tag elutions from two experiments

Locus tag	Name[a]	Alias[b]	Subcomplex[c]	Unique peptides	Coverage
Tb11.01.8620	MRB8620	TbGRBC3	MRB1 core	25	45%
Tb11.02.5390	MRB5390	TbGRBC4	MRB1 core	54	38.6%
Tb927.5.3010	MRB3010	TbGRBC6	MRB1 core	24	36.6%
Tb927.4.4150/Tb927.8.8180[d]	MRB4150/MRB8180	TbREMC4	TbRGG2	21	25.8%
Tb927.4.4160/ Tb927.8.8170[d]	MRB4160/ MRB8170	TbREMC5/ TbREMC5A	TbRGG2	20	24.6%
Tb927.2.3800	GAP1	TbGRBC2	MRB1 core	18	33.7%
Tb927.10.11870	MRB11870	TbGRBC5	MRB1 core	14	45.8%
Tb927.7.2570	GAP2	TbGRBC1	MRB1 core	14	39.3%
Tb927.7.800	MRB800	TbREMC3	TbRGG2	10	19.3%
Tb927.10.10130	MRB10130	TbREMC1	None	8	19.8%
Tb927.10.10830	TbRGG2		TbRGG2	5	24.1%

[a]Nomenclature according to Ammerman et al. (2012).
[b]Nomenclature according to Aphasizheva et al. (2014).
[c]MRB1 subcomplex to which protein is assigned according to Ammerman et al. (2012).
[d]Peptides that could have arisen from either of the two highly homologous proteins.

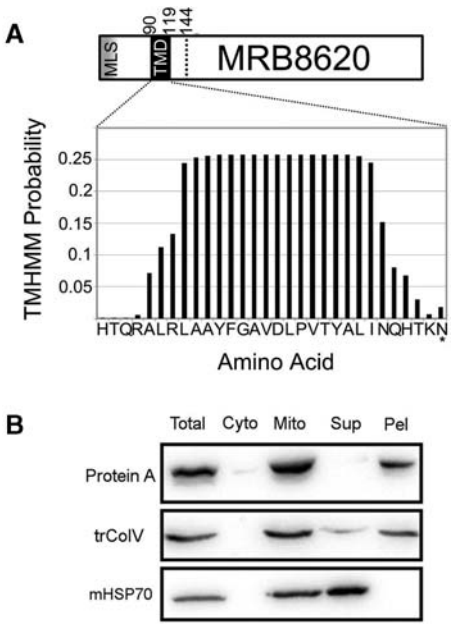

FIGURE 1. MRB8620 is a mitochondrial membrane-associated protein. (*A*) An N-terminal transmembrane domain (TMD) predicted in MRB8620. TMD predicted by TMHMM 2.0 program is located between the 90th and 119th amino acid sites with the probability of each residue being part of the TMD peaking ~0.25. Predicted N-terminal mt localization signal (MLS) shown on the *left*. A stretch of amino acids with small probability of being part of a TMD extends to the 144th amino acid (dotted line) with the same score as the amino acid marked with the asterisk. Numbering of amino acid residues is from the starting methionine. (*B*) Western blot analysis of digitonin fractionation of cytoplasm (Cyto) and mitochondrial (Mito), as well as Triton X-100 fractionation of mt proteins into soluble and membrane fractions, containing in the supernatant (Sup) phases or pellet (Pel), respectively. Proportional volumes of each fraction were loaded as described in Material and Methods along with an equivalent amount of lysate from whole cells (Total) taken for comparison. Antibodies used are indicated on the *left*.

a medium containing ample glucose (Coustou et al. 2008). To determine whether any negative impact of MRB8620 depletion on parasite's fitness is masked in the energy-rich milieu of SDM79, the RNAi cell line was transferred to SDM80 medium, which does not contain glucose. The RNAi silencing of MRB8620 in SDM80 was verified on the protein (Fig. 2E) and RNA levels (Fig. 2F). A reproducible reduction in growth was observed after Day 4 of RNAi induction in a glucose-poor medium (Fig. 2D), with a doubling time from Days 4–6 post-induction of 32.95 ± 0.93 h in the MRB8620-silenced cells, versus 20.52 ± 0.59 h in the noninduced controls. After 6 d post-induction, there is a recovery of the growth rate in MRB8620-depleted trypanosomes (22.55 ± 0.49 h doubling time at Days 6–8 versus 20.87 ± 0.26 h at Days 8–10), although it still lags when compared with the noninduced controls (19.66 ± 1.02 h doubling time at Days 6–8 versus 18.87 ± 0.86 h at Days 8–10). Thus, down-regulation of MRB8620 inhibits growth under glucose-poor conditions, in which oxidative phosphorylation is required for energy production.

Ablation of MRB8620 affects editing in procyclic stage

Upon RNAi silencing of MRB8620, the growth of PS is affected in SDM80 as opposed to SDM79. Hence, we investigated the effect of MRB8620 silencing on steady-state levels of mt RNAs under both growth conditions, in order to explain lower fitness of PS flagellates under conditions in which they depend on a functional respiratory chain for energy generation.

To address this question, RNA was harvested from uninduced and MRB8620 RNAi-induced cells grown in glucose-poor SDM80 for 4 d. Some of the RNA was converted to cDNA by reverse transcription to serve as a template for the qPCR assay of mt mRNA and rRNA steady-state levels (Carnes et al. 2005). Figure 3A depicts the relative abundances of the assayed transcripts in the RNAi silenced cells when compared with the noninduced controls. The never-edited 9S and 12S rRNAs as well as cytochrome *c* oxidase 1 (CO1) and NADH dehydrogenase subunit 4 (ND4) mRNAs were not affected by MRB8620 ablation. From the mRNAs that require only modest U insertions, called minimally edited, only cytochrome *c* reductase subunit b (CYB) shows a ~30% decrease and ~20% increase in the edited and pre-edited species, respectively. The persistence of CO2 editing upon ablation of MRB8620 is notable, because it uniquely does not require a *trans*-acting gRNA for its editing, but uses a gRNA-like element within its 3′-UTR (Golden and Hajduk 2005). The pan-edited mRNAs, which require U insertion/deletion throughout the transcript, are most affected in the MRB8620 knockdowns (Fig. 3A). Furthermore, with the exception of ND7, there is a concomitant accumulation of pre-edited forms of the followed transcripts. Equivalent results were obtained from another clone examined in parallel (data not shown).

To eliminate the possibility that editing is affected because of the destabilization of gRNAs in the MRB8620-depleted trypanosomes, as was the case when GAP1 was RNAi-silenced (Weng et al. 2008; Hashimi et al. 2009), we assayed the steady-state levels of gRNAs by Northern blot analysis (Fig. 3B). In the tetracycline-treated cells, there was an almost twofold increase in the levels of gRNAs for the editing of ATP synthase subunit 6 (A6), mitochondrial unidentified reading frame 2 (MURF2), and CO3 when compared with the constant levels of the cytosolic 5.8S rRNA between the RNAi-induced and noninduced cells. Similar accumulation of these small transcripts has been previously observed when editing is impaired by knockdown of other MRB1 subunits (Ammerman et al. 2013; Aphasizheva et al. 2014).

After establishing that there is indeed a defect in RNA editing upon MRB8620 silencing in PS grown in glucose-poor SDM80, we decided to address whether such a phenotype is observed when the cells are grown in glucose-supplemented SDM79, a condition in which depletion of this MRB1 subunit does not affect cell growth. RNA harvested from these cells as before was converted to cDNA for the qPCR assay (Fig. 3C).

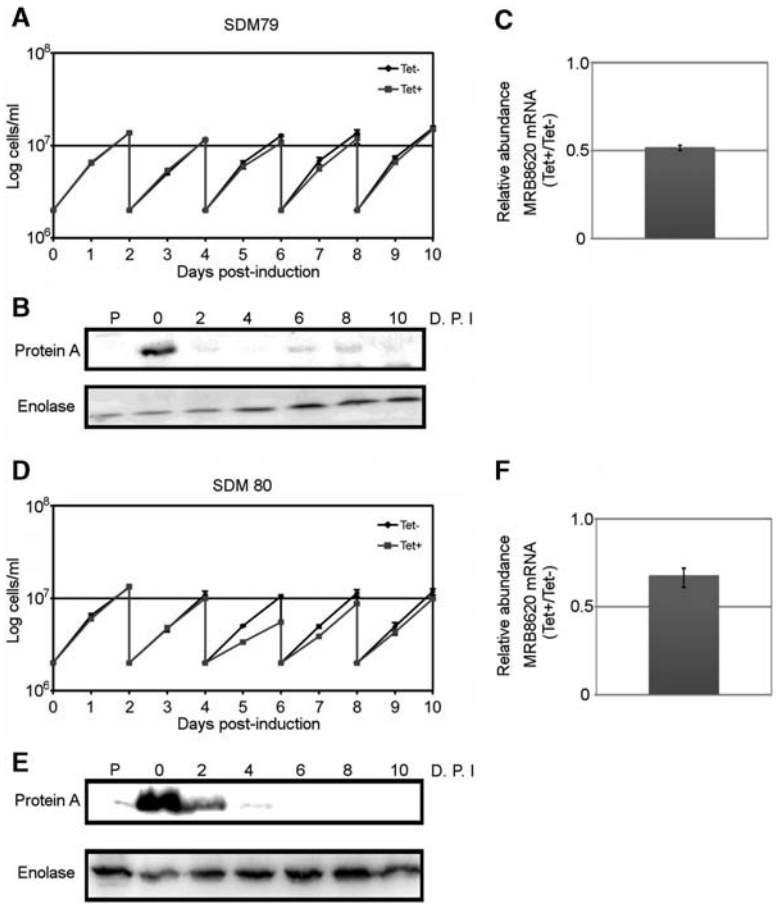

FIGURE 2. *T. brucei* growth is inhibited upon silencing of MRB8620 in glucose-poor SDM80 but not in glucose-containing SDM79. (*A*) Growth of PS cells in SDM79 in the presence (gray square and line) and absence (black diamond and line) of tetracycline (*tet*), which induces MRB8620 RNAi silencing, over a 10 d time course. The cells were diluted to the starting density of 2×10^6 cells/mL every 2 d. (*B*) Western blot analysis of the RNAi silencing of MRB8620-PTP by α-protein A antibody, with α-enolase shown as a loading control. Cell lysates were collected from the parental cell line (P) as well as the MRB8620 knockdowns every even day 0 to 10 d post-induction (DPI) with tetracycline. (*C*) Bar graph indicating the relative MRB8620 RNA levels in the RNAi-induced versus uninduced-control cells as determined by quantitative RT-PCR and normalized to 18S. Whiskers denote range of obtained relative abundancies within technical triplicates. (*D–F*) The same as *A–C* above, respectively, except that the cells were grown in SDM80.

Overall, these RNAs are affected similarly to those from the MRB8620 knockdown grown in SDM80: never-edited RNAs are not impacted, whereas minimally edited CYB and the assayed pan-edited mRNAs show the down-regulation of edited products and the concurrent accumulation of pre-edited transcripts.

To summarize this part, RNAi silencing of MRB8620 leads to a defect in RNA editing. There is a decrease in pan-edited transcripts as well as in the corresponding form of minimally edited CYB. This phenotype is accompanied by an accumulation of pre-edited transcripts, which are not processed when RNA editing is impeded, as well as gRNAs, suggesting that they may be turned over when utilized to guide editing events on an mRNA. This impact on RNA editing is independent of the energy metabolism state of the PS, although cell fitness is compromised only when the trypanosomes rely on oxidative phosphorylation for ATP generation. Subsequent experiments were performed on cells grown in SDM80.

MRB8620 is required for MRB1 integrity

As MRB8620 is a subunit of the MRB1 complex, we wondered whether its depletion by RNAi would affect the integrity of the whole complex. To this end, macromolecules isolated from tetracycline-induced MRB8620 and GAP1 RNAi cells in addition to the parental line from which they were derived were separated on a 10%–30% glycerol gradient by ultracentrifugation. Twelve fractions of increasing density were probed with antibodies recognizing MRB1 core subunits GAP1 and MRB3010, as well as TbRGG2 (Ammerman et al. 2012). The RECC subunit KREPA3 was also immunodecorated to serve as a marker for 20 Svedberg (S) sedimentation within the gradient, taking advantage of this biochemical property of the complex (Golas et al. 2009). As shown in Figure 4A, the ablation of MRB8620 affects the distribution of GAP1 and MRB3010 in the gradients (cf. parental and MRB8620 RNAi). In the case of GAP1, the protein is equally distributed throughout the gradient (fractions 1–21) upon MRB8620 silencing, which is in contrast to the pattern observed in the parental control. Signal from MRB3010 appears in lighter fractions than what was observed in the parental cell line (fractions 13–21), indicating that a significant fraction of this core subunit is not-assembled into larger complexes. A very slight shift to lighter fractions was also observed for TbRGG2 (Fig. 4A). KREPA3 mostly retained its characteristic 20S sedimentation, indicating that the ablation of MRB8620 does not affect the integrity of RECC.

The observation that the sedimentation rate of the assayed MRB1 proteins is affected upon MRB8620 ablation prompted us to investigate intra-MRB1 interactions in this background. Toward this goal, we generated a cell line in which one of the *MRB3010* alleles was in situ C-terminally tagged with the V5 epitope to facilitate the immunoprecipitation (IP) of the respective protein by a cross-reacting α-V5 antibody. In this way, we were able to determine which proteins co-IP with MRB3010-V5 in the presence and absence of

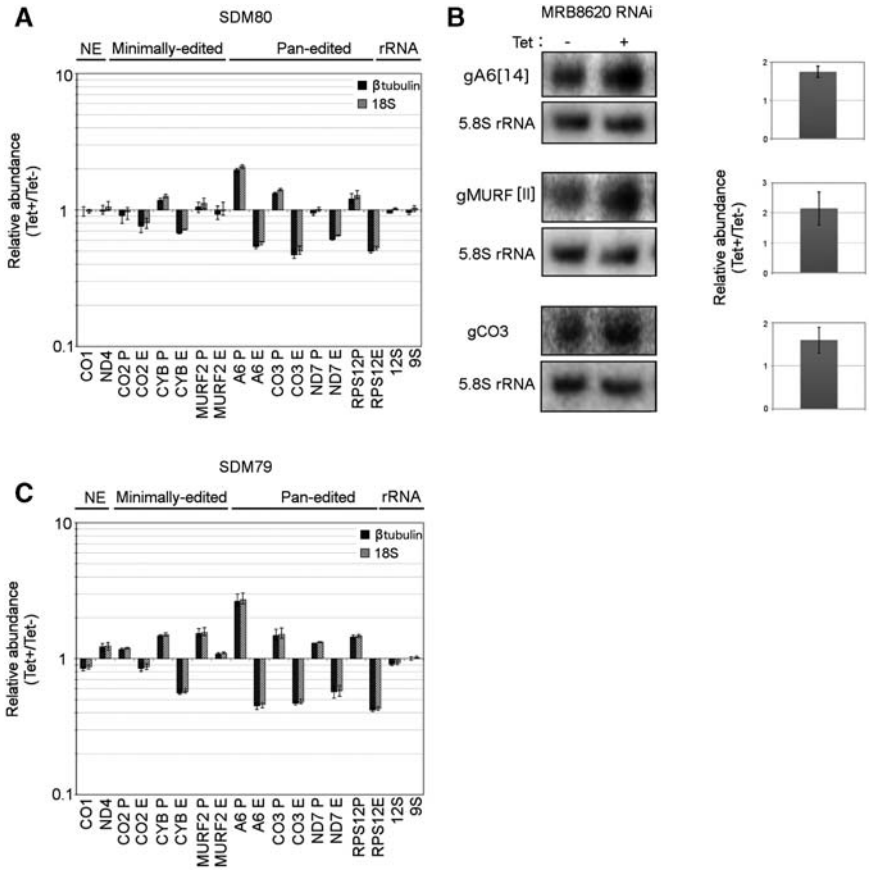

FIGURE 3. MRB8620 plays a role in RNA editing. (*A*) RNA was isolated from PS cultured in SDM80 to Day 4 post-induction. RNA abundance was quantified by qRT-PCR using primer pairs specific for selected never-edited, minimally edited, pan-edited, and ribosomal RNAs, as labeled on the *x*-axis. The bar graph depicts the relative abundance of RNA levels in tetracycline-induced *T. brucei* compared to uninduced-control cells. RNA levels were standardized to β-tubulin (black bar) or 18S (striped bar) cDNA. Whiskers denote range of obtained relative abundances within technical triplicates. (*B*) Levels of gRNAs in MRB8620 RNAi *T. brucei* grown in SDM80. Nylon membranes were probed with 5′ end labeled oligonucleotides complementary to gA6[14], gMURF2[II], or gCO3 gRNAs, with 5.8S rRNA set as a loading control for each membrane. The signals were quantified and normalized to the levels of 5.8S RNA from the same sample. The bar graph on the *right* depicts fold change in RNAi-induced cells compared with uninduced-control *T. brucei* and whiskers the error between duplicates. (*C*) As in *A*, where the cells were cultured in SDM79. *Top* of the graph indicates whether species of RNA assayed is never-edited (NE), minimally, pan-edited, or mitochondrial rRNA. The following abbreviations were used for mRNAs assayed by qPCR: ATPase subunit 6 (A6), cytochrome *c* oxidase subunits 1 (CO1), 2 (CO2), and 3 (CO3), cytochrome reductase subunit b (CYB), maxicircle unknown reading frame 2 (MURF2), NADH dehydrogenase subunits 4 (ND4) and 7 (ND7), and ribosomal protein S12 (RPS12). (P) Pre-edited RNA; (E) edited RNA.

MRB8620 (Fig. 4B). Interaction of MRB3010-V5 with GAP1 and MRB11870, another core MRB1 protein, is reduced when MRB8620 is down-regulated (Fig. 4B), which is consistent with the previous observation that in this background a portion of MRB3010 does not assemble into larger complexes and GAP1's sedimentation is affected. This experiment also indicates that the association of TbRGG2 and MRB8170, another member of the TbRGG2 subcomplex, is also reduced, albeit to a small degree in the former case (Fig. 4B). A decreased association of the TbRGG2 subcomplex with MRB3010-V5 in the MRB8620 knockdown is also in agreement with the apparent shift of TbRGG2 to lighter glycerol gradient fractions. The more dramatic decrease of MRB8170 association with MRB1 core upon MRB8620 depletion, compared with that of TbRGG2, is consistent with the strong direct interaction detected between MRB8170 and MR8620 in yeast two-hybrid studies (Ammerman et al. 2012.) The steady-state levels of the proteins examined in Figure 4 were not affected by the MRB8620 knockdown as evidenced by their equivalent signals in the loading of the glycerol gradients (Fig. 4A) or the IP inputs (Fig. 4B).

Because the integrity of the MRB1 core is compromised upon knockdown of its MRB8620 and MRB11870 subunits (Ammerman et al. 2013), we checked whether RNAi silencing of GAP1 has a similar phenotype in this respect. Unlike other core MRB1 proteins, GAP1/2 proteins form a heterotetrameric complex that binds gRNAs, the depletion of which leads to destabilization of these small, noncoding transcripts (Weng et al. 2008; Hashimi et al. 2009). Furthermore, GAP1/2 exhibits a heterodisperse distribution on glycerol gradients when compared with the other core subunits (Fig. 4A), suggesting that their interactions are not restricted to the MRB1 core. GAP1 RNAi did not result in a shift of MRB3010 or TbRGG2 to lighter fractions, the latter observation being agreement with a previous study (Aphasizheva et al. 2014), despite its demonstrated protein depletion (Fig. 4A, cf. GAP1 RNAi and parental). Next, we introduced a C-terminal V5-tagged *MRB3010* allele into a PS cell line containing GAP1 RNAi construct (Hashimi et al. 2009). The IP of MRB3010-V5 was performed as with the MRB8620-depleted samples (Fig. 4C), and immunoprecipitated proteins probed with the same panel of antibodies. As expected, due to RNAi silencing, GAP1 was not detected in the MRB3010-V5 IP (Fig. 4C). Interestingly, MRB11870 interaction with MRB3010-V5 persisted, perhaps even up-regulated, in the GAP1-depleted cells, indicating that GAP1 is not required for assembly of the MRB1 core. The extent of TbRGG2 and MRB8170 co-IP was equivalent in the GAP1-silenced cells and noninduced controls (Fig. 4C).

Thus, MRB8620 appears to be a central player in the integrity of the MRB1 core as well as core-TbRGG2 subcomplex

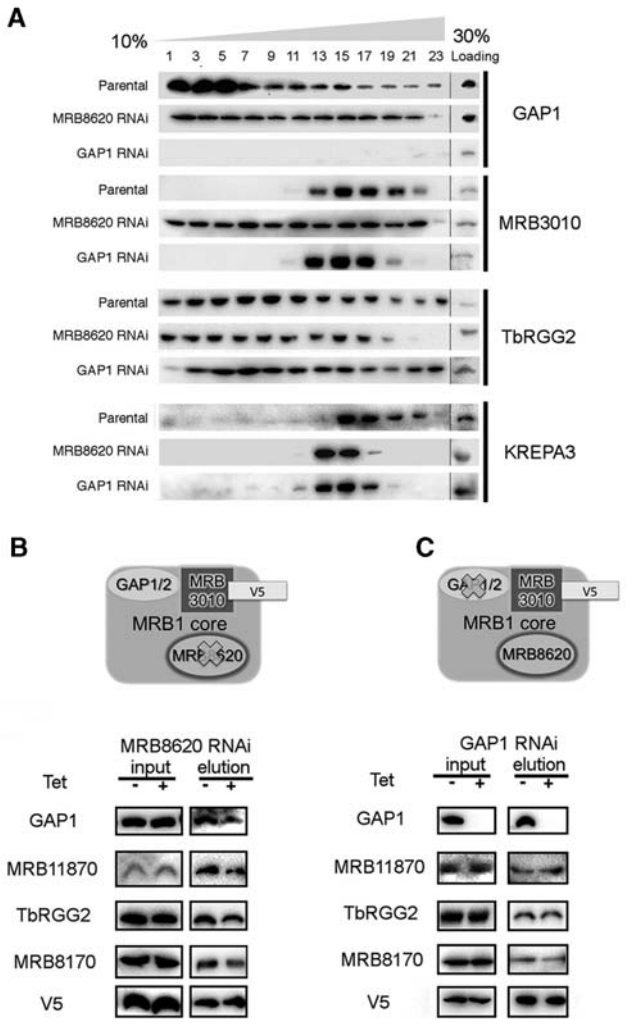

FIGURE 4. MRB8620 is required for MRB1 core integrity. (*A*) The effect of MRB8620 and GAP1 depletion on the sedimentation of GAP1, MRB3010, TbRGG2, and RECC subunit KREPA3. Mitochondrial lysates from the parental cell line (*top* images), RNAi-silenced MRB8620 (*middle* images), and GAP1 (*lower* images) *T. brucei* were loaded on 10%–30% glycerol gradients for their fractionation. Alternate gradient glycerol fractions were analyzed by immunodecoration of Western blots with the indicated antibodies indicated on the *right*. To the *right* of the 23rd fraction (loading) is a sample from the lysis step before loading onto the gradient to demonstrate equivalent amounts of protein were used among samples. (*B*) Scheme of MRB1 core complex components in cells harboring MRB8620 RNAi with MRB3010 V5 tagged at an endogenous allele. MRB3010-V5 and associated proteins were isolated by Protein G-Dynabead from extracts of mitochondria from either uninduced (tet−) or RNAi-induced (tet+) MRB8620 RNAi cells. Both input and elutions (indicated above images) were analyzed by Western blot for MRB1 complex components using the antibodies indicated on the *right*. (*C*) As in *B*, except that the cells harbor the GAP1 RNAi construct with MRB3010 V5 tagged at an endogenous allele.

interactions. Its ablation by RNAi results in a portion of the core subunit MRB3010 appearing in lower density fractions, indicating their compromised incorporation. This result was further confirmed by pull-down of MRB3010-V5 in a MRB8620-depleted background. In contrast, the MRB1 core can assemble in the absence of GAP1, because MRB3010-V5 interacts to the same degree with the other core protein MRB11870 upon RNAi silencing. Similar results were observed for interactions between core subunit MRB3010 and subunits of the TbRGG2 subcomplex in the presence and absence of MRB8620 and GAP1.

Down-regulation of MRB8620 results in an accumulation of mRNAs requiring editing associated with GAP1/2

The integrity of MRB1 core is compromised upon RNAi silencing of MRB8620, eventually giving rise to disrupted RNA editing. We next investigated whether MRB8620 depletion affects the abundance of mt mRNAs associated with GAP1/2, given the loss of GAP1/2 association with the MRB1 core in this milieu. It has been shown that gRNA-bound GAP1/2 heterotetramer is associated with mRNA bound protein (e.g., KREL1 and MERS1 [Weng et al. 2008]). This result indicates that edited mRNAs may associate with GAP1/2 subcomplex, given the annealed gRNA: mRNA duplexes as the substrate of RNA editing. The copurification of gRNAs and mRNAs with MRB3010 protein is precedent for this notion (Madina et al. 2014).

To assess the effect of MRB8620 depletion on GAP1/2-mRNA association, we performed a GAP1 IP from mt lysates of MRB8620-silenced and untreated *T. brucei* (Fig. 5A). Dynabeads cross-linked with specific α-GAP1 antibody (Hashimi et al. 2009) were used. IP of GAP1 was equally efficient from both RNAi-induced and untreated samples, as shown by Western blot analysis using the α-GAP1 antibody (Fig. 5A). RNA isolated from the IP eluates was converted into cDNA to serve as a template for the aforementioned real-time qPCR assay for mt mRNA levels (Carnes et al. 2005).

To demonstrate the enrichment of mRNA from the GAP1 IP, a comparison was performed between mRNA precipitated from antibody-conjugated Dynabeads and that from blank beads as a mock. As performed in a previous study (Madina et al. 2014), we confirmed that cDNAs from mt RNAs were enriched in the GAP1 IP when compared with the mock (Supplemental Fig. 1). Interestingly, pre-edited and edited A6, CO3, and ND7 were more abundant in the GAP1 IP when compared with the mock, whereas the never-edited mt mRNAs CO1 and ND4, plus nuclear 18S rRNA and cytosolic β-tubulin mRNA, were equally represented in both samples. Thus, GAP1 associates with mRNAs that hybridize with gRNAs for their maturation.

Next, we compared the amount of pre-edited and edited mRNAs pulled down by GAP1 IP in the presence and down-regulation of MRB8620 by relative qPCR quantification (Pfaffl 2001). Consistent with never-edited CO1 and ND4 RNAs being carried over during the IP procedure, cDNAs representing these transcripts were equally present in the RNAi-silenced and untreated samples (data not shown) and thus were used to normalize the relative abundancies of

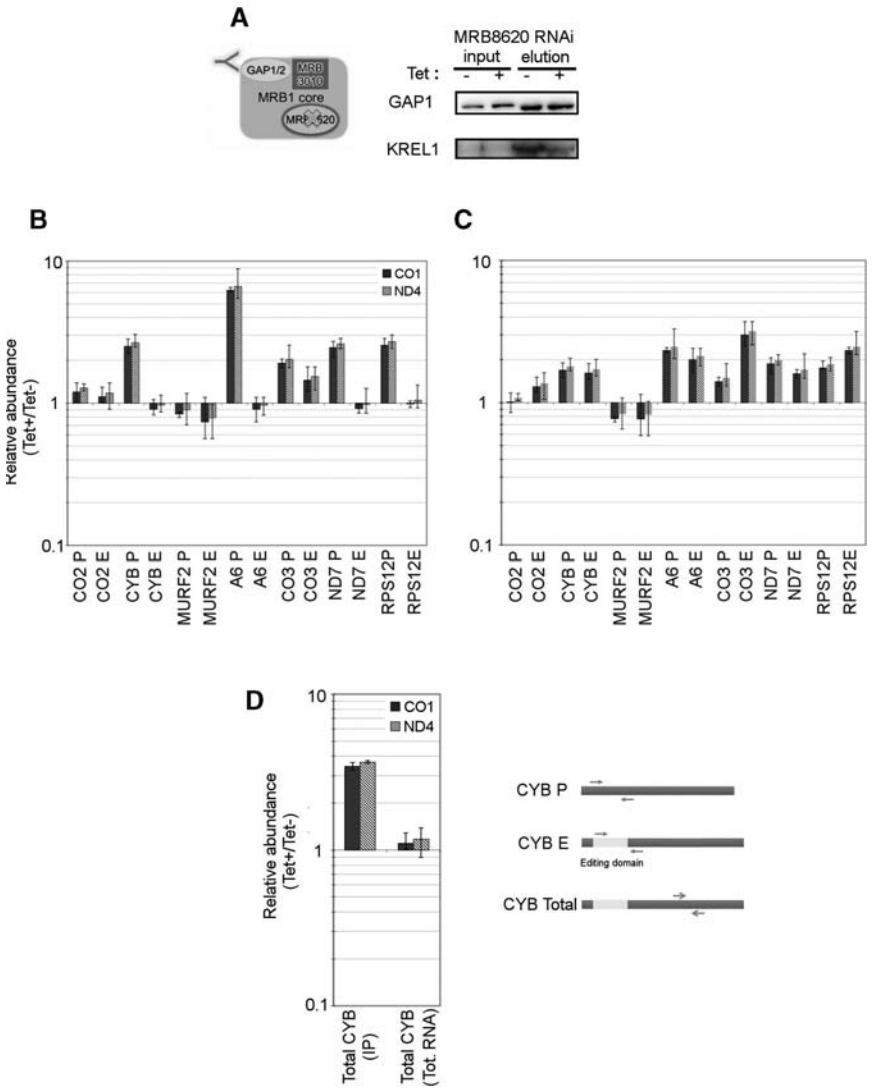

FIGURE 5. GAP1/2 heterotetramer exhibits accumulation of mRNAs undergoing RNA editing and reduced association with RECC upon MRB1 core disassembly by MRB8620 RNAi. (*A*) Scheme depicting GAP1/2 IP in MRB8620 RNAi-silenced cells (*left*). Western blot (*right*) of GAP1 IPs performed in MRB8620 RNAi-induced (Tet+) and uninduced cells (Tet−) were immunodecorated with antibodies against GAP1 and RECC subunit KREL1. (*B*) GAP1/2-bound RNAs isolated from the elutions from *A* were converted to cDNA for quantification by real-time PCR with selected primer sets for minimally edited and pan-edited RNAs. The bar graph indicates fold changes in RNA isolated from MRB8620 RNAi-induced cells compared to that from uninduced cells normalized to never-edited mRNAs CO1 (black bars) and ND4 (striped bars). Whiskers denote range of obtained relative abundances within technical triplicates. (*C*) Relative abundance of pre-edited and edited mRNAs pulled down in GAP1/2 IPs as in *B* but when normalized to the levels of the same transcripts from total RNA (Fig. 3A) in MRB8620-depleted and uninduced controls. This normalization is elaborated in Materials and Methods. (*D*) Relative abundance of total CYB transcripts pulled down with GAP1 in the IP as well as total RNA (Tot. RNA) from MRB8620-depleted and uninduced controls, and depicted as in *B*. The scheme on the *right* in *D* indicates the primers designed to detect the pre-edited (P), edited (E), and total CYB transcripts. All qPCR graphs are representative data from one of two IPs.

the assayed pre-edited and edited transcripts. Figure 5B reveals a consistent accumulation of pre-edited transcripts associated with GAP1 in the MRB8620 knockdown. Such a buildup of pre-edited mRNAs is consistent with the hypothesis that RNA editing is blocked upon MRB8620 depletion. Edited mRNAs are associated with GAP1 in equal measure in the presence or ablation of MRB8620, with the exception of CO3, which shows an accumulation. Because the levels of many RNAs differ in the input samples in response to MRB8620 depletion, we next normalized the relative levels of RNAs associating with GAP1 in the knockdown and control cells to their relative levels as assayed from total RNA isolated from the same sample types (Fig. 3A). As seen in Figure 5C, the enrichment of pre-edited mRNAs persists when the data are processed in this way. In addition, we observed that the relative abundance of many edited mRNAs associating with GAP1 also appears to be enriched in MRB8620 knockdown versus control cells, suggesting that the small amount of edited RNAs present in these cells also accumulates in association with GAP1/2 when MRB8620 is depleted. The exceptions to this pattern are the pre-edited and edited forms of MURF2, which exhibit a decrease in association with GAP1 upon MRB8620 depletion.

To circumvent the complication of changing RNA levels in the input in MRB8620-depleted cells, we next measured total CYB mRNA, using qPCR primers annealing to the CYB mRNA sequence outside of its short editing domain (Fig. 5D), which are expected to reflect the combined relative abundance of pre-edited, edited transcripts and intermediates. These primers were utilized on the cDNA generated from the GAP1 IP eluates as well as the total RNA in the knockdown and untreated controls, as described thus far in this section. Figure 5D shows that CYB mRNA measured using this primer pair was ~2.5-fold enriched in GAP1 IPs in MRB8620 knockdown cells compared with control cells, despite the constant levels measured in total RNA. From these data and those in Figure 5B,C, we conclude that both pre-edited and edited mRNAs accumulate in association with GAP1/2 when the MRB1 core is disrupted by MRB8620 depletion.

The accumulation of pre-edited mt mRNAs in association with GAP1 is consistent with an impairment in RNA editing. As the GAP1 heterotetramer has been demonstrated to associate with RECC via RNA linkers (Aphasizheva et al. 2014), and the latter complex confers the catalytic activities needed

for RNA editing, we assayed whether RECC and GAP1/2 associate upon MRB8620 silencing. Western blots of GAP IP eluates from MRB8620-down-regulated and untreated cells were immunodecorated with the KREL1 protein to serve as marker for RECC as it represents one of the RNA ligases of the complex (Schnaufer et al. 2001). This signal is weaker in the MRB8620 knockdown (Fig. 5A), suggesting that RECC association with GAP1/2 is compromised in this background, leading to an accumulation of preprocessed RNAs bound to GAP1/2.

In summary, the GAP1/2 heterotetramer associates with mRNAs that require RNA editing for their maturation. When the MRB1 core is disrupted upon MRB8620 silencing, there is an accumulation of mRNAs undergoing editing in association with GAP1/2. Furthermore, there is also a decreased association between the immunoprecipitated GAP1/2 and RECC, which provides the core enzymatic activities needed for RNA editing.

MRB8620 is necessary for editing in bloodstream stage *T. brucei*

Our observation that RNAi silencing of MRB8620 impacts RNA editing in PS, regardless of the metabolic status of the cells, contradicts a previous report (Aphasizheva et al. 2014). To verify this phenotype, we set out to determine whether MRB8620 is also required for RNA editing in BS. Our initial attempts to create a double *MRB8620* gene knockout (DKO) in BS failed (data not shown), suggesting that this protein is essential for the parasite.

Given this complication, we opted to take advantage of a BS cell line bearing a L262P site mutation in the ATP synthase γ-subunit, which allows *T. brucei* at this life-cycle stage to be viable despite blocked kDNA inheritance or expression (Dean et al. 2013; Schnarwiler et al. 2014). We predicted that the knockout of both *MRB8620* alleles would be achievable as RNA editing is rendered redundant in this genetic background. After creating the cell line bearing the L262P site mutation in one of the γ-subunit gene alleles, we confirmed that this genetic modification indeed rendered this cell line kDNA-independent (see Materials and Methods).

To determine whether BS MRB8620 knockout cells exhibit RNA editing, we replaced both *MRB8620* ORFs with constructs bearing the phleomycin and hygromycin resistance cassettes in L262P-mutant bearing BS, as shown by PCR with primer pair I annealing to genomic sequence just outside of the integration sites (Fig. 6A,B). More significantly, sequence within the *MRB8620* ORF was not PCR amplified by primer pair II from genomic DNA extracted from the DKO (Fig. 6A,C). This amplicon was detected in the genomic DNA from BS in which only a single *MRB8620* ORF was deleted and in the parental cell lines.

Demonstrating that we indeed generated a *MRB8620* DKO, we harvested RNA from these cells and the parental L262P-mutant bearing cells in which both *MRB8620* alleles were intact, both grown under the same conditions. This material was converted to cDNA for use in the qPCR assay measuring steady-state levels of maxicircle-encoded RNAs. Neither never-edited CO1 and ND4 mRNAs nor 9S and 12S rRNAs were affected in the DKO when compared with

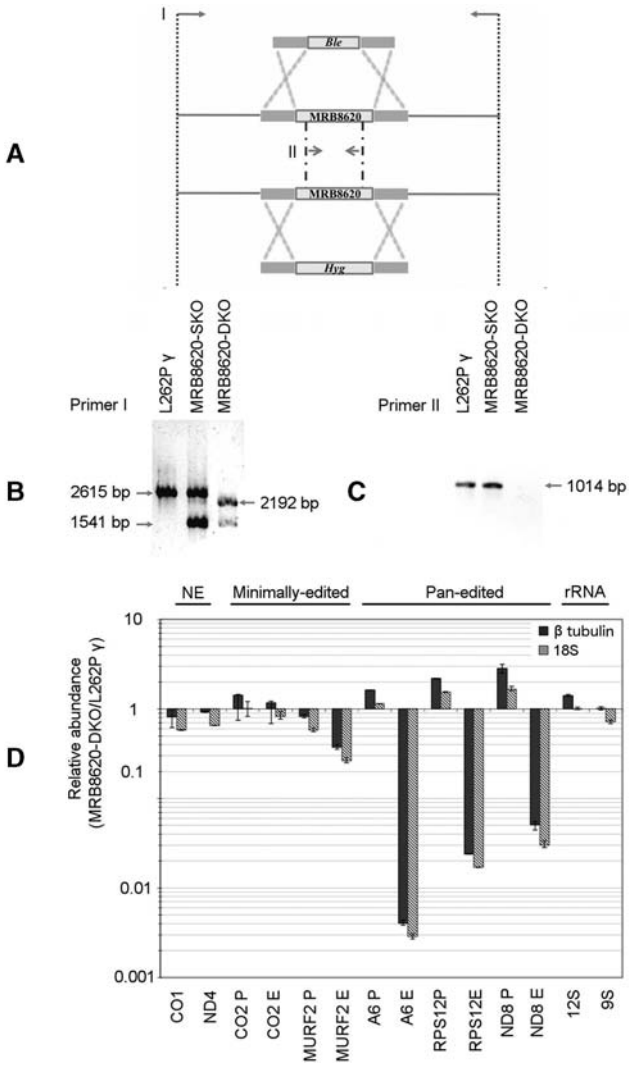

FIGURE 6. MRB8620 is essential for RNA editing in BS *T. brucei*. (*A*) Scheme depicting how MRB8620 double knockout was generated. Arrows indicate the locations of PCR primer pairs I and II, just flanking the knockout loci and amplifying the *MRB8620* ORF, respectively, used to identify the single and double knockouts generated by homologous recombination in the cell line in which one of the ATP synthase γ-subunit alleles bears a L262P site mutation. (*B*) Agarose gel-resolved PCR products of primer pair I flanking the genomic integration site of the constructs from genomic DNA isolated from the parental hemizygous L262P-mutant BS *T. brucei*, single knockout (SKO) and MRB8620 double knockout (DKO). The size of each amplicon is indicated by the arrow. Primer pairs for identification are depicted in *A*. (*C*) As in *B*, but showing the PCR amplicon from primer pair II amplifying sequence from within the MRB8620 ORF. (*D*) Relative abundance of mitochondrial mRNAs in MRB8620 double knockout cells compared with the parental hemizygous ATP synthase L262P γ-subunit mutant cell line. Whiskers denote range of obtained relative abundances within technical triplicates. Labeled as in Figure 3A.

the parental cell line (Fig. 6D), indicating that maxicircle kDNA was not lost in the L262P-mutant bearing cells grown for the time period of the experiment. However, a decrease in the levels of minimally edited MURF2 mRNA and pan-edited A6, ND8, and RPS12 RNAs was observed (Fig. 6D). The defect in editing of pan-edited RNAs was quite dramatic, with an almost two order of magnitude reduction in their levels when compared with the parental, L262P γ-subunit heterozygote controls. It should be noted that there was a concomitant accumulation of pre-edited mRNAs in the DKOs in relation to the parental cell lines that was on par with what was observed in PS when MRB8620 was down-regulated compared with the noninduced controls. To elaborate, pre-edited A6 in the BS DKO was 1.1–1.6 times the parental levels versus PS RNAi-induced (grown in SDM79) showing approximately two times the noninduced control levels for the same transcript. Similarly, RPS12 pre-edited in the BS DKO was 1.5–2.2 times the parental control compared to PS induced showing 1.2–1.3 times the noninduced level. Thus, it appears that RNA editing is compromised in *MRB8620* DKO, indicating it plays a role in this process in BS.

DISCUSSION

We have studied in detail MRB8620, a subunit of the MRB1 core subcomplex that functions in trypanosome RNA editing. However, the findings we describe here are not just restricted to this subunit but also contribute to our understanding of the complex in general.

Disruption of MRB1 core integrity by MRB8620 knockdown leads to a reduction in mt RNA editing in *T. brucei*. The obvious phenotype in this condition is a down-regulation of edited mRNAs, which was observed in our study in both PS and BS, in contrast to previous work (Aphasizheva et al. 2014). Yet, impairment of editing also led to other consequences. For example, gRNAs exhibited an increase in their steady-state levels, as was observed when other MRB1 proteins were silenced by RNAi (Ammerman et al. 2013; Aphasizheva et al. 2014), suggesting that these small noncoding transcripts are consumed after fulfilling their guiding role during the normal, unimpeded course of RNA editing.

We did not observe any effect on doubling time in PS *T. brucei* when the MRB8620 knockdown was grown in SDM79 medium. Under these culture conditions, glycolysis seems to be sufficient to cover cellular ATP demands (Coustou et al. 2008). Thus, it is not surprising that the relatively modest effect we observed upon MRB8620 silencing on RNA editing, which is essential for the maturation of mRNAs encoding subunits of the respiratory chain, would not result in reduced fitness of flagellates that do not rely on oxidative phosphorylation for energy generation. This metabolic pathway rises to prominence under the low glucose condition of SDM80. Indeed, here we do observe a slight growth inhibition of PS upon MRB8620 silencing. This moderate effect on flagellate fitness may be due to the low penetrance of RNAi in this study. Alternatively, the observed reduction in MRB1 complex integrity upon MRB8620 silencing may itself result in suboptimal editing. The other MRB1 proteins are still present in this background but are less efficient in their contribution to the process, which nevertheless occurs at sufficient levels to allow unaltered growth. MRB8620 may also be a particularly stable protein that persists at lower but still adequate doses during the course of RNAi silencing (i.e., residual MRB8620 still functions despite being diluted by RNAi targeting de novo protein during cell growth). We speculate that the finding that MRB8620 is membrane associated, and bears a predicted hydrophobic domain that may serve as a transmembrane domain, could also contribute to a possible higher degree of protein stability. The membrane association of MRB8620 would not be unprecedented, as other proteins involved in *T. brucei* mt RNA processing also exhibit this property. Several pentatricopeptide proteins, which are so named because they contain the eponymous RNA-binding motif, have been shown to be membrane associated along with mt ribosomal RNA (Pusnik et al. 2007). Among these is the kinetoplast polyadenylation/uridylation factor 1 (kPAF1), also known as PPR1, which interacts with both MRB1 and mt ribosomes (Aphasizheva et al. 2011; Ammerman et al. 2012).

As demonstrated by the RNAi-mediated knockdown, MRB8620 plays a central role in MRB1 core integrity. This condition may be due to disrupted assembly of the constituent subunits during construction of the core and/or it may reflect a core that is especially unstable in the absence of MRB8620. Nevertheless, when MRB8620 is down-regulated, partner proteins GAP1, MRB11870, and MRB3010 exhibit a decreased associated with each other as a MRB1 core. The core's association with the TbRGG2 subcomplex, which appears to be the MRB1 component responsible for the processivity of pan-editing (Ammerman et al. 2010; Hashimi et al. 2013), is also reduced and its integrity somewhat disrupted upon MRB8620 depletion. The phenotype differs when the GAP1/2 heterotetramer is depleted by RNAi. In this case, MRB11870 interacts with MRB3010 to the same degree or more than in the untreated controls, implying that the MRB1 core remains intact despite the depletion of the GAP1/2 heterotetramer and the downstream effects manifested by gRNA degradation and pre-edited mRNA accumulation. Furthermore, association of the TbRGG2 subcomplex with the MRB1 core also persists, in agreement with its density gradient sedimentation remaining unperturbed upon GAP1 silencing (Aphasizheva et al. 2014), as well as its interaction with the core via MRB3010 or MRB8620, as demonstrated in a yeast two-hybrid screen (Ammerman et al. 2012). Taken together, these data indicate that MRB1 core integrity is dependent on subunits such as MRB8620 and MRB11870 (Ammerman et al. 2013), whereas the presence of the GAP1/2 heterotetramer is dispensable for its assembly or stability and even its association with TbRGG2. This finding plus the heterodispersion of the GAP1/2 subcomplex in

density gradients (Acestor et al. 2009; Hashimi et al. 2009; Ammerman et al. 2011, 2012; Kafková et al. 2012; Aphasizheva et al. 2014) and the association of GAP1/2 with REH2 (Madina et al. 2014) or TbRGG3 (McAdams et al. 2015) suggest that GAP1/2 interactions are not restricted to the MRB1 core and that the heterotetramer represents a functionally distinct entity.

Another consequence of impaired MRB1 core fabrication is the accumulation of pre-edited mRNAs in association with the GAP1/2 heterotetramer. The two GAPs are the only established RBPs of the MRB1 core, as they have been shown to bind gRNAs to promote their stability, hence their aliases (Weng et al. 2008; Hashimi et al. 2009). This work also shows that the heterotetramer associates with pre-edited and edited mRNAs, although the nature of their interaction remains unknown (e.g., whether they are directly bound to the proteins or indirectly bound via gRNA hybridization or another bound protein partner). As the gRNA:mRNA duplex represents the substrate for RNA editing, it is plausible that GAP1/2 would pull down both transcript species. Upon disruption of the MRB1 core, pre-edited mRNAs that are slated for maturation via this process could become clogged on the GAP1/2 heterotetramer as they do not proceed along this pathway. Consistent with this hypothesis is the redistribution of GAP1 sedimentation throughout the glycerol gradient performed on samples from the MRB8620-silenced trypanosomes. The shift of GAP1 to more dense fractions upon MRB8620 silencing may reflect its increased accumulation on mRNA as described above. Because GAP1 associates with additional proteins outside the MRB1 complex (Madina et al. 2014; McAdams et al. 2015), these larger GAP1-containing complexes may also comprise non-MRB1 ribonucleoprotein complexes. Similar shifts of GAP1 sedimentation to larger glycerol gradient fractions has been reported previously in response to depletion of specific MRB1 proteins (Aphasizheva et al. 2014).

However, we observe that GAP1/2-bound edited RNAs are present at the same level in both MRB8620-down-regulated and untreated controls, or even increased in the former when normalized to the reduced level of these transcripts when the whole mt transcriptome is concerned. One explanation is that the cDNAs annealing to what we term edited primers may not be fully edited. Another explanation that is not mutually exclusive to the previous one is that RNAi silencing does not fully deplete MRB8620, letting RNA editing occur at a lower level than normally. In this background, residual edited RNAs are enriched in association with the GAP heterotetramer. Supporting this finding is that KREL1, one of the RECC enzymes providing the machinery for U insertion/deletion, still associates with GAP1 when MRB8620 is down-regulated, although to a lesser degree as compared to the untreated control. In the untreated controls, the pool of edited mRNA sequence that is sequestered by GAP1/2 may represent only a small fraction of these transcripts. The residual amounts of edited RNA remaining in the MRB8620-depleted background could associate with GAP1/2 to a similar degree as in the controls, where edited RNAs may not reside long with MRB1 after completion of the editing process.

MRB1 has been interpreted to be a platform for the various components of the RNA editing and other RNA processes to assemble (Hashimi et al. 2013) or a vital part of the RNA editing holoenzyme along with RECC (Aphasizheva et al. 2014). Regardless of one's point of view, it is clear that cooperation among several protein subcomplexes is needed for RNA editing to work. In this study, we show that MRB8620 is required for proper assembly of the MRB1 core. A model arising from the investigated consequences of MRB1 core disassembly is shown in Figure 7, to suggest

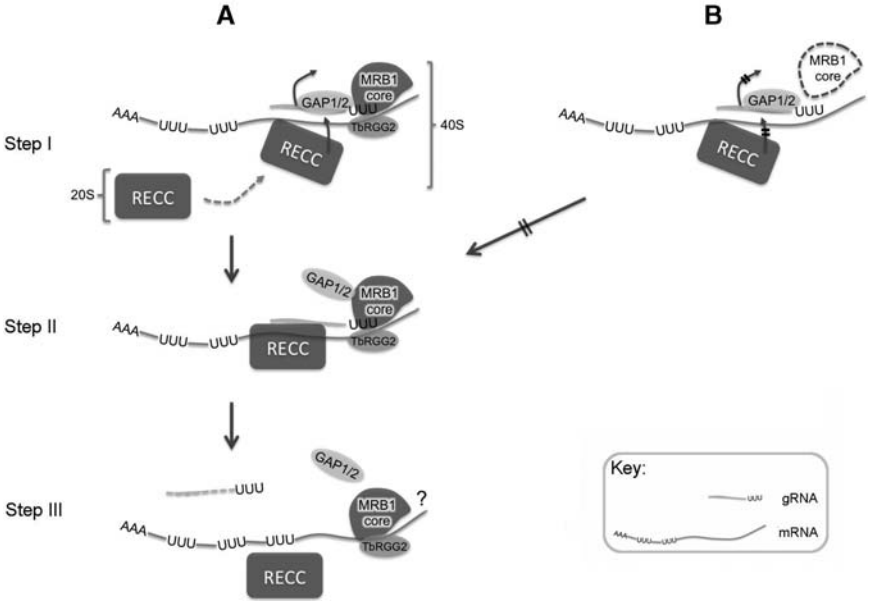

FIGURE 7. Proposed role of MRB1 core assembly in RNA editing. (*A*) Assembly of editing machinery on duplexed gRNA:mRNA in the native state of untreated *T. brucei*. 3′-Oligo(U) bearing gRNA strand on top with 3′-poly(A/U) tail appended, partially edited mRNA on bottom. Step I: 20 S RECC assembled with gRNA-bound GAP1/2 and MRB1 core as well as TbRGG2 subcomplex bound to mRNA to form 40 S particle. Arrows indicate conformational change removing GAP1/2 from gRNA to allow RECC access to editing site as defined by gRNA:mRNA duplex. Step II: RECC processes mRNA:gRNA free of obstructive GAP1/2 heterotetramer. Step III: gRNA is degraded after use in editing of prior mRNA/gRNA duplex. RECC and GAP1/2 assumed to disassociate. Question mark (?) indicates that MRB1 core and TbRGG2 remaining attached to still partially edited mRNA remains unknown. (*B*) Consequence of MRB1 core disassembly (dashed outline) caused by MRB8620 silencing on editing. Crossed arrows indicate that the conformational change freeing GAP1/2 from the gRNA:mRNA duplex, allowing RECC to bind to the hybridized transcripts, does not occur because of disassembly of MRB1 core.

how this core subcomplex may serve to facilitate RNA editing.

We demonstrated that while GAP1/2 undoubtedly interacts with the MRB1 core, it may represent a separate entity that is functionally distinguishable from the other core subunits (Fig. 7A, Step I). Furthermore, when GAP1 is RNAi silenced, interaction between the core protein MRB3010 and TbRGG2 persists. Because gRNA and edited RNAs are depleted in this background, we presume the interaction between MRB3010 and TbRGG2 is dependent on protein–protein interactions enhanced by the presence of pre-edited and/or partially edited mRNAs (Fig. 7A, Step I), consistent with previous results (Ammerman et al. 2012; Foda et al. 2012). Thus, our results suggest that the association of the MRB1 core with mRNA is facilitated by interaction with the TbRGG2 subcomplex (Fig. 7, Step I).

We have also shown that GAP1/2 associates with mRNA undergoing RNA editing, and that these transcripts appear to accumulate on the heterotetramer when MRB1 core assembly is disrupted. This observation is a further testament to GAP1/2 being functionally distinct to the MRB1 core. Decreased RECC association with GAP1/2 in this background is also consistent with the mRNA accumulation phenotype, because this protein complex provides the catalytic activities for the processing of these transcripts (Fig. 7B).

To explain these findings, we propose that in the native state, the MRB1 core may serve to facilitate a conformational change so that GAP1/2 is removed from the gRNA:mRNA duplex so that it does not sterically hinder RECC access to ESs along the hybridized transcripts (Fig. 7A, Steps I and II). It has been previously shown that although RECC sedimenting at 20S fractions is depleted of RNAs, thus having its catalytic sites free for in vitro RNA editing assays, the heavier 40S RECC fractions do contain RNA and associate with GAP1/2 (Golas et al. 2009; Aphasizheva et al. 2014). Thus, we propose that although the GAP1/2 heterotetramer may be shifted away from a processed ES, it remains anchored to the mRNA undergoing processing via the MRB1 and TbRGG2 subcomplexes (Fig. 7A, Step II). In the MRB8620-depleted background, in which the MRB1 core cannot be properly assembled, mRNAs that undergo editing accumulate on GAP1/2 because RECC access to the gRNA:mRNA duplex is hindered (Fig. 7B).

GAP1/2 release from the RECC processed gRNA:mRNA duplex is also supported by the finding that gRNAs are degraded after they have been used by RNA editing (Fig. 7A, Step III; Ammerman et al. 2013; Aphasizheva et al. 2014), because the binding of these small RNAs to the heterotetramer promotes their stability (Weng et al. 2008; Hashimi et al. 2009). How the discussed protein complexes behave after editing of a block as defined by a gRNA:mRNA duplex remains unknown. RECC and the GAPs most likely dissociate from the processed RNA (Fig. 7A, Step III). Perhaps the MRB1 core remains associated with a partially edited mRNA to facilitate steps I and II as depicted in Figure 7A for the next round of editing. Collectively, the data presented here demonstrate an important role for the MRB1 core in RNA trafficking during kinetoplastid RNA editing.

MATERIALS AND METHODS

Generation of cell lines and their manipulation

A 575-bp-long portion of the 3′ part of the MRB8620 open reading frame excluding the stop codon was cloned into the pC-PURO-PTP vector, a variation on pC-NEO-PTP, via the ApaI and NotI sites in the polylinker (Schimanski et al. 2005). This construct was linearized by cutting with SphI, whose single restriction site is within the MRB8620 sequence, to create homology flanks for in situ tagging of the gene product for affinity purification. Cells with proper integration of the construct were selected by their resistance to puromycin. In situ C-terminal tagging of MRB8620 and MRB3010 was facilitated by previously described vectors (Huang et al. 2014). To generate RNAi knockdowns, PCR primers were designed using the RNAit tool (Redmond et al. 2003) for amplifying an appropriate region of the MRB8620 ORF from *T. brucei* genomic DNA, for cloning into the p2T7-177 vector (Wickstead et al. 2002) allowing inducible RNAi. The linearized constructs were electroporated into the PS 29–13 strain by an established protocol (Kafková et al. 2012). Cell density in SDM79 (Brun and Schönenberger 1979) and in glucose-poor SDM80 (Coustou et al. 2008) was measured daily with a Coulter counter as described previously (Kafková et al. 2012).

For the double knockout of MRB8620 in the BS 427 strain, a kDNA-independent cell line was first generated by replacing an endogenous ATP synthase F_1 γ-subunit locus with an ORF bearing the L262P mutation, which was selected with puromycin (Dean et al. 2013). To verify that the generated cell line was truly kDNA-independent, it was grown in the presence of 20 nM ethidium bromide for 5 d. The lack of 4′,6-diamidino-2-phenylindole (DAPI) stained kDNA confirmed that the L262P γ-subunit mutation allowed survival despite loss of the organellar genome (data not shown). The MRB8620 knockout constructs were generated using a fusion PCR method (Merritt and Stuart 2013) to generate either the hygromycin or phleomycin resistance marker cassettes flanked by *MRB8620* 5′- and 3′-untranslated regions to facilitate homologous recombination. These constructs were sequentially electroporated into the kDNA-independent BS *T. brucei* by an established protocol (Ammerman et al. 2013). The PCR primers amplifying elements incorporated into the described constructs used to generate the various cell lines are summarized in Supplemental Table 2.

RNA detection assays

RNA isolation and gRNA detection by probing of Northern blots with 5′-P^{32} labeled oligonucleotide probes (sequences are given in Supplemental Table 2) were conducted as described elsewhere (Kafková et al. 2012). Quantitative real-time PCR was also performed according to this study except the generation of template cDNA from the RNAi-silenced and knockout cells. The QuantiTech Reverse Transcription kit (QIAGEN) was used for generating cDNA from 4 μg of RNA, with a prior genomic DNA degradation step, according to the manufacturer's instructions. Primers

for detection of MRB8620 cDNA by qPCR are given in Supplemental Table 2. Other primers used in this study, along with a description of relative abundances of cDNAs between treated and untreated samples, were described previously (Carnes et al. 2005).

Protein detection assays and cell fractionation

Tandem affinity purification (TAP) of MRB8620 via its C-terminal PTP (ProtC-TEV-ProtA) (Schimanski et al. 2005) tag was performed following an established protocol (Ammerman et al. 2011) to yield eluates that were analyzed by LC-MS/MS mass spectroscopy as previously described (Kafková et al. 2012). The separation of mitochondria and cytosolic components, as well as further fractionation of the former into soluble and insoluble parts, was performed as described elsewhere (Schnaufer et al. 2005). In brief, 1×10^8 cells were treated with 1 mL of 0.015% digitonin in SoTE buffer (20 mM Tris, pH 7.5; 0.6 M sorbitol; and 2 mM EDTA) on ice and then separated by centrifugation into the cytosolic (supernatant) and organellar (pellet) fractions. The volume of the cytosolic fraction was measured and the pellet was resuspended in an equal volume of 1% Triton X-100 and separated into soluble (supernatant) and insoluble (pellet) fractions by centrifugation; the pellet was again resuspended in the same volume as the supernatant. Equal volumes from each fraction, representing the same proportion of each fraction, was loaded onto a SDS-PAGE gel along with a cell equivalent of total lysate from *T. brucei*.

Glycerol gradients and immunoprecipitation

Mitochondria were isolated from 10^{10} MRB8620 and GAP RNAi knockdown and parental control flagellates as described previously (Hashimi et al. 2008). The resulting vesicles corresponding to 5 mg of protein were lysed in 1 mL of the lysis buffer (10 mM Tris at pH 7.2, 10 mM $MgCl_2$, 100 mM KCl, 1 mM DTT, 1 mg/mL pepstatin, and 2 mg/mL leupeptin) with 1% Triton X-100 and treated with 20U RNaseOUT™ (Life Technology) for 60 min at 4°C. The lysate was cleared and loaded on an 11-mL 10%–30% glycerol gradient, which was centrifuged at 32,000 rpm in a Beckman SW41 rotor for 16 h at 4°C. Twelve 0.5-mL fractions were then collected from the top of the gradient for Western blot analysis.

Mitochondria from 2×10^9 MRB3010-V5 PS cells were harvested and lysed as for the glycerol gradients. IP of MRB3010-YFP was performed as previously described (Huang et al. 2014), and elutions were analyzed by Western blotting. Equal volumes from the IP eluates generated from an equal amount of cells were loaded onto 12% or 15% SDS-polyacrylamide gels for the resolution of the constituent proteins.

The cross-linking of α-GAP1 antibody to Protein G Dynabeads (Life Technology) was done with dimethyl pimelimidate (DMP) (Sigma-Aldrich) as follows. Beads were washed two times with phosphate-buffered saline (PBS) at 1:1 ratio by rotation for 10 min at 4°C. After discarding the supernatant, dilution buffer (PBS + 1mg/mL BSA) was added at 1:1 ratio and rotated for 10 min at 4°C. Approximately 20 µg of α-GAP1 antibody in dilution buffer was then added at a 1:1 ratio to the beads and rotated 1 h at 4°C. Afterward, the beads were washed again in PBS as before. Thirteen milligrams per milliliter DMP solution pH 8 was prepared immediately prior to cross-linking and mixed with equal volume of 0.2 M triethanolamine in PBS. The cross-linking solution was added to the beads at a 1:1 ratio and rotated for 30 min at room temperature (RT). Then the beads were washed three times with PBS as before. A quenching buffer of 50 mM ethanolamine in PBS was added to beads at a 1:1 ratio and rotated 5 min at RT three times and then washed with PBS as before. The beads were then treated twice with 1 M glycine pH 3 and then rotated for 10 min at RT. The beads were then ready for IP after a last PBS wash. RNA IP was performed as the MRB3010-YFP IP, with the addition of a preclearing step by gentle agitation with Protein G Dynabeads for 30 min and three subsequent stringent washing steps (10 mM Tris, pH 7.4; 1 mM EDTA; 1 mM EGTA; NaCl 300 mM; and 1% Triton X-100) for reduction of background. RNA from the IP was recovered by acid phenol–chloroform extraction and a successive ethanol precipitation. The RNA IP was performed two times. RNAs were then processed for the qPCR assay for mt transcript levels as described above and performed in technical triplicates.

The formula for normalization of RNA IP to mt RNA levels in the MRB8620 knockdown (Fig. 3A) is as follows: V_{IP}, representing abundance value of one tested transcript from the elution, V_T as the same transcript from the lysis, relative GAP1/2-associated mRNA fraction value $V_f = V_{IP}/V_T$, the GAP1/2-associated mRNA fraction fold number $R_f = (V_{IP\text{-induced}}/V_{T\text{-induced}})/(V_{IP\text{-noninduced}}/V_{T\text{-noninduced}}) = (V_{IP\text{-induced}}/V_{IP\text{-noninduced}})/(V_{T\text{-induced}}/V_{T\text{-noninduced}}) = (2 \times \text{PCR efficiency percent})^{(\text{CtIPnoninduced-CtIPinduced})}/(2 \times \text{PCR efficiency percent})^{(\text{Ctnon-induced-Ctinduced})}$.

Western blot analysis and antibodies

Forty micrograms of proteins from hypotonically isolated mitochondrial vesicles were loaded on 12% or 15% SDS-polyacrylamide gels and then transferred to a PVDF membrane. Western blot analysis was performed with the following polyclonal antibodies, all at 1:1000: α-MRB3010, α-MRB11870, and α-MRB8170 (Ammerman et al. 2012); α-GAP1 (Hashimi et al. 2009); α-TbRGG2 (Fisk et al. 2008); α-trCoIV (Maslov et al. 2002); α-protein A (Sigma-Aldrich); and α-V5 (Life Technologies). Anti-enolase antibody was used at a 1:10,000 dilution. In addition, monoclonal antibodies immunodecorating KREL1 and KREPA3 (Panigrahi et al. 2001) were also used at 1:50 dilutions.

SUPPLEMENTAL MATERIAL

Supplemental material is available for this article.

ACKNOWLEDGMENTS

We thank Achim Schnaufer (University of Edinburgh) for providing constructs and protocols for creating the kDNA-independent BS cell line used in this study, Ken Stuart (Seattle Biomed) and Paul Michels (Universidad de los Andes/University of Edinburgh) for the kind gift of antibodies, and Peter Koník (University of South Bohemia) for help with mass spectroscopy. This work was supported by the Grant Agency of the Czech Republic (15-21974S), RNPnet FP7 program (289007), and Praemium Academiae to J.L., and the National Institutes of Health (NIH) (RO1 AI061580) to L.K.R.

Received April 24, 2015; accepted September 9, 2015.

REFERENCES

Acestor N, Panigrahi AK, Carnes J, Zíková A, Stuart KD. 2009. The MRB1 complex functions in kinetoplastid RNA processing. *RNA* **15:** 277–286.

Ammerman ML, Presnyak V, Fisk JC, Foda BM, Read LK. 2010. TbRGG2 facilitates kinetoplastid RNA editing initiation and progression past intrinsic pause sites. *RNA* **16:** 2239–2251.

Ammerman ML, Hashimi H, Novotná L, Čičová Z, McEvoy SM, Lukeš J, Read LK. 2011. MRB3010 is a core component of the MRB1 complex that facilitates an early step of the kinetoplastid RNA editing process. *RNA* **17:** 865–877.

Ammerman ML, Downey KM, Hashimi H, Fisk JC, Tomasello DL, Faktorová D, Kafková L, King T, Lukeš J, Read LK. 2012. Architecture of the trypanosome RNA editing accessory complex, MRB1. *Nucleic Acids Res* **40:** 5637–5650.

Ammerman ML, Tomasello DL, Faktorová D, Kafková L, Hashimi H, Lukeš J, Read LK. 2013. A core MRB1 complex component is indispensable for RNA editing in insect and human infective stages of *Trypanosoma brucei*. *PLoS One* **8:** e78015.

Aphasizheva I, Maslov D, Wang X, Huang L, Aphasizhev R. 2011. Pentatricopeptide repeat proteins stimulate mRNA adenylation/uridylation to activate mitochondrial translation in trypanosomes. *Mol Cell* **42:** 106–117.

Aphasizheva I, Zhang L, Wang X, Kaake RM, Huang L, Monti S, Aphasizhev R. 2014. RNA binding and core complexes constitute the U-insertion/deletion editosome. *Mol Cell Biol* **34:** 4329–4342.

Blum B, Bakalara N, Simpson L. 1990. A model for RNA editing in kinetoplastid mitochondria: "guide" RNA molecules transcribed from maxicircle DNA provide the edited information. *Cell* **60:** 189–198.

Brown SV, Hosking P, Li J, Williams N. 2006. ATP synthase is responsible for maintaining mitochondrial membrane potential in bloodstream form *Trypanosoma brucei*. *Eukaryot Cell* **5:** 45–53.

Brun R, Schönenberger. 1979. Cultivation and in vitro cloning or procyclic culture forms of *Trypanosoma brucei* in a semi-defined medium. *Acta Trop* **36:** 289–292.

Carnes J, Trotter JR, Ernst NL, Steinberg A, Stuart K. 2005. An essential RNase III insertion editing endonuclease in *Trypanosoma brucei*. *Proc Natl Acad Sci* **102:** 16614–16619.

Carnes J, Trotter JR, Peltan A, Fleck M, Stuart K. 2008. RNA editing in *Trypanosoma brucei* requires three different editosomes. *Mol Cell Biol* **28:** 122–130.

Coustou V, Biran M, Breton M, Guegan F, Rivière L, Plazolles N, Nolan D, Barrett MP, Franconi JM, Bringaud F. 2008. Glucose-induced remodeling of intermediary and energy metabolism in procyclic *Trypanosoma brucei*. *J Biol Chem* **283:** 16342–16354.

Dean S, Gould MK, Dewar CE, Schnaufer AC. 2013. Single point mutations in ATP synthase compensate for mitochondrial genome loss in trypanosomes. *Proc Natl Acad Sci* **110:** 14741–14746.

Ernst NL, Panicucci B, Igo RP Jr, Panigrahi AK, Salavati R, Stuart K. 2003. TbMP57 is a 3′ terminal uridylyl transferase (TUTase) of the *Trypanosoma brucei* editosome. *Mol Cell* **11:** 1525–1536.

Ernst NL, Panicucci B, Carnes J, Stuart K. 2009. Differential functions of two editosome exoUases in *Trypanosoma brucei*. *RNA* **15:** 947–957.

Fisk JC, Ammerman ML, Presnyak V, Read LK. 2008. TbRGG2, an essential RNA editing accessory factor in two *Trypanosoma brucei* life cycle stages. *J Biol Chem* **283:** 23016–23025.

Foda BM, Downey KM, Fisk JC, Read LK. 2012. Multifunctional G-rich and RRM-containing domains of TbRGG2 perform separate yet essential functions in trypanosome RNA editing. *Eukaryot Cell* **11:** 1119–1131.

Golas MM, Böohm C, Sander B, Effenberger K, Brecht M, Stark H, Göoringer HU. 2009. Snapshots of the RNA editing machine in trypanosomes captured at different assembly stages in vivo. *EMBO J* **28:** 766–778.

Golden DE, Hajduk SL. 2005. The 3′-untranslated region of cytochrome oxidase II mRNA functions in RNA editing of African trypanosomes exclusively as a *cis* guide RNA. *RNA* **11:** 29–37.

Hashimi H, Zíková A, Panigrahi AK, Stuart KD, Lukeš J. 2008. TbRGG1, an essential protein involved in kinetoplastid RNA metabolism that is associated with a novel multiprotein complex. *RNA* **14:** 970–980.

Hashimi H, Čičová Z, Novotná L, Wen YZ, Lukeš J. 2009. Kinetoplastid guide RNA biogenesis is dependent on subunits of the mitochondrial RNA binding complex 1 and mitochondrial RNA polymerase. *RNA* **15:** 588–599.

Hashimi H, Benkovičová V, Čermáková P, Lai DH, Horváth A, Lukeš J. 2010. The assembly of F_1F_O-ATP synthase is disrupted upon interference of RNA editing in *Trypanosoma brucei*. *Int J Parasitol* **40:** 45–54.

Hashimi H, Zimmer SL, Ammerman ML, Read LK, Lukeš J. 2013. Dual core processing: MRB1 is an emerging kinetoplast RNA editing complex. *Trends Parasitol* **29:** 91–99.

Hernandez A, Madina BR, Ro K, Wohlschlegel JA, Willard B, Kinter MT, Cruz-Reyes J. 2010. REH2 RNA helicase in kinetoplastid mitochondria: ribonucleoprotein complexes and essential motifs for unwinding and guide RNA (gRNA) binding. *J Biol Chem* **285:** 1220–1228.

Huang Z, Kaltenbrunner S, Šimková E, Staněk D, Lukeš J, Hashimi H. 2014. Dynamics of mitochondrial RNA-binding protein complex in *Trypanosoma brucei* and its petite mutant under optimized immobilization conditions. *Eukaryot Cell* **13:** 1232–1240.

Kafková L, Ammerman ML, Faktorová D, Fisk JC, Zimmer SL, Sobotka R, Read LK, Lukeš J, Hashimi H. 2012. Functional characterization of two paralogs that are novel RNA binding proteins influencing mitochondrial transcripts of *Trypanosoma brucei*. *RNA* **18:** 1846–1861.

Lai DH, Hashimi H, Lun ZR, Ayala FJ, Lukeš J. 2008. Adaptations of *Trypanosoma brucei* to gradual loss of kinetoplast DNA: *Trypanosoma equiperdum* and *Trypanosoma evansi* are petite mutants of *T. brucei*. *Proc Natl Acad Sci* **105:** 1999–2004.

Madina BR, Kumar V, Metz R, Mooers BHM, Bundschuh R, Cruz-Reyes J. 2014. Native mitochondrial RNA-binding complexes in kinetoplastid RNA editing differ in guide RNA composition. *RNA* **20:** 1142–1152.

Maslov DA, Simpson L. 1992. The polarity of editing within a multiple gRNA-mediated domain is due to formation of anchors for upstream gRNAs by downstream editing. *Cell* **70:** 459–467.

Maslov DA, Zíková A, Kyselová I, Lukeš J. 2002. A putative novel nuclear-encoded subunit of the cytochrome *c* oxidase complex in trypanosomatids. *Mol Biochem Parasitol* **125:** 113–125.

McAdams NM, Ammerman ML, Nanduri J, Lott K, Fisk JC, Read LK. 2015. An arginine-glycine-rich RNA binding protein impacts the abundance of specific mRNAs in the mitochondria of *Trypanosoma brucei*. *Eukaryot Cell* **14:** 149–157.

McManus MT, Adler BK, Pollard VW, Hajduk SL. 2000. *Trypanosoma brucei* guide RNA poly(U) tail formation is stabilized by cognate mRNA. *Mol Cell Biol* **20:** 883–891.

Merritt C, Stuart K. 2013. Identification of essential and non-essential protein kinases by a fusion PCR method for efficient production of transgenic *Trypanosoma brucei*. *Mol Biochem Parasitol* **190:** 44–49.

Möller S, Croning MD, Apweiler R. 2001. Evaluation of methods for the prediction of membrane spanning regions. *Bioinformatics* **17:** 646–653.

Nebohá̌cová M, Maslov DA, Falick AM, Simpson L. 2004. The effect of RNA interference down-regulation of RNA editing 3′-terminal uridylyl transferase (TUTase) 1 on mitochondrial de novo protein synthesis and stability of respiratory complexes in *Trypanosoma brucei*. *J Biol Chem* **279:** 7819–7825.

Nilsson D, Gunasekera K, Mani J, Osteras M, Farinelli L, Baerlocher L, Roditi I, Ochsenreiter T. 2010. Spliced leader trapping reveals widespread alternative splicing patterns in the highly dynamic transcriptome of *Trypanosoma brucei*. *PLoS Pathog* **6:** e1001037.

Panigrahi AK, Schnaufer A, Carmean N, Igo RP, Jr, Gygi SP, Ernst NL, Palazzo SS, Weston DS, Aebersold R, Salavati R, et al. 2001. Four

related proteins of the *Trypanosoma brucei* RNA editing complex. *Mol Cell Biol* **21:** 6833–6840.

Pfaffl MW. 2001. A new mathematical model for relative quantification in real-time RT-PCR. *Nucleic Acids Res* **29:** e45.

Pusnik M, Small I, Read LK, Fabbro T, Schneider A. 2007. Pentatricopeptide repeat proteins in *Trypanosoma brucei* function in mitochondrial ribosomes. *Mol Cell Biol* **27:** 6876–6888.

Redmond S, Vadivelu J, Field MC. 2003. RNAit: an automated web-based tool for the selection of RNAi targets in *Trypanosoma brucei*. *Mol Biochem Parasitol* **128:** 115–118.

Schimanski B, Nguyen TN, Guünzl A. 2005. Highly efficient tandem affinity purification of trypanosome protein complexes based on a novel epitope combination. *Eukaryot Cell* **4:** 1942–1950.

Schnarwiler F, Niemann M, Doiron N, Harsman A, Kaäser S, Mani J, Chanfon A, Dewar CE, Oeljeklaus S, Jackson CB, et al. 2014. Trypanosomal TAC40 constitutes a novel subclass of mitochondrial β-barrel proteins specialized in mitochondrial genome inheritance. *Proc Natl Acad Sci* **111:** 7624–7629.

Schnaufer A, Panigrahi AK, Panicucci B, Igo RP Jr, Wirtz E, Salavati R, Stuart K. 2001. An RNA ligase essential for RNA editing and survival of the bloodstream form of *Trypanosoma brucei*. *Science* **291:** 2159–2162.

Schnaufer A, Clark-Walker GD, Steinberg AG, Stuart K. 2005. The F1-ATP synthase complex in bloodstream stage trypanosomes has an unusual and essential function. *EMBO J* **24:** 4029–4040.

Siegel TN, Hekstra DR, Wang X, Dewell S, Cross GA. 2010. Genome-wide analysis of mRNA abundance in two life-cycle stages of *Trypanosoma brucei* and identification of splicing and polyadenylation sites. *Nucleic Acids Res* **38:** 4946–4957.

Verner Z, Basu S, Benz C, Dixit S, Dobáková E, Faktorová D, Hashimi H, Horáková E, Huang Z, Paris Z, et al. 2015. Malleable mitochondrion of *Trypanosoma brucei*. *Int Rev Cell Mol Biol* **315:** 73–151.

Weng J, Aphasizheva I, Etheridge RD, Huang L, Wang X, Falick AM, Aphasizhev R. 2008. Guide RNA-binding complex from mitochondria of trypanosomatids. *Mol Cell* **32:** 198–209.

Wickstead B, Ersfeld K, Gull K. 2002. Targeting of a tetracycline-inducible expression system to the transcriptionally silent minichromosomes of *Trypanosoma brucei*. *Mol Biochem Parasitol* **125:** 211–216.

Zíková A, Horáková E, Jirků M, Dunajčíková P, Lukeš J. 2006. The effect of down-regulation of mitochondrial RNA-binding proteins MRP1 and MRP2 on respiratory complexes in procyclic *Trypanosoma brucei*. *Mol Biochem Parasitol* **149:** 65–73.

Attached Publications

Part I. Trypanosome RNA editing

Hassan Hashimi, Sara L. Zimmer, Michelle L. Ammerman, Laurie K. Read and Julius Lukeš (2013). Dual core processing: MRB1 is an emerging kinetoplast RNA editing complex. *Trends in Parasitol.* 29: 91-99.

This review summarizes the current state of knowledge of MRB1 in light of the newly elucidated architecture of the complex in the enclosed Nucleic Acids Research paper. It puts forth working hypotheses of how MRB1 may also help integrate RNA editing to other processing events in the mitochondrion of kinetoplastids.

Review

Dual core processing: MRB1 is an emerging kinetoplast RNA editing complex

Hassan Hashimi[1], Sara L. Zimmer[2], Michelle L. Ammerman[2], Laurie K. Read[2], and Julius Lukeš[1]

[1] Institute of Parasitology, Biology Center, Czech Academy of Sciences, and Faculty of Science, University of South Bohemia, České Budějovice (Budweis) 370 05, Czech Republic
[2] Department of Microbiology and Immunology, School of Medicine, State University of New York at Buffalo, NY 14214, USA

Our understanding of kinetoplastid RNA (kRNA) editing has centered on this paradigm: guide RNAs (gRNAs) provide a blueprint for uridine insertion/deletion into mitochondrial mRNAs by the RNA editing core complex (RECC). The characterization of constituent subunits of the mitochondrial RNA-binding complex 1 (MRB1) implies that it too is vital to the editing process. The recently elucidated MRB1 architecture will be instrumental in putting functional data from individual subunits into context. Our model depicts two functions for MRB1: mediating multi-round kRNA editing by coordinating the exchange of multiple gRNAs required by RECC to edit lengthy regions of mRNAs, and then linking kRNA editing with other RNA processing events.

Kinetoplastid RNA editing and the mitochondrial RNA binding complex 1

Much has been learned about kRNA editing since its discovery in the mitochondrion of trypanosomes by Benne and colleagues in 1986 [1], such as the role of small guide RNAs (gRNAs; see Glossary) in providing information for each uridine (U) insertion or deletion [2], validation of the enzyme cascade model [3], as well as detailed characterization of RECC (Box 1), the molecular machine that orchestrates the required enzymatic steps [4–6]. As a process shared by causative agents of African sleeping sickness, Chagas disease, leishmaniases, and other serious illnesses, kRNA editing is being explored as a possible drug target [7]. Nonetheless, perplexing questions remain about both the mechanism of kRNA editing and about how this process is integrated into the general mitochondrial RNA metabolism.

Another complex known as MRB1 is also required for editing, and rivals RECC in terms of complexity. The current state of knowledge we review here indicates that MRB1 may be the key to many unanswered questions. Several of the proteins that comprise MRB1 bear signature motifs and domains that clearly indicate a role in RNA metabolism; others lack identifiable domains and, furthermore, are unique to the excavate order Kinetoplastida [8–11]. Intense work has revealed a dizzying array of potential functions of these proteins in kRNA editing and metabolism [11–20], making it difficult to pinpoint the function(s) of MRB1. Recently the architecture of MRB1 was reported [16], which has allowed us to better interpret functional analysis of the constituents identified thus far. Here, we present a model of how MRB1 may work in kRNA metabolism by mediating the exchange of gRNAs required by RECC in processing mRNAs that need multi-round kRNA editing, and by linking kRNA editing with other RNA processing events.

Glossary

Anchor domain: a 5′-proximal part of a gRNA that facilitates the formation of a gRNA:mRNA duplex by hybridizing to a mRNA that is to undergo editing.
ARM/HEAT repeats: repeat motifs initially described from the *Drosophila* Armadillo protein and four cytoplasmic proteins in mammals and yeast, respectively, which often act in protein–protein interactions.
Editing block: a stretch of sequence on an edited mRNA that contains several ESs, as determined by the information domain of a gRNA.
Editing site (ES): cleavage site on a mRNA where either a uridine insertion or deletion takes place, as defined by the first base-pair mismatch on the mRNA;gRNA duplex.
Fully edited mRNA: transcripts in which all the needed editing steps have been completed.
Guide RNA (gRNA): small RNAs that act in *trans* to supply sequence information for decrypting edited mRNAs (one gRNA contained in the 3′-UTR of the coxII mRNA acts in *cis*).
Information domain: the part of the gRNA that dictates the ESs along an editing block on an edited mRNA; the fully processed editing block is complementary to the anchor domain via normal and non-canonical Watson–Crick base-pairing.
Maxicircle DNA: the approximately 22 Kb component of kDNA that encodes mRNA and rRNA genes; there are tens of copies of these DNAs, and the gene-encoding region is homogenous in sequence.
Minicircle DNA: the approximately 1 Kb component making up the bulk of kDNA encoding gRNA genes; the thousands of copies are heterogeneous in sequence because they represent all the gRNAs needed to decrypt edited mRNAs.
Minimally-edited mRNA: transcripts that require kRNA editing only in a small portion of their sequence requiring few gRNAs; sometime also termed moderately-edited.
Never-edited mRNA: transcripts that forgo kRNA editing.
Pan-edited mRNA: transcripts that undergo kRNA editing throughout their sequence and require many gRNAs.
Partially edited mRNA: intermediates of pan-edited transcripts undergoing kRNA editing, in which the 5′-proximal sequence remains 'pre-edited' whereas the 3′-proximal sequence is 'edited'.
Pre-edited (pre-) mRNA: edited transcripts before they undergo kRNA editing, thus having the same sequence as the kDNA maxicircle cryptogene; also termed unedited.

Corresponding author: Lukeš, J. (jula@paru.cas.cz).
Keywords: kinetoplastida; trypanosome; RNA editing; protein complexes; RECC; MRB1.

Box 1. RNA editing core complex (RECC)

The RECC complex is also referred to in the literature as the L-complex [4] or the 20S editosome [5]. The latter name reflects the size of the editosome in ultracentrifugation studies. The complex contains about 20 proteins that encapsulate the enzymatic activities needed for a single round of U-insertion/deletion editing (Figure 1a and described in main text). In comparison to MRB1, the composition of RECC appears to be static. Nevertheless, recent work has shown that there are three major forms of RECC, each bearing a defining endonuclease [44,45]. One of them specifically cleaves edited sites (ESs) that require U-insertion, whereas another does so for ESs slated to undergo U-deletion. A third is special in that it cleaves coxII transcripts. The editing of coxII does not need traditional gRNAs because it bears its own within its 3′-UTR, thus acting in *cis* [37]. The deletion endonuclease associates with a U-specific exonuclease that trims superfluous Us from the ES. It is still not clear whether these three RECCs represent stable complexes, or if the appropriate endonuclease, and associated proteins, are recruited by a RECC already processing a gRNA:mRNA duplex.

Herein, we use the MRB1 nomenclature for some of the constituent subunits as introduced elsewhere [14] – the 'MRB' prefix followed by the last digits of the trypanosome genome database TriTrypDB (http://tritrypdb.org/tritrypdb/) accession number. Some proteins, such as the gRNA-associated proteins (GAPs), TbRGG2, and RNA editing helicase 2 (REH2), were named before this nomenclature was introduced.

The basic mechanism of kRNA editing mediated by RECC

In *Trypanosoma brucei*, 12 of 18 protein-coding mitochondrial genes require kRNA editing for their maturation. Editing initiates with the 5′-most portion of the small gRNA, termed the anchor domain, hybridizing with a complementary part of the pre-edited (pre)-mRNA, with some additional interactions within the gRNA 3′ oligo(U) tail (Figure 1a) [21]. The editing site (ES) where a U-insertion/deletion occurs on the pre-mRNA is indicated by the first base-pair mismatch between the gRNA:mRNA duplex (Figure 1a). The pre-mRNA is cleaved here, in the first RECC-catalyzed kRNA editing step, to yield 5′ and 3′ fragments that are bridged by the bound gRNA. Depending on the gRNA information domain sequence downstream of the anchor, one or more Us are added or removed from the 5′ fragment. RECC enzymes catalyze both events: a 3′-terminal uridylyltransferase (TUT) adds Us, and a U-specific exonuclease deletes them. After the ES has been edited, the pre-mRNA fragments are sealed together by a RECC RNA ligase. A single gRNA carries information for several ESs along a stretch of the pre-mRNA termed the

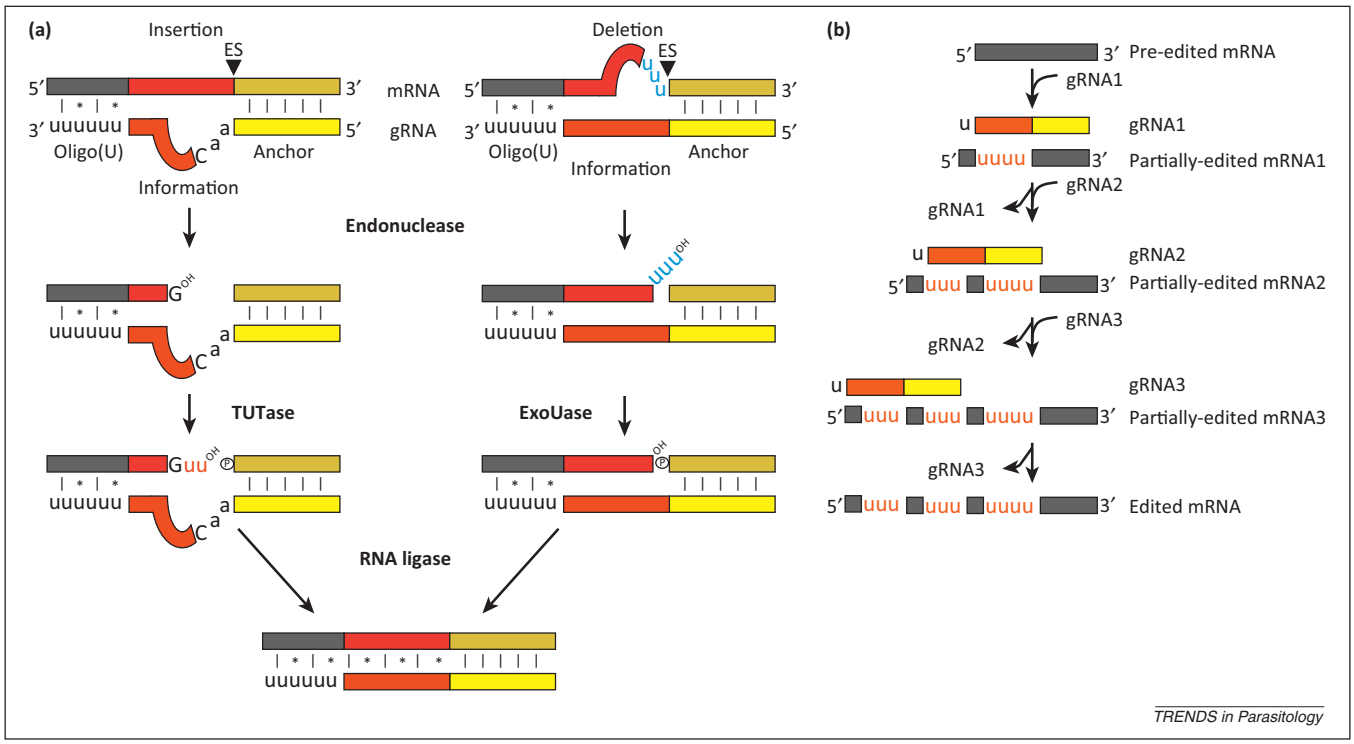

Figure 1. Single- versus multi-round kRNA editing. **(a)** A single round of kRNA editing as mediated by one of the appropriate RECCs through an enzyme cascade. The first base-pair mismatch in the duplex between gRNA (lower strand; domains in solid colors; yellow, anchor; red, information; black U, 3′-oligo(U) tail) and mRNA (top strand; regions on mRNA are indicated in a different shade of color to that of the corresponding gRNA domains) define the editing site (ES; arrowhead), which is then cleaved on the mRNA by an endonuclease (all enzymatic activities in bold). In U-insertion, Us (in red) are added to the 3′ end of the 5′-mRNA cleavage product by a terminal uridylyltransferase (TUTase) as guided by the gRNA. In U-deletion, a U-specific exonuclease (exoUase) prunes away extra Us (in blue) on the 3′ end of the 5′-mRNA cleavage product. An RNA ligase then seals the two mRNA fragments back together after the appropriate editing event is completed. **(b)** Pan-edited mRNAs require multi-rounds of kRNA editing. A cascade of gRNAs is required to decrypt a pan-edited mRNA (black striped strand). The first gRNA [solid colors using same scheme to distinguish domains as in (a); black U signifies 3′-oligo(U) tail] guides RNA editing (signified by inserted red Us) along a block defining several editing sites. When the editing events dictated by the gRNA are completed, the gRNA is unwound from the mRNA. A second gRNA binds to a newly edited sequence on the mRNA that can now hybridize its anchor domain. As this process is repeated, editing progresses in the 3′ to 5′ direction until the mRNA is fully edited. The mRNA intermediates between the pre-edited molecule and the fully edited form are referred to as partially edited. Abbreviations: OH, 3′-hydroxyl group; P, 5′-phosphate group; *, non-canonical base pairing; |, canonical Watson–Crick base pairing.

editing block; as editing progresses, the mRNA becomes complementary to the gRNA via both normal and non-canonical Watson–Crick base-paring.

Massively processed pan-edited mRNAs require a cascade of gRNAs

Three quarters of the edited mRNAs in *T. brucei* are pan-edited, an extreme form of kRNA editing. For example, 547 Us are inserted and 41 are deleted over 223 ESs in the cytochrome *c* oxidase (cox) III transcript, representing more than half of the mature mRNA [22]. Pan-editing occurs in the 3′ to 5′ direction along the pre-mRNA and requires numerous gRNAs, unlike the one or two needed by less-edited transcripts [23]. When editing requires multiple gRNAs (Figure 1b), a portion of the fully processed pre-mRNA editing block generated from the first gRNA sequence serves as the annealing site for the anchor domain of the next gRNA. This process is repeated until the pre-mRNA is fully edited, and contains the decrypted open reading frame (ORF) ready for translation. The pan-editing intermediates, in which the 5′-proximal sequences remain unedited, are referred to as partially-edited transcripts. When provided with an mRNA and cognate gRNA, the core editing activities encapsulated in RECC can be reconstituted *in vitro* [3]. However, *in vitro* editing is limited to one ES rather than the entire editing block specified by the gRNA. Consequently, the cascade of gRNA exchange also cannot take place *in vitro*. Together, these findings suggest that other factors are required for editing *in vivo*. Furthermore, the mechanisms of gRNA removal from a fully processed editing block and recruitment and binding of the next required gRNA are unknown. Because this process involves the unwinding of a tightly bound gRNA:edited mRNA duplex, helicase activity is likely required. The RNA helicase, REH1, appears to act in gRNA removal in some capacity [24], although it does not contribute the majority of the unwinding activity in the mitochondria [13].

Other steps in kRNA metabolism

Although due to its uniqueness, editing stands out as a kRNA maturation process, it is but one step from the mitochondrial genome to translation of the encoded proteins (Figure 2). Transcription of *T. brucei* maxi- and

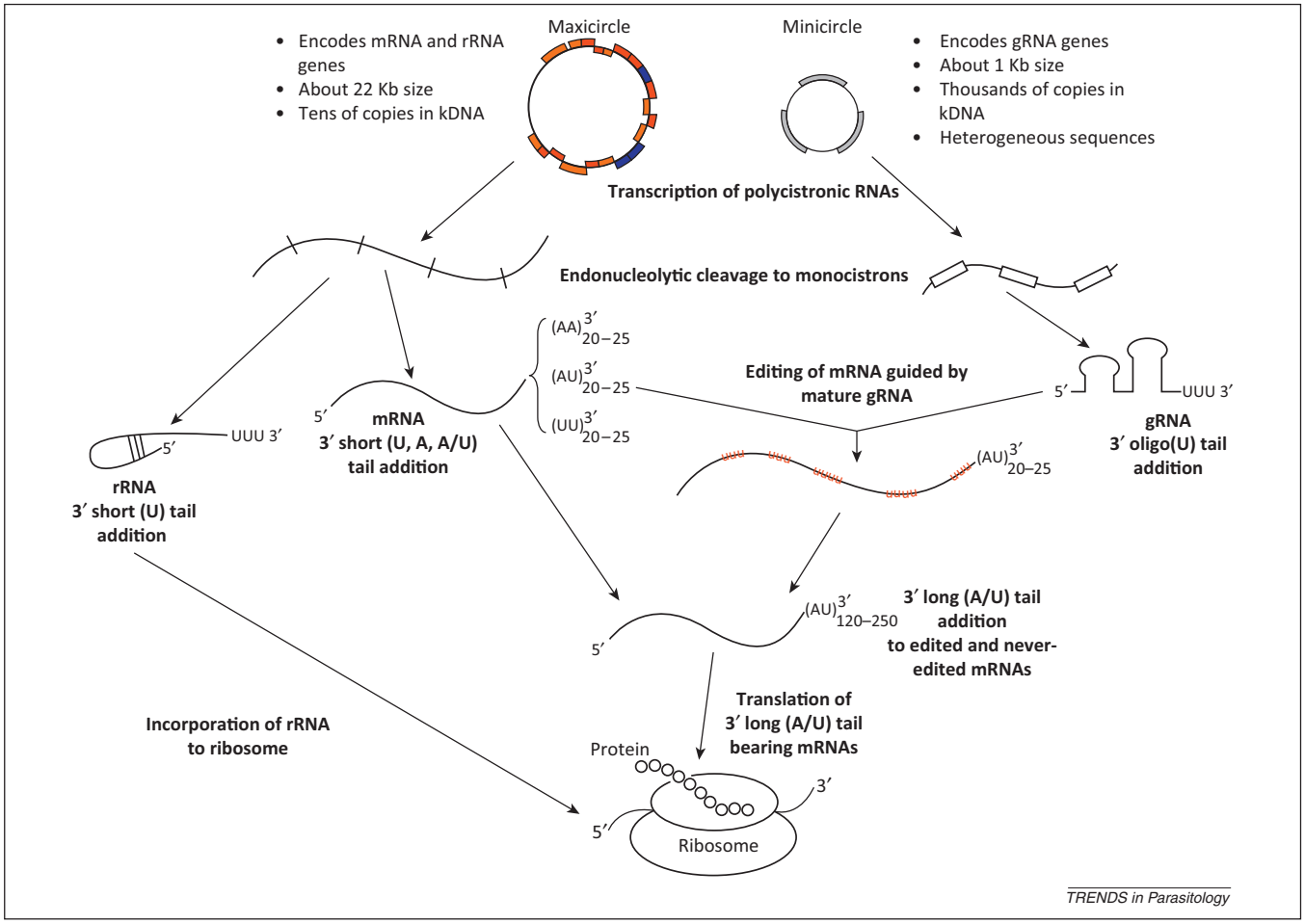

Figure 2. Summary of kRNA metabolism. The maxi- and minicircles of the kDNA are depicted on the top with a summary of their major characteristics adjacent. Genes encoding pan-edited mRNAs are in red, minimally edited in blue, and never-edited in orange. Genes encoding gRNAs are grey on the minicircles. RNA metabolism steps are indicated in bold. Transcription of both yields polycistronic transcripts that are subsequently cleaved to yield monocistronic RNAs. The rRNAs obtain short 3′ (U) tails and are incorporated into ribosomes; mRNAs initially get short 3′ tails (up to 20–25 nt, composed of U, A, or A/U as indicated in subscript next to tails in the figure); gRNAs get short 3′-oligo(U) tails. The mature gRNAs mediate editing of mRNAs. Fully edited and never-edited mRNAs are eventually marked with long 3′ (A/U) tails (120–250 nt) for translation. Turnover of mRNAs could occur at any step of this process.

minicircle kinetoplast DNAs (kDNAs), which encode all mRNAs and rRNAs, or virtually all gRNAs, respectively, is performed by a single RNA polymerase [12,25]. Because maxicircle and minicircle transcripts are polycistronic, endonucleolytic cleavage is needed to free individual cistrons. An endonuclease called mitochondrial RNA precursor-processing endonuclease 1(mRPN1) is involved in processing minicircle pre-RNAs into single gRNAs [26]. The genes on polycistronic maxicircle transcripts are very close together or overlapping, and are cleaved into cistrons by a hitherto unknown enzyme(s) [27].

RNA turnover and physical shuttling of RNA between relevant complexes and binding proteins are two other processes occurring in the mitochondria. Both may be influenced by a further post-transcriptional event: the addition of non-encoded 3′ tails composed of adenine (A), U, or some combination thereof to most mitochondrial RNAs [10,28–31]. The kinetoplast poly(A) polymerase 1 (KPAP1) attaches the As, whereas the TUTase RET1 adds the Us into these tails. These structures occur in two different populations according to their lengths. Short 3′ mRNA tails appear to impact transcript stability in a variety of ways [10,28,32,33], whereas long tail addition, facilitated by two pentatricopeptide (PPR) proteins, likely marks mRNAs as translationally competent [34]. Long A/U tail addition is hypothesized to serve as a bridge between editing and translation [34]. Several of the protein players mentioned in these processes, plus RECC, associate to some degree with the MRB1 complex. However, very little is known about how mRNAs are physically transcribed or the transition from processing to editing, degradation, and translation.

The architecture of MRB1

Reports of MRB1 purification from *T. brucei* and *Leishmania tarentolae* have described both overlapping and varying subunits [8–11,13–16]. In the former category are GAPs 1 and 2 (also known as GRBC2 and 1), MRB3010, MRB8620, MRB5390, and MRB11870, which have been reassuringly present in virtually all MRB1 purifications. Others, such as the DExD-box RNA helicase REH2 plus the RNA-binding proteins TbRGG2 and MRB1680, associate with MRB1 in a variable fashion. Many interactions were found to be due to proteins binding to the same RNA. We propose that some of the more tenuous interactions reflect a dynamic composition of MRB1, in which proteins were incorporated into several subcomplexes [16]. This notion that MRB1 is made up of several subcomplexes, and/or that some subunits shuttle between those involved in other aspects of RNA metabolism, is supported by the observed heterodispersion of individual parts in ultracentrifugation sedimentation studies [8,9,12–14,16].

To address the confusing nature of the MRB1 composition, a comprehensive yeast two-hybrid screen was used to map the interactions between the 31 proteins found in various MRB1 isolations [16]. Surprisingly, only six proteins were responsible for the majority of interactions. Four of these are components of a core identified by multiple RNase-resistant copurification steps (Figure 3). Subunits from this core interact with the TbRGG2 subcomplex, composed of the eponymous protein and either one of the paralogs MRB8170 or MRB4160; in addition, TbRGG2 interacts with MRB8180 and MRB10130, although the temporal association of all of these proteins is unknown [15,16,26]. The TbRGG2 subcomplex interacts with the MRB1 core in an RNase-sensitive manner, in contrast to the direct binding exhibited among most of the core subunits. MRB10130, a polypeptide almost entirely composed of ARM/HEAT repeats that often act in protein–protein interactions, also associates with the core subcomplex and with proteins involved in other steps in kRNA metabolism [35].

As mentioned previously, many of the intra-MRB1 interactions are enhanced or even dependent on the presence of RNA. One such protein is MRB6070, which contains zinc fingers, suggesting that it is an RNA-binding protein. Although it does not interact with other MRB1 proteins via yeast two-hybrid analysis, it does associate with MRB1 complex purified from cells in an RNA-dependent manner [16]. The RNA-dependent interactions within the MRB1 complex, and the observation that several subunits self-interact in the yeast two-hybrid screen and/or seem to form oligomers *in vivo*, make it difficult to pinpoint the MRB1 subunit stoichiometry. In addition, it remains an open question whether the *bona fide* protein–protein interactions among the MRB1 subunits reflect constant interactions, as is observed for many RECC constituents, or are dynamic.

MRB1 interaction with other protein complexes involved in kRNA metabolism

In addition to intra-complex interactions, several MRB1 subunits have been found to interact with proteins of other complexes acting in the various kRNA metabolic processes enumerated above. Substoichiometric amounts of RECC have been retained in TbRGG2, REH2, and core MRB1 component purifications in an RNase-sensitive manner [11,13,18]. The complex containing KPAP1 and the kinetoplast polyadenylation/uridylation factor 1 (KPAF1) PPR protein associates with MRB1 in a similar fashion [10,11,13,34]. Furthermore, KPAF1 was shown to interact with the MRB1 core and the TbRGG2 subcomplex in the yeast two-hybrid screen (Figure 3) [16]. MRB1 subunit purifications from *T. brucei* also intermittently co-purify mitochondrial edited mRNA stability factor 1, a protein named according to its apparent function in the organelle [8,11]. Thus it seems that MRB1 (sub)complexes are also involved with those playing a role in mitochondrial mRNA maturation and stability.

Interestingly, KPAP1 and the PPR protein KPAF1 associate with the mitochondrial ribosomes, the endpoint for all translatable mRNAs, in addition to MRB1. MRB1 proteins also pulled down substoichiometric amounts of ribosomal proteins [8,11,13], although it must be noted that ribosomal proteins are common contaminants in proteomic analyses of protein purifications in general. A more refined study demonstrated a preferential association of the MRB1 core GAPs, along with the TUTase RET1 and RECC, with the large subunit of the ribosome [34]. These observations support a model in which MRB1 physically and functionally

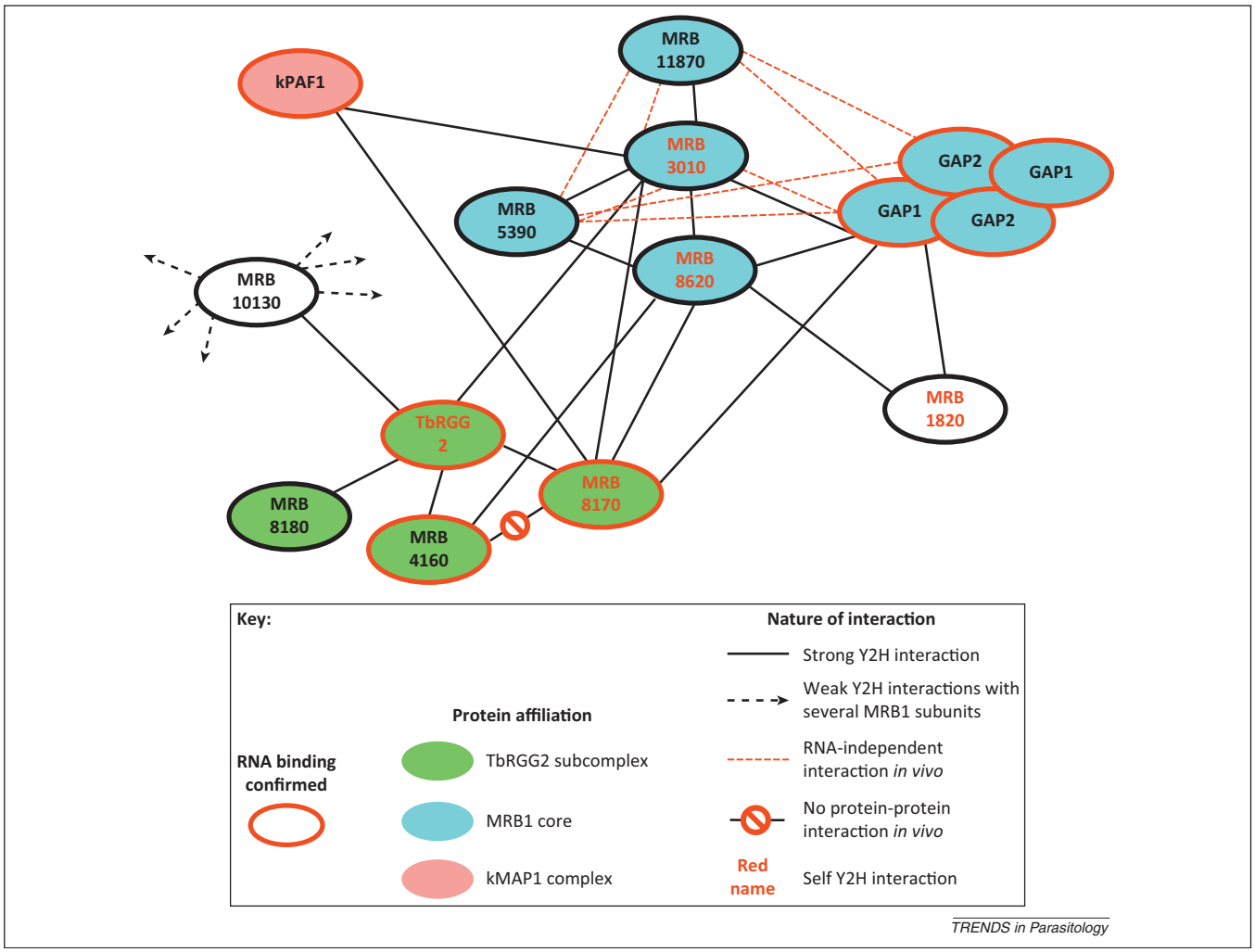

Figure 3. Architecture of MRB1. A summary of the pairwise yeast two-hybrid (Y2H) mapped MRB1 subunit interactions, plus those determined *in vivo,* as adapted from Ammerman and colleagues [16]. The figure is updated to reflect the mutually exclusive interaction of MRB8170 and MRB4160 with TbRGG2 [15] and the heterotetrameric nature of the GAP1 and GAP2 interaction [11]. A key to the figure is shown at the bottom. The black lines represent 'strong' Y2H interactions in at least one direction. The promiscuous 'weak' Y2H interactions of the ARM/HEAT domain containing MRB10130 with various MRB1 subunits are also indicated by broken black lines projecting out.

interacts with the mitochondrial protein translation machinery.

Because MRB1 contains subunits that have RNA-binding activity (e.g., GAPs and REH2; see below), it is perhaps not surprising that the complex associates with other RNA-interacting proteins and complexes. For example, the endonuclease mRPN1 involved in processing gRNAs has been reported to associate with the TbRGG2 subcomplex [26]. In addition, the mitochondrial-RNA-binding-proteins 1/2 complex, which is an mRNA:gRNA matchmaker *in vitro*, has a substoichiometric, RNase-sensitive association with MRB1 [13,15,36]. Therefore, these associations link MRB1 to the processes of gRNA biogenesis and utilization.

Nuts and bolts: the functional characterization of MRB1 subunits

Functional studies of MRB1 subunits based on RNAi-mediated depletion of individual components reveal multifarious phenotypes. Of the six MRB1 core proteins, GAP1, GAP2, MRB3010, MRB5390, MRB8620, and MRB11870, all but the last two have been analyzed in this way. These proteins proved to be essential for the viability of *T. brucei* by affecting different aspects of the RNA editing process (Table 1).

GAP1 and 2 are paralogs that associate in a heterotetramer, and repression of either results in loss of both proteins [11,12]. The GAPs bind gRNAs *in vitro* despite lacking domains known to confer this activity [11]. Consistent with this finding, their repression results in decreased gRNA levels, which subsequently affect editing of mRNAs that require these *trans*-elements. As such, the minimally edited coxII, whose gRNA acts in *cis* because it is contained in the 3′-UTR of the mRNA [37], is not affected. Unlike the GAPs, the core protein MRB3010 does not have *in vitro* RNA-binding activity, and its downregulation in *T. brucei* did not affect bulk gRNA levels [14]. However, RNAi did result in depletion of both pan- and minimally-edited RNAs, although the latter were affected to a lesser degree. Simultaneously, there was an increase in pre-edited and early partially-edited RNAs, consistent with MRB3010 playing a role at an early step in editing. MRB5390

Table 1. Summary of MRB1 subunit RNAi phenotypes

		RNAi growth inhibition		RNA abundance effect due to RNAi				RNA binding?				
Name[a]	TriTrypDB accession number	PF[d]	BF[d]	Never-edited RNA	Pan-edited RNA	Minimally edited RNA	gRNA	Proven	Predicted domain[b]	Complex	Notes	Refs
GAP1 (GRBC2)	Tb927.2.3800	Y	Y	N	Y	Y (not coxII)	Y	Y		MRB1 core	gRNA binding Paralog GAP2	[11,12]
GAP2 (GRBC1)	Tb927.7.2570	Y	Y	N	Y	Y (not coxII)	Y	Y		MRB1 core	gRNA binding Paralog GAP1	[11,12]
MRB3010	Tb927.5.3010	Y	Y	N	Y	Y	N	N		MRB1 core	Role in early step kRNA editing	[14]
MRB5390	Tb11.02.5390	Y	ND	N	Y (subset)	Y (subset)	ND	ND		MRB1 core		[17]
TbRGG2	Tb927.10.10830	Y	Y	N	Y	N	N	Y	RGG, RRM	TbRGG2 subcomplex	3′–5′ Progression of RNA editing	[17–20]
MRB8170	Tb927.8.8170	N	ND	N	Y	N	N	Y		TbRGG2 subcomplex	Paralog MRB4160	[15]
MRB4160	Tb927.4.4160	N	ND	N	N	N	N	Y		TbRGG2 subcomplex	Paralog MRB8170	[15]
MRB8170/MRB4160[c]	–	Y	Y	N	Y	Y	N	–		–	RNAi affects pan-edited more than minimally edited	[15]
MRB1680	Tb927.6.1680	Y	ND	N	Y	N	ND	ND	C2H2 Zn finger			[17]
REH2	Tb927.4.1500	Y	ND	N	Y	Y (not coxII)	Y	Y	dsRBP, DExD box		gRNA binding RNA-unwinding activity	[12,13]

[a]Aliases given in parentheses.

[b]Common abbreviations of motifs.

[c]Describes simultaneous RNAi-mediated silencing of the paralogs MRB8170 and MRB4160.

[d]Abbreviations: BF, bloodstream form; gRNA, guide RNA; N, no; ND, not determined; PF, procyclic form; Y, yes.

repression similarly resulted in depletion of edited transcripts, although to a more modest effect [17].

Like the core MRB1 proteins, TbRGG2 is essential for RNA editing [17–20]. However, unlike the aforementioned knockdowns, TbRGG2 RNAi-mediated silencing only affects pan-edited transcripts, resulting in a buildup of partially edited RNAs at the expense of the fully edited forms. This observation suggests a role in promoting the 3′ to 5′ progression of editing, a notion supported by the *in vitro* characterization of its N-terminal G-rich region, with GWG and RG repeats, and C-terminal RRM domain [19,20]. TbRGG2 has an N-terminal RNA-annealing activity, which is crucial for editing, while the C-terminal domain confers an RNA-melting activity.

The TbRGG2 subcomplex also contains either MRB8170 or MRB4160 in a mutually exclusive fashion [15,16]. These two proteins are highly similar paralogs in *T. brucei*, having arisen from a chromosomal duplication in this clade, being a single copy in other trypanosomatids [15,38]. Like TbRGG2, both paralogs have *in vitro* RNA-binding activity. Furthermore, their simultaneous RNAi-mediated silencing preferentially results in a decrease of pan-edited RNAs, without affecting gRNAs. Although this phenotype is ostensibly reminiscent of TbRGG2, there is an important contrast: minimally edited RNAs are also affected (but not when either MRB8170 or MRB4160 are individually silenced), and some pre-edited forms of the pan-edited mRNAs are also decreased [15].

Some MRB1 subunits that are neither part of the core nor TbRGG2 subcomplex have also been characterized by RNAi. The RNA helicase REH2 is a gRNA-binding protein and, like the GAPs, its depletion results in a decrease of gRNAs [12,13]. Furthermore, REH2 associates with the bulk of RNA-unwinding activity from mitochondrial lysates, which distinguishes it from REH1. MRB1680, a putative RNA-binding protein with five zinc-finger domains, has a RNAi phenotype that resembles that of TbRGG2: a decrease of pan-edited RNAs with minor effects on minimally-edited transcripts [17].

Building models of MRB1 function from the nuts and bolts

The determined architecture of MRB1 has been instrumental in putting all of the RNAi studies into context. By combining these two datasets, we propose one model describing two functions for MRB1, namely mediating the recruitment and exchange of gRNAs required by RECC in processing pan-edited mRNAs that require multiple rounds of the process, and linking kRNA editing to other kRNA processing events (Figure 4).

The first function has MRB1 acting in tandem with RECC as dual core processors of pan-edited RNAs. This notion is supported by the predominant MRB1 RNAi phenotype, in which pan-edited RNAs are more severely compromised than their minimally-edited counterparts because they require more gRNAs for editing. Although the paucity of data makes predicting exactly what the core MRB1 subcomplex is doing in this scenario challenging, the gRNA-binding GAPs may serve to bring these molecules to or maintain them within the reaction center. In this model, the MRB1 core serves as a scaffold for creating

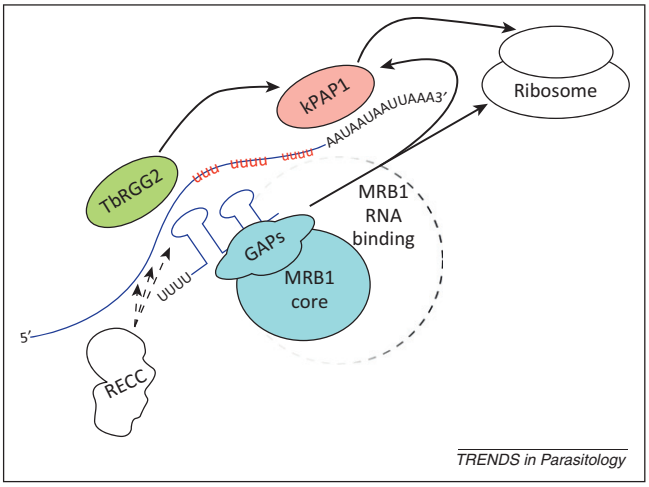

Figure 4. Proposed model of MRB1 function. The assembly of the MRB1 core and TbRGG2 subcomplex(es), plus RECC and the kPAP1 complex, onto an mRNA is depicted using the same color scheme as in Figure 3. The GAPs bring gRNAs to the reaction center. The core associates with the transcript via the putative RNA-binding proteins of MRB1 (depicted as a broken circle radiating from the MRB1 core). The TbRGG2 subcomplex(es) promotes gRNA:mRNA annealing and/or unwinding of these double-stranded structures. The kPAP1 complex is responsible for 3′-tail addition. The unbroken black arrows signify verified interactions among complexes. Substrate RNAs are depicted in blue. Red 'u' stretches denote sequences already edited within the mRNA. Broken arrows from RECC indicate that it associates with RNAs in cooperation with MRB1. This scheme does not depict the potential dynamic movement of particular proteins among the complexes.

the reaction center, because the core MRB3010 protein seems to halt an early step(s) in editing, possibly linked to RECC via the mRNA undergoing pan-editing. The TbRGG2 subcomplex serves as an engine for the 3′ to 5′ progression by promoting proper gRNA:mRNA duplex unwinding after an editing block for a given gRNA has been completed and/or promoting the formation of the next duplex. The *in vitro* characterized RNA-binding, annealing, and unwinding activities of TbRGG2 could potentially be employed in such a task, aided by either of the RNA-binding MRB8170 and MRB4160 subunits.

The second function of MRB1 is to link kRNA editing to other processing events required for the expression of mitochondrial genes. The available data suggest an entanglement between the protein players in kRNA editing, gRNA processing, and in mRNA 3′-tail addition, RNA stability/turnover and translation, because MRB1 subunits are always present in association with these processes [10,11,13,26,34]. Furthermore, there is evidence for functional coordination between multiple steps in kRNA metabolism. For instance, a short oligo(A) tail stabilizes mRNA only following the editing of the first gRNA-dictated editing block [10,33]. The addition of a long (A/U) tail occurs after an RNA is completely edited (or nearly so), and this 3′ extension is thought to act as an important factor signaling the transition from editing to translation [10,32,34]. It seems reasonable to assume that shuttling between different steps of kDNA gene expression is a necessary process for organellar biogenesis, and MRB1 appears to be a strong candidate for such a role.

Additional components of MRB1 may very well affect RNA editing, and/or link it to other metabolic processes, but are not specified in our model. REH2 and MRB1680 are

Box 2. Outstanding questions

- What are the precise mechanisms by which MRB1 impacts kRNA editing?
- What are the spatial and temporal distributions of MRB1 and other complexes within the single reticulated mitochondrion?
- How is RNA routed into the appropriate complexes devoted to a specific processing step?
- What are the regulatory elements in the whole pathway of kDNA gene expression from transcription via editing, processing and turnover to translation?

putative RNA-binding proteins, the depletion of which impacts kRNA editing [13,17]. Furthermore, it is difficult at this time to proffer whether the identified subcomplexes represent static or dynamic structures, although the described studies seem to indicate the latter. It will be interesting to see how future results will refine this model.

Our data can also be used to exclude some putative MRB1 functions, such as roles in transcription or cleavage of polycistronic maxicircle RNAs into individual cistrons. We presume that if one of these were true, changes in abundance of never-edited mRNAs would be a predominant MRB1 RNAi phenotype, which is not the case. The MRB1 subunits that were examined by RNAi in both *T. brucei* bloodstream and procyclic *in vitro* cell cultures exhibited comparable phenotypes, indicating that MRB1 may not play a major role in regulation of editing among the life-cycle stages (Table 1). However, not all MRB1 subunits have been analyzed in this way.

MRB1 contributes to the irremediable complexity of RNA editing

Future studies will likely refine our current MRB1 functional model (Box 2); however, even now it is clear that MRB1 is an emerging key player in kRNA editing in conjunction with RECC. The discovery of MRB1 certainly adds to kRNA editing complexity. More than 70 proteins – and counting – are required for editing mitochondrial RNAs and generating gRNAs in *T. brucei* [39]. This tally is in addition to the presumably large number of proteins required for maturation of never-edited mRNAs as well as rRNAs, the latter of which are assembled into mitochondrial ribosomes, requiring more than 100 proteins to construct this machine that ultimately translates the mature mRNAs [40].

Why would so many proteins be needed for the expression of only a handful of gene products in a eukaryotic cell? According to the most plausible adaptive explanations, kRNA editing generates mitochondrial protein diversity via an alternative editing strategy [41], or it provides another level of gene regulation among life stages [42]. Nevertheless, these appealing theories remain unsupported.

An alternative view, albeit one that is also difficult to address experimentally, suggests that the irremediable complexity of kRNA editing has arisen due to constructive neutral evolution [39,43]. In essence, this idea suggests that the complexity that typifies many biochemical systems can emerge even in the absence of any positive selection pressure. Thus, as a biological process like kRNA editing grows more complex over time, various interacting components become essential without serving any adaptive advantage. These components have become interdependent, and the cell is consequently stuck with an intricate clockwork in which each gear is intrinsically essential to its proper running. In the case of kRNA metabolism, MRB1 and RECC, together with other players involved in the processing of the various kRNA species, are each essential players in the expression of kDNA-encoded genes.

Acknowledgments

This work was supported by the Grant Agency of the Czech Republic (204/09/1667 and P305/12/2261), the RNPnet FP7 program (289007), a Praemium Academiae award to J.L., as well as National Institutes of Health awards RO1 AI061580 to L.K.R. and F32 AI092902 to S.L.Z.. J.L. is a Fellow of the Canadian Institute for Advanced Research.

References

1 Benne, R. *et al.* (1986) Major transcript of the frameshifted coxII gene from trypanosome mitochondria contains four nucleotides that are not encoded in the DNA. *Cell* 46, 819–826
2 Blum, B. *et al.* (1990) A model for RNA editing in kinetoplastid mitochondria: 'guide' RNA molecules transcribed from maxicircle DNA provide the edited information. *Cell* 60, 189–198
3 Seiwert, S.D. and Stuart, K. (1994) RNA editing: transfer of genetic information from gRNA to precursor mRNA in vitro. *Science* 266, 114–117
4 Simpson, L. *et al.* (2004) Mitochondrial proteins and complexes in *Leishmania* and *Trypanosoma* involved in U-insertion/deletion RNA editing. *RNA* 10, 159–170
5 Stuart, K.D. *et al.* (2005) Complex management: RNA editing in trypanosomes. *Trends Biochem. Sci.* 30, 97–105
6 Lukeš, J. *et al.* (2010) The remarkable mitochondrion of trypanosomes and related flagellates. In *Structures and Organelles in Pathogenic Protists* (de Souza, W., ed.), pp. 227–252, Springer
7 Salavati, R. *et al.* (2012) Inhibitors of RNA editing as potential chemotherapeutics against trypanosomatid pathogens. *Int. J. Parasitol. Drugs Drug Res.* 2, 36–46
8 Hashimi, H. *et al.* (2008) TbRGG1, an essential protein involved in kinetoplastid RNA metabolism that is associated with a novel multiprotein complex. *RNA* 14, 970–980
9 Panigrahi, A.K. *et al.* (2008) Mitochondrial complexes in *Trypanosoma brucei*: a novel complex and a unique oxidoreductase complex. *Mol. Cell. Proteomics* 7, 534–545
10 Etheridge, R.D. *et al.* (2008) 3′ Adenylation determines mRNA abundance and monitors completion of RNA editing in *T. brucei* mitochondria. *EMBO J.* 27, 1596–1608
11 Weng, J. *et al.* (2008) Guide RNA-binding complex from mitochondria of trypanosomatids. *Mol. Cell* 32, 198–209
12 Hashimi, H. *et al.* (2009) Kinetoplastid guide RNA biogenesis is dependent on subunits of the mitochondrial RNA binding complex 1 and mitochondrial RNA polymerase. *RNA* 15, 588–599
13 Hernandez, A. *et al.* (2010) REH2 RNA helicase in kinetoplastid mitochondria: ribonucleoprotein complexes and essential motifs for unwinding and guide RNA (gRNA) binding. *J. Biol. Chem.* 285, 1220–1228
14 Ammerman, M.L. *et al.* (2011) MRB3010 is a core component of the MRB1 complex that facilitates an early step of the kinetoplastid RNA editing process. *RNA* 17, 865–877
15 Kafková, L. *et al.* (2012) Functional characterization of two paralogs that are novel RNA binding proteins influencing mitochondrial transcripts of *Trypanosoma brucei*. *RNA* 18, 1846–1861
16 Ammerman, M.L. *et al.* (2012) Architecture of the trypanosome RNA editing accessory complex, MRB1. *Nucleic Acids Res.* 40, 5637–5650
17 Acestor, N. *et al.* (2009) The MRB1 complex functions in kinetoplastid RNA processing. *RNA* 15, 277–286
18 Fisk, J.C. *et al.* (2008) TbRGG2, an essential RNA editing accessory factor in two *Trypanosoma brucei* life cycle stages. *J. Biol. Chem.* 283, 23016–23025

19 Ammerman, M.L. *et al.* (2010) TbRGG2 facilitates kinetoplastid RNA editing initiation and progression past intrinsic pause sites. *RNA* 16, 2239–2251
20 Foda, B.M. *et al.* (2012) Multifunctional G-rich and RRM-containing domains of TbRGG2 perform separate yet essential functions in trypanosome RNA editing. *Eukaryot. Cell* 11, 1119–1131
21 McManus, M.T. *et al.* (2000) *Trypanosoma brucei* guide RNA poly(U) tail formation is stabilized by cognate mRNA. *Mol. Cell. Biol.* 20, 883–891
22 Feagin, J.E. *et al.* (1987) Developmentally regulated addition of nucleotides within apocytochrome *b* transcripts in *Trypanosoma brucei*. *Cell* 49, 337–345
23 Maslov, D.A. and Simpson, L. (1992) The polarity of editing within a multiple gRNA-mediated domain is due to formation of anchors for upstream gRNAs by downstream editing. *Cell* 70, 459–467
24 Li, F. *et al.* (2011) Trypanosome REH1 is an RNA helicase involved with the 3′–5′ polarity of multiple gRNA-guided uridine insertion/deletion RNA editing. *Proc. Natl. Acad. Sci. U.S.A.* 108, 3542–3547
25 Grams, J. *et al.* (2002) A trypanosome mitochondrial RNA polymerase is required for transcription and replication. *J. Biol. Chem.* 277, 16952–16959
26 Madina, B.R. *et al.* (2011) Guide RNA biogenesis involves a novel RNase III family endoribonuclease in *Trypanosoma brucei*. *RNA* 17, 1821–1830
27 Koslowsky, D.J. and Yahampath, G. (1997) Mitochondrial mRNA 3′ cleavage/polyadenylation and RNA editing in *Trypanosoma brucei* are independent events. *Mol. Biochem. Parasitol.* 90, 81–94
28 Aphasizheva, I. and Aphasizhev, R. (2010) RET1-catalyzed uridylylation shapes the mitochondrial transcriptome in *Trypanosoma brucei*. *Mol. Cell. Biol.* 30, 1555–1567
29 Adler, B.K. *et al.* (1991) Modification of *Trypanosoma brucei* mitochondrial rRNA by posttranscriptional 3′ polyuridine tail formation. *Mol. Cell. Biol.* 11, 5878–5884
30 Blum, B. and Simpson, L. (1990) Guide RNAs in kinetoplastid mitochondria have a nonencoded 3′ oligo(U) tail involved in recognition of the preedited region. *Cell* 62, 391–397
31 Ryan, C.M. and Read, L.K. (2005) UTP-dependent turnover of *Trypanosoma brucei* mitochondrial mRNA requires UTP polymerization and involves the RET1 TUTase. *RNA* 11, 763–773
32 Zimmer, S.L. *et al.* (2012) Additive and transcript-specific effects of KPAP1 and TbRND activities on 3′ non-encoded tail characteristics and mRNA stability in *Trypanosoma brucei*. *PLoS ONE* 7, e37639
33 Kao, C.Y. and Read, L.K. (2005) Opposing effects of polyadenylation on the stability of edited and unedited mitochondrial RNAs in *Trypanosoma brucei*. *Mol. Cell. Biol.* 25, 1634–1644
34 Aphasizheva, I. *et al.* (2011) Pentatricopeptide repeat proteins stimulate mRNA adenylation/uridylation to activate mitochondrial translation in trypanosomes. *Mol. Cell* 42, 106–117
35 Andrade, M.A. *et al.* (2001) Comparison of ARM and HEAT protein repeats. *J. Mol. Biol.* 309, 1–18
36 Aphasizhev, R. *et al.* (2003) A 100-kD complex of two RNA-binding proteins from mitochondria of *Leishmania tarentolae* catalyzes RNA annealing and interacts with several RNA editing components. *RNA* 9, 62–76
37 Golden, D.E. and Hajduk, S.L. (2005) The 3′-untranslated region of cytochrome oxidase II mRNA functions in RNA editing of African trypanosomes exclusively as a *cis* guide RNA. *RNA* 11, 29–37
38 Jackson, A.P. (2007) Tandem gene arrays in *Trypanosoma brucei*: comparative phylogenomic analysis of duplicate sequence variation. *BMC Evol. Biol.* 7, 54
39 Lukeš, J. *et al.* (2011) How a neutral evolutionary ratchet can build cellular complexity. *IUBMB Life* 63, 528–537
40 Zíková, A. *et al.* (2008) *Trypanosoma brucei* mitochondrial ribosomes: affinity purification and component identification by mass spectrometry. *Mol. Cell. Proteomics* 7, 1286–1296
41 Ochsenreiter, T. *et al.* (2008) Alternative mRNA editing in trypanosomes is extensive and may contribute to mitochondrial protein diversity. *PLoS ONE* 3, e1566
42 Speijer, D. (2006) Is kinetoplastid pan-editing the result of an evolutionary balancing act? *IUBMB Life* 58, 91–96
43 Gray, M.W. *et al.* (2010) Cell biology. Irremediable complexity? *Science* 330, 920–921
44 Carnes, J. *et al.* (2011) Endonuclease associations with three distinct editosomes in *Trypanosoma brucei*. *J. Biol. Chem.* 286, 19320–19330
45 Carnes, J. *et al.* (2008) RNA editing in *Trypanosoma brucei* requires three different editosomes. *Mol. Cell. Biol.* 28, 122–130

Attached Publications

Part I. Trypanosome RNA editing

Laurie K. Read, Julius Lukeš, Hassan Hashimi (2016). Trypanosome RNA editing: the complexity of getting U in and taking U out. *Wiley Interdiscip. Rev. RNA* 7: 33-51.

A review that brings together the latest data from our laboratories and others studying the complexes involved in RNA editing, RECC and MRB1.

Advanced Review

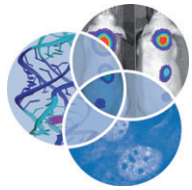

Trypanosome RNA editing: the complexity of getting U in and taking U out

Laurie K. Read,[1]* Julius Lukeš[2,3,4] and Hassan Hashimi[2,3]

RNA editing, which adds sequence information to RNAs post-transcriptionally, is a widespread phenomenon throughout eukaryotes. The most complex form of this process is the uridine (U) insertion/deletion editing that occurs in the mitochondria of kinetoplastid protists. RNA editing in these flagellates is specified by *trans*-acting guide RNAs and entails the insertion of hundreds and deletion of dozens of U residues from mitochondrial RNAs to produce mature, translatable mRNAs. An emerging model indicates that the machinery required for trypanosome RNA editing is much more complicated than previously appreciated. A family of RNA editing core complexes (RECCs), which contain the required enzymes and several structural proteins, catalyze cycles of U insertion and deletion. A second, dynamic multiprotein complex, the Mitochondrial RNA Binding 1 (MRB1) complex, has recently come to light as another essential component of the trypanosome RNA editing machinery. MRB1 likely serves as the platform for kinetoplastid RNA editing, and plays critical roles in RNA utilization and editing processivity. MRB1 also appears to act as a hub for coordination of RNA editing with additional mitochondrial RNA processing events. This review highlights the current knowledge regarding the complex molecular machinery involved in trypanosome RNA editing.

How to cite this article:
WIREs RNA 2015. doi: 10.1002/wrna.1313

INTRODUCTION

The term 'RNA editing' describes site-specific post-transcriptional changes in an RNA sequence other than pre-mRNA splicing and 3′-polyadenylation.[1] RNA editing was first described in trypanosomatids, when it was found that four nonencoded uridine (U) residues were added to the mitochondrial (mt) mRNA-encoding cytochrome *c* oxidase 2 (cox2), thus repairing a frameshift in the gene.[2] This process, whose discovery was quite surprising, stood out because information not encoded within a gene unexpectedly appears in its transcript. A year after this report, a cytidine (C) base in the mRNA-encoding apolipoprotein B (apoB) expressed in the mammalian small intestine was shown to be converted into a U.[3] This 'C-to-U' type editing occurs through a simple deamination of the C and results in the creation of an internal stop codon and a truncated, functionally altered apoB protein.

Later studies revealed that the RNA editing phenomenon is a widespread occurrence throughout eukaryotes (Figure 1). C-to-U conversion editing is a common processing event for transcripts of plant chloroplasts and mitochondria, and a few U-to-C substitutions also occur in the latter organelle.[5] Another common type of RNA editing involving deamination is adenosine (A) to inosine (I) conversion. A-to-I editing represents the most common form of editing in metazoans.[6,7] Insertion/

*Correspondence to: lread@buffalo.edu

[1]University at Buffalo School of Medicine, Buffalo, NY, USA

[2]Institute of Parasitology, Biology Centre, Czech Academy of Sciences, České Budějovice, Czech Republic

[3]Faculty of Science, University of South Bohemia, České Budějovice, Czech Republic

[4]Canadian Institute for Advanced Research, Toronto, ON, Canada

Conflict of interest: The authors have declared no conflicts of interest for this article.

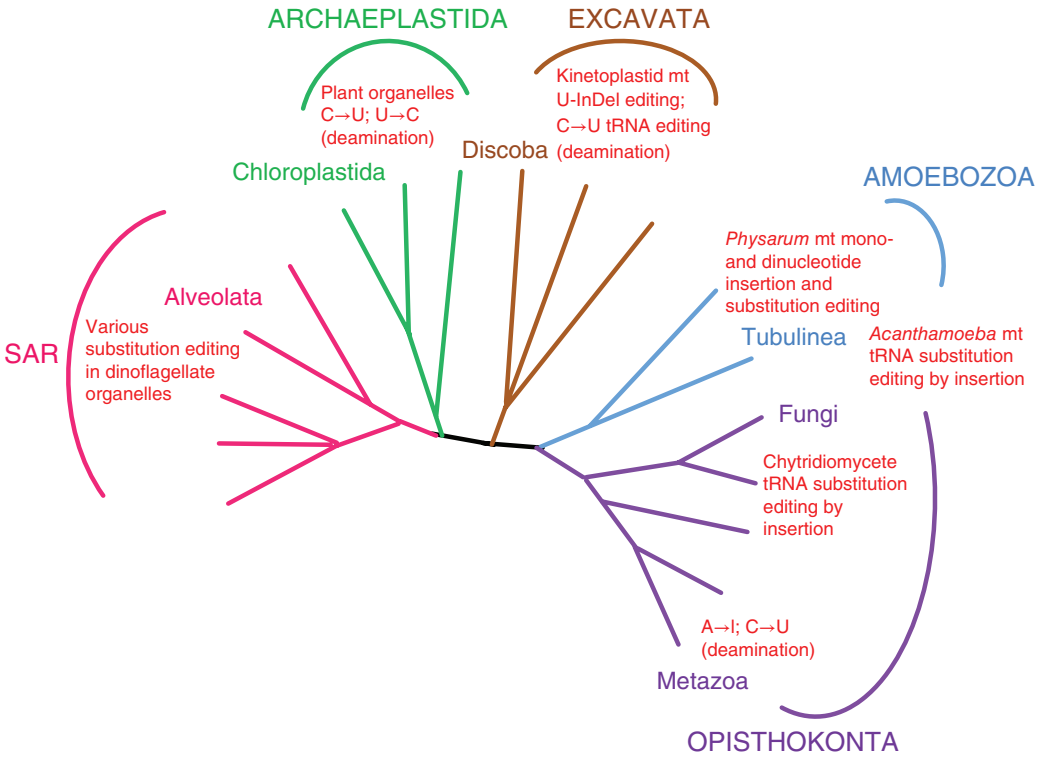

FIGURE 1 | Distribution of multiple types of RNA editing across eukaryotes. Phylogenetic tree based on Adl et al.[4] Only branches with clades that have a demonstrated type of RNA editing are labeled. Adjacent red text summarizes the type of editing.

deletion editing, as seen in trypanosomes, is not as widely distributed throughout eukaryotes as nucleotide substitution editing, although insertion/deletion editing coexists with substitution-type editing in mtRNAs of the slime mold *Physarum polycephalum*, albeit through a different mechanism not involving *trans*-acting RNAs.[8] RNA editing is not restricted to mRNAs, as tRNA[9] and rRNA[8,10] also have been reported to undergo this process.

When these phenomena were discovered, it was not clear how information could be added to or changed in an RNA molecule after it has been transcribed from a gene. Decades of research into the various types of RNA editing have begun to reveal their respective underlying mechanisms.[11,12] Despite the diversity of RNA editing systems, two recurrent features of the molecular machinery ensure the site-specificity of modifications. The first is the utilization of double-stranded RNAs to designate the RNA editing site. This can occur either in *trans*, by hybridization of two separate transcripts, or in the form of intramolecular hairpin loops. The second is the interplay of the substrate RNAs with protein complexes to recognize editing sites and facilitate their modification. The most complicated of these systems, in terms of the numbers of RNAs and proteins involved, remains trypanosome U insertion/deletion editing.

In this review, we summarize the current state of knowledge about the machinery underlying the bewilderingly complex process of RNA editing in trypanosomes. In addition to the well-characterized catalytic machinery, termed the editosome or RNA editing core complex (RECC),[13,14] numerous additional dynamically interacting ribonucleoprotein complexes that are essential for RNA editing and further maturation of edited RNAs have been recently uncovered. This review will focus on work performed primarily in *Trypanosoma brucei*, the causative agent of human African trypanosomiasis, which has become a model trypanosomatid thanks to its possessing a robust RNAi pathway, a feature lacking in most easily cultured trypanosomes and related flagellates.[15]

URIDINE INSERTION/DELETION RNA EDITING AND THE RECC

Basic Mechanism of Uridine Insertion/Deletion RNA Editing

Mt DNA of *T. brucei* and related trypanosomatid flagellates, also known as kinetoplast DNA, is

composed of two types of mutually interlocked circular DNA molecules: about a dozen identical maxicircles encode all 18 protein-coding genes and two truncated mt rRNAs, while thousands of heterogenous minicircles carry most guide (g) RNA genes.[16] Although six maxicircle transcripts exist as standard open reading frames, 12 require U-insertion/deletion RNA editing to generate translatable RNAs. Nine of these transcripts undergo an extreme form of the process called pan-editing. For example, cox3 RNA is remodeled by the insertion of 547 Us and deletion of 41 Us, and thus editing essentially creates the open reading frame of the RNA.[17] The remaining three edited RNAs are each modified in small domains, and thus called minimally edited RNAs. The sequence information for editing is provided by small *trans*-acting gRNAs that act as templates for U-insertion/deletion[18,19] (Figure 2(a)). The sole exception is the cox2 RNA, which contains in its own 3′ UTR the template that guides insertion of four Us in its protein-coding sequence.[20] Deep sequencing of the gRNA population of the insect vector stage (procyclic form; PF) *T. brucei* identified 642 major classes of gRNAs, accounting for complete sets of gRNAs for the majority of edited RNAs.[21] This study revealed significant redundancy in the gRNA population, which is possible because guiding interactions comprise both Watson–Crick and G–U base pairing, and very substantial variation in the abundances of different gRNA classes.

Editing ensues when the 5′ anchor domain of a gRNA forms a primarily Watson–Crick duplex with its cognate mRNA just downstream of the regions whose editing it will direct (Figure 2(a)). Apart from the anchor region, the remainder of the gRNA has only sporadic complementarity to the mRNA. This includes the 3′-oligo(U) tail, which has been postulated to base pair with the mRNA downstream of the region to be edited, thereby strengthening the gRNA–mRNA interaction.[22] The enzymes that catalyze editing are contained within RECC,[23–33] and editing proceeds via an 'enzyme cascade.' Following gRNA–mRNA anchor duplex formation, an editing endonuclease recognizes a mismatch between the gRNA and mRNA and cleaves the mRNA at this editing site (Figure 2(a)). Depending on the sequence of the gRNA, Us will then either be added to the 3′ end of the 5′ cleavage product by a terminal uridylyltransferase (TUTase) or deleted by a U-specific exoribonuclease. At this point, the 5′ and 3′ mRNA fragments are bridged by the gRNA, and the two fragments are subsequently resealed by an RNA ligase.

One gRNA specifies the edited sequence at multiple adjacent editing sites, and following the

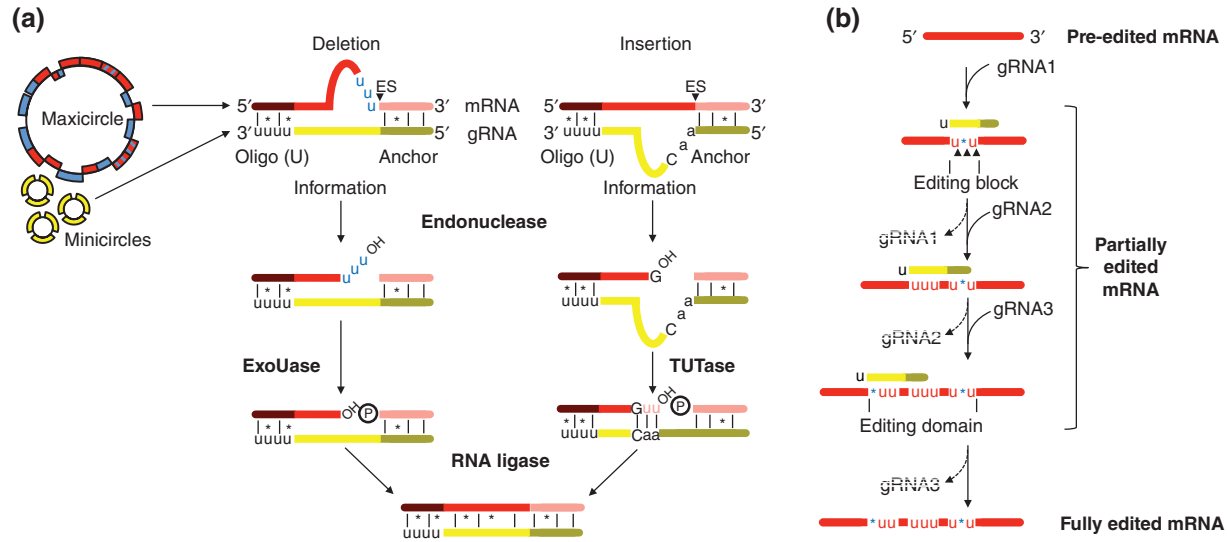

FIGURE 2 | Mechanism of U insertion/deletion editing. (a) Pre-edited mRNAs are transcribed from mitochondrial maxicircles, while the majority of gRNAs are transcribed from the minicircle component of mitochondrial DNA. The gRNA 5′ anchor region (olive) base pairs with the mRNA and the gRNA information region (yellow) directs the number of Us inserted or deleted. The gRNA 3′ oligo(U) tail stabilizes the gRNA/mRNA interaction. Enzymes contained within the RNA editing core complex (RECC) catalyze mRNA endonucleolytic cleavage at an editing sites, U insertion by a 3′ TUTase, and U deletion by a U-specific exoribonuclease as directed by the sequences of gRNAs. Cleaved mRNAs are resealed by RNA ligases. (b) Multi-round editing entails sequential utilization of multiple gRNAs. Because the anchor region of a given gRNA base pairs with edited mRNA sequence specified by the prior gRNA, editing progresses in a 3′–5′ direction along an mRNA. Multiple black arrowheads symbolize multiple editing sites within an editing block, as defined by the hybridized gRNA. Dashed gRNA labels indicate that they are turned over during/after an editing block has been processed. An editing domain is a stretch of mRNA sequence that requires the gRNA cascade for its processing.

utilization of a given gRNA, it is complementary to the edited RNA. Pan-edited mRNAs require the sequential utilization of dozens of gRNAs for their complete editing (Figure 2(b)). For example, editing of cox3 and ATP synthase subunit 6 (A6) mRNAs requires 40 and 32 different gRNAs, respectively.[21] The first gRNA–mRNA anchor is formed between the gRNA anchor domain and the small 3′ never edited sequence present in all pan-edited mRNAs. Subsequent gRNAs form anchor duplexes with the edited mRNA sequences directed by the 3′-proximal gRNA, dictating that editing progress in the 3′–5′ direction along the mRNA (Figure 2(b)). This scenario necessitates the removal of fully base-paired gRNAs to free up the single stranded sequence for binding the next gRNA. The REH1 helicase appears to function in this capacity to some extent[34] (see *Other Complexes Associated with MRB1* section). However, the precise mechanism of gRNA removal and recruitment remain pressing questions.

Sequential gRNA utilization and resultant 3′–5′ editing progression produce a highly complex steady-state RNA population containing large numbers of partially edited RNAs that are processed to different extents at their 3′-ends and unedited at their 5′-ends[35] (Figure 2(b)). In addition, partially edited RNAs typically contain 'junction regions' between the 5′ unedited and 3′ fully edited sequences. Junctions contain edited RNA sequence that matches neither the unedited nor the fully edited sequence, and are believed to be regions of active editing that are ultimately corrected to the proper sequence, although their precise origins are unknown. It has been postulated that junctions arise from inaccurate pairing between cognate mRNA and gRNA or utilization of noncognate gRNAs.[35] Experiments aimed at defining the origin and role of junction sequences, using next generation sequencing of editing intermediates in cells depleted of specific components of the editing machinery, will provide important mechanistic insights into the process.

The RNA Editing Core Complex

RECC contains the enzymes that catalyze an editing cycle.[23–33] Extensive biochemical and genetic experiments over the past 15 years have revealed three distinct types of RECC (Figure 3), which share a common set of twelve proteins, including four enzymes: RNA editing ligases 1 and 2 (KREL1 and KREL2), 3′-TUTase (KRET2), and a U-specific exoribonuclease (KREX2). Also present are six interaction proteins containing predicted OB-folds (KREPA1-6) and two proteins with degenerate RNase III motifs (KREPB4 and KREPB5) (Figure 3). Two heterotrimeric subcomplexes with stable protein–protein interactions exist within the common RECC proteins. These subcomplexes are comprised of (1) KRET2–KREPA1–KREL2, which catalyzes gRNA-directed U-insertion *in vitro*, and (2) KREX2–KREPA2–KREL1, which catalyzes gRNA-directed U deletion *in vitro*.[36] Within these subcomplexes, KREPA1 and KREPA2 bind and stimulate the activities of their partner proteins.[29,36–39] KREPA1 and KREPA2 also bind directly to the KREPA3 and KREPA6 interaction proteins to bridge the insertion and deletion subcomplexes within RECC[40] (Figure 3(a)).

A major advance in our understanding of RECC architecture was the discovery that the complex comprising the 12 common RECC proteins interacts with three RNase III family endonucleases (KREN1, KREN2, and KREN3) and their partner proteins (KREPB8, KREPB7, and KREPB6, respectively) to form three RECC variants with differing functions[26,41] (Figure 3(b)). KREN1/KREPB8 is also joined by a U-specific exoribonuclease, KREX1. Remarkably, both *in vitro* and *in vivo* studies show that KREN1/KREPB8/KREX1 RECC functions in U deletion, KREN2/KREPB7 RECC functions in U insertion, and KREN3/KREPB6 RECC is specific for the *cis*-editing of cox2 mRNA.[26,42] Interestingly, KREX1, present only in KREN1/KREPB8/KREX1 RECC variants, is apparently the primary exoribonuclease in RNA editing. Although KREX2 is a component of the heterotrimeric deletion subcomplex and is active *in vitro*, this enzyme is dispensable in both PF and mammalian bloodstream form (BF) *T. brucei*,[43] and harbors a deletion that renders it catalytically inactive in *Leishmania*.[44] With regard to RECC endonuclease activities, several lines of evidence support a model in which KREN1–3 form heterodimers with the KREPB4 and KREPB5 proteins that possess degenerate RNase III motifs.[45] Interestingly, RNase III family endoribonucleases typically act as a homodimers cleaving double-stranded RNA.[46] Thus, the model in which catalytically active KREN1-3 molecules form heterodimers with inactive KREPB4 and/or KREPB5 is especially satisfying because it explains why only the mRNA strand duplexed to gRNA is cleaved during the editing cycle.

In vitro editing reactions with purified RECC result in precise, gRNA-directed U-insertion or deletion into a single editing site.[19] However, neither site-to-site progression nor gRNA exchange takes place in these reactions (with the exception of one report of two-site editing[47]), thereby implicating additional factors in the editing process *in vivo*. Research over

the past several years has uncovered another multiprotein complex that is essential for RNA editing, termed the mt RNA binding complex 1[48] [MRB1; a.k.a. RNA editing substrate binding complex (RESC)[49]]. Evidence to date suggests that MRB1 is the key to understanding RNA recruitment to RECC and the mechanism of editing progression.[48–51] Next, we describe the discovery of MRB1 and the current model of its function in kinetoplastid RNA editing. MRB1 is thought to serve as the platform for kinetoplastid RNA editing and, additionally, as a hub for coordination of editing with other mt RNA processing machineries.[48,49,51–53]

DISCOVERY OF THE MRB1 COMPLEX AND ITS CONNECTION TO RNA EDITING

Concurrent Discovery of the MRB1 Complex

The MRB1 complex was discovered in 2008 in three independent studies, each of which used different purification techniques, thus leading to differing proposed compositions.[52,54,55] Panigrahi and colleagues[54] used a monoclonal antibody (McAb) generated against a 20S fraction of *T. brucei* mitochondria to immunoprecipitate a complex of 16 proteins, all of unknown function. Within this set of proteins was the target of the McAb, Tb927.7.2570 (later termed GAP2 or GRBC1; Table 1), and a related protein with 31% sequence identity (GAP1; a.k.a. GRBC2), both of which contained no recognizable motifs. TAP tagging of GAP2 and two other proteins from the original purification identified 14 common proteins. Of these, several suggested the ability to interact with RNA, including a DEAD box RNA helicase (REH2; Tb927.4.1500), a C2H2 zinc finger protein (Tb927.6.1680), and a protein with an RRM RNA binding domain and an RGG box (TbRGG2; Tb927.10.10830). The majority of the other proteins lacked recognizable motifs or homologues outside the kinetoplastid flagellates. Based on the presence of several putative RNA binding proteins, the complex was named put-MRB1 (putative Mt RNA Binding complex 1).

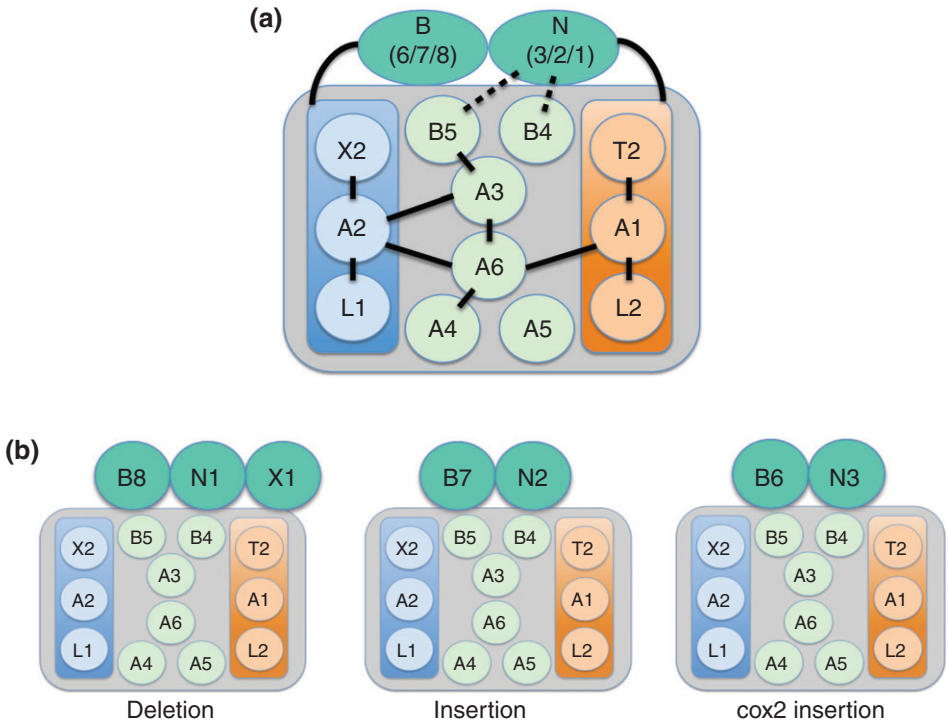

FIGURE 3 | RNA editing core complex (RECC or editosome). (a) RECC contains 12 common proteins, of which three (KREX2, KREPA2, and KREL1) comprise a deletion subcomplex and three (KRET2, KREPA1, and KREL2) comprise an insertion subcomplex. OB-fold containing proteins KREPA3, KREPA6, KREPA4, and KREPA5 maintain protein–protein interactions. Zinc-finger containing KREPB4 and KREPB5 are thought to interact with endonucleases KREN1, KREN2, and KREN3 and their respective partners KREPB8, KREPB7, and KREPB6. KRENs interact with the insertion subcomplex and their KRPEB partners interact with the deletion subcomplex. (b) There are three distinct classes of RECC, which differ in the associated KREN endonuclease and KREP partner proteins. KREN1/KRENB8 also associate with exoribonuclease KREX1. KREN1 containing RECCs catalyze U deletion, KREN2 containing RECCs catalyze U insertion, and KREN3 containing RECCs catalyze insertion specifically into cox2 mRNA.

TABLE 1 | MRB1 Complex Subunits

Subcomplex	Name	Alias	Domains	TriTrypDB #	References[1]
Core	GAP1	GRBC2		Tb927.2.3800	49,52–57
Core	GAP2	GRBC1		Tb927.7.2570	49,52–57
Core	MRB3010	GRBC6	RPS2	Tb927.5.3010	49,51,53,58–60
Core	MRB5390	GRBC4		Tb11.02.5390	49,53,61
Core	MRB8620	GRBC3		Tb927.11.16860	49,53,62
Core	MRB11870	GRBC5	pentein	Tb927.10.11870	49,53,60
Core	MRB0880	GRBC7		Tb927.11.9140	49,53
Core[2]	RBP30	none	RRM	Tb927.5.2100	na
Core[2]	none	none		Tb927.9.1420	na
Core[2]	none	none		Tb927.10.10120	na
TbRGG2	TbRGG2	none	RRM, RGG	Tb927.10.10830	49,50,53,61,63,64
TbRGG2	MRB1860	REMC2		Tb927.2.1860	49,53
TbRGG2	MRB4160[3]	REMC5		Tb927.4.4160	49,53,65
TbRGG2	MRB800	REMC3		Tb927.7.800	49,53
TbRGG2	MRB8170[3]	REMC5A		Tb927.8.8170	49,53,65
TbRGG2	MRB8180[4]	REMC4		Tb927.8.8180	49,53
TbRGG2	PhyH	none	PhyH	Tb927.9.7260	na
Unknown	MRB10130	REMC1	ARM/HEAT	Tb927.10.10130	49,53,54

[1] Listed are publications in which a given protein was either analyzed by RNAi-silencing, used as bait in a protein–protein interaction study, or in which recombinant protein was characterized.
[2] Designated as core components in Ref 48, but not found in any other MRB1 purifications.
[3] MRB4160 and MRB8170 are paralogues arising from a gene duplication that share ~85% amino acid identity.
[4] MRB8180 is paralogous with Tb927.4.4150. These paralogues share ~99% amino acid identity, and thus are designated as a single protein here.

Hashimi and co-workers[55] identified GAP1 and GAP2 in a TAP purification of TbRGG1, a mt protein that binds synthetic oligo(U) ribonucleotide *in vitro*.[66] Reciprocal purifications of GAP1 and GAP2 returned a set of 14 proteins, of which 10 overlapped with those in the Panigrahi *et al*. study.[54] This 14-protein complex was again termed put-MRB1. Finally, Weng et al.[52] purified a related complex from the model kinetoplastid, *Leishmania tarentolae*. These authors originally isolated the *L. tarentolae* homologues of *T. brucei* GAP1/2 in immunoprecipitates of the MRP1/2 RNA binding proteins that impact cytochrome *b* (cyB) mRNA editing.[67,68] Reciprocal TAP purifications of *L. tarentolae* GAP1 and GAP2 revealed 12 proteins interacting in an RNA-independent manner, of which six or seven were also present in purifications of put-MRB1 from other laboratories. Weng et al.[52] referred to the co-purified proteins resembling put-MRB1 as the GRBC (guide RNA binding complex) for reasons discussed below. Thus, three separate studies identified similar mt complexes, and the tantalizing presence of several proteins with predicted RNA binding domains piqued great interest in its function. However, the disparate lists of proteins from each laboratory left the composition of the complex unresolved, and suggested that association of some of the components might be substoichiometric or transient. This ill-defined complex is now commonly referred to as the MRB1 complex,[48,58,61] and its composition has been refined and its function probed. Although the MRB1 complex was originally identified by association with the TbRGG1[55] or MRP1/2[52] proteins, these interactions were shown to be strictly RNA-dependent and these proteins have not often been identified with the MRB1 complex in subsequent studies. Thus, TbRGG1 and MRP1/2 will not be further discussed here.

Evidence Linking the MRB1 Complex to RNA Editing

The MRB1 complex was initially linked to U-insertion/deletion RNA editing by functional analyses of the GAP1 and GAP2 proteins. Both proteins are essential for growth in PF and BF *T. brucei*.[52,56] Strikingly, RNAi-mediated depletion of either protein causes massive destabilization of the entire gRNA population and consequent inhibition of editing of all RNAs that require *trans*-acting gRNAs (i.e., all

RNAs except cox2).[52,56] This finding accounts for the naming of these proteins GAP1/2 (guide RNA associated proteins)[56] or GRBC2/1 (guide RNA binding complex),[52] and hereafter they will be referred to by their more common name, GAP1/2.[48,58] GAP1 and GAP2 are mutually dependent for their stability,[56] form a stable complex, and are resolved in native PAGE as an ~200 kDa particle, the predicted size of a tetramer.[52] *In vitro* transcription/translation studies showed that, while GAP1 can form a dimer, both GAP1 and GAP2 are required for optimal formation of the tetramer.[52] Moreover, GAP1/2 co-expressed in *E. coli* form a ~200 kDa complex, consistent with a heterotetramer of α2/β2 configuration.[57] In accordance with their ability to stabilize gRNAs, GAP1/2 interact with RNA *in vivo*. In cells lacking organellar RNA due to depletion of the mt RNA polymerase, the sedimentation coefficient of GAP1/2 on glycerol gradients is significantly reduced.[56] Endogenous gRNAs are associated with TAP-purified GAP1/2.[52] Finally, *in vitro*, the recombinant GAP1/2 heterotetramer binds synthetic gRNAs with a K_d of about 200 nM.[57] Together, these studies identified a gRNA binding and stabilizing complex in the mitochondria of kinetoplastid protozoa, with the GAP1/2 heterotetramer as the likely gRNA binding component. The definition of the MRB1 complex remained in flux, however, pending more in depth analysis of its composition as described below.

Interestingly, the MRB1 complex is evolutionarily ancestral as it is apparently present already in the earliest-branching kinetoplastid *Perkinsela*, an aflagellar endosymbiont of another protist *Paramoeba*.[69] All six protein-coding transcripts of *Perkinsela* undergo editing, and the level of conservation between RECC and the MRB1 complex of *T. brucei* on one side and *Perkinsela* on the other is about the same, because in the latter flagellate we were able to identify homologues of more than half of the subunits of both complexes.[70]

ARCHITECTURE OF THE MRB1 COMPLEX

Global Studies Reveal Overall MRB1 Architecture

The physical and functional association of GAP1/2 with gRNAs, plus their interaction with other potential RNA binding proteins within the MRB1 complex, spurred a flurry of studies into the organization and function of the complex. Of the 31 potential MRB1 components, only six proteins were in common in all three original studies.[52,54,55] Thus, to understand the function of the MRB1 complex, it first became imperative to elucidate its composition, including the identification of stable subcomplexes, RNA-dependent and -independent contacts, and transiently associating proteins.

To this end, Ammerman et al.[53] embarked on a comprehensive yeast two-hybrid screen to define direct protein–protein contacts. Each protein was given the designation MRBXXX, where XXX denotes the last 3–5 digits of the gene identifier in TriTrypDB (http://tritrypdb.org), unless it was known by a previously published name (Table 1). In all, 961 protein–protein pairs were tested in both bait and prey directions and screened for weak and strong interactions. In this screen, 19 of the 31 proteins exhibited interactions in at least one direction, with a total of 61 interactions. Remarkably, a small number of proteins accounted for the majority of interactions. GAP1, MRB3010, MRB8620, MRB8170, MRB4160, and TbRGG2 were involved in 30 of 31 strong interactions and 24 of 31 weak interactions, while MRB10130 engaged in a large number of weak interactions.[53] To confirm yeast two-hybrid results, the genes of MRB1 subunits that exhibited interactions were *in situ* tagged and resultant proteins tandem affinity purified. Purifications were performed in the presence or absence of RNases to determine interactions involving RNA. Co-purifying proteins identified by western blot analysis or mass spectrometry validated numerous yeast two-hybrid contacts, and importantly, revealed RNase-resistant interactions between some MRB1 components that did not exhibit direct interactions in the yeast two-hybrid screen. The combined yeast two-hybrid and *in vivo* studies thus defined an RNA-independent particle containing GAP1/2 and at least four other proteins, termed the MRB1 core (Table 1 and Figure 4).

The same study identified a second MRB1 subcomplex containing TbRGG2, an RNA binding protein previously reported to significantly impact RNA editing[63] (Table 1 and Figure 4). In contrast to the MRB1 core, TbRGG2 exhibited interactions with GAP1/2 and other core components that were partially sensitive to RNase treatment, and thus termed 'RNA-enhanced.' Consistent with the observation that a small amount of TbRGG2 remains in association with the core after RNase treatment, TbRGG2 exhibited yeast two-hybrid interactions with MRB1 core components, GAP1, MRB3010 and MRB8620. TbRGG2 also displayed strong yeast two-hybrid interactions with MRB4160 and MRB8170, paralogues arising from a chromosome-region duplication

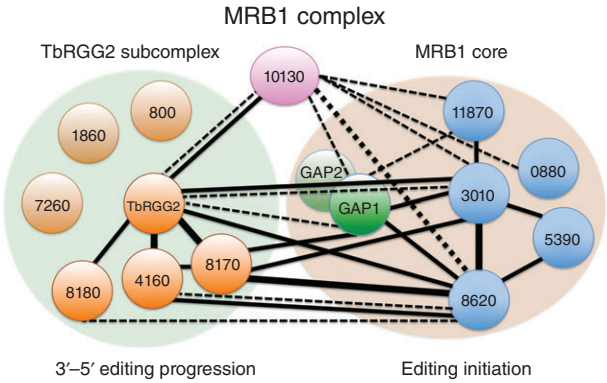

FIGURE 4 | MRB1 complex organization. MRB1 is comprised of a core that facilitates editing initiation, a TbRGG2 subcomplex that functions in 3′–5′ editing progression, and the MRB10130 protein that may bridge and organize the two subcomplexes. MRB1 core contains the GAP1/2 heterotetramer (bright green) that binds and stabilizes gRNAs and which appears to be dissociable and engages in additional interactions. Light green circle (TbRGG2 subcomplex) and light brown circle (MRB1 core) represent largely RNA-independent interactions determined in studies by Ammerman et al.[53] and Aphasizheva et al.[49] Black lines indicate direct interactions by yeast two-hybrid screen.[53] Solid lines, strong interactions; dotted lines, weak interactions; thin lines, interaction in one direction; thick lines, interaction in both directions. The MRB1 complex has also been referred to as RESC (RNA editing substrate binding complex), MRB1 core as GRBC (gRNA binding complex), and TbRGG2 subscomplex as REMC (RNA editing mediator complex).[49]

in *T. brucei*,[71] and with MRB8180. Like TbRGG2, the interaction between MRB8170 and the MRB1 core was strongly RNA-enhanced in pulldown experiments. In addition, co-purifications of tagged and endogenous TbRGG2 and MRB8170 were somewhat RNase-sensitive, suggesting that multiple TbRGG2 subcomplexes are present on a given mRNA, and/or interactions between TbRGG2 subcomplex components are not as stable as those between MRB1 core proteins. Together, these data suggested that a TbRGG2 subcomplex(es), comprising at least TbRGG2, MRB4160, MRB8170, and MRB8180 associates with the MRB1 core in a manner that is significantly strengthened by RNA (Figure 4).

One protein that could not be confidently placed in either the MRB1 core or TbRGG2 subcomplex is MRB10130, a protein comprised almost entirely of α-helical repeats resembling Armadillo (ARM) or HEAT repeats. MRB10130 emerged from the MRB1 yeast two-hybrid screen as a protein exhibiting one of the highest numbers of interactions.[53] It displayed weak interactions with numerous components of the MRB1 core, a strong interaction with TbRGG2, and weak interactions with a few proteins that were reportedly components of the KPAP1 polyadenylation and MERS1 RNA decay complexes.[52] *In vivo* pulldowns of MRB10130 indicated relatively RNase-sensitive interactions with GAP1/2 and MRB8170, and somewhat less RNase-sensitive interactions with TbRGG2 and the MRB1 core protein, MRB3010. The wide array of weak MRB10130 protein contacts is noteworthy in light of known functions of several ARM/HEAT family proteins, which often act as protein complex organizers.[72] It will be of interest to determine whether MRB10130 plays a similar role in organizing MRB1 function. Finally, several proteins consistently co-purified with MRB1 complex components in pulldown experiments from Ammerman and colleagues, yet could not be confidently placed in either the core or TbRGG2 subcomplexes because they failed to interact in the yeast two-hybrid screen and specific antibodies to these proteins were not available. These include MRB800, MRB1860, MRB0880, and Tb927.9.7260 (also known as Tb09.160.5320).

More recently, Aphasizheva et al.[49] reported an extensive study combining *in vivo* tagging and mass spectrometry of MRB1 complex proteins. Label-free quantitative mass spectrometry of both untreated and RNase-treated samples was used to place proteins within each complex and to quantify their interactions. Importantly, this approach validated the model put forth by the Ammerman study[53] of the overall architecture of the MRB1 complex, again revealing the presence of an MRB1 core mediated by direct protein–protein interactions that interacts with the TbRGG2 subcomplex through RNA-enhanced contacts (Table 1 and Figure 4). Assignment of specific proteins to each complex, which was also in agreement with the earlier study, was followed by inclusion of additional proteins in the subcomplexes. Specifically, MRB0880 makes numerous contacts with MRB1 core components, while MRB800, MRB1860, and Tb927.9.7260 cluster with TbRGG2 subcomplex proteins (Figure 4). Also labeled as MRB1 core components were three additional proteins (Tb927.10.10120, Tb927.5.2100, and Tb927.9.1420) that were not identified in any other MRB1 study. These proteins appear to have relatively few and weak contacts, and so are not designated here as *bone fide* MRB1 core proteins. This group also places MRB10130 as part of the TbRGG2 subcomplex. However, their mass spectrometry results are entirely consistent with the aforementioned yeast two-hybrid study, showing MRB10130 making numerous contacts with several components of both the MRB1 core and TbRGG2 subcomplexes. Thus, we consider the role of

MRB10130 in the architecture of the MRB1 complex to be unresolved and more consistent with a role as a complex organizer (Figure 4). We note that the Aphasizheva study[49] introduces new nomenclature for all MRB1 complexes and proteins based on their putative functions (Table 1). However, we prefer to stay with the more common MRB designations until the functions of these exciting but poorly understood complexes and proteins are better defined.

Some proteins that were reported in the original MRB1 purifications were not present in either of the more in-depth studies of MRB1 architecture. MRB6070, MRB1590, and TbRGG3 (previously MRB1820) were shown to engage in entirely RNA-dependent interactions with MRB1, and thus do not represent *bone fide* components of the complex.[53,73,74] The REH2 RNA helicase also comprises a complex separate from MRB1,[51] and its essential role in RNA editing is reviewed in *Other Complexes Associated with* MRB1 section. Collectively, the two global studies[49,53] provide very strong evidence for the existence of an MRB1 complex comprised of the core of about seven proteins that interact in an RNA-independent manner and a TbRGG2 subcomplex, which itself contains seven proteins that associate with the MRB1 core in an RNA-enhanced manner (Figure 4).

Roles of Specific Proteins in Maintaining MRB1 Complex Architecture

MRB1 subcomplex size and integrity have been commonly investigated by analysis of their sedimentation within a density gradient upon ultracentrifugation. While this approach is subject to variability, it is especially useful in examining the impact of RNAi-silencing of specific components on the sedimentation, and thus integrity, of an examined subcomplex. Typically, components of both the MRB1 core and TbRGG2 subcomplex tend to sediment between 20 and 30S, and this distribution markedly shifts toward lighter fractions upon RNase treatment, likely reflecting both the contribution of RNA to the complex's sedimentation value and the RNA-enhanced interaction between the MRB1 core and TbRGG2 subcomplex.[49,53,59,65] Analysis of GAP1/2 sedimentation patterns is somewhat complicated, however, by their extraordinarily heterodisperse pattern on glycerol density gradients, which reveals a distribution that does not entirely coincide with that of other MRB1 complex components.[49,53,56,59,61,65] Indeed, in addition to their roles as integral MRB1 core components, GAP1/2 are present in association with the REH2 RNA helicase[51,58] and, separately, the TbRGG3 RNA binding protein[73] in the absence of some MRB1 core components, suggesting additional roles for GAP1/2 in mt RNA metabolism in addition to their functions in the MRB1 core. Furthermore, GAP1/2 downregulation does not appear to affect the interaction of the other MRB1 core subunits with each other.[62] The incorporation of GAP1/2 into higher molecular weight complexes, like other MRB1 components, requires mt RNA.[56,61]

Initial studies implicate MRB3010 and MRB11870 as important structural components of the MRB1 core. Knockdown of MRB3010 causes both GAP1 and GAP2 to shift from a broad distribution between 10–40S and 10–20S fractions on glycerol gradients.[59] Moreover, the MRB3010–GAP1 interaction requires MRB11870, because MRB3010 immunoprecipitates contain substantially less GAP1 when MRB11870 is depleted.[60] In contrast, knockdown of either MRB5390 or MRB0880 failed to greatly affect the sedimentation of GAP1/2 on glycerol gradients, suggesting that these may be peripheral components of the MRB1 core.[49,61]

The core proteins MRB0880 and MRB11870 likely play integral roles in the association between the MRB1 core and TbRGG2 subcomplex. Upon MRB0880 depletion, TbRGG2 markedly shifts to lighter gradient fractions and its overall abundance is modestly decreased.[49] Additionally, co-immunoprecipitations demonstrated that the association between the core protein MRB3010 and the TbRGG2 subcomplex is significantly decreased when MRB11870 is depleted.[60] Several components of the TbRGG2 subcomplex have also been implicated in bridging its interaction with the MRB1 core. For example, when either TbRGG2 or MRB8180 is downregulated, sedimentation of GAP1/2 shifts toward the top of the gradient.[49,61] Likewise, MRB8180 depletion causes TbRGG2 to shift to lighter gradient fractions,[49] likely reflecting a disruption of the complete MRB1 complex. Kafkova et al.[65] showed that knockdown of MRB8170 causes both GAP1/2 and MRB3010 to redistribute to lighter gradient fractions, and co-depletion of the paralogous MRB8170 and MRB4160 lead to an even more pronounced shift in these core proteins. Thus, within the TbRGG2 subcomplex, TbRGG2, MRB8180, MRB4160, and MRB8170 all appear to be important in maintaining the interaction between the MRB1 core and the TbRGG2 subcomplex. Because TbRGG2, MRB4160, and MRB8170 all bind RNA *in vitro*,[63,65] it cannot be distinguished whether the impact of these proteins involves direct protein–protein contacts or whether it is secondary via the loss of RNAs that are required for the enhanced

interaction between the core and TbRGG2 subcomplexes. Future experiments with defined mutants defective in binding either RNA or specific proteins will be important in answering this question.

It is difficult to disentangle the roles of specific proteins in the maintenance of the TbRGG2 subcomplex, as its structure and composition are somewhat elusive, and evidence suggests the existence of distinct variants. For example, MRB4160 and MRB8170 share 77% amino acid identity, with major differences primarily located in their N-termini.[65] Using antibodies specific to MRB8170, Kafkova et al.[65] showed that MRB8170 is entirely absent from immunoprecipitations of tagged MRB4160, indicating that these two proteins are present in mutually exclusive variants of the TbRGG2 subcomplex. Additional evidence suggests that the TbRGG2 subcomplex is dynamic. TbRGG2, MRB8170, and MRB4160, but not other TbRGG2 subcomplex proteins, were identified in association with the mRPN1 endoribonuclease that may function in gRNA processing in PF *T. brucei*.[75,76] Furthermore, MRB8170 does not entirely co-sediment with TbRGG2,[53] consistent with additional interactions of this protein. As with the MRB1 core, RNA clearly contributes to incorporation of the TbRGG2 subcomplex into higher order complexes, as RNase treatment of mt extracts causes both TbRGG2 and MRB8170 to dramatically redistribute to lighter gradient fractions.[63,65] Potential heterogeneity notwithstanding, the impacts of both MRB8180[49] and MBB8170/4160[65] knockdowns on TbRGG2 gradient sedimentation have been investigated. Interestingly, neither has a very dramatic impact on TbRGG2-containing complexes. In fact, depletion of MRB8170/4160 actually shifts the peak of TbRGG2 toward slightly heavier fractions of the gradient, hinting at complicated dynamics between components of the MRB1 complex. Moreover, the observation that MRB8170/4160 knockdown has only modest effects on TbRGG2 sedimentation, but relatively large effects on the sedimentation of MRB1 core components, is somewhat paradoxical given that it is not considered a *bona fide* subunit of the core.

As described above, MRB10130 exhibits numerous contacts with both MRB1 core and TbRGG2 subcomplex proteins.[49,53] Consistent with a potential role in complex organization, MRB10130 depletion causes redistribution of GAP1/2 to heavier glycerol gradient fractions,[49] suggesting that GAP1/2 fail to properly interact with MRB1 and become free to engage in non-MRB1 interactions. The abundance of TbRGG2 as visualized in glycerol gradient fractions is significantly reduced upon MRB10130 RNAi.[49] Additional studies showed that depletion of the core MRB11870 subunit caused disruption of core MRB10130 binding, as well as core TbRGG2 subcomplex interactions.[60] In light of the direct MRB10130-MRB11870 interaction identified by yeast two-hybrid analysis,[53] these observations suggest that loss of TbRGG2 subcomplex components upon MRB11870 disruption is secondary to disruption of MRB10130 interactions with the MRB1 core. These data are consistent with a model in which MRB10130 bridges the MRB1 core and TbRGG2 subcomplex, and/or facilitates their interaction (Figure 4).

MRB1 Complex Interaction with RECC

The MRB1 complex clearly interacts with gRNAs[51,52] and mRNAs,[49,51,58] and knockdown studies reveal its important role in RNA editing (see MRB1 Complex Function section). Nevertheless, its interactions with the RECC complex are highly transitory. MRB1 complex proteins have been observed in RECC purifications and *vice versa*,[24,52,63] but this is not common and entire complexes are not represented. Furthermore, sedimentation of 20S RECC is essentially unperturbed by depletion of MRB1 complex proteins, including those of both the MRB1 core and TbRGG2 subcomplex.[49,52,61,63,65] Nevertheless, recent evidence indicates that RECC does interact with at least GAP1/2. RECC present in 30–40S regions of glycerol gradients co-precipitates with GAP1/2 in an RNase-sensitive manner and is quantitatively super-shifted with anti-GAP1/2 antibodies.[49] It will be of interest to define the precise nature of complex(es) associated with RECC. More precisely, do GAP1/2 interact with RECC by themselves, or in the context of the MRB1 core particle, the entire MRB1 complex, or some other particle?

MRB1 COMPLEX FUNCTION

Emerging evidence points to the MRB1 complex as the platform for RNA editing.[48,49,51] While early studies assumed that RECC was the complex on which editing occurred, it was always paradoxical that purified 20S RECC contains little or no mRNA or gRNA.[14,23,49] Furthermore, in *in vitro* RNA editing assays, purified RECC performs very poorly and is essentially nonprocessive. In contrast to RECC, affinity purified MRB1 complex contains readily detectable mRNA and gRNA.[49,51,52,58,62] The presence of these RNA species in association with MRB1, together with functional studies on complex components as described next, are consistent with

the MRB1 complex acting as the site of kinetoplastid RNA editing.

MRB1 Core

As previously stated, the GAP1/2 component of the MRB1 core binds and stabilizes gRNAs. The functions of other MRB1 core components have been examined in *T. brucei* engineered for inducible RNAi-silencing of individual proteins.[49,59–62] When gRNA abundance is examined in these cells, it is clear that all other MRB1 core proteins are dispensable for gRNA stabilization. Thus, the GAP1/2 heterotetramer is the gRNA-binding and stabilizing component of the MRB1 core.

To determine whether depletion of other MRB1 core proteins impacts RNA editing, a commonly used assay is qRT-PCR with two primer sets: one that targets pre-edited mRNA sequences near their 3′ ends and another targeting edited mRNA sequences near their 5′ ends. Because editing progresses from 3′ to 5′ along an mRNA, the latter primers assess the generation of nearly fully edited mRNAs. Using this assay, cells depleted of MRB3010 or MRB11870 typically exhibit an 80–90% decrease in edited mRNAs and two- to fourfold increases in pre-edited RNAs, especially for pan-edited transcripts.[49,59,60] Minimally edited RNAs sometimes show lesser, but still obvious, defects. Remarkably, editing of cox2 mRNA is also substantially affected in MRB3010 or MRB11870 knockdown, despite the reliance of this mRNA only on a *cis*-acting gRNA.[20] Because cox2 mRNA editing is independent of *trans*-acting gRNAs, and thus GAP1/2, this finding indicates that the MRB1 core has a function in RNA editing that extends beyond simply presenting GAP1/2-bound gRNAs to RECC.

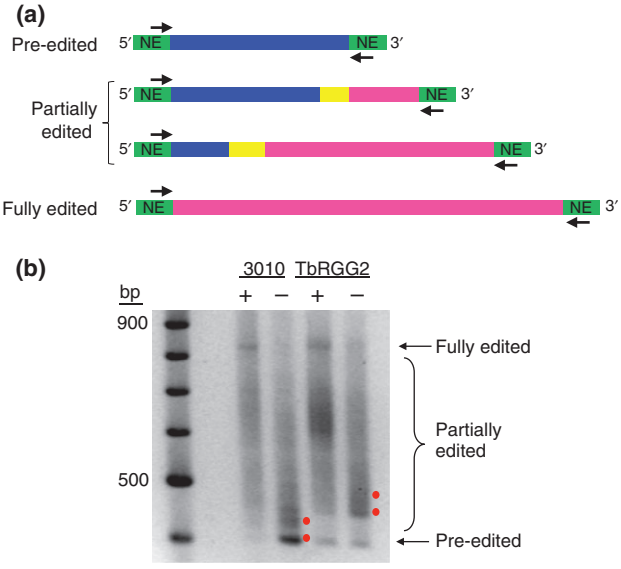

FIGURE 5 | Full gene PCR assay used to analyze the step of editing in which a given MRB1 protein functions. (a) End point PCR is performed with primers targeting the 5′ and 3′ never edited regions present at the ends of all pan-edited RNAs to amplify all versions of a given RNA (pre-edited, partially edited, fully edited). Green, never edited; pink, fully edited; yellow, junction region; blue, pre-edited. (b) Agarose gel analysis of full gene PCR amplicons of ATPase 6 RNA in cells either expressing (+) or depleted of (–) MRB3010 or TbRGG2. Red dots indicate products that accumulate in the absence of each protein. Note that pre-edited RNA accumulates upon MRB3010 depletion but not upon TbRGG2 depletion, signifying a role in editing initiation for the former, but not the latter.

To assess in more detail the relative impacts of MRB1 core proteins on editing initiation as opposed to the 3′–5′ progression of editing, Ammerman and colleagues[50,59,60] employed a 'full gene PCR' assay. Here, end point PCR is performed with primers annealing to 5′ and 3′ never-edited regions present on all edited RNAs (Figure 5). Because U-insertion is ten times more common than U-deletion, gel-resolution of the amplicons reveals pre-edited, partially edited, and fully edited RNA populations and indicates approximate points at which editing is compromised upon RNAi-silencing (Figure 5). Full gene PCRs for MRB3010- and MRB11870-depleted cells reveal defects at 3′-most editing sites, indicating a defect in editing initiation, consistent with significantly increased pre-edited RNAs in MRB3010 and MRB11870 knockdowns.[59,60] Deep sequencing of mt mRNA populations currently underway will provide more detailed information regarding the precise editing intermediates that accumulate in cells depleted of specific MRB1 components.

The RNAi-silencing phenotypes of two other MRB1 core proteins, MRB0880 and MRB5390, appear somewhat less dramatic and more mRNA-specific than those following the depletion of MRB3010 or MRB11870.[49,61] Results regarding MRB5390 are inconsistent, as one qRT-PCR study reports modest decreases in only edited cox3, ribosomal protein subunit 12 (RPS12), and maxicircle unknown reading frame 2 (MURF2) mRNAs, while at the same time observing increases in almost all pre-edited RNAs, suggesting possible effects on pre-edited mRNA stabilization.[61] Another study reported substantial decreases in many edited mRNAs by qRT-PCR, while concurrent Northern blot analysis of RPS12 mRNA revealed little increase in pre-edited or partially edited mRNA.[49] These differences may reflect different RNAi-efficiencies in the two studies. The role of another MRB1 core component, MRB8620 has been somewhat paradoxical based on

one study. In this report,[49] edited RNAs are either unaffected or increased 1.5- to 2-fold when MRB8620 is knocked down. Mass spectrometry studies by these authors indicate that MRB8620 maintains numerous contacts with the large ribosomal subunit; thus, it may play a more substantial role in post-editing events than other MRB1 core components. However, a more recent study has shown that RNAi-mediated repression of MRB8620 indeed results in an inhibition of editing due to the comprised integrity of the MRB1 core, albeit to a lesser degree than when the other studied core MRB1 subunits are downregulated.[62] In this background, transcripts requiring RNA editing accumulated on the GAP1/2 heterotetramer, indicating a disruption of RNA trafficking during the RNA editing process when the MRB1 core is disrupted. The MRB1 core components are essential for growth of PF[49,52,56,59–61] and, when examined, BF[56,59,60] *T. brucei*. Only under culturing conditions that induces the PF to rely entirely on the mitochondrion for its energy metabolism did MRB8620 downregulation affect flagellate fitness, most likely due to its subtle RNAi phenotype.[62] Interestingly, depletion of most of these proteins also results in a slight increase in gRNA abundance,[49,60,62] suggesting that gRNAs are consumed in the editing process (Figure 2(b)) and, thus, build up when editing is inhibited by MRB1 core protein knockdown. Finally, all of the studies described above analyzed the effects of MRB1 core protein depletion on never-edited mt mRNAs and rRNAs, with little or no apparent effects on these RNA populations. Thus, the MRB1 core contains GAP1/2 as its gRNA-binding component, impacts early events in the editing process apart from gRNA delivery, and possesses a function restricted to RNA editing.

TbRGG2 Subcomplex

This subcomplex, which interacts with the MRB1 core in an RNA-enhanced manner[49,53] (and see above), is named for the first of its components to be studied: TbRGG2. This protein was initially identified by mass spectrometry of immunoprecipitated RECC complexes,[24] and it is one of the few MRB1 components with recognizable domains.[63] It contains a G-rich N-terminus comprising GWG and RG/RGG repeats and a canonical RRM type RNA binding domain at its C-terminus. Recombinant TbRGG2 binds synthetic pre-edited mRNA, edited mRNA, and gRNA *in vitro*, and exhibits an almost 10-fold higher affinity for pre-edited mRNA ($K_d \sim 4$ nM) than for the latter two transcripts.[63,64] Surprisingly, high affinity RNA binding maps to the G-rich N-terminus, and requires both GWG and RGG repeats. The RRM domain displays lower affinity RNA binding (K_ds = 80–150 nM), with a relative preference for gRNA compared to the full-length protein or N-terminus. Because of the requirement for iterative mRNA–gRNA annealing and unwinding events during RNA editing, Ammerman et al.[50] also tested whether recombinant TbRGG2 possesses these activities. Indeed, TbRGG2 displays robust mRNA–gRNA annealing activity *in vitro*, and exhibits RNA unwinding activity in an *E. coli* reporter assay. Subsequent deletion studies mapped annealing activity to the protein's G-rich N-terminus and unwinding to the RRM-containing C-terminus.[64] Thus, *in vitro* studies show that TbRGG2 binds pre-edited mRNA with high affinity and possesses the ability to modulate RNA–RNA interactions.

To address the role of TbRGG2 in RNA editing, three different groups analyzed mRNA levels in TbRGG2 knockdowns by qRT-PCR with essentially the same results.[49,61,63] Editing of pan-edited RNAs is dramatically compromised in TbRGG2-depleted cells, whereas editing of the three minimally edited RNAs remains unaffected. Furthermore, when measured, large decreases in the abundance of edited mRNAs were often not accompanied by increases in corresponding pre-edited mRNAs.[61,63] These findings suggested a role for TbRGG2 in the 3′–5′ progression of editing with minimal effects on editing initiation. Utilizing full gene PCRs and primer extension assays with primers targeted to different parts of the RPS12 and A6 editing domains, Ammerman et al.[50] confirmed that TbRGG2 depletion has minimal effects on editing initiation, modest effects at mRNA 3′ editing sites, and much more dramatic effects on 5′ editing sites, consistent with an impact on the 3′–5′ progression of editing (see also Figure 5). Conventional sequence analysis of ~100 cDNAs derived from RPS12 full gene PCRs in TbRGG2 replete versus depleted cells revealed two regions of the RPS12 mRNA where editing was prone to stalling. Referencing cDNA sequences with a then available gRNA database[77] suggested that sites of stalling corresponded both to the 3′ end of one gRNA and to internal regions of another gRNA. Thus, it was not possible from this small cDNA dataset to distinguish whether TbRGG2 functions in gRNA exchange or in utilization of adjacent editing sites within a single mRNA–gRNA duplex. Deep sequencing analyses of edited mRNAs from TbRGG2 replete and depleted cells are currently underway to resolve this question. In addition to revealing stalling at specific points during editing progression, the sequences of the cDNA

clones from the TbRGG2-silenced cells displayed significant decreases in the lengths of the junction regions that lie between 3′ fully edited and 5′ unedited regions. Junction regions are thought to be sites of active editing at the time when RNA is harvested from the cells, and their reduction upon ablation of TbRGG2 is consistent with impaired gRNA utilization. *In vivo* complementation studies of these RNAi knockdowns with TbRGG2 deletion and point mutants showed that the RRM domain-containing C-terminus is completely incapable of rescuing the knockdown, while the N-terminus harboring high affinity RNA-binding and annealing activities can partially complement cell growth and RNA editing.[64] A point mutant lacking RNA unwinding activity provided full complementation, suggesting that the RNA annealing function of TbRGG2 is more important in editing than its *in vitro* RNA unwinding activity. Collectively, *in vivo* studies implicate TbRGG2 in facilitating gRNA utilization critical for active editing and its resulting 3′–5′ progression.

The only other TbRGG2 subcomplex proteins that have been studied in detail are the paralogous MRB4160 and MRB8170 proteins,[65] which are devoid of any motifs or homology to known proteins. Nevertheless, *in vitro* UV cross-linking assays with synthetic RNAs demonstrated that both recombinant proteins possess RNA-binding activity. Like TbRGG2, MRB8170 displayed five to sixfold higher affinity for mRNA than gRNA in filter binding assays, although in contrast to TbRGG2 the K_ds of MRB8170 for pre-edited and edited mRNA are similar (15–20 nM). *In vivo*, only the MRB4160/8170 double knockdown exhibits a growth defect, and the two proteins are partially redundant with respect to mt mRNA levels. No defects in mRNA levels were observed in MRB4160 knockdowns, whereas the ablation of MRB8170 resulted in modest defects in MURF2 and A6 mRNA editing and cox3 and NADH dehydrogenase subunit 7 (ND7) pre-edited mRNA stability. The double MRB4160/8170 knockdown exhibited widespread editing defects including both pan-edited mRNAs, and to a lesser extent minimally edited RNAs, and also exhibited the likely defect in the stability of pre-edited cox3 mRNA that was observed in the MRB8170 single knockdown. Similar to TbRGG2 knockdowns, pre-edited mRNA levels were not increased for pan-edited RNAs whose editing was affected by concurrent MRB4160/8170 knockdown.[65] This suggests MRB4160/8170 may play a role in editing progression similar to TbRGG2, although this hypothesis has not been directly tested. Analysis of mRNA levels by qRT-PCR in cells depleted of other TbRGG2 subcomplex components, namely MRB8180, MRB800, and MRB1860, has been reported, with the caveat that the latter two proteins were only depleted to 60% of wild type levels and pre-edited mRNA levels were not reported.[49] MRB1860 depletion impacted only edited ND7 mRNA, while MRB8180 and MRB800 had distinct transcript-specific effects on edited mRNA levels. Importantly, depletion of TbRGG2 subcomplex components does not affect gRNA levels. Thus, the effects of TbRGG2 subcomplex on RNA editing likely reflect roles in RNA trafficking and utilization.

MRB10130

One published study has touched on the impact of depleting the ARM/HEAT repeat protein, MRB10130.[49] qRT-PCR analyses revealed a dramatic decrease in almost all edited mRNAs. While pre-edited mRNAs were not tested this way, Northern blot analysis of RPS12 mRNA showed substantial accumulation of pre-edited mRNA. In addition, the levels of several gRNAs were increased. These authors also reported modest decreases in some never-edited RNAs upon MRB10130 depletion, although this may be due to the analysis being performed at a time point after the dramatic growth defect had already ensued. In general, the phenotype of MRB10130 is more reminiscent of MRB1 core proteins than TbRGG2 subcomplex proteins, consistent with this protein's numerous physical interactions with core components.

Current Model for MRB1 Complex Function

Even though we are still far from understanding the mechanisms by which the MRB1 complex manifests its essential role(s) in RNA editing, a model is emerging based on the above data[48,49,51] (Figures 4 and 6). The MRB1 core appears to be critical for the initiation of editing and very early editing events. One function of the core is likely to present GAP1/2-bound gRNAs to RECC. However, the effects of MRB1 component knockdowns on cox2 mRNA editing indicate that it has additional key functions in initial editing events. The TbRGG2 subcomplex apparently functions in gRNA utilization, thus facilitating 3′ to 5′ editing progression. The RNA binding and annealing capacity of TbRGG2 almost certainly contributes to this function. The roles of other TbRGG2 subcomplex components may be more RNA-related, potentially facilitating specific mRNA–gRNA interactions via their own RNA-binding

activities (e.g., MRB8170 and MRB4160). Numerous outstanding questions remain, including the precise nature of the RNA-enhanced interaction between the MRB1 core and TbRGG2 subcomplex and the potential role of MRB10130 in its coordination. Other key unanswered questions are the route of gRNA and mRNA trafficking, the precise involvement of distinct proteins in this process, and the nature of the interaction between MRB1 and RECC.

OTHER COMPLEXES ASSOCIATED WITH MRB1

In addition to its role as a platform for the RNA editing reaction, the MRB1 complex appears to act as a hub for numerous mt RNA processing reactions[48] (Figure 6). Several proteins interact with MRB1 transiently and/or substoichiometrically, and below we describe the evidence for the physical and functional interaction of these complexes with MRB1.

RNA Helicases

Soon after the discovery that the site-specificity of trypanosome RNA editing is mediated by the hybridization of gRNAs to their cognate mRNAs, the participation of RNA helicases in the process was hypothesized. Helicase activity is likely required to unwind tight duplexes comprised of gRNA-edited mRNA, so that subsequent gRNAs can anchor, thereby permitting editing progression[78,79] (Figure 2 (b)). RNA helicases have also been proposed to be involved in the remodeling of the ribonucleoprotein complexes that interact with transcripts during the course of RNA editing. So far, two mt RNA editing helicases have been characterized.

RNA editing helicase 1 (REH1), originally called mHel61p, is among the first proteins involved in RNA editing to be cloned from *T. brucei*.[78] This DExD/H box family protein exhibits *in vitro* RNA unwinding activity, consistent with a potential role in melting duplexed gRNA–mRNA to enable subsequent editing by the next gRNA[34] (Figure 2(b)). Further support for this role is that ablation of REH1 results in a decrease of some edited mRNAs, with the 3′–5′ progression being compromised.[34,78] However, while REH1 appears to exhibit some RNA-dependent interaction with RECC,[34] it does not associate with the bulk of mt RNA helicase activity.[78,79]

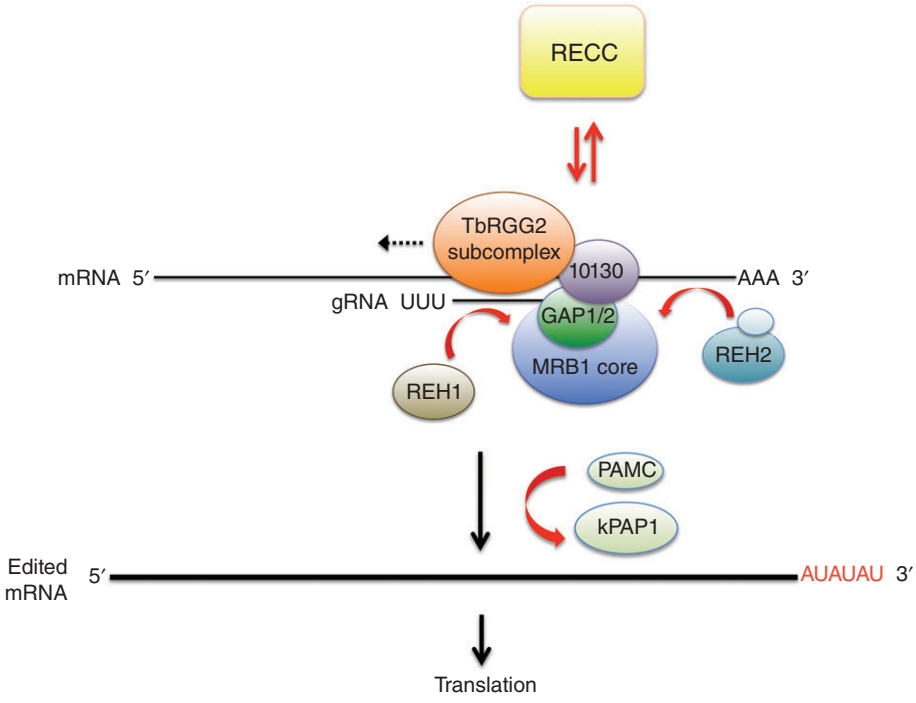

FIGURE 6 | Current model for the coordination of numerous complexes in mitochondrial U insertion/deletion RNA editing and mRNA processing. The MRB1 complex [comprised of MRB1 core (including GAP1/2), TbRGG2 subcomplex, and MRB10130] serves as a platform for the editing reaction. RECC, containing the catalytic enzymes, associates transiently with MRB1-associated RNAs. TbRGG2 subcomplex facilitates editing 3′–5′ progression (dotted arrow). RNA helicases REH1 and REH2 appear to promote RNA association with MRB1. Following the completion of editing, kPAP1, potentially with assistance from PAMC, catalyzes a long A/U tail on the 3′ end of fully edited mRNA, rendering it competent for translation.

REH2 is a much larger mt DExD/H box helicase (~240 kDa as compared to the ~60 kDa REH1 in *T. brucei*) that associates with the majority of mt RNA unwinding activity.[80] This finding agrees with REH2 being discovered due to its association with MRB1 and RECC. These interactions appear to be via RNA linkers[58] as was also demonstrated for REH1.[34,49] REH2 interacts with gRNAs in a manner dependent on its double stranded RNA binding domain and DExD/H box helicase motifs. Ablation of REH2 leads to a decrease in edited RNAs. gRNA stability may also be compromised,[56,80] although this has not been observed in all studies.[51] Interestingly, RNA immunoprecipitation/RNAseq studies showed that REH2 appears to associate with a cohort of gRNAs that direct later editing blocks, compared to MRB3010, which associates with gRNAs biased toward those directing early editing blocks.[51] Moreover, REH2 depletion leads to a decrease in pre-edited and partially edited RNAs associated with MRB3010, suggesting that REH2 acts in *trans* to facilitate mRNA recruitment to the MRB1 core.[58] In sum, emerging evidence suggests that REH1 and REH2 helicases play important roles in RNA editing, although the mechanistic details await further investigation.

Nudix Hydrolase

A protein dubbed mt edited mRNA stability factor 1 - (MERS1) was initially found, along with GAP1/2, associated substoichiometrically with the MRP1/2 complex in *Leishmania*.[68] This protein was later shown to be associated in an RNA-dependent manner with MRB1 in isolations of GAP1 and GAP2.[52,55] MERS1 bears a motif that places it in the Nudix Hydrolase superfamily of proteins. Such proteins are found throughout prokaryotes, eukaryotes and even viruses, and are mainly pyrophosphohydrolases that cleave nucleotide di- and triphosphates linked to another 'X' moiety (hence the name NUDIX), i.e., NDP-X to NMP and P-X, and thus are involved in many metabolic pathways involving sugars.[81] In terms of participation in RNA metabolism, a Nudix hydrolase conserved among opisthokonts called Dcp2 is involved in the mRNA decapping. To date, little is known about the role of MERS1 in shaping the mt transcriptome of trypanosomes. RNAi-silencing of the protein in *T. brucei* leads to a destabilization of edited mRNAs,[52] although further studies will be required to establish the mechanistic connections between MERS1 and other mt RNA processing events, including RNA editing.

kPAP

Mt RNAs possess nonencoded 3′ tails, and the presence of two RNA populations with short (~20 nt) and longer (~120 nt) tails was reported two decades ago.[82] More recent studies have revealed that these tails are comprised of A, U, or A/U, with the longer tails generally having a higher percentage of U, and tail composition apparently being quite RNA-specific.[83–85] Short A-tails stabilize edited RNAs, but not pre-edited RNAs, both *in vitro* and *in vivo*, and only a small amount of editing is required for A-tail mediated stabilization.[85,86] Long tails, present primarily on never-edited and fully edited RNAs, appear to facilitate mRNA association with the small ribosomal subunit, and thus translation.[84]

Kinetoplast poly(A) polymerase 1 (kPAP1) functions in both long and short 3′-tail synthesis, and it resides in the kPAP complex with a heterodimer of two pentatricopeptide (PPR) proteins, termed kPAF1 and kPAF2.[84,85] *In vitro* assays demonstrated that kPAF1/2 promotes long 3′-tail synthesis.[84] kPAF1/2 does not stimulate long A-tail synthesis, but rather requires interspersed Us added by RET1 to generate long tails. The kPAP1 complex engages in transient and RNA-mediated interactions with RECC and MRB1.[49,52,85] kPAP1 also apparently makes several weak contacts with the mt ribosome, assisting the connection between poly A/U tail synthesis and translation.[49] Numerous questions remain regarding the interactions between the kPAP complex and others involved in mt RNA processing. At what point and with which proteins does kPAP1 add short tails to mt RNAs? How does the kPAP complex recognize only translatable (fully edited and never-edited) RNAs for long A/U tail synthesis?

PAMC

The so-called polyadenylation mediator complex (PAMC) exhibited protein-mediated interactions with the MRB1 core in one recent study,[49] although its components had not been previous identified in association with MRB1. While this complex does not strongly interact with the kPAP complex, ablation of one of its subunits (but not others) suggested a role in both short and long 3′-tail synthesis, thereby leading to its name. The role of the PAMC complex in mt RNA polyadenylation and processing await further investigation.

CONCLUSION

The discovery of MRB1 provided important clues to longstanding questions in the kinetoplastid RNA

editing field, such as why RECC appeared to lack stable RNA association and why it failed to catalyze processive RNA editing *in vitro*. Evidence to date suggests that MRB1 is the platform for editing, and that it facilitates RNA recruitment to RECC and 3′–5′ progression of editing. However, these studies are in their infancy. Future work is needed to address the degree of heterogeneity and dynamism within the MRB1 complex, the biochemical functions of MRB1 complex components, and the precise protein–RNA interactions that facilitate the byzantine process that is U-insertion/deletion RNA editing. Interactions between MRB1 and other RNA processing machineries provide a further layer of complexity in kinetoplastid mt gene expression.

ACKNOWLEDGMENTS

This work was supported by National Institutes of Health (RO1 AI061580) to L.K.R., and Czech Grant Agency (15-21974S), RNPnet FP7 program (289007), and Praemium Academiae award to J.L.

REFERENCES

1. Gott JM, Emeson RB. Functions and mechanisms of RNA editing. *Annu Rev Genet* 2000, 34:499–531.
2. Benne R, Van den Burg J, Brakenhoff JP, Sloof P, Van Boom JH, Tromp MC. Major transcript of the frame-shifted coxII gene from trypanosome mitochondria contains four nucleotides that are not encoded in the DNA. *Cell* 1986, 46:819–826.
3. Powell LM, Wallis SC, Pease RJ, Edwards YH, Knott TJ, Scott J. A novel form of tissue-specific RNA processing produces apolipoprotein-B48 in intestine. *Cell* 1987, 50:831–840.
4. Adl SM, Simpson AG, Lane CE, Lukes J, Bass D, Bowser SS, Brown MW, Burki F, Dunthorn M, Hampl V, et al. The revised classification of eukaryotes. *J Eukaryot Microbiol* 2012, 59:429–493.
5. Maier RM, Zeltz P, Kossel H, Bonnard G, Gualberto JM, Grienenberger JM. RNA editing in plant mitochondria and chloroplasts. *Plant Mol Biol* 1996, 32:343–365.
6. Maas S, Rich A, Nishikura K. A-to-I RNA editing: recent news and residual mysteries. *J Biol Chem* 2003, 278:1391–1394.
7. Bazak L, Haviv A, Barak M, Jacob-Hirsch J, Deng P, Zhang R, Isaacs FJ, Rechavi G, Li JB, Eisenberg E, et al. A-to-I RNA editing occurs at over a hundred million genomic sites, located in a majority of human genes. *Genome Res* 2014, 24:365–376.
8. Gott JM, ed. *Mechanisms and Functions of RNA Editing in Physarum polycephalum*. Norfolk: Caister Academic Press; 2013, 17–40.
9. Jackman JE, Alfonzo JD. Transfer RNA modifications: nature's combinatorial chemistry playground. *Wiley Interdiscip Rev RNA* 2013, 4:35–48.
10. Valach M, Moreira S, Kiethega GN, Burger G. Trans-splicing and RNA editing of LSU rRNA in Diplonema mitochondria. *Nucleic Acids Res* 2014, 42:2660–2672.
11. Stefl R, Oberstrass FC, Hood JL, Jourdan M, Zimmermann M, Skrisovska L, Maris C, Peng L, Hofr C, Emeson RB, et al. The solution structure of the ADAR2 dsRBM–RNA complex reveals a sequence-specific readout of the minor groove. *Cell* 2010, 143:225–237.
12. Maris C, Masse J, Chester A, Navaratnam N, Allain FH. NMR structure of the apoB mRNA stem-loop and its interaction with the C to U editing APOBEC1 complementary factor. *RNA* 2005, 11:173–186.
13. Simpson L, Aphasizhev R, Lukes J, Cruz-Reyes J. Guide to the nomenclature of kinetoplastid RNA editing: a proposal. *Protist* 2010, 161:2–6.
14. Stuart KD, Schnaufer A, Ernst NL, Panigrahi AK. Complex management: RNA editing in trypanosomes. *Trends Biochem Sci* 2005, 30:97–105.
15. Barnes RL, Shi H, Kolev NG, Tschudi C, Ullu E. Comparative genomics reveals two novel RNAi factors in Trypanosoma brucei and provides insight into the core machinery. *PLoS Pathog* 2012, 8:e1002678.
16. Jensen RE, Englund PT. Network news: the replication of kinetoplast DNA. *Annu Rev Microbiol* 2012, 66:473–491.
17. Feagin JE, Abraham JM, Stuart K. Extensive editing of the cytochrome c oxidase III transcript in Trypanosoma brucei. *Cell* 1988, 53:413–422.
18. Blum B, Bakalara N, Simpson L. A model for RNA editing in kinetoplastid mitochondria: "guide" RNA molecules transcribed from maxicircle DNA provide the edited information. *Cell* 1990, 60:189–198.
19. Seiwert SD, Stuart K. RNA editing: transfer of genetic information from gRNA to precursor mRNA in vitro. *Science* 1994, 266:114–117.
20. Golden DE, Hajduk SL. The 3'-untranslated region of cytochrome oxidase II mRNA functions in RNA editing of African trypanosomes exclusively as a cis guide RNA. *RNA* 2005, 11:29–37.

21. Koslowsky D, Sun Y, Hindenach J, Theisen T, Lucas J. The insect-phase gRNA transcriptome in Trypanosoma brucei. *Nucleic Acids Res* 2014, 42:1873–1886.
22. Koslowsky DJ, Reifur L, Yu LE, Chen W. Evidence for U-tail stabilization of gRNA/mRNA interactions in kinetoplastid RNA editing. *RNA Biol* 2004, 1:28–34.
23. Rusche LN, Cruz-Reyes J, Piller KJ, Sollner-Webb B. Purification of a functional enzymatic editing complex from Trypanosoma brucei mitochondria. *EMBO J* 1997, 16:4069–4081.
24. Panigrahi AK, Allen TE, Stuart K, Haynes PA, Gygi SP. Mass spectrometric analysis of the editosome and other multiprotein complexes in Trypanosoma brucei. *J Am Soc Mass Spectrom* 2003, 14:728–735.
25. Panigrahi AK, Schnaufer A, Ernst NL, Wang B, Carmean N, Salavati R, Stuart K. Identification of novel components of Trypanosoma brucei editosomes. *RNA* 2003, 9:484–492.
26. Carnes J, Trotter JR, Peltan A, Fleck M, Stuart K. RNA editing in Trypanosoma brucei requires three different editosomes. *Mol Cell Biol* 2008, 28:122–130.
27. Carnes J, Trotter JR, Ernst NL, Steinberg A, Stuart K. An essential RNase III insertion editing endonuclease in Trypanosoma brucei. *Proc Natl Acad Sci USA* 2005, 102:16614–16619.
28. Trotter JR, Ernst NL, Carnes J, Panicucci B, Stuart K. A deletion site editing endonuclease in Trypanosoma brucei. *Mol Cell* 2005, 20:403–412.
29. Ernst NL, Panicucci B, Igo RP Jr, Panigrahi AK, Salavati R, Stuart K. TbMP57 is a 3' terminal uridylyl transferase (TUTase) of the Trypanosoma brucei editosome. *Mol Cell* 2003, 11:1525–1536.
30. McManus MT, Shimamura M, Grams J, Hajduk SL. Identification of candidate mitochondrial RNA editing ligases from Trypanosoma brucei. *RNA* 2001, 7:167–175.
31. Aphasizhev R, Aphasizheva I, Nelson RE, Gao G, Simpson AM, Kang X, Falick AM, Sbicego S, Simpson L. Isolation of a U-insertion/deletion editing complex from Leishmania tarentolae mitochondria. *EMBO J* 2003, 22:913–924.
32. Rusche LN, Huang CE, Piller KJ, Hemann M, Wirtz E, Sollner-Webb B. The two RNA ligases of the Trypanosoma brucei RNA editing complex: cloning the essential band IV gene and identifying the band V gene. *Mol Cell Biol* 2001, 21:979–989.
33. Cruz-Reyes J, Zhelonkina AG, Huang CE, Sollner-Webb B. Distinct functions of two RNA ligases in active Trypanosoma brucei RNA editing complexes. *Mol Cell Biol* 2002, 22:4652–4660.
34. Li F, Herrera J, Zhou S, Maslov DA, Simpson L. Trypanosome REH1 is an RNA helicase involved with the 3'–5' polarity of multiple gRNA-guided uridine insertion/deletion RNA editing. *Proc Natl Acad Sci USA* 2011, 108:3542–3547.
35. Koslowsky DJ, Bhat GJ, Read LK, Stuart K. Cycles of progressive realignment of gRNA with mRNA in RNA editing. *Cell* 1991, 67:537–546.
36. Schnaufer A, Ernst NL, Palazzo SS, O'Rear J, Salavati R, Stuart K. Separate insertion and deletion subcomplexes of the Trypanosoma brucei RNA editing complex. *Mol Cell* 2003, 12:307–319.
37. Ernst NL, Panicucci B, Carnes J, Stuart K. Differential functions of two editosome exoUases in Trypanosoma brucei. *RNA* 2009, 15:947–957.
38. Park YJ, Budiarto T, Wu M, Pardon E, Steyaert J, Hol WG. The structure of the C-terminal domain of the largest editosome interaction protein and its role in promoting RNA binding by RNA-editing ligase L2. *Nucleic Acids Res* 2012, 40:6966–6977.
39. Gao G, Rogers K, Li F, Guo Q, Osato D, Zhou SX, Falick AM, Simpson L. Uridine insertion/deletion RNA editing in Trypanosomatids: specific stimulation *in vitro* of Leishmania tarentolae REL1 RNA ligase activity by the MP63 zinc finger protein. *Protist* 2010, 161:489–496.
40. Schnaufer A, Wu M, Park YJ, Nakai T, Deng J, Proff R, Hol WG, Stuart KD. A protein–protein interaction map of trypanosome ~20S editosomes. *J Biol Chem* 2010, 285:5282–5295.
41. Panigrahi AK, Ernst NL, Domingo GJ, Fleck M, Salavati R, Stuart KD. Compositionally and functionally distinct editosomes in Trypanosoma brucei. *RNA* 2006, 12:1038–1049.
42. Carnes J, Zelaya Soares C, Wickham C, Stuart K. Endonuclease associations with three distinct editosomes in Trypanosoma brucei. *J Biol Chem* 2011, 286:19320–19330.
43. Carnes J, Lewis Ernst N, Wickham C, Panicucci B, Stuart K. KREX2 is not essential for either procyclic or bloodstream form Trypanosoma brucei. *PLoS One* 2012, 7:e33405.
44. Rogers K, Gao G, Simpson L. Uridylate-specific 3' 5'-exoribonucleases involved in uridylate-deletion RNA editing in trypanosomatid mitochondria. *J Biol Chem* 2007, 282:29073–29080.
45. Guo X, Carnes J, Ernst NL, Winkler M, Stuart K. KREPB6, KREPB7, and KREPB8 are important for editing endonuclease function in Trypanosoma brucei. *RNA* 2012, 18:308–320.
46. MacRae IJ, Doudna JA. Ribonuclease revisited: structural insights into ribonuclease III family enzymes. *Curr Opin Struct Biol* 2007, 17:138–145.
47. Alatortsev VS, Cruz-Reyes J, Zhelonkina AG, Sollner-Webb B. Trypanosoma brucei RNA editing: coupled cycles of U deletion reveal processive activity of the editing complex. *Mol Cell Biol* 2008, 28:2437–2445.
48. Hashimi H, Zimmer SL, Ammerman ML, Read LK, Lukes J. Dual core processing: MRB1 is an emerging

kinetoplast RNA editing complex. *Trends Parasitol* 2013, 29:91–99.

49. Aphasizheva I, Zhang L, Wang X, Kaake RM, Huang L, Monti S, Aphasizhev R. RNA binding and core complexes constitute the U-insertion/deletion editosome. *Mol Cell Biol* 2014, 34:4329–4342.
50. Ammerman ML, Presnyak V, Fisk JC, Foda BM, Read LK. TbRGG2 facilitates kinetoplastid RNA editing initiation and progression through intrinsic pause sites. *RNA* 2010, 16:2239–2251.
51. Madina BR, Kumar V, Metz R, Mooers BH, Bundschuh R, Cruz-Reyes J. Native mitochondrial RNA-binding complexes in kinetoplastid RNA editing differ in guide RNA composition. *RNA* 2014, 20:1142–1152.
52. Weng J, Aphasizheva I, Etheridge RD, Huang L, Wang X, Falick AM, Aphasizhev R. Guide RNA-binding complex from mitochondria of trypanosomatids. *Mol Cell* 2008, 32:198–209.
53. Ammerman ML, Downey KM, Hashimi H, Fisk JC, Tomasello DL, Faktorova D, Kafkova L, King T, Lukes J, Read LK. Architecture of the trypanosome RNA editing accessory complex, MRB1. *Nucleic Acids Res* 2012, 40:5637–5650.
54. Panigrahi AK, Zikova A, Dalley RA, Acestor N, Ogata Y, Anupama A, Myler PJ, Stuart KD. Mitochondrial complexes in Trypanosoma brucei: a novel complex and a unique oxidoreductase complex. *Mol Cell Proteomics* 2008, 7:534–545.
55. Hashimi H, Zikova A, Panigrahi AK, Stuart KD, Lukes J. TbRGG1, an essential protein involved in kinetoplastid RNA metabolism that is associated with a novel multiprotein complex. *RNA* 2008, 14:970–980.
56. Hashimi H, Cicova Z, Novotna L, Wen YZ, Lukes J. Kinetoplastid guide RNA biogenesis is dependent on subunits of the mitochondrial RNA binding complex 1 and mitochondrial RNA polymerase. *RNA* 2009, 15:588–599.
57. Aphasizheva I, Aphasizhev R. RET1-catalyzed uridylylation shapes the mitochondrial transcriptome in Trypanosoma brucei. *Mol Cell Biol* 2010, 30:1555–1567.
58. Madina BR, Kumar V, Mooers BH, Cruz-Reyes J. Native variants of the MRB1 complex exhibit specialized functions in kinetoplastid RNA editing. *PLoS One* 2015, 10:e0123441.
59. Ammerman ML, Hashimi H, Novotna L, Cicova Z, McEvoy SM, Lukes J, Read LK. MRB3010 is a core component of the MRB1 complex that facilitates an early step of the kinetoplastid RNA editing process. *RNA* 2011, 17:865–877.
60. Ammerman ML, Tomasello DL, Faktorova D, Kafkova L, Hashimi H, Lukes J, Read LK. A core MRB1 complex component is indispensable for RNA editing in insect and human infective stages of Trypanosoma brucei. *PLoS One* 2013, 8:e78015.
61. Acestor N, Panigrahi AK, Carnes J, Zikova A, Stuart KD. The MRB1 complex functions in kinetoplastid RNA processing. *RNA* 2009, 15:277–286.
62. Huang Z, Faktorova D, Krizova A, Kafkova L, Read LK, Lukes J, Hashimi H. Integrity of the core mitochondrial RNA binding complex 1 is vital for trypanosome RNA editing. *RNA* (Epub ahead of print; October 7, 2015).
63. Fisk JC, Ammerman ML, Presnyak V, Read LK. TbRGG2, an essential RNA editing accessory factor in two Trypanosoma brucei life cycle stages. *J Biol Chem* 2008, 283:23016–23025.
64. Foda BM, Downey KM, Fisk JC, Read LK. Multifunctional G-rich and RRM-containing domains of TbRGG2 perform separate yet essential functions in trypanosome RNA editing. *Eukaryot Cell* 2012, 11:1119–1131.
65. Kafkova L, Ammerman ML, Faktorova D, Fisk JC, Zimmer SL, Sobotka R, Read LK, Lukes J, Hashimi H. Functional characterization of two paralogs that are novel RNA binding proteins influencing mitochondrial transcripts of Trypanosoma brucei. *RNA* 2012, 18:1846–1861.
66. Vanhamme L, Perez-Morga D, Marchal C, Speijer D, Lambert L, Geuskens M, Alexandre S, Ismaili N, Goringer U, Benne R, et al. Trypanosoma brucei TBRGG1, a mitochondrial oligo(U)-binding protein that co-localizes with an in vitro RNA editing activity. *J Biol Chem* 1998, 273:21825–21833.
67. Vondruskova E, van den Burg J, Zikova A, Ernst NL, Stuart K, Benne R, Lukes J. RNA interference analyses suggest a transcript-specific regulatory role for mitochondrial RNA-binding proteins MRP1 and MRP2 in RNA editing and other RNA processing in Trypanosoma brucei. *J Biol Chem* 2005, 280:2429–2438.
68. Aphasizhev R, Aphasizheva I, Nelson RE, Simpson L. A 100-kD complex of two RNA-binding proteins from mitochondria of Leishmania tarentolae catalyzes RNA annealing and interacts with several RNA editing components. *RNA* 2003, 9:62–76.
69. Tanifuji G, Kim E, Onodera NT, Gibeault R, Dlutek M, Cawthorn RJ, Fiala I, Lukes J, Greenwood SJ, Archibald JM. Genomic characterization of Neoparamoeba pemaquidensis (Amoebozoa) and its kinetoplastid endosymbiont. *Eukaryot Cell* 2011, 10:1143–1146.
70. David V, Flegontoc P, Gerasimov E, Tanifuji G, Hashimi H, Logacheva MD, Maruyama S, Onodera NT, Gray MW, Archibald JM, Lukes J. Gene loss and error-prone RNA editing in the mitochondrion of Perkinsela, an endosymbiont kinetoplastid. *mBio* 2015. In press.
71. Jackson AP. Evolutionary consequences of a large duplication event in Trypanosoma brucei: chromosomes 4 and 8 are partial duplicons. *BMC Genomics* 2007, 8:432.

72. Xu W, Kimelman D. Mechanistic insights from structural studies of beta-catenin and its binding partners. *J Cell Sci* 2007, 120:3337–3344.
73. McAdams NM, Ammerman ML, Nanduri J, Lott K, Fisk JC, Read LK. An arginine–glycine-rich RNA binding protein impacts the abundance of specific mRNAs in the mitochondria of Trypanosoma brucei. *Eukaryot Cell* 2015, 14:149–157.
74. Shaw PL, McAdams NM, Hast MA, Ammerman ML, Read LK, Schumacher MA. Structures of the T. brucei kRNA editing factor MRB1590 reveal unique RNA-binding pore motif contained within an ABC-ATPase fold. *Nucleic Acids Res* 2015, 43:7096–7109.
75. Carnes J, Lerch M, Kurtz I, Stuart K. Bloodstream form Trypanosoma brucei do not require mRPN1 for gRNA processing. *RNA* 2015, 21:28–35.
76. Madina BR, Kuppan G, Vashisht AA, Liang YH, Downey KM, Wohlschlegel JA, Ji X, Sze SH, Sacchettini JC, Read LK, et al. Guide RNA biogenesis involves a novel RNase III family endoribonuclease in Trypanosoma brucei. *RNA* 2011, 17:1821–1830.
77. Ochsenreiter T, Cipriano M, Hajduk SL. KISS: the kinetoplastid RNA editing sequence search tool. *RNA* 2007, 13:1–4.
78. Missel A, Souza AE, Norskau G, Goringer HU. Disruption of a gene encoding a novel mitochondrial DEAD-box protein in Trypanosoma brucei affects edited mRNAs. *Mol Cell Biol* 1997, 17:4895–4903.
79. Missel A, Goringer HU. Trypanosoma brucei mitochondria contain RNA helicase activity. *Nucleic Acids Res* 1994, 22:4050–4056.
80. Hernandez A, Madina BR, Ro K, Wohlschlegel JA, Willard B, Kinter MT, Cruz-Reyes J. REH2 RNA helicase in kinetoplastid mitochondria: ribonucleoprotein complexes and essential motifs for unwinding and guide RNA (gRNA) binding. *J Biol Chem* 2010, 285:1220–1228.
81. McLennan AG. The Nudix hydrolase superfamily. *Cell Mol Life Sci* 2006, 63:123–143.
82. Bhat GJ, Souza AE, Feagin JE, Stuart K. Transcript-specific developmental regulation of polyadenylation in Trypanosoma brucei mitochondria. *Mol Biochem Parasitol* 1992, 52:231–240.
83. Zimmer SL, McEvoy SM, Menon S, Read LK. Additive and transcript-specific effects of KPAP1 and TbRND activities on 3' non-encoded tail characteristics and mRNA stability in Trypanosoma brucei. *PLoS One* 2012, 7:e37639.
84. Aphasizheva I, Maslov D, Wang X, Huang L, Aphasizhev R. Pentatricopeptide repeat proteins stimulate mRNA adenylation/uridylation to activate mitochondrial translation in trypanosomes. *Mol Cell* 2011, 42:106–117.
85. Etheridge RD, Aphasizheva I, Gershon PD, Aphasizhev R. 3'-Adenylation determines mRNA abundance and monitors completion of RNA editing in *T. brucei* mitochondria. *EMBO J* 2008, 27:1596–1608.
86. Kao CY, Read LK. Opposing effects of polyadenylation on the stability of edited and unedited mitochondrial RNAs in Trypanosoma brucei. *Mol Cell Biol* 2005, 25:1634–1644.

Attached Publications

Part II.

DYSKINETOPLASTIC

TRYPANOSOMA BRUCEI

Attached Publications

Part II. DYSKINETOPLASTIC *TRYPANOSOMA BRUCEI*

De-Hua Lai, Hassan Hashimi, Zhao-Rong Lun, Francisco J. Ayala and Julius Lukeš (2008). Adaptations of *Trypanosoma brucei* to gradual loss of kinetoplast DNA: *Trypanosoma equiperdum* and *Trypanosoma evansi* are petite mutants of *T. brucei. Proc. Natl. Acad. Sci. U.S.A.* 105:1999-2004.

This paper examines several strains of *T. brucei evansi* and *T. brucei equiperdum* to demonstrate the many stages that these subspecies undergo to get from the Dk state, in which kDNA minicircles are homogenized and maxicircles accumulate deletions, to the Ak state when all kDNA is gone. The paper identifies several compensatory mutations to the γ subunit of F_OF_1-ATP synthase that were later verified to allow these trypanosomes to achieve the Dk and Ak condition.

Adaptations of *Trypanosoma brucei* to gradual loss of kinetoplast DNA: *Trypanosoma equiperdum* and *Trypanosoma evansi* are *petite* mutants of *T. brucei*

De-Hua Lai*†, Hassan Hashimi*‡, Zhao-Rong Lun†, Francisco J. Ayala§¶, and Julius Lukeš*‡¶

*Biology Centre, Institute of Parasitology, Czech Academy of Sciences, and ‡Faculty of Sciences, University of South Bohemia, 37005 České Budějovice, Czech Republic; †Center for Parasitic Organisms, State Key Laboratory of Biocontrol, School of Life Sciences, and Key Laboratory of Tropical Diseases Control, Zhongshan Medical College, Sun-Yat Sen University, 510275 Guangzhou, China; and §Department of Ecology and Evolutionary Biology, University of California, Irvine, CA 92697

Contributed by Francisco J. Ayala, December 14, 2007 (sent for review November 21, 2007)

***Trypanosoma brucei* is a kinetoplastid flagellate, the agent of human sleeping sickness and ruminant nagana in Africa. Kinetoplastid flagellates contain their eponym kinetoplast DNA (kDNA), consisting of two types of interlocked circular DNA molecules: scores of maxicircles and thousands of minicircles. Maxicircles have typical mitochondrial genes, most of which are translatable only after RNA editing. Minicircles encode guide RNAs, required for decrypting the maxicircle transcripts. The life cycle of *T. brucei* involves a bloodstream stage (BS) in vertebrates and a procyclic stage (PS) in the tsetse fly vector. Partial [dyskinetoplastidy (Dk)] or total [akinetoplastidy (Ak)] loss of kDNA locks the trypanosome in the BS form. Transmission between vertebrates becomes mechanical without PS and tsetse mediation, allowing the parasite to spread outside the African tsetse belt. *Trypanosoma equiperdum* and *Trypanosoma evansi* are agents of dourine and surra, diseases of horses, camels, and water buffaloes. We have characterized representative strains of *T. equiperdum* and *T. evansi* by numerous molecular and classical parasitological approaches. We show that both species are actually strains of *T. brucei*, which lost part (Dk) or all (Ak) of their kDNA. These trypanosomes are not monophyletic clades and do not qualify for species status. They should be considered two subspecies, respectively *T. brucei equiperdum* and *T. brucei evansi*, which spontaneously arose recently. Dk/Ak trypanosomes may potentially emerge repeatedly from *T. brucei*.**

dourine | mitochondria | protozoa | RNA editing | surra

Trypanosoma brucei is a kinetoplastid flagellate responsible for human sleeping sickness and the ruminant disease nagana in Africa. The mitochondrial (mt) or kinetoplast DNA (kDNA) of trypanosomatids consists of a huge network of interlocked circular DNA molecules of two types: maxicircles and minicircles. The former encode classical mt genes, the transcripts of most of which are rendered translatable only upon the uridine insertion/deletion type of RNA editing. Minicircles encode small RNA molecules termed guide (g) RNAs, necessary for decoding encrypted maxicircle transcripts (1–3).

The kDNA is one of the largest mt genomes known. A sophisticated machinery ensures faithful replication of the kDNA of *T. brucei*, which is represented by thousands of minicircles (each ≈1.0 kb in size) and dozens of maxicircles (≈23 kb) (4, 5). Because it supplies the substrate gRNAs required for RNA editing, the possibility that *T. brucei* would lose its kDNA would seem unlikely. Yet a partial or even full loss of kDNA, termed dyskinetoplastidy (Dk) and akinetoplastidy (Ak), occurs in nature and can be induced in the laboratory (6).

T. brucei has a complex life cycle. It proliferates in vertebrates as the bloodstream stage (BS), which relies on glycolysis and has down-regulated mitochondria; in the tsetse fly vector, it exists as the procyclic stage (PS) with a fully active organelle (7). The partial or total loss of kDNA locks the trypanosome in the BS form, because the information in the kDNA network is essential for the PS (2). The reduction of a heteroxenous life cycle to a monoxenous one has had dramatic consequences, such as the elimination of the tsetse vector (or any other similar insect vector) from the life cycle, which paradoxically allowed trypanosomes to leave the African tsetse belt and spread to other continents (8). Recombination or genetic exchange does not occur in Dk/Ak trypanosomes (6, 9).

Dk/Ak trypanosomes are categorized into three species: *Trypanosoma equiperdum*, *Trypanosoma evansi*, and *Trypanosoma equinum* (10). *T. equinum* has now been synonymized with *T. equiperdum* (11, 12) and will not be further discussed herein. A widely accepted paradigm holds that *T. evansi* evolved, via *T. equiperdum*, when camels infected with *T. brucei* moved to tsetse-free areas (10). *T. equiperdum* and *T. evansi* are responsible for dourine and surra, respectively, economically significant diseases infecting horses, camels, and water buffaloes, transmitted in the BS by bloodsucking insects or coitus (9). Surra is the most widespread and serious disease of camels. Apart from causing different clinical diseases, *T. equiperdum* (dourine) and *T. evansi* (surra) differ only in that the former contains at least fragments of kDNA maxicircles (Dk), missing from *T. evansi* (Ak). Hundreds of studies on the epidemiology, pathology, and prevalence of both diseases have been published (6, 9, 13). Yet the existence of *T. equiperdum* has been questioned, because no new strains have been isolated for a long time (ref. 13, but see refs. 14 and 15).

We have performed a multifarious characterization of representative strains of *T. equiperdum* and *T. evansi*. Our results reveal that both species are strains of *T. brucei*, which independently lost parts of their kDNA. Neither the Dk nor Ak trypanosomes are monophyletic clades, and thus they would not qualify for species status. We suggest they be considered as subspecies, respectively, *T. brucei equiperdum* and *T. brucei evansi*. Our findings provide important insights into the mt functions and reveal the enormous plasticity of *T. brucei*.

Results

It has been shown that some *T. equiperdum* strains contain a deletion in their kDNA maxicircle (16–18), whereas ambiguity remained whether other strains have an intact or disrupted maxicircle (19). We first sequenced the maxicircle coding region in two strains of *T. equiperdum*. The analysis of strain STIB818 (Table 1) confirmed the occurrence of a 9-kb deletion, flanked by truncated 12S rRNA and cytochrome oxidase subunit 1 (cox1) genes; all other retained genes are intact [supporting information (SI) Fig. 8*C*]. The second strain, STIB842, is a representative of strains with the whole

Author contributions: D.-H.L., H.H., and J.L. designed research; D.-H.L. and H.H. performed research; Z.-R.L. contributed new reagents/analytic tools; and F.J.A. and J.L. wrote the paper.

The authors declare no conflict of interest.

¶To whom correspondence may be addressed. E-mail: fjayala@uci.edu or jula@paru.cas.cz.

This article contains supporting information online at www.pnas.org/cgi/content/full/0711799105/DC1.

Table 1. Strains of *Trypanosoma* spp. investigated in this study

Strains	Species	Host	Origin	Date
29–13*	*T. brucei*	Cattle	Tanzania	1956
EATRO HN	*T. brucei*	n.a.	n.a.	n.a.
STIB 920	*T. brucei*	Hartebeest	Tanzania	1971
BoTat1.1	*T. equiperdum*	Horse	Morocco	1924
STIB 842	*T. equiperdum*	n.a.	n.a.	n.a.
OVI	*T. equiperdum*	Horse	South Africa	1975
STIB 841	*T. equiperdum*	n.a.	South Africa	n.a.
STIB 818	*T. equiperdum*	Horse	China	1979
ATCC30019	*T. equiperdum*	n.a.	France	1903
ATCC30023	*T. equiperdum*	n.a.	France	1903
AnTat4.1	*T. equiperdum*	n.a.	n.a.	n.a.
STIB 784	*T. equiperdum*	n.a.	n.a.	n.a.
STIB 810	*T. evansi*	Water buffalo	China	1985
STIB 805	*T. evansi*	Water buffalo	China	1985
STIB 807	*T. evansi*	Water buffalo	China	1979
CPOgz1	*T. evansi*	Water buffalo	China	2005
GDH	*T. evansi*	Horse	China	1964
GDB2	*T. evansi*	Water buffalo	China	1981
GXM	*T. evansi*	Mule	China	1979
JSB2	*T. evansi*	Water buffalo	China	1986
AS131M	*T. evansi*	Horse	Philippines	2006
SS73M	*T. evansi*	Water buffalo	Philippines	2006
SS143M	*T. evansi*	Water buffalo	Philippines	2006
Ted3	*T. evansi*	Dog	Brazil	1992
Teh2	*T. evansi*	Horse	Brazil	1996
Teh3	*T. evansi*	Horse	Brazil	1996
RoTat1.2	*T. evansi*	Water buffalo	Indonesia	1982
Stock Kazakh	*T. evansi*	Camel	Kazakhstan	1995
Stock Viet	*T. evansi*	Water buffalo	Vietnam	1998
KETRI 2479	*T. evansi*	Camel	Kenya	1980

n.a., information not available.
*Derived from strain Lister 427.

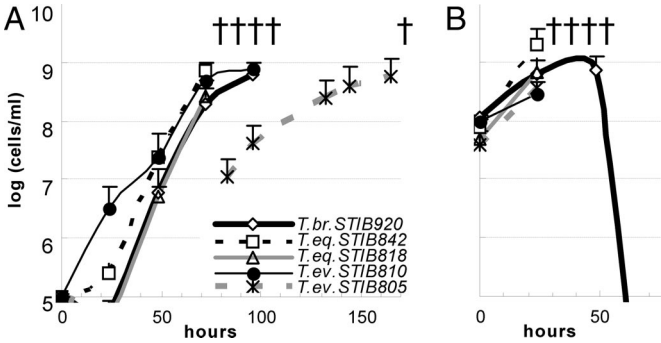

Fig. 1. Parasitaemia growth curves. (*A*) Growth curve of parasitaemia caused by representative strains in mice. The cell density in blood is indicated. (*B*) Growth curve of parasitaemia of the same strains as in *A* in mice with concurrent i.p. injection of 10 μg of EtdBr per gram of weight.

assortment of maxicircle genes, as shown by a PCR-based screen of nine *T. equiperdum* strains (Table 2; SI Table 3). Sequencing confirmed the presence of all apparently functional maxicircle genes in STIB842 (SI Fig. 8*B*), with 97% nucleotide identity with *T. brucei* (SI Fig. 8*A*). No maxicircle genes could be amplified from three other strains labeled as *T. equiperdum* (American Type Culture Collection nos. ATCC30023, STIB784, and AnTat 4.1; Table 2), yet the presence of maxicircle genes is the only molecular feature that would distinguish *T. equiperdum* from *T. evansi* (6, 9, 12). The absence of the maxicircle genes in all tested *T. evansi* strains was anticipated (Table 2).

To rule out the possibility that some *T. equiperdum* strains are mislabeled *T. brucei* strains, mice were experimentally infected with the *T. brucei* strain STIB920, *T. equiperdum* strains STIB818 and STIB842, and *T. evansi* strains STIB805 and STIB810. With the exception of Ak STIB805, all strains showed very similar dynamics of parasitaemia and invariably killed the mice within 3–4 days (Fig. 1*A*). To test the ability of the studied trypanosomes to lose kDNA, mice were injected with ethidium bromide (EtdBr) in the early phase of infection. Indeed, all tested Dk strains were prone to the loss: 90% of cells had no detectable kDNA within 48 h (SI Fig. 9*B*). The absence of kDNA had no effect on pathogenicity, because the parasitaemia progressed equally with and without EtdBr treatment (Fig. 1*B*). However, the *T. brucei* STIB920 infection performed with EtdBr treatment was not lethal for the mice, because the parasites were eliminated from the blood (Fig. 1*B*).

To corroborate that the studied *T. equiperdum* are morphologically indistinguishable *T. brucei*, transformation from the BS to PS was performed *in vitro* in the SDM-79 medium supplemented with citrate and *cis*-aconitate (20). Although the transformation of *T. brucei* STIB920 started within 12 h, and at 60 h virtually all cells had transformed into the PS, no transformation was observed in the Dk strains, which all perished after 4 days (SI Fig. 10).

An extensive restriction analysis to assess minicircle complexity revealed sequence heterogeneity of the *T. brucei* minicircles and their apparent homogeneity in *T. equiperdum* and *T. evansi* (Fig. 2*A* and SI Fig. 11). Note that the *T. equiperdum* strains with full-size maxicircles (STIB841 and STIB842) (Table 2) exhibit the same extent of minicircle homogenization as other Dk strains (Fig. 2*A*). The lack of minicircle heterogeneity was confirmed by sequence analysis, because all 14 and 7 AsuII-linearized minicircles of strains STIB818 (class A *T. equiperdum*) and STIB842 (class B *T. equiperdum*), respectively, were virtually identical within each strain (SI Fig. 12). The class A minicircles contain three putative gRNA genes, whereas a nonoverlapping set of five gRNAs is encoded by

Table 2. Presence/absence of maxicircle-encoded genes in selected *Trypanosoma* spp. strains

Species	Strains	ND7	A6	CO2	ND5	12S rRNA	ND7-Cyb	MURF1-ND1	ND1-MURF2	MURF2-CO1	ND4-ND5
T. brucei	STIB 920	+	+	+	+	+	+	+	+	+	+
T. equiperdum	BoTat1.1	+	+	+	+	+	+	+	+	+	+
T. equiperdum	STIB 842	+	+	+	+	+	+	+	+	+	+
T. equiperdum	OVI	+	+	+	+	+	ND	ND	+	+	ND
T. equiperdum	STIB 841	+	+	+	+	+	+	+	+	+	+
T. equiperdum	STIB 818	–	–	–	+	+	–	–	–	–	+
T. equiperdum	ATCC30019	–	–	–	+	+*	–*	–*	–*	–*	+
T. equiperdum	ATCC30023†	–	–	–	–	–	–	–	–	–	–
T. equiperdum	STIB 784†	–	–	–	–	–	–	–	–	–	–
T. equiperdum	AnTat4.1	–	–	–	–	–	–	–	–	–	–
T. evansi	STIB 810	–	–	–	–	–	–	–	–	–	–
T. evansi	STIB 805†	–	–	–	–	–	–	–	–	–	–

ND, not determined.
*Ref. 18.
†Akinetoplastic strains.

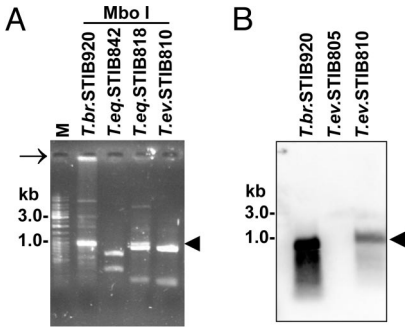

Fig. 2. Minicircle homogenization (*A*) and/or absence (*B*). (*A*) EtdBr-stained agarose gel showing restriction analysis of kDNA minicircles from representative strains using MboI (see also SI Fig. 11). Linearized minicircles are indicated by an arrowhead. Note the presence of kDNA network in the slot of the *T. brucei* lane (arrow). (*B*) Southern blotting of total DNA isolated from representative strains and digested with restriction enzyme TaqI. The membrane was hybridized with a radiolabeled probe prepared from total *T. brucei* minicircles.

class B minicircles (SI Fig. 11). With the whole *T. brucei* minicircle population as a template for random hexamer labeling, Southern hybridization confirmed the total absence of minicircles in the Ak strains of *T. evansi* (Fig. 2*B*).

To assess the consequences of the alterations of the mini- and maxicircle components of kDNA on the RNA level, we analyzed the transcription and editing of selected mt transcripts. Using probes specific for preedited, edited, and never-edited mRNAs, we performed Northern blot analysis of ATPase subunit 6 (A6) and cytochrome oxidase subunits 1–3 (cox1, -2, and -3). All probes gave the strongest signal in the PS *T. brucei* 29–13 cells. The preedited A6 and cox3 and never-edited cox1 mRNAs were also abundant in the BS *T. brucei* strain STIB920 (Fig. 3*A*). However, the only mt transcripts detected in the Dk trypanosomes were the preedited A6 and cox3 mRNA in the *T. equiperdum* strain STIB842 and never-edited cox1 in STIB818, both known to contain the respective genes in their maxicircles (Table 2).

To determine whether the mt mRNAs in the full-size maxicircle strain STIB842 undergo editing, we performed quantitative real-time (q)PCR on cDNA from these cells with primers directed against selected preedited [A6; ribosomal protein S12 (RPS12); cox2; maxicircle unknown reading frame 2 (MURF2)], edited (A6; RPS12; cox2; MURF2), and never-edited transcripts [cox1; NADH-dehydrogenase subunit 4 (ND4) (SI Table 3)]. All reactions were performed in triplicate, including those for determination of the expression of nuclear-encoded β-tubulin and 18S rRNA transcripts, used as references for calculations of the relative abundances of the mt mRNAs. The levels of all examined transcripts in the PS and BS of *T. brucei* strain 29–13 were as described (2), and the A6, MURF2, RPS12, and cox2 mRNAs were edited (Fig. 3*B*). However, although the *T. equiperdum* STIB842 has a full set of maxicircle genes, editing was confined to transcripts that require only maxicircle-encoded gRNAs, namely cox2 and MURF2 (Fig. 3*B*). The *T. equiperdum* strain STIB818 has a 9-kb deletion in maxicircle but still retains genes for RPS12, cox1, and ND4; the mRNAs testify to the ongoing transcription of the maxicircle (Fig. 3*A*). Only preedited RPS12 mRNA was detected in this strain (Fig. 3*B*). Because missing minicircle-encoded gRNAs have restricted editing in the STIB842 strain to the usage of maxicircle-encoded gRNA genes, we wondered which components of the editing machinery are present in these Dk cells. We confirmed the presence of all tested proteins involved in editing (MRP1, MRP2, TbRGG1, RBP16, and TbTUT1) in the essayed strains, including Ak *T. evansi* STIB805 (Fig. 4*A*). Moreover, even in the total absence of minicircles in this strain (Fig. 2*B*), the minicircle-binding protein UMSBP and the mt DNA polymerase IC are still produced and imported into the organelle (Fig. 4*A*).

We tested the presumption that the metabolism of Dk/Ak trypanosomes is similar to that of the BS of *T. brucei*. Trypanosome alternative oxidase (TAO), which is strongly up-regulated in the BS, was revealed to be similarly abundant in the Dk/Ak cells (Fig. 4*A*). Antibodies against subunits of ATPase (F_1 subunit β and F_0 subunit b) recognized their target in all lysates, but this essential complex was down-regulated in *T. evansi* (Fig. 4*A*). Proteins confined to the PS *T. brucei* (see also Northern blot in Fig. 3*A*), such as the nuclear-encoded cox6, Rieske Fe-S protein, trypanosome-specific subunit of cytochrome oxidase (trCO4), cytochrome *c* (CytC), and apocytochrome c_1 (apoC_1), were absent from the BS, regardless of their species affiliation (Fig. 4*A*). Both insect (PS) and mammalian stages (BS) of *T. brucei* differ strikingly in their sensitivity to KCN and salicylhydroxamic acid (SHAM), the inhibitors of respiratory complexes and TAO, respectively. The BS of *T. brucei* STIB920 and the *T. equiperdum* and *T. evansi* strains use TAO as their sole electron acceptor (Fig. 4*B*; SI Fig. 13).

Because the membrane potential was shown to be upheld by F_1-ATP synthase in the DK strain 164, which contains a mutated γ subunit to compensate for the loss of the putative A6 subunit (21), we sequenced the gene for the γ subunit in 19 Dk/Ak strains. In the relevant region, which is highly conserved among all known members of the genus *Trypanosoma* (Fig. 5 *Top*), the Dk/Ak strains show either a deletion or a mutation. With one exception (STIB842), the deletion or mutation was present only in one allele of what is a single-copy gene in *T. brucei* (Fig. 5 *Middle*). Sequence analysis of the γ subunit cDNAs in STIB810 confirmed that both alleles are transcribed, but 90% mRNAs are derived from the mutated allele, indicating it is more highly expressed (Fig. 5 *Bottom*). Membrane potential was virtually identical in all tested Dk/Ak strains and *T.*

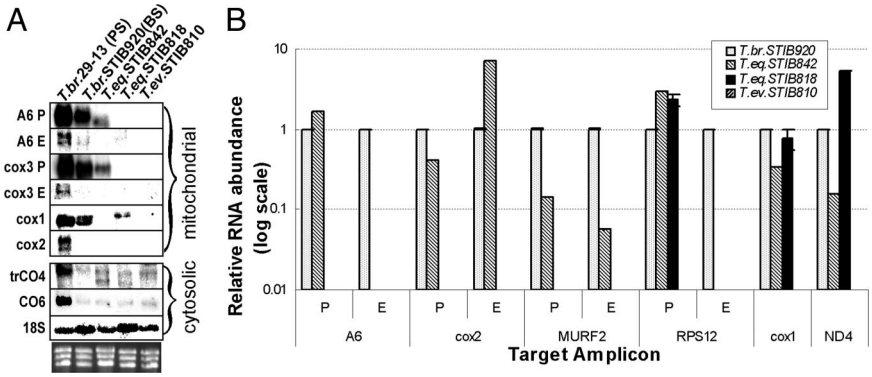

Fig. 3. Transcript levels (*A*) and RNA editing (*B*). (*A*) Levels of mt and cytosolic transcripts detected by Northern blotting in representative strains of *T. brucei*, *T. equiperdum*, and *T. evansi*. P, preedited; E, edited; A6, ATP synthase subunit 6; cox1–3, cytochrome oxidase subunits 1–3; trCO4, trypanosome cytochrome oxidase subunit 4; CO6, cytochrome oxidase subunit 6; 18S, 18S ribosomal RNA. As a control, the gel was stained with EtdBr to visualize rRNA bands. (*B*) RNA editing of some mRNAs is affected in the Dk/Ak cells. Real-time PCR analysis of preedited, edited, and never-edited mRNAs, performed in triplicate on cDNAs. For each target amplicon, the relative change in RNA abundance was determined by using cytosolic transcripts of β-tubulin and 18S rRNA (data not shown) as internal references, because their transcription was not affected. The relative abundance of each examined transcript was plotted on a logarithmic scale: 1.0 represents the level in BS of *T. brucei* STIB920; A6, ATPase subunit 6; cox2, cytochrome oxidase subunit 2; MURF2, maxicircle unknown reading frame 2; RPS12, ribosomal protein S12; never-edited cox1 mRNA; and ND4, NADH-dehydrogenase subunit 4.

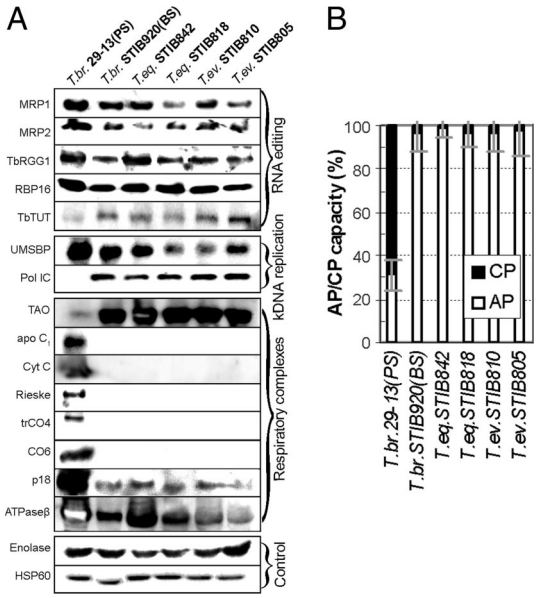

Fig. 4. Protein levels (*A*) and respiration (*B*). (*A*) Levels of mt and cytosolic proteins detected by Western blotting in strains of *T. brucei*, *T. equiperdum*, and *T. evansi*. MRP1/2, mtRNA-binding proteins 1/2; TbRGG1, editing-associated RGG1 protein; RBP16, RNA-binding protein 16; TbTUT, terminal uridyl transferase; UMSBP, universal minicircle sequence binding protein; POL IC, mt DNA polymerase IC; apo C_1, apocytochrome Cyt C_1; Cyt C, cytochrome *c*; Rieske, Rieske Fe-S protein; trCO4, trypanosome cytochrome oxidase subunit 4; CO6, cytochrome oxidase subunit 6; p18, ATP synthase subunit b; ATPase β, ATP synthase subunit β; hsp60, heat shock protein 60. (*B*) Relative contribution of TAO-mediated pathway (AP) and cytochrome-mediated pathway (CP) in *T. brucei* PS and BS, and the Dk/Ak strains. The amount of O_2 consumption inhibited by KCN was measured as the CP capacity. The mean and the SD values of three experiments are shown.

brucei, showing that a noncanonically composed ATP synthase (Fig. 4*A*) is sufficient for its maintenance (SI Fig. 14).

Neither the deletion nor the absence of the maxicircle kDNA has an impact on kinetoplast morphology, which retains its characteristic disk-like structure in the Dk strains (Fig. 6 *A–D*). The only cells in which electron microscopy failed to detect any kDNA disk were the Ak strains, which completely lack minicircles (Fig. 6*E*).

We addressed the controversial issue of taxonomy and species assignment of the Dk/Ak trypanosomes using the spliced leader

Fig. 5. Amino acid (*Top* and *Middle*) and nucleotide (*Bottom*) alignment of a highly conserved part of the γ subunit of ATP synthase.

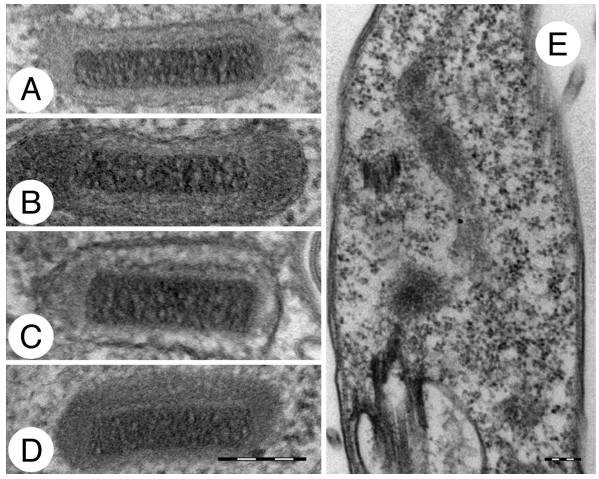

Fig. 6. Electron microscopy of kinetoplasts in fixed cells. (*A*) *T. brucei* STIB920, (*B*) *T. equiperdum* STIB842, (*C*) *T. equiperdum* STIB818, (*D*) *T. evansi* STIB810, and (*E*) *T. evansi* STIB805. (Scale bar, 200 nm.)

(SL) RNA gene. We sequenced 59 nonreiterative SL RNA genes with their intergenic regions from 21 Dk/Ak strains. Because pronounced intragenomic variability was confined to the most variable part of the intergenic region, the amplicons could always be unambiguously aligned. Sequences were aligned with a complete set of 26 SL RNA genes from *T. brucei* 927, incomplete sets of newly sequenced (14 SL RNA sequences), and available SL RNA genes for *T. brucei* strains 29–13, EATRO-HN and STIB920, and *T. brucei gambiense*, analyzed by neighbor joining and shown as an unrooted tree (Fig. 7). Because of a limited amount of phylogenetic information in the ≈1.4-kb region, bootstrap support is generally low. However, two distant clusters of the *T. brucei* SL RNA sequences obtained from the EATRO-HN and 29–13 strains are intermingled with *T. equiperdum* sequences. The *T. evansi* sequences are confined to half of the tree but are interspersed with *T. equiperdum* and *T.b. gambiense* SL RNA sequences (Fig. 7).

Discussion

For >100 years *T. brucei*, *T. equiperdum*, and *T. evansi* have been considered separate species, based on differences in the mode of transmission, host range and pathogenicity, and longstanding understanding that *T. equiperdum* retains at least a part of maxicircle kDNA, whereas *T. evansi* completely lost it (6, 9, 12). Our data show that the Dk/Ak strains of *T. equiperdum* and *T. evansi* have evolved from *T. brucei* after losing the capacity to faithfully replicate their kDNA.

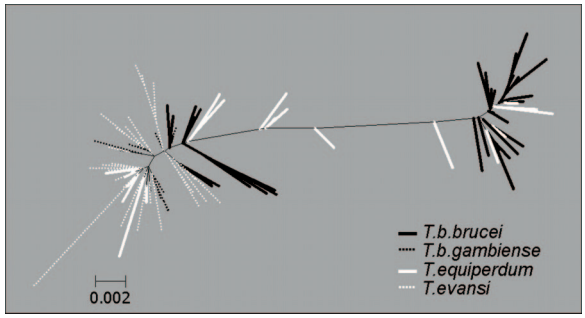

Fig. 7. Neighbor-joining clustering of the SL RNA repeats from *Trypanosoma* species. Alignment was performed by using CLUSTALW with gap opening weight = 15 and gap extension weight = 6.6.

RNA editing is essential in *T. brucei* for both PS and BS (22). However, the selective pressure to retain the full array of minicircle gRNA genes, a prerequisite for fully functional editing, will no longer exist in the absence of the tsetse fly infective stage (PS). This possibility exists because respiratory complexes III and IV are down-regulated in the BS, and many of the mt-encoded genes are subunits of these complexes. A notable exception is the putative A6 subunit of ATP synthase, which is essential for maintaining membrane potential in both PS and BS (21, 23). Its mRNA is edited by ≈20 gRNAs located on numerous kDNA minicircles, whereas hundreds of gRNAs needed for decoding of at least 11 mRNAs in the PS are unnecessary for the BS (2, 3). Therefore, in the mammalian stage, the minicircles may no longer be essential. Although unfaithful kDNA replication in the PS will result in the loss of essential gRNA(s) (24), leading to death, the BS may lose many gRNAs, because most encode information not essential in this stage, with the exception of the A6-specific gRNAs.

The loss of gRNA genes entails the inability of the parasite to transform into the insect PS. Therefore, transmission can only be by haematophagous insects or blood exchange during coitus. The subsequent homogenization of minicircles will lead to the loss of the A6-specific gRNAs, disrupting editing of the still essential A6 subunit. This pressure will likely select cells with a mutation in the γ subunit of ATP synthase, enabling the parasite to compensate for the lack of the A6 subunit, thus allowing survival. Computer simulations of minicircle-sequence class plasticity show that many unnecessary classes may be lost within a few hundred generations, whereas it may take tens of thousands of generations before the last few classes are lost (24), showing how vulnerable trypanosomes are in their vertebrate host to the loss of gRNA genes unnecessary for the BS (see below).

Our data show that the first step toward Dk is the homogenization of minicircles, followed by some deletion in the maxicircles. Because we found no strains with maxicircles that progressively accumulated mutations, we assume that fragility of the mt genome makes it prone to deletions. The maxicircles are thereafter lost altogether, and the demise of kDNA is completed by a total elimination of minicircles in the Ak cells. A consequence of minicircle homogenization is that the mt RNAs cannot be properly edited. Even with the number of minicircle-encoded gRNA genes dropping from several hundreds in *T. brucei* to only approximately eight in the Dk strains, the protein machinery underlying editing remains intact, using maxicircle-encoded gRNAs. This is the case in the maturation of cox2 and MURF2 mRNAs, which are edited by *cis*- and *trans*-acting maxicircle gRNAs, respectively. In the latter case, editing is drastically reduced, presumably because the MURF2 gRNAs are also supplied by minicircle genes. Unexpectedly, components of all of the characterized multiprotein complexes involved in editing are still present in the Ak strains, which lack any nucleic acids in their organelle, a situation mimicked in laboratory-induced Dk *T. brucei* (25).

RNA editing and kDNA replication are baroque processes, requiring dozens to hundreds of proteins (2, 3, 5). However, it is the unfaithful replication and/or segregation of minicircles that is the trigger of kDNA loss. As with the editosome proteins, replication proteins such as mtDNA polymerase IC and UMSBP remain abundantly present even in the absence of their substrates. (Note that the absence of maxicircles does not impact the structure of the kDNA disk.) Without selective pressure, the now-useless organellar nucleic acids are doomed, with the weird twist that proteins involved in their replication, transcription, and editing remain despite an apparent redundancy. Because not even the Ak strains are devoid of these proteins, dozens of such proteins continue to be synthesized and imported into the DNA-lacking mitochondrion, testifying to a stunning lack of "communication" between the organelle and the nucleus in these primitive flagellates.

This situation may be an indication that the Dk/Ak trypanosomes diverged from *T. brucei* fairly recently, because they still retain genes rendered unnecessary by the loss of the mt genome. However, another factor may account for the persistence of these unneeded genes. In contrast to other eukaryotes, trypanosome protein-coding genes are organized as polycistronic transcription units (26). Comparative analysis of the genomes of *T. brucei*, *T. cruzi*, and *Leishmania major* has revealed a tendency for maintaining gene order (27). It may be difficult to lose specific editing and kDNA replication/maintenance genes without major rearrangements of the chromosomes.

We have discovered intermediate steps in the process of kDNA loss, which was unexpected because *T. brucei* is an ancient protist, split from *T. cruzi* ≈100 Mya (28), whereas the loss of nonessential parts of the kDNA may have happened within decades (24). One would expect *T. brucei* either with intact kDNA or totally devoid of it. This conundrum can be resolved by postulating a continuous appearance of new strains outside Africa with nonfunctional kDNA that at some point reach the Ak state. The loss of kDNA, combined with the lack of the genetic recombination in the insect vector, amounts to a selective disadvantage of these strains, eventually leading to their elimination and replacement by newly evolved strains following the same path. An alternative explanation would be that humans have caused this process recently, by transporting infected animals out of the African tsetse belt. The transformation into the Dk and eventually the Ak cells enabled these flagellates to spread out of Africa and become the most widespread pathogenic trypanosome (8).

No substantial differences have been found between *T. brucei* and the Dk/Ak strains other than in the kDNA (9, 12, 29). The SL RNA intergenic region is a multicopy marker suitable for discrimination between closely related trypanosomatid isolates (30, 31). The SL RNA sequences derived from *T. equiperdum* and *T. evansi* strains are intermingled with the *T. brucei* and *T.b. gambiense* sequences, none of which form a species-specific cluster. The paraphyly of *T. equiperdum* and *T. evansi* is further supported by the strain-specific mutations in the highly conserved γ subunit and by the fact that the *T. equiperdum* strains differ in the last abundant minicircle class. These independent genetic traits suggest that any strain of *T. brucei* can serve as a source of a Dk/Ak lineage.

The absence of monophyly and the short genetic distance from *T. brucei* strains imply that the species category is inappropriate for *T. equiperdum* and *T. evansi*. The available evidence suggests they are the equivalents in *T. brucei* of the *petite* mutants of *Saccharomyces cerevisiae* and other yeasts. Similarly as the *petite* mutants, the Dk/Ak cells are respiratory-deficient, have an accelerated mutation rate in the γ subunit of ATP synthase, and a disrupted mt genome, which can be easily and completely lost upon EtdBr treatment (32). In the *petite* mutants of yeast, it has been postulated that allele-specific mutations in the α and γ subunits result in the formation of an aberrant ATP synthase that can prevent proton leakage, which allows their survival (33). A similar effect of one such mutation has been experimentally confirmed (21).

We propose that the Dk/Ak mutants occur spontaneously and frequently in *T. brucei*, which is the case for the *petite* mutants in *S. cerevisiae*. In both systems, the mutants do not represent a monophyletic assembly but rather strains arising independently and by (slightly) different mechanisms. It would not be practical for the veterinary community to label *T. equiperdum* and *T. evansi* as *petite* mutants of *T. brucei*. It has been proposed that single or a few gene(s) conferring the ability to occupy a new niche is sufficient to justify the rank of subspecies in a trypanosome (12). We propose that the rank of subspecies may be assigned in the case of the absence, rather than presence, of some gene(s). In any case, *T. equiperdum* and *T. evansi* do not constitute monophyletic groups. We propose to rename them *T.b. equiperdum* and *T.b. evansi*. Our data strongly suggest that *T.b. equiperdum* and *T.b. evansi* represent intermediate stages of the continuous adjustments of *T. brucei* cells to life without kDNA.

Materials and Methods

Strains, DNA Analysis, and Light and Electron Microscopy. Trypanosomes were purified from mice by DE52 DEAE cellulose (Whatman) (ref. 34, with slight modifications). The kDNA network was isolated by sucrose gradient ultracentrifugation (35). MspI, MboI, HindIII, EcoRI, BamHI, HhaI, AsuII, TaqI, HaeIII, and RsaI were used for restriction analysis. Linearized mini- and maxicircles were ligated into pBlueScript SK$^-$ vector and sequenced (EU155057-EU155060 and EU185799-EU185800). Light and electron microscopy was as in ref. 36.

Southern, Northern, and Western Blot Analyses. Total DNA digested with TaqI was resolved in agarose gel, blotted, and hybridized with a radiolabeled probe. Total RNA was isolated by using Trireagent (Sigma); 10 μg was loaded on a 1% formaldehyde agarose gel, blotted, and cross-linked. Hybridization with a radiolabeled probe was as in ref. 37. Cell lysates were analyzed on a 12% SDS/PAGE gradient gel, blotted, and probed with a panel of antibodies following conditions described elsewhere (37, 38).

Sequence Analysis of ATP Synthase Subunit γ and SL RNA. Subunit γ of ATP synthase (EU185790–EU185798) and SL RNA (GeneBank accession nos. EU180634–EU180706) were amplified and sequenced as in refs. 21 and 31.

qPCR. Total RNA was isolated from cells and treated with the Turbo DNA-free kit (Ambion). Then cDNA was synthesized by using the SuperScript III reverse transcriptase (Invitrogen) with random hexamers. qPCR analysis was as in ref. 39. The relative abundance of RNAs was determined as in ref. 40.

Growth Curve of Strains and Post-Dyskinetoplastic Treatment. Mice were randomly grouped, and each group of four mice was infected with different strains through i.p. inoculation. Selected mice with parasitemia of $\approx 10^8$ cells per milliliter were inoculated with 10 μg/g of EtdBr (41). Parasitemia was assayed by counting trypanosomes from tail blood. Blood smears were stained with DAPI to determine the percentage of Dk/Ak cells.

Measurement of Respiration Rate and Membrane Potential. BS cells were collected via the DE52 column, washed, and resuspended in PSG at 1×10^7 cells per ml. Oxygen consumption and membrane potential of PS cells were as in ref. 37. Conditions for BS cells were adapted: incubation temperature increased to 37°C, inhibitors were added at 1.5-min intervals, and final concentration of SHAM was raised to 0.09 mM.

Transformation of Bloodstream Trypanosomes to PS. BS cells from infected blood were cultivated as in ref. 20. For the next 4 days, living cells were observed by fluorescence microscopy after 15-min staining with 250 nM Mitotracker red at 27°C.

ACKNOWLEDGMENTS. R. Brun (Swiss Tropical Institute, Basel), F. Claes (Institute of Tropical Medicine, Antwerp, Belgium), A. Dargantes (University of Gent, Merelbeke, Belgium), W. Gibson (University of Bristol, Bristol, U.K.), L. McInnes (Murdoch University, Murdoch, Perth, Western Australia), M. M. G. Teixeira (University of Sao Paulo, Sao Paulo, Brazil), and J.-L. Zhou (Shanghai Veterinary Research Institute, Shanghai, China) kindly provided strains or DNA; and P. T. Englund (Johns Hopkins University, Baltimore), M. D. Ginger (Lancaster University, Lancaster, U.K.), S. L. Hajduk (University of Georgia, Athens), G. C. Hill (Vanderbilt University, Nashville, TN), M. M. Klingbeil (University of Massachusetts, Amherst), P. A. M. Michels (University Catholique Louvain, Brussels), L. K. Read (State University of New York, Buffalo), J. Shlomai (Hebrew University, Jerusalem), L. Simpson (University of California, Los Angeles), and L. Vanhamme (Université Libre Brussels, Gosselies, Belgium) kindly provided antibodies. This work was supported by the Czech Republic (Grant 204/06/1558), the Czech Academy of Sciences (Grant A500960705), the Czech Ministry of Education (Grants LC07032 and 2B06129, to J.L.), and the National Science Foundation of China (Grants 30570245 and 30670275, to Z.-R.L.).

1. Simpson AGB, Stevens JR, Lukeš J (2006) The evolution and diversity of kinetoplastid flagellates. *Trends Parasitol* 22:168–174.
2. Lukeš J, Hashimi H, Zíková A (2005) Unexplained complexity of the mitochondrial genome and transcriptome in kinetoplastid flagellates. *Curr Genet* 48:277–299.
3. Stuart KD, Schnaufer A, Ernst NL, Panigrahi AK (2005) Complex management: RNA editing in trypanosomes. *Trends Biochem Sci* 30:97–105.
4. Shlomai J (2004) The structure and replication of kinetoplast DNA. *Curr Mol Med* 4:623–647.
5. Liu BY, Liu YN, Motyka SA, Agbo EEC, Englund PT (2005) Fellowship of the rings: the replication of kinetoplast DNA *Trends Parasitol* 21:363–369.
6. Schnaufer A, Domingo GJ, Stuart K (2002) Natural and induced dyskinetoplastic trypanosomatids: how to live without mitochondrial DNA. *Int J Parasitol* 32:1071–1084.
7. Besteiro S, Barrett MP, Riviere L, Bringaud F (2005) Energy generation in insect stages of *Trypanosoma brucei*: metabolism in flux. *Trends Parasitol* 21:185–191.
8. Lun Z-R, Desser SS (1995) Is the broad range of hosts and geographical distribution of *Trypanosoma evansi* attributable to the loss of maxicircle kinetoplast DNA? *Parasitol Today* 11:131–133.
9. Brun R, Hecker H, Lun Z-R (1998) *Trypanosoma evansi* and *T. equiperdum*: distribution, biology, treatment and phylogenetic relationship. *Vet Parasitol* 79:95–107.
10. Hoare CA (1972) *The Trypanosomes of Mammals* (Blackwell Scientific, Oxford).
11. Ventura RM, *et al.* (2000) Molecular and morphological studies of Brazilian *Trypanosoma evansi* stocks: The total absence of kDNA in trypanosomes from both laboratory stocks and naturally infected domestic and wild mammals. *J Parasitol* 86:1289–1298.
12. Gibson W (2007) Resolution of the species problem in African trypanosomes. *Int J Parasitol* 37:829–838.
13. Claes F, Buscher P, Touratier L, Goddeeris BM (2005) *Trypanosoma equiperdum*: master of disguise or historical mistake? *Trends Parasitol* 21:316–321.
14. Li F-J, Lai D-H, Lukeš J, Chen X-G, Lun Z-R (2006) Doubts about *Trypanosoma equiperdum* strains classed as *Trypanosoma brucei* or *Trypanosoma evansi. Trends Parasitol* 22:55–56.
15. Vanhollebeke B, *et al.* (2006) Human *Trypanosoma evansi* infection linked to a lack of apolipoprotein L-1. *N Engl J Med* 355:2752–2756.
16. Frasch ACC, *et al.* (1980) The kinetoplast DNA of *Trypanosoma equiperdum. Biochim Biophys Acta* 607:397–401.
17. Lun Z-R, Brun R, Gibson W (1992) Kinetoplast DNA and molecular karyotypes of *Trypanosoma evansi* and *Trypanosoma equiperdum* from China. *Mol Biochem Parasitol* 50:189–196.
18. Shu HH, Stuart K (1994) Mitochondrial transcripts are processed but are not edited normally in *Trypanosoma equiperdum* (ATCC 30019), which has kDNA sequence deletion and duplication. *Nucleic Acids Res* 22:1696–1700.
19. Riou GF, Saucier J -M (1979) Characterization of the molecular components in kinetoplast-mitochondrial DNA of *Trypanosoma equiperdum. J Cell Biol* 82:248–263.
20. Brun R, Schönenberger M (1981) Stimulating effect of citrate and cis-aconitate on the transformation of *Trypanosoma brucei* bloodstream forms to procyclic forms in vitro. *Z Parasitenkd* 66:17–24.
21. Schnaufer A, Clark-Walker GD, Steinberg AG, Stuart K (2005) The F_1-ATP synthase complex in bloodstream stage trypanosomes has an unusual and essential function. *EMBO J* 24:4029–4040.
22. Schnaufer A, *et al.* (2001) An RNA ligase essential for RNA editing and survival of the bloodstream form of *Trypanosoma brucei. Science* 291:2159–2162.
23. Brown SV, Hosking P, Li JL, Williams N (2006) ATP synthase is responsible for maintaining mitochondrial membrane potential in bloodstream form *Trypanosoma brucei. Eukaryot Cell* 5:45–53.
24. Simpson L, Thiemann OH, Savill NJ, Alfonzo JD, Maslov DA (2000) Evolution of RNA editing in trypanosome mitochondria. *Proc Natl Acad Sci USA* 97:6986–6993.
25. Domingo GJ, *et al.* (2003) Dyskinetoplastic *Trypanosoma brucei* contains functional editing complexes. *Eukaryot Cell* 2:569–577.
26. Tschudi C, Ullu E (1988) Polygene transcripts are precursors to calmodulin mRNAs in trypanosomes. *EMBO J* 7:455–463.
27. El-Sayed NM, *et al.* (2005) Comparative genomics of trypanosomatid parasitic protozoa. *Science* 309:404–409.
28. Stevens JR, Rambaut A (2001) Evolutionary rate differences in trypanosomes. *Infect Genet Evol* 1:143–150.
29. Artama WT, Agey MW, Donelson JE (1992) DNA comparisons of *Trypanosoma evansi* (Indonesia) and *Trypanosoma brucei* spp. *Parasitology* 104:67–74.
30. Thomas S, Westenberger SJ, Campbell DA, Sturm NR (2005) Intragenomic spliced leader RNA array analysis of kinetoplastids reveals unexpected transcribed region diversity in *Trypanosoma cruzi. Gene* 352:100–108.
31. Maslov DA, Westenberger SJ, Xu X, Campbell DA, Sturm NR (2007) Discovery and barcoding by analysis of spliced leader RNA gene sequences of new isolates of Trypanosomatidae from Heteroptera in Costa Rica and Ecuador. *J Eukaryot Microbiol* 54:57–65.
32. Chen XJ, Clark-Walker GD (2000) The petite mutations in yeasts: 50 years on. *Int Rev Cytol* 194:197–237.
33. Chen XJ, Clark-Walker GD (1995) Specific mutations in α and γ-subunits of F_1-ATPase affect mitochondrial genome integrity in the petite-negative yeast *Kluyveromyces lactis. EMBO J* 14:3277–3286.
34. Lanham SM, Godfrey DG (1970) Isolation of salivarian trypanosomes from man and other mammals using DEAE-cell. *Exp Parasitol* 28:521–534.
35. Pérez-Morga D, Englund PT (1993) The structure of replicating kinetoplast DNA networks. *J Cell Biol* 123:1069–1079.
36. Yurchenko V, Lukeš J, Xu X, Maslov DA (2006) An integrated morphological and molecular approach to a new species description in the Trypanosomatidae: the case of *Leptomonas podlipaevi* n. sp., a parasite of *Boisea rubrolineata* (Hemiptera: Rhopalidae). *J Euk Microbiol* 53:103–111.
37. Horváth A, *et al.* (2005) Down-regulation of the nuclear-encoded subunits of the complexes III, IV disrupts their respective complexes but not complex I in procyclic *Trypanosoma brucei. Mol Microbiol* 58:116–130.
38. Vondrušková E, *et al.* (2005) RNA Interference analyses suggest a transcript-specific regulatory role for mitochondrial RNA-binding proteins MRP1 and MRP2 in RNA editing and other RNA processing in *Trypanosoma brucei. J Biol Chem* 280:2429–2438.
39. Carnes J, Trotter JR, Ernst NL, Steinberg A, Stuart K (2005) An essential Rnase III insertion editing endonuclease in *Trypanosoma brucei. Proc Natl Acad Sci USA* 102:16614–16619.
40. Pfaffl MW (2001) A new mathematical model for relative quantification in real-time RT-PCR. *Nucleic Acids Res* 29:2002–2007.
41. Agbe SA, Yielding KL (1993) Effect of verapamil on antitrypanosomal activity of drugs in mice. *Acta Trop* 55:11–19.

Attached Publications

Part II. DYSKINETOPLASTIC *TRYPANOSOMA BRUCEI*

Hassan Hashimi, Vladislava Benkovičová, Petra Čermáková, De-Hua Lai, Anton Horváth and Julius Lukeš (2010). The assembly of F_OF_1-ATP synthase is disrupted upon interference of RNA editing in *Trypanosoma brucei*. *Int. J. Parasitol.* 40: 45-54.

This paper experimentally proves, albeit indirectly, that kDNA maxicircles indeed encode the A6 subunit, which is important to establish in light of the existence of Dk and Ak *T. brucei*. The study gets around the problem of net being able to directly manipulate the trypanosome mt genome by taking advantage of the differential phenotypes of RNAi-silencing of proteins involved in RNA editing and stability.

International Journal for Parasitology 40 (2010) 45–54

Contents lists available at ScienceDirect

International Journal for Parasitology

journal homepage: www.elsevier.com/locate/ijpara

The assembly of F_1F_O-ATP synthase is disrupted upon interference of RNA editing in *Trypanosoma brucei*

Hassan Hashimi [a], Vladislava Benkovičová [b], Petra Čermáková [b], De-Hua Lai [a], Anton Horváth [b], Julius Lukeš [a,*]

[a] Biology Centre, Institute of Parasitology, Czech Academy of Sciences, and Faculty of Biology, University of South Bohemia, České Budějovice (Budweis), Czech Republic
[b] Department of Biochemistry, Faculty of Natural Sciences, Comenius University, Bratislava, Slovakia

ARTICLE INFO

Article history:
Received 27 April 2009
Received in revised form 18 June 2009
Accepted 7 July 2009

Keywords:
RNA editing
ATP synthase
Mitochondrion
Trypanosoma
Respiratory complex
Membrane potential

ABSTRACT

Throughout eukaryotes, the gene encoding subunit 6 (ATP6) of the F_1F_O-ATP synthase (complex V) is maintained in mitochondrial (mt) genomes, presumably because of its high hydrophobicity due to its incorporation into the membrane-bound F_O moiety. In *Trypanosoma* species, a mt transcript that undergoes extensive processing by RNA editing has a very low sequence similarity to ATP6 from other organisms. The notion that the putative ATP6 subunit is assembled into the F_O sub-complex is ostensibly challenged by the existence of naturally occurring dyskinetoplastic (Dk) and akinetoplastid (Ak) trypanosomes, which are viable despite lacking the mtDNA required for its expression. Taking advantage of the different phenotypes between RNA interference knock-down cell lines in which the expression of proteins involved in mtRNA metabolism and editing can be silenced, we provide support for the view that ATP6 is encoded in the mt genome of *Trypanosoma* species and that it is incorporated into complex V. The reduction of the F_1F_O oligomer of complex V coincides with the accumulation of the F_1 moiety in ATP6-lacking cells, which also appear to lack the F_O ATP9 multimeric ring. The oligomycin sensitivity of ATPase activity of complex V in ATP6-lacking cells is reduced, reflecting the insensitivity of the Dk and Ak cells to this drug. In addition, the F_1 moiety of complex V appears to exist as a dimer in steady state conditions and contains the ATP4 subunit traditionally assigned to the F_O sub-complex.

1. Introduction

Trypanosoma brucei is a pathogen with a broad impact on the inhabitants of sub-Saharan Africa, sub-species of which are the causative agents of human sleeping sickness and ruminant nagana. The haemoflagellate switches between the tsetse fly vector and mammalian host, where it exists in the procyclic and bloodstream stages (PS and BS, respectively), respectively, and has to adapt to the different environments of the insect midgut and mammalian bloodstream. During its life cycle the parasite undergoes substantial physiological and morphological changes (Matthews, 2005), the transformation of its single mitochondrion belonging to the most dramatic of those (Vickerman, 1985). The mitochondrion in the BS is considerably reduced and appears to lack cristae (Schneider, 2001; Hannaert et al., 2003). This morphological difference, in addition to the absence of cytochrome-containing respiratory complexes III and IV, reflects the exclusivity of glycolysis in the energy metabolism of *T. brucei* in the glucose-rich bloodstream of the mammalian host. In contrast, the PS contains a fully developed mitochondrion, appearing as a reticulated structure meandering throughout the cytoplasm, with the participation of complexes III and IV in the generation of ATP via oxidative phosphorylation (Besteiro et al., 2005).

Although the BS has a reduced mitochondrion, it is hardly a dormant organelle, as it still requires the expression of the mitochondrial (mt) (kinetoplast) DNA (kDNA), consisting of thousands of interlocked minicircles and dozens of maxicircles (Shlomai, 2004; Liu et al., 2005). The latter molecules are the equivalents of classical mtDNA, containing genes required for the organelle's biogenesis, most of which encode subunits of the respiratory complexes. The expression of the majority of these genes is not as straightforward as in other eukaryotes however, as their maturation requires extensive RNA editing in the form of post-transcriptional insertion and/or deletion of uridines (U) in pre-ordained positions within the mRNA sequence. A diverse population of minicircles encode small guide (g) RNAs, which direct the enzymatic machinery encompassed by the editosome protein complex to properly edit the mRNAs (Lukeš et al., 2005; Stuart et al., 2005).

* Corresponding author. Address: Biology Centre, Institute of Parasitology, Czech Academy of Sciences, and Faculty of Biology, University of South Bohemia, Branišovská 31, 37005 České Budějovice (Budweis), Czech Republic. Tel.: +420 38 7775416; fax: +420 38 5310388.
E-mail address: jula@paru.cas.cz (J. Lukeš).

0020-7519/$36.00
doi:10.1016/j.ijpara.2009.07.005

Trypanosomes maintain the mt membrane potential ($\Delta\Psi$m) required for the import of essential proteins (Nolan and Voorheis, 1992; Bertrand and Hajduk, 2000) and Ca^{2+} (Vercesi et al., 1992). Typically, eukaryotes rely on respiratory complexes I, III and IV to pump protons outside of the mt matrix to generate $\Delta\Psi$m, and the latter two complexes indeed have such a role in the PS (Horváth et al., 2005). However, noteworthy experiments have shown that in the BS it is the F_OF_1-ATP synthase (complex V) that adopts the role of sustaining $\Delta\Psi$m (Vercesi et al., 1992; Schnaufer et al., 2005; Brown et al., 2006).

In a typical mitochondrion, complex V acts as a dynamo, driven by the flux of protons down the electrochemical gradient inherent in $\Delta\Psi$m, which is coupled to the production of ATP. Its mechanism of action can be explained by exploring the remarkably conserved structure of complex V. An extensive compositional study of the F_OF_1-ATP synthase in *T. brucei* (Zíková et al., 2009) has demonstrated the presence of most of the subunits comprising the core structure of the complex in bacteria, archea and eukaryotes (Boyer, 1997; Velours and Arselin, 2000), as well as several proteins that are unique to kinetoplastids. Complex V is composed of two parts: the hydrophobic F_O moiety embeds the complex into the mt inner membrane, while the F_1 sub-complex extends into the mt matrix. The F_O part is composed of one ATP6 subunit (subunit *a* in the mammalian nomenclature), one or two ATP4 (*b*) subunits and a ring of 10–15 ATP9 (*c*) subunits. Interaction between the F_O ATP4 and F_1 oligomycin sensitivity-conferring protein (OSCP) subunits forms the peripheral stalk, which is believed to comprise part of a stator running parallel to the central stalk (Mulkidjanian et al., 2007). The action of complex V is reversed in the BS, in which ATP is consumed in order to pump protons out of the matrix (Schnaufer et al., 2005; Brown et al., 2006).

The essential ATP6 subunit is retained in virtually all mt genomes, presumably due to its extreme hydrophobicity (Funes et al., 2002). In *T. brucei*, a pan-edited mt transcript, requiring information from an estimated 21 gRNAs for the insertion of 448 Us and deletion of 28 Us to render a translatable open reading frame (ORF), has been hypothesised to encode ATP6 (Bhat et al., 1990; Corell et al., 1993). Such an assignment was supported by analysis of the in silico translated product, revealing a similar hydropathy profile and low sequence similarity of the C-terminus to ATP6 orthologues from other species (Bhat et al., 1990). However, conclusive evidence for this speculative designation is missing (Stuart et al., 1997).

The notion that this pan-edited mRNA encodes the ATP6 subunit, and that it is assembled into the F_O moiety is, however, further complicated by the existence of natural and laboratory-induced dyskinetoplastic (Dk) and akinetoplastic (Ak) trypanosomes, which are viable despite a partial and complete loss of kDNA, respectively (Schnaufer et al., 2002). These cells are locked in the BS because they lack the mitochondrial-encoded subunits of the cytochrome-containing complexes III and IV, and are viable despite the absence of the ATP6 gene (Schnaufer et al., 2002). Yet RNA editing is essential in the BS of *T. brucei* (Schnaufer et al., 2001), suggesting that the product of ATP6 is not entirely dispensable. Furthermore, the consumption of ATP by the F_1 moiety of complex V is required for maintaining $\Delta\Psi$m, which is considered indispensable for the survival of any trypanosome, including the Dk and Ak strains (Schnaufer et al., 2005). One interpretation of these findings is that the protein product of the edited mRNA putatively assigned as ATP6 in the mt genome of *Trypanosoma* spp. is not incorporated into the F_O moiety, perhaps because it does not encode this subunit. Another explanation postulates that in the Ak cells mutations have evolved in the nuclear-encoded subunits of the complex to offset the absence of ATP6, in which the ATPase activity of the F_1 is uncoupled from the incomplete F_O that lacks proton pumping capacity. A single amino acid substitution in the C-terminus of the γ subunit from a laboratory-induced Dk strain was elegantly demonstrated to be such a mutation (Schnaufer et al., 2005), while additional mutations in the same region with a putative compensatory role were identified in several natural Ak strains (Lai et al., 2008). Consistent with such a scenario is the insensitivity of *Trypanosoma brucei evansi* to oligomycin, a specific inhibitor of F_O, to which the BS *T. brucei* remains susceptible (Opperdoes et al., 1976; Schnaufer et al., 2005). Furthermore, the putative ATP6 mRNA is edited in both PS and BS trypanosomes, while other transcripts are preferentially edited only in one of these stages (Stuart et al., 1997; Schnaufer et al., 2002).

Despite significant efforts during the last two decades, proteins translated from edited mRNAs remain elusive. To date, apocytochrome B (cyB) and cytochrome *c* oxidase subunit 2 (cox2) from the model trypanosomatid *Leishmania tarentolae* remain the only directly observed translation products of a moderately edited mRNA, as detected by Edman degradation of conspicuous protein signals (Horváth et al., 2000, 2002), whereas those translated from a pan-edited mRNA have yet to be found (Horváth et al., 2002; Panigrahi et al., 2009). Underscoring the invisible nature of these mt-encoded proteins is that they have not been detected in a proteomics survey of the organelle (Panigrahi et al., 2009). Furthermore, ATP6 was not detected in any of the isolations of complex V from *T. brucei* (Zíková et al., 2009) or the monoxenous flagellate *Crithidia fasciculata* (Speijer et al., 1997). Attempts to generate antibodies against proteins predicted from pan-edited RNAs using synthetic oligopeptides were also ineffective (A. Horváth and J. Lukeš unpublished data; Rob Benne and Dave Speijer, personal communication). Unfortunately, direct recombinant manipulation of kDNA is still not feasible despite valiant efforts (Sbicego et al., 1998; Schnaufer et al., 2000).

We have thus decided to address the translation and incorporation of the predicted ATP6 protein by taking advantage of the different phenotypes resulting from RNA interference (RNAi)-mediated silencing of two nuclear-encoded proteins involved in mtRNA metabolism: mtRNA binding protein 2 (MRP2) and kRNA editing proteins KREPA6 (summarised in Table 1). MRP2 with its partner MRP1 forms a heterotetrameric MRP1/2 complex, which facilitates annealing of gRNAs to their cognate mRNAs (Schumacher et al., 2006). RNAi knock-down (KD) of MRP2 in the PS resulted in the down-regulation of a subset of never-edited and edited mRNAs, with the important exception of ATP6 (Vondrušková et al., 2005), which consequently caused the disruption of complexes III and IV (Table 1) (Zíková et al., 2006). Since KREPA6 is a subunit of the editosome (Stuart et al., 2005), its depletion in the PS results in a general reduction of RNA editing, affecting mRNAs for subunits of complexes III and IV, as well as ATP6 (Table 1) (Tarun et al., 2008). Although the secondary effect of its silencing on the respiratory complexes was not directly investigated, their disruption is considered inevitable, since this outcome is observed

Table 1
Summary of mitochondrial transcripts affected by the RNA interference (RNAi) silencing of mitochondrial RNA binding protein 2 (MRP2) and kinetoplastid RNA editing protein 6 (KREPA6).

RNAi KD	Effect on mitochondrial RNAs						Reference
	I	III	IV	rRNA	RPS12	ATP6	
KREPA6	E	E	E	ND	E	E	Tarun et al. (2008)
MRP2	NE and E	E	NE	0	E	0	Vondrušková et al. (2005)

Mitochondrial RNAs: I = subunit of complex I (NADH dehydrogenase); III = subunit of complex III (cytochrome *c* reductase); IV = subunit of complex IV (cytochrome *c* oxidase); rRNA = mitoribosomal RNA; RPS12 = ribosomal protein subunit 12.
Effect: E = decrease in edited mRNA; NE = decrease in never-edited RNA; 0 = no effect; ND = not determined; KD – knock-down.

in the RNAi KD of the terminal uridylyl transferase required for gRNA maturation, which affected all edited mRNAs in a similar fashion (Aphasizhev et al., 2002; Nebohacova et al., 2004). Here we present several lines of evidence, albeit indirect, for the existence of a genuine ATP6 subunit of an apparently non-canonical complex V in the mitochondrion of PS *T. brucei*.

2. Materials and methods

2.1. Strains, cultivation and isolation of mitochondria

The *T. brucei* MRP2 and KREPA6 RNAi cell lines were described elsewhere (Vondrušková et al., 2005; Tarun et al., 2008). The PCR-generated fragment (forward primer with BamHI restriction site: 5′-TGGGATCCAACACTGCACCATGGATTG-3′; reverse primer with XhoI site: 5′-AAGCTCGAGTGGATGTTCTTTCCCCTC-3′; both restriction sites underlined) of ATP4 (p18) was cloned into the p2T7–177 vector. The ATP4 knock-down cell line was established by transformation of the parental 29-13 cell line with resulting cassette, as described elsewhere (Hashimi et al., 2008). All transgenic cells, as well as the 29-13 cell line, were cultivated in semi-defined media (SDM)-79 medium under conditions described elsewhere (Vondrušková et al., 2005). The *T. brucei* strain 920, *Trypanosoma brucei equiperdum* strain 818 and *T. b. evansi* strain 810 were described previously (Lai et al., 2008). The kinetoplast-mt vesicles from 5×10^8 non-induced and induced PS cells were isolated by hypotonic lysis as described elsewhere (Horváth et al., 2005). Pelleted mt vesicles were stored at −70 °C until required.

2.2. Quantitative real-time PCR

Quantitative real-time PCR (qPCR) reactions were performed as in Hashimi et al. (2008). Primers for amplification of pre-edited and edited mt mRNAs are as described elsewhere (Carnes et al., 2005), as are those for KREPA6 (Tarun et al., 2008). The primer pair for detection of MRP2 cDNA is MRP2-qPCR-Fw (5′-GAAGCTTGGCTG TGTCCTTC-3′) and MRP2-qPCR-Rv (5′-TGCGTCCGAATACGATTACA-3′). Relative RNA abundance between RNAi-induced and non-induced samples were calculated as described previously (Carnes et al., 2005; Hashimi et al., 2008; Lai et al., 2008; Tarun et al., 2008).

2.3. Measurement of ATPase activity and inhibition experiments

One milligram of mt proteins was resuspended in 1 ml of the TC buffer (0.2 M KCl; 10 mM Tris–HCl, pH 8.2; 2 mM $MgCl_2$). The reaction was started at room temperature by adding ATP to a the final concentration of 5 mM and after 5 min was stopped by mixing 95 µl aliquots with 5 µl of 3 M $CHCl_3$—COOH, incubated for 30 min on ice, and spun (16,000*g* for 10 min at 4 °C). Ninety microlitres of the supernatant were added to 1 ml of the Sumner reagent (8.8% [w/v] $FeSO_4$; 375 mM H_2SO_4; 6.6% [w/v] $(NH_4)Mo_7O_{24}$). After 15 min incubation at room temperature, absorbance of free P_i was measured at 610 nm. Parallel experiments were performed with untreated samples and those in the presence of 10 µg/ml oligomycin or 1 mM azide. Inhibition experiments were reproduced in 10 independent measurements from four RNAi inductions with parallel non-induced controls. Statistical significance of observed differences in inhibition data were determined by Student's *t*-test. $P < 0.05$ was considered significant.

2.4. In-gel activity staining and two-dimensional gel electrophoresis

For activity staining, 100 µg of mitochondrial lysate in 0.5 M aminocaproic acid and 2% dodecylmaltoside was loaded per lane and analysed on a 4–15% gradient blue native polyacrylamide (BN) PAGE gel as described elsewhere (Horváth et al., 2005). Immediately after the run, the gel was transferred into either ATPase reaction buffer (35 mM Tris; 270 mM glycine; 19 mM $MgSO_4$; 0,3% [w/v] $Pb(NO_3)_2$; 11 mM ATP) for overnight incubation, or into cytochrome oxidase buffer (50 mM sodium phosphate, pH 7.4; 1 mg/ml 3,3′-diaminobenzidine; 24 U/ml catalase; 1 mg/ml cytochrome *c*; 75 mg/ml sucrose) for 3 h staining, both by slow agitation. The ATPase activity appears as white and cytochrome *c* oxidase activity as brown precipitate. The resulting bands were quantified with the scanning densitometry ImageQuant program (Molecular Dynamics). The BN-PAGE gels for the first dimension of two-dimensional gel electrophoresis were prepared in the aforementioned fashion. The second dimension was resolved on 10% Tricine–SDS–PAGE gels as in Horváth et al. (2005) and Zíková et al. (2006).

2.5. Western blot analysis

After electrophoresis, the BN-PAGE gel was blotted on a nitrocellulose membrane and probed with polyclonal rabbit antibodies raised against complex V subunits (designation in parenthesis) of *C. fasciculata* (F_1 moiety) (Speijer et al., 1997), *L. tarentolae* (ATP4) (Bringaud et al., 1995) and *T. brucei* (ATP9) (Brown et al., 2006) were used at 1:1,000, 1:3,000 and 1:500 dilutions, respectively. Secondary α-rabbit antibodies (1:2,000) (Sevapharma) coupled to horseradish peroxidase were visualised according to the manufacturer's protocol using the ECL kit (Pierce).

2.6. Isolation of F_1 moiety of complex V by chloroform extraction

In a protocol adapted from Linnett et al. (1979), hypotonically-isolated mt vesicles from 4×10^8 cells were resuspended in 300 µl STE buffer (0.25 M sucrose; 20 mM Tris·HCl, pH 7.9; 2 mM EDTA), and sonicated 4 × 10 s with 30 s intervals. The sonicate was centrifuged at 100,000*g* for 30 min at 4 °C, and the pellet was then resuspended in 300 µl STE buffer. A 150 µl vol. of chloroform was added; the two phases were emulsified by vortexing for 10 s and spun in a microcentrifuge at maximum speed for 5 min at room temperature. The aqueous phase was transferred into a new centrifuge tube and ultracentrifuged at 100,000*g* for 30 min at 25 °C. The proteins present in the supernatant were concentrated to 0.4 µg/µl using Microcon YM-30 centrifugation filters (Millipore), in which the solvent buffer was replaced with the resuspension solution (0.5 M aminocaproic acid; 0.25% dodecylmaltoside). This sample was divided and stored overnight at either 0 °C or room temperature to assay for the cold lability of the isolated F_1 moiety. Approximately 5 µg of extracted proteins were loaded per lane of the BN-PAGE gel.

3. Results

3.1. Differential effect of KREPA6 and MRP2 RNAi silencing on ATP6 editing

Inhibition of cell growth was re-evaluated in the PS cells, in which the KREPA6 or MRP2 transcripts were down-regulated by RNAi (Figs. 1A and C). In agreement with previous reports (Vondrušková et al., 2005; Tarun et al., 2008), tetracycline-induced targeting of these transcripts by double-stranded RNA resulted in slower growth. Based on these results, subsequent experiments were performed using cells grown for 6 days in the presence or absence of tetracycline. This time-point was chosen since our study concerns a secondary phenotype affecting the respiratory complexes, a strategy already employed in similar studies (Aphasizhev et al., 2002; Nebohacova et al., 2004), taking advantage of the consequential results of the direct effect of these RNAi KDs on mtRNAs.

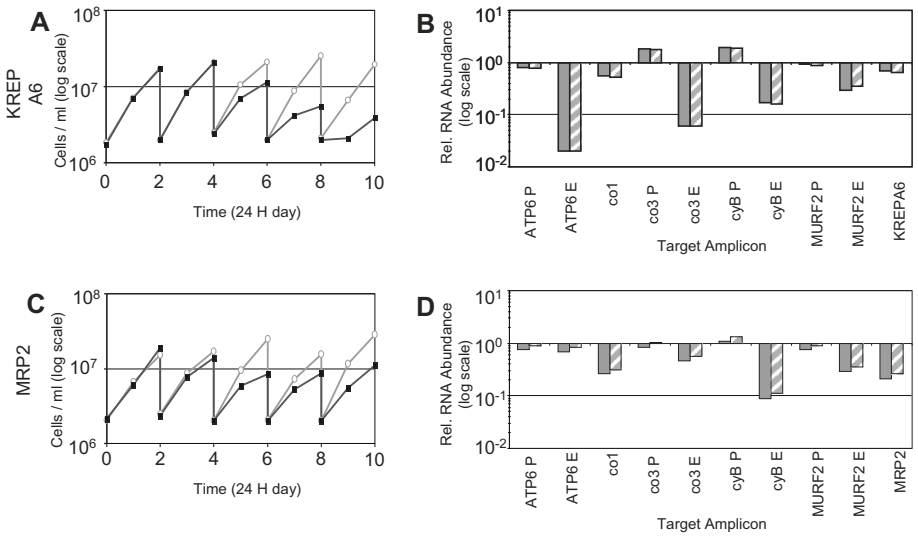

Fig. 1. Effect of RNA interference (RNAi) of mitochondrial RNA binding protein 2 (MRP2) and kinetoplastid RNA editing protein 6 (KREPA6) on procyclic stage (PS) *Trypanosoma brucei* cell growth and editing of ATP6 mRNA. The growth curves for non-induced (grey open circles) and induced KREPA6 (A) and MRP2 (C) RNAi knock-downs (black filled squares) are shown for a period of 10 days. The *y* axis is depicted on a log scale and represents the cell densities of the cultures measured every 24 h, as specified on the *x* axis. Real-time quantitative PCR analysis of a subset of mitochondrial-encoded RNAs, including pre-edited and edited ATP6 mRNAs, as well as the levels of the particular nuclear-encoded and RNAi-targeted mRNA (KREPA6 – B; MRP2 – D) was performed in triplicate on cDNAs generated from cells grown for 6 days in the presence or absence of tetracycline. For each target amplicon, the relative change in RNA abundance due to induction of RNAi-silencing of the particular transcript was determined by using cytosolic transcripts of β-tubulin (striped bar) and 18S rRNA (grey bar) as internal references, since their transcription was not affected by treatment. The following pre-edited (P) and edited (E) mRNAs were assayed: ATPase subunit 6 (ATP6), cytochrome oxidase subunits 1 (co1) and 3 (co3), cytochrome reductase subunit b (cyB) and maxicircle unknown reading frame 2 (MURF2). The average and median SD of the measured triplicate cycle threshold (C_t) values are 0.13 and 0.10, respectively.

In the original report, mtRNAs were assayed in the MRP2-silenced cells by poisoned primer extension (Vondrušková et al., 2005), showing reduction of edited and never-edited subunits of complexes III and IV, without an apparent effect on the ATP6 mRNA (Table 1). We have verified the differential effect on ATP6 editing in the KREPA6 and MRP2 KDs using a more sensitive method based on qPCR (Fig. 1B and D). Using previously described primers against pre-edited and edited ATP6 mRNAs (Carnes et al., 2005), editing of this transcript is virtually abolished in the KREPA6 KD 6 days after tetracycline induction compared with its non-induced counterpart (Fig. 1B). In contrast, MRP2-silencing only slightly reduces the levels of pre-edited and edited ATP6 mRNAs (Fig. 1D), perhaps reflecting a general role in RNA stability and/or processing, suggested for its eponymous complex (Schumacher et al., 2006; Vondrušková et al., 2005). Nonetheless, the level of the translatable ATP6 transcript is considerably closer to the wild-type level upon the depletion of MRP2 compared with KREPA6.

A subset of the mt-encoded RNAs for subunits of respiratory complexes III and IV, plus the edited maxicircle unidentified reading frame 2 (MURF2), were also assayed by reverse transcription-qPCR to confirm that they are affected as originally reported in the KREPA6 and MRP2 KDs (Vondrušková et al., 2005; Tarun et al., 2008) (summarised in Table 1). As expected, the never-edited transcript of complex IV co1 and the edited RNA of the complex III cyB were down-regulated upon MRP2 silencing (Fig. 1D). Editing of co3 and cyB was also reduced in the cells with down-regulated KREPA6 (Fig. 1B). Moreover, editing of the MURF2 transcript, encoding a protein of unknown function, was equally affected in both KDs (Fig. 1B and D).

3.2. The accumulation of the F_1 moiety and reduction of the F_1F_O oligomer of complex V in ATP6-depleted cells

Mitoplasts from the non-induced and tetracycline-induced KREPA6 and MRP2 KDs were subjected to BN-PAGE/in-gel ATPase activity experiments. Complex V was visualised by running these lysates on the BN gels, followed by staining for the in-gel ATPase activity (Fig. 2A). In all samples except the KREPA6-silenced one, relatively strong upper (~2,700 kDa) and lower (~900 kDa) activity bands are present, separated by a triplet of weaker bands. To investigate the identity of these bands, Western blots of parallel BN-PAGE gels were probed with antibodies immunodecorating subunits of complex V (Fig. 2B and C). The α-F_1 β subunit and α-ATP4 antibodies, used in previous studies of *T. brucei* (Schnaufer et al., 2005; Lai et al., 2008), were originally raised against the F_1 moiety of *C. fasciculata* (Speijer et al., 1997), and the F_O-subunit of *L. tarentolae* (Bringaud et al., 1995; Nelson et al., 2004). Both antibodies positively labelled all of the bands with the same relative intensities as the in-gel activity stain. Polyclonal antibodies raised against the *Saccharomyces cerevisiae* ATP4, 6 and 9 subunits did not cross-react with antigens present in *T. brucei* (data not shown).

Multiple bands are resolved by native gel electrophoresis that correspond to different forms of complex V in yeast, such as oligomers, dimers and monomers of F_1F_O, as well as free F_1 particles (Rak et al., 2007). We attempted to identify the form of complex V corresponding to the upper and lower bands by LC–MS/MS. However, only peptides from the catalytic F_1 moiety were identified in all three samples, plus ATP4, possibly because the technique is not amenable to identification of the hydrophobic peptides comprising F_O (data not shown). The presence of the canonical F_O ATP4 in all bands also complicated this task. We resorted to the assignment of these bands by how their estimated molecular weights match the canonical stoichiometry (Boyer, 1997; Velours and Arselin, 2000; Mulkidjanian et al., 2007) of the currently annotated complex V subunits in the GeneDB *T. brucei* genome database (http://www.genedb.org/genedb/tryp/). The top ~2,700 kDa band has been provisionally assigned as an oligomer of complex V. The identity of the lower ~900 kDa band was more difficult to ascertain, since its migration could correspond to either a monomer of complex V or a dimer of the F_1 sub-complex. We favour the latter interpretation, since the isolated F_1 moiety from *L. tarentolae* has been reported to have a similar ~900 kDa size and was also

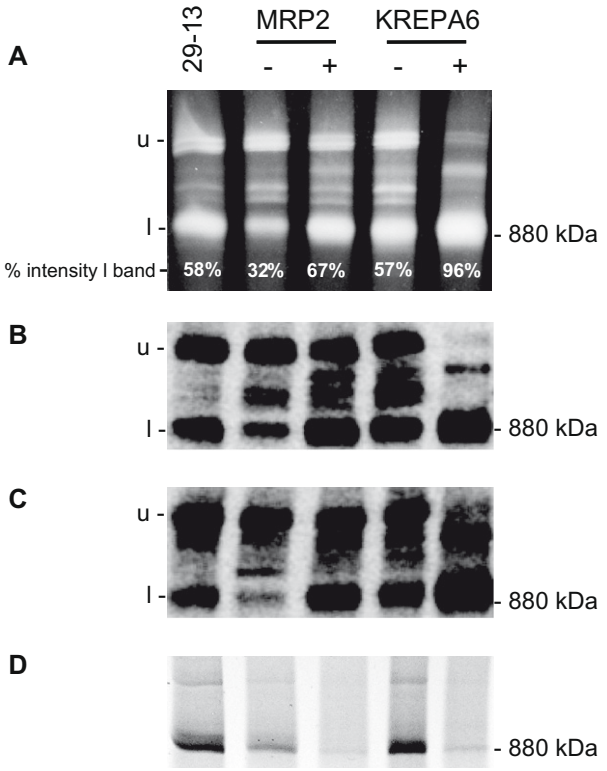

Fig. 2. Decrease in complex V F_1F_O oligomers and accumulation of free F_1 dimers in the ATP6-deficient cells. Mitochondrial complexes from mitochondrial RNA binding protein 2 (MRP2) and kinetoplastid RNA editing protein 6 (KREPA6) knock-down cells, grown for 6 days in the absence (–) or presence (+) of 1 μg/ml tetracycline (tet), respectively, were separated by 4–15% blue native gel electrophoresis and stained for in-gel ATPase activity. Protein (100 μg) was loaded in each lane. 29-13, procyclic *Trypanosoma brucei* strain 29-13. The position of the ferritin dimer molecular weight marker is indicated on the left; u – upper activity bands (~2,700 kDa); l – lower activity bands (~900 kDa). (A) In-gel ATPase activity. The percentage of density of the lower activity bands relative to that of total density of the combined bands is indicated at the bottom. (B) Western blot analysis with antibody against the F_1 β subunit. (C) Western blot analysis with antibody against the F_O subunit ATP4. (D) In-gel cytochrome *c* oxidase (complex IV) activity. The presence of complex IV on blue native gels was detected by incubation with the reaction buffer (see Section 2.4), which yields a dark precipitate upon catalysis by the complex. In both knock-down cell lines, the density of the activity band is reduced by ~70% compared with their non-induced counterparts.

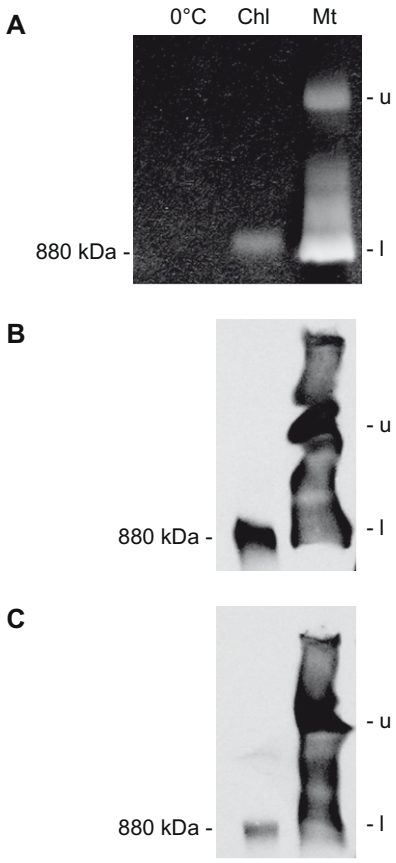

Fig. 3. ATP4 is present in the chloroform-extracted F_1 moiety of procyclic *Trypanosoma brucei*. Protein (100 μg) from lysates of hypotonically-isolated mitochondria and the equivalent of 5 μg of the F_1 moiety after chloroform extraction were resolved on a 4–15% blue native gel. The position of the ferritin dimer (Sigma) used as molecular weight marker is indicated on the left. 0 °C, F_1 moiety isolated by chloroform extraction and incubated overnight at 0 °C; Chl, F_1 moiety isolated by chloroform extraction and incubated overnight at room temperature; Mt, lysates from hypotonically-isolated mitochondria; u – upper activity bands (~2,700 kDa); l – lower activity bands (~900 kDa). After the run, the gel was either stained for in-gel ATPase activity (A), or transferred onto a nitrocellulose membrane and immunodecorated with polyclonal antibodies against either the F_1 β subunit (B) or the F_O subunit ATP4 (C).

proposed to be a dimer (Nelson et al., 2004), which corresponds with our results presented in Fig. 3.

The cells interfered against KREPA6 (in which editing of ATP6 is virtually abolished (Fig. 1B)), exhibit a reduction in oligomerization of complex V and a corresponding accumulation of free F_1 dimers (Fig. 2A). Semi-quantification of the ATPase bands reveal that the lowest doublet represents 96% of the sum density of the upper and lower bands in the lane containing the RNAi-silenced sample, while it comprises 57% and 58% in-gel activity from the untreated and parental cell lines, respectively (Fig. 2A). A similar enrichment of the free F_1 dimers was observed in KREN1 KD cells, in which one of the endonucleases essential for RNA editing has been ablated (data not shown) (Trotter et al., 2005). Such a disruption of complex V is not observed in the MRP2 KDs, in which editing of ATP6 persists, while the amounts of never-edited, pre-edited and edited mRNAs of the other mt-encoded subunits of respiratory complexes are decreased (Vondrušková et al., 2005; Zíková et al., 2006). The in-gel activity of free F_1 represents 32% and 67% of the sum density of the upper and lower bands observed in the non-induced and RNAi-induced samples, respectively (Fig. 2A). It should be noted that the percentage of the free F_1 moiety in the MRP2 KD cells grown in the absence of tetracycline is lower than that observed in the parental strain, while this particle represents a portion of the in-gel ATPase activity that is similar to that observed in the parental cell lines. Such a phenomenon has been previously reported in comparing the in-gel activities of complex IV in the non-induced and RNAi-induced KDs of complex III subunits (Horváth et al., 2005).

Western blot analyses with antibodies against the β and ATP4 subunits of the F_1 and F_O sub-complexes (Fig. 2B and C), respectively, also revealed the predominant accumulation of the F_1 moiety upon RNAi-silencing of KREPA6 compared with that in MRP2 KD as well as the parental cell lines. Furthermore, the immunopositive signals from either antibody are not observed in the upper band of the KREPA6-silenced samples, while they are in the other lanes. Interestingly, a signal corresponding to the uppermost of the three middle bands is observed in the KREPA6-silenced lane of both immunodecorated blots. As expected, the in-gel activity of complex IV was dramatically reduced by approximately 70% when either MRP2 or KREPA6 were down-regulated (Fig. 2D).

3.3. ATP4 is required for the integrity of F_1 moiety

The presence of ATP4, traditionally assigned to the F_O moiety (Boyer, 1997; Velours and Arselin, 2000), in the F_1 sub-complex

prompted us to further investigate this issue. The soluble F_1 moiety was obtained from hypotonically-isolated mt from the 29-13 cells, a method that purifies the sub-complex from the membrane-bound hydrophobic subunits (Linnett et al., 1979). The F_1 moiety was resolved on a BN gel together with the whole mt lysate. Upon staining by the in-gel ATPase activity assay, the lower band from the mt lysate migrates the same distance as the isolated F_1 moiety, whose activity is cold labile (Fig. 3A), a typical characteristic of the isolated F_1 sector. Western blot analyses using antibodies against the F_1 β subunit and F_O subunit ATP4 showed that both are present in the chloroform-extracted F_1 sub-complex (Fig. 3B and C). ATP4 was also reported to be present in the chloroform-extracted F_1 moiety of *C. fasciculata* (Speijer et al., 1997). Migration of the isolated F_O moiety in relation to the ferritin dimer suggests that it exists as a dimer, taking into account the sizes and stoichiometry of the F_1 subunits. This result is in agreement with the size of this particle in *L. tarentolae*, as determined by biochemical isolation (Nelson et al., 2004) or its visualisation by adenylylation with [α-^{32}P] ATP in native gels (Peris et al., 1997).

We also generated an RNAi KD of ATP4 to examine its position within the complex. Silencing of ATP4 resulted in slower growth of the PS cells (Fig. 4A). After 90 h of RNAi-induction, the steady-state level ATP4 protein was virtually eliminated (Fig. 4A, inset), which was the time-point chosen for subsequent experiments. In-gel ATPase activity and Western blot analysis using an antibody against the β subunit showed that the level of the catalytic portion of complex was decreased upon down-regulation of ATP4 (Figs. 4B and C). This result is reminiscent of the apparent destabilization of the β subunit of F_1 upon silencing of its partner, the α subunit, and vice versa (Schnaufer et al., 2005; Brown et al., 2006), which may be an indication that ATP4 also interacts directly with this moiety. This interpretation is consistent with its apparent association with the chloroform-isolated F_1 particle, as well as its interaction with the F_1 OSCP subunit of complex V. Another possibility is that this antibody recognises a genuine F_1 subunit and not the canonical F_O ATP4 subunit. In any case, it is clear that this protein plays a role in maintaining the integrity of the F_1 moiety.

3.4. Formation of the F_O ATP9 multimeric ring is disrupted in the absence of ATP6

Two-dimensional gel electrophoresis was employed to further examine complex V in the KREPA6 KDs, since a polyclonal antibody against ATP9, a subunit forming the multimeric ring of the F_O sub-complex, appears to recognise proteins resolved under denaturing conditions. Native complexes of RNAi cell lines grown in the presence or absence of tetracycline were separated on BN gels in the first dimension followed by SDS–PAGE in the second dimension to break apart individual subunits. As seen in the Western blot in Fig. 5A, the β subunit and ATP4 have been detected in the upper and lower bands (as visualised by in-gel ATPase activity), as well as in the middle bands. However, ATP9 is confined to the region corresponding to the upper bands, and is present to a lesser degree in the middle bands (Fig. 5A). In the KREPA6-silenced samples, ATP4 and F_1 are concentrated in the lowest bands, while ATP9 is undetectable, presumably because in the absence of ATP6, it cannot be assembled into the complex and is degraded (Fig. 5B). This finding further supports the notion that the lower band represents the F_1 moiety.

3.5. Sensitivity to oligomycin is decreased in ATP6-depleted mitoplasts

The Ak trypanosome *T. b. evansi* is insensitive to oligomycin, a specific inhibitor of the F_O subunit (Schnaufer et al., 2005; Opperdoes et al., 1976). We investigated the possibility that the KREPA6-depleted cells may exhibit a decrease in sensitivity to oligomycin

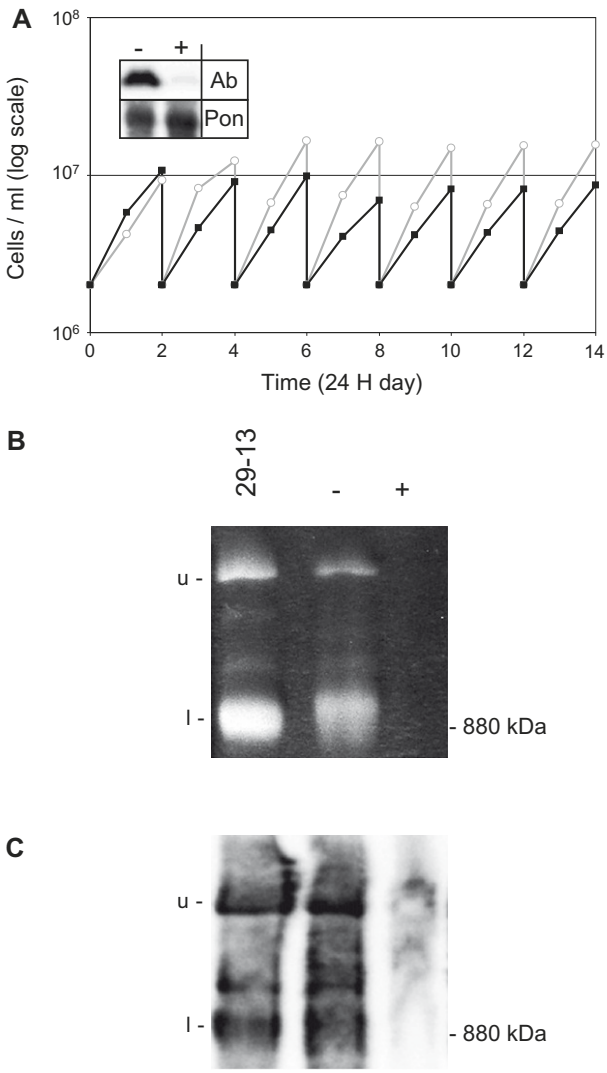

Fig. 4. Down-regulation of ATP4 results in slower growth and disassembly of the F_1 moiety. (A) The growth curves for non-induced (grey open circles) and RNA interference (RNAi)-induced cells (black filled squares) are shown for a period of 14 days and depicted as in Fig. 1A. Inset displays the down-regulation of the ATP4 protein after 90 h of RNAi-induction (+) compared with the non-induced cells (−), as determined by Western blot analysis (Ab). Ponceau staining of the membrane is shown as a loading control (Pon). (B) Complex V from mitochondrial lysates of the *Trypanosoma brucei* 29-13 parental cell line, as well as the ATP4 RNAi knock-down cell line grown for 90 h in the absence (−) and presence (+) of tetracycline, was resolved on a 4–15% blue native gel and visualised by the in-gel ATPase activity assay, as in Fig. 2A. The upper (u, ~2,700 kDa) and lower (l, ~900 kDa) bands, in addition to the position of the ferritin dimer marker (880 kDa), are indicated on the left and right, respectively. Protein (100 μg) was loaded in each lane. (C) Visualisation of F_1 β subunit after the blue native gel was transferred to nitrocellulose and probed with specific antibody. Labelling as in Fig. 2B.

that would be reminiscent of the behaviour of the ATP6-lacking Ak cells. The ATPase activity of hypotonically-isolated mt from the non-induced and RNAi-induced KREPA6 and MRP2 KDs, as well as the parental 29-13 cells, were assayed for the release of P_i in the presence of 10 μg/ml oligomycin and 1 mM azide, which inhibit the F_1 sub-complex (Fig. 6), compared with samples without inhibitors. The observed ~40% reduction of ATPase activity by either inhibitor in mt from the 29-13 cell is similar to what has been previously reported for the BS trypanosomes (Schnaufer et al., 2005). Down-regulation of KREPA6 results in more than 50% lower sensitivity to oligomycin, compared with the non-induced cells, while both cell lines do not differ in their sensitivity to azide (Fig. 6). The observed changes in oligomycin sensitivity are statistically

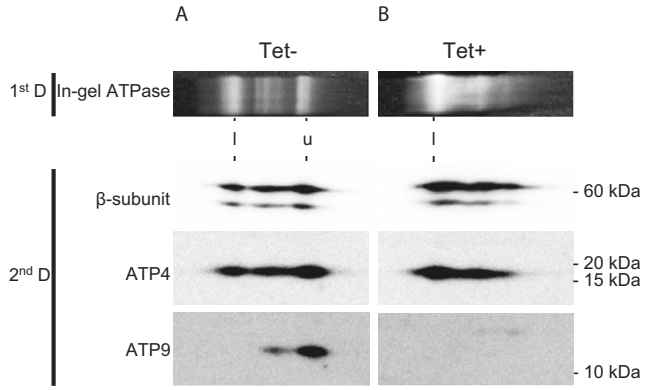

Fig. 5. Incorporation of F_O ATP9 into complex V in the presence and absence of ATP6. Complex V from *Trypanosoma brucei* kinetoplastid RNA editing protein 6 (KREPA6) knock-down cell lines grown for 6 days in the absence (A) and presence (B) of 1 μg/ml tetracycline, were resolved by two-dimensional (2D) gel electrophoresis. Native mitochondrial complexes were separated on a 4–15% blue native gel (1st D), as described in Fig. 1. Complex V was subsequently visualised by in-gel ATPase activity and the upper ~2,700 kDa (u) and lower ~900 kDa (l) bands are indicated just below. The individual subunits of the complexes were separated by 10% Tricine–SDS–PAGE (2nd D), transferred to nitrocellulose and probed with antisera against the F_1 β-subunit, ATP4 and ATP9. These antibodies are indicated on the left. Molecular weight markers are specified on the right.

significant ($P = 0.0288$), while fluctuations in azide inhibition are not ($P = 0.4907$), as determined by the Student's *t*-test. The MRP2 KD cells also exhibit somewhat reduced sensitivity to oligomycin, although they remain more susceptible to the drug than the KREPA6-silenced cells. This relatively minor decrease in sensitivity of the MRP2-silenced cells is not statistically significant (oligomycin $P = 0.1810$; azide $P = 0.5199$), and may be due to the slight decrease of edited ATP6 mRNA, as revealed by qPCR (Fig. 1D).

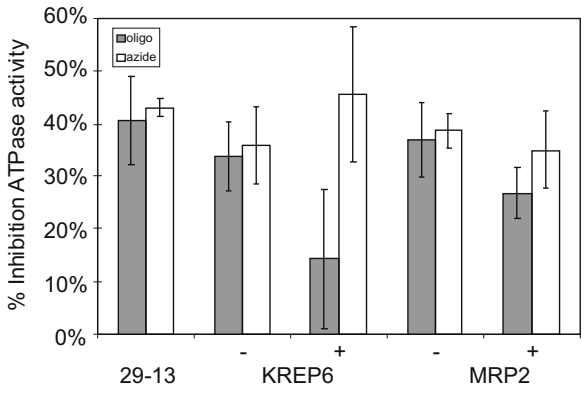

Fig. 6. ATP6-depleted cells exhibit reduced sensitivity to the F_O inhibitor oligomycin. Inhibition of the in vitro ATPase activity of complex V by 10 μg/ml of oligomycin (grey bar), which targets the F_O moiety and 1 mM azide (white bar), interfering with the F_1 moiety, was assayed. Hypotonically-isolated mitochondria from the parental *Trypanosoma brucei* 29-13 cell line and from the mitochondrial RNA binding protein 2 (MRP2) and kinetoplastid RNA editing protein 6 (KREPA6) knock-down (KD) cells, grown for 6 days in the absence (−) and presence (+) of 1 μg/ml tetracycline, were solubilised and incubated with 5 mM ATP. The release of free P_i was measured by absorbance at 610 nm. The vertical axis depicts average percentage of inhibition of ATPase compared with the untreated samples. For both inhibitors, three independent experiments using mitochondria from the 29-13 cells and six each from individual RNA interference-induced and non-induced KREPA6 and MRP2 KDs were performed. Error bars indicate the SD among the 10 individual experiments. The statistical significance of % inhibition of ATPase activity by oligomycin was $P = 0.0288$ and $P = 0.1810$ between induced (+) and non-induced (−) KREPA6 and MRP2 KD cells, respectively, as determined by Student's *t*-test. *P*-values for changes in sensitivity to azide inhibition were $P = 0.4907$ and $P = 0.5199$ for KREPA6 and MRP2 tet + and − samples, respectively.

3.6. Prevalence of the uncoupled F_1 moiety in Dk and Ak trypanosomes

In the induced KREPA6 KD cells, the accumulation of the F_1 moiety is apparent in the absence of the edited ATP6 mRNA (Fig. 2A). Therefore, in the BN-PAGE gels we have assayed the in-gel ATPase activity of lyzed mt purified from the Ak and Dk strains of *T. b. evansi* and *T. b. equiperdum*, respectively, as well as from the PS and BS of *T. brucei* (Fig. 7A). Two prominent bands are apparent in the BS that correspond to the top ~2,700 kDa F_1F_O-oligomer and the bottom ~900 kDa F_1-dimer present in the PS cells. In the Dk and Ak strains only the lower ATPase activity band is apparent, however, with a higher intensity than that found in the BS cells (Fig. 7A). The BS and the Dk trypanosomes show considerably lower in-gel ATPase activity than the PS cells, which is in agreement with previous observations that complex V is down-regulated in the stages infecting mammals (Brown et al., 2001). The native forms of complex V were also visualised by Western blot analysis using an antibody directed against the β subunit, revealing the predominance of the F_1 dimer in the Dk and Ak trypanosomes (Fig. 7B). This finding was confirmed by Western blot analysis of two-dimensional gels resolving complex V, as in Fig. 4, showing that in the Ak *T. b. evansi* strain, the ATP4 subunit is restricted to the lower ATPase activity band.

4. Discussion

Since its seminal discovery (Benne et al., 1986), RNA editing in the mitochondrion of kinetoplastid flagellates has become an intensely studied process (Lukeš et al., 2005; Stuart et al., 2005). There was very little doubt that the edited transcripts are translated into mt proteins. Still, to date only two proteins produced from a moderately edited and never-edited mt mRNA were shown to exist (Horváth et al., 2000, 2002), while all attempts to detect predicted protein products of pan-edited mRNAs failed. An extensive analysis of mt transcripts in *T. brucei* and *L. tarentolae*, however, detected a widespread occurrence of partially edited molecules, with fully edited ones representing only a tiny fraction of the mtRNA population (Decker and Sollner-Webb, 1990; Sturm and Simpson, 1990). In the particular case of pan-edited ATP6, only 10% of analysed molecules could serve as blueprints for the synthesis of the canonical ATP6 subunit of complex V (Ochsenreiter et al., 2008).

Although perhaps inefficiently produced, the product of pan-edited ATP6 mRNA appears to be incorporated into the complex V of *Trypanosoma* species, as supported by several lines of evidence presented in this study. The PS cells, in which the 20S editosome subunit KREPA6 was RNAi-silenced, are deficient of ATP6 compared with cells with down-regulated MRP2. Indeed, RNA editing is generally inhibited by silencing proteins directly involved in the process, invariably affecting mt mRNAs encoding subunits of respiratory complexes, whereas complex V escaped such interference in the latter KD. The absence of the ATP6 protein caused by the disruption of RNA editing significantly reduces the level of F_1F_O oligomers of complex V, while an accumulation of the released F_1 moiety, the soluble portion of the ATP synthase, takes place. The KREPA6 KD represents an ATP6-lacking background compared with the MRP2-silenced cells, in which oligomerization occurs at approximately the wild-type level. This situation is also apparent in Dk and Ak trypanosomes, which naturally lack the capacity to express ATP6, since they also exhibit an accumulation of the free F_1 moiety compared with BS *T. brucei* containing the F_1F_O oligomers. Furthermore, we show that ATP9, the subunit responsible for the formation of the multimeric ring of the F_O moiety, is reduced in the absence of ATP6. Finally, the sensitivity of complex V to oligomycin is reduced in cells lacking the capacity

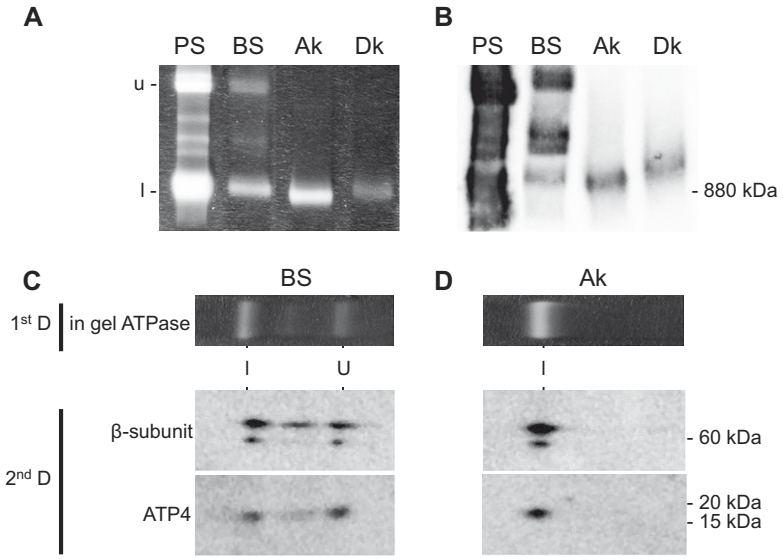

Fig. 7. The prevelance of the F_1 moiety in naturally akinetoplastic *Trypanosoma brucei evansi* and dyskinetoplastic *Trypanosoma brucei equiperdum*. (A) In-gel ATPase activity. Mitochondrial protein complexes were resolved and stained as described in Fig. 1. Protein (100 μg) was loaded in each lane. BS, bloodstream *T. brucei*, strain 920; PS, procyclic *T. brucei* strain 29-13; Ak, akinetoplastic bloodstream *T. b. evansi*, strain 810; Dk, dyskinetoplastic bloodstream *T. b. equiperdum*, strain 818; u – upper activity band (~2,700 kDa); l – lower activity bands (~900 kDa). (B) Western blot analysis with antibody against the F_1 β subunit under the conditions described in Fig. 2. The position of the ferritin dimer molecular weight marker is indicated on the left. (C) Two-dimensional (2D) gel electrophoresis resolution of complex V in the bloodstream *T. brucei* (BS) was performed and labelled as described in detail in Fig. 5. Western blots were probed with antisera against ATP4. (D) Two-dimensional gel electrophoresis resolution of complex V in the akinetoplastic bloodstream *T. b. evansi*, strain 810 (Ak) was performed and labelled as described in detail in Fig. 5. Western blots were probed with antisera against ATP4.

to edit ATP6 mRNAs, which correlates with the situation documented for the Dk trypanosomes naturally lacking ATP6 (Schnaufer et al., 2005).

The deletion of ATP6 in *S. cerevisiae* resulted in the loss of F_1F_O dimers and monomers and the appearance of free F_1, as revealed by in-gel ATPase activity staining (Rak et al., 2007). Our findings in *T. brucei* are consistent with these results. However, ATP9 appears to still be assembled into complex V in the yeast null mutants (Rak et al., 2007). In trypanosomes, the absence of ATP6 appears to destabilise the F_O moiety, as implied by the diminished ATP9 ring, leading to the apparent deficiency of F_1F_O formation. This observation indicates that ATP6 may not be the last subunit incorporated into complex V as has been suggested for the yeast orthologue, as a measure to prevent a premature leakage of protons by the incomplete sub-complex (Tzagoloff et al., 2004; Rak et al., 2007).

Several other differences between kinetoplastid and canonical complex V were underscored by this study. It appears that ATP4, a subunit traditionally assigned to F_O, is firmly associated with F_1 in these flagellates, confirming the same observation made in *C. fasciculata* (Speijer et al., 1997). This situation is possible given its role in the formation of the peripheral stalk by direct interaction with the F_1 OSCP subunit. Alternatively, the designation of this protein associated with the F_1 particle as ATP4 may have been premature. However, it is clear that this protein is associated with the soluble portion of complex V.

This study also suggests that the F_1 subunit exists as a dimer across kinetoplastid flagellates, as originally reported for *L. tarentolae* (Peris et al., 1997; Nelson et al., 2004). While this notion varies from the report of Zíková and colleagues (2009), who show that the *T. brucei* F_1 moiety migrates at the same rate as the ferritin monomer (440 kDa) by native gel electrophoresis, it is consistent with the size of a complex with self-adenylylating activity in both of these trypanosomatid species (Peris et al., 1997), which was later shown to be the F_1 particle (Nelson et al., 2004). This inconsistency may be due to technical aspects of the electrophoresis, such as differences in the range of the acrylamide gradient. Dimerization of this moiety has been reported in other eukaryotes (Dienhart et al., 2002). However, in these organisms it is promoted by an inhibitor protein in response to conditions that lead to diminished $\Delta\Psi$m, such as oxygen deprivation, in order to conserve ATP that would otherwise be spent by reversal of complex V (Dienhart et al., 2002). The chloroform-extracted F_1 moiety of *T. brucei*, whose migration in native gels also suggests a dimer conformation, is apparently not inhibited, since they maintain in-gel ATPase activity. Thus, its apparent dimerization is formed by another mechanism. Homodimers of the ATP4 subunit, assigned to the membrane-bound F_O sub-complex, have been demonstrated to form between two adjacent complexes in yeast (Spannagel et al., 1998). The possibility that this subunit is present in the F_1 sector in trypanosomes may mediate the dimerization of this moiety. Nonetheless, the occurrence of F_1 as a dimer appears to be unique to these organisms.

Although the presented data suggest, to our knowledge for the first time, that a protein product of a pan-edited RNA is indeed translated, and in this case assembled into complex V, due to the limitations of our system, we were unable to directly address the question whether ATP6 is essential for ATP synthesis. A logical experiment would be to test in vitro ATP synthase activity (Allemann and Schneider, 2000) from mt isolated from the analysed KDs. However, this assay requires that the capacity to generate $\Delta\Psi$m is preserved, which both KDs lack due to the inevitable disruption of proton pumping complexes III and IV. Nevertheless, the notion that ATP6 is indispensable is further supported by reports that RNA editing is essential in the BS *T. brucei*, which uses complex V to sustain $\Delta\Psi$m (Schnaufer et al., 2001). The maturation of the ATP6 mRNA by this process is redundant in the Dk and Ak trypanosomes because compensatory mutations in some of the F_1 subunits allow the conversion of ATP^{4-} to ADP^{3-} (Schnaufer et al., 2005; Lai et al., 2008). The antipodal exchange of these substrates by the ATP/ADP carrier appears to maintain $\Delta\Psi$m along the inner mt membrane.

Acknowledgements

We thank Salvador Tarun, Yuko Ogata and Ken Stuart (Seattle Biomedical Research Institute, USA) for the gift of the KREPA6 and KREN1 cell lines and for facilitating mass spectroscopy analysis. We also thank Noreen Williams (State University of New York, Buffalo, USA), Larry Simpson (University of California, Los Angeles, USA), Jean Velours (Institut de Biochimie et Génétique Cellulaires, Bordeaux, France), Rob Benne and Dave Speijer (University of Amsterdam, Netherlands) for kindly providing antibodies. We thank Alena Zíková and Zdeněk Verner for fruitful discussions, Achim Schnaufer (University of Edinburgh, Scotland) for critical reading of the manuscript and Alexander Tzagoloff (Columbia University, New York City, USA) for helpful comments. This work was supported by the Grant Agency of the Czech Republic (204/06/1558), the Grant Agency of the Czech Academy of Sciences (A500960705), the Czech Ministry of Education (LC07032, 2B06129 and 6007665801), the Grant Agency of the Slovak Ministry of Education and the Slovak Academy of Sciences (1/3241/06 and 1/0393/09).

References

Allemann, N., Schneider, A., 2000. ATP production in isolated mitochondria of procyclic *Trypanosoma brucei*. Mol. Biochem. Parasitol. 111, 87–94.

Aphasizhev, R., Sbicego, S., Peris, M., Jang, S.-H., Aphasizheva, I., Simpson, A.M., Rivlin, A., Simpson, L., 2002. Trypanosome mitochondrial 3′ terminal uridylyl transferase (TUTase): the key enzyme in U-insertion/deletion RNA editing. Cell 108, 637–648.

Benne, R., Van den Burg, J., Brakenhoff, J.P., Sloof, P., Van Boom, J.H., Tromp, M.C., 1986. Major transcript of the frameshifted *coxll* gene from trypanosome mitochondria contains four nucleotides that are not encoded in the DNA. Cell 46, 819–826.

Bertrand, K.I., Hajduk, S.L., 2000. Import of a constitutively expressed protein into mitochondria from procyclic and bloodstream forms of *Trypanosoma brucei*. Mol. Biochem. Parasitol. 106, 249–260.

Besteiro, S., Barrett, M.P., Riviere, L., Bringaud, F., 2005. Energy generation in insect stages of *Trypanosoma brucei*: metabolism in flux. Trends Parasitol. 21, 185–191.

Bhat, G.J., Koslowsky, D.J., Feagin, J.E., Smiley, B.L., Stuart, K., 1990. An extensively edited mitochondrial transcript in kinetoplastids encodes a protein homologous to ATPase subunit-6. Cell 61, 885–894.

Boyer, P.D., 1997. The ATP synthase – a splendid molecular machine. Ann. Rev. Biochem. 66, 717–749.

Bringaud, F., Peris, M., Zen, K.H., Simpson, L., 1995. Characterization of two nuclear-encoded protein components of mitochondrial ribonucleoprotein complexes from *Leishmania tarentolae*. Mol. Biochem. Parasitol. 71, 65–79.

Brown, S.V., Chi, T.B., Williams, N., 2001. The *Trypanosoma brucei* mitochondrial ATP synthase is developmentally regulated at the level of transcript stability. Mol. Biochem. Parasitol. 115, 177–187.

Brown, S.V., Hosking, P., Li, J., Williams, N., 2006. ATP synthase is responsible for maintaining mitochondrial membrane potential in bloodstream form *Trypanosoma brucei*. Eukaryot. Cell 5, 45–53.

Carnes, J., Trotter, J.R., Ernst, N.L., Steinberg, A., Stuart, K., 2005. An essential RNase III insertion editing endonuclease in *Trypanosoma brucei*. Proc. Natl. Acad. Sci. USA 102, 16614–16619.

Corell, R.A., Feagin, J.E., Riley, G.R., Strickland, T., Guderian, J.A., Myler, P.J., Stuart, K., 1993. *Trypanosoma brucei* minicircles encode multiple guide RNAs which can direct editing of extensively overlapping sequences. Nucleic Acids Res. 21, 4313–4320.

Decker, C.J., Sollner-Webb, B., 1990. RNA editing involves indiscriminate U changes throughout precisely defined editing domains. Cell 61, 1001–1011.

Dienhart, M., Pfeiffer, K., Schagger, H., Stuart, R.A., 2002. Formation of the yeast F_1F_0-ATP synthase dimeric complex does not require the ATPase inhibitor protein, Inh1. J. Biol. Chem. 277, 39289–39295.

Funes, S., Davidson, E., Claros, M.G., van Lis, R., Perez-Martinez, X., Vazquez-Acevedo, M., King, M.P., Gonzales-Halphen, D., 2002. The typically mitochondrial DNA-encoded ATP6 subunit of the F_1F_0-ATPase is encoded by a nuclear gene in *Chlamydomonas reinhardtii*. J. Biol. Chem. 277, 6051–6058.

Hannaert, V., Bringaud, F., Opperdoes, F.R., Michels, P.A.M., 2003. Evolution of energy metabolism and its compartmentation in kinetoplastida. Kinetopl. Biol. Dis. 2, 11–42.

Hashimi, H., Zíková, A., Panigrahi, A.K., Stuart, K.D., Lukeš, J., 2008. TbRGG1, a component of a novel multi-protein complex involved in kinetoplastid RNA editing. RNA 14 (14), 970–980.

Horváth, A., Berry, E.A., Maslov, D.A., 2000. Translation of the edited mRNA for cytochrome *b* in trypanosome mitochondria. Science 287, 1639–1640.

Horváth, A., Horáková, E., Dunajčíková, P., Verner, Z., Pravdová, E., Šlapetová, I., Cuninková, L., Lukeš, J., 2005. Down-regulation of the nuclear-encoded subunits of the complexes III and IV disrupts their respective complexes but not complex I in procyclic *Trypanosoma brucei*. Mol. Microbiol. 58, 116–130.

Horváth, A., Neboháčová, M, Lukeš, J., Maslov, D.A., 2002. Unusual polypeptide synthesis in the kinetoplast-mitochondria from *Leishmania tarentolae* – identification of individual de novo translation products. J. Biol. Chem. 277, 7222–7230.

Lai, D.-H., Hashimi, H., Lun, Z.-R., Ayala, F.J., Lukeš, J., 2008. Adaptation of *Trypanosoma brucei* to gradual loss of kinetoplast DNA: *T. equiperdum* and *T. evansi* are petite mutants of *T. brucei*. Proc. Natl. Acad. Sci. USA 105, 1999–2004.

Linnett, P.E., Mitchell, A.D., Partis, M.D., Beechey, R.B., 1979. Preparation of the soluble ATPase from mitochondria, chloroplasts, and bacteria by the chloroform technique. Methods Enzymol. 55, 337–343.

Liu, B., Liu, Y., Motyka, S.A., Agbo, E.E.C., Englund, P.T., 2005. Fellowship of the rings: the replication of kinetoplast DNA. Trends Parasitol. 21, 363–369.

Lukeš, J., Hashimi, H., Zíková, A., 2005. Unexplained complexity of the mitochondrial genome and transcriptome in kinetoplastid flagellates. Curr. Genet. 48, 277–299.

Matthews, K.R., 2005. The developmental cell biology of *Trypanosoma brucei*. J. Cell Sci. 118, 283–290.

Mulkidjanian, A.Y., Makarova, K.S., Galperin, M.Y., Koonin, E.V., 2007. Inventing the dynamo machine: the evolution of the F-type and V-type ATPases. Nat. Rev. Microbiol. 5, 892–899.

Nebohacova, M., Maslov, D.A., Falick, A.M., Simpson, L., 2004. The effect of RNA interference down-regulation of RNA editing 3′-terminal uridylyl transferase (TUTase) 1 on mitochondrial de novo protein synthesis and stability of respiratory complexes in *Trypanosoma brucei*. J. Biol. Chem. 279, 7819–7825.

Nelson, R.E., Aphasizheva, I., Falick, A.M., Nebohacova, M., Simpson, L., 2004. The I-complex in *Leishmania tarentolae* is an uniquely-structured F_1-ATPase. Mol. Biochem. Parasitol. 135 (35), 219–222.

Nolan, D.P., Voorheis, H.P., 1992. The mitochondrion in blood-stream forms of *Trypanosoma brucei* is energized by the electrogenic pumping of protons catalyzed by the F_1F_0-ATPase. Eur. J. Biochem. 209, 207–216.

Ochsenreiter, T., Cipriano, M., Hajduk, S.L., 2008. Alternative mRNA editing in trypanosomes is extensive and may contribute to mitochondrial protein diversity. PLoS One 3, e1566.

Opperdoes, F.R., Borst, P., Derijke, D., 1976. Oligomycin sensitivity of the mitochondrial ATPase as a marker for fly transmissibility and the presence of functional kinetoplast DNA in African trypanosomes. Comp. Biochem. Physiol. B – Biochem. Mol. Biol. 55, 25–30.

Panigrahi, A.K., Ogata, Y., Zíková, A., Anupama, A., Dalley, R.A., Acestor, N., Myler, P.J., Stuart, K.D., 2009. A comprehensive analysis of *Trypanosoma brucei* mitochondrial proteome. Proteomics 9, 434–450.

Peris, M., Simpson, A.M., Grunstein, J., Liliental, J.E., Frech, G.C., Simpson, L., 1997. Native gel analysis of ribonucleoprotein complexes from a *Leishmania tarentolae* mitochondrial extract. Mol. Biochem. Parasitol. 85, 9–24.

Rak, M., Tetaud, E., Godard, F., Sagot, I., Salin, B., Duvezin-Caubet, S., Slonimski, P.P., Rytka, J., di Rago, J.-P., 2007. Yeast cells lacking the mitochondrial gene encoding the ATP synthase subunit 6 exhibit a selective loss of complex IV and unusual mitochondrial morphology. J. Biol. Chem. 282, 10853–10864.

Sbicego, S., Schnaufer, A., Blum, B., 1998. Transient and stable transfection of *Leishmania* by particle bombardment. Mol. Biochem. Parasitol. 94, 123–126.

Schnaufer, A., Clark-Walker, G.D., Steinberg, A.G., Stuart, K., 2005. The F_1-ATP synthase complex in bloodstream stage trypanosomes has an unusual and essential function. EMBO J. 24, 4029–4040.

Schnaufer, A., Domingo, G.J., Stuart, K., 2002. Natural and induced dyskinetoplastic trypanosomatids: how to live without mitochondrial DNA. Int. J. Parasitol. 32, 1071–1084.

Schnaufer, A., Panigrahi, A.K., Panicucci, B., Igo Jr., R.P., Wirtz, E., Salavati, R., Stuart, K., 2001. An RNA ligase essential for RNA editing and survival of the bloodstream form of *Trypanosoma brucei*. Science 291, 2159–2162.

Schnaufer, A., Sbicego, S., Blum, B., 2000. Antimycin A resistance in a mutant *Leishmania tarentolae* strain is correlated to a point mutation in the mitochondrial apocytochrome *b* gene. Curr. Genet. 37, 234–241.

Schneider, A., 2001. Unique aspects of mitochondrial biogenesis in trypanosomatids. Int. J. Parasitol. 31, 1403–1415.

Schumacher, M.A., Karamooz, E., Zíková, A., Trantírek, L., Lukeš, J., 2006. Crystal structures of *Trypanosoma brucei* MRP1/MRP2 guide-RNA-binding complex reveals RNA matchmaking mechanism. Cell 126, 701–711.

Shlomai, J., 2004. The structure and replication of kinetoplast DNA. Curr. Mol. Med. 4, 623–647.

Spannagel, C., Vaillier, J., Arselin, G., Graves, P.-V., Grandier-Vazeille, X., Velours, J., 1998. Evidence of a subunit 4 (subunit b) dimer in favor of the proximity of ATP synthase complexes in yeast inner mitochondrial membrane. Biochim. Biophys. Acta 1414 (14), 260–264.

Speijer, D., Breek, C.K., Muijsers, A.O., Hartly, A.F., Berden, J.A., Albrecht, S.P., Samyn, B., Van Beeumen, J., Benne, R., 1997. Characterization of the respiratory chain from cultured *Crithidia fasciculata*. Mol. Biochem. Parasitol. 85, 171–186.

Stuart, K.D., Allen, T.E., Heidmann, S., Seifert, S.D., 1997. RNA editing in kinetoplastid protozoa. Microbiol. Mol. Biol. Rev. 61, 105–120.

Stuart, K.D., Schnaufer, A., Ernst, N.L., Panigrahi, A.K., 2005. Complex management: RNA editing in trypanosomes. Trends Biochem. Sci. 30, 97–105.

Sturm, N.R., Simpson, L., 1990. Partially edited mRNAs for cytochrome *b* and subunit III of cytochrome oxidase from *Leishmania tarentolae* mitochondria: RNA editing intermediates. Cell 61, 871–878.

Tarun Jr., S.Z., Schnaufer, A., Ernst, N.L., Proff, R., Deng, J., Hol, W., Stuart, K., 2008. KREPA6 is an RNA-binding protein essential for editosome integrity and survival of *Trypanosoma brucei*. RNA 14, 347–358.

Trotter, J.R., Ernst, N.L., Carnes, J., Panicucci, B., Stuart, K., 2005. A deletion site editing endonuclease in *Trypanosoma brucei*. Mol. Cell 20, 403–412.

Tzagoloff, A., Barrientos, A., Neupert, W., Hermann, J.M., 2004. Atp10p assists assembly of atp6p into the F_0 unit of the yeast mitochondrial ATPase. J. Biol. Chem. 279, 19775–19780.

Velours, J., Arselin, G., 2000. The *Saccharomyces cerevisiae* ATP synthase. J. Bioenerg. Biomembr. 32, 383–390.

Vercesi, A.E., Docampo, R., Moreno, S.N., 1992. Energization-dependent Ca^{2+} accumulation in *Trypanosoma brucei* bloodstream and procyclic trypomastigotes mitochondria. Mol. Biochem. Parasitol. 56, 251–257.

Vickerman, K., 1985. Developmental cycles and biology of pathogenic trypanosomes. Med. Bull. 41, 105–114.

Vondrušková, E., van den Burg, J., Zíková, A., Ernst, N.L., Stuart, K., Benne, R., Lukeš, J., 2005. RNA interference analyses suggest a transcript-specific regulatory role for MRP1 and MRP2 in RNA editing and other RNA processing in *Trypanosoma brucei*. J. Biol. Chem. 280, 2429–2438.

Zíková, A., Horáková, E., Jirků, M., Dunajčíková, P., Lukeš, J., 2006. The effect of down-regulation of mitochondrial RNA-binding proteins MRP1 and MRP2 on respiratory complexes in procyclic *Trypanosoma brucei*. Mol. Biochem. Parasitol. 149, 65–73.

Zíková, A., Schnaufer, A., Dalley, R.A., Panigrahi, A.K., Stuart, K.D., 2009. The F_0F_1-ATP synthase complex contains novel subunits and is essential for procyclic *Trypanosoma brucei*. . 5, e1000436.

Attached Publications

Part II. DYSKINETOPLASTIC *TRYPANOSOMA BRUCEI*

Zdeněk Paris[†], Hassan Hashimi[†], Sijia Lun, Juan D. Alfonzo and Julius Lukeš (2011). Futile import of tRNAs and proteins into the mitochondrion of *Trypanosoma brucei evansi. Mol. Biochem. Parasitol.* 176: 116-120.

This paper shows that mtRNA polymerase, GAPs 1 and 2 plus even tRNAs are imported into the mitochondrion of *Trypanosoma brucei evansi* even though the substrates for their function, mRNA, gRNA and fully assembled ribosomes (due to a lack of rRNA) are not present. I am co-first author on this publication.

[†]Co-first author

Molecular & Biochemical Parasitology 176 (2011) 116–120

Contents lists available at ScienceDirect

Molecular & Biochemical Parasitology

Short communication

Futile import of tRNAs and proteins into the mitochondrion of *Trypanosoma brucei evansi*

Zdeněk Paris[a,1], Hassan Hashimi[a,b,1], Sijia Lun[a,2], Juan D. Alfonzo[c], Julius Lukeš[a,b,*]

[a] Biology Centre, Institute of Parasitology, Czech Academy of Sciences, 37005 České Budějovice (Budweis), Czech Republic
[b] Faculty of Science, University of South Bohemia, 37005 České Budějovice (Budweis), Czech Republic
[c] Department of Microbiology and OSU Center for RNA Biology, The Ohio State University, Columbus, OH 43210, USA

ARTICLE INFO

Article history:
Received 22 June 2010
Received in revised form
17 December 2010
Accepted 22 December 2010
Available online 30 December 2010

Keywords:
Trypanosoma
tRNA
Protein import
Mitochondrion
Kinetoplast

ABSTRACT

Trypanosoma brucei brucei has two distinct developmental stages, the procyclic stage in the insect and the bloodstream stage in the mammalian host. The significance of each developmental stage is punctuated by specific changes in metabolism. In the insect, *T. b. brucei* is strictly dependent on mitochondrial function and thus respiration to generate the bulk of its ATP, whereas in the mammalian host it relies heavily on glycolysis. These observations have raised questions about the importance of mitochondrial function in the bloodstream stage. Peculiarly, akinetoplastic strains of *Trypanosoma brucei evansi* that lack mitochondrial DNA do exist in the wild and are developmentally locked in the glycolysis-dependent bloodstream stage. Using RNAi we show that two mitochondrion-imported proteins, mitochondrial RNA polymerase and guide RNA associated protein 1, are still imported into the nucleic acids-lacking organelle of *T. b. evansi*, making the need for these proteins futile. We also show that, like in the *T. b. brucei* procyclic stage, the mitochondria of both bloodstream stage of *T. b. brucei* and *T. b. evansi* import various tRNAs, including those that undergo thiolation. However, we were unable to detect mitochondrial thiolation in the akinetoplastic organelle. Taken together, these data suggest a lack of connection between nuclear and mitochondrial communication in strains of *T. b. evansi* that lost mitochondrial genome and that do not required an insect vector for survival.

1. Introduction

Trypanosoma brucei brucei is an evolutionary ancestral parasite, transmitted from one mammalian host to another by the blood-sucking tse-tse fly. While *T. b. brucei* is responsible for n'gana of livestock, African sleeping sickness of humans is caused by its subspecies *T. b. rhodesiense* and *T. b. gambiense*. Two other subspecies (*T. b. evansi* and *T. b. equiperdum*) are causative agents of surra and dourine, serious diseases afflicting mostly horses, water buffaloes and camels [1,2].

The single mitochondrion of *T. b. brucei* undergoes dramatic changes in the course of the life cycle. In the reticulated cristae-rich organelle of the procyclic stage parasitizing the tse-tse vector, functional cytochrome *c*-containing respiratory complexes capable of energy transduction are present [3]. The mitochondrion also contains alternative terminal oxidase (TAO), incomplete Krebs cycle and acetate:succinate CoA transferase cycle and other metabolic pathways. For energy production this active mitochondrion can utilize glycolytic substrates as well as various amino acids [4]. However, the bloodstream stage responsible for the disease in its vertebrate hosts harbors a mitochondrion, which is dramatically different from its procyclic counterpart by being repressed in numerous functions. The organelle is reduced in size, contains just a few cristae and lacks both Krebs cycle and respiratory complexes III and IV [5]. TAO is the only terminal oxidase [6] and membrane potential is upheld by the reverse action of the ATPase complex [7]. Yet even this mitochondrion is far from dormant, as replication and transcription of its kinetoplast (k) DNA, and extensive RNA editing and RNA processing remain fully active and essential [1,8–10]. This dual metabolism, in distinct life cycle stages, of a mitochondrion that occurs in a single copy per cell, makes it a very interesting and tractable model for exploring mechanisms that govern the switch from an active to an inactive mode.

Another approach that is particularly suitable for examining stage-specific differences of the mitochondrion involves comparisons of subspecies of *T. b. brucei*, which differ in terms of their kDNA content. One of these strains, *T. b. equiperdum*, has lost sig-

* Corresponding author at: Biology Centre, Institute of Parasitology, Branisovska 31, Czech Academy of Sciences, 37005 České Budějovice (Budweis), Czech Republic. Tel.: +420 38 7775416.
E-mail address: jula@paru.cas.cz (J. Lukeš).
[1] These authors contributed equally to this work.
[2] Present address: PROOF Centre of Excellence, St. Paul's Hospital, Vancouver, Canada.

0166-6851/$ – see front matter © 2010 Elsevier B.V. All rights reserved.
doi:10.1016/j.molbiopara.2010.12.010

nificant portions of its mitochondrial genome, while the organelle of some strains of *T. b. evansi* is totally devoid of kDNA [11–13]. These trypanosomes are therefore incapable of transmission by tsetse flies, and are locked into the bloodstream stage. Although their spreading among ungulate hosts relies solely on mechanical means of transmission, the lost dependence on the insect vector paradoxically allowed spreading of these trypanosomes outside of Africa [11,12,14]. Without the kDNA-encoded subunits a switch to the metabolically fully active procyclic organelle is impossible and *T. b. evansi* permanently depends on the glucose-rich environment of the vertebrate blood [11]. One can therefore postulate that any process found in its mitochondrion is genuinely associated with the bloodstream stage.

In a previous study, we have demonstrated that the akinetoplastic mitochondrion keeps importing proteins that are involved in kDNA replication, mitochondrial RNA editing and RNA processing [13]. While this occurrence is indeed not surprising for the organelle of the *T. b. brucei* bloodstream stage, it seems to be a counterintuitive phenomenon for *T. b. evansi*, as one would not predict efficient import of these proteins into a mitochondrion permanently devoid of DNA and RNA. As we show in this work, proteins involved in RNA synthesis and processing are still imported into the akinetoplastic mitochondrion of *T. b. evansi*, but in contrast to *T. b. brucei*, are non-essential. We also show for the first time that tRNAs are imported into and thiolated within the mitochondrion of *T. b. brucei* bloodstream stage, and imported into but not thiolated within the mitochondrion of *T. b. evansi*. This further supports the conclusion that subunits of respiratory complexes are required for neither tRNA [15], nor protein import.

2. Results and discussion

2.1. Proteins required for the bloodstream stage of T. b. brucei are non-essential for T. b. evansi

Despite its functional down-regulation and morphological reduction, numerous proteins are still imported into the mitochondrion of the bloodstream stage of *T. b. brucei*. Indeed, the RNA editing machinery, composed of proteins imported from the cytosol, is essential both at this and at the procyclic stage [8]. However, at least one key protein component, RNA editing ligase 1, of the editing machinery is dispensable in the mitochondrion of *T. b. evansi* [7]. It was of interest to test whether a ubiquitous protein, such as the mitochondrial RNA polymerase (mtRNAP) is also non-essential in these cells. To test this, we used dyskinetoplastic strain of *T. b. evansi* genetically engineered for overexpression of double-stranded RNA to facilitate RNA interference (RNAi) [7]. A p2T7-177 construct containing the same mtRNAP gene fragment used previously for RNAi in the *T. b. brucei* procyclic stage [16] was electroporated into both the *T. b. brucei* bloodstream stage and the *T. b. evansi* and transformants were selected using phleomycin. As no antibody is available against mtRNAP, the efficiency of RNAi was confirmed by quantitative real time PCR as described previously [10,13], with cDNA reverse-transcribed from RNA isolated from knockdown cell lines grown in medium that contained or lacked the RNAi-induction agent tetracycline (Fig. 1A, inset). Three days after RNAi induction similar downregulation of mtRNAP mRNA, namely 71 and 75% of the non-induced mRNA levels, was observed in *T. b. brucei* and *T. b. evansi* RNAi-silenced cells, respectively. This level of mtRNAP mRNA reduction was sufficient to inhibit growth of the bloodstream stage of *T. b. brucei* (Fig. 1A), which was expected as its expression was earlier shown to be essential in the procyclic stage [16]. However, ablation of the target mRNA in the dyskinetoplastic cells did not have any impact on their growth (Fig. 1A). Therefore, in contrast to *T. b. brucei*, mtRNAP is dispensable in *T. b. evansi*.

This result led us to a similar question with the guide (g) RNA associated protein 1 (GAP1), which is essential for both the procyclic and the bloodstream stages of *T. b. brucei* [10]. After electroporation with a linearized p2T7-177 vector containing a previously used fragment of the GAP1 gene [10], clonal cell lines were selected and RNAi induced as described above. At two and four days after RNAi induction, total cell lysates were collected and separated by SDS-PAGE and transferred to PVDF membranes, which were subsequently immunoprobed with anti-GAP1 antibodies, as well as with antibodies against cytosol-specific enolase. Under these conditions GAP1 expression is efficiently down-regulated when compared to the non-induced control (Fig. 1B; inset). Despite this down-regulation (Fig. 1B), no effect on cell growth was observed in the GAP1-silenced *T. b. evansi* cells, even after 10 days following RNAi induction. This result is in contrast to GAP1 down-regulation in *T. b. brucei* bloodstream cells, which exhibit growth inhibition after three days of RNAi induction [10]. We can therefore conclude that the elimination of mtRNAP and GAP1, two essential proteins in the *T. b. brucei* bloodstream stage, has no effect in the dyskinetoplastic *T. b. evansi*.

To confirm that GAP1 is imported into the mitochondrion of bloodstream *T. b. brucei* and *T. b. evansi*, as has been shown in the procyclic stage of the former sub-species, digitonin fractionation was performed [17,18] to separate the cell contents into their mitochondrial and cytosolic constituents using protocols slightly modified for a given stage. Proteins from total, cytosolic and mitochondrial fractions (10 μg/lane) were used for Western analysis as described above. The purity of fractions was assayed using antibodies against enolase and prohibitin [19], which are specific for cytosol and mitochondrion, respectively (Fig. 1C). An immunopositive signal was detected with the anti-GAP1 specific antibody in mitochondrial and total cell fractions in both cell-types (Fig. 1C), indicating its import into the organelle in the dyskinetoplastic trypanosomes despite its apparent redundancy (Fig. 1B).

GAP1, like the RNA editing ligase, is a highly specialized and rather unique mitochondrial protein [8,10,20]. However, mtRNAP is a virtually ubiquitous component of the aerobic eukaryotic mitoproteomes, with undisputed essentiality [16]. Therefore, its apparent futile import into a mitochondrion devoid of a genome in *T. b. evansi* has important consequences. Firstly, it is obvious that these proteins do not have any moonlighting functions other than in RNA metabolism. Second, the protein import machinery is totally independent on the genomic status of the organelle, as it apparently imports dozens or even hundreds of different proteins with no function in this mitochondrion and thus produced and imported in vain. It is puzzling that in an organism with an 8 h generation time, which thrives in an environment where it is under constant selective pressure from the host immune response and from competition for nutrients with other trypanosomes, no mechanism exists that would prevent this obviously wasteful behavior. It is also plausible that stringent regulation of protein-specific import may be more energy demanding than futile import of the non-essential proteins.

2.2. tRNAs are imported into the T. b. brucei bloodstream mitochondrion

It is now widely accepted that in procyclic *T. b. brucei*, due to the absence of tRNA genes in the kDNA network, all tRNAs have to be imported from the cytosol into the mitochondrion for translation to occur [21]. However, nothing is known about this process in the bloodstream stage. It is expected that despite significant differences in mitochondrial metabolism between both stages, protein translation and therefore tRNA import are still required. To date, indirect evidence is available for mitochondrial translation of at least one protein in this life cycle stage [7,22]. Furthermore, nothing is known

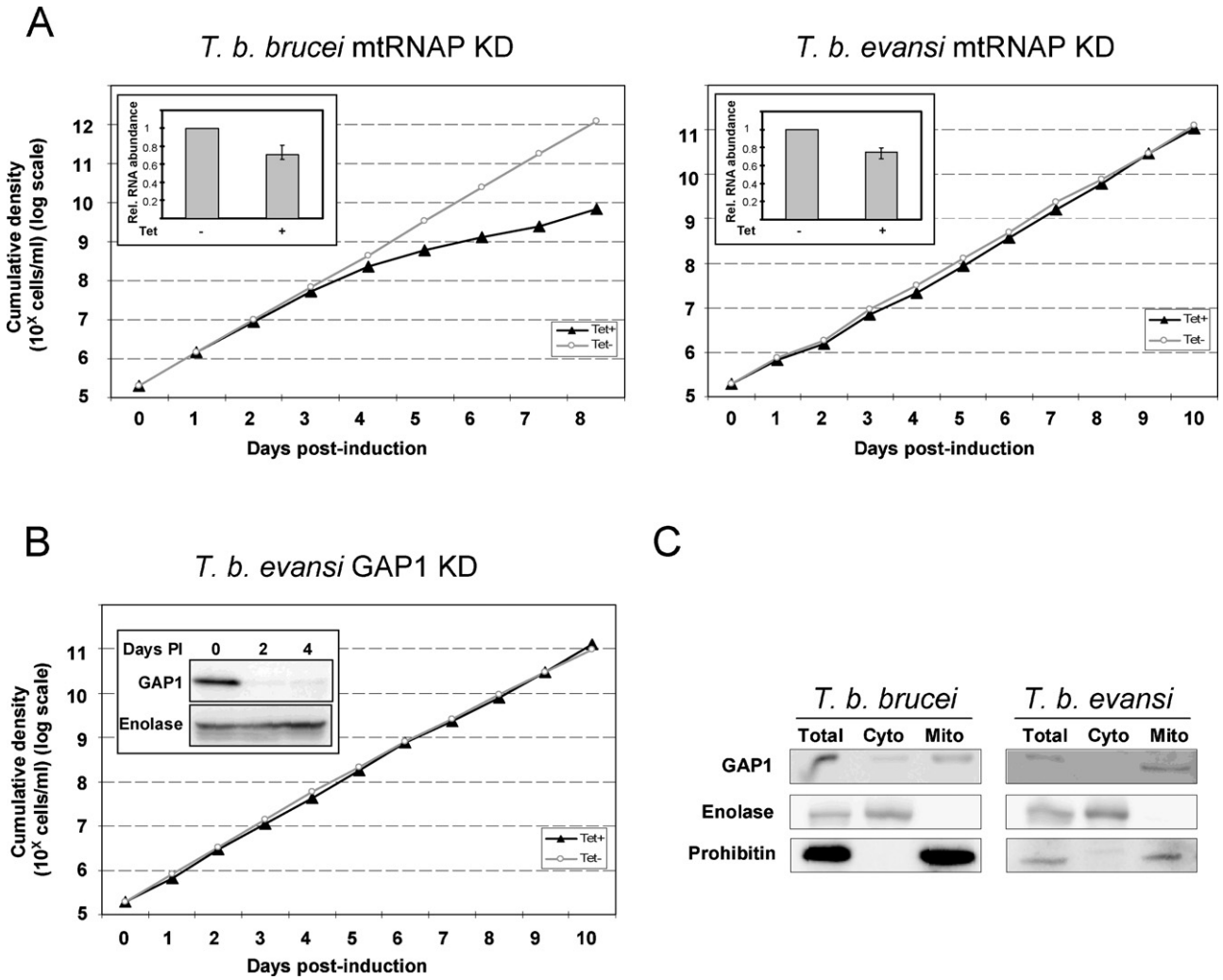

Fig. 1. Mitochondrial RNA polymerase (mtRNAP) and guide RNA associated protein 1 (GAP1) are not essential for *T. b. evansi*. (A) A comparison of the growth effect of RNAi-silencing of mitochondrial RNA polymerase in *T. b. brucei* bloodstream stage and *T. b. evansi*. The cumulative density of trypanosomes is depicted on the *y*-axis on a log scale and the days after tetracycline (Tet) induction are shown on the *x*-axis. Growth of RNAi-induced cells is plotted with the black line and full triangles, while the non-induced controls are shown as a grey line with open circles. Growth of *T. b. brucei* cells is in the left panel and *T. b. evansi* is in the right panel. Insets depict graphs showing the relative abundance of mtRNAP mRNA from cells grown three days in the presence of the RNAi-induction agent tetracycline (tet+) as compared to cells grown for the same time in medium lacking the drug (tet−). The abundance was determined by quantitative real-time (q) PCR using as a template cDNA generated by random hexamer primers from total RNA isolated from both samples using the following primer pair (forward 5′-CAGCATGAA GATCTCGGTGA-3′ and reverse 5′-CGTACAATGGCTTCCCAGTT-3′). The relative mRNA levels were normalized using qPCR data obtained with the previously described primers amplifying β-tubulin [10,13] from the same cDNA. All qPCR reactions were done in triplicate and in parallel with a negative control to ensure that the signal was not due to genomic DNA contamination. Standard deviations for the determined relative levels of mtRNAP mRNA in tet+ as compared to tet− samples are shown by error bars. (B) RNAi-silencing of GAP1 does not influence cell division. Graph plotted and labeled as described for (A). Inset shows a Western blot of cells grown in the absence (0) and presence of tet for two (2) and four (4) days. The membrane was immunodecorated with either anti-GAP1 (top) or anti-enolase antibodies (bottom), and visualized via peroxidase-conjugated secondary antibodies against rabbit IgGs. (C) GAP1 is imported into the mitochondria of *T. b. brucei* (left) and *T. b. evansi* (right). Digitonin fractions were obtained as described in the text and 10 μg of protein from total, cytosolic (Cyto) and mitochondrial (Mito) fractions were separated by SDS-PAGE and transferred onto PVDF membrane, which was immunodecorated and visualized with antibodies against GAP1 (top), enolase (middle), and prohibitin (bottom) as described in (B).

about the state of tRNA import into the akinetoplastic strains. Logically in these strains, the lack of mitochondrial genome obviates the need for organellar translation and conversely tRNA import. Before addressing tRNA import in *T. b. evansi*, we decided to first clarify the situation in the bloodstream stage of *T. b. brucei*.

To this end, approximately 10^9 *T. b. brucei* cells were purified from the blood of an intraperitoneally infected rat using a DEAE column. Similar amounts of procyclic *T. b. brucei* were also obtained by cultivation in SDM-79 medium. Mitochondria were then isolated from the procyclic and bloodstream cells by digitonin fractionation. The relative purity of the resulting mitochondrial and cytosolic fractions was confirmed by the aforementioned Western blot analysis using the compartment-specific antibodies against GAP1 and prohibitin (mitochondrial markers) and enolase (cytosolic markers) (Fig. 1C). Next, using guanidinium extraction, total and mitochondrial RNAs were purified from cell lysates and digitonin-extracted organelles, respectively. Northern blot analysis detected individual RNA species by probing with specific labeled oligonucleotides (Fig. 2). Mitochondrial-encoded 12S rRNA and the spliced leader RNA, used as mitochondrion and cytosol specific controls, respectively, verified the purity of the analyzed fractions. The set of five probes specific for individual tRNAs ($tRNA^{Phe}$, $tRNA^{Gle}$, $tRNA^{Ile}$, $tRNA^{Glu}$ and $tRNA^{Gly}$) showed that all these species are present in the organelle of either stage, at comparable amounts (Fig. 2), demonstrating that tRNA import occurs in bloodstream trypanosomes.

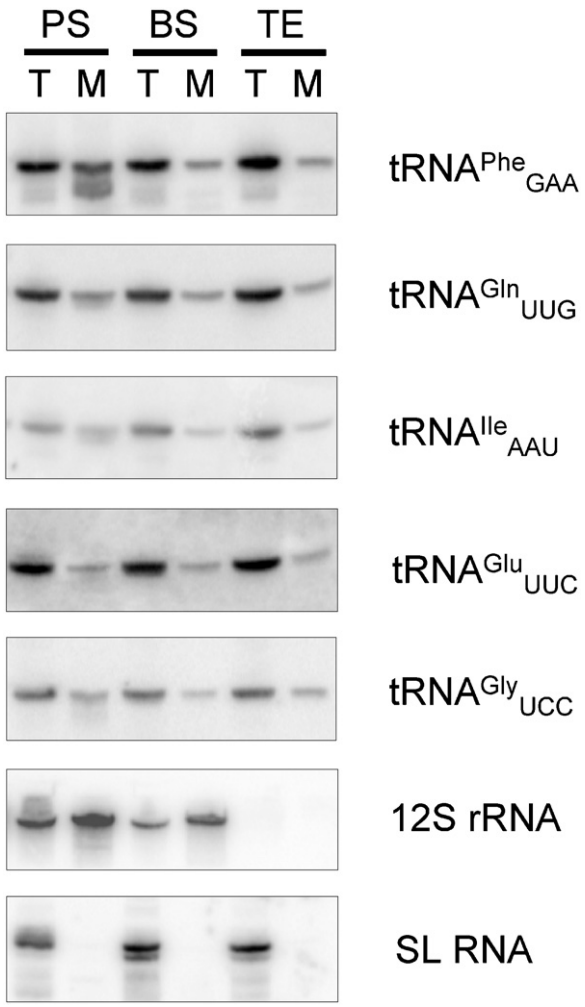

Fig. 2. tRNAs are imported into the *T. b. evansi* mitochondrion. Total and/or mitochondrial RNA was purified using guanidinium extraction. Mitochondria were isolated from 4×10^8 cells using fractionation with 0.05% final concentration of digitonin in the SoTE buffer. Obtained vesicles were subsequently treated with 2 μg/ml RNAse A in the SoTE buffer to remove contaminating cytosolic RNA. Samples of total (10 μg) and mitochondrial RNA (2.5 μg) were separated on denaturing 8% polyacrylamide gel with 8 M urea and electrobloted to Zeta probe membranes, which were subsequently probed with [^{32}P]5′ end-labeled oligonucleotides specific for a given RNA. After the run, total (T) and mitochondrial (M) RNAs from procyclic (PS) and bloodstream stages of *T. b. brucei* (BS) and *T. b. evansi* (TE), blotted and visualized with radioactively labeled oligonucleotides specific for tRNA^{Phe}, tRNA^{Gle}, tRNA^{Ile}, tRNA^{Glu} and tRNA^{Gly}. 12S rRNA and spliced leader (SL) RNA were used as controls specific for mitochondrial and cytosolic fractions, respectively.

2.3. tRNAs are imported into the T. b. evansi mitochondrion

The only *T. b. evansi* strain engineered for inducible expression of transgenes is dyskinetoplastic, which means that it contains residual kDNA minicircles [7], whereas the strain for which tRNA import and modification has been herein assayed is the akinetoplastic 805 strain originally isolated from a water buffalo in China [13]. This strain completely lost its mitochondrial genome and consequently does not contain any RNA molecules derived from organellar transcription. Since neither translation nor tRNAs are required in this mitochondrion, it was reasonable to assume that their import does not occur. To corroborate this, a rat was inoculated with the 805 strain and parasites were purified at a terminal stage of infection. Total as well as mitochondrial RNAs obtained by digitonin fractionation were analyzed by Northern blot hybridization (Fig. 2). A spliced leader RNA-specific oligonucleotide probe showed that the mitochondrial fractions were devoid of cytosolic contamination, while the lack of any signal obtained with a 12S rRNA-specific probe confirmed that kDNA is absent from the 805 strain (Fig. 2). However, contrary to our expectations, signals were obtained by subsequent hybridization with five probes specific for individual aforementioned tRNAs, demonstrating that despite the lack of a mitochondrial genome, tRNA import is unabated in the akinetoplastic trypanosomes.

2.4. tRNAs are thiolated only in the T. b. brucei mitochondrion

It was shown recently that tRNAs are thiolated in the procyclic *T. b. brucei* but this modification plays no role in tRNA import [15,23]. These observations significantly differ from a previous report obtained with *Leishmania tarentolae*, a flagellate related to the genus *Trypanosoma*, where tRNA thiolation may serve as a negative determinant for mitochondrial tRNA import [24]. In light of the current results, we tested whether tRNA thiolation also occurs in the bloodstream stage of *T. b. brucei* and *T. b. evansi*.

Thiolation of different tRNAs was analyzed by APM gels as previously described [25]. These gels permit separation of thiolated and non-thiolated tRNAs on the basis of differential mobility during electrophoresis (Fig. 3). Northern blots of tRNAs obtained from total and mitochondrial cell fractions of *T. b. brucei* (both the procyclic and the bloodstream stage) and *T. b. evansi*, resolved in the presence of APM, showed that cytosolic tRNA^{Gln} was thiolated to similar levels in all fractions tested (Fig. 3A). This tRNA species is known to be thiolated solely in the cytosol. We also analyzed the thiolation levels of tRNA^{Trp}, the only tRNA known to be thiolated exclusively in the mitochondrion following import [15,23,25]. Although this tRNA is highly thiolated in the mitochondrion of procyclic *T. b. brucei*, its thiolation is somewhat lower in the organelle of the bloodstream stage. With the method used, which is able to detect down to ~0.5% of thiolated species, and even with double amount of mitochondrial RNA loaded (5 μg; data not shown), we were unable to detect the band corresponding to the thiolated tRNA^{Trp} in *T. b. evansi* (Fig. 3B).

The fact that thiolation occurs in the bloodstream stage testifies indirectly to the presence of cysteine desulfurase, an enzyme that is essential for Fe-S cluster assembly [18] and thiolation of both cytosolic and mitochondrial tRNAs in procyclic *T. b. brucei* [25]. Moreover, this cysteine desulfurase also has a limited selenocysteine lyase activity in the insect stage trypanosomes [26], yet its function(s) in the mammalian stage remain(s) to be established. The thiolation status of mitochondrial tRNA is revealing in several respects. As has been shown previously, the *T. b. brucei* bloodstream stage lacks any respiratory complexes in its mitochondrion [3–5], yet this has apparently no impact on tRNA import. Therefore, we posit that the Rieske Fe-S protein, as well as other subunits of respiratory complexes, do not play any role in the import of the tRNAs in *T. b. brucei* regardless of developmental stage, a conclusion contradicting results published for the *Leishmania* species [27]. In further support of this notion, the absence of the Rieske Fe-S protein and a subunit of respiratory complex IV has been confirmed in numerous *T. b. evansi* strains [13]. Furthermore, our data strongly suggest the absence of the interdependence between mitochondrial translation and tRNA import. The latter process apparently operates by a default mechanism, regardless of the situation "within" the organelle in terms of DNA content and translation requirements. It is also worth noting that thiolation is the only process, with the exception of the status of kDNA, which differs, at least to some extent, between the *T. b. brucei* bloodstream stage and the *T. b. evansi*. As apparent from their comparison, thiolation of mitochondrial tRNAs, consistently weaker in the *T. b. brucei* bloodstream stage as compared to the insect stages, was undetectable in the akinetoplastic *T. b. evansi* (Fig. 3B). We propose that this is caused by a progressive degeneration of the apparently dysfunctional *T.*

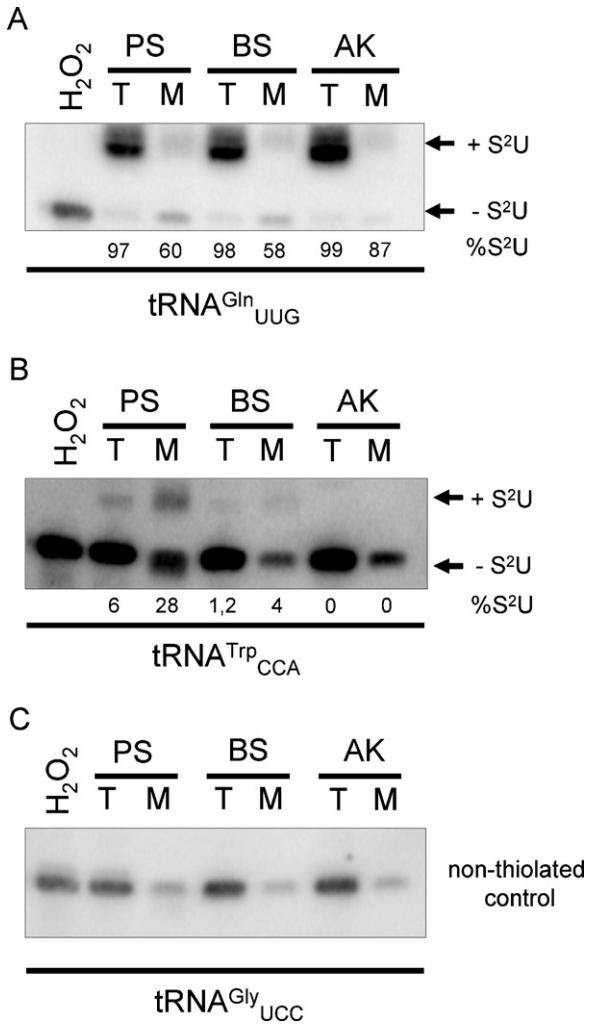

Fig. 3. tRNAs are thiolated in cytosol but not in the mitochondrion of *T. b. evansi*. Total (T) and mitochondrial (M) RNA from procyclic (PS) and bloodstream stages of *T. b. brucei* (BS), and *T. b. evansi* (TE) was separated in APM-containing polyacrylamide gels. Northern blots were probed for $tRNA^{Gln}$ (A) and $tRNA^{Trp}$ (B). Bands corresponding to thiolated (+S^2U) and non-thiolated tRNAs (−S^2U) are indicated. H_2O_2 was used as a control to show complete oxidation of thiolation, eliminating the mobility shift. The $tRNA^{Gly}$ (C) served as a loading control. Percent thiolation (% S^2U) was calculated by dividing the signal from the shifted band by the total signal of shifted (thiolated) and non-shifted and multiplied by 100.

b. evansi mitochondrion, which imports tRNAs to no purpose. It has been suggested elsewhere that *T. b. evansi* may not be monophyletic, but rather an assembly of strains that for one reason or another started loosing their capacity to faithfully replicate, transcribe or edit their organellar nucleic acids [11–13], with mitochondrial tRNA thiolation now added to the list of possible triggers of dys/akinetoplastidy.

3. Conclusions

Our results further strengthen the argument that *T. b. evansi* represents the bloodstream stage of *T. b. brucei* that lost (part of) its kinetoplast DNA. We propose that organelles of both trypanosomes, likely having a relationship reminiscent of that between the yeast *Saccharomyces cerevisiae* and its petite mutants, are an ideal object for study of interactions between the mitochondrion and the nucleus. Our data further stress the impression that the organelle is much more independent of the nucleus than appreciated so far.

Acknowledgements

We thank Achim Schnaufer (University of Edinburgh) for sharing *T. b. evansi* RNAi cell line. This work was supported by the Grant Agency of the Czech Republic 204/09/1667 and 560/3092, the Ministry of Education of the Czech Republic (2B06129, LC07032 and 6007665801), and the Praemium Academiae award to J.L., and NIH grant GM084065 to J.D.A.

References

[1] Schnaufer A, Domingo GJ, Stuart K. Natural and induced dyskinetoplastic trypanosomatids: how to live without mitochondrial DNA. Int J Parasitol 2002;32:1071–84.
[2] Claes F, Buscher P, Touratier L, Goddeeris BM. *Trypanosoma equiperdum*, master of disguise or historical mistake. Trends Parasitol 2005;21:316–21.
[3] Besteiro S, Barrett MP, Rivière L, Bringaud F. Energy generation in insect stages of *Trypanosoma brucei*: Metabolism in flux. Trends Parasitol 2005;21:185–91.
[4] Tielens AGM, van Hellemond JJ. Surprising variety in energy metabolism within Trypanosomatidae. Trends Parasitol 2009;25:482–90.
[5] Hannaert V, Bringaud F, Opperdoes FR, Michels PAM. Evolution of energy metabolism and its compartmentation in Kinetoplastida. Kinetopl Biol Dis 2003;2:11.
[6] Chaudhuri M, Ott RD, Hill GC. Trypanosome alternative oxidase: from molecule to function. Trends Parasitol 2006;22:484–91.
[7] Schnaufer A, Clark-Walker JD, Steinberg AG, Stuart K. The F1-ATP synthase complex in bloodstream stage trypanosomes has an unusual and essential function. EMBO J 2005;24:4029–40.
[8] Schnaufer A, Panigrahi AK, Panicucci B, et al. An RNA ligase essential for RNA editing and survival of the bloodstream form of *Trypanosoma brucei*. Science 2001;291:2159–62.
[9] Fisk JC, Ammerman ML, Presnyak V, Read LK. TbRGG2, an essential RNA editing accessory factor in two *Trypanosoma brucei* life cycle stages. J Biol Chem 2009;283:23016–25.
[10] Hashimi H, Čičová Z, Novotná L, Wen Y-Z, Lukeš J. Kinetoplastid guide RNA biogenesis is dependent on subunits of the mitochondrial RNA binding complex 1 and mitochondrial RNA polymerase. RNA 2009;15:588–99.
[11] Jensen RE, Simpson L, Englund PT. What happens when *Trypanosoma brucei* leaves Africa. Trends Parasitol 2008;24:428–31.
[12] Lun ZR, Lai DH, Li FJ, Lukeš J, Ayala FJ. *Trypanosoma brucei*: two steps to spread out from Africa. Trends Parasitol 2010;26:434–7.
[13] Lai DH, Hashimi H, Lun ZR, Ayala FJ, Lukeš J. Adaptations of *Trypanosoma brucei* to gradual loss of kinetoplast DNA: *T. equiperdum* and *T.evansi* are petite mutants of *T. brucei*. Proc Natl Acad Sci USA 2008;105:1999–2004.
[14] Schnaufer A. Evolution of dyskinetoplastic trypanosomes: how, and how often? Trends Parasitol 2010;26:557–8.
[15] Paris Z, Rubio MAT, Lukeš J, Alfonzo JD. Mitochondrial tRNA import in *Trypanosoma brucei* is independent of thiolation and the Rieske protein. RNA 2009;15:1398–406.
[16] Grams J, Morris JC, Drew ME, Wang Z, Englund PT, Hajduk SL. A trypanosome mitochondrial RNA polymerase is required for transcription and replication. J Biol Chem 2002;277:16952–9.
[17] Charrière F, Helgadóttir S, Horn EK, Söll D, Schneider A. Dual targeting of a single tRNATrp requires two different tryptophanyl-tRNA synthesis in *Trypanosoma brucei*. Proc Natl Acad Sci USA 2006;103:6847–52.
[18] Smíd O, Horáková E, Vilímová V, et al. Knock-downs of iron-sulfur cluster assembly proteins IscS and IscU down-regulate the active mitochondrion of procyclic *Trypanosoma brucei*. J Biol Chem 2006;281:28679–86.
[19] Týč J, Faktorová D, Kriegová E, et al. Probing for primary functions of prohibitin in *Trypanosoma brucei*. Int J Parasitol 2010;40:73–83.
[20] Amaro RE, Schnaufer A, Interthal H, Hol W, Stuart KD, McCammon JA. Discovery of drug-like inhibitors of an essential RNA-editing ligase in *Trypanosoma brucei*. Proc Natl Acad Sci USA 2008;105:17278–83.
[21] Schneider A, Martin JA, Agabian N. A nuclear encoded tRNA of *Trypanosoma brucei* is imported into mitochondria. Mol Cell Biol 1994;4:2317–22.
[22] Hashimi H, Benkovičová V, Čermáková P, Lai DH, Horváth A, Lukeš J. The assembly of F_1F_0-ATP synthase is disrupted upon interference of RNA editing in *Trypanosoma brucei*. Int J Parasitol 2010;40:45–54.
[23] Bruske EI, Sendfeld F, Schneider A. Thiolated tRNAs of *Trypanosoma brucei* are imported into mitochondria and dethiolated after import. J Biol Chem 2009;6284:36491–9.
[24] Kaneko T, Suzuki T, Kapushoc ST, Rubio MA, Ghazvini J, Watanabe K. Wobble modification differences and subcellular localization of tRNAs in *Leishmania tarentolae*: implication for tRNA sorting mechanism. EMBO J 2003;22:657–67.
[25] Wolgamuth-Benedum JM, Rubio MAT, Paris Z, et al. Thiolation controls cytoplasmic tRNA stability and acts as a negative determinant for tRNA editing in mitochondria. J Biol Chem 2009;284:23947–53.
[26] Poliak P, Van Hoewyk D, Oborník M, et al. Functions and cellular localization of cysteine desulfurase and selenocysteine lyase in *Trypanosoma brucei*. FEBS J 2010;277:383–93.
[27] Mukherjee S, Basu S, Home P, Dhar G, Adhya S. Necessary and sufficient factors for the import of transfer RNA into the kinetoplast mitochondrion. EMBO Rep 2007;8:589–95.

Attached Publications

Part II. DYSKINETOPLASTIC *TRYPANOSOMA BRUCEI*

Zhenqiu Huang, Sabine Kaltenbrunner, Eva Šimková, David Staněk, Julius Lukeš[†], Hassan Hashimi[†] (2014). The Dynamics of Mitochondrial RNA-binding Protein Complex in *Trypanosoma brucei* and its Petite Mutant Under Optimized Immobilization Conditions. *Euk. Cell* 13: 1232-40.

This paper describes how RNA can affect the in vivo dynamics of mt RNA binding proteins in *T. brucei* and Ak *T. brucei evansi*. In order to perform this study, a method to immobilize these highly motile cells without compromising their viability was established.

[†]Co-corresponding author

EC Journals.ASM.org

Dynamics of Mitochondrial RNA-Binding Protein Complex in *Trypanosoma brucei* and Its Petite Mutant under Optimized Immobilization Conditions

Zhenqiu Huang,[a,b] Sabine Kaltenbrunner,[b] Eva Šimková,[c] David Staněk,[c] Julius Lukeš,[a,b] Hassan Hashimi[a,b]

Institute of Parasitology, Biology Centre, Czech Academy of Sciences, České Budějovice (Budweis), Czech Republic[a]; Faculty of Sciences, University of South Bohemia, České Budějovice (Budweis), Czech Republic[b]; Institute for Molecular Genetics, Czech Academy of Sciences, Prague, Czech Republic[c]

There are a variety of complex metabolic processes ongoing simultaneously in the single, large mitochondrion of *Trypanosoma brucei*. Understanding the organellar environment and dynamics of mitochondrial proteins requires quantitative measurement *in vivo*. In this study, we have validated a method for immobilizing both procyclic stage (PS) and bloodstream stage (BS) *T. brucei brucei* with a high level of cell viability over several hours and verified its suitability for undertaking fluorescence recovery after photobleaching (FRAP), with mitochondrion-targeted yellow fluorescent protein (YFP). Next, we used this method for comparative analysis of the translational diffusion of mitochondrial RNA-binding protein 1 (MRP1) in the BS and in *T. b. evansi*. The latter flagellate is like petite mutant *Saccharomyces cerevisiae* because it lacks organelle-encoded nucleic acids. FRAP measurement of YFP-tagged MRP1 in both cell lines illuminated from a new perspective how the absence or presence of RNA affects proteins involved in mitochondrial RNA metabolism. This work represents the first attempt to examine this process in live trypanosomes.

The kinetoplastid flagellates belonging to the *Trypanosoma brucei* group have been a focus of research because they are etiological agents of human African trypanosomiasis, a serious disease commonly referred to as sleeping sickness, which is spread among humans and large mammals by the *Glossina* fly in sub-Saharan Africa. Yet, *T. brucei* has also emerged as a powerful model for eukaryotic cell biology as efforts to understand it as a pathogen have revealed many fascinating biological properties. For example, its simple cell architecture (1) has been exploited to understand organelle biogenesis (2, 3).

The single, large mitochondrion of *T. brucei* has also become known for a number of divergent characteristics that have been a subject of intense research (4). Its mitochondrial genome, called kinetoplast DNA (kDNA), is a compact network composed of thousands of the mutually concatenated DNA minicircles and maxicircles adjacent to the flagellar basal body. Many of the protein-coding genes located on the kDNA maxicircles require extensive RNA editing of the uridine (U) insertion and/or deletion type, eventually yielding translatable open reading frames (ORFs). Small noncoding transcripts called guide RNAs (gRNAs), encoded almost exclusively by the minicircles, provide the information for each U insertion/deletion event via binding to its cognate mRNA. The resulting proteins are involved in mitochondrial respiratory complexes and translation. During its life cycle, the mitochondrion of *T. brucei* undergoes a transition from the large, reticulated organelle of the insect midgut-dwelling procyclic stage (PS), which is equipped with the electron transport chain complexes, to a morphologically reduced organelle devoid of cristae, which is characteristic for the glycolysis-dependent slender bloodstream stage (BS) that infects mammalian hosts (1, 5).

Live-cell imaging is increasingly employed to study eukaryotic cellular function, enabling real-time tracking of biological processes of individual cells. Advanced microscopy techniques such as fluorescence recovery after photobleaching (FRAP), fluorescence correlation spectroscopy (FCS), and fluorescence resonance energy transfer (FRET) can provide informative and critical insights into protein dynamics such as diffusion, assembly, and interaction with partners (6). In order to apply these powerful techniques to *T. brucei* and other flagellates, the vigorous motility of these cells must be accommodated (7), calling into need techniques that efficiently immobilize cells yet maintain them in an appropriate physical state.

Immobilization of the BS on agarose has been employed to study apolipoprotein L1-mediated lysis and mitochondrial membrane potential in live cells (8, 9). The PS flagellates have been embedded in low-melting-point agarose to study Golgi compartment duplication and bilobe protein turnover (10) or sandwiched between a slide and a coverslip to examine intraflagellar transport by FRAP (11). While these methods were utilized to great effect in their respective studies, the influence of the immobilization techniques on cell viability was not specifically addressed. A study in which kinetoplastid protists were immobilized in a CyGEL matrix did systematically assay cell viability, claiming its suitability for the PS and *Leishmania major* but not for the BS (12). This immobilization method was later used to study the trafficking of surface proteins in *L. major* by FRAP (13).

Here, we describe a rapid, economical, and reproducible immobilization method that can be used with an inverted microscope and compensates for the absence of a dedicated chamber for

Received 21 June 2014 Accepted 21 July 2014

Published ahead of print 25 July 2014

Address correspondence to Julius Lukěs, jula@paru.cas.cz, or Hassan Hashimi, hassan@paru.cas.cz.

Supplemental material for this article may be found at http://dx.doi.org/10.1128/EC.00149-14.

doi:10.1128/EC.00149-14

maintenance of carbon dioxide tension. The method is suitable for application to both PS and BS cells, as they remain in a viable state for an extended time period. Furthermore, this technique facilitates FRAP, as shown by the full fluorescence recovery of photobleached mitochondrion-targeted yellow fluorescent protein (MT-YFP), indicating the healthy physical state of cells immobilized by our technique.

Establishing this platform for imaging of live *T. b. brucei* has allowed us to analyze the dynamics of the mitochondrial RNA-binding protein 1 and 2 (MRP1/2) complex in the nanostructured compartment of the mitochondrial matrix. This abundant complex is a heterotetramer consisting of two each of the MRP1 (TriTrypDB accession no. Tb927.11.1710) and MRP2 (accession no. Tb927.11.13280) subunits (14, 15). Although these two proteins have low sequence identity, they remarkably share a tertiary structure that forms a "Whirly" transcription factor fold. The tetramerization of MRP1 and -2 creates an electropositive face that allows the complex's nonspecific interaction with the negatively charged phosphate groups of the RNA backbone. This mode of binding exposes the bases of each nucleotide outward, which would be amenable to a suggested role for the MRP1/2 complex as an RNA matchmaker, which facilitates annealing of gRNA and mRNA molecules (14–17). However, functional analysis of MRP1/2 has suggested that this complex may play a wider role in mitochondrial RNA metabolism in addition to or instead of RNA editing (18–20).

Here we address for the first time mitochondrial RNA metabolism in live trypanosomes by studying the motility and dynamics of MRP1 under two strikingly different conditions. We contrast the *T. b. brucei* BS, which has an intact kDNA encoding transcripts that are duly processed by the elaborate pathway residing in the mitochondrion, with *T. b. evansi*. The mitochondrion of this akinetoplastic (AK) subspecies is devoid of any organellar DNA or RNA. Thus, these trypanosomes can be considered an analog to rho^0 petite mutant *Saccharomyces cerevisiae*, which also lacks mitochondrial DNA (9, 21, 22). Yet, AK *T. b. evansi* still imports the protein machinery required for RNA processing despite the lack of substrate nucleic acids, as well as all tRNAs (21, 23–25). Among the imported macromolecular complexes assembled from the imported proteins are the MRP1/2 heterotetramer and a catalytically active RNA-editing core complex (RECC) that coordinates the enzymatic steps required for U insertion/deletion (21, 25). Indeed, C-terminally tagged MRP1, serving as a proxy for the whole complex, exhibits less translational diffusion within the BS mitochondrion than in AK *T. b. evansi*, which can be explained by the lack of mitochondrion-encoded nucleic acids in the latter compartment. These results provide a novel insight into the environment of the organelle and may be applicable to the study of other mitochondrial proteins.

MATERIALS AND METHODS

Generation of cell lines. Lister 427 strains of PS and BS *T. b. brucei* and Antat 3/3 *T. b. evansi* were cultured, transfected, and screened for the appropriate drug resistance of a given construct as described previously (9, 26). The construct pMT-YFP, modified from the pDEX557-Y plasmid (27) to include the mitochondrial signal peptide from the *Naegleria gruberi* iron dehydrogenase gene between the HindIII and XhoI restriction sites upstream of the YFP gene, was employed to generate MT-YFP cell lines. For *in situ* C-terminal tagging of MRP1 with YFP, the full ORF excluding the stop codon was PCR amplified with forward primer 5′-TATAGGGCGAATTGGATGATTCGACTCGCATGCCTGCGT-3′ and reverse primer 5′-ACCATTCCGCCACCGGAATGGTATCGCGATGTGTCACTTAC-3′. The PCR amplicon was cloned into the p2937 vector (27) via the homology flanks introduced into the PCR primers (underlined) with the GeneArt Seamless Cloning kit according to the manufacturer's (Invitrogen) protocol.

Confocal microscopy. In order to visualize mitochondria, 5×10^6 to 1×10^7 PS *T. brucei* cells were incubated in semidefined medium 79 (SDM-79) supplemented with 200 nM MitoTracker Red CMXRos (Molecular Probes) for 20 min at 27°C, while 5×10^6 to 1×10^7 BS *T. brucei* cells were incubated in Hirumi's modified Iscove's medium 9 (HMI-9) with 20 nM MitoTracker Red for 20 min at 37°C. Cells were subsequently immobilized by the method described below. They were examined on an Olympus FluoView FV1000 confocal microscope with the accompanying FluoView v1.7 software and a 488-nm laser for YFP scanning and a 559-nm laser for the propidium iodide (PI) and Mitotracker Red CMXRos dyes, respectively. All images were processed and collected with a 100× oil immersion objective at 25°C. Line scanning of the merged images was done by drawing a test line across the cell intersecting the mitochondrion and measuring the relative fluorescence intensity along the line with the ImageJ software (28).

Trypanosome immobilization. Research grade agarose (Serva) was dissolved in heated phosphate-buffered saline (PBS) supplemented with 6 mM D-glucose (PBSG) to a concentration of 1% (wt/vol). A 12-ml volume was poured into a 9.2-cm-diameter petri dish (SPL) and left to solidify, which ensures a sheet of agarose with a thickness of about 2 mm. The agarose block can be prepared in advance and stored for 1 month sealed at 4°C until use. In the meantime, PS, BS, and *T. b. evansi* cells were centrifuged at 900 × *g* for 2 min and washed once with prewarmed PBSG (25°C for PS cells and 37°C for BS and AK *T. b. evansi* cells) under the same centrifugation conditions. The cells were gently suspended in 200 μl of phenol red-free Iscove's modified Dulbecco's medium (IMDM; Invitrogen) prewarmed to the appropriate temperature based on a given cell stage. Five microliters was dropped onto a 24-by-60-mm coverslip (Prestige), which was immediately and gently covered with a 1-by-1-cm agarose block cut from the petri dish. The coverslip was fixed onto an inverted Olympus FluoView FV1000 confocal microscope on top of two microscope slides with Plasticine (see Fig. 1A; also see Fig. S1 in the supplemental material). Cells were kept at the appropriate temperature with a heat block before immobilization.

FRAP analysis. Cells that were immobilized for up to 30 min were used in FRAP experiments. A series of 250 images (800 by 800 pixels, 10 μs/pixel; frame time, 0.336 s) were acquired with a 170-μm pinhole and sequential multitrack imaging with a 488-nm laser (5% transmission for acquisition). The simultaneous-scanning SIM Scanner system was used with a 405-nm laser whose intensity was adjusted for 50 to 75% photobleaching in a circular region of interest (ROI) with a diameter of 0.35 μm. Per replicate, an individual cell was bleached only once. The average fluorescence intensity $F(t)$ within the bleached region was calculated with the FRAP accessory tool in the FluoView v1.7 program (Olympus). The $F(t)$ in the background and in the unbleached region of the same cell were measured to normalize FRAP recovery curves by using the following equation (28, 29): $F(t)_{\mathrm{norm}} = [F(t)_{\mathrm{ROI}} - F(t)_{\mathrm{bkgd}}](F_{\mathrm{i,non}} - F_{\mathrm{i.bkgd}})/[F(t)_{\mathrm{non}} - F(t)_{\mathrm{bkgd}}](F_{\mathrm{i},ROI} - F_{\mathrm{i.bkgd}})$.

The bleached ROI intensity $[F(t)_{\mathrm{ROI}}]$ and the nonbleached region intensity $[F(t)_{\mathrm{non}}]$ are corrected with the background intensity $[F(t)_{\mathrm{bkgd}}]$ at each time point (t) and divided by the corrected intensity of the nonbleached region for the loss of fluorescence during the time course of the experiment. Next, the data are normalized to the background-corrected prebleach intensity (F_{i}) in the nonbleached region, the background region, and the ROI ($F_{\mathrm{i.non}}$, $F_{\mathrm{i.bkgd}}$, and $F_{\mathrm{i.ROI}}$, respectively). By using the first time point after the bleach set as $t = 0$, the fluorescence intensity recovery ratio $[F(t)_{\mathrm{R}}]$ at each time point can be calculated to generate mean recovery curves (see Fig. 2D to F and 3E to F) by using the mean value of every five sequential scanning measurements as follows: $F(t)_{\mathrm{R}} = [F(t)_{\mathrm{norm}} - F(0)]/[1 - F(0)]$.

In order to obtain the $T_{50\%}$ and R_{max} values, which indicate the translational diffusion and motile fraction of the photobleached fluorescent protein, the FRAP recovery curve from each replicate per sample was fitted by the single-component exponential model in the equation $F(t) = A(1 - e^{-t/TFRAP})$ (29).

$T_{50\%}$ was calculated from the fitted-curve model for each FRAP experiment. The mobile fraction was equal to R_{max}, the maximal recovery of fluorescence compared to the prebleach values from this equation when $t = \infty$ (29–31). The values obtained from each FRAP experiment, see Tables S1 to S6 in the supplemental material, and the means and standard deviations (SDs) of these values are shown below the FRAP images in Fig. 2D to F and 3E to F. The statistical significance of the difference between the MRP1-YFP R_{max} values of BS and AK *T. b. evansi* was calculated by unpaired Student *t* test by using the determined mean R_{max}, SD, and number of replicates (*n*).

Immunoprecipitation and Western blot analysis. Immunoprecipitation was carried out with 1×10^8 BS and *T. b. evansi* protozoa expressing MRP1-YFP. Lysates from these cells were incubated with anti-green-fluorescent-protein (anti-GFP) monoclonal antibody 3E6 (Molecular Probes) bound to Dynabeads protein G (Invitrogen) for 12 h at 4°C in the presence of Complete protease inhibitor according to the manufacturer's (Roche) recommendation. The flowthrough fraction was collected for subsequent Western blot analysis, and the column was washed three times with 200 μl of PBS with 0.05% Tween 40. The antibody-antigen interaction was disrupted by elution three times with 50 μl of 100 mM glycine (pH 2.5), and the eluates were neutralized with 1 M Tris buffer (pH 8.7) and analyzed by Western blotting as previously described (26).

RESULTS

Viability of PS and BS trypanosomes under immobilizing conditions. Cells constitutively expressing MT-YFP were gently centrifuged, and after the growth medium was discarded, they were resuspended in IMDM. In addition to lacking the phenol red present in the growth medium for BS and PS *in vitro* cultures, which can interfere with fluorescence assays, IMDM contains D-glucose and HEPES, a buffer that maintains a physiological pH despite changes in the concentration of carbon dioxide (32). A drop of the cell suspension was applied to a coverslip fixed onto an inverted confocal microscope (Fig. 1A; see Fig. S1 in the supplemental material). This drop was immediately covered with a thin layer of agarose to restrain the cells and also mitigate cell desiccation.

The viability of immobilized *T. b. brucei* was first determined by staining with PI added to IMDM. Because of selective penetration of the compound into dead cells, the number of viable cells was determined by counting PI staining-negative cells. Initially, about 99% of the PS and BS protozoa were fully viable, reflecting the mild harvesting and immobilizing process (Fig. 1B and C). Within 3 h under the immobilization condition at room temperature, the percentage of viable PS cells remained above 90%, with the surviving cells exhibiting normal morphology and a homogeneous distribution of MT-YFP, a reflection of the vitality of the organelle. Viability dropped to 80 and 60% after 4 and 6 h, respectively. At this final time point, dead cells exhibited a swollen morphology and the MT-YFP showed a fragmented distribution, representing the disintegration of mitochondria.

For BS, the percentage of viable cells remained above 90% for the first 2 h of immobilization, with MT-YFP evenly distributed throughout the organelle (Fig. 1D). Hence, this time frame can be recommended for live-cell imaging experiments. After 3 h, viability under these conditions declined sharply, with the overall appearance of swollen cell morphology and mitochondrial fragmentation. Under our established immobilization conditions, viable cells at both stages exhibited limited membrane and/or flagellar undulation, although they were fixed in place (see Movies S1 and S2 in the supplemental material). Furthermore, the procedure developed promotes a population of consistently immobilized and evenly distributed cells.

Trypanosome immobilization facilitates FRAP experiments. Although the viability assays showed that the absolute majority of both PS and BS cells was healthy and viable for at least 2 h, the potential effect of immobilization on mitochondrial physiology remained unknown. Therefore, we decided first to test whether our immobilization protocol allows the application of FRAP to the mitochondrion, which is the organelle of interest to us. Using the results of the previous experiments as a guideline, we performed immobilization within 30 min in all subsequent experiments.

We started with the measurement of the translational diffusion of YFP, equipped with the mitochondrial import signal from *N. gruberi* iron hydrogenase (MT-YFP) (33), in immobilized PS and BS plus AK *T. b. evansi* cells. In all cases, MT-YFP exhibited consistent colocalization with the Mitotracker Red dye, indicating an even distribution of the tagged protein within the mitochondrion (Fig. 2A to C). On the basis of this, the photobleaching spots for the FRAP analysis were randomly selected in the mitochondrial compartment of an individual cell. In PS cells, MT-YFP reached 50% recovery ($T_{50\%}$) of the prebleaching fluorescence intensity within the bleached ROI at 4.44 ± 2.82 s after bleaching (Fig. 2D), as well as achieving full recovery of fluorescence over the time course (R_{max} = 1.02 ± 0.128), indicating that diffusion of YFP is unhindered in the matrix.

In BS and AK *T. b. evansi* cells, the YFP recovery profiles in the ROI appeared to be almost identical, with $T_{50\%}$ values of 2.96 ± 2.30 and 3.44 ± 1.67 s, respectively, and virtually full recovery of prebleaching fluorescence intensity (R_{max} = 0.97 ± 0.169 and 0.94 ± 0.165, respectively) (Fig. 2E and F). In summary, these data show that our immobilization method is appropriate for FRAP analysis of BS and PS, as well as AK *T. b. evansi*, cells. The recovery of MT-YFP fluorescence in these immobilized trypanosomes is also indicative of their viable condition, as no such recovery was detected in the photobleached ROIs of PS cells exhibiting a fragmented mitochondrial morphology (see Fig. S2 in the supplemental material), which also stained with the dead-cell marker PI (Fig. 1D). Moreover, since a substantial fraction of YFP remained in a diffused state and recovered rapidly after bleaching, this protein qualifies as a suitable fluorescent tag for tracking the mobility of other mitochondrial proteins in *T. brucei*.

The MRP1/2 complex exhibits different dynamics in *T. b. brucei* and AK *T. b. evansi*. In order to investigate the dynamics of the MRP1/2 complex, we generated both BS and AK *T. b. evansi* cell lines carrying *in situ* C-terminally YFP-tagged MRP1 (MRP1-YFP). Because the latter cell type is locked in the slender pathogenic stage (9, 21), only BS *T. b. brucei* was used in the comparative FRAP analysis, which capitalized on the dramatic difference between these cell lines in terms of the absence or presence of nucleic acids in their respective organelles.

First, we compared the abundance of MRP1-YFP in BS and AK protozoa by immunodecoration of Western blot assays of respective whole-cell lysates with anti-GFP antibody, which showed no differences in expression between the two cell lines (Fig. 3A). Next, to confirm that YFP tagging does not interfere with the incorporation of MRP1 into the MRP1/2 complex *in vivo*, we immunoprecipitated tagged MRP1 with an anti-GFP

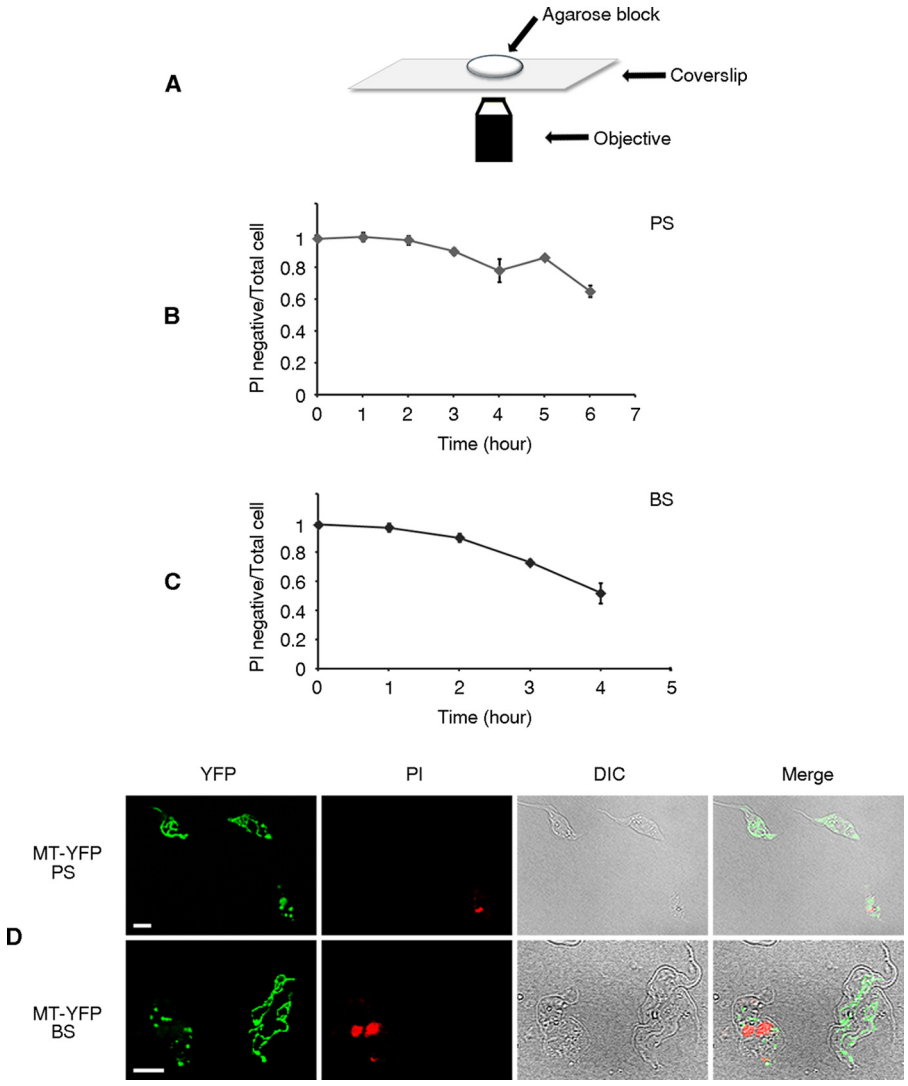

FIG 1 Parasite viability under agarose block immobilization conditions. (A) Schematic depicting the apparatus used to monitor trypanosomes immobilized with a 1% agarose block with an inverted microscope. (B) *T. b. brucei* PS viability was determined following immobilization as depicted in panel A. Harvested trypanosomes were resuspended gently in IMDM containing 5 μg/ml PI. PI exclusion was used as a marker of viability, and cell viability is plotted on the *y* axis as PI-negative cells/total cells. More than 200 cells were counted per time point in triplicate. (C) BS *T. b. brucei* viability was determined as described for panel B. (D) Representative imagines of PS and BS trypanosomes immobilized for 1 h. Scale bars, 10 μm.

antibody (Fig. 3B) and looked for the presence of endogenous MRP1 and MRP2 with antibodies against each of these subunits (20). Since C-terminally tagged MRP1 coimmunoprecipitated with the endogenous subunits in both BS *T. b. brucei* and AK *T. b. evansi*, MRP1-YFP is properly assembled into the MRP1/2 complex. The band intensities of the MRP1-YFP versus the endogenous MRP1 suggest that the stoichiometry of the former ranges from two to one copies. Thus, the subsequent FRAP experiment is relevant for the MRP1/2 complex as a whole. Furthermore, coimmunoprecipitation of the intact MRP1/2 complex in AK *T. b. evansi* (Fig. 3B) indicates that the complex is properly assembled even in the absence of RNA. The MRP1-YFP protein consistently colocalized with the Mitotracker Red signal, proving that there is an even distribution of the tagged protein in the mitochondrial lumen of both cell lines and that this localization pattern is independent of the presence or absence of organelle-encoded RNA (Fig. 3C and D).

The photobleached ROIs for FRAP were selected randomly as in the case of MT-YFP. Hence, the results reflect the general profile of MRP1 throughout the organelle. In the FRAP analysis, MRP1-YFP did not show full recovery in BS *T. b. brucei* or in AK *T. b. evansi*. The mobile fraction of the YFP-tagged protein, as reflected in the R_{max} value in the BS ROI, was 0.47 ± 0.188 (Fig. 3E), while that of AK *T. b. evansi* was 0.71 ± 0.175 (Fig. 3F). This difference between the mean R_{max} values obtained from fitted curves from all of the replicates of each sample is statistically significant ($P = 0.001$). The MRP1/2 complex thus exhibits significantly higher motility in the mitochondrial lumen of *T. b. evansi*, which differs from the BS by the absence of organellar RNA. Furthermore, the presence of an immobile fraction, as demonstrated by the *T. b.*

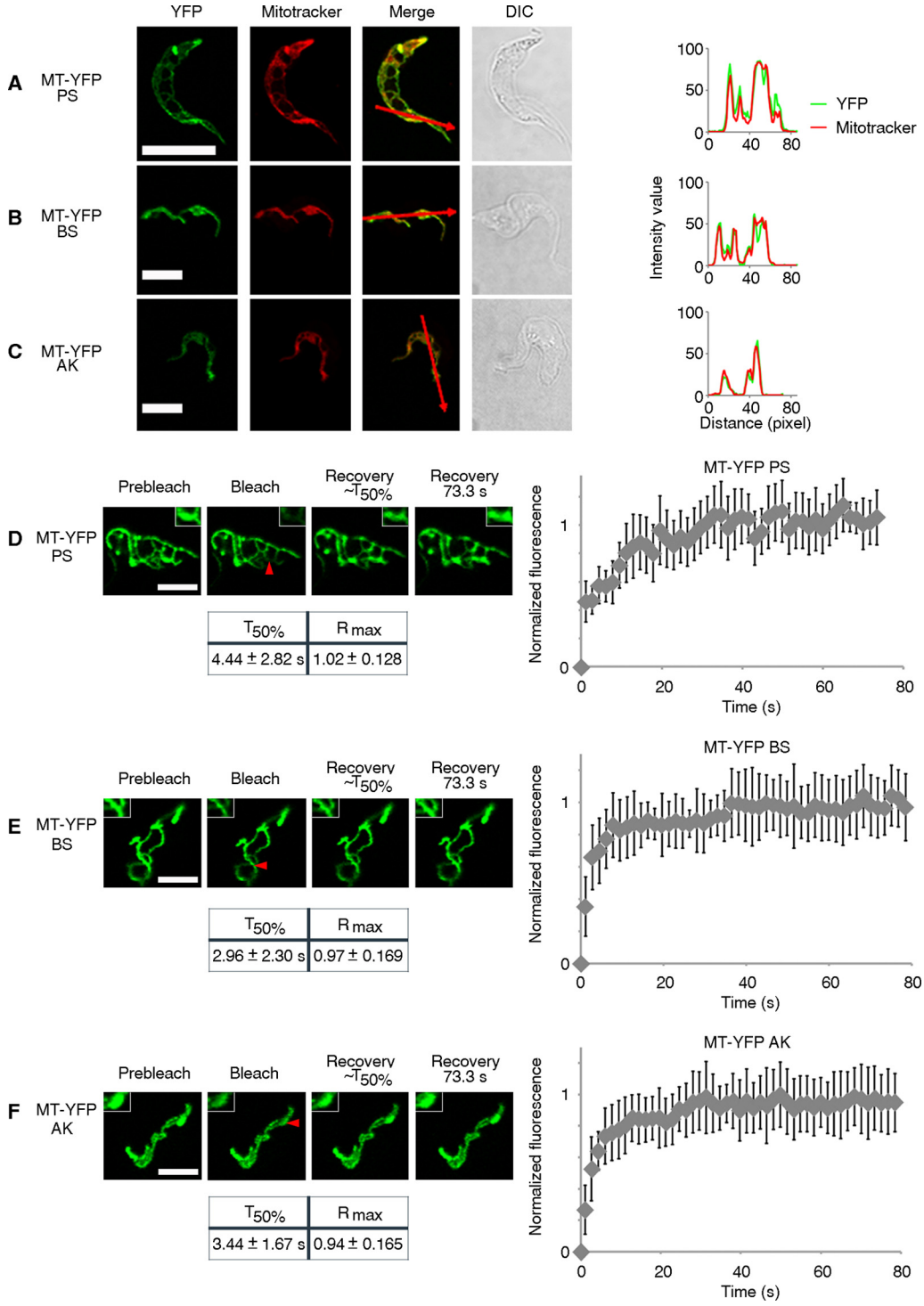

FIG 2 FRAP analysis of mitochondrion-targeted YFP in live immobilized trypanosomes. (A to C) Mitochondrial localization and distribution of MT-YFP in PS *T. b. brucei* (A), BS *T. b. brucei* (B), and AK *T. b. evansi* (C). From left to right, the YFP and Mitotracker Red channels are indicated at the top, followed by a merged view of both images in which the trace of the line scan used to measure each channel's fluorescence intensity is indicated by a red arrow. The plotted intensities along the line are shown to the right of the differential interference contrast (DIC) images of the trypanosomes. (D to F) FRAP analysis of MT-YFP in PS *T. b. brucei* (D), BS *T. b. brucei* (E), and AK *T. b. evansi* (F). To the left are representative images acquired in a FRAP experiment during, from left to right, the prebleaching, bleached, and approximate $T_{50\%}$ and maximal-recovery time points. The photobleached ROI is indicated by the red arrowhead in the bleached image and is enlarged ×2.5 in the insets. To the right are the average fluorescence recovery curves from PS (n = 14 cells) plus BS and AK (n = 15 cells) trypanosomes, normalized as described in Materials and Methods. The mean $T_{50\%}$ and R_{max} values ± SDs determined from the fitted curves generated from these measurements (for data obtained from the fitted curves for each replicate of PS, BS, and AK trypanosomes, see Tables S1 to S3 in the supplemental material) are shown below the FRAP images. Scale bars, 10 μm (A) and 5 μm (B to F).

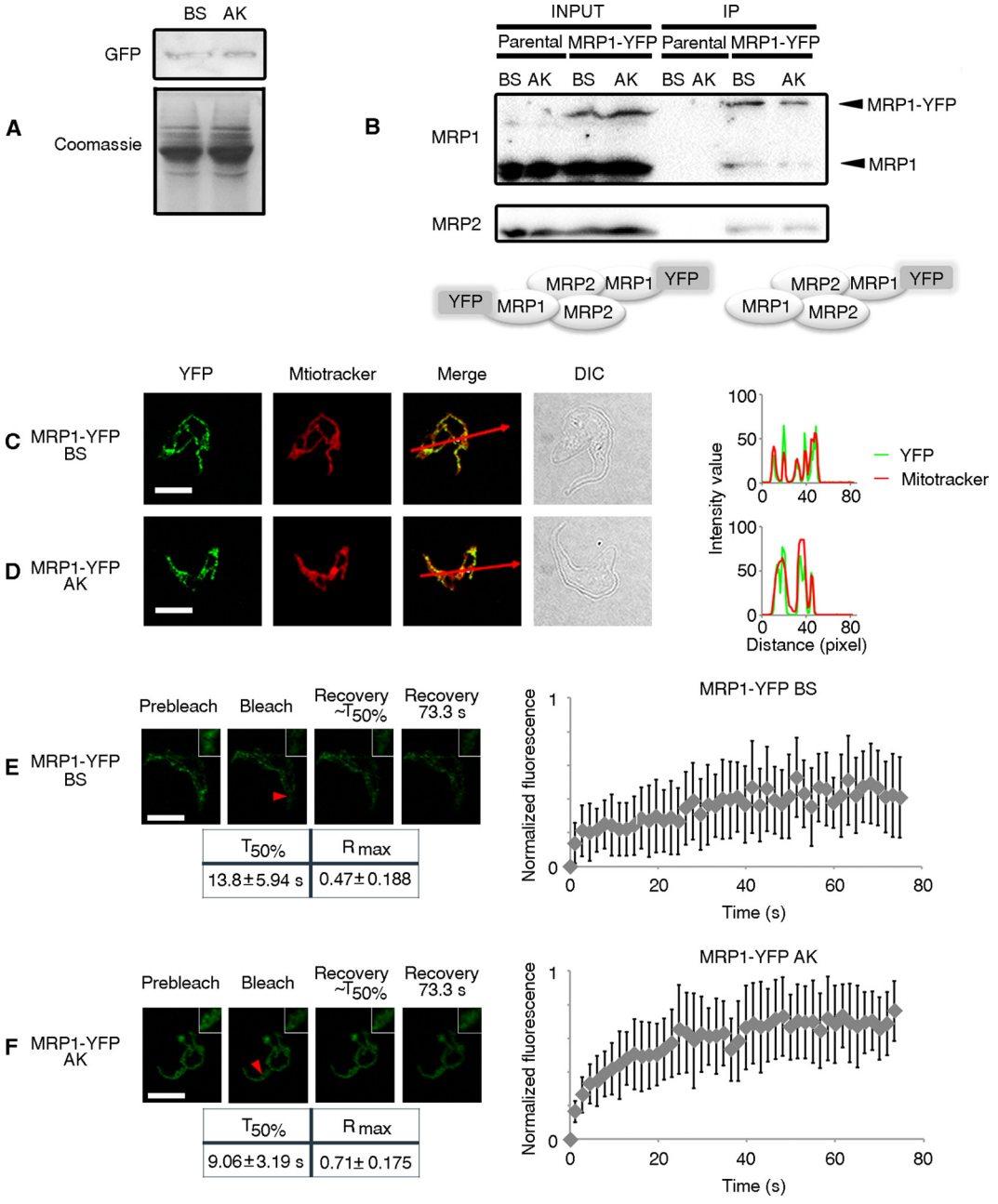

FIG 3 FRAP analysis of *in situ* YFP-tagged MRP1 in BS and AK trypanosomes. (A) Comparison of levels of MRP1-YFP expression in BS and AK trypanosomes with polyclonal anti-GFP antibody (top) and Coomassie staining of these samples as a control to ensure equal loading (bottom). (B) Coimmunoprecipitation of endogenous MRP1/2 with MRP1-YFP in BS *T. b. brucei* and AK *T. b. evansi*. The input and immunoprecipitated (IP) fractions of the parental cell lines, from which the MRP1-YFP fractions are derived, and the MRP1-YFP cell lines are indicated at the top. The signal from the antibody raised against either MRP1 or -2 is indicated to the left of each Western blot. Below is a schematic depiction of the two configurations of the MRP1/2 complex bearing MRP1-YFP. (C, D) Mitochondrial localization and distribution of MRP1-YFP in BS *T. b. brucei* (C) and AK *T. b. evansi* (D) shown as in Fig. 2A to C. (E, F) FRAP analysis of MRP1-YFP in BS *T. b. brucei* ($n = 17$ cells) (E) and AK *T. b. evansi* ($n = 14$ cells) (F) shown as in Fig. 2D to F. The mean $T_{50\%}$ and R_{max} values ± SDs obtained from individual fitted curves for each replicate (see Tables S4 and S5 in the supplemental material for BS and AK data, respectively) are shown below the representative FRAP images. Scale bars, 5 μm.

evansi MRP1-YFP recovery curve, revealed that RNA is not the only factor that affects the mobility of the MRP1/2 complex, implying interactions with other structures and/or molecules enclosed by the mitochondrial inner membrane.

We decided also to address this phenomenon in PS *T. b. brucei*. As in the BS, MRP1-YFP was properly assembled into the MRP1/2 complex and localized throughout the mitochondrial lumen (see Fig. S3A and B in the supplemental material). While there was indeed an immobile fraction in the PS ($R_{max} = 0.797 \pm 0.173$) as well, it was smaller than that in the BS ($R_{max} = 0.47 \pm 0.188$) (see Fig. S3C).

DISCUSSION

The development of live-imaging techniques such as FRAP and FCS has been instrumental in advancing our knowledge of cell biology, such as addressing spliceosome assembly in HeLa cells (28, 34). In contrast to the situation in adherent cell types, the use of these techniques in *T. brucei* and related flagellates has been hampered by their highly motile nature, which is an essential part of their biology (7, 12). In this work, we describe an immobilization method that overcomes this problem and opens an opportunity to exploit the simple architecture of trypanosomes for this line of research (1). The method is rapid, economical, and reproducible, using a thin agarose block to restrain cells on top of a coverslip for visualization with an inverted microscope. The gentle preparation protocol, which avoids the brief drying steps of other immobilization protocols (2, 8), is robust enough for application to both PS and BS *in vitro* cultures, which are life stages with very different physiological states (5).

An essential prerequisite for such studies is that the cells be maintained in a vital state. In order to validate the method, we assayed the viability of trypanosomes by scoring for the percentage of dead cells that incorporate PI in the two life cycle stages tested. According to this assay, cell viability is maintained for 3 h for the PS and 2 h for the BS. These results were confirmed by the morphology of the mitochondrion, which eventually took on a fragmented appearance as cells began to regress, as visualized by leader sequence-directed MT-YFP.

The MT-YFP-expressing cell lines were further investigated by FRAP in order to better assess the condition of the trypanosomes, as well as test the suitability of this type of immobilization for such live-imaging techniques. In contrast to the situation with cytosolic GFP-expressing *L. major* embedded in a CyGEL matrix (12), the photobleached ROI exhibited full recovery in PS, BS, and AK MT-YFP trypanosomes. This observation is consistent with a healthy state of the immobilized flagellates, as it reproduces robust recovery results from FRAP with mitochondrion-targeted GFP in adherent mammalian cell lines (29, 35), a system that does not require immobilization steps that could affect cell viability. Furthermore, no such recovery was seen in dying trypanosomes upon FRAP of MT-YFP. The immobilization technique also proved to restrain cells in a manner suitable for recording of fluorescence recovery within an approximately 0.1-μm^2 ROI.

With the utility of FRAP on trypanosomes immobilized by our new technique confirmed, we decided to investigate the dynamics of the *in situ* C-terminally tagged MRP1-YFP, which was verified to be incorporated into the abundant RNA-binding MRP1/2 complex (14, 15, 17). The dynamics of the MRP1/2 complex were compared in BS and AK *T. b. evansi* cells to determine the influence of mitochondrion-encoded RNAs, which are absent from the latter subspecies (9, 21, 23). In the BS, more of the MRP1/2 complex was in an immobile fraction than in AK *T. b. evansi*, as it achieved an R_{max} of 0.47 ± 0.188 of the prebleach fluorescence within the photobleached ROI compared to an R_{max} of 0.71 ± 0.175 in AK cells. The presence of mitochondrion-encoded RNA clearly hinders the dynamics of the MRP1/2 complex (Fig. 4A). We exclude the possibility that physiological changes in the AK mitochondrion that are due to loss of the mitochondrion-encoded subunit of F_0F_1-ATP synthase and compensatory mutations in the nucleus-encoded γ subunit (9, 22) underlie this difference in the translational diffusion of MRP1/2 because MT-YFP exhibits similar dynamics within the matrix compartment of both types of organelles. Other proteins simultaneously coating RNAs bound to MRP1/2 may contribute to this apparent drag in BS, as the MRP1/2 complex has been shown in the related trypanosomatid *Leishmania tarentolae* to associate via RNA with the RECC, conferring the core enzymatic activities needed for RNA editing, and members of mitochondrial RNA-binding complex 1 (17), which plays an ancillary role in the process (36).

Surprisingly, the MRP1/2 complex in AK *T. b. evansi* does not fully recover to prephotobleached levels within the MRP1-YFP1

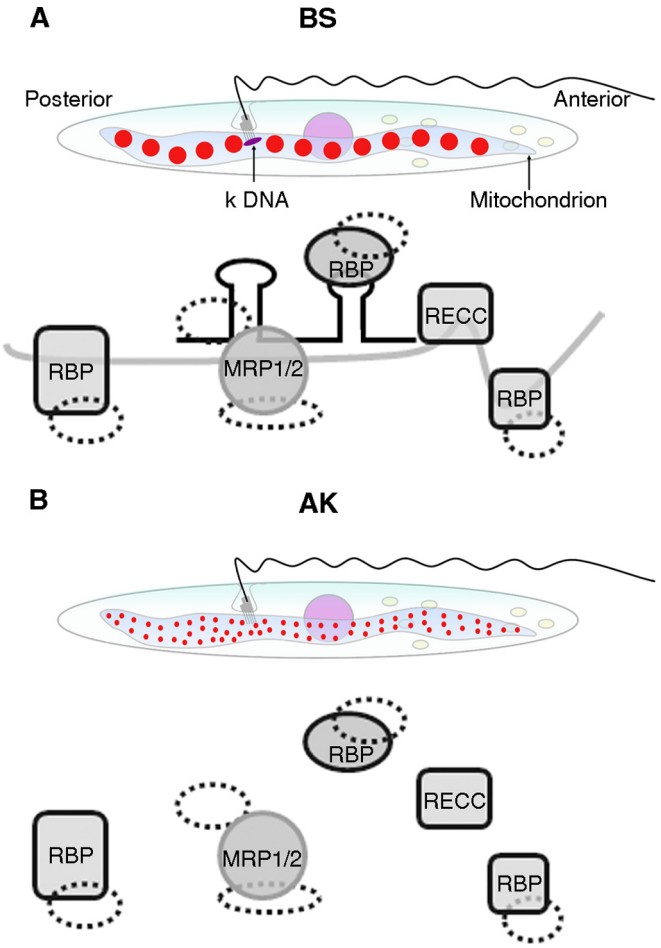

FIG 4 Schematic illustration of RNA-processing protein complexes in BS and AK trypanosomes. (A) RNA-protein complex distribution in the BS. In the presence of kDNA and its encoded RNA, MRP1/2 exists in RNA-protein complexes (large red circles), which are evenly distributed throughout the whole mitochondrial matrix and associated with other proteins coating the same RNA. The gray schemes below the cell models show that MRP1/2-bound RNA is undergoing the RNA-editing process with the RECC, gRNA, and other RNA-binding proteins (RBP) bound to the same RNA molecule. The dashed circles represent speculated proteins bound directly to MRP1/2 and other proteins. (B) Distribution and construction of the RNA-processing protein complex with the absence of RNA in AK *T. b. evansi*. In the absence of kDNA and organelle-encoded RNA, identical proteins involved in RNA processing shown in panel A are still scattered throughout the mitochondrial matrix but as smaller complexes not aggregating around RNA (small red circles). The gray scheme below the cell model shows that MRP1/2 is perhaps bound to other proteins, depicted as dashed circles as in panel A. Other proteins that interact with MRP1/2 via RNA linkers in panel A are shown but are independent of MRP1/2 in AK *T. b. evansi*.

ROI. Even in this environment without mitochondrion-encoded RNA, there is an immobile fraction of the heterotetramer. There are some possible explanations for this phenomenon (Fig. 4B). The first one postulates that the MRP1/2 complex interacts with other proteins in an RNA-independent manner. However, there is very little evidence thus far that the MRP1/2 complex interacts with any polypeptides outside the complex (37). Alternatively, the MRP1/2 complex may interact with tRNAs that are futilely imported into the AK mitochondrion, although proteins that normally bind these nucleic acids to facilitate their role in translation are also present (23, 24), likely sequestering them from spurious interaction with MRP1/2. Another possibility is that the 125- to 150-kDa MRP1/2 complex, bearing one or two copies of MRP1-YFP, is more prone to molecular sieving effects within the matrix than MT-YFP is, leading to an apparent immobile fraction. Finally, association with another structure within the mitochondrion, such as the inner membrane, may hinder a fraction of MRP1/2. Mitochondrial RNA metabolism pathways could be located in proximity to the inner membrane, where translation of mature mRNAs by mitochondrial ribosomes occurs to facilitate the incorporation of nascent polypeptides into the lipid bilayer (38). MRP1/2 association with this part of the organelle in the AK trypanosome could be a vestige of this now obsolete process.

The translational diffusion of the MRP1/2 complex was also assayed in PS *T. b. brucei*. While an immobile fraction of the complex was observed, it was much smaller than that in the BS. However, direct comparison of these results between the BS and the PS is more complicated than that made between BS and AK *T. b. evansi*. For instance, the two life cycle stages harbor mitochondria that have very different morphological and physiological states, which could have differing impacts on the translational diffusion of the matrix proteins. Furthermore, the mitochondrial transcriptomes differ between the PS and the slender BS by a still unknown mechanism and extent (39). Perhaps this observation may be due in part to this phenomenon.

The immobilization technique developed for this study has allowed us to exploit the availability of AK *T. b. evansi in vitro* cultures to study the impact of RNA on the dynamics of the abundant RNA-binding MRP1/2 complex. Until now, the behaviors of proteins involved in mitochondrial RNA metabolism have not been explored in live cells. The use of FRAP has brought a different perspective not only to our current knowledge about the MRP1/2 tetramer but also to how RNA can affect the dynamics of proteins involved in the byzantine RNA metabolism of the trypanosome mitochondrion, in which hundreds of proteins in several complexes are coordinated to express the few proteins encoded by kDNA.

ACKNOWLEDGMENTS

We thank Michael Ginger (University of Lancaster, Lancaster, United Kingdom) and Mark Carrington (University of Cambridge, Cambridge, United Kingdom) for pDEX577-Y and p2937 and Achim Schnaufer (University of Edinburgh, Edinburgh, United Kingdom) for providing the *T. b. evansi* cell line. We thank Martin Hof and Jan Sýkora (J. Heyrovský Institute of Physical Chemistry, Czech Republic), as well as Maria Carmo-Fonseca and José Rino (Instituto de Medicina Molecular, Portugal) and Radek Kaňa (Institute of Microbiology, Czech Republic), for enlightening discussions and valuable advice.

This work was supported by the Czech grant agency (P305/12/2261), the RNPnet FP7 program (289007), Bioglobe grant CZ.1.07/2.3.00/30.0032, and a Praemium Academiae award to J.L., who is also a Fellow of the Canadian Institute for Advanced Research. We acknowledge the use of research infrastructure funded from EU 7th Framework program 316304.

REFERENCES

1. **Matthews KR.** 2005. The developmental cell biology of *Trypanosoma brucei*. J. Cell Sci. **118:**283–290. http://dx.doi.org/10.1242/jcs.01649.
2. **Ho HH, He CY, de Graffenried CL, Murrells LJ, Warren G.** 2006. Ordered assembly of the duplicating Golgi in *Trypanosoma brucei*. Proc. Natl. Acad. Sci. U. S. A. **103:**7676–7681. http://dx.doi.org/10.1073/pnas.0602595103.
3. **He CY, Pypaert M, Warren G.** 2005. Golgi duplication in *Trypanosoma brucei* requires Centrin2. Science **310:**1196–1198. http://dx.doi.org/10.1126/science.1119969.
4. **Lukeš J, Hashimi H, Verner Z, Čičová Z.** 2010. The remarkable mitochondrion of trypanosomes and related flagellates, p 227–252. *In* de Souza W (ed), Structures and organelles in pathogenic protists. Springer, Berlin, Germany.
5. **Bringaud F, Riviere L, Coustou V.** 2006. Energy metabolism of trypanosomatids: adaptation to available carbon sources. Mol. Biochem. Parasitol. **149:**1–9. http://dx.doi.org/10.1016/j.molbiopara.2006.03.017.
6. **Gordon GW, Berry G, Liang XH, Levine B, Herman B.** 1998. Quantitative fluorescence resonance energy transfer measurements using fluorescence microscopy. Biophys. J. **74:**2702–2713. http://dx.doi.org/10.1016/S0006-3495(98)77976-7.
7. **Broadhead R, Dawe HR, Farr H, Griffiths S, Hart SR, Portman N, Shaw MK, Ginger ML, Gaskell SJ, McKean PG, Gull K.** 2006. Flagellar motility is required for the viability of the bloodstream trypanosome. Nature **440:**224–227. http://dx.doi.org/10.1038/nature04541.
8. **Pérez-Morga D, Vanhollebeke B, Paturiaux-Hanocq F, Nolan DP, Lins L, Homble F, Vanhamme L, Tebabi P, Pays A, Poelvoorde P, Jacquet A, Brasseur R, Pays E.** 2005. Apolipoprotein L-I promotes trypanosome lysis by forming pores in lysosomal membranes. Science **309:**469–472. http://dx.doi.org/10.1126/science.1114566.
9. **Schnaufer A, Clark-Walker GD, Steinberg AG, Stuart K.** 2005. The F1-ATP synthase complex in bloodstream stage trypanosomes has an unusual and essential function. EMBO J. **24:**4029–4040. http://dx.doi.org/10.1038/sj.emboj.7600862.
10. **Esson HJ, Morriswood B, Yavuz S, Vidilaseris K, Dong G, Warren G.** 2012. Morphology of the trypanosome bilobe, a novel cytoskeletal structure. Eukaryot. Cell **11:**761–772. http://dx.doi.org/10.1128/EC.05287-11.
11. **Buisson J, Chenouard N, Lagache T, Blisnick T, Olivo-Marin JC, Bastin P.** 2013. Intraflagellar transport proteins cycle between the flagellum and its base. J. Cell Sci. **126:**327–338. http://dx.doi.org/10.1242/jcs.117069.
12. **Price HP, MacLean L, Marrison J, O'Toole PJ, Smith DF.** 2010. Validation of a new method for immobilising kinetoplastid parasites for live cell imaging. Mol. Biochem. Parasitol. **169:**66–69. http://dx.doi.org/10.1016/j.molbiopara.2009.09.008.
13. **Maclean LM, O'Toole PJ, Stark M, Marrison J, Seelenmeyer C, Nickel W, Smith DF.** 2012. Trafficking and release of *Leishmania* metacyclic HASPB on macrophage invasion. Cell. Microbiol. **14:**740–761. http://dx.doi.org/10.1111/j.1462-5822.2012.01756.x.
14. **Zíková A, Kopečná J, Schumacher MA, Stuart K, Trantírek L, Lukeš J.** 2008. Structure and function of the native and recombinant mitochondrial MRP1/MRP2 complex from *Trypanosoma brucei*. Int. J. Parasitol. **38:**901–912. http://dx.doi.org/10.1016/j.ijpara.2007.12.009.
15. **Schumacher MA, Karamooz E, Zíková A, Trantírek L, Lukeš J.** 2006. Crystal structures of *T. brucei* MRP1/MRP2 guide-RNA binding complex reveal RNA matchmaking mechanism. Cell **126:**701–711. http://dx.doi.org/10.1016/j.cell.2006.06.047.
16. **Müller UF, Lambert L, Goringer HU.** 2001. Annealing of RNA editing substrates facilitated by guide RNA-binding protein gBP21. EMBO J. **20:**1394–1404. http://dx.doi.org/10.1093/emboj/20.6.1394.
17. **Aphasizhev R, Aphasizheva I, Nelson RE, Simpson L.** 2003. A 100-kD complex of two RNA-binding proteins from mitochondria of *Leishmania tarentolae* catalyzes RNA annealing and interacts with several RNA editing components. RNA **9:**62–76. http://dx.doi.org/10.1261/rna.2134303.
18. **Fisk JC, Presnyak V, Ammerman ML, Read LK.** 2009. Distinct and overlapping functions of MRP1/2 and RBP16 in mitochondrial RNA metabolism. Mol. Cell. Biol. **29:**5214–5225. http://dx.doi.org/10.1128/MCB.00520-09.
19. **Lambert L, Müller UF, Souza AE, Goringer HU.** 1999. The involvement of gRNA-binding protein gBP21 in RNA editing—an *in vitro* and *in vivo*

analysis. Nucleic Acids Res. **27:**1429–1436. http://dx.doi.org/10.1093/nar/27.6.1429.
20. **Vondrusková E, van den Burg J, Zíková A, Ernst NL, Stuart K, Benne R, Lukeš J.** 2005. RNA interference analyses suggest a transcript-specific regulatory role for mitochondrial RNA-binding proteins MRP1 and MRP2 in RNA editing and other RNA processing in *Trypanosoma brucei*. J. Biol. Chem. **280:**2429–2438. http://dx.doi.org/10.1074/jbc.M405933200.
21. **Lai DH, Hashimi H, Lun ZR, Ayala FJ, Lukeš J.** 2008. Adaptations of *Trypanosoma brucei* to gradual loss of kinetoplast DNA: *Trypanosoma equiperdum* and *Trypanosoma evansi* are petite mutants of *T. brucei*. Proc. Natl. Acad. Sci. U. S. A. **105:**1999–2004. http://dx.doi.org/10.1073/pnas.0711799105.
22. **Dean S, Gould MK, Dewar CE, Schnaufer AC.** 2013. Single point mutations in ATP synthase compensate for mitochondrial genome loss in trypanosomes. Proc. Natl. Acad. Sci. U. S. A. **110:**14741–14746. http://dx.doi.org/10.1073/pnas.1305404110.
23. **Paris Z, Hashimi H, Lun S, Alfonzo JD, Lukeš J.** 2011. Futile import of tRNAs and proteins into the mitochondrion of *Trypanosoma brucei evansi*. Mol. Biochem. Parasitol. **176:**116–120. http://dx.doi.org/10.1016/j.molbiopara.2010.12.010.
24. **Cristodero M, Seebeck T, Schneider A.** 2010. Mitochondrial translation is essential in bloodstream forms of *Trypanosoma brucei*. Mol. Microbiol. **78:**757–769. http://dx.doi.org/10.1111/j.1365-2958.2010.07368.x.
25. **Domingo GJ, Palazzo SS, Wang B, Pannicucci B, Salavati R, Stuart KD.** 2003. Dyskinetoplastic *Trypanosoma brucei* contains functional editing complexes. Eukaryot. Cell **2:**569–577. http://dx.doi.org/10.1128/EC.2.3.569-577.2003.
26. **Hashimi H, McDonald L, Stříbrná E, Lukeš J.** 2013. Trypanosome Letm1 protein is essential for mitochondrial potassium homeostasis. J. Biol. Chem. **288:**26914–26925. http://dx.doi.org/10.1074/jbc.M113.495119.
27. **Kelly S, Reed J, Kramer S, Ellis L, Webb H, Sunter J, Salje J, Marinsek N, Gull K, Wickstead B, Carrington M.** 2007. Functional genomics in *Trypanosoma brucei*: a collection of vectors for the expression of tagged proteins from endogenous and ectopic gene loci. Mol. Biochem. Parasitol. **154:**103–109. http://dx.doi.org/10.1016/j.molbiopara.2007.03.012.
28. **Martins SB, Rino J, Carvalho T, Carvalho C, Yoshida M, Klose JM, de Almeida SF, Carmo-Fonseca M.** 2011. Spliceosome assembly is coupled to RNA polymerase II dynamics at the 3′ end of human genes. Nat. Struct. Mol. Biol. **18:**1115–1123. http://dx.doi.org/10.1038/nsmb.2124.
29. **Dieteren CE, Gielen SC, Nijtmans LG, Smeitink JA, Swarts HG, Brock R, Willems PH, Koopman WJ.** 2011. Solute diffusion is hindered in the mitochondrial matrix. Proc. Natl. Acad. Sci. U. S. A. **108:**8657–8662. http://dx.doi.org/10.1073/pnas.1017581108.
30. **Kaňa R.** 2013. Mobility of photosynthetic proteins. Photosynth. Res. **116:**465–479. http://dx.doi.org/10.1007/s11120-013-9898-y.
31. **Goodwin JS, Kenworthy AK.** 2005. Photobleaching approaches to investigate diffusional mobility and trafficking of Ras in living cells. Methods **37:**154–164. http://dx.doi.org/10.1016/j.ymeth.2005.05.013.
32. **Baicu SC, Taylor MJ.** 2002. Acid-base buffering in organ preservation solutions as a function of temperature: new parameters for comparing buffer capacity and efficiency. Cryobiology **45:**33–48. http://dx.doi.org/10.1016/S0011-2240(02)00104-9.
33. **Fritz-Laylin LK, Prochnik SE, Ginger ML, Dacks JB, Carpenter ML, Field MC, Kuo A, Paredez A, Chapman J, Pham J, Shu S, Neupane R, Cipriano M, Mancuso J, Tu H, Salamov A, Lindquist E, Shapiro H, Lucas S, Grigoriev IV, Cande WZ, Fulton C, Rokhsar DS, Dawson SC.** 2010. The genome of *Naegleria gruberi* illuminates early eukaryotic versatility. Cell **140:**631–642. http://dx.doi.org/10.1016/j.cell.2010.01.032.
34. **Huranová M, Ivani I, Benda A, Poser I, Brody Y, Hof M, Shav-Tal Y, Neugebauer KM, Staněk D.** 2010. The differential interaction of snRNPs with pre-mRNA reveals splicing kinetics in living cells. J. Cell Biol. **191:**75–86. http://dx.doi.org/10.1083/jcb.201004030.
35. **Partikian A, Olveczky B, Swaminathan R, Li Y, Verkman AS.** 1998. Rapid diffusion of green fluorescent protein in the mitochondrial matrix. J. Cell Biol. **140:**821–829. http://dx.doi.org/10.1083/jcb.140.4.821.
36. **Hashimi H, Zimmer SL, Ammerman ML, Read LK, Lukeš J.** 2013. Dual core processing: MRB1 is an emerging kinetoplast RNA editing complex. Trends Parasitol. **29:**91–99. http://dx.doi.org/10.1016/j.pt.2012.11.005.
37. **Panigrahi AK, Zíková A, Dalley RA, Acestor N, Ogata Y, Anupama A, Myler PJ, Stuart KD.** 2008. Mitochondrial complexes in *Trypanosoma brucei*: a novel complex and a unique oxidoreductase complex. Mol. Cell. Proteomics **7:**534–545. http://dx.doi.org/10.1074/mcp.M700430-MCP200.
38. **Maslov D, Agrawal R.** 2012. Mitochondrial translation in trypanosomatids, p 215–236. *In* Bindereif A (ed), RNA metabolism in trypanosomes. Springer, Berlin, Germany.
39. **Schnaufer A, Domingo GJ, Stuart K.** 2002. Natural and induced dyskinetoplastic trypanosomatids: how to live without mitochondrial DNA. Int. J. Parasitol. **32:**1071–1084. http://dx.doi.org/10.1016/S0020-7519(02)00020-6.

Attached Publications

Part III.

TRYPANOSOME MITOCHONDRIAL TRANSLATION

Attached Publications

Part III. TRYPANOSOME MITOCHONDRIAL TRANSLATION

Marina Cristodero, Jan Mani, Silke Oeljeklaus, Lukas Aeberhard, Hassan Hashimi, David J. F. Ramrath, Julius Lukeš, Bettina Warscheid and André Schneider (2013). Mitochondrial translation factors of *Trypanosoma brucei*: Elongation factor-Tu has a unique subdomain that is essential for its function. *Mol. Microbiol.* 90: 744-755.

This paper describes the functional analysis of elongation factors EF-Tu, EF-Ts and EF-G1 plus the release factor RF1 in trypanosome mitochondrial translation. All of these proteins are essential for the process, and surprisingly, EF-Tu has a unique subdomain that may allow this protein to interact with tRNAs that must be imported from the cytosol. Furthermore, interference of mitochondrial translation leads to a downregulation of nucleus-encoded subunits of the respiratory chain and upregulation of cytosolic ribosome proteins.

Molecular Microbiology (2013) 90(4), 744–755 ■
doi:10.1111/mmi.12397
First published online 30 September 2013

Mitochondrial translation factors of *Trypanosoma brucei*: elongation factor-Tu has a unique subdomain that is essential for its function

Marina Cristodero,[1†] Jan Mani,[1] Silke Oeljeklaus,[2] Lukas Aeberhard,[1‡] Hassan Hashimi,[3,4] David J. F. Ramrath,[5] Julius Lukeš,[3,4] Bettina Warscheid[2] and André Schneider[1*]

[1]*Department of Chemistry and Biochemistry, University of Bern, Freiestrasse 3, CH-3012 Bern, Switzerland.*
[2]*Faculty of Biology and BIOSS Centre for Biological Signalling Studies, University of Freiburg, 79104 Freiburg, Germany.*
[3]*Institute of Parasitology, Biology Center, Czech Academy of Sciences, 370 05 České Budějovice (Budweis), Czech Republic.*
[4]*Faculty of Science, University of South Bohemia, 370 05 České Budějovice (Budweis), Czech Republic.*
[5]*Institute of Molecular Biology and Biophysics, Swiss Federal Institute of Technology (ETH Zürich), Zürich, Switzerland.*

Summary

Mitochondrial translation in the parasitic protozoan *Trypanosoma brucei* relies on imported eukaryotic-type tRNAs as well as on bacterial-type ribosomes that have the shortest known rRNAs. Here we have identified the mitochondrial translation elongation factors EF-Tu, EF-Ts, EF-G1 and release factor RF1 of trypanosomatids and show that their ablation impairs growth and oxidative phosphorylation. *In vivo* labelling experiments and a SILAC-based analysis of the global proteomic changes induced by EF-Tu RNAi directly link EF-Tu to mitochondrial translation. Moreover, EF-Tu RNAi reveals downregulation of many nuclear encoded subunits of cytochrome oxidase as well as of components of the bc1-complex, whereas most cytosolic ribosomal proteins were upregulated. Interestingly, *T. brucei* EF-Tu has a 30-amino-acid-long, highly charged subdomain, which is unique to trypanosomatids. A combination of RNAi and complementation experiments shows that this subdomain is essential for EF-Tu function, but that it can be replaced by a similar sequence found in eukaryotic EF-1a, the cytosolic counterpart of EF-Tu. A recent cryo-electron microscopy study revealed that trypanosomatid mitochondrial ribosomes have a unique intersubunit space that likely harbours the EF-Tu binding site. These findings suggest that the trypanosomatid-specific EF-Tu subdomain serves as an adaption for binding to these unusual mitochondrial ribosomes.

Accepted 7 September, 2013. *For correspondence. E-mail andre.schneider@ibc.unibe.ch; Tel. (+41) 31 631 4253; Fax (+41) 31 631 4887. †Present address: Institute of Cell Biology, University of Bern, Baltzerstrasse 4, CH-3012 Bern, Switzerland. ‡Present address: Robert Koch-Institut, Nordufer 20, 13353 Berlin, Germany.

Introduction

Mitochondria derive from an α-proteobacterial endosymbiont that during evolution either has transferred most of its genes to the nucleus or lost them for good. Most of the mitochondrial proteome, consisting of 1000 or more proteins, is therefore produced in the cytosol and subsequently imported into the organelle. However, a typical mitochondrial genome still encodes a small set of proteins (8 in yeast and 13 in humans) that is essential for oxidative phosphorylation (OXPHOS), the main function of mitochondria. To produce these proteins, mitochondria need their own translation system consisting of ribosomes, a full set of tRNAs and soluble translation factors. In line with their evolutionary descent the translation system of mitochondria is of the bacterial type (Gray, 2012). However, mitochondria and bacteria diverged approximately 2 billion years ago, resulting in many unique features of the mitochondrial translation system. Mitochondrial ribosomes are anchored to the membrane, have much shorter rRNAs and a larger number of ribosomal proteins. Mitochondrial mRNAs lack Shine–Dalgarno sequences and often are translated by a variant genetic code. Translation uses a reduced set of tRNAs that generally are shorter than their bacterial or cytosolic counterparts (Agrawal and Sharma, 2012; Gray, 2012).

The soluble mitochondrial translation factors, such as elongation factor Tu (EF-Tu), elongation factor Ts (EF-Ts), elongation factor G (EF-G) and release factor 1 (RF1) are orthologues of the corresponding factors in bacteria (Spremulli *et al.*, 2004). The small GTPase EF-Tu forms a complex with GTP and aminoacylated elongator tRNAs,

bringing the latter to the A site of the ribosome. There the GTPase activity of EF-Tu is stimulated, causing a conformational change that eventually leads to the release of the aminoacylated tRNA. The GTP exchange factor EF-Ts binds to the GDP-form of EF-Tu and induces its recycling by exchanging GDP for GTP. The conserved bacterial GTPase EF-G has two functions. It catalyses the translocation step after peptide bond formation and is involved in ribosome recycling. Interestingly, mitochondria have two orthologues of EF-G: EF-G1 and EF-G2, which are required for ribosomal translocation and recycling respectively. Finally, translation is terminated by binding of RF1 to the stop codons UAA and UAG, which releases the completed polypeptide (Spremulli *et al.*, 2004; Rorbach *et al.*, 2007).

Most of what we know about mitochondrial translation stems from work in yeast and mammals, which are quite closely related. To understand the conserved features of mitochondrial translation and the evolutionary forces that shaped it, it is important to study the process in a more diverse group of eukaryotes. The parasitic protozoan *Trypanosoma brucei* and its relatives are excellent systems to do so, since they appear to have diverged from other eukaryotes very early in evolution (Dacks *et al.*, 2008). This is reflected in a number of unusual features of its organellar translation system. The ribosomes of trypanosomal mitochondria for example have very unique structural features including the shortest rRNAs found in nature and a very high protein content (Sharma *et al.*, 2009; Agrawal and Sharma, 2012). Unlike yeast and mammals, the mitochondria of trypanosomatids lack tRNA genes and therefore need to import all tRNAs from the cytosol. Imported tRNAs represent a small fraction of the tRNA population that is used for cytosolic translation. Thus, in trypanosomatids the bacterial-type translation system of the mitochondrion must function exclusively with imported tRNAs, all of which are of the eukaryotic type (Alfonzo and Söll, 2009; Schneider, 2011). This creates problems for mitochondrial translation initiation, which requires a bacterial-type initiator $tRNA^{Met}$. Another conflict arises from the fact that in mitochondria the universal UGA stop codon has been reassigned to tryptophan and therefore cannot be decoded by the $tRNA^{Trp}$(CCA) that is imported from the cytosol. In order to cope with these challenges, trypanosomatids evolved adaptations in their mitochondrial translation system. They have a $tRNA^{Met}$ formyl-transferase that recognizes the imported elongator $tRNA^{Met}$ and allows it to function in organellar translation initiation (Tan *et al.*, 2002a). In the case of the $tRNA^{Trp}$, trypanosomatids acquired an RNA editing enzyme that changes the anticodon of the imported $tRNA^{Trp}$ from CCA to UCA (Alfonzo *et al.*, 1999) and a specific tryptophanyl-tRNA synthetase that is able to charge the edited $tRNA^{Trp}$ (Charrière *et al.*, 2006).

Here we present an *in vivo* analysis of the conserved mitochondrial translation factors EF-Tu, EF-Ts, EF-G1 and RF1 in *T. brucei*. Individual ablation of each of these factors inhibits OXPHOS and consequently normal growth of the procyclic form of the parasite. *In vivo* labelling experiments demonstrate the requirement of EF-Tu for mitochondrial protein synthesis and a quantitative proteomic analysis of the EF-Tu RNAi cell line documents the central role mitochondrially encoded subunits play for the stability and/or assembly of respiratory complexes. Finally, a bioinformatic analysis identified a trypanosomatid-specific motif of EF-Tu that is critical for EF-Tu function but dispensable for its interaction with EF-Ts.

Results

EF-Tu, EF-Ts, EF-G1 and RF1 are essential for normal growth of T. brucei

In silico analysis using the BLAST algorithm readily identifies the trypanosomal orthologues of the mitochondrial translation factors EF-Tu (Tb927.10.13360), EF-Ts (Tb927.3.3630), EF-G1 (Tb927.10.5010) and RF1 (Tb927.3.1070) (Figs S1–S4) (Berriman *et al.*, 2005). In order to determine their localization, we prepared transgenic cell lines allowing the expression of variants of the four proteins carrying either the haemagglutinin (HA) or the cMYC tag at their C-termini. Subsequent digitonin extractions were used to prepare crude mitochondrial and cytosolic fractions (Charrière *et al.*, 2006), which were analysed by immunoblotting. The results showed that, as expected, all four tagged proteins co-purify with mitochondrial heat shock protein 70 (mHSP70) that was used as a mitochondrial marker (Fig. 1). To study their importance for growth, we established stable transgenic cell lines allowing inducible RNAi-mediated ablation of each of the four proteins in procyclic *T. brucei*. For each cell line, the efficiency of RNAi was verified by Northern blot analysis. Figure 2 shows that ablation of all four translation factors resulted in an impairment of normal growth. Whereas for EF-Tu, EF-G1 and RF1 we observe a growth arrest, the ablation of EF-Ts caused a less severe slow growth phenotype. In summary these results show that in procyclic *T. brucei* all four mitochondrial translation factors are essential for normal growth.

Ablation of mitochondrial translation factors impairs OXPHOS

At early time points after induction ablation of mitochondrial translation factors should interfere with mitochondrial protein synthesis without affecting cytosolic translation. All known mitochondrially encoded proteins of *T. brucei* either function directly in OXPHOS or are components of

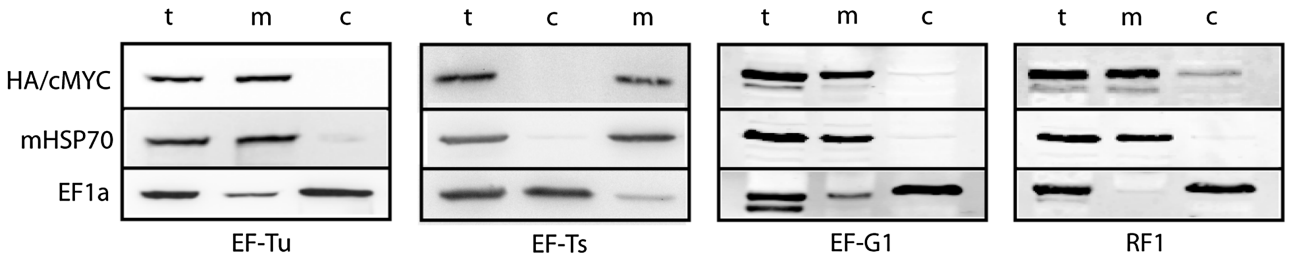

Fig. 1. Localization of epitope-tagged EF-Tu, EF-Ts, EF-G1 and RF1. A total of 0.3×10^7 cell equivalents each of total cellular (t), cytosolic (c) and crude mitochondrial extracts (m) of cell lines expressing C-terminally HA-tagged versions of EF-Tu, EF-G1 and RF1 or cMYC-tagged EF-Ts were analysed by immunoblots using anti-HA- or anti-cMYC-antibodies (top panels). Comparison with molecular mass markers showed that the sizes of the tagged proteins were consistent with the prediction. mHSP70 served as a mitochondrial marker (middle panels) and eukaryotic translation elongation factor 1a (EF1a) was used as a cytosolic marker (bottom panels). Only the relevant regions of the blots are shown.

the mitochondrial ribosomes that produce them (Feagin, 2000). Thus, inhibition of mitochondrial translation will primarily affect OXPHOS but not substrate level phosphorylation (SUBPHOS), which relies exclusively on nuclear-encoded proteins. Measuring OXPHOS activity can therefore be used as a proxy for the functionality of the mitochondrial translation system. The mitochondrion of procyclic *T. brucei* produces ATP by OXPHOS as well as by SUBPHOS catalysed by the citric acid cycle enzyme succinyl-CoA synthetase (Bochud-Allemann and Schneider, 2002). We have established an assay that allows quantification of both modes of ATP production. Extraction of whole cells with low concentrations of digitonin was used to obtain crude mitochondrial fractions that are incubated either with α-ketoglutarate, the substrate for SUBPHOS, or with succinate, a substrate for OXPHOS. Atractyloside, which prevents mitochondrial import of ADP, inhibits both types of mitochondrial ATP production, whereas antimycin an inhibitor of complex III of the respiratory chain selectively blocks OXPHOS (Schneider *et al.*, 2007). Figure 3 shows that ablation of each of the four mitochondrial translation factors of *T. brucei* abolishes OXPHOS without significantly impairing mitochondrial SUBPHOS. These results suggest that the growth phenotypes that are observed in the four RNAi cell lines (Fig. 2) are caused by the inhibition of mitochondrial protein synthesis.

Ablation of EF-Tu abolishes mitochondrial protein synthesis

EF-Tu was studied in more detail. To that end we produced a cell line, termed EF-Tu-3′UTR RNAi, in which in contrast to the cell line shown in Fig. 1A the RNAi was targeting the 3′UTR of the EF-Tu mRNA. Induction of RNAi in this cell line causes essentially the same growth phenotype (Fig. 7A) than was observed in the original RNAi cell line, in which the coding region of EF-Tu was targeted (Fig. 2). The advantage of this new RNAi cell line is that it allows complementation experiments (see below). Uninduced as well as induced EF-Tu-3′UTR RNAi cell lines were subjected to [^{35}S]-methionine labelling of *de novo* synthesized mitochondrially encoded proteins. The labelled proteins were subsequently resolved on a 9%/14% two-dimensional denaturing acrylamide gel (Horváth *et al.*, 2002; Hashimi *et al.*, 2013). The results in Fig. 4 show that in uninduced cells spots corresponding to mitochondrially encoded cytochrome b (CYTB) and cytochrome oxidase subunit 1 (COX1), as well as a number of still unidentified mitochondrial gene products were detected. Induction of EF-Tu RNAi for 5.5 days, the time of the onset of the growth arrest, abolishes this labelling, indicating that EF-Tu as expected is essential for mitochondrial protein synthesis.

Quantitative proteomic analysis of the EF-Tu RNAi cell line

In order to get a more detailed, unbiased and global picture on the effects of ablation of EF-Tu in trypanosomes, we devised a powerful proteomics approach which comprises RNAi combined with stable isotope labelling by amino acids in cell culture (SILAC) and high-resolution mass spectrometry (MS). Uninduced and induced EF-Tu RNAi cells were grown in media containing heavy or light isotopes of lysine and arginine respectively. Equal cell numbers of both populations were then mixed and mitochondria-enriched fractions were prepared by digitonin extraction. Quantitative MS-based analysis allowed to accurately determine the abundance ratio of proteins in uninduced and induced RNAi cells. The experiment was performed in triplicate and statistical analysis allowed us to identify, on a global scale, which proteins exhibit significant changes in abundance in the induced EF-Tu RNAi cell line (Table S1). All in all 1848 proteins were quantified in at least two replicates (data not shown). After 4 days of induction, at the time point the growth arrest becomes

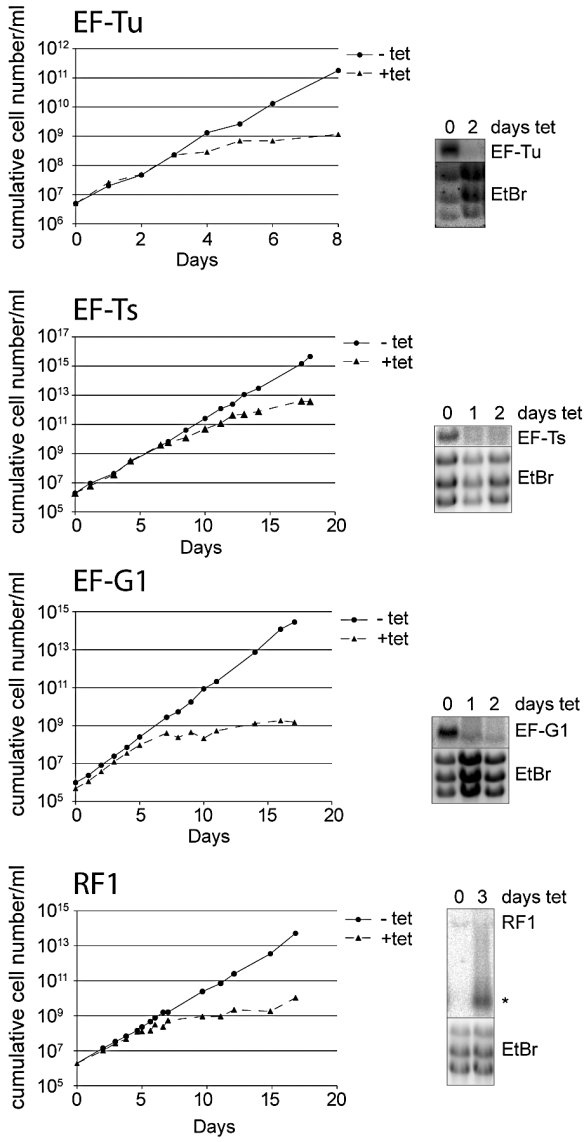

Fig. 2. EF-Tu, EF-Ts, EF-G1 and RF1 are required for normal growth of procyclic *T. brucei*. Growth curves of uninduced (– tet) and induced (+ tet) representative clonal RNAi cell lines directed against the translation factors indicated at the top are shown. The panels on the right depict Northern blots of the corresponding mRNAs isolated at the indicated time points after induction of RNAi. The ethidium bromide (EtBr) stained rRNAs in the lower panels serve as loading controls.

apparent, 21 proteins were more than twofold downregulated (Fig. 5A). As expected the most highly downregulated protein was EF-Tu itself (20-fold), the direct target of the RNAi. Moreover, mitochondrially encoded COX2 was also among the top hits (4.3-fold downregulated). The mitochondrial gene product COX3 was threefold downregulated but only detected in a single replicate (data not shown). A total of 55% of the remaining downregulated proteins are predicted subunits or assembly factors of COX or the bc1-complex (Fig. 5A), which contain three and one mitochondrially encoded subunits respectively. The results were confirmed by blue-native gel analysis which show a decline of the levels of COX4 and cytochrome C1, a subunit of the bc1-complex, in the corresponding respiratory complexes (Fig. 5B). In summary, the proteome-wide quantitative EF-Tu RNAi analysis and the [^{35}S]-methionine *in vivo* labelling experiments allow to directly link the expression of EF-Tu to mitochondrial protein synthesis.

Interestingly, we also report 61 proteins that are more than twofold upregulated upon EF-Tu RNAi (Fig. 5C). Approximately 60% of these are cytosolic ribosomal proteins, suggesting that ablation of mitochondrial translation causes a global upregulation of cytosolic protein synthesis. The remaining more than twofold upregulated proteins include two glucose transporters, alternative oxidase and fumarate hydratase (Table S1). The latter two may indicate that in the absence of a functional respiratory chain the cell tries to balance the redox state by other means.

EF-Tu of T. brucei *contains a trypanosomatid-specific motif*

Unlike in other eukaryotes, mitochondrial translation in *T. brucei* and its relatives has to function with imported cytosolic tRNAs and with highly derived ribosomes having ultra-short rRNAs (Niemann *et al*., 2011). Of all the translation factors mentioned above, EF-Tu is therefore of special interest since it must directly interact with both imported, eukaryotic-type tRNAs and the uniquely structured ribosome. EF-Tu of trypanosomatids is highly similar to EF-Tu of other species (Fig. S1). However, a multiple sequence alignment of EF-Tu orthologues from bacteria and mitochondria of various organisms reveals a trypanosomatid-specific motif of approximately 30 amino acids in length, located 100 amino acid residues from the C-terminus (aa 370–400) (Fig. 6A; Fig. S1). This subdomain is conserved within trypanosomatids and consists of almost 50% charged amino acids, with nine basic and eight acidic residues in *T. brucei*. EF-Tu has a three domain structure consisting of domain 1 (position 1–199 in *Escherichia coli* EF-Tu), which includes the GTP binding site, and domains 2 (aa: 209–296 in *E. coli* EF-Tu) and 3 (aa: 300–393 in *E. coli* EF-Tu) that consist of β-strands only (Krab and Parmeggiani, 1998, Krab & Parmeggiani, 2002). A high-resolution structure of *Thermus thermophilus* EF-Tu in complex with aminoacyl-tRNA and GDP bound to the 70S ribosome has been solved (Schmeing *et al*., 2009). Using the alignment shown in Fig. 6A it is therefore possible to map the trypanosomatid-specific subdomain onto the structure of EF-Tu. This analysis shows that the subdomain localizes to domain 3, where it most likely contributes to a loop that connects two beta-folds (data not shown).

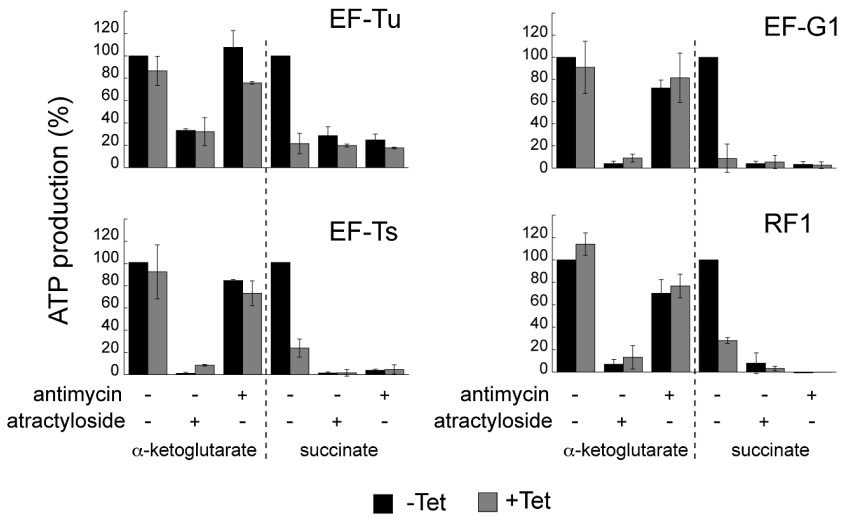

Fig. 3. EF-Tu, EF-Ts, EF-G1 and RF1 are required for OXPHOS but not for mitochondrial SUBPHOS. *In organello* mitochondrial ATP production triggered by α-ketoglutarate and succinate of the indicated uninduced (– Tet) and induced (+ Tet) RNAi cell lines was determined using luciferase-mediated luminescence. The substrates tested and the additions of antimycin and atractyloside are indicated at the bottom. ATP production in mitochondria isolated from uninduced cells tested without antimycin or atractyloside is set to 100%. The bars represent means expressed as percentages. Standard errors of at least three independent biological replicates are indicated. Induction times were: 5 days for EF-Tu; 8 days for EF-Ts; 5 days for EF-G1 and 7 days for RF1.

Eukaryotic translation elongation factor 1a (EF1a) is the orthologue of EF-Tu in the eukaryotic cytosol. Interestingly, a multiple sequence alignment of trypanosomal EF-Tu with cytosolic EF1a orthologues from a number of eukaryotes allows the identification of a conserved sequence segment in EF1a that shows similarity to the trypanosomatid-specific EF-Tu motif (Fig. 6B). With 18 amino acids in length it is shorter than its EF-Tu counterpart, but it is found 60 amino acids from the C-terminus of EF1a in domain 3, which is the same relative position as is seen for the trypanosomatid-specific motif in EF-Tu. Interestingly, the sequence segments in EF-Tu and EF1a consist of almost 50% of charged amino acids and have a high degree of similarity in their central regions.

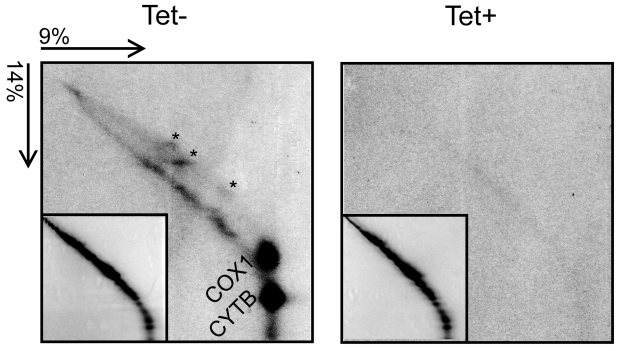

Fig. 4. RNAi silencing of EF-Tu results in inhibition of mitochondrial translation. *De novo* synthesized mitochondrial proteins from parallel uninduced (Tet–) and induced (Tet+, 5.5 days) EF-Tu-3′UTR RNAi cell lines were labelled with S^{35}-methionine and subsequently resolved by two-dimensional SDS-PAGE electrophoresis. Acrylamide concentrations of each gel dimension are indicated in the upper left-hand corner. Identified spots corresponding to CYTB and COX1 are indicated along with unidentified polypeptides (*). Insets show same gels with Coomassie-stained cytoplasmic proteins as loading control.

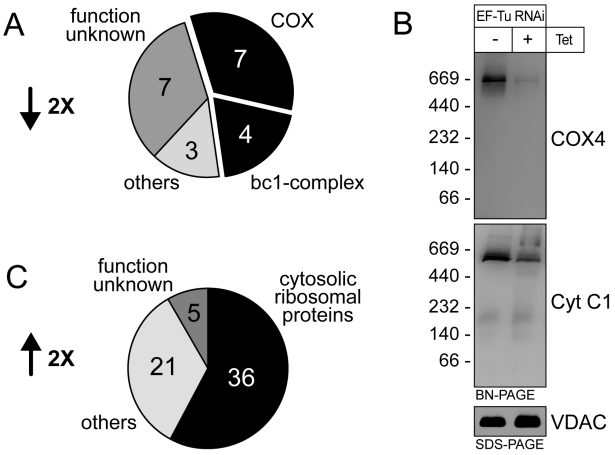

Fig. 5. Global proteomic changes in EF-Tu RNAi cells analysed by SILAC and blue-native gel electrophoresis of respiratory complexes. Equal numbers of uninduced and induced (4 days) EF-Tu RNAi cells, grown in the presence of light or heavy isotopes of lysine and arginine, were mixed and fractionated using digitonin prior to mass spectrometric analysis.
A. Pie chart depicting the 21 proteins that are downregulated at least twofold upon ablation of EF-Tu. Seven proteins are putative components or assembly factors of COX. Four proteins are putative subunits or assembly factors of the bc1-complex. Seven proteins are annotated as hypothetical proteins with unknown function in TriTrypDB (http://tritrypdb.org/tritrypdb/) and three proteins show homology to proteins of known function. The latter include EF-Tu.
B. Blue-native gel immunoblot analysis of COX (COX4) and the bc1-complex (Cyt C1) in uninduced (– Tet) and induced (+ Tet; 4 days) EF-Tu RNAi cells. An immunoblot of an SDS-gel containing the same samples was decorated with voltage-dependent anion channel (VDAC) antiserum to serve as a loading control. Molecular weight markers (kDa) are indicated.
C. Pie chart depicting the 62 proteins that are upregulated at least twofold following induction of EF-Tu RNAi. Thirty-six proteins are putative components of the cytosolic ribosome. Five proteins are annotated as hypothetical proteins with unknown function in TriTrypDB and 21 other proteins show homology to proteins of known function. See Table S1 for the complete data set.

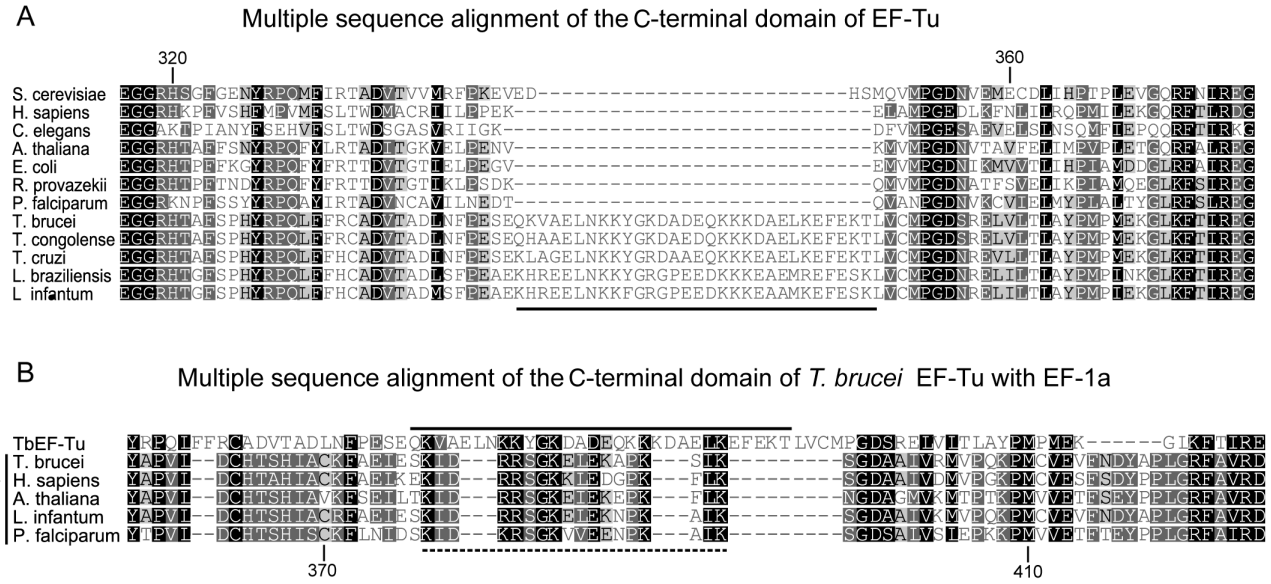

Fig. 6. Multiple sequence alignment reveals a trypanosomatid-specific motif in EF-Tu.
A. Multiple sequence alignment of a domain 3 subregion of the indicated mitochondrial and bacterial EF-Tu orthologues. The five trypanosomatid proteins are listed at the bottom. The trypanosomatid-specific motif is underlined. Numbers at the top indicate the amino acid positions in *E. coli* EF-Tu.
B. Multiple sequence alignment of a domain 3 subregion of *T. brucei* EF-Tu with its eukaryotic orthologue EF1a. The trypanosomatid-specific subdomain of EF-Tu is overlined and the segment of EF1a that was used to replace EF-Tu subdomain is indicated by the dashed line. Numbers at the bottom indicate the amino acid positions in the human EF1a.

The trypanosomatid-specific motif of EF-Tu is essential for function

The presence of the trypanosomatid-specific subdomain in EF-Tu raises the questions whether it is required for EF-Tu function and whether it is connected to the similar sequence segment that is found in EF1a. These questions can be addressed using the EF-Tu-3′UTR RNAi cell line, since it allows complementation experiments with wild-type and mutant versions of EF-Tu provided that they are expressed in a different genomic context. The experiment in Fig. 7B shows that ectopic expression of wild-type EF-Tu (EF-Tu-WT) fully restores growth of the EF-Tu-3′UTR RNAi cell line and therefore serves as a positive control. Ectopic expression of an EF-Tu variant lacking the trypanosomatid-specific subdomain (EF-Tu-ΔELKE), on the other hand, was not able to complement the growth arrest (Fig. 7C). However, if a chimeric EF-Tu was expressed, in which the trypanosomatid-specific motif was replaced by the corresponding sequence segment of EF1a (EF-Tu-1a), growth was restored to wild-type levels (Fig. 7D). *In vivo* labelling experiments and blue native gels furthermore showed that the complemented cell line was able to synthesize mitochondrial protein and that it had an intact COX and bc1-complex (Fig. S5).

Northern blots were performed to confirm that in all tested cell lines addition of tetracycline results in (i) ablation of the endogenous EF-Tu mRNA and (ii) induction of the expression of the ectopic EF-Tu gene copy. Ectopically expressed EF-Tu and its two variants all contained a C-terminal HA-tag, which allows us to confirm that the proteins are efficiently targeted to mitochondria (Fig. 8A). In summary these experiments demonstrate that the trypanosomatid-specific subdomain is essential for EF-Tu function and that it can be replaced by the corresponding sequence segment in EF1a.

One explanation for these results would be that removal of the trypanosomatid-specific motif simply results in the misfolding and potential collapse of the EF-Tu tertiary structure. The resolved structure of the *E. coli* EF-Tu/EF-Ts complex shows that both domain 1 and domain 3 of EF-Tu are in contact with EF-Ts (Kawashima *et al.*, 1996). Thus, misfolding of these EF-Tu domains would impair interaction with EF-Ts and inhibit cell growth.

In order to test whether the EF-Tu variants can still interact with EF-Ts, we used cell lines that simultaneously expresses the HA-tagged EF-Tu variants and cMYC-tagged EF-Ts.

Immunoprecipitation experiments using anti-HA antiserum showed that cMYC tagged EF-Ts efficiently interacts with wild-type EF-Tu as well as with the two EF-Tu variants (Fig. 8B). Interestingly, interaction of EF-Ts with the EF-Tu variant that lack the trypanosomatid-specific domain was even slightly more efficient than with the chimeric EF-Tu, in which the trypanosomatid-specific subdomain was replaced by the corresponding sequence

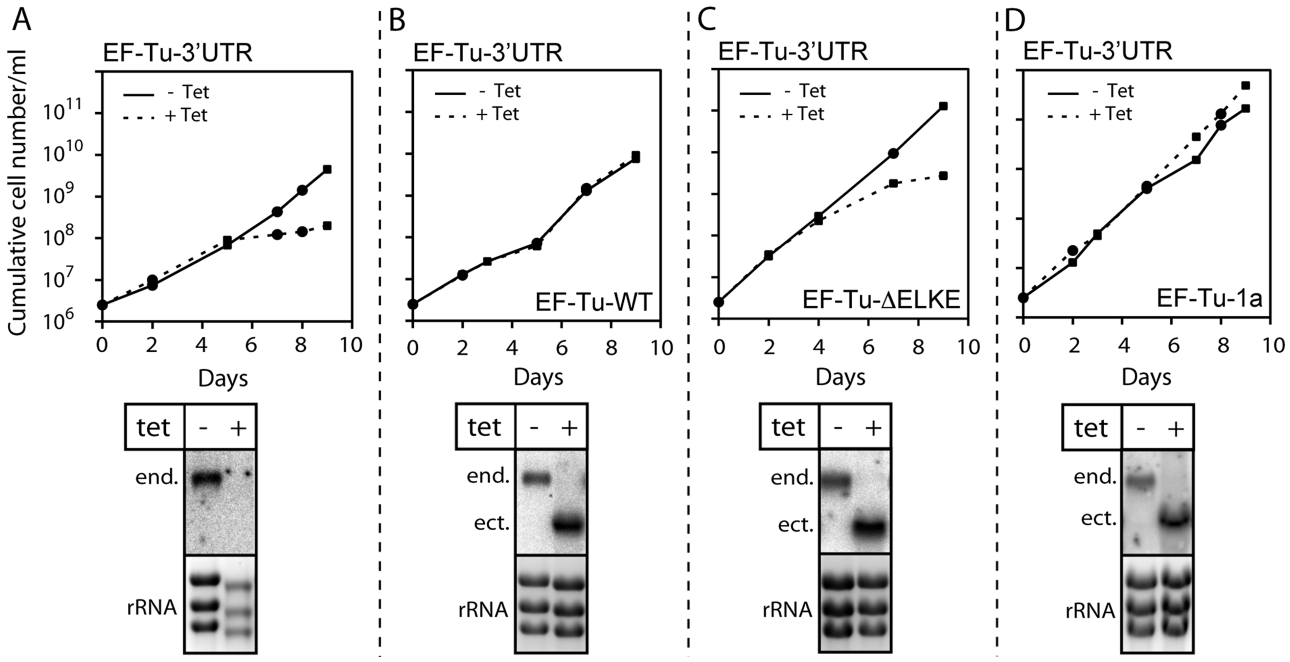

Fig. 7. Complementation experiments using an EF-Tu RNAi cell line targeting the 3′UTR.
A. Top panel, growth curve of uninduced (– Tet) and induced (+ Tet) EF-Tu-3′UTR RNAi cell line. Bottom panel, Northern blots probed for the coding region of the EF-Tu mRNA (end.). The EtBr-stained rRNAs in the lower panels serve as loading controls.
B. EF-Tu-3′UTR RNAi cell line ectopically expressing C-terminally HA-tagged versions of wild-type EF-Tu (EF-Tu-WT) under Tet control. The addition of Tet induces simultaneous downregulation of the endogenous EF-Tu mRNA (end.) and upregulation of the ectopic copy (ect.) of the EF-Tu gene respectively.
C. As in (B) but the complementation was performed using a C-terminally HA-tagged version of EF-Tu lacking the trypanosomatid-specific motif (EF-Tu-ΔELKE).
D. As in (B) but the complementation was done using a HA-tagged version of EF-Tu in which the trypanosomatid-specific subdomain was replaced by the corresponding region of EF1a (EF-Tu-1a).

segment of EF1a, even though only the latter could complement growth. These results strongly suggest that removal of the trypanosomatid-specific subdomain does not result in misfolding of domain 3 of EF-Tu but interferes with its function in a more subtle way.

Discussion

In contrast to mitochondrial RNA editing, which has been a major focus of research in trypanosomes during the last two decades, the study of mitochondrial translation has been largely neglected. This is somewhat ironic since the only function of RNA editing is to convert transcripts of mitochondrially encoded cryptogenes into functional mRNAs that can be translated. Here, we provide the first analysis of four *T. brucei* mitochondrial translation factors, with a special emphasis on EF-Tu. All four proteins are essential for normal growth of procyclic trypanosomes. Whereas EF-Tu has previously been shown to be essential for the bloodstream from Cristodero *et al.* (2010), the other three proteins have not been studied in this life cycle stage yet. However, since it is well established that mitochondrial translation is essential in bloodstream forms of the parasite, we would expect EF-G1, EF-Ts and RF1 to be essential in this pathogenic stage as well. The requirement of EF-Ts for normal growth is interesting in the light of the fact that the genome of *Saccharomyces cerevisiae* lacks an EF-Ts orthologue, indicating that its EF-Tu has the capability for self-recycling (Chiron *et al.*, 2005). In contrast, mitochondrial translation in *Schizosaccharomyces pombe* and humans depends on EF-Ts and therefore, in this respect, groups together with the *T. brucei* system.

In order to get a more precise picture of the proteomic changes that are caused by the EF-Tu RNAi, we developed a SILAC-based method that in principle is applicable to any inducible RNAi cell line of trypanosomes. It allowed to quantify the changes in the abundance levels of 1721 proteins that were induced by EF-Tu RNAi. The results show a strong downregulation of mitochondrially encoded COX2 and COX3. The remaining 16 predicted mitochondrially encoded proteins were not detected. This is not surprising since trypanosomal proteins encoded by mitochondrial genes are notoriously difficult to detect due to their small size and extreme hydrophobicity (Horváth *et al.*, 2000; 2002). In fact the only MS-based study that identified mitochondrially encoded proteins before also

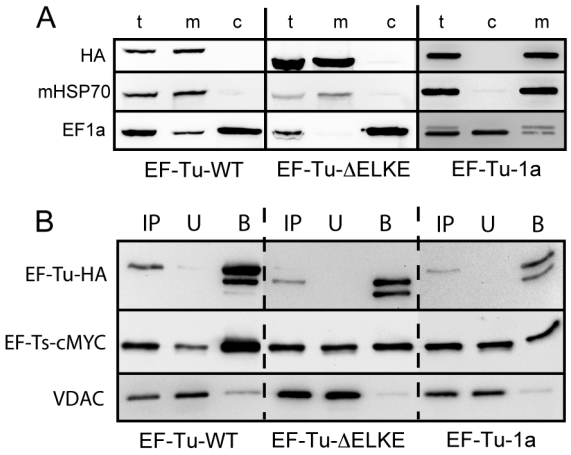

Fig. 8. All versions of EF-Tu localize to mitochondria and interact with EF-Ts.
A. A total of 0.3×10^7 cell equivalents each of total cellular (t), cytosolic (c) and crude mitochondrial extracts (m) of cell lines expressing C-terminally HA-tagged wild-type EF-Tu (EF-Tu-WT) or mutated EF-Tu versions (EF-Tu-ΔELKE, EF-Tu-1a) were analysed by immunoblots as in Fig. 1.
B. Digitonin extracts of cell lines expressing EF-Ts carrying a C-terminal cMYC-tag and the indicated HA-tagged EF-Tu variants were immunoprecipitated using anti-HA antibodies and analysed by immunoblotting. Ten per cent each of total extract (IP) and unbound fraction (U) as well as 95% of the bound fraction (B) were analysed by immunoblot. The panels were probed with anti-HA, anti-cMYC and anti-VDAC antibodies, as indicated.

only detected COX2 and COX3, even though in this case isolated respiratory complexes were analysed (Acestor *et al*., 2011). Thus, the strong reduction of COX2 and COX3 levels upon RNAi strongly suggest that EF-Tu is directly required for their synthesis. In addition, we also observed a decrease in abundance of many nuclear-encoded subunits of both COX and the bc1-complex (Fig. 5A), which is consistent with the results from immunoblots of blue-native gels in which the two complexes essentially cannot be detected anymore after induction of RNAi. In summary, this suggests that the mitochondrially encoded subunits play a central role in the assembly and/or stability of these two respiratory complexes and that in their absence most of their nuclear-encoded subunits are degraded. Global proteomic analysis of the changes caused by the EF-Tu RNAi is also an excellent tool to study potential compensatory mechanism with which the cell tries to counteract the loss of mitochondrial protein synthesis. Indeed we observed a co-ordinated increase in expression of essentially all cytosolic ribosomal proteins detected in the EF-Tu RNAi proteome (Fig. 5C, Table S1). This suggests that upregulation of cytosolic protein synthesis is one of the main responses induced by the absence of mitochondrial translation and/or the subsequent loss of OXPHOS.

EF-Tu of *T. brucei* contains a short, highly charged insertion of approximately 30 amino acids close to the C-terminus that is essential for its function. EF-Tu functions in bringing charged elongator tRNAs to the ribosomes. It must therefore interact with both, tRNAs and ribosomes. We have purified recombinant trypanosomal wild-type EF-Tu from *E. coli*. However, despite extensive efforts we were not able to show that it binds tRNAs of any source. Moreover, the purification of native mitochondrial ribosomes of trypanosomatids in amounts that would be required for EF-Tu binding assays, is also very challenging (Zíková *et al*., 2008; Sharma *et al*., 2009). Thus, direct biochemical interrogation of tRNA/EF-Tu or EF-Tu/ribosome interactions is at the moment not possible. However, a comparative analysis of the trypanosomatid mitochondrial translation system with that of other eukaryotes suggests that the trypanosomatid-specific EF-Tu motif may be linked to features of mitochondrial translation that are unique to these flagellates and therefore sheds light on its possible function.

An interesting deviation of mitochondrial translation in trypanosomatids in comparison with other systems is that it functions exclusively with imported tRNAs that are of the eukaryotic-type (Salinas *et al*., 2008; Alfonzo and Söll, 2009; Schneider, 2011). This means that trypanosomal EF-Tu, in contrast to its homologues in other species, has to bind eukaryotic-type tRNAs. It is therefore tempting to speculate that the trypanosomatid-specific EF-Tu motif represents an adaptation of the bacterial-type mitochondrial translation system to the eukaryotic-type tRNAs. This notion is supported by the fact that it can be replaced by the corresponding sequence of eukaryotic EF1a. However, whereas bacterial-type and eukaryotic-type initiator tRNAs are very different (RajBhandary, 1994) this is not the case for the elongator tRNAs. Some have identity elements that differ between the two domains and therefore must be charged by the matching eukaryotic-type or bacterial-type aminoacyl-tRNA synthetases. Once charged, however, the elongator tRNAs of eukaryotes and bacteria are functionally largely interchangeable. Furthermore, the loss of mitochondrial tRNA genes is not restricted to trypanosomatids but also occurred in another group of parasitic protozoa, the apicomplexans (Crausaz-Esseiva *et al*., 2004; Pino *et al*., 2010). These organisms are therefore faced with the same problem than trypanosomatids, namely to use of eukaryotic-type tRNAs in mitochondrial translation. However, apicomplexans have a standard EF-Tu that lacks the C-terminal motif found in trypanosomatids (see *P. falciparum* row in Fig. 6A), indicating that this subdomain cannot stringently be required to recognize eukaryotic-type tRNAs.

Another unique feature of trypanosomatids is their mitochondrial ribosomes, which are smaller than bacterial ribosomes, have very short rRNAs and hence show a very low RNA to protein ratio (Sharma *et al*., 2009; Agrawal and Sharma, 2012). It is therefore feasible that the

trypanosomatid-specific subdomain is required for binding of EF-Tu to these unique ribosomes. A recent cryo-electron microscopy study of mitochondrial ribosomes of the trypanosomatid *Leishmania tarentolae* supports this notion, as it showed that despite the generally conserved structure, they are more porous when compared with their counterparts in mammalian mitochondria (Sharma *et al*., 2009). Most important in the context of our study is the finding that the intersubunit space is dramatically remodelled in the mitochondrial ribosome of *L. tarentolae*, when compared with any other ribosome. Based on this distinctive intersubunit space, which accommodates the interactions of tRNAs and translational factors, the authors predicted that translational elongation factors in the *Leishmania* mitochondrion should be quite distinctive (Sharma *et al*., 2009).

EF-Tu of *T. brucei* and *T. thermophilus* are highly homologous. A high-resolution structure of the ribosome bound to EF-Tu and aminoacyl-tRNA is available for *T. thermophilus* (Schmeing *et al*., 2009). Thus, the overall localization of the ELKE-motif can be assigned in the *T. thermophilus* EF-Tu ribosome complex (Fig. S6). On the basis of this structural analysis the ELKE-motif would be localized in close proximity to ribosomal protein L11, which is consistent with the notion that the ELKE-motif is required for ribosome binding. L11 builds the basis of the L7/L12 stalk, a structurally flexible region of the large subunit of the ribosome that contributes to the intersubunit space. However, since the ELKE-motif would also be in close proximity to the tRNA elbow, it cannot be excluded that it is also involved in the interaction between tRNA and EF-Tu.

In summary, we believe it most likely that the trypanosomatid-specific EF-Tu subdomain may serve as an adaptation that allows the protein to fit into the distinctive intersubunit space of mitochondrial ribosomes. The observation that it can be replaced with the corresponding sequence of EF1a may be explained by the similar charge distribution that is observed in both sequences.

Trypanosomes have a unique evolutionary history. They may represent the earliest diverging eukaryotes with mitochondria capable of OXPHOS (Dacks *et al*., 2008; Cavalier-Smith, 2010). Understanding their highly unusual mitochondrial translation system is therefore expected to provide insight into both fundamentally conserved and evolutionary flexible aspects of mitochondrial protein synthesis and perhaps also translation in general. Moreover, bacterial EF-Tu – after the ribosome itself – is the major target for antibiotics affecting protein synthesis (Krab and Parmeggiani, 1998). Thus, since mitochondrial translation is essential for the pathogenic bloodstream form of *T. brucei*, its unique features are also of interest for the hunt of novel drug targets (Brun *et al*., 2011).

Experimental procedures

Culture of cells

Procyclic transgenic cell lines are based on *T. brucei* 29-13. They were grown at 27°C in SDM-79 supplemented with 15% fetal calf serum and the required antibiotics. Transformation and cloning of transgenic cell lines were done as described (Beverley and Clayton, 1993). The concentration of antibiotics used to select transgenic cell lines was 5 μg ml^{-1} for blasticidin and 0.1 μg ml^{-1} for puromycin. Expression of tagged proteins or double-stranded RNAs for RNAi was induced with 1 μg ml^{-1} tetracycline.

Constructs for inducible RNAi

All RNAi cell lines were stem-loop constructs based on pLew-100 carrying the blasticidin resistance gene (Wirtz *et al*., 1999; Bochud-Allemann and Schneider, 2002). RNAi against the coding region of EF-Tu (Tb927.10.13360) was performed as previously described (Cristodero *et al*., 2010). RNAi directed against the 3′UTR of EF-Tu (EF-Tu-3′UTR) was done using a 465 bp region immediately downstream of the stop codon. The 3′UTR of the EF-Tu mRNA is estimated to be longer than 1 kb (Kolev *et al*., 2010). For the three remaining RNAi cell lines we used the following inserts: a 455 bp fragment (nucleotides 4–459) of the EF-Ts gene (Tb927.3.3630); a 626 bp fragment (nucleotides 1051–1677) of the EF-G1 gene (Tb927.10.5010) and a 653 bp fragment (nucleotides 3–656) of the RF1 gene (Tb927.3.1070).

Constructs for epitope tagging

Tet-inducible expression of C-terminally HA-tagged EF-Tu, EF-G1 and RF1 was achieved using pLew-100-derived constructs carrying the puromycin resistance marker (Wirtz *et al*., 1999; Bochud-Allemann and Schneider, 2002). C-terminal *in situ* tagging of EF-Ts with the cMYC epitope was done as already described (Oberholzer *et al*., 2005). For generation of the EF-Tu-DELKE mutant a 28-amino-acid region, comprising amino acids 372–399 of EF-Tu (encoded by: AAGGTT GCTGAGTTGAACAAAAAGTATGGGAAGGACGCGGATGA GCAAAAGAAGAAGGATGCAGAGTTGAAGGAGTTCGAAA AG), was deleted by fusion PCR. The mutant EF-Tu-1a chimera was produced by deleting 24 amino acids of EF-Tu (position 372–395) and by replacing them with 18 amino acids (position 365–382, encoded by AGATCGACCGTCG CTCTGGCAAGGAGCTGGAGAAGGCTCCCAAGTCGATCA AGT) of trypanosomal *T. brucei* EF1a.

Culture of cells for SILAC proteomics

EF-Tu RNAi cells grown in SDM-79 containing 15% FCS were washed in PBS and cultured in modified SDM-80 (Lamour *et al*., 2005) containing 5.55 mM glucose and supplemented with the normal light (L) or heavy (H) amino acids [$^{13}C/^{15}N$]Arg (1.1 mM) and [$^{13}C/^{15}N$]Lys (0.4 mM) (Cambridge Isotope Laboratories, USA) in the presence of 20% dialysed FCS (BioConcept, Switzerland) for 2 days. Cultures were induced with tetracycline (Tet) for 4 days and uninduced and

induced cells mixed in a 1:1 ratio (L – Tet/H + Tet; L – Tet/H + Tet; L + Tet/H – Tet). Cells were extracted using digitonin to obtain a crude mitochondrial fraction (Bochud-Allemann and Schneider, 2002) for mass spectrometric analyses.

Quantitative mass spectrometry and data analysis

SILAC-labelled proteins (30 μg) of crude mitochondrial fractions ($n = 3$) resuspended in urea buffer (30 mM Tris-HCl, 7 M urea, 2 M thiourea, pH 8.5) were separated by SDS-PAGE and visualized using colloidal Coomassie Blue. Gel lanes were cut into 12 slices of equal size. Following reduction of disulphide bonds (10 mM DTT in 10 mM NH_4HCO_3, 30 min at 65°C) and subsequent alkylation of free thiol groups (55 mM iodoacetamide in 10 mM NH_4HCO_3, 30 min at RT, in the dark), proteins were in-gel digested with trypsin and the resulting peptide mixtures analysed by UHPLC-ESI-MS/MS on an LTQ-Orbitrap XL (Thermo Scientific, Bremen, Germany) online coupled to an Ultimate 3000 RSLCnano system (Thermo Scientific, Idstein, Germany) essentially as described before (Mick *et al*., 2012).

Mass spectrometric raw data were processes with MaxQuant (version 1.3.0.5; Cox and Mann, 2008) and its integrated search algorithm Andromeda (Cox *et al*., 2011). Proteins were identified by correlating MS/MS spectra with a database containing the entries of the *T. brucei* protein database (TriTrypDB, release 4.2) as well as the amino acid sequences of the currently known mitochondrially encoded proteins as described before (Niemann *et al*., 2013) including carbamidomethylation of cysteine residues as fixed modification. Proteins were identified with ≥ one unique peptide of at least six amino acids and a false discovery rate of < 0.01 on peptide and protein level. SILAC-based relative protein quantification was based on unique peptides and ≥ one SILAC peptide pair. Protein abundance ratios (induced/uninduced) normalized to the median of the respective replicate were $\log_{10}$-transformed and mean $\log_{10}$ ratios across all three replicates as well as the p-value of each protein were calculated.

Immunoprecipitations

Cell lines allowing simultaneous RNAi-mediated depletion of EF-Tu (EF-Tu-3′UTR), overexpression of HA-tagged EF-Tu variants (EF-Tu-WT, EF-Tu-ΔELKE and EF-Tu-1a) and cMYC tagged EF-Ts were induced for 48 h and harvested by centrifugation. Pellets from 3.75×10^8 cells were resuspended in 470 μl of 25 mM Tris-HCl, pH 7.5, 50 mM KCl, 1× protease inhibitor mix (Roche, Switzerland), 0.25% (w/v) Nonidet-40 (NP-40) and 1 mM EDTA and lysed by incubation for 5 min at 4°C with constant mixing. Samples were cleared by centrifugation at 500 *g* for 2 min and the resulting supernatant was adjusted to 1.25% (w/v) of NP-40. After incubation for 10 min at 4°C the supernatants were centrifuged again at 16 000 *g* for 40 min. The cleared supernatants (500 μl each) were added to pre-washed beads containing covalently linked anti-HA antibodies (40 μl of 1:1 slurry) (Roche, Switzerland) and incubated for 2 h at 4°C under constant mixing. Subsequently, the beads were extensively washed in the same buffer containing 0.1% (w/v) of NP-40. Final eluates were obtained by boiling the beads in SDS sample buffer.

Miscellaneous

Digitonin extractions and ATP production assays were performed as previously described (Bochud-Allemann and Schneider, 2002; Schneider *et al*., 2007). RNA isolation, and Northern blot analysis were performed according to Tan *et al*. (2002b).

[^{35}S]-methionine *in vivo* labelling of mitochondrially synthesized proteins was done as described (Horváth *et al*., 2002; Hashimi *et al*., 2013). Multiple sequence alignments were done using CLUSTAL omega from EBI (Sievers *et al*., 2011). The following antibodies were used for immunoblots (working dilutions are indicated in parentheses): monoclonal anti-HA antiserum (HA11, Covance Research Products, Princeton, USA) (1:1000), monoclonal anti-cMYC antiserum (Invitrogen, USA) (1:1000), monoclonal anti-EF1a antiserum (Santa Cruz Biotechnology, USA) (1:10 000), polyclonal anti-mHSP70 antiserum (1:1000) (provided by R. Jensen), polyclonal anti-VDAC antiserum (1:1000), polyclonal anti-COX4 antiserum (1:1000) and polyclonal anti-Cyt C1 antiserum.

Acknowledgements

We thank R. Jensen (John Hopkins School of Medicine) for the mHSP70 antiserum and Kurt Lobenwein for technical assistance. M.C. gratefully acknowledges a fellowship of the VELUX foundation. Research in the lab of A.S. was supported by Grant 138355 of the Swiss National Foundation. Work in the lab of B.W. was supported by the Deutsche Forschungsgemeinschaft, Excellence Initiative of the German Federal & State Governments (EXC 294 BIOSS). J.L. is a Fellow of the Canadian Institute for Advanced Research and was supported by the Praemium Academiae award and the Czech grant agency (P305/12/2261). D.J.F.R. was supported by a long-term fellowship of the Federation of European Biochemical Societies (FEBS).

References

Acestor, N., Zíková, A., Dalley, R.A., Anupama, A., Panigrahi, A.K., and Stuart, K.D. (2011) *Trypanosoma brucei* mitochondrial respiratome: composition and organization in procyclic form. *Mol Cell Proteomics* **10:** M110.006908. doi:10.1074/mcp.M1110.006908

Agrawal, R.K., and Sharma, M.R. (2012) Structural aspects of mitochondrial translational apparatus. *Curr Opin Struct Biol* **22:** 797–803.

Alfonzo, J.D., and Söll, D. (2009) Mitochondrial tRNA import – the challenge to understand has just begun. *Biol Chem* **390:** 717–722.

Alfonzo, J.D., Blanc, V., Estevez, A.M., Rubio, M.A.T., and Simpson, L. (1999) C to U editing of anticodon of imported mitochondrial $tRNA^{Trp}$ allows decoding of UGA stop codon in *Leishmania*. *EMBO J* **18:** 7056–7062.

Berriman, M., Ghedin, E., Hertz-Fowler, C., Blandin, G., Renauld, H., Bartholomeu, D.C., *et al*. (2005) The genome of the African trypanosome *Trypanosoma brucei*. *Science* **309:** 416–422.

Beverley, S.M., and Clayton, C.E. (1993) Transfection of

Leishmania and *Trypanosoma brucei* by electroporation. *Methods Mol Biol* **21:** 333–348.
Bochud-Allemann, N., and Schneider, A. (2002) Mitochondrial substrate level phosphorylation is essential for growth of procyclic *Trypanosoma brucei*. *J Biol Chem* **277:** 32849–32854.
Brun, R., Don, R., Jacobs, R.T., Wang, M.Z., and Barrett, M.P. (2011) Development of novel drugs for human African trypanosomiasis. *Future Microbiol* **6:** 677–691.
Cavalier-Smith, T. (2010) Kingdoms Protozoa and Chromista and the eozoan root of the eukaryotic tree. *Biol Lett* **6:** 342–345.
Charrière, F., Helgadóttir, S., Horn, E.K., Söll, D., and Schneider, A. (2006) Dual targeting of a single tRNATrp requires two different tryptophanyl-tRNA synthetases in *Trypanosoma brucei*. *Proc Natl Acad Sci USA* **103:** 6847–6852.
Chiron, S., Suleau, A., and Bonnefoy, N. (2005) Mitochondrial translation: elongation factor tu is essential in fission yeast and depends on an exchange factor conserved in humans but not in budding yeast. *Genetics* **169:** 1891–1901.
Cox, J., and Mann, M. (2008) MaxQuant enables high peptide identification rates, individualized p.p.b.-range mass accuracies and proteome-wide protein quantification. *Nat Biotechnol* **26:** 1367–1372.
Cox, J., Neuhauser, N., Michalski, A., Scheltema, R.A., Olsen, J.V., and Mann, M. (2011) Andromeda: a peptide search engine integrated into the MaxQuant environment. *J Proteome Res* **10:** 1794–1805.
Crausaz-Esseiva, A., Naguleswaran, A., Hemphill, A., and Schneider, A. (2004) Mitochondrial tRNA import in *Toxoplasma gondii*. *J Biol Chem* **279:** 42363–42368.
Cristodero, M., Seebeck, T., and Schneider, A. (2010) Mitochondrial translation is essential in bloodstream forms of *Trypanosoma brucei*. *Mol Microbiol* **78:** 757–769.
Dacks, J.B., Walker, G., and Field, M.C. (2008) Implications of the new eukaryotic systematics for parasitologists. *Parasitol Int* **57:** 97–104.
Feagin, J.E. (2000) Mitochondrial genome diversity in parasites. *Int J Parasitol* **30:** 371–390.
Gray, M.W. (2012) Mitochondrial evolution. *Cold Spring Harb Perspect Biol* **4:** a011403.
Hashimi, H., McDonald, L., Stríbrná, E., and Lukeš, J. (2013) Trypanosome Letm1 protein is essential for mitochondrial potassium homeostasis. *J Biol Chem*. PMID: 23893410.
Horváth, A., Berry, E.A., and Maslov, D.A. (2000) Translation of the edited mRNA for cytochrome b in trypanosome mitochondria. *Science* **287:** 1639–1640.
Horváth, A., Nebohacova, M., Lukeš, J., and Maslov, D.A. (2002) Unusual polypeptide synthesis in the kinetoplast-mitochondria from *Leishmania* tarentolae. Identification of individual *de novo* translation products. *J Biol Chem* **277:** 7222–7230.
Kawashima, T., Berthet-Colominas, C., Wulff, M., Cusack, S., and Leberman, R. (1996) The structure of the *Escherichia coli* EF-Tu.EF-Ts complex at 2.5 A resolution. *Nature* **379:** 511–518.
Kolev, N.G., Franklin, J.B., Carmi, S., Shi, H., Michaeli, D., and Tschudi, G. (2010) The transcriptome of the human pathogen *Trypanosoma brucei* at single-nucleotide resolution. *PLoS Pathog* **6:** e1001090.
Krab, I.M., and Parmeggiani, A. (1998) EF-Tu, a GTPase odyssey. *Biochim Biophys Acta* **1443:** 1–22.
Krab, I.M., and Parmeggiani, A. (2002) Mechanisms of EF-Tu, a pioneer GTPase. *Prog Nucleic Acid Res Mol Biol* **71:** 513–551.
Lamour, N., Riviere, L., Coustou, V., Coombs, G.H., Barrett, M., and Bringaud, F. (2005) Proline metabolism in procyclic *Trypanosoma brucei* is down-regulated in the presence of glucose. *J Biol Chem* **280:** 11902–11910.
Mick, D.U., Dennerlein, S., Wiese, H., Reinhold, R., Lorenzi, I., Sasarman, F., *et al*. (2012) Respiratory chain assembly is linked to protein import and translational regulation via the MITRAC complex. *Cell* **151:** 1528–1541.
Niemann, M., Schneider, A., and Cristodero, M. (2011) Mitochondrial translation in trypanosomatids: a novel target for chemotherapy? *Trends Parasitol* **27:** 429–433.
Niemann, M., Wiese, S., Mani, J., Chanfon, A., Jackson, C., Meisinger, C., *et al*. (2013) Mitochondrial outer membrane proteome of *Trypanosoma brucei* reveals novel factors required to maintain mitochondrial morphology. *Mol Cell Proteomics* **12:** 515–528.
Oberholzer, M., Morand, S., Kunz, S., and Seebeck, T. (2005) A vector series for rapid PCR-mediated C-terminal in situ tagging of *Trypanosoma brucei* genes. *Mol Biochem Parasitol* **145:** 117–120.
Pino, P., Aeby, E., Foth, B.J., Sheiner, L., Soldati, T., Schneider, A., and Soldati-Favre, D. (2010) Mitochondrial translation in absence of local tRNA aminoacylation and methionyl tRNA formylation in Apicomplexa. *Mol Microbiol* **76:** 706–718.
RajBhandary, U.L. (1994) Initiator transfer RNAs. *J Bacteriol* **176:** 547–552.
Rorbach, J., Soleimanpour-Lichaei, R., Lightowlers, R.N., and Chrzanowska-Lightowlers, Z.M. (2007) How do mammalian mitochondria synthesize proteins? *Biochem Soc Trans* **35:** 1290–1291.
Salinas, T., Duchêne, A.M., and Maréchal-Drouard, L. (2008) Recent advances in tRNA mitochondrial import. *Trends Biochem Sci* **33:** 320–329.
Schmeing, T.M., Voorhees, R.M., Kelley, A.C., Gao, Y.-G., Murphy, F.V., Weir, J.R., and Ramakrishnan, V. (2009) The crystal structure of the ribosome bound to EF-Tu and aminoacyl-tRNA. *Science* **326:** 688–694.
Schneider, A. (2011) Mitochondrial tRNA import and its consequences for mitochondrial translation. *Annu Rev Biochem* **80:** 1033–1053.
Schneider, A., Bouzaidi-Tiali, N., Chanez, A.-L., and Bulliard, L. (2007) ATP production in isolated mitochondria of procyclic *Trypanosoma brucei*. *Methods Mol Biol* **372:** 379–387.
Sharma, M.R., Booth, T.M., Simpson, L., Maslov, D.A., and Agrawal, R.K. (2009) Structure of a mitochondrial ribosome with minimal RNA. *Proc Natl Acad Sci USA* **106:** 9637–9642.
Sievers, F., Wilm, A., Dineen, D., Gibson, T.J., Karplus, K., Li, W., *et al*. (2011) Fast, scalable generation of high-quality protein multiple sequence alignments using Clustal Omega. *Mol Syst Biol* **11:** 539.
Spremulli, L.L., Coursey, A., Navratil, T., and Hunter, S.E. (2004) Initiation and elongation factors in mammalian mitochondrial protein biosynthesis. *Prog Nucleic Acid Res Mol Biol* **77:** 211–261.

Tan, T.H.P., Bochud-Allemannn, N., Horn, E.K., and Schneider, A. (2002a) Eukaryotic-type elongator tRNAMet of *Trypanosoma brucei* becomes formylated after import into mitochondria. *Proc Natl Acad Sci USA* **99:** 1152–1157.

Tan, T.H.P., Pach, R., Crausaz, A., Ivens, A., and Schneider, A. (2002b) tRNAs in *Trypanosoma brucei*: genomic organization, expression and mitochondrial import. *Mol Cell Biol* **22:** 3707–3717.

Wirtz, E., Leal, S., Ochatt, C., and Cross, G.A. (1999) A tightly regulated inducible expression system for conditional gene knock-outs and dominant-negative genetics in *Trypanosoma brucei*. *Mol Biochem Parasitol* **99:** 89–101.

Zíková, A., Panigrahi, A.K., Dalley, R.A., Acestor, N., Anupama, A., Ogata, Y., *et al.* (2008) *Trypanosoma brucei* mitochondrial ribosomes: affinity purification and component identification by mass spectrometry. *Mol Cell Proteomics* **7:** 1286–1296.

Supporting information

Additional supporting information may be found in the online version of this article at the publisher's web-site.

Attached Publications

Part III. TRYPANOSOME MITOCHONDRIAL TRANSLATION

Hassan Hashimi[†], Sabine Kaltenbrunner, Alena Zíková, Julius Lukeš (2016). Trypanosome mitochondrial translation and tetracycline: No sweat about Tet. *PLoS Pathog.* 12: e1005492.

In this PLoS Pearl article, we discuss the recent finding the tetracycline affects mitochondrial translation in opisthokonts and plants, causing the "mitonuclear" imbalance that has both positive and negative consequences for these organisms. This side-effect however complicates the interpretation of data using Tet-On/Off systems of gene control in biomedical research. We show experimentally and with cited literature that *T. brucei* mitochondrial translation is not sensitive to the antibiotic. We hypothesize that this insensitivity is due to the lack of mitochondrial rRNA elements, present in opisthokonts and plants, which are the binding sites of tetracycline.

[†]Corresponding author

PLOS | PATHOGENS

PEARLS

Trypanosome Mitochondrial Translation and Tetracycline: No Sweat about Tet

Hassan Hashimi[1,2]*, Sabine Kaltenbrunner[2], Alena Zíková[1,2], Julius Lukeš[1,2,3]

1 Institute of Parasitology, Biology Centre, Czech Academy of Sciences, University of South Bohemia, Czech Republic, **2** Faculty of Science, University of South Bohemia, Czech Republic, **3** Canadian Institute for Advanced Research, Toronto, Canada

* hassan@paru.cas.cz

Overview

A recent study vividly demonstrates the unintended impact of the antibiotic tetracycline (Tet) on animal and plant mitochondrial translation, which corresponds to the α-proteobacterial origin of the organelle. This effect was ultimately manifested by an impact on the cellular, and even organismal, levels in the studied eukaryotes. Thus, widespread use of Tet in agriculture and biomedical research is now under scrutiny. Interestingly, Tet does not affect this process in trypanosomatids. The highly divergent nature of trypanosomatid mitochondrial ribosomes may explain why these flagellates are insensitive to Tet.

Citation: Hashimi H, Kaltenbrunner S, Zíková A, Lukeš J (2016) Trypanosome Mitochondrial Translation and Tetracycline: No Sweat about Tet. PLoS Pathog 12(4): e1005492. doi:10.1371/journal.ppat.1005492

Editor: Laura J Knoll, University of Wisconsin Medical School, UNITED STATES

Published: April 21, 2016

Funding: This work was funded by Grant Agency of the Czech Republic (grant number: 15-21974S), ERC CZ (grant number: LL1205). The funders had no role in study design, data collection and analysis, decision to publish, or preparation of the manuscript.

Competing Interests: The authors have declared that no competing interests exist.

How Does Tetracycline Affect Mitochondria?

A study recently published by Moullan and coauthors [1] pronounced that even low doses in the μg/ml range of tetracycline (Tet) have an adverse effect on mitochondrial function in several model eukaryotes, ranging from metazoa to plants to in vitro human cultures. This paper brought into the limelight the danger of profuse usage of this class of antibiotics not only prophylactically, e.g., to maintain and promote growth in livestock, but also in biomedical research. The emergence of elegant platforms for Tet-controlled transcription by Tet-On and Tet-Off systems for inducing and suppressing gene expression, respectively, in a variety of eukaryotic models underlies the widespread use of this antibiotic in experimental biology. Importantly, as illustrated by these authors, even low, single-digit μg/ml concentrations of Tet also induced what has been termed "mitonuclear protein imbalance," in which the proportion of nucleus-encoded proteins imported into the organelle versus those arising from mitochondrial genes increases [1]. This subtle but perceptible phenotype, long overlooked, consequently impairs mitochondrial functions, such as respiration, and also induces significant detrimental changes at the organismal level, such as diminished growth and delayed development. Interestingly, a beneficial impact was observed in *Caenorhabditis elegans*, in which treatment with the Tet-class antibiotic doxycycline (Dox) mitigated the age-related decline in motility. Thus, the authors concluded that the vast amount of data produced using Tet-controlled gene expression may be confounded by the unintended disruption of the given model's mitochondria. They also cautioned against the future use of Tet-On and Tet-Off systems [1].

How Does Tetracycline Inhibit Mitochondrial Translation?

The mitonuclear protein imbalance caused by the antibiotic in question arises from its long-ago established inhibition of mitochondrial translation [2], which coheres to the α-proteobacterial origin of the organelle. More specifically, Tet prevents the accommodation of aminoacylated

(aa-) tRNA into its entry point to the mitochondrial ribosome, the A-site [3,4]. Two solved structures of the bacterium *Thermus thermophilis* 30S ribosomal small subunit (SSU) bound by Tet share two sites where the antibiotic attaches to facilitate its inhibitory action [5,6]. In the first location adjacent to the A-site, the compound intercalates into a pocket formed by the double-stranded (ds) helices H31 and H34 of 16S ribosomal (r) RNA, the polyribonucleotide component of the SSU, and binds to the sugar-phosphate backbone of H34. Within this position, Tet sterically hinders aa-tRNA attachment into the A-site of the ribosome, thus inhibiting translation [3,5,6]. A second Tet-binding position identified in both structures involves another ds 16S rRNA helix designated H27, a switch region that plays a role in selection of the proper aa-tRNA at the A-site [7]. Although this would not directly hinder aa-tRNA accommodation into the ribosome, it may still contribute to the disruption of this translational step [3]. These secondary structural motifs of the bacterial SSU 16S rRNA that interact with Tet are conserved in the homologous SSU rRNA of plant and animal mitochondrial ribosomes (Fig 1) [8,9]. Thus, the inhibitory effect of Tet on mitochondrial translation leading to the consequences described by Moullan and coauthors [1] could rely on a very similar mechanism as described for bacterial ribosomes [3,5,6].

How Does Tetracycline Affect Trypanosomes?

What does all this mean for the large community of molecular parasitologists studying *Trypanosoma brucei*? The development of Tet-controlled transcription for functional analysis of nuclear genes, mostly via straightforward application of RNA interference and the expression of exogenous genes, represented a major breakthrough for the field [10]. This platform has been so successful in *T. brucei* that it has also been implemented to study various *Leishmania* species [11]. However, are all these data, acquired over two decades, confounded by the recently reported Tet-triggered mitonuclear protein imbalance plaguing typical model systems of biomedical research [1]? Should the future application of this useful platform be reconsidered? Reassuringly, the answer to both questions is no. As seen in Fig 2, Dox exhibits a very high EC_{50} value of about 620 μg/ml in cultured procyclic *T. brucei*, the life cycle stage residing in the tsetse fly midgut that bears an actively respiring mitochondrion [12]. Indeed, up to 50 μg/ml of Dox does not negatively impact parasite fitness. This observation recapitulates tacit knowledge in the field that Tet treatment at the standard induction dose of 1 μg/ml, considerably lower than the aforementioned concentration, does not hamper *T. brucei* cell division. In contrast, when mitochondrial gene expression is down-regulated, ultimately decreasing the levels of the organellar gene products that are generated by mitochondrial ribosomes, an obvious growth-inhibition phenotype is observed (e.g., [13] and [14]).

Is Trypanosome Mitochondrial Translation Affected by Tetracycline?

The seeming insensitivity of trypanosomatids to Tet treatment occurs because mitochondrial translation is not susceptible to the antibiotic. Studies done on procyclic *T. brucei* and the related species *Leishmania tarentolae* have demonstrated that their mitochondrial translation is not affected even when they are grown in the presence of 100 μg/ml Tet [13,15], a concentration greatly exceeding those used by Moullan and coauthors [1], but half that of the maximal concentration not affecting procyclic *T. brucei* fitness (Fig 2).

Could one of the mechanisms of bacterial Tet resistance, Tet efflux, Tet degradation, rRNA mutations, or the participation of ribosomal protection proteins (RPPs) [3,4] underlie the Tet resistance of trypanosomatid mitochondrial translation? Most RPPs are homologous to prokaryotic elongation factors EF-Tu and EF-G, a structural feature that allows these proteins to

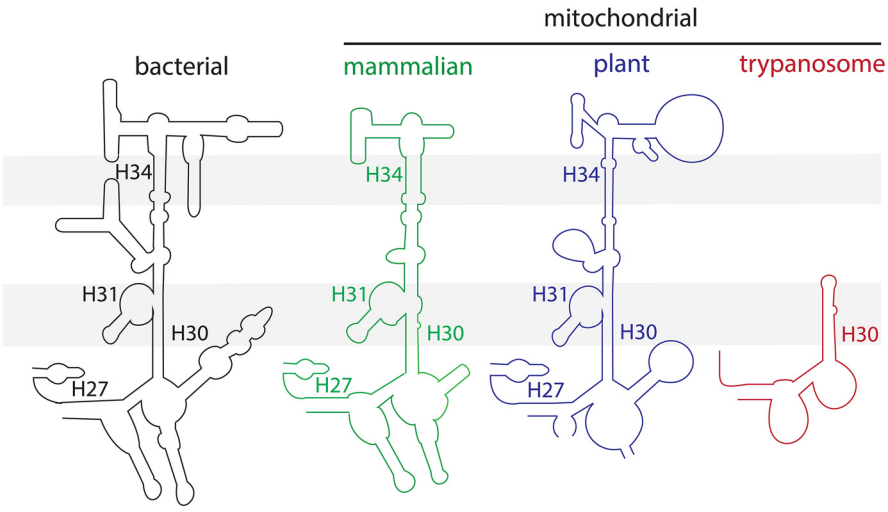

Fig 1. The ribosomal small subunit rRNA loops containing H31 and H34, as well as H27, double-stranded helices from bacteria (black) plus the mitochondria of mammals (green), plants (blue) and trypanosomes (red). Grey shading highlights the location of H31 and H34 in the SSU rRNAs bearing these motifs, as well as their absence in the same region of the trypanosomatid SSU rRNA. Helix H30, which is conserved throughout all the depicted rRNAs, is also indicated as a reference point. Adapted from [8] and [9].

doi:10.1371/journal.ppat.1005492.g001

access and dislodge Tet from the ribosome A-site [3,4]. However, only genes encoding mitochondrial EF-Tu, EF-G1, and EF-G2 have been identified in trypanosomatid genomes [14], implying the lack of RPPs to perform the same function on trypanosomatid mitochondrial ribosomes. With the current state of knowledge, it is still not possible to rule out Tet efflux of the mitochondrion or Tet degradation within the organelle with confidence. However, available data allow exploring the last possibility that key differences in the SSU rRNA sequence may underlie the Tet insensitivity of trypanosomatid mitochondrial translation.

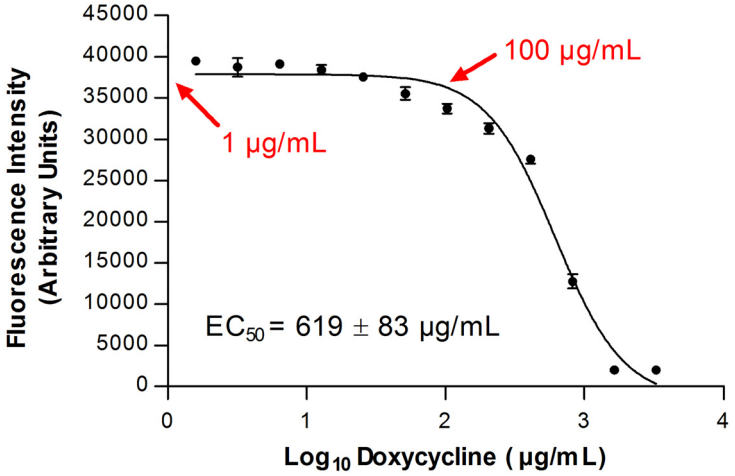

Fig 2. Effect of 24 hour doxycycline exposure on the viability of procyclic stage *T. brucei*. Data points represent the mean cell viability ± standard error of the mean (SEM) ($n = 4$), as measured by the Alamar Blue fluorescent dye assay. *X*-axis, µg/ml doxycycline (log scale); *y*-axis Alamar Blue fluorescence intensity in arbitrary units; doxycycline EC_{50} value calculated from curve given on lower left. Red arrows indicate points corresponding to 1 and 100 µg/ml concentrations on the *x*-axis. The assay was performed as previously described [19].

doi:10.1371/journal.ppat.1005492.g002

Are Unique Features of Trypanosome Mitochondrial Ribosomes Responsible for the Insensitivity of Mitochondrial Translation to Tetracycline?

The mitochondrial ribosomes of both *T. brucei* and *L. tarentolae* are quite different from their counterparts in animals, plants, and bacteria. The 9S SSU and 12S large subunit (LSU) rRNAs are considerably reduced as compared to the rRNAs of aforementioned organisms, representing the smallest known orthologs of these molecules [9,16]. To compensate for this deficiency in the rRNA component of the ribosome, trypanosomatids have experienced an expansion in the number of mitochondrial ribosomal proteins, most of which are unique to these kinetoplastid flagellates. The solved structure of the *L. tarentolae* mitochondrial ribosome [9] further refines this information in terms of the lack of Tet-sensitivity of the ribosome. Here, we see that the loop of the 9S rRNA, which encompasses the important Tet-binding H31 and H34 helices present in other SSU rRNAs, is significantly truncated (Fig 1). This loop, which also contains rRNA elements normally needed for aa-tRNA accommodation into the A-site, is replaced in mitochondrial ribosomes by trypanosomatid-specific proteins [9]. In this milieu, the Tet-binding site is ablated by the lack of the H31 and H34 helices, the latter of which ordinarily provides the sugar-phosphate backbone for attachment of the antibiotic [3,5,6]. Furthermore, the H27 helix that represents another Tet-binding site is considerably reduced in trypanosomatid 9S rRNA.

The observation that the contact points for Tet-binding are lacking in the trypanosomatid mitochondrial SSU is not proof that these structural features are completely responsible for organellar translation's insensitivity to treatment with this antibiotic. However, their conspicuous absence represents the most parsimonious hypothesis for this phenomenon considering the current state of knowledge. If this hypothesis is true, trypanosomatid mitochondrial ribosomes may be informative in comparative studies further investigating the mechanism of Tet inhibition of translation in other bacterial and organellar systems. Certainly, the insensitivity of trypanosomatid mitochondrial translation to Tet represents yet another exquisite example of the extreme evolutionary divergence of this group of protists, considering this trait is found in the bacterial domain of life, which gave rise to mitochondria, and remains conserved in the widely separated plant and mammalian eukaryotic clades. This phenomenon also belongs to a long line of discoveries made in trypanosomatids that have contributed to our understanding of biological processes vital to eukaryotes as a whole, epitomized by renowned examples, including the linkage of glycoproteins to the plasma membrane via glycosylphosphatidylinositol anchors [17] and the shaping of transcriptomes by RNA editing [18]. It is also reassuring to know that as we unravel more about the fascinating biology of trypanosomatids, our genetic tools are precise.

References

1. Moullan N, Mouchiroud L, Wang X, Ryu D, Williams EG, et al. (2015) Tetracyclines disturb mitochondrial function across eukaryotic models: A call for caution in biomedical research. Cell Reports 10: 1681–1691.
2. Clark-Walker GD, Linnane AW (1966) In vivo differentiation of yeast cytoplasmic and mitochondrial protein synthesis with antibiotics. Biochemical and Biophysical Research Communications 25: 8–13. PMID: 5971759
3. Connell SR, Tracz DM, Nierhaus KH, Taylor DE (2003) Ribosomal protection proteins and their mechanism of tetracycline resistance. Antimicrobial Agents and Chemotherapy 47: 3675–3681. PMID: 14638464
4. Chopra I, Roberts M (2001) Tetracycline antibiotics: mode of action, applications, molecular biology, and epidemiology of bacterial resistance. Microbiology and Molecular Biology Reviews 65: 232–260. PMID: 11381101

5. Pioletti M, Schlunzen F, Harms J, Zarivach R, Gluhmann M, et al. (2001) Crystal structures of complexes of the small ribosomal subunit with tetracycline, edeine and IF3. The EMBO Journal 20: 1829–1839. PMID: 11296217
6. Brodersen DE, Clemons WM Jr., Carter AP, Morgan-Warren RJ, Wimberly BT, et al. (2000) The structural basis for the action of the antibiotics tetracycline, pactamycin, and hygromycin B on the 30S ribosomal subunit. Cell 103: 1143–1154. PMID: 11163189
7. Lodmell JS, Dahlberg AE (1997) A conformational switch in *Escherichia coli* 16S ribosomal RNA during decoding of messenger RNA. Science 277: 1262–1267. PMID: 9271564
8. Spencer DF, Schnare MN, Gray MW (1984) Pronounced structural similarities between the small subunit ribosomal RNA genes of wheat mitochondria and *Escherichia coli*. Proceedings of the National Academy of Sciences of the United States of America 81: 493–497. PMID: 6364144
9. Sharma MR, Booth TM, Simpson L, Maslov DA, Agrawal RK (2009) Structure of a mitochondrial ribosome with minimal RNA. Proceedings of the National Academy of Sciences of the United States of America 106: 9637–9642. doi: 10.1073/pnas.0901631106 PMID: 19497863
10. Matthews KR (2015) 25 years of African trypanosome research: From description to molecular dissection and new drug discovery. Molecular and Biochemical Parasitology 200: 30–40. doi: 10.1016/j.molbiopara.2015.01.006 PMID: 25736427
11. Kraeva N, Ishemgulova A, Lukeš J, Yurchenko V (2014) Tetracycline-inducible gene expression system in *Leishmania mexicana*. Molecular and Biochemical Parasitology 198: 11–13. doi: 10.1016/j.molbiopara.2014.11.002 PMID: 25461484
12. Verner Z, Basu S, Benz C, Dixit S, Dobáková E, et al. (2015) Malleable mitochondrion of *Trypanosoma brucei*. International Review of Cell and Molecular Biology 315: 73–151. doi: 10.1016/bs.ircmb.2014.11.001 PMID: 25708462
13. Nebohácová M, Maslov DA, Falick AM, Simpson L (2004) The effect of RNA interference down-regulation of RNA editing 3'-terminal uridylyl transferase (TUTase) 1 on mitochondrial de novo protein synthesis and stability of respiratory complexes in *Trypanosoma brucei*. The Journal of Biological Chemistry 279: 7819–7825. PMID: 14681226
14. Cristodero M, Mani J, Oeljeklaus S, Aeberhard L, Hashimi H, et al. (2013) Mitochondrial translation factors of *Trypanosoma brucei*: elongation factor-Tu has a unique subdomain that is essential for its function. Molecular Microbiology 90: 744–755. doi: 10.1111/mmi.12397 PMID: 24033548
15. Horváth A, Nebohácová M, Lukeš J, Maslov DA (2002) Unusual polypeptide synthesis in the kinetoplast-mitochondria from Leishmania tarentolae. Identification of individual de novo translation products. The Journal of Biological Chemistry 277: 7222–7230. PMID: 11773050
16. Zíková A, Panigrahi AK, Dalley RA, Acestor N, Anupama A, et al. (2008) *Trypanosoma brucei* mitochondrial ribosomes: affinity purification and component identification by mass spectrometry. Molecular & Cellular Proteomics 7: 1286–1296.
17. Ferguson MA (1999) The structure, biosynthesis and functions of glycosylphosphatidylinositol anchors, and the contributions of trypanosome research. Journal of Cell Science 112: 2799–2809. PMID: 10444375
18. Read LK, Lukeš J, Hashimi H (2016) Trypanosome RNA editing: the complexity of getting U in and taking U out. Wiley Interdisciplinary Reviews RNA 7: 33–51. doi: 10.1002/wrna.1313 PMID: 26522170
19. Alkhaldia AAM, Martínek J, Panicucci B, Dardonville C, Zíková A, et al. (2016) Trypanocidal action of bisphosphonium salts through a mitochondrial target in bloodstream form Trypanosoma brucei. International Journal for Parasitology: Drugs and Drug Resistance 6: 23–34.

Attached Publications

Part IV.

TRYPANOSOME MITOCHONDRIAL PHYSIOLOGY

Attached Publications

Part IV. TRYPANOSOME MITOCHONDRIAL PHYSIOLOGY

Hassan Hashimi[†], Lindsay McDonald, Eva Střibrná and Julius Lukeš[†] (2013). Trypanosome Letm1 Protein Is Essential for Mitochondrial Potassium Homeostasis. *J. Biol Chem.* 288: 26914-25.

In this paper, we demonstrate that the ancestral role of the highly conserved Letm1 is K^+/H^+ antiport to prevent the sequestering of the abundant monovalent cation in the negatively charged mitochondrial matrix, which would lead to osmotic swelling of the organelle. Moreover, the RNAi-silencing of *T. brucei* Letm1 is complemented by the human ortholog. This paper may help to clear up the controversy surrounding the function of this protein, which has been implicated in seizure symptoms of the human congenital disease Wolf-Hirschhorn syndrome.

[†]Co-corresponding author

THE JOURNAL OF BIOLOGICAL CHEMISTRY VOL. 288, NO. 37, pp. 26914–26925, September 13, 2013

Trypanosome Letm1 Protein Is Essential for Mitochondrial Potassium Homeostasis*[S]

Received for publication, June 19, 2013, and in revised form, July 23, 2013 Published, JBC Papers in Press, July 26, 2013, DOI 10.1074/jbc.M113.495119

Hassan Hashimi[‡§1], **Lindsay McDonald**[‡2], **Eva Stříbrná**[‡], **and Julius Lukeš**[‡§3]

From the [‡]*Institute of Parasitology, Biology Centre, Czech Academy of Sciences and the* [§]*Faculty of Science, University of South Bohemia, 370 05 České Budějovice (Budweis), Czech Republic*

Background: Letm1 is a mitochondrial protein attributed disparate roles, including cation/proton antiport and translation.
Results: Letm1 RNAi silencing in *Trypanosoma brucei* triggers swelling mitochondria and translation arrest that is ameliorated by chemical potassium/proton exchangers.
Conclusion: The ancestral function of Letm1, to maintain mitochondrial potassium homeostasis, shows remarkable conservation.
Significance: Results from diverged *T. brucei* provide a better understanding of Letm1 function throughout eukaryotes.

Letm1 is a conserved protein in eukaryotes bearing energized mitochondria. Hemizygous deletion of its gene has been implicated in symptoms of the human disease Wolf-Hirschhorn syndrome. Studies almost exclusively performed in opisthokonts have attributed several roles to Letm1, including maintaining mitochondrial morphology, mediating either calcium or potassium/proton antiport, and facilitating mitochondrial translation. We address the ancestral function of Letm1 in the highly diverged protist and significant pathogen, *Trypanosoma brucei*. We demonstrate that Letm1 is involved in maintaining mitochondrial volume via potassium/proton exchange across the inner membrane. This role is essential in the vector-dwelling procyclic and mammal-infecting bloodstream stages as well as in *Trypanosoma brucei evansi*, a form of the latter stage lacking an organellar genome. In the pathogenic bloodstream stage, the mitochondrion consumes ATP to maintain an energized state, whereas that of *T. brucei evansi* also lacks a conventional proton-driven membrane potential. Thus, Letm1 performs its function in different physiological states, suggesting that ion homeostasis is among the few characterized essential pathways of the mitochondrion at this *T. brucei* life stage. Interestingly, Letm1 depletion in the procyclic stage can be complemented by exogenous expression of its human counterpart, highlighting the conservation of protein function between highly divergent species. Furthermore, although mitochondrial translation is affected upon Letm1 ablation, it is an indirect consequence of K^+ accumulation in the matrix.

Letm1 (leucine zipper EF hand-containing transmembrane protein 1) is evolutionarily conserved in diverse eukaryotic lineages bearing energized mitochondria, ranging from opisthokonts, comprising metazoa and fungi, to plastid-containing plants and apicomplexans (1, 2). Letm1, a protein predicted to be embedded into the mitochondrial (mt)[4] inner membrane (IM) via a predicted transmembrane domain (1, 3, 4), came into prominence because its gene locus is often within a deletion, occurring to different extents, on the short arm of human chromosome 4, causing Wolf-Hirschhorn syndrome (5). Symptoms of this disease, affecting 1 in 20,000–50,000 births, are multifarious but often include facial abnormalities, various degrees of mental retardation, and seizures (6). The loss of *Letm1* has been implicated in the development of the final symptom because patients with deletions that exclude this locus do not exhibit seizures (7, 8).

The first hint of the role of Letm1 on the cellular level emerged from a deletion mutant screen for mt defects performed in *Saccharomyces cerevisiae* (9). The swollen appearance of the organelle in the *Letm1* knock-out yeast strains prompted the authors to dub it MDM38, representing another alias for the protein, to reflect its effect on mitochondrial distribution and morphology. RNAi silencing of *Letm1* in other opisthokont models like human cell cultures, *Drosophila melanogaster*, and *Caenorhabditis elegans* also resulted in swollen and fragmented mitochondria (3, 10–12), suggesting a conservation of function at least within this clade. This notion is further supported by the successful complementation of yeast *Letm1* knockout by expression of the human ortholog (1).

However, how Letm1 operates on the cellular level remains debated. Given its dramatic effect on mt morphology, it has been proposed to play an undefined structural role in the human organelle, particularly in maintaining the cristae that form inner membrane invaginations into the matrix (12). This morphological function was determined to operate indepen-

* This work was supported in part by Czech Grant Agency Grant P305/12/2261 and a Praemium Academiae award (to J. L.).
[S] This article contains supplemental Figs. 1 and 2.
[1] To whom correspondence may be addressed: Institute of Parasitology, Biology Centre, Branišovska 31, 370 05 České Budějovice, Czech Republic. Tel.: 420-38-777-5416; Fax: 420-38-531-0388; E-mail: hassan@paru.cas.cz.
[2] Present address: Institute of Immunology and Infection Research, School of Biological Sciences, Ashworth Laboratories, University of Edinburgh, Edinburgh EH9 3JT, United Kingdom.
[3] Fellow of the Canadian Institute for Advanced Research. To whom correspondence may be addressed: Institute of Parasitology, Biology Centre, Branišovska 31, 370 05 České Budějovice, Czech Republic. Tel.: 420-38-777-5416; Fax: 420-38-531-0388; E-mail: jula@paru.cas.cz.

[4] The abbreviations used are: mt, mitochondrial; IM, inner membrane; KHE, potassium/proton exchange; PS, procyclic stage; BS, bloodstream stage; SMP, submitochondrial particle; mHSP70, mitochondrial heat shock protein 70; HsLetm1 and TbLetm1, human and *T. brucei* Letm1, respectively.

dently of the fission and fusion machineries that maintain the mt network in these cells (3, 12).

Letm1 has also been hypothesized to take part in maintaining matrix volume as a cation/proton (H^+) antiporter. This function would also be consistent with the observed swollen mitochondria phenotype upon depletion of Letm1 because this treatment would negatively impact ion homeostasis and cause organellar osmotic stress. However, the identity of the cation that is translocated by Letm1 remains controversial. Several compelling studies in yeast, *Drosophila*, and human cell culture have shown that it has a central part in potassium/proton exchange (KHE), which maintains matrix volume by regulating potassium (K^+) extrusion (1, 3, 10, 13). In all of these model systems, treatment with the chemical K^+/H^+ exchanger nigericin compensates for the loss of Letm1-mediated KHE. However, Letm1 was also identified as a calcium (Ca^{2+})/H^+ antiporter in the genome-wide RNAi screen in *Drosophila* S2 cells (14), a finding corroborated in a later report (15).

Yet another role that has been attributed to Letm1 in *S. cerevisiae* is the anchoring of mt ribosomes to the inner membrane, into which it facilitates the incorporation of hydrophobic *de novo* translated subunits of the respiratory chain (4, 16, 17). This path of inquiry began with an observed reduction of the steady-state levels of a subset of mitochondrially encoded proteins in *Letm1* knockouts (4). A similar phenomenon was also reported in *Arabidopsis thaliana* bearing simultaneous homozygous and hemizygous knockouts of its two *Letm1* paralogs (18). Further support for this role, albeit indirect, was the report that Letm1 silencing in HeLa cells resulted in the disassembly of some respiratory chain complexes (12), which was nevertheless contradicted by another similar study on the same cell type (3).

To date, our understanding of Letm1 is rather convoluted. To shed light on this situation, we have undertaken functional analysis of Letm1 (TriTrypDB genome database accession number Tb927.3.4920 (19)) in the protozoan flagellate *Trypanosoma brucei*. As a member of the Kinetoplastea, it has a long and independent evolutionary history, perhaps due to its early branching from other eukaryotic lineages (20, 21). Kinetoplastids contain a single mitochondrion, with its organellar genome located in a discrete place as the giant kinetoplast DNA (kDNA) network (22). Most of the kDNA-encoded transcripts undergo elaborate post-transcriptional processing called RNA editing.

Research on kinetoplastids has proven to be invaluable to the field of mt comparative biochemistry. Notably, seminal work described Ca^{2+} influx into the trypanosome mitochondrion in a ruthenium red-sensitive fashion (23, 24). These data became critical for the algorithm to identify conserved proteins responsible for Ca^{2+} uptake, by testing a pool of mt proteins shared by kinetoplastids and vertebrates but absent in yeast, which lack this activity. Thus, after half a century of characterizing this activity, some of the responsible proteins have been identified (25–28).

T. brucei subspecies are the causative agents of a human disease with the familiar name sleeping sickness as well as the veterinarian disease nagana (29). These diseases are spread by the tsetse fly vector in sub-Saharan Africa. The parasite undergoes several morphological and physiological changes as it cycles between the mammalian host and insect vector (30), notably within its mitochondrion (22). In the procyclic stage (PS) that resides in the midgut of the vector, the organelle engages in oxidative phosphorylation to generate ATP, as in canonical mitochondria. The proliferative long slender bloodstream stage (BS) that is pathogenic for the mammalian host generates energy exclusively by glycolysis. In this milieu, the mitochondrion is not only reduced, as exemplified by its paucity of cristae and lack of cytochrome-containing respiratory complexes, but also becomes an energy consumer. Membrane potential is maintained by the remaining F_OF_1-ATP synthase, which hydrolyzes ATP to pump H^+ out of the matrix (31, 32). However, the BS mitochondrion is not dormant because organellar gene expression is still needed for cell viability (33–36), and a handful of essential mt biochemical pathways have been revealed (31, 32, 37–39).

Interestingly, a subspecies called *T. brucei evansi* is a naturally occurring form of *T. brucei* without kDNA and the causative agent of the ungulate disease surra (31, 40). This parasite is the equivalent of petite mutant (ρ^0) yeast, viable only in the fermentable medium of the bloodstream. As a consequence, it has lost the capacity to transform to the PS, which requires an energy-producing organelle and is instead spread mechanically by biting insects. *T. brucei evansi* bears compensatory mutations to the γ-subunit in the stalk of F_oF_1-ATP synthase, most likely facilitating the complex's competence for ATP hydrolysis in the absence of the mitochondrially encoded subunit A6 (31, 40). This activity in concert with that of the mt ATP/ADP carrier protein maintains the electrogenic component of the membrane potential by the antipodal exchange of ATP^{4-} and ADP^{3-}.

In this study, we take advantage of RNAi permissibility and ease of transgenesis of PS, BS, and *T. brucei evansi* in *in vitro* cultures to generate conditional knockdown cell lines to test the effect of Letm1 silencing in three different physiological states of the mitochondrion. We also compare our results in this highly diverged organism with the previously enumerated results from opisthokont model systems in order to elucidate the basal function of the evolutionarily conserved Letm1. Although this study does not represent the first one performed outside of the opisthokont clade, as the aforementioned report in Plantae can attest (18), this is for the first time when almost complete silencing of Letm1 has been achieved, yielding a clear and robust phenotype. This study also reveals yet another essential function of the *T. brucei* BS mitochondrion: the maintenance of ion homeostasis.

EXPERIMENTAL PROCEDURES

Cloning, Cultivation, Transfection, Growth Curves, and 5′-End Mapping of Letm1 mRNA—PS and BS *T. brucei* as well as *T. brucei evansi* were cultured, transfected, and selected for the relevant drug resistance for each of the given constructs and counted as described elsewhere (31, 34). A *Letm1* gene fragment amplified using forward primer GGATCCGGTCAAGCCTACCCGATACA (introduced BamHI site underlined) and reverse primer AGGCCTTCGGTAATTGCCTTCACTCC (HindIII site underlined) was cloned into the p2T7-177 vector, bearing opposing T7 polymerase promoters/tetracycline oper-

ators and targeted to a transcriptionally silent part of the *T. brucei* genome (41), via the indicated restriction sites. For *in situ* C-terminal tagging of Letm1 with YFP, the full open reading frame (ORF) excluding the stop codon was PCR-amplified with the forward primer GGTACCATGTTGG CAGCAACGGGGTT (Acc65I restriction site underlined) and reverse primer GGATCCATTT TTTGCAATCACCTCTGAAGGCT (BamHI site underlined) and cloned into the p2937 vector, derived from the p2710 vector bearing the blasticidin resistance marker (42). The construct was linearized using the unique NcoI restriction site within the Letm1 ORF to yield homology flanks for integration into the endogenous locus. The full ORF of HsLetm1 was PCR-amplified from cDNA (clone FLJ81927AAAF) supplied by the National Institute of Technology and Evaluation Biological Resource Center (Japan) using the forward primer TCAGATCTGCTCTTCACCTCTGCGA and reverse primer TCAGATCTTTGCTTCATGGC GTTGA and cloned into the pABPURO vector (43) via the underlined BglII restriction sites. We took advantage of every mRNA bearing a spliced leader RNA sequence by amplifying the 5′-end of Letm1 with the canonical spliced leader RNA forward primer and the reverse primer AGACATTAAACGGCCCTTCC, as described previously (44).

Indirect Immunofluorescence and Confocal and Electron Microscopy—Indirect immunofluorescence was performed as described elsewhere (34) except that the fixed samples were permeabilized with 0.15% Triton X-100 in PBS (v/v). Samples were decorated with primary rabbit antibodies against either GFP or HA_3, depending on the epitope and then subsequently with Alexa-488-conjugated anti-rabbit secondary antibody. Prior to this procedure, 2×10^6 live PS cells were incubated for 20 min at 27 °C with 100 nM MitoTracker Red CMXRos. All antibodies and dyes were from Molecular Probes. Transmission electron microscopy was performed as before (40).

Digitonin Fractionation, Western Blot Analysis, and Triton X-114 Separation of Membrane Proteins—Digitonin fractionation of cells into cytosolic and mitochondrial compartments and Western blots were performed as described previously (36). Antibodies against the *T. brucei* mitochondrial heat shock protein, cytochrome *c*, TrCOIV, and the β-subunit of F_1-ATPase (31, 45) were used at 1:1000 dilutions, whereas enolase was used at 1:10,000 dilutions. The Triton X-114 isolation of membrane and soluble proteins was performed as described previously (46) on mitochondria hypotonically isolated from PS *T. brucei* by an established method (47). Acetone-precipitated proteins from the fractions were resuspended in equal volumes of ultrapure water.

Isolation of Submitochondrial Particles and Proteinase K Protection Assay—Hypotonically isolated mitochondria were further processed to generate submitochondrial particles (SMPs) by adapting procedures described previously (13, 45). Briefly, a mitochondria suspension corresponding to 2.4 mg/ml protein was sonicated with three 10-s pulses (50% amplitude, 1 Hz) followed by 1-min pauses in ice water using a UP200S Ultrasonic Processor (Hielscher Ultrasound Technology). The SMPs were sedimented at 31,000 × *g* for 5 h at 4 °C. For the proteinase K protection assay, the SMPs were resuspended at a concentration of 1 mg/ml protein and incubated with or without 200 μg/ml proteinase K for 15 min on ice and then treated with 1 mM PMSF for another 15 min on ice.

Treatment of PS T. brucei with Nigericin, Monensin, and Valinomycin—For the nigericin (all ionophores used were from Sigma-Aldrich) rescue experiment described in the legend of Fig. 4*A*, PS *T. brucei* were grown for 2 days in SDM-79 medium supplemented with tetracycline. Cells were subsequently diluted to 2×10^6 cells/ml into various media with a stepwise doubling of nigericin concentrations in the 0–100 nM range. The 0 nM medium was mock-treated with the nigericin solvent ethanol. This procedure was done in order to ensure that all cells had the same initial degree of Letm1 down-regulation before ionophore exposure. Cell density was then measured at each nigericin concentration every 24 h over a 3-day time course. The procedure for monensin treatment (Fig. 4*B*) was the same, except there was a stepwise 10-fold increase in this ionophore concentration at the 0–1000 ng/ml range. For the valinomycin treatment of PS cells described in the legend to Fig. 5, the PS cells were incubated with a 1 μM concentration of the compound for 2 h. A subset of the cells was pretreated with 2 μM of nigericin prior to valinomycin application.

Flow Cytometry for Membrane Potential—PS *T. brucei* incubated with MitoTracker Red CMXRos, as described above, were diluted 1:5 in PBS and placed into a FACSCanto II flow cytometer (BD Biosciences) for measurement of fluorescence. Twenty thousand cells were counted in each measurement. Controls in which membrane potential was collapsed by the simultaneous addition of 20 μM carbonyl cyanide *p*-trifluoromethoxyphenylhydrazone to cells were also measured. Data were analyzed using the Flowing Software program (Turku Centre for Biotechnology, Finland).

Quantitative Real-time PCR and Northern Blot Analysis—Quantitative real-time PCR was performed as described previously (34), using primers homologous to mt mRNAs as designed by Carnes *et al.* (48). Letm1 mRNA was measured using specific primers CGGAATACCTGTCGTCCACT and AGACATTAAACGGCCCTTCC. The relative abundance of the assayed mRNA in the induced RNAi knockdowns, as compared with the non-induced controls and normalized to either 18 S rRNA or β-tubulin levels, was determined by standard protocols (34, 48). Northern blots were done as described previously (44), using an antisense probe generated via the aforementioned Letm1 quantitative PCR primers. Both primers were used to amplify a product from *T. brucei* genomic DNA, which was subsequently used as a template for a 45-cycle PCR with the ^{32}P-end-labeled reverse primer in the presence of [α-^{32}P]dATP (6000 μCi/ml).

Mitochondrial Translation Assay—The mitochondrial translation assay is discussed in detail elsewhere (49). Briefly, 4×10^6 cells were incubated with [^{35}S]methionine for 1 h (Easy Tag Express Protein Labeling Kit, PerkinElmer Life Sciences) in the presence of 10 mg/ml cyclohexamide to suppress cytoplasmic translation. The cells were lysed at 37 °C for 20 min in the loading buffer (2% SDS, 125 mM Tris-HCl, pH 6.8, 2% β-mercaptoethanol, 27% glycerol (v/v)) and then run on a 9% acrylamide SDS gel in the first dimension. Each lane was cut out and placed in a denaturing solution (1% SDS, 125 mM Tris-HCl, pH 6.8, 1% β-mercaptoethanol) at 37 °C for 1 h before being run in the

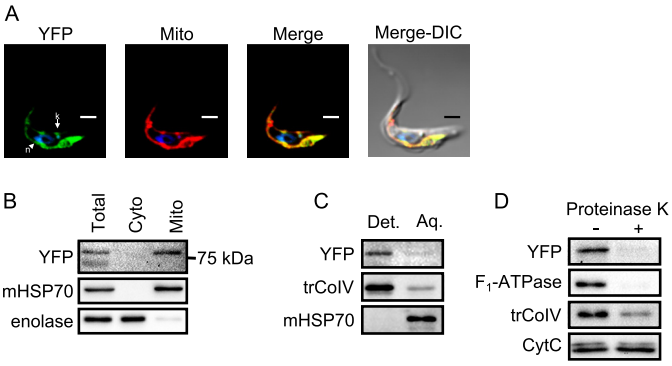

FIGURE 1. **Localization of C-terminally YFP-tagged Letm1 to *T. brucei* mitochondrial inner membrane.** *A*, indirect immunofluorescence of fixed PS *T. brucei* labeled with MitoTracker Red, which visualizes the single reticulated organelle. *Labels above pictures* indicate signal from YFP antibody (*YFP*), MitoTracker (*Mito*), and both (*Merge*) and signals overlaid with a differential contrast image (*Merge-DIC*). DAPI-stained nucleus (*n*) and kDNA (*k*) are indicated by an *arrowhead* and *arrow*, respectively. *Scale bar*, 2 μm. *B*, Western blot analysis of digitonin fractionation of cytoplasm (*Cyto*) and mitochondrial (*Mito*) compartments in comparison with an equivalent amount of lysate from whole cells (*Total*). The 75 kDa marker is indicated on the *right*. *C*, Western blot analysis of Triton X-114 fractionation of mitochondrial proteins into membrane and soluble fractions, which reside in the detergent (*Det.*) or aqueous (*Aq.*) phases, respectively. *D*, Western blot analysis of SMPs treated with proteinase K (+) or untreated controls (−). Antibodies used are indicated on the *left*.

second dimension on a 14% acrylamide-SDS gel. The gels were Coomassie-stained, incubated for 1 h in 1 M salicylate (Sigma-Aldrich), and then dried before exposure to BioMax Film (Eastman Kodak Co.).

RESULTS

Letm1 Is a Mitochondrial Inner Membrane Protein—In order to confirm that the annotated *T. brucei* Letm1 ortholog is targeted to the mitochondrion, cell lines were generated in which one of the gene loci was *in situ* tagged with sequence encoding a C-terminal YFP extension. Indirect immunofluorescence confocal microscopy revealed that Letm1 is indeed localized throughout the organelle because its signal overlaps with the specific marker MitoTracker Red CMXRos dye (Fig. 1*A*). This result was confirmed by digitonin permeabilization of cells into cytosolic and mitochondrial fractions, using antibodies immunodecorating mitochondrial heat shock protein 70 (mHSP70) and enolase as markers of these compartments, respectively (Fig. 1*B*). To verify that Letm1 is a membrane protein, isolated mitochondria from the YFP-tagged cell line were partitioned by Triton X-114 phase separation into membrane and soluble proteins, the former of which was retained in the detergent phase (Fig. 1*C*). The YFP antibody signal appeared in the detergent phase with the trypanosomatid-specific subunit of respiratory complex IV (trCOIV) (50), whereas the matrix marker mHSP70 remained in the aqueous phase (Fig. 1*C*). To determine the protein's IM localization, SMPs from the cell line where subjected to a proteinase K protection assay. In most SMPs, the inner leaflet of the IM faces outward, exposed to the protease. Indeed, trCOIV and matrix-facing F_1-ATPase are susceptible to enzyme degradation, in contrast to cytochrome *c*, located in the intermembrane space, which is protected by the IM (Fig. 1*D*). The C-terminal YFP tag is also degraded by this treatment, indicating that this portion of the protein extrudes into the matrix from the IM (Fig. 1*D*), a topology kept by the human ortholog (3).

Because the *in situ* tagged protein is bigger than the predicted size of the tagged Letm1 protein (Fig. 1*A*), about 80 *versus* 68 kDa, respectively, we decided to map the 5′-end of the mature *Letm1* mRNA to define its ORF. The start codon is actually further upstream than predicted (supplemental Fig. 1*A*), encoding a protein with the observed size and of a length comparable with that of the ortholog from the related *Trypanosoma cruzi* (supplemental Fig. 1*B*). The revised ORF contains the transmembrane domain that defines all Letm1 orthologs and other well conserved features, such as a putative protein kinase C phosphorylation site and C-terminal coiled-coil regions, but lacks the two Ca^{2+}-binding EF-hand domains present in orthologs of some other eukaryotes.

RNAi Silencing of Letm1 in Procyclic Stage Results in Mitochondrial Swelling and Inhibited Growth—To test whether Letm1 is an essential protein for the PS cells, a conditional RNAi cell line was generated using an established system in which dsRNA overexpression is induced by the addition of tetracycline, as described elsewhere (34). To test whether the dsRNA successfully targets *Letm1* mRNA for degradation, RNA was harvested from cells grown in the presence and absence of the antibiotic for 48 h for subsequent Northern analysis using a radioactively labeled antisense probe that anneals to the *Letm1* sequence. The transcript is undetectable in the RNAi-induced cells as compared with the non-induced controls (Fig. 2*A*). Ethidium bromide-stained rRNA was used as a control for equal loading. Next, we measured the growth of RNAi-induced and uninduced PS cells every 24 h over a 10-day course. Fig. 2*B* depicts a representative line graph showing absolute cell density at each time point, including the dilution of cultures every other day to 2×10^6 cells/ml. Reproducible growth inhibition is apparent 3 days after RNAi induction.

The impairment of Letm1-depleted cells is most likely due to the appearance of a swollen mitochondrion, as revealed by transmission electron microscopy (Fig. 2*C*, *1*). The identity of this massive, electron-lucent organelle, as compared with the unaltered mt electrodensity in the untreated controls (Fig. 2*C*, *3*), is supported by the surrounding double membranes (Fig. 2*C*, *2*, *arrowheads*). The discoidal cristae, which are characteristic for *T. brucei* and other members of the phylum Euglenozoa (21), remain upon Letm1 down-regulation in the periphery of the swollen organelle (Fig. 2*C*, *1* and *2*, *arrows*).

Human Letm1 Complements the Endogenous Trypanosome Ortholog—To exclude the possibility that the Letm1-silencing phenotype is due to off target effects and also to determine the protein's functional homology across the enormous evolutionary distance separating kinetoplastids from opisthokonts, we examined whether a constitutively expressed human Letm1 (HsLetm1) could complement the depletion of its *T. brucei* ortholog (TbLetm1). First, we confirmed that the exogenous HsLetm1, bearing a 3× hemagglutinin (HA_3) epitope tag on its C terminus, is targeted to the flagellate mitochondrion. Indirect immunofluorescence shows that HsLetm1 indeed co-localizes with the MitoTracker Red dye (Fig. 3*A*). This result was confirmed by digitonin subfractionation of cells into the cytosolic and mitochondrial compartments, in which the α-HA antibody

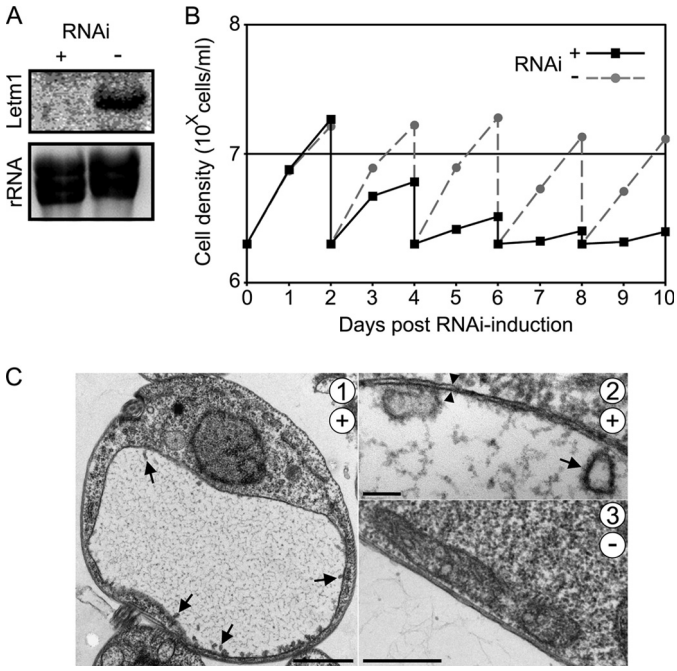

FIGURE 2. **Knockdown of Letm1 in PS *T. brucei* results in growth inhibition and mitochondrial swelling.** *A*, Northern blot analysis showing that Letm1 mRNA is depleted in cells grown with the RNAi-inducing tetracycline (+) as compared with the untreated controls (−) in the *upper image* (*Letm1*). The ethidium bromide-stained rRNA from the corresponding *lanes* is shown *below* as a loading control. *B*, PS *T. brucei* grown in the presence (*RNAi*+) or absence (*RNAi*−) of tetracycline. The *x* axis shows days post-RNAi induction; the *y* axis shows cell density in 10^X cells/ml plotted on a logarithmic scale. *C*, transmission electron micrographs of cells grown in the presence (+; *pictures 1* and *2*) or absence (−; *picture 3*) of tetracycline for 3 days. Cristae and double membranes are indicated by *arrows* and *double arrowheads*, respectively. *Scale bars*, 1 μm, 100 nm, and 500 nm for *pictures 1*, *2*, and *3*, respectively.

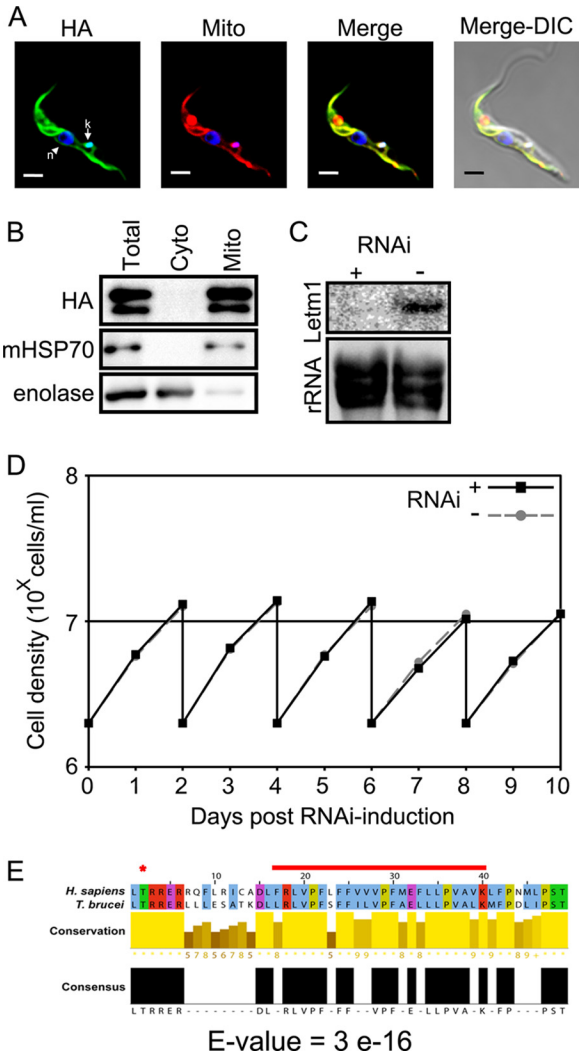

FIGURE 3. **Expression of human Letm1 rescues knockdown of the *T. brucei* ortholog.** *A* and *B*, indirect immunofluorescence and digitonin subfractionation of PS *T. brucei* confirm mitochondrial localization of the C-terminal HA_3-tagged human Letm1 (*HA*). Other labels and the *scale bar* in *A* are as described for Fig. 1, *A* and *B*. *C*, Northern blot analysis confirms the ablation of the endogenous *T. brucei* Letm1 mRNA in cells constitutively overexpressing exogenous human Letm1. Labeling is as in Fig. 2*A*. *D*, growth of PS *T. brucei* constitutively overexpressing human Letm1 grown in the presence (*RNAi*+) or absence (*RNAi*−) of tetracycline. Labeling is as in Fig. 2*B*. *E*, alignment of the predicted transmembrane domain of the human and *T. brucei* orthologs. *, conserved predicted protein kinase C phosphorylation site; *red line*, transmembrane domain. The *E*-value of BLAST alignment of the two sequences is shown at the bottom.

signal associates with that of the mitochondrial marker mHSP70 (Fig. 3*B*). The abundant upper band migrated at the expected ~90 kDa size with a less intense one just below, a pattern also observed when the protein was expressed in *Escherichia coli* (14).

After verifying that the endogenous TbLetm1 is still silenced in cells expressing HsLetm1 (Fig. 3*C*), the growth of cell lines with and without TbLetm1 down-regulation was compared. As shown in the line graph in Fig. 3*D*, both samples grew at the same rate. This result indicates that HsLetm1 can fully complement the ablation of TbLetm1 in *T. brucei*, suggesting functional homology of the two orthologs. Indeed, the two orthologs share sequence homology in the region of the predicted transmembrane domain (Fig. 3*E*).

The Nigericin Ionophore Restores Cell Viability and Mitochondrial Function in Letm1 Knockdowns—The manifested swollen mitochondria upon Letm1 ablation may be due to a consequent accumulation of ions. To test whether K^+ is the cation in question, we attempted to treat RNAi-induced *T. brucei* with varying doses of nigericin, an ionophore that acts as an antiporter of K^+ and H^+ across membranes, as described under "Experimental Procedures." Fig. 4*A* depicts a line graph in which average cell density among quadruplicates is plotted against nigericin concentration. Each line presents measurements made 1–3 days after ionophore treatment. Growth rates at each nigericin concentration are inferred from the difference between points relative to the *y* axis and also depicted in supplemental Fig. 2*A*.

In the cells depleted for Letm1 (RNAi+), there is a dose-dependent increase in growth from 0 to 50 nM nigericin, after which there is a decrease in growth. This latter trend is probably due to the intrinsic toxicity of the ionophore to *T. brucei*, as demonstrated by a line graph showing the dose-dependent decrease in growth of cells grown in the absence of tetracycline (RNAi−) throughout the whole concentration range. However, it should be mentioned that the Letm1-depleted cells grown in 100 nM nigericin still exhibit more rapid growth than those grown without the drug, indicating that this ionophore is able to partially restore cell viability upon loss of Letm1. The cells

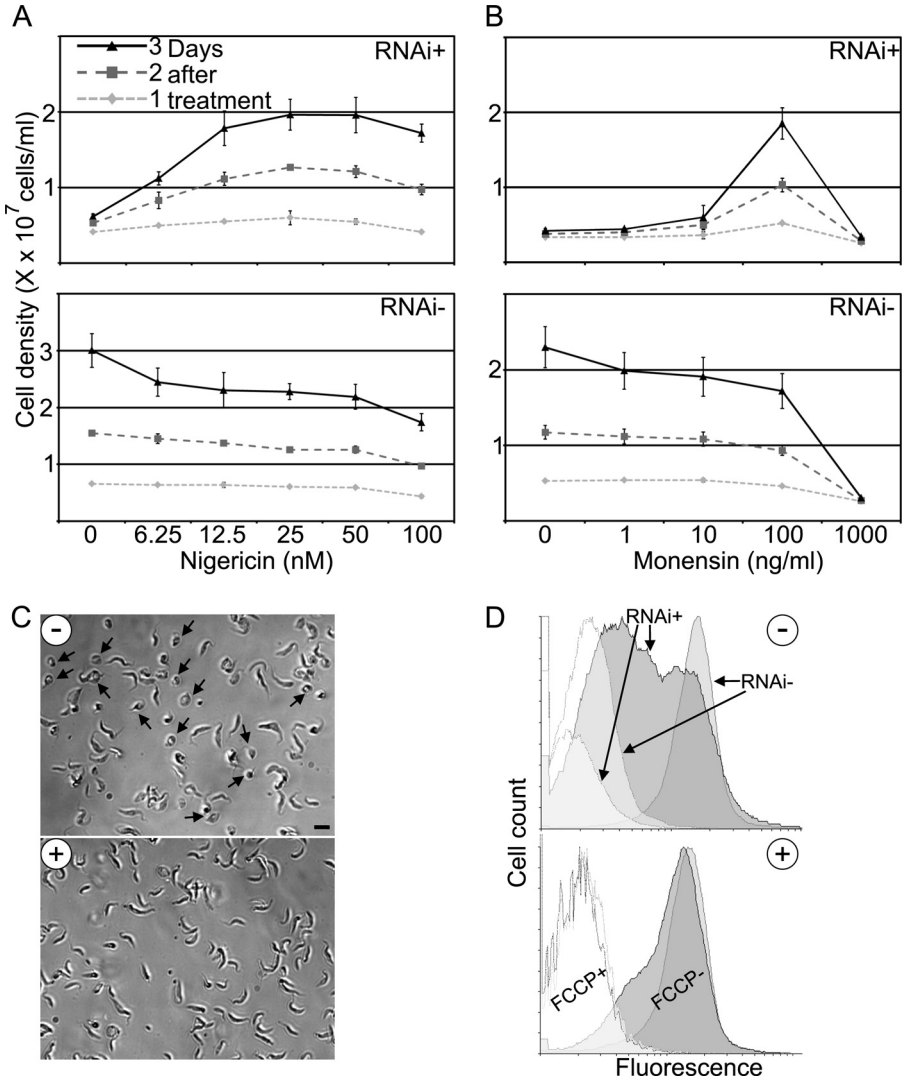

FIGURE 4. **Treatment with the ionophore nigericin rescues the Letm1 knockdown in PS *T. brucei*.** *A*, cell growth in a 0–100 nM range of nigericin concentrations (*x* axis), as measured by density (10^x cells/ml, along the *y* axis) of cells grown in the presence (*RNAi*+) or absence of tetracycline (*RNAi*−). Each *shaded line* represents 1–3 days after treatment. $n = 4$; *error bars* indicate S.D. *B*, cell growth in a 0–100 ng/ml range of monensin concentrations (*x* axis); otherwise as in *A*. *C*, light micrographs showing cells after 3 days of RNAi induction either treated with 25 nM nigericin (+) or mock-treated with ethanol (−). *Scale bar*, 10 μm. *D*, flow cytometry histogram following membrane potential in MitoTracker-labeled PC *T. brucei* grown in the presence (*RNAi*+) or absence of tetracycline (*RNAi*−) and either mock-treated with ethanol (*top plot*; −) or treated with 25 nM nigericin (*bottom plot*; +). An increase in fluorescence is depicted on the *x* axis from *left* to *right* on a logarithmic scale plotted against a cell count on the *y* axis. *Unfilled curves* are measurements of cells also treated with 20 μM carbonyl cyanide *p*-trifluoromethoxyphenylhydrazone (*FCCP*), an uncoupler of mitochondrial membrane potential.

ablated for Letm1 exhibited comparable growth rates as compared with their RNAi-uninduced counterparts when treated with 25, 50, and 100 nM nigericin (supplemental Fig. 2*A*).

We next looked to see whether nigericin treatment restores mt morphology and physiology. Cells grown for 2 days in the presence of tetracycline to induce Letm1 silencing were subsequently diluted into media with or without 25 nM nigericin and grown for 24 h before being subjected to assays comparing RNAi-treated and untreated samples. Light microscopy reveals that about half of the cells grown in the absence of the ionophore (Fig. 4*C*, −) exhibit a rounded shape with lucent center, representing the swollen mitochondrion (*arrows*), whereas all of the treated cells exhibit normal gross morphology (Fig. 4*C*, +). The physiological state of the organelle in both samples was also determined using the MitoTracker Red dye, whose intercalation into the matrix correlates with membrane potential. According to the flow cytometry histogram (Fig. 4*D*, −), the membrane potential of Letm1-depleted cells (*RNAi*+) not treated with nigericin exhibits various degrees of membrane potential reduction compared with their non-induced counterparts (*RNAi*−), as represented by two broad fluorescence peaks. The broad range of membrane potential reduction also reflects the various morphological effects 3 days after Letm1 down-regulation. However, nigericin-treated cells with reduced or endogenous Letm1 levels exhibited the same membrane potential (Fig. 4*D*, +), suggesting that the ionophore mediates restoration of the physiological state of the organelle.

These results were further confirmed by treatment with monensin, a less specific ionophore that exchanges H^+ and monovalent cations, such as K^+. Using the same previously described scheme, 100 ng/ml was determined to restore growth in the Letm1-depleted cells compared with the uninduced cells

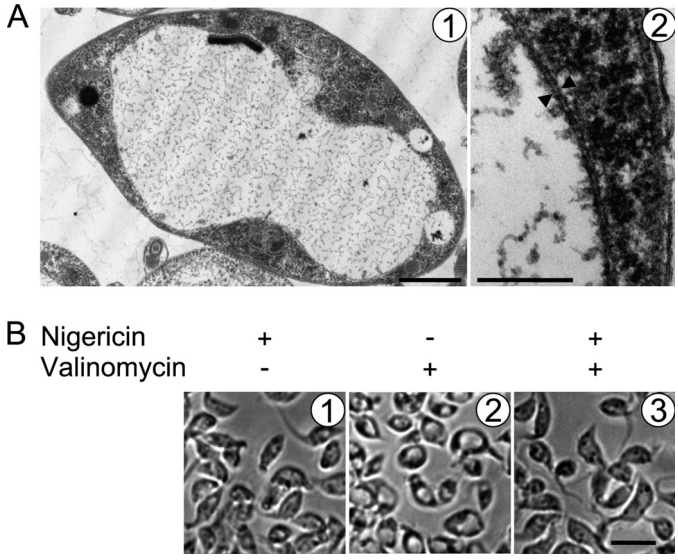

FIGURE 5. **Treatment of PS *T. brucei* with the K^+ ionophore valinomycin results in mitochondrial swelling.** *A*, transmission electron micrographs of PS *T. brucei* treated with a 1 μM concentration of the K^+ ionophore valinomycin. Double membranes are indicated by *opposing arrowheads*. *Scale bars*, 2 μm and 200 nm for *pictures 1* and *2*, respectively. Note the peripherally located kinetoplast DNA *disk*. *B*, light micrographs showing cells treated with either 2 μM nigericin or 1 μM valinomycin alone or pretreated with the former and then treated with the latter, as indicated at the *top* of the *images* from *left* to *right*. *Scale bar*, 10 μm.

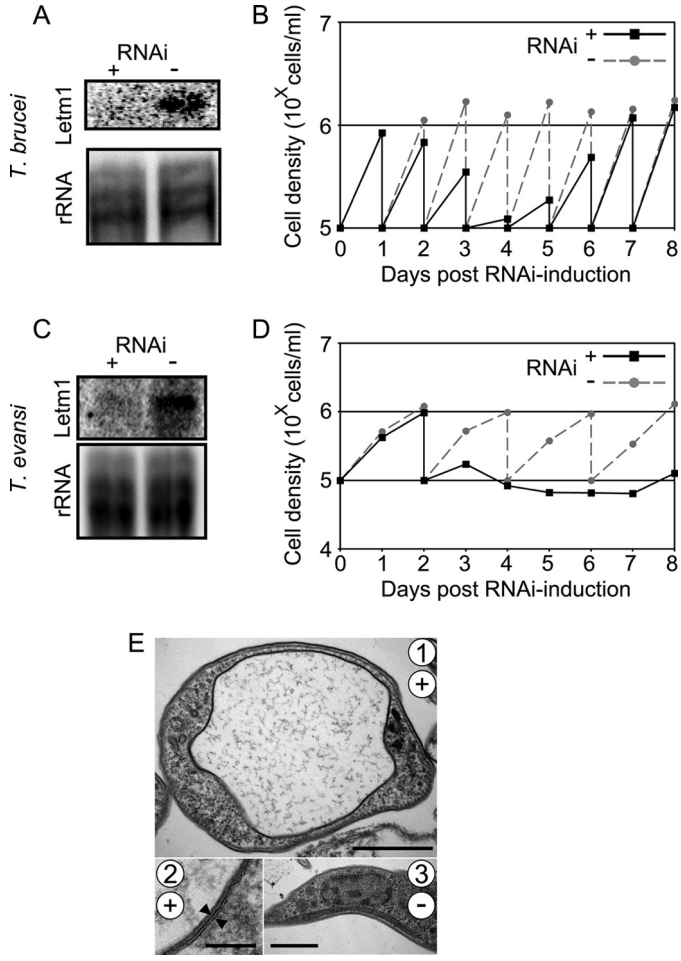

FIGURE 6. **Knockdown of Letm1 in BS *T. brucei* and *T. brucei evansi* results in growth inhibition and mitochondrial swelling.** *A–D*, Northern blot analysis confirming ablation of Letm1 mRNA in RNAi-induced cells *versus* non-induced controls plus growth analysis comparing these two samples in BS *T. brucei* (*A* and *B*) and *T. brucei evansi* (*C* and *D*). Labeling is as in Fig. 2, *A* and *B*. *E*, transmission electron micrographs of *T. brucei evansi* grown in the presence (+; *pictures 1* and *2*) or absence (−; *picture 3*) of tetracycline for 3 days. Double membranes are indicated by *opposing arrowheads*. *Scale bars*, 1 μm, 100 nm, and 1 μm for *pictures 1*, *2*, and *3*, respectively.

treated with the same dose (Fig. 4*B* and supplemental Fig. 2*B*). Taken together, these results suggest that upon Letm1 silencing, K^+ cations accumulate in the mt matrix, which cause subsequent osmotic stress and swelling mitochondria. The chemical action of the ionophores nigericin and monensin compensates for the ablation of Letm1 by mediating KHE across the inner membrane. Consequently, these cells exhibit normal mt morphology and physiology.

Depletion of Letm1 Phenocopies the K^+ Ionophore Valinomycin—As further support for the notion that matrix K^+ accumulation is behind the swelling of the PS *T. brucei* mitochondrion upon Letm1 silencing, the parental cell line used in the generation of the conditional RNAi knockdown was treated with the ionophore valinomycin. In contrast to nigericin, valinomycin acts in a Nerstian fashion by transporting K^+ across lipid membranes down an electrochemical gradient. Thus, this compound is often used in other systems to dissipate mt membrane potential (3, 51). Valinomycin supplementation (1 μM) to SDM-79 medium was fatal to *T. brucei* after 2 h of exposure. As seen by subsequent observation by transmission electron microscopy, these cells exhibit a swollen mitochondrion in a manner reminiscent of the Letm1 knockdown (Fig. 5*A*).

We next asked whether nigericin pretreatment can prevent valinomycin-mediated swelling mitochondria. Cells were incubated with 2 μM nigericin for 15 min and then split into those exposed to or lacking valinomycin treatment as described above; cells without nigericin pretreatment prior to valinomycin exposure were included in this experiment. As visualized by light microscopy, *T. brucei* incubated only with this concentration of nigericin exhibit a shrunken appearance, possibly due to unspecified cell-wide effects (Fig. 5, *B1*). Nigericin pretreatment prevents the visible swelling of mitochondria caused by valinomycin (Fig. 5*B*, *2* and *3*). It appears that Letm1 knockdown in PS phenocopies the swelling mitochondria effect of the K^+ ionophore valinomycin in the parental cell line, including the susceptibility of this swelling to the K^+/H^+ antiporter nigericin.

Letm1 Is Essential for T. brucei evansi and the Bloodstream Stage of T. brucei—To gain insight into the role of Letm1 in mitochondria bearing different physiological states, we generated conditional RNAi knockdowns in *T. brucei* BS and *T. brucei evansi*, a petite mutant of *T. brucei* lacking any kDNA and hence a canonical proton gradient across the inner mt membrane (31, 52). Efficient degradation of the *Letm1* transcript in either cell line was verified by Northern blot analysis (Fig. 6, *A* and *C*). Growth in the presence and absence of the RNAi induction agent was subsequently assayed as in PS, with a lower starting concentration of 5×10^5 cells/ml. As seen in the line graph in Fig. 6*B*, Letm1 depletion in BS resulted in growth inhibition already 2 days after RNAi induction, after the first daily dilution. A recovery of growth often occurring when essential pro-

teins are down-regulated (34) is also observed to begin at day 4 of the time course. Obvious growth inhibition is also observed on day 3 after the first cell passage in *T. brucei evansi* (Fig. 6*D*), which is performed every other day due to the slower growth rate of these trypanosomes as compared with BS. Both cell types exhibited swelling mitochondria at these time points, as shown in a representative picture from *T. brucei evansi* (Fig. 6*E*, *1* and *2*), a very dramatic contrast to the thin morphology of the organelle in the untreated controls (Fig. 6*E*, *3*). Thus, Letm1 plays the same role in mediating KHE in the mitochondrion of trypanosome stages that lack a respiratory chain and cristae, as exemplified by the results in BS *T. brucei*. Furthermore, this ion exchange functions even in the absence of a canonical proton gradient across the inner membrane, which is not a component of the mitochondrial membrane potential in *T. brucei evansi* (31).

Letm1 Is Dispensable for Mitochondrial Translation—Because *T. brucei evansi* has lost its mt genome, components responsible for gene expression in the organelle have been rendered redundant (31, 36). Thus, the essential nature of Letm1 in these ρ^0 trypanosomes argues ostensibly against a primary function in mt translation via its interaction with ribosomes. To further investigate, we decided to assay *de novo* translated apocytochrome *b* (CytB) and cytochrome *c* oxidase subunit 1 (Cox1) in PS (49), the *T. brucei* life cycle stage that assembles the respiratory complexes into which these proteins are incorporated (22).

Letm1 RNAi knockdowns grown in the presence of tetracycline for 2–4 days plus a non-induced control were subjected to the [^{35}S]methionine labeling of *de novo* synthesized mt proteins, which were subsequently resolved on a 9%/14% acrylamide two-dimensional denaturing gel. A steady decrease in the labeled Cox1 and CytB, as well as still unidentified products, was observed over the time course (Fig. 7*A*). This decrease in ^{35}S signal is compared with the Coomassie-stained cytosolic proteins (Fig. 7*A*, *insets*), which remain at a constant level in all samples. To ensure that this decrease was due to translational rather than transcriptional defects, steady-state levels of these transcripts were also determined by real-time quantitative PCR. *Cox1* mRNA, which does not undergo RNA editing, and *CytB* mRNA, which is processed by moderate RNA editing, complemented by the massively edited *Cox3* transcript, were virtually unaffected 3 days after RNAi induction (Fig. 7*B*). Therefore, it appears that mt translation is indeed compromised in Letm1-depleted *T. brucei.*

To resolve whether this phenomenon is directly due to the depletion of Letm1 or a downstream effect, mt translation was assayed in RNAi cell lines induced by tetracycline for 4 days with or without 25 nM nigericin treatment for the last 2 days plus the non-induced controls. As shown in Fig. 8*A*, translation proceeds in the Letm1-silenced cells, in which KHE is restored by nigericin. *Letm1* mRNA was measured in the nigericin-treated cells to confirm that it was degraded upon RNAi induction (Fig. 8*B*). We conclude from these experiments that the observed hindering of mt translation in Letm1-depleted *T. brucei* is a secondary consequence of the disrupted ion homeostasis.

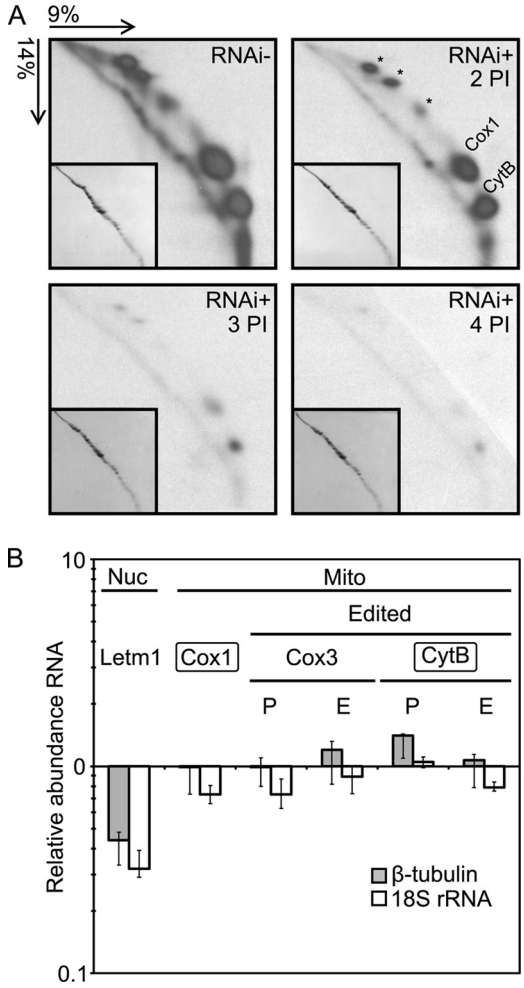

FIGURE 7. **Knockdown of Letm1 has an effect on mitochondrial translation in PS *T. brucei.*** *A*, resolution of *de novo* [^{35}S]methionine-labeled mitochondrial proteins by two-dimensional SDS-PAGE. Acrylamide composition and the direction of each dimension are indicated at the *top left*. *Insets* show the same gels in which the cytoplasmic proteins are Coomassie-stained. Gels are RNAi− and RNA+ 2, 3, and 4 days postinduction (*PI*) by tetracycline. The identified *spots* corresponding to apocytochrome *b* (*CytB*) and cytochrome *c* oxidase subunit 1 (*Cox1*) are indicated along with hitherto unidentified mitochondrial proteins (*). *B*, quantitative real-time PCR assaying steady state levels of selected mitochondrial (*Mito*) and nucleus-encoded Letm1 mRNAs (*Nuc*). Transcripts undergoing RNA editing are indicated, and the pre-edited (*P*) and edited (*E*) forms were individually assayed. *Boxed transcripts* are those whose protein products were followed in *A*. The mean relative levels of the assayed amplicons in the RNAi-induced cells relative to the levels in the uninduced control are plotted logarithmically and normalized to the same calculation performed for the nucleus-encoded β-tubulin (*gray bars*) and 18 S rRNA cDNAs (*white bars*), which were unaffected by the Letm1 RNAi silencing. *Error bars*, range of obtained relative abundances; $n = 3$.

DISCUSSION

Mitochondria are ancient organelles of an endosymbiotic origin that are, in one form or another, maintained in all extant eukaryotes living in very different ecological niches. As such, although mitochondria have undergone divergent evolution in these various organisms, they still retain basal characters that are common to them, such as being bound by double membranes (53). Using the highly diverged *T. brucei* as a study model, we have exploited its amenabilities and its evolutionary divergence to determine the ancestral function of the ubiquitous Letm1 protein, which exhibits remarkable conservation of

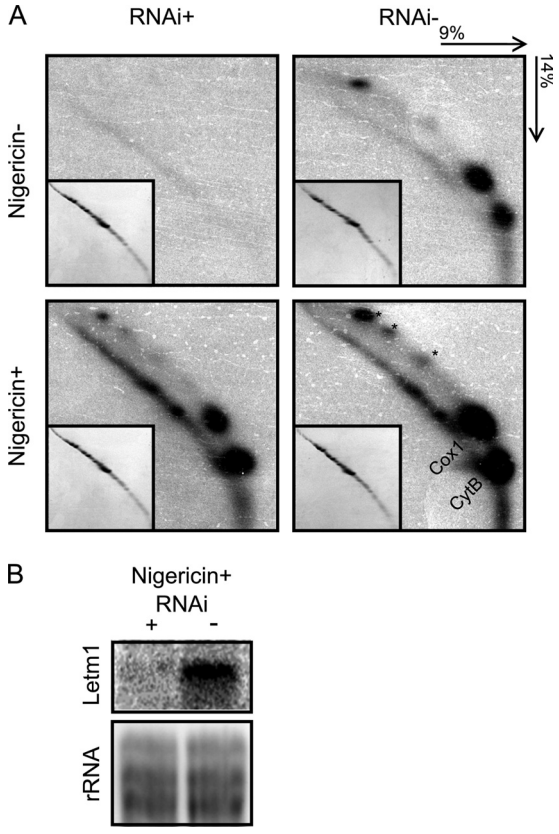

FIGURE 8. **Mitochondrial translation persists in nigericin-treated PS *T. brucei* Letm1 knockdowns.** *A*, resolution of *de novo* [^{35}S]methionine-labeled mitochondrial proteins by two-dimensional SDS-PAGE. Acrylamide composition and the direction of each dimension are indicated at the *top right*. Other labels and features are as described for Fig. 7*A*. Gels corresponding to protein products from RNAi-induced cells (*RNAi*+) and uninduced controls (*RNAi*−) are indicated at the *top*, and those treated with 25 μM nigericin (*Nigericin*+) and untreated (*Nigericin*−) are designated on the *left*. *B*, Northern blot analysis showing that Letm1 mRNA is down-regulated in cells grown in the presence of tetracycline (+) as compared with the untreated controls (−), both grown in the presence of nigericin. Labeling is as in Fig. 2*A*.

function in different organellar contexts and across large evolutionary distances.

The *T. brucei* organelle is present in a single copy and carries discoidal cristae (21), and its energy metabolism undergoes dramatic alterations during the life cycle (22). However, despite such differences, our studies reproduced a phenotype seen in some of those previously carried out in other eukaryotes, namely that ablation of the Letm1 protein results in swelling mitochondria (1, 3, 10–12). This condition is alleviated by treatment with chemical monovalent cation/proton exchangers, such as nigericin or monensin. These results strongly suggest that Letm1 mediates KHE, the coupling of K^+ extrusion from the mt matrix against its natural concentration gradient with the downhill movement of H^+ into this space. In a Letm1-depleted background, K^+ accumulates in the organelle, causing the osmotic stress that leads to the striking effect on organellar morphology. This RNAi phenotype is akin to the mt swelling observed when *T. brucei* is treated with a large dose of valinomycin, an ionophore that allows K^+ to penetrate polarized membranes and accumulate in the enclosed space.

Peter Mitchell (54) originally recognized the hazard of cation sequestering within the negatively charged matrix of energized mitochondria as a consequence of membrane potential and predicted the existence of H^+-driven mechanisms to mitigate this possibility as one of the postulates of his chemiosmotic hypothesis. The trypanosomatid organelle has a proven K^+ uptake activity with pharmacological properties that are reminiscent of those possessed by an ATP-sensitive K^+ channel embedded in the IM of other eukaryotes (55–57). Thus, the need for K^+ efflux from the matrix via KHE is a logical requirement for the organelle in trypanosomes, and our results suggest that Letm1 has a role in this process.

Another study has implicated Letm1 in Ca^{2+} translocation across the IM (14, 15). Our results suggest otherwise, agreeing with those that have postulated a role in KHE (1, 3, 10). The reason for this disparity is unclear. Jiang and colleagues described Ca^{2+} translocation function in HeLa cell cultures and used liposome reconstitution of the recombinant protein (14), although it should be noted that this study described a significantly more limited effect on mt morphology than previous reports. However, in our study, the aforementioned ability of the K^+/H^+-exchanging ionophores nigericin and monensin to rescue the Letm1-depleted *T. brucei* presents convincing evidence that it is indeed K^+ homeostasis that is disrupted. Also, in contrast to K^+, which represents the most concentrated intracellular cation (58, 59), Ca^{2+} is a carefully regulated secondary messenger whose intracellular concentration is in the micromolar range (60), making its accumulation in the matrix a less likely cause of the swelling mitochondria phenotype. Finally, yeast still retain an ortholog of the *Letm1* gene despite lacking an active Ca^{2+} uptake mechanism (25–27, 60), presumably removing the evolutionary pressure to maintain the protein in this organellar context.

In *T. brucei*, Letm1 does not appear to play a direct role in mitochondrial translation as has been suggested for the yeast ortholog (4, 16, 17). Although this process is indeed compromised in the Letm1 knockdowns, it persists when these cells are treated with nigericin. Because mitochondrial ribosomes disassociate in high K^+ concentration environments (61, 62), we propose that the apparent effect on mitochondrial translation represents an epiphenomenon to the accumulation of the cation in the matrix upon Letm1 ablation. Furthermore, the similar growth rates of the Letm1-depleted and uninduced controls in the optimal doses of the ionophores nigericin and monensin suggest that additional processes are not affected besides mt K^+/H^+ antiport.

Taking all into account, we conclude that the ancestral function of Letm1 is KHE to maintain and/or regulate K^+ homeostasis and consequently mt volume. This conservation of function throughout eukaryotes is underscored by the ability of the human Letm1 ortholog to complement the down-regulation of the *T. brucei* ortholog. This evidence of common function in trypanosomes and humans is also interesting, given the wide structural variation between the two orthologs; although they share sequence homology in the defining trans-membrane domain, only human Letm1 bears two EF hands, indicating that they are superfluous to Letm1 function in the parasite. This result suggests that the motif does not directly contribute to cation extrusion from the organelle but perhaps serves a regulatory role for the human protein.

Our model system provided additional insight into conserved Letm1 function in different mt physiological states, as represented by the BS *T. brucei* and the ρ^0 *T. brucei evansi*, both of which we show require function of this protein. In the BS stage, mt membrane potential is exclusively generated by the F_oF_1-ATP synthase via ATP hydrolysis, whereas *T. brucei evansi* is quite extreme in that only the electrogenic component of mt membrane potential is responsible for maintaining the energized mitochondrion of the parasite. Interestingly, this component of the proton motive force appears to be sufficient to drive Letm1-mediated KHE.

The essentiality of Letm1 offers new insight into the functions of the BS mitochondrion, known to be massively reduced in function and morphology (22) yet still indispensable. Among the few active pathways in the BS organelle requiring the preservation of mt membrane potential are the maintenance of the glycosomal redox balance via the glycerol-3-phosphatase/dihydroxyacetone phosphate shuttle, fatty acid synthesis, and thymidylate production for DNA synthesis (31, 32, 37–39). Although Ca^{2+} uptake activity has previously been described in the BS mitochondrion, the essentiality of this pathway was not explored, and we are now therefore able to add ion homeostasis to the list of indispensable functions of the BS organelle. The requirement for Letm1 is perhaps more surprising still in the even further reduced mitochondrion of *T. brucei evansi*, because it suggests that one reason why this petite mutant undergoes extraordinary lengths to maintain an energized mitochondrion (31, 40) is to maintain mt matrix K^+, an irony, considering that it is this very feature that predisposes the organelle to cation accumulation.

This study exploited many features of the *T. brucei* subspecies complex that makes it a suitable model for studying mitochondrial function that extends from its role in this neglected pathogen to other eukaryotes. Its high evolutionary divergence allows it to serve as a valuable outgroup for establishing whether pathways described in opisthokont models are well conserved and serve as a foundation for organelle function and biogenesis. The availability of genetically tractable *in vitro* cultures bearing very different mitochondrial states allows one to easily address the potential persistence or modulation of protein function in these milieus. Thus, we show that Letm1 serves an essential and extremely conserved function in *T. brucei* to maintain mitochondrial volume by KHE.

Acknowledgments—We thank Dmitri Maslov (University of California) for advice on the de novo mt protein labeling assay; Achim Schnaufer (University of Edinburgh) for providing the T. brucei evansi cell line used in the study and sequence information; Zhenqiu Huang (University of South Bohemia) for the Letm1-YFP construct made from a plasmid provided by Mark Carrington (Cambridge University); Julius Lukeš IV (Charles University) for help with initial experiments; Luděk Kořeny (Cambridge University) for assistance with the alignment of the human and T. brucei Letm1 orthologs; and Ken Stuart (Seattle Biomed), Paul Michels (Universidad de los Andes/University of Edinburgh), and Steve Hajduk (University of Georgia) for α-mHSP70, enolase, and cytochrome c antibodies, respectively.

REFERENCES

1. Nowikovsky, K., Froschauer, E. M., Zsurka, G., Samaj, J., Reipert, S., Kolisek, M., Wiesenberger, G., and Schweyen, R. J. (2004) The LETM1/YOL027 gene family encodes a factor of the mitochondrial K^+ homeostasis with a potential role in the Wolf-Hirschhorn syndrome. *J. Biol. Chem.* **279,** 30307–30315
2. Schlickum, S., Moghekar, A., Simpson, J. C., Steglich, C., O'Brien, R. J., Winterpacht, A., and Endele, S. U. (2004) LETM1, a gene deleted in Wolf-Hirschhorn syndrome, encodes an evolutionarily conserved mitochondrial protein. *Genomics* **83,** 254–261
3. Dimmer, K. S., Navoni, F., Casarin, A., Trevisson, E., Endele, S., Winterpacht, A., Salviati, L., and Scorrano, L. (2008) LETM1, deleted in Wolf-Hirschhorn syndrome is required for normal mitochondrial morphology and cellular viability. *Hum. Mol. Genet.* **17,** 201–214
4. Frazier, A. E., Taylor, R. D., Mick, D. U., Warscheid, B., Stoepel, N., Meyer, H. E., Ryan, M. T., Guiard, B., and Rehling, P. (2006) Mdm38 interacts with ribosomes and is a component of the mitochondrial protein export machinery. *J. Cell Biol.* **172,** 553–564
5. Endele, S., Fuhry, M., Pak, S. J., Zabel, B. U., and Winterpacht, A. (1999) LETM1, a novel gene encoding a putative EF-hand Ca^{2+}-binding protein, flanks the Wolf-Hirschhorn syndrome (WHS) critical region and is deleted in most WHS patients. *Genomics* **60,** 218–225
6. Battaglia, A., Filippi, T., and Carey, J. C. (2008) Update on the clinical features and natural history of Wolf-Hirschhorn (4p-) syndrome. Experience with 87 patients and recommendations for routine health supervision. *Am. J. Med. Genet. C Semin. Med. Genet.* **148C,** 246–251
7. South, S. T., Bleyl, S. B., and Carey, J. C. (2007) Two unique patients with novel microdeletions in 4p16.3 that exclude the WHS critical regions. Implications for critical region designation. *Am. J. Med. Genet. A* **143A,** 2137–2142
8. Zollino, M., Lecce, R., Fischetto, R., Murdolo, M., Faravelli, F., Selicorni, A., Buttè, C., Memo, L., Capovilla, G., and Neri, G. (2003) Mapping the Wolf-Hirschhorn syndrome phenotype outside the currently accepted WHS critical region and defining a new critical region, WHSCR-2. *Am. J. Hum. Genet.* **72,** 590–597
9. Dimmer, K. S., Fritz, S., Fuchs, F., Messerschmitt, M., Weinbach, N., Neupert, W., and Westermann, B. (2002) Genetic basis of mitochondrial function and morphology in *Saccharomyces cerevisiae*. *Mol. Biol. Cell* **13,** 847–853
10. McQuibban, A. G., Joza, N., Megighian, A., Scorzeto, M., Zanini, D., Reipert, S., Richter, C., Schweyen, R. J., and Nowikovsky, K. (2010) A *Drosophila* mutant of LETM1, a candidate gene for seizures in Wolf-Hirschhorn syndrome. *Hum. Mol. Genet.* **19,** 987–1000
11. Hasegawa, A., and van der Bliek, A. M. (2007) Inverse correlation between expression of the Wolfs Hirschhorn candidate gene Letm1 and mitochondrial volume in *C. elegans* and in mammalian cells. *Hum. Mol. Genet.* **16,** 2061–2071
12. Tamai, S., Iida, H., Yokota, S., Sayano, T., Kiguchiya, S., Ishihara, N., Hayashi, J., Mihara, K., and Oka, T. (2008) Characterization of the mitochondrial protein LETM1, which maintains the mitochondrial tubular shapes and interacts with the AAA-ATPase BCS1L. *J. Cell Sci.* **121,** 2588–2600
13. Froschauer, E., Nowikovsky, K., and Schweyen, R. J. (2005) Electroneutral K^+/H^+ exchange in mitochondrial membrane vesicles involves Yol027/Letm1 proteins. *Biochim. Biophys. Acta* **1711,** 41–48
14. Jiang, D., Zhao, L., and Clapham, D. E. (2009) Genome-wide RNAi screen identifies Letm1 as a mitochondrial Ca^{2+}/H^+ antiporter. *Science* **326,** 144–147
15. Waldeck-Weiermair, M., Jean-Quartier, C., Rost, R., Khan, M. J., Vishnu, N., Bondarenko, A. I., Imamura, H., Malli, R., and Graier, W. F. (2011) Leucine zipper EF hand-containing transmembrane protein 1 (Letm1) and uncoupling proteins 2 and 3 (UCP2/3) contribute to two distinct mitochondrial Ca^{2+} uptake pathways. *J. Biol. Chem.* **286,** 28444–28455
16. Bauerschmitt, H., Mick, D. U., Deckers, M., Vollmer, C., Funes, S., Kehrein, K., Ott, M., Rehling, P., and Herrmann, J. M. (2010) Ribosome-binding proteins Mdm38 and Mba1 display overlapping functions for regulation of mitochondrial translation. *Mol. Biol. Cell* **21,** 1937–1944

17. Lupo, D., Vollmer, C., Deckers, M., Mick, D. U., Tews, I., Sinning, I., and Rehling, P. (2011) Mdm38 is a 14-3-3-like receptor and associates with the protein synthesis machinery at the inner mitochondrial membrane. *Traffic* **12,** 1457–1466
18. Zhang, B., Carrie, C., Ivanova, A., Narsai, R., Murcha, M. W., Duncan, O., Wang, Y., Law, S. R., Albrecht, V., Pogson, B., Giraud, E., Van Aken, O., and Whelan, J. (2012) LETM proteins play a role in the accumulation of mitochondrially encoded proteins in *Arabidopsis thaliana* and AtLETM2 displays parent of origin effects. *J. Biol. Chem.* **287,** 41757–41773
19. Aslett, M., Aurrecoechea, C., Berriman, M., Brestelli, J., Brunk, B. P., Carrington, M., Depledge, D. P., Fischer, S., Gajria, B., Gao, X., Gardner, M. J., Gingle, A., Grant, G., Harb, O. S., Heiges, M., Hertz-Fowler, C., Houston, R., Innamorato, F., Iodice, J., Kissinger, J. C., Kraemer, E., Li, W., Logan, F. J., Miller, J. A., Mitra, S., Myler, P. J., Nayak, V., Pennington, C., Phan, I., Pinney, D. F., Ramasamy, G., Rogers, M. B., Roos, D. S., Ross, C., Sivam, D., Smith, D. F., Srinivasamoorthy, G., Stoeckert, C. J., Jr., Subramanian, S., Thibodeau, R., Tivey, A., Treatman, C., Velarde, G., and Wang, H. (2010) TriTrypDB. A functional genomic resource for the Trypanosomatidae. *Nucleic Acids Res.* **38,** D457–D462
20. Philippe, H., Lopez, P., Brinkmann, H., Budin, K., Germot, A., Laurent, J., Moreira, D., Müller, M., and Le Guyader, H. (2000) Early-branching or fast-evolving eukaryotes? An answer based on slowly evolving positions. *Proc. Biol. Sci.* **267,** 1213–1221
21. Cavalier-Smith, T. (2010) Kingdoms Protozoa and Chromista and the eozoan root of the eukaryotic tree. *Biol. Lett.* **6,** 342–345
22. Lukeš, J., Hashimi, H., Verner, Z., and Čičová, Z. (2010) The remarkable mitochondrion of trypanosomes and related flagellates. in *Structures and Organelles in Pathogenic Protists* (de Souza, W., ed) pp. 227–252, Springer, Berlin
23. Xiong, Z. H., Ridgley, E. L., Enis, D., Olness, F., and Ruben, L. (1997) Selective transfer of calcium from an acidic compartment to the mitochondrion of *Trypanosoma brucei*. Measurements with targeted aequorins. *J. Biol. Chem.* **272,** 31022–31028
24. Vercesi, A. E., Docampo, R., and Moreno, S. N. (1992) Energization-dependent Ca^{2+} accumulation in *Trypanosoma brucei* bloodstream and procyclic trypomastigotes mitochondria. *Mol. Biochem. Parasitol.* **56,** 251–257
25. Perocchi, F., Gohil, V. M., Girgis, H. S., Bao, X. R., McCombs, J. E., Palmer, A. E., and Mootha, V. K. (2010) MICU1 encodes a mitochondrial EF hand protein required for Ca^{2+} uptake. *Nature* **467,** 291–296
26. Baughman, J. M., Perocchi, F., Girgis, H. S., Plovanich, M., Belcher-Timme, C. A., Sancak, Y., Bao, X. R., Strittmatter, L., Goldberger, O., Bogorad, R. L., Koteliansky, V., and Mootha, V. K. (2011) Integrative genomics identifies MCU as an essential component of the mitochondrial calcium uniporter. *Nature* **476,** 341–345
27. De Stefani, D., Raffaello, A., Teardo, E., Szabò, I., and Rizzuto, R. (2011) A forty-kilodalton protein of the inner membrane is the mitochondrial calcium uniporter. *Nature* **476,** 336–340
28. Docampo, R., and Lukeš, J. (2012) Trypanosomes and the solution to a 50-year mitochondrial calcium mystery. *Trends Parasitol.* **28,** 31–37
29. Barrett, M. P., Burchmore, R. J., Stich, A., Lazzari, J. O., Frasch, A. C., Cazzulo, J. J., and Krishna, S. (2003) The trypanosomiases. *Lancet* **362,** 1469–1480
30. Matthews, K. R. (2005) The developmental cell biology of *Trypanosoma brucei*. *J. Cell Sci.* **118,** 283–290
31. Schnaufer, A., Clark-Walker, G. D., Steinberg, A. G., and Stuart, K. (2005) The F_1-ATP synthase complex in bloodstream stage trypanosomes has an unusual and essential function. *EMBO J.* **24,** 4029–4040
32. Brown, S. V., Hosking, P., Li, J., and Williams, N. (2006) ATP synthase is responsible for maintaining mitochondrial membrane potential in bloodstream form *Trypanosoma brucei*. *Eukaryot. Cell* **5,** 45–53
33. Cristodero, M., Seebeck, T., and Schneider, A. (2010) Mitochondrial translation is essential in bloodstream forms of *Trypanosoma brucei*. *Mol. Microbiol.* **78,** 757–769
34. Hashimi, H., Cicová, Z., Novotná, L., Wen, Y. Z., and Lukes, J. (2009) Kinetoplastid guide RNA biogenesis is dependent on subunits of the mitochondrial RNA binding complex 1 and mitochondrial RNA polymerase. *RNA* **15,** 588–599
35. Schnaufer, A., Panigrahi, A. K., Panicucci, B., Igo, R. P., Jr., Wirtz, E., Salavati, R., and Stuart, K. (2001) An RNA ligase essential for RNA editing and survival of the bloodstream form of *Trypanosoma brucei*. *Science* **291,** 2159–2162
36. Paris, Z., Hashimi, H., Lun, S., Alfonzo, J. D., and Lukeš, J. (2011) Futile import of tRNAs and proteins into the mitochondrion of *Trypanosoma brucei evansi*. *Mol. Biochem. Parasitol.* **176,** 116–120
37. Clayton, A. M., Guler, J. L., Povelones, M. L., Gluenz, E., Gull, K., Smith, T. K., Jensen, R. E., and Englund, P. T. (2011) Depletion of mitochondrial acyl carrier protein in bloodstream-form *Trypanosoma brucei* causes a kinetoplast segregation defect. *Eukaryot. Cell* **10,** 286–292
38. Helfert, S., Estévez, A. M., Bakker, B., Michels, P., and Clayton, C. (2001) Roles of triosephosphate isomerase and aerobic metabolism in *Trypanosoma brucei*. *Biochem. J.* **357,** 117–125
39. Roldán, A., Comini, M. A., Crispo, M., and Krauth-Siegel, R. L. (2011) Lipoamide dehydrogenase is essential for both bloodstream and procyclic *Trypanosoma brucei*. *Mol. Microbiol.* **81,** 623–639
40. Lai, D. H., Hashimi, H., Lun, Z. R., Ayala, F. J., and Lukes, J. (2008) Adaptations of *Trypanosoma brucei* to gradual loss of kinetoplast DNA. *Trypanosoma equiperdum* and *Trypanosoma evansi* are petite mutants of *T. brucei*. *Proc. Natl. Acad. Sci. U.S.A.* **105,** 1999–2004
41. Wickstead, B., Ersfeld, K., and Gull, K. (2002) Targeting of a tetracycline-inducible expression system to the transcriptionally silent minichromosomes of *Trypanosoma brucei*. *Mol. Biochem. Parasitol.* **125,** 211–216
42. Kelly, S., Reed, J., Kramer, S., Ellis, L., Webb, H., Sunter, J., Salje, J., Marinsek, N., Gull, K., Wickstead, B., and Carrington, M. (2007) Functional genomics in *Trypanosoma brucei*. A collection of vectors for the expression of tagged proteins from endogenous and ectopic gene loci. *Mol. Biochem. Parasitol.* **154,** 103–109
43. Long, S., Jirků, M., Mach, J., Ginger, M. L., Sutak, R., Richardson, D., Tachezy, J., and Lukes, J. (2008) Ancestral roles of eukaryotic frataxin. Mitochondrial frataxin function and heterologous expression of hydrogenosomal Trichomonas homologues in trypanosomes. *Mol. Microbiol.* **69,** 94–109
44. Kafková, L., Ammerman, M. L., Faktorová, D., Fisk, J. C., Zimmer, S. L., Sobotka, R., Read, L. K., Lukes, J., and Hashimi, H. (2012) Functional characterization of two paralogs that are novel RNA-binding proteins influencing mitochondrial transcripts of *Trypanosoma brucei*. *RNA* **18,** 1846–1861
45. Speijer, D., Breek, C. K., Muijsers, A. O., Hartog, A. F., Berden, J. A., Albracht, S. P., Samyn, B., Van Beeumen, J., and Benne, R. (1997) Characterization of the respiratory chain from cultured *Crithidia fasciculata*. *Mol. Biochem. Parasitol.* **85,** 171–186
46. Mathias, R. A., Chen, Y. S., Kapp, E. A., Greening, D. W., Mathivanan, S., and Simpson, R. J. (2011) Triton X-114 phase separation in the isolation and purification of mouse liver microsomal membrane proteins. *Methods* **54,** 396–406
47. Schneider, A., Charrière, F., Pusnik, M., and Horn, E. K. (2007) Isolation of mitochondria from procyclic *Trypanosoma brucei*. *Methods Mol. Biol.* **372,** 67–80
48. Carnes, J., Trotter, J. R., Ernst, N. L., Steinberg, A., and Stuart, K. (2005) An essential RNase III insertion editing endonuclease in *Trypanosoma brucei*. *Proc. Natl. Acad. Sci. U.S.A.* **102,** 16614–16619
49. Nebohácová, M., Maslov, D. A., Falick, A. M., and Simpson, L. (2004) The effect of RNA interference Down-regulation of RNA editing 3′-terminal uridylyl transferase (TUTase) 1 on mitochondrial de novo protein synthesis and stability of respiratory complexes in *Trypanosoma brucei*. *J. Biol. Chem.* **279,** 7819–7825
50. Maslov, D. A., Zíková, A., Kyselová, I., and Lukes, J. (2002) A putative novel nuclear-encoded subunit of the cytochrome c oxidase complex in trypanosomatids. *Mol. Biochem. Parasitol.* **125,** 113–125
51. Malka, F., Guillery, O., Cifuentes-Diaz, C., Guillou, E., Belenguer, P., Lombès, A., and Rojo, M. (2005) Separate fusion of outer and inner mitochondrial membranes. *EMBO Rep.* **6,** 853–859
52. Wirtz, E., Leal, S., Ochatt, C., and Cross, G. A. (1999) A tightly regulated inducible expression system for conditional gene knock-outs and dominant-negative genetics in *Trypanosoma brucei*. *Mol. Biochem. Parasitol.* **99,** 89–101

53. Vafai, S. B., and Mootha, V. K. (2012) Mitochondrial disorders as windows into an ancient organelle. *Nature* **491,** 374–383
54. Mitchell, P. (2011) Chemiosmotic coupling in oxidative and photosynthetic phosphorylation. 1966. *Biochim. Biophys. Acta* **1807,** 1507–1538
55. Paucek, P., Mironova, G., Mahdi, F., Beavis, A. D., Woldegiorgis, G., and Garlid, K. D. (1992) Reconstitution and partial purification of the glibenclamide-sensitive, ATP-dependent K^+ channel from rat liver and beef heart mitochondria. *J. Biol. Chem.* **267,** 26062–26069
56. Costa, A. D., and Krieger, M. A. (2009) Evidence for an ATP-sensitive K^+ channel in mitoplasts isolated from *Trypanosoma cruzi* and *Crithidia fasciculata*. *Int. J. Parasitol.* **39,** 955–961
57. Inoue, I., Nagase, H., Kishi, K., and Higuti, T. (1991) ATP-sensitive K^+ channel in the mitochondrial inner membrane. *Nature* **352,** 244–247
58. Haddy, F. J., Vanhoutte, P. M., and Feletou, M. (2006) Role of potassium in regulating blood flow and blood pressure. *Am. J. Physiol. Regul. Integr. Comp. Physiol.* **290,** R546–R552
59. Rodríguez-Navarro, A. (2000) Potassium transport in fungi and plants. *Biochim. Biophys. Acta* **1469,** 1–30
60. Rizzuto, R., De Stefani, D., Raffaello, A., and Mammucari, C. (2012) Mitochondria as sensors and regulators of calcium signalling. *Nat. Rev. Mol. Cell Biol.* **13,** 566–578
61. Spremulli, L., and Kraus, B. L. (1987) Bovine mitochondrial ribosomes. Effect of cations and heterologous dissociation factors on subunit interactions. *Biochem. Biophys. Res. Commun.* **147,** 1077–1081
62. Maslov, D., and Agrawal, R. (2012) Mitochondrial translation in trypanosomatids. in *RNA Metabolism in Trypanosomes* (Bindereif, A., ed) pp. 215–236, Springer, Berlin

Attached Publications

Part IV. TRYPANOSOME MITOCHONDRIAL PHYSIOLOGY

Zdeněk Verner, Somsuvro Basu, Corinna Benz, Sameer Dixit, Eva Dobáková, Drahomíra Faktorová, Hassan Hashimi, Eva Horáková, Zhenqiu Huang, Zdeněk Paris, Priscila Peña-Diaz, Lucie Ridlon, Jiří Týč, David Wildridge, Alena Zíková, Julius Lukeš (2015). Malleable mitochondrion of *Trypanosoma brucei*. *Int. Rev. Cell Mol. Biol.* 315:73-151.

An excerpt from a review (pp. 102-104) about trypanosome mitochondrial biology summarizing the current state of knowledge of mitochondrial Ca^{2+} and K^{+} uptake and homeostasis.

3.3 Transport of Ions

It was established in the early 1960s that mammalian mitochondria have the ability to uptake calcium cations (Ca^{2+}) in a manner that relies on the inner membrane potential generated by the electron transport chain and sensitive to the ruthenium red dye (Deluca and Engstrom, 1961). Consistent with the role of Ca^{2+} as a potent secondary messenger in various cell signaling pathways (Clapham, 2007), an increase of the cation in the matrix directly stimulates the Krebs cycle enzymes isocitrate dehydrogenase and 2-oxoglutarate dehydrogenase and indirectly the pyruvate dehydrogenase (PDH) complex (Hansford, 1994). This process in turn increases the $NADH/NAD^+$ ratio, which boosts oxidative phosphorylation. In addition to being a target of Ca^{2+} stimulation, mitochondria play a role in shaping the spatiotemporal distribution and levels of the cation in the cytosol (Rizzuto et al., 2012). Mitochondrial calcium uptake can occur within microdomains of high Ca^{2+} concentration at sites in close proximity to the endoplasmic reticulum or plasma membrane (Rizzuto et al., 1998, 1993). Yet, the concentration of matrix Ca^{2+} must be carefully regulated as a high load sensitizes the opening of the permeability transition pore, which commits a cell to the mitochondria-dependent apoptosis (Haworth and Hunter, 1979; Szalai et al., 1999).

Strangely, this mt Ca^{2+} uptake mechanism is not present in yeast (Carafoli and Lehninger, 1971), even though these belong to the opisthokonts. Even more surprisingly, mitochondria isolated from *T. cruzi* did demonstrate this activity in exactly the same manner as the mammalian organelle (Docampo and Vercesi, 1989a,b). A series of follow-up studies established that this biochemical property is conserved throughout trypanosomatids (Docampo and Lukeš, 2012). Of particular interest was the observation that mitochondria isolated from BSF retained this activity, despite not having the energy-producing Krebs cycle or classical electron transport chain (Vercesi et al., 1992).

Studies on mt Ca^{2+} uptake in kinetoplastids became vital almost a quarter of a century later in identifying the protein components underlying this activity. Of the 1098 mouse proteins making up the MitoCarta (Pagliarini et al., 2008), only a handful fit the criteria for proteins putatively involved in mt calcium uptake: (1) inner membrane localization; (2) expression in most mammalian tissues; (3) orthologs present in vertebrates and kinetoplastids, but not yeast. This procedure led to the discovery of two proteins that were part of calcium uptake mechanism conserved between vertebrate and

trypanosome mitochondria. The mitochondrial calcium uptake protein 1 (MICU1) is an EF-hand-containing protein with a single transmembrane domain (Perocchi et al., 2010). Later studies in mammals have demonstrated that MICU1 regulates the opening of the bona fide calcium channel by sensing Ca^{2+} concentration in the IMS, which presumably reflects the situation in the cytosol (Csordás et al., 2013; Mallilankaraman et al., 2012). The actual pore is formed by oligomers of the mitochondrial calcium uniporter (MCU) protein (Baughman et al., 2011; De Stefani et al., 2011; Raffaello et al., 2013).

Studies of the MCU ortholog in PCF and BSF showed that mt calcium uptake is essential for viability (Huang et al., 2013). The authors concluded that as in mammalian mitochondria, matrix calcium stimulates energy metabolism in PCF as the MCU-depleted trypanosomes suffered from a higher intracellular AMP/ATP ratio and an upregulation of autophagy markers, a common cell response to starvation. The enzymes that are regulated by matrix calcium in mammalian cells are also present in PCF, albeit separated into different metabolic fluxes (Section 4.1). The function of mt calcium uptake is not so straightforward in the BSF, as the mitochondrion switches to an ATP consumer. However, PDH remains present in BSF to convert pyruvate from glycolysis to acetyl-CoA, which is then used for essential FA synthesis via acetate or directly by the FAS II pathway (Mazet et al., 2013; Stephens et al., 2007). As this protein complex is stimulated by matrix Ca^{2+} in mammals, perhaps it is as well in trypanosomes, giving MCU at least one raison d'etre in this stage (Huang et al., 2013). While mt calcium uptake mediated by MCU appears to shape cytosolic Ca^{2+} in *T. brucei* (Xiong et al., 1997), a possible interplay between the *T. brucei* mitochondrion and endoplasmic reticulum remains mysterious (Docampo and Lukeš, 2012; Vercesi et al., 1993).

In contrast to the tightly regulated Ca^{2+}, potassium (K^+) is the most abundant cation in the cell (Haddy et al., 2006; Rodríguez-Navarro, 2000). In the initial proposition of chemiosmotic theory, the danger that oxidative phosphorylation would pose in terms of cation sequestration in the negatively charged matrix was recognized (Mitchell, 2011). Several protein channels whose molecular identity remains unknown are believed to exist that mediate the entry of K^+ into the matrix across the inner membrane (Szewczyk et al., 2009). Evidence for their existence is based on the sensitivity of mammalian inner membrane potassium conductance to ATP, Ca^{2+}, and compounds such as glibenclamide (Inoue et al., 1991; Paucek et al., 1992). Indeed, mitoplasts isolated

from *T. cruzi* also exhibited such properties, suggesting this phenomenon is conserved throughout a wide range of eukaryotes (Costa and Krieger, 2009).

A mechanism to alleviate matrix monovalent cation overloading as driven in an electroneutral fashion by the proton motive force generated by oxidative phosphorylation was also described as part of the chemiosmotic theory (Mitchell, 2011). A protein called Leucine zipper EF-hand-containing protein 1 (Letm1) was shown to be a component of K^+/H^+ exchange (KHE), as its gene knockout in *S. cerevisiae* caused massive mt swelling that was ameliorated by the ionophore nigericin, which enables KHE chemically (Nowikovsky et al., 2004). This protein has orthologs across eukaryotes, including *T. brucei* (Hashimi et al., 2013a). As in yeast and humans (Dimmer et al., 2008), downregulation of Letm1 initiated mt swelling in both life cycle stages, although it is reversed by nigericin treatment. Interestingly, the swelling was also observed in the petite mutant *T. b. evansi*, which does not possess the ΔpH component of the mt proton motive force (Hashimi et al., 2013a). An alternative hypothesis was proposed in which Letm1 is a mt Ca^{2+}/H^+ exchanger that may regulate KHE (Jiang et al., 2009; Tsai et al., 2014), although this idea remains controversial (Nowikovsky and Bernardi, 2014).

While much of this chapter is devoted to differences between the mt proteomes of *T. brucei* and better-studied model systems such as mammalian cells and yeast, this section also underscores how similarities between diverse eukaryotic clades can further increase our understanding of the biology of the organelle. The regulation of K^+ in the mt matrix by the highly conserved Letm1 and the putative proteins(s) comprising an influx channel for the cation may be a mechanism to modulate mt volume (Nowikovsky and Bernardi, 2014; Nowikovsky et al., 2004), suggesting an ancient origin of this mechanism. Furthermore, a comparative approach of mt proteomes of kinetoplastids and the opisthokont vertebrates and yeast led to the discovery of the proteins responsible for mt Ca^{2+} uptake.

4. MITOCHONDRIAL METABOLISM

Import of proteins and metabolites feeds mt metabolism. Due to the presence of carbohydrate metabolism coupled to oxidative phosphorylation, the mitochondrion represents a powerhouse of the cell. However,